ROYAL AIRCRAFT ESTABLISHMENT
BEDFORD.

R. & M. No. 3095
(18,788)
A.R.C. Monograph

MINISTRY OF SUPPLY

AERONAUTICAL RESEARCH COUNCIL

REPORTS AND MEMORANDA

An Investigation of the Hydrodynamic Stability and Spray Characteristics of High Length/Beam Ratio Seaplane Hulls with High Beam Loadings

BY

D. M. RIDLAND, A.F.R.Ae.S., J. K. FRISWELL, B.Sc.,
and A. G. KURN.

LONDON: HER MAJESTY'S STATIONERY OFFICE

PRICE £6 6s 0d NET

MINISTRY OF SUPPLY

AERONAUTICAL RESEARCH COUNCIL
REPORTS AND MEMORANDA

An Investigation of the Hydrodynamic Stability and Spray Characteristics of High Length/Beam Ratio Seaplane Hulls with High Beam Loadings

By

D. M. RIDLAND, A.F.R.Ae.S., J. K. FRISWELL, B.Sc.,
and A. G. KURN

LONDON: HER MAJESTY'S STATIONERY OFFICE
1959

© *Crown copyright 1959*

Printed and published by
HER MAJESTY'S STATIONERY OFFICE

To be purchased from
York House, Kingsway, London W.C.2
423 Oxford Street, London W.1
13A Castle Street, Edinburgh 2
109 St. Mary Street, Cardiff
39 King Street, Manchester 2
Tower Lane, Bristol 1
2 Edmund Street, Birmingham 3
80 Chichester Street, Belfast
or through any bookseller

Printed in Great Britain

An Investigation of the Hydrodynamic Stability and Spray Characteristics of High Length/Beam Ratio Seaplane Hulls with High Beam Loadings

By

D. M. RIDLAND, A.F.R.AE.S., J. K. FRISWELL, B.SC., and A. G. KURN

COMMUNICATED BY THE DIRECTOR-GENERAL OF SCIENTIFIC RESEARCH (AIR)
MINISTRY OF SUPPLY

*Reports and Memoranda No. 3095**
March, 1956

Summary

Tests have been made on a series of high length/beam ratio seaplane hulls with high beam loadings. The effects of varying the hull parameters, forebody warp, afterbody length and afterbody angle, together with the interaction of these effects, and of tailoring the afterbody, on the calm water hydrodynamic stability and spray characteristics of the series have been determined. To amplify this work, investigations have been made into the effects of load, moment of inertia and radius of gyration, and slipstream, together with a limited assessment of longitudinal hydrodynamic stability characteristics in waves.

Dynamic models were used and tests for the main investigation consisted of assessments of longitudinal hydrodynamic stability characteristics, both undisturbed and disturbed, at two weights, of spray behaviour at these weights, and of directional hydrodynamic stability characteristics at the higher weight only. Improvements in test techniques are described and, where appropriate, reference is made to earlier work on hulls of low length/beam ratio.

* M.A.E.E. Report F/Res/269, received October, 1956.

LIST OF CONTENTS

LIST OF APPENDICES

LIST OF TABLES

LIST OF ILLUSTRATIONS

CHAPTER 1

Introduction

This report describes a series of experiments on high length/beam ratio seaplane hulls, which are defined to be hulls for which the ratio

$$\frac{\text{distance from forward perpendicular to aft step}}{\text{maximum beam at chine}}$$

(*i.e.*, the ratio of overall length as far as the aft step to the maximum wetted beam) is greater than 10. These hulls came into prominence when it was found that by the use of a high length/beam ratio a considerable reduction in the aerodynamic surface-area drag coefficient was possible, thus enabling higher flying speeds to be attained. Further investigations showed that a reduction in percentage hull-structure weight was also feasible and that when chine immersion occurred, as would usually be the case, landing impact forces were reduced.

The aim of the present investigation was to add to the existing information by providing data on the hydrodynamic stability and spray characteristics of this class of hull. In addition to this, data was obtained which also applied to conventional hulls and consolidated earlier work on similar lines. The investigation was made by determining the effects of varying a number of standard seaplane hull parameters on a basic hull of high length/beam ratio. This was complemented by extensive tests on the effects of several non-geometric parameters (such as load), important in themselves but subsidiary to the main investigation, and by a limited series of tests in waves.

The report is divided into twelve chapters. Chapter 2 deals with test techniques, Chapters 3, 4 and 5 cover the subsidiary investigations, while the main work on the hull shape parameters is considered in Chapters 6 to 10. The tests in waves are discussed at length in Chapter 11 and a few full-scale applications of the results, together with some general conclusions, are given in Chapter 12.

The discussion on techniques in Chapter 2 is quite extensive. It commences with an outline of the scope of the tests and this is followed by a description of both the aerodynamic and hydrodynamic aspects of the model design. The methods used for the measurement of aerodynamic lift are then considered and the next section deals with the determination of longitudinal stability characteristics. It includes a review of previous techniques for the assessment of longitudinal stability characteristics with disturbance and a consideration of the effects of disturbance, both of which should help in the understanding of the phenomenon of disturbed stability. The method used to evaluate spray characteristics is then described and this is followed by a section on directional stability measurements. The chapter ends with a statement of the manner in which values of elevator effectiveness were obtained.

The investigation of load effects considered in Chapter 3 was carried out to permit a more enlightened interpretation of the limited assessments which were made on each model of the main series. It was found that in general the variation with load of the important characteristics was linear and was what would be expected from experience on low length/beam ratio hulls. In Chapter 4 it is verified that pitching moment of inertia is not a significant parameter in the investigation and the effects of moment of inertia, radius of gyration and mass are correlated. Chapter 5 deals with the remaining subsidiary parameter, slipstream, and indicates generally the effects of this parameter on the stability characteristics of high length/beam ratio hulls. It is shown that with increase in thrust coefficient both critical trim and trim generally are reduced, while both resistance to disturbance and elevator effectiveness are increased. At the same time the spray blister in the propeller plane is raised and broken.

That part of the main investigation in which a determination was made of the effects of variations in the primary hull shape parameters, forebody warp, afterbody length and afterbody angle, is described in Chapters 6, 7 and 8. It was found that the outstanding effect of forebody warp is to improve spray characteristics considerably. This is accompanied by a useful improvement in longitudinal, and a negligible deterioration in directional, stability characteristics. The effects of lengthening the afterbody are to reduce critical trim and amplitudes of porpoising, and to increase considerably resistance to disturbance. This is accompanied, however, by poor directional stability, bad spray and low elevator effectiveness. The afterbody-angle results show that higher afterbody angles give rise to good characteristics generally, but when the aim is to reduce afterbody angle, as might well be the case, great care would have to be taken. The effects are not independent of load and the lowest afterbody angle tested gave rise to extremely bad disturbed stability characteristics, poor spray and low elevator effectiveness.

The interaction of the effects of the hull shape parameter variations is discussed in Chapter 9. The main conclusion is that, while there is no simple law governing the combination of individually advantageous parameters, it is true in the general case to say that combining the most beneficial values of the various parameters will give the hull with the best stability characteristics.

In Chapter 10 the tailored afterbody is discussed, a tailored afterbody being one designed to fit in the forebody wake in such a manner that no afterbody suctions are generated, the object being to alleviate disturbed instability. In the present case the technique of tailoring has been found sound, disturbed instability being much

reduced, and it is concluded that to obtain maximum benefit from this procedure not only the afterbody but the main step also should be considered. A further interesting result of afterbody tailoring is a large improvement in directional stability characteristics.

Chapter 11, dealing with the tests in waves, is detailed and represents a large number of tank tests, but even so there is scope for much more work on this topic. The main conclusions reached are that the risk of instability in waves is lessened by high speeds and nose-down elevator angles and that for mid-planing speeds there exists a resonant wavelength equal to two and a half times the hull length.

Finally, in Chapter 12, a number of more general points based on the work as a whole are discussed.

In addition to the main body of the report there are five appendices which illustrate or describe points of interest not directly connected with the main theme of the investigation. The first, on static margin effects, shows that even quite large variations in static margin have little effect on undisturbed longitudinal stability characteristics, while the second is a précis of the methods used to obtain the hull lines for models of this series. In the third Appendix the effects of changes in mass, moment of inertia and radius of gyration are treated theoretically and correlated with the experimental results of Chapter 4. The agreement between theory and experiment is extremely good.

An assessment is made in Appendix 4 of the degree of correlation between the effects of disturbance and waves on longitudinal stability. It is definitely established that no practical correlation exists. The last Appendix gives a very brief account of the individual hydrodynamic characteristics of each model and special note is made of any peculiarities in behaviour. A very quick appreciation of the outstanding features of any of the parameters investigated can thus be obtained.

CHAPTER 2

Test Techniques

1. **Introduction.**—The tests on which this investigation is based were made in the Royal Aircraft Establishment Seaplane Tank on complete dynamic models and the apparatus and test methods used were basically those described in Ref. 1. Several modifications were made, however, both to the apparatus and to the methods, and in one or two cases it was found necessary to carry out limited subsidiary investigations to establish individual techniques for use in this programme.

Thirteen different models were used in the investigation and general details of these, together with the grouping of the models for test purposes, are given in Table 2. The tests actually carried out on the models of the series are listed in Table 3 and, except for those made on the interaction models (Chapter 9), consisted of assessments of aerodynamic lift, hydrodynamic longitudinal stability, spray and hydrodynamic directional stability characteristics.

Consideration is given first in the present section of the report to both the aerodynamic and hydrodynamic aspects of the design of the models, and the methods used to determine aerodynamic lift characteristics are then described. In this connection it may be remarked that the lift assessment was subsidiary in that it was made mainly to ensure consistent loads on water during stability tests. The techniques used in the longitudinal stability tests are discussed next and it is here that the most extensive modifications to earlier methods have been made: the tests without disturbance were carried out in accordance with Ref. 1, but additional observations were made on each test run; the tests with disturbance were made with a revised maximum-disturbance technique; the tests in waves, while resembling those of Ref. 1 in some details, were conducted with an overall approach different from that of tests made hitherto and the technique may thus be regarded as completely new. A description of two recording systems which were used during the wave tests completes the section on longitudinal stability test techniques. The method of assessing spray characteristics is then described and a comprehensive discussion of the directional stability tests follows. Finally, the method used to obtain the curves of mean elevator effectiveness against speed is detailed.

The presentation used for the results of each type of test is considered with the relevant technique, but it may be remarked here that results have in general been presented non-dimensionally. Should it be desired to interpret these results in terms of full-scale values then, for a flying boat of 150,000 lb and 9·5 ft beam (these are considered to be reasonable dimensions for a hull of the present type), the models are 1/20 scale and full-scale values may be obtained by multiplying C_v by 10·35 to give speed in knots and C_Δ by 54,500 to give load in pounds.

2. **Model Design.**—2.1. **Aerodynamic.**—As only hull characteristics were under investigation, model wing and tail design was arbitrary except for the need to produce a reasonably stable craft with lift and moments of the right order, and the aerodynamics of all models of the series were identical, as far as manufacture would allow, with those of the basic model. Aerodynamic data are given in Table 1.

A 1/15 scale *Sunderland* wing with cropped tips was chosen for the mainplane and provision was made for the fitting of four compressed-air driven turbine-propeller units when it was desired to simulate slipstream effects, leading-edge slats being fitted outboard of the outer nacelles in this case to increase $C_{L\max}$ and approximate to the higher Reynolds-number lift characteristics appertaining full scale. To represent the zero-thrust case for the slipstream investigation the propellers were replaced by fairings and the tip slats retained, but for the main tests of the series, which were made without slipstream, the nacelles and turbines were completely removed and full-span slats were fitted, the tip slats being insufficient by themselves to remove a kink from the lift curve (Fig. 30c), which was presumably due to the low Reynolds numbers at which the tests were made. The various configurations are illustrated in Fig. 28.

The tailplane was that of a 1/15 scale *Sunderland* apart from the elevators, the chord of which was increased to give better coverage of the attitude range and improve aerodynamic stability (this effective increase in tail area should not alter the lower critical trim, *i.e.*, the trim of a point on the lower stability limit[2]). The position of the tailplane, high on the fin (Fig. 1), was chosen to avoid interference from spray at high planing attitudes.

The fin and rudder were combined in one vertical surface, but moments could be induced by the bending of a metal tab slotted into the trailing edge.

With a keel attitude of zero degrees, the standard-mean-chord quarter-chord point was 0·04 ft forward of and 0·28 ft above the c.g. (Table 1). The model was thus aerodynamically stable, having a stick-fixed static margin of approximately $0{\cdot}15c$ in the case without slipstream. Brief consideration is given in Appendix I to the variation of static margin with attitude and to the general effects of this variation on the hydrodynamic longitudinal stability characteristics of the models.

2.2. **Hydrodynamic.**—For the hydrodynamic investigation successive variations were made on the basic hull form while retaining the same forebody length and beam.

The methods used to obtain the hull lines for each model of the series were, apart from the changes in afterbody shape, essentially similar; they are described in Appendix II and hull lines for the basic model (Model A) are given in Fig. 41. The variations made on the basic hull form may be seen in Table 2.

In order to produce clean breakaway of spray, model scale, with negligible effect on stability, chine strips were fitted to all of the model hulls. They consisted of strips of foil inserted along the chine so as to bisect the hull wall-planing bottom angle and to stand proud to the order of 0·003 in.

3. **Aerodynamic Lift.**—For the measurement of aerodynamic lift runs were made in all the configurations concerned at constant speeds with the model at fixed incidences, appropriate ranges of speed, incidence and elevator angle being covered. In the power-on slipstream case, air was supplied to the turbines at constant pressure, the value being chosen to give a reasonable take-off propeller thrust. Additionally, a representative tailplane lift curve was obtained by making a series of runs on the basic model with its tail unit removed, the model otherwise being in the normal test configuration (*see* Table 3). The required lift curve was then determined as the difference between these results and the corresponding ones with the tailplane in position.

Throughout the lift runs the model was suspended so as to keep the mainplane at a constant height (about 1·5*c*) above the water surface. No allowance was made for ground effect, but earlier work on this subject by Clark and Tye[3], using a model with an unslatted wing, shows an error in C_L value at 10-deg wing incidence (wing chord to horizontal) of about 4 per cent, for values of height above water corresponding to the present case. The error is zero at 4-deg incidence, and approximately linear up to $C_{L\max}$ which is unchanged by ground effect. In the present hydrodynamic stability tests, therefore, at 16-deg incidence, corresponding generally to upper-limit attitudes, one can expect to have actual lift values of the order of 8 per cent greater than those at similar attitudes obtained by measurement in the lift rig. The lift curves are used primarily for estimation of load on water, so the maximum error will be found at take-off speeds and high attitudes. At increasing distances from this region of the stability diagram the error will be progressively less.

The lift curves without slipstream have been plotted in the usual manner. An example, showing the effect of elevator, is given in Fig. 126. The points plotted are check points in respect of which the curves have been modified from those of the first wing tested. The tailplane lift curve is shown in Fig. 2 and the lift curves with slipstream have been plotted at different thrust coefficients, T_c, in Fig. 30a.

4. **Hydrodynamic Longitudinal Stability.**—Throughout this investigation all assessments of longitudinal stability characteristics, both with and without disturbance, and in waves, have been made by means of constant-speed runs with different elevator settings, over a range of speeds from 4 to 40 ft/sec. Each run was made with zero flap and one centre-of-gravity position and the model was towed from the wing tips on the lateral axis through the centre of gravity, being free in pitch and heave only. During each run the speed, elevator angle, trim and stability characteristics were noted. In each case the motion was defined as unstable when the resulting oscillation (if any) was apparently divergent or had a constant amplitude of more than 2 degrees (This 2-deg limit has been chosen arbitrarily as the maximum permissible for safety under operational conditions[4]). The tests in waves gave rise, as might be expected, to motions which differed greatly from those of the calm-water cases and which were for the most part irregular. The classification of such motions as stable or otherwise is dealt with in Chapter 11, Section 1.3.

The calm-water tests*, which form the main part of the investigation, were made with a smooth, undisturbed, water surface. From the results of these tests, undisturbed and disturbed stability diagrams were built up in the usual manner as described below. Also it was found that, in the majority of cases of instability, the oscillation maintained a constant amplitude which could be read to within 5 per cent and on plotting these observations the unstable part of the diagram could be divided into natural regions of equal steady oscillations as in Fig. 4. Similar diagrams have been included for each model of the series, but only individual test points with amplitudes have been given; no zones have been drawn. Special forms of diagram, unlike those for the undisturbed and disturbed cases, have been devised for the presentation of the results of the wave tests and these are described in Chapter 11, Section 1.5.

4.1. **Longitudinal Stability without Disturbance.**—For the assessment of longitudinal stability characteristics without disturbance, test runs were made in the manner described in the previous Section, all oscillations being allowed to develop naturally with no external aid, and the stability data for each model have been presented as in Figs. 121, 124 and 125. In the first type of Figure the stability limits, trim curves and test points are given, the latter being marked stable, unstable or border-line as appropriate (it may be noted that separate figures are given for the undisturbed and disturbed cases contrary to usual practice; this enables a clearer appreciation of the undisturbed and disturbed qualities to be gained); in the second are shown load-coefficient curves which are based on the trim curves of the preceding Figure and are calculated from the lift curves for the particular model concerned; in the third type of Figure the amplitudes of porpoising for each test point are shown in conjunction with the stability limits.

No flying region is indicated on the stability diagrams because, except on extremely rare occasions, the models did not fly, but a good idea of flying speeds for each

* Tests other than those made in waves, *i.e.*, tests with and without disturbance.

elevator setting can be obtained from the corresponding load-coefficient diagrams. The load-coefficient curves serve for the case with disturbance as well as for that without. In the computation of load coefficients no correction was applied for ground effect, but allowance was made for the effect of elevator.

Comparisons of stability limits for the assessment of the effects of one or other of the parameters under investigation have in general been made on a C_v base at different loads, but consideration was given earlier in the investigation to the use of another base, namely the hydrodynamic lift coefficient $C_\Delta^{1/2}/C_v$, and this type of presentation has been retained in one or two appropriate instances. It has been claimed (Refs. 5 and 6) that stability limits obtained without disturbance for one model at different weights will collapse when plotted on a $C_\Delta^{1/2}/C_v$ base, that is to say that, as the effect of weight is considered implicitly in the parameter $C_\Delta^{1/2}/C_v$, it will not be seen as a separation of the limits. In this connection an interesting comparison is made in Fig. 5, where undisturbed stability limits for Model B at different weights are shown both on a C_v and on a $C_\Delta^{1/2}/C_v$ base. The tendency for the limits to collapse in the latter case is evident, but that a complete collapse is not obtained is equally clear and for this reason this type of plot has not been generally adopted in the present investigation. Further consideration is given to this matter in Chapter 9.

4.2. **Longitudinal Stability with Disturbance.**—The experimental techniques in use prior to the commencement of this programme for the assessment of disturbed stability characteristics left a great deal to be desired and were unsuitable for a major research investigation. The techniques have accordingly been modified and to help in appreciating the difficulties involved in this type of test a brief review of earlier methods has been given below. This is followed by a description of the modified methods used in this investigation and, in an attempt to advance the understanding of disturbed instability, the next Section is devoted to a résumé of disturbance effects. The last Section gives a probable explanation of the mechanism by which the large amplitude oscillations associated with disturbed instability are sustained.

The test results are presented in the same way as are those for the undisturbed case; examples may be seen in Fig. 122, which is a disturbed stability diagram, and in Fig. 125, where the corresponding porpoising amplitude diagram is given. As has been previously mentioned, each load-coefficient diagram serves for both undisturbed and disturbed cases; the diagram corresponding to Fig. 122 can be seen in Fig. 124.

Previous Disturbance Techniques

Disturbance techniques for stability testing have been used in the R.A.E. Seaplane Tank for some time. In Ref. 7 (1935) it was suggested that, as calm water conditions would seldom be realised full scale, some disturbance of the water during a model test was desirable. This was achieved by doing each test run while the water surface was still disturbed from the previous run. If instability did not develop, however, the model was ' disturbed fairly violently ' (by hand) and the subsequent motion was observed. It was noted that sometimes the large disturbance caused instability where the smaller one (that due to the disturbed water surface) did not; on such occasions the interpretation of the results was to some extent a matter of judgment and it was found that a slightly pessimistic prediction of the full-scale behaviour was often made.

A more detailed technique was necessitated by the fact that in 1938 two seaplanes, the *Lerwick* and the *Saunders-Roe R2/33*, stable model scale with the techniques then used, became unstable full scale, the latter crashing as a result of this instability. The revision of technique is reported by Gott[8] who states that ' a serious difficulty appears when it is necessary to decide what is a suitable disturbance to give the model ' and that ' it has always been generally agreed that the model disturbance should be correctly scaled down from the maximum disturbance the full-scale flying boat can receive in service. Unfortunately, individual judgment as to what this means in practice shows enormous variation and disturbances given to models have varied from a gentle touch with one finger to a push which changed the attitude of the model by perhaps 5 degrees '. The apparent discrepancy between model and full-scale behaviour of the *Lerwick* was explained when the method of applying disturbance, as well as the amount given, was found to be of fundamental importance. It was noted that a nose-down disturbance was more effective in producing instability than a tail-down disturbance of equal magnitude and that a train of about six waves could cause the onset of instability, quite as well as a manual disturbance, even though they were waves of small height, as long as the wave length was of the right order to produce a resonance effect*. It was concluded, however, that the wave technique is too time-consuming and that a suitable manual disturbance must be given to the model. This disturbance must not be too small in case an unstable region is missed; it must not be too large, so that the aircraft under consideration is not unduly penalised, *i.e.*, so that the aircraft under consideration is not made to appear worse than it is under normal operating conditions, and it must be of the right kind. What the right disturbance is must be determined by trial.

The disturbance in general use in 1944[4] is quoted by Smith and White, in a review of porpoising phenomena, as being a severe nose-down angular disturbance of the order of 10-deg amplitude though, in the more recent tests on the *Saunders-Roe E6/44*[9], the applied disturbances were of the general order of 6 to 8-deg nose down, except at fine angles of trim, when the keel attitude was lowered to 0-deg, *i.e.*, the disturbance was less than 6-deg. The latter is substantially the same as the method described in the most recent review of tank-testing tech-

* So-called ; it is not suggested by the authors of the present report that true resonance occurs but, the term being commonly used in this context, it will be retained.

nique (Ref. 1), where it is stated that ' if no oscillation develops, the rear cord (model guide string) is jerked to give the model an impulsive nose-down disturbance of about 6-deg, or sufficient to reduce the keel attitude to zero, whichever is the smaller '.

It can be seen that the above techniques are not well defined and leave a great deal to the judgment of the operator, quite apart from the difficulty of applying a given degree of disturbance. While they may be satisfactory for tests on individual specific aircraft they are not suitable for tests on a research series of models; furthermore, the significance of applying a given degree of disturbance is not fully understood. The revised techniques described below were therefore used in the present investigation.

Present Investigation

In order to obtain limits which were both reproducible and comparable from model to model, two sets of limits were obtained for each model at each weight, one being for the undisturbed case and the other for the case with maximum disturbance as defined below. The undisturbed limits indicate what can be expected full scale in very calm water without disturbance and are precise, and the test conditions are those on which theoretical treatments are based. The disturbed limits are similarly precise and reproducible when obtained by the method used, which was:

(*a*) to give a nose-down impulsive disturbance to the model by jerking on the rear guide string

(*b*) to give the maximum disturbance possible consistent with safety so that instability was induced at all speeds and attitudes at which it was feasible to do so,

and were obtained for use in conjunction with the undisturbed limits to give a complete picture of the calm-water stability characteristics.

That both sets of limits are necessary for a complete representation of calm-water stability characteristics is illustrated by the comparison of limits in Fig. 6 for two of the models, C and N, which were used in this programme. In the undisturbed case C appears to be the better model, but only just, whereas N is much superior under disturbed conditions. For good all-round stability N is unquestionably the better hull form, but no such clear-cut decision could have been formed from a comparison of the undisturbed limits alone.

It was hoped that in addition to helping towards a complete understanding of calm-water stability characteristics the disturbed limits could be used as an indication of rough-water behaviour. Details of experiments conducted to determine whether this was in fact possible are given later in the report and the extent to which the two sets of results can be correlated is examined in Appendix IV; the remainder of this Section is concerned with disturbed limits and the mechanism of disturbed instability.

The Effect of Disturbance on Stability Limits

The effect of disturbance in that region of the stability diagram which is unstable without disturbance is to produce a discontinuous increase in the amplitude of steady porpoising (Figs. 4, 62 and 76). There must, therefore, be a critical disturbance in this region, such that if it is exceeded, the model will oscillate at the higher amplitude. Also, as the degree of disturbance is increased, so is the magnitude of the unstable region, until a limit is reached when no further instability can be induced regardless of the disturbance; this is referred to as the limit with maximum disturbance. Partial limits for various degrees of disturbance for Models A and D are shown in Fig. 7 and illustrate this point; a complete set of graded limits could have been obtained, but this was considered unnecessary. It can be seen that the limit with maximum disturbance is, by its nature, a completely reproducible limit, since to render a configuration unstable it is only necessary to exceed the critical disturbance*, not reproduce it. Furthermore, it appears that a slight misjudgment of what constitutes the maximum disturbance is unlikely to be significant, as evidenced by Fig. 7, where an almost correct final limit is obtained with 6 deg of disturbance, so that the error in a limit obtained with greater amounts of disturbance should be very small.

The limits in Fig. 7 are based on observations taken during normal stability tests and the marked similarity of the two diagrams may be noted (Model D differs from Model A only with respect to afterbody length; that of Model D is one beam less than that of Model A). The number 0 indicates the limit obtained with zero disturbance, at which the amplitude of porpoising is 2 deg; each of the other numbers indicates the limits defining unstable regions which were obtained with that number of degrees of disturbance, but the amplitude of porpoising at the limit is not necessarily 2 deg; in fact, it is generally greater. This is shown in Fig. 4 where the unstable regions have been divided into zones of equal steady oscillations, or in Figs. 62 and 76, where porpoising amplitudes at specific points are marked This feature is worth noting; in the undisturbed case there is a natural gradation of amplitudes from stable to unstable regions and to talk of a 2-deg limit implies that everywhere along the limit porpoising amplitudes of 2 deg will be found. In the disturbed case to speak of a 2-deg limit implies only that porpoising outside the limit is of greater amplitude than 2 deg. It would be better to talk of a limit obtained with x deg of disturbance, or an x-deg disturbance limit.

Examination of Fig. 7 also shows that with increasing disturbance the mid-planing region becomes unstable first, reaching a maximum width with about 5 deg of disturbance; further increases in the degree of applied disturbance only raise the high-speed lower limit. In the vicinity of the latter it has been noted that the greater

* *i.e.*, the minimum disturbance necessary to induce instability at any particular speed and attitude.

the disturbance necessary to produce instability, the more violent is the resulting porpoising; in particular, following a disturbance at high speeds and low attitudes, the porpoising of every model of this series has been violent with the model leaping well clear of the water during each cycle. Again, when a hull modification is introduced which increases resistance to disturbance, this is characterised by the reduction or disappearance of disturbed instability in the mid-planing region; the high-speed low-attitude unstable region may be modified to some extent, but instability here appears always to be attainable if sufficient disturbance is given.

It is concluded in Appendix IV that disturbed limits cannot be interpreted in terms of stability in waves; they do, however, indicate full-scale stability characteristics with disturbance and the question of what constitutes a full-scale disturbance therefore deserves closer examination. The wash of a boat, such as that which caused the crash of the *Saunders-Roe* R2/33[8], or a sudden yaw, such as that which caused porpoising and finally damage to the *Solent* N.J.201[10] are acceptable examples, but a type of disturbance which occurs regularly full scale is that encountered during landing. The suggestion that every landing constitutes a disturbance was considered in essence by Gott[11] and upheld in the light of his experience, and it is made (quite independently) in Chapter 7, Section 2.3. and is supported by American evidence. It is considered, therefore, that limits with maximum disturbance indicate either stability characteristics in take-off or planing when a severe disturbance is encountered, or the worst stability characteristics in landing.

An investigation by Locke and Hugli[12] into disturbance effects substantiates the existence of different limits for different degrees of disturbance and of a final limit which further increases in magnitude of disturbance do not alter. This work is interesting because it was restricted to the upper-limit region, where the present data are rather sparse, yet led to the same conclusions.

Mechanism of Disturbed Instability

So far, no mathematical theory has been advanced for the case of stability with disturbance and the phenomenon is not well understood. Gott has offered an explanation of the unstable motion following a disturbance, in terms of afterbody suctions which may occur under certain conditions of air and water flow round the afterbody[13]. His account is clear and, as it is generally supported by recent experience, it is repeated below.

> 'Consider a model oscillating with a small amplitude, so that the motion is damped, and then let the amplitude be increased until it includes an attitude at which suction effects occur. If the suction effect is sufficiently localised it will act like an impulse applied at a particular phase in the oscillation and it is not difficult to show, from the usual expressions for a damped harmonic oscillation, that if the phase of the impulse is suitable the model will then execute a continuous undamped oscillation . . .
>
> According to this theory the essential feature is not the disturbance required to start porpoising considered as a force or a moment, but the amplitude of oscillation required to reach an attitude at which suction effects occur. An indication of the correctness of this view was obtained on an unstable model which was made to oscillate at small steady amplitudes by running through a long and very shallow wave. Whenever the double amplitude reached about 5 deg, porpoising of much larger amplitude commenced. The critical condition need only be reached once and could be reached full scale due to any number of chance circumstances which do not exist at all under the controlled conditions of tank testing.'

As has been seen, the existence of the critical condition referred to by Gott is confirmed by the present investigation, in which it has been referred to as the critical disturbance.

4.3. **Longitudinal Stability in Waves.**—The limited tests which were made to assess the longitudinal stability characteristics in waves of the high length/beam ratio class of hulls now under investigation are considered in Chapter 11. The techniques used were, except for the presence of waves in the tank and for modifications occasioned thereby, the same as those used in the calm-water tests without disturbance. For convenience the test methods are described in Chapter 11 in association with the discussion on wave effects.

4.4. **Recording Systems.**—As an aid in stability testing generally, two desynn systems were attached to the model rig, one for height, using a flap type transmitter, and the other for attitude, using a miniature transmitter. Rapid-response indicators were used and these were fitted in an automatic observer which, by means of a Bell and Howell A.4 cine camera, also recorded time and speed. The systems had the normal desynn limitations[14] but the required working frequencies, 3 or 4 per second, were low and, as the indicators were damped, the trends of height or attitude changes were fairly well shown. An example is given in Fig. 3, which shows a recorded disturbance at $C_v = 7{\cdot}16$ with an elevator angle of -8 deg. The observed amplitude of porpoising was 8 deg and this agrees well with the recorded amplitude.

5. **Spray.**—In an attempt to get spray photographs of reasonable value for comparison purposes F.24 cameras were positioned off the starboard bow, the starboard beam forward of the wing and the starboard beam aft of the wing. A chequered pattern, consisting of alternate black and white squares $\frac{1}{4}$-beam wide with the step point as origin, was painted on the starboard side of each model to aid subsequent analysis. An exposure time of 1/50 of a second was used in order to get photographs of apparently continuous spray envelopes instead of the discrete drops without sense of direction which result from using, say, an electronic flash with an open camera shutter. As the cameras were close to the model, the depth of focus was small and roughly only one plane, chosen as that con-

taining the grid on the hull side, could be in focus. The photographs therefore show parts of the spray and model wing as being considerably out of focus, but against the chequered background the spray profile is sufficiently well defined for a reasonable comparison to be made.

The photographs from the different cameras were taken simultaneously during the undisturbed longitudinal stability assessments, with $\eta = -8$ deg, mainly over the displacement range of speeds. An example is given in Fig. 51.

The spray characteristics of any of the models at a given speed can best be assessed by inspection of the spray photographs for that speed, while a good overall impression of the model spray characteristics at a given weight may be obtained from the projection of the envelope of the spray profiles for the various speeds on the median plane of the model. Such an envelope has been drawn for each model at each load tested and forms a convenient basis for the comparison of spray characteristics. The spray profiles used were taken straight from the side-view photographs and a limited parallax error was accepted; where this error tended to become large the curves were not drawn. The projections have been plotted using the non-dimensional co-ordinates C_X and C_Z, that is, in the median plane only ($C_Y = 0$); the absence of projections orthogonal to these, which cannot be obtained from the photographs, is not serious, since the photographs enable the positions of the spray blisters to be judged qualitatively, and in any case the curves are intended for comparison purposes rather than for absolute measurements. It should be noted that, in plotting the projections, velocity spray was included when it was integral with the main spray blister, otherwise it was ignored. An example of spray projections for one model at different weights may be seen in Fig. 19.

In addition to the spray photographs, photographs were on occasion also taken of the wake formation from two suitable positions. No analysis of these photographs was attempted but, where appropriate, several of them have been reproduced in the present report to illustrate points of interest.

6. **Hydrodynamic Directional Stability.**—For the directional stability assessment the model was towed and pivoted at the c.g. so that it was free in pitch, yaw and heave. A constraint was applied in roll so that subsequent analysis and comparison would not be unduly complicated. Steady-speed runs were made over a range of speeds from 4 to 40 ft/sec and at each speed the model was yawed in steps up to not more than 18 deg, moments being applied through strings attached to the wing-tips level with the c.g. The direction and order of magnitude of the resulting hydrodynamic moment was judged by the operator through the pull in the strings, and the angle of yaw was read off a scale on the tailplane with an accuracy of about $\pm\frac{1}{2}$ deg. These observations were used to prepare a stability diagram of the type described below. This type of test was carried out earlier on a dynamic model of the *Princess*[15] but owing to the large undetermined scale effect it was stated to be somewhat inconclusive. As in the present case comparative rather than absolute values are primarily required, however, this is not of immediate importance.

The type of test now under consideration is not common and the associated presentation of results will probably not be so readily appreciated as that of the results of the undisturbed longitudinal stability tests. For this reason a typical directional stability diagram is shown in Fig. 8. It was obtained for the basic model with an elevator setting which gave a low stable take-off trim, and explanatory notes, based on observation, have been added.

Unlike the longitudinal stability diagram, which is divided into definite stable and unstable zones, the directional stability diagram, with degrees of yaw as ordinates and velocity coefficients as abscissae, represents a plane of instability which is crossed by lines of both stable and unstable equilibrium. If the model is positioned (in effect) at any point in this plane and then given complete freedom in yaw at constant speed, it will swing round to the nearest line of stable equilibrium that it can reach without crossing an unstable line. In other words, it will swing towards a line of stable equilibrium and away from a line of unstable equilibrium. The present tests have been made with no rudder tab, *i.e.*, with zero aerodynamic yawing moment, and the directional stability diagrams are for this case only. Similar diagrams could have been obtained for different rudder settings, but they are not necessary to the present investigation and it is considered that they would differ by very little from the zero applied aerodynamic yawing-moment case.

It was decided in the initial stages of the investigation to determine the effects on directional stability of attitude, roll constraint, load and breaker strips; the strips consisted of six forward-sloping strips of wood of thin triangular section suitably positioned at about 30-deg to the vertical on the afterbody wall to deflect any water flowing over this part of the hull and so alleviate suction forces which might otherwise yaw the model. These effects were found to be small and were therefore neglected in the remaining directional stability tests; they are discussed below.

The effect of attitude can be seen without roll constraint by comparing Figs. 9 and 10, and with roll constraint by comparing Figs. 11 and 12. Before considering these Figures it may be remarked that the attitude in pitch of the model is governed by the elevator setting, which was kept constant throughout the speed range. Two elevator settings were chosen to give extremes of trim within the stable undisturbed region. Comparing Figs. 9 and 10, the only effect of attitude change with no roll constraint is to move the high-speed unstable equilibrium line by a small amount. This effect would not be significant in a practical case and does not warrant separate investigation. The effect is similar and of a comparable order when the roll constraint is introduced (*cf.* Figs. 11 and 12).

The effect of roll constraint can be judged for low and high attitudes by comparing Figs. 9 and 10 with Figs. 11 and 12. In both cases the effects are relatively small; there is again a small displacement of the high-speed unstable equilibrium line and at lower speeds, $C_v = 4$ and 5, roll constraint causes the unstable equilibrium line to be moved nearer to the stable one. The main result of introducing roll constraint is thus a slight improvement in hump directional stability, but the change is insufficient to justify separate investigations on each model.

The effect of breaker strips may be seen by comparing Figs. 12 and 13, but before dicussing them a few preliminary remarks may be helpful. It has been suggested that, although the type of stability diagram now being considered is useful for a model-to-model comparison, because of the large scale effect (completely undetermined through lack of full-scale data), model directional stability tests should be repeated with side breaker strips [1, 15] in position and that the two sets of diagrams so obtained would represent limiting conditions between which the full-scale cases lie. In the present tests without breaker strips, at the larger angles of yaw and higher speeds, the water flowing over the hull side presented to the direction of motion attached itself to and covered the whole of the side for the length of the afterbody, sometimes running up the vertical tail surface; in view of this and the aforementioned suggestion, tests on the basic model with roll constraint and at high attitudes (Fig. 12) were repeated with breaker strips in position (Fig 13). The breaker strips functioned well, but as their effect on stability was merely to remove the outer high-speed equilibrium lines, leaving an exact reproduction of part of the normal stability diagram, *i.e.*, the curve below $C_v = 3$, no further tests of this kind were made. It is interesting to note that with breaker strips, heavy porpoising occurred above $C_v = 7$, where it did not occur without. This was evidently due to the change in flow and consequent change in pressure distribution. Tests with various numbers and positions of breaker strips showed the high-speed directional instability to be due to hydrodynamic suction over a small area of the afterbody side near the rear step.

The effect of load on directional stability characteristics may be ascertained from Figs. 14 and 15, which are for low and high loadings respectively; there are no differences of major practical significance between the two diagrams. The continuous line of unstable equilibrium for the high loading is not maintained at the lower weight, a short stable equilibrium line being introduced at $C_v = 4\frac{1}{2}$. There is thus a slight deterioration in directional qualities with the decrease in weight, but the speed band over which it occurs is very narrow. In a detailed investigation of the stability characteristics of a specific hull form it would probably be worthwhile to check load effects, but in the present series of tests this was not considered necessary.

The main directional tests in this programme have thus been made with roll constraint at one weight ($C_{\Delta 0} = 2{\cdot}75$) and c.g. position, without slipstream, at one elevator setting ($\eta = 0$ deg) and one rudder setting ($\zeta = 0$ deg) and without breaker strips. Results are presented as in the Figures just considered.

7. **Elevator Effectiveness.**—As the aerodynamic characteristics of each model of the series are the same, the effect of changes in hull parameters, such as forebody warp, on elevator effectiveness can easily be ascertained. Corresponding to each model weight, therefore, a plot of elevator effectiveness has been given. The analysis has been made in some detail because the curves of attitude against elevator angle appeared initially to be of definite form and to have little scatter. The method used was to obtain a curve of attitude against elevator angle for a given speed, to plot the slope of this curve and to obtain the mean ordinate, *i.e.*, the mean elevator effectiveness; finally, the mean values of elevator effectiveness were plotted on a speed base. Specific values of elevator effectiveness obtained in the second stage have been used in discussions in later Sections of the report and it may be noted that to obtain the mean value of effectiveness for a given speed the summation was made in each case from $\eta = -12$ deg to $\eta = +4$ deg. An example of the final type of plot may be seen in Fig. 20, where curves of mean elevator effectiveness are given for various loadings on a C_v base.

CHAPTER 3

The Effects of Load

1. **Introduction.**—All models of the main series were tested at two loads, $C_{\Delta 0} = 2{\cdot}25$ and $2{\cdot}75$, but in view of the large differences normally found between characteristics at different loads, tests were carried out on one model at additional loadings to give closer coverage of the range, $C_{\Delta 0} = 2{\cdot}00$ to $3{\cdot}00$, to enable the linearity or otherwise of the load effects to be ascertained. The results also bring out a number of points of interest apart from the direct question of linearity of the various effects and these are considered in some detail. Model B was selected for the tests because it allowed a greater range of loads to be investigated than the basic model and it was felt to be representative of the series. Relevant aerodynamic and hydrodynamic data are given in Tables 1 and 2 respectively and the hull lines for this model are shown in Fig. 41.

The beam-loading coefficient was increased by increments of $0{\cdot}25$ from $2{\cdot}00$ to $3{\cdot}00$ and at each stage the longitudinal stability characteristics of the model were fully determined and photographs were taken of the spray. The results of these tests show the effects of load on the longitudinal stability limits, both undisturbed and disturbed, on trim, on the amplitudes of porpoising in both undisturbed and disturbed cases, on elevator effectiveness and on spray. Throughout the tests the pitching moment of inertia of Model B was held constant at $21{\cdot}30$ lb/ft^2.

Reference is made to five other load investigations, which are concerned with hulls of low length/beam ratio, and the results are compared with those of the present tests.

2. **Longitudinal Stability.**—2.1. **Present Tests.**—The detailed effects of a 50 per cent increase in weight on the longitudinal stability characteristics of Model B may be seen in the undisturbed case by comparing Figs. 127 and 135, which are for $C_{\Delta 0} = 2{\cdot}00$ and $3{\cdot}00$ respectively, and in the disturbed case by comparing Figs. 128 and 136.

At $C_{\Delta 0} = 2{\cdot}00$ the undisturbed stability characteristics of this model are very good. There is a very wide stable band extending from zero to take-off speeds, the smallest attitude range between the two limits at any speed being $7\frac{1}{2}$ deg, which is considerable. Lower-limit instability is only encountered below $\alpha_K = 6$ deg and the extent of upper-limit instability is very small. Hump attitude, $9\frac{1}{2}$ deg, is quite reasonable and the trim curves show no irregularities. With the increase in loading to $C_{\Delta 0} = 3{\cdot}00$ the stability has deteriorated to a state which is just acceptable. The lower limit is found at higher attitudes and the unstable area has increased in extent sufficiently to cut the continuous stable band in a narrow neck of instability. It is obvious from the diagram that this neck has just formed and that a slight decrease in weight would remove it. The high-speed region of upper-limit instability remains roughly unchanged, but the limit itself has been raised slightly and moved up the speed axis. Hump attitude has been increased by $1\frac{1}{2}$ deg and, apart from a slight kink in the curve $\eta = -8$ deg, the trim curves are still regular. Similar details of the effects of intermediate load increases can be obtained from the corresponding stability diagrams (Figs. 129, 131 and 133).

Considering the undisturbed longitudinal stability limits for all the loadings as a whole, the effect of progressive weight increases is shown in Figure 16. The greatest change in the lower limit occurs between $C_{\Delta 0} = 2{\cdot}00$ and $2{\cdot}25$, but for the remaining regular weight increases the change is almost constant at a given speed, e.g., at $C_v = 7$, from $C_{\Delta 0} = 2{\cdot}25$ to $3{\cdot}00$, the limit is raised by $0{\cdot}9°$ per $0{\cdot}25$ increase in $C_{\Delta 0}$. The upper limits show less regularity but, apart from $C_{\Delta 0} = 3{\cdot}00$, there is a general increase in attitude and speed with increasing load. At $C_{\Delta 0} = 3{\cdot}00$ the tendency for the upper limit to increase in attitude is reversed, but it should be noted that at this weight the form of the diagram is beginning to change in that there is a complete band of instability across it, and again, the upper limits are more difficult to obtain experimentally (*i.e.*, the model is prone to fly if instability increases these attitudes) and are based on fewer points than the lower limits.

Undisturbed porpoising amplitudes (Fig. 18) show little change as a result of weight increases except in the region of upper-limit instability, where small but definite increases in amplitudes are obtained.

Longitudinal stability with disturbance for $C_{\Delta 0} = 2{\cdot}00$ is good. A band of instability appears across the diagram due to disturbance, but it is not wide and it is followed by a relatively large stable region. The depth of this stable region is initially 5 deg, but this decreases with increase of speed, due mainly to the curling up of the lower limit.

The effect of a 50 per cent increase in weight to give $C_{\Delta 0} = 3{\cdot}00$ is shown by Fig. 136 to be drastic. The unstable band has increased in width and the lower limit has been raised to such an extent that only a small stable area is left at the high-speed end of the diagram. These characteristics would be unacceptable full scale. Intermediate effects of load can be seen in the relevant stability diagrams with disturbance (Figs. 130, 132 and 134).

Rates of change of the position of the disturbed limits with respect to weight may be roughly assessed from Fig. 16, but it should be remembered that there is more room for experimental error in the determination of the

disturbed limits than in the undisturbed case and, in any case, there is no reason to believe that the limits should show a consistent variation. It can be said, however, that there is a tendency for the limits to lie in order and it can be generally expected that increase in weight will increase the unstable area.

Porpoising amplitudes with disturbance (Fig. 18) are of the same order throughout the weight range covered, *i.e.*, loading has negligible effect on disturbed porpoising amplitudes.

Changes in the effects of disturbance due to load variations can be gauged by comparing undisturbed and disturbed stability limits for $C_{\Delta 0} = 2{\cdot}00$ and $C_{\Delta 0} = 3{\cdot}00$. For $C_{\Delta 0} = 2{\cdot}00$ (Figs. 127 and 128) the effect of disturbance generally is to reduce the initially large stable region by more than half; the upper limit is unaltered, a vertical band of instability is introduced and elsewhere the lower limit is raised to about 5 deg. In the higher weight case, $C_{\Delta 0} = 3{\cdot}00$ (Figs. 135 and 136), disturbance reduces the stable region to roughly one fifth of its original area; the upper limit is mainly unchanged, the initial narrow vertical unstable band is greatly widened and the lowest stable attitude is 7 deg. For this model, therefore, a 50 per cent weight increase considerably increases the severity of disturbance effects on stability limits. An examination of the corresponding pairs of diagrams for intermediate loadings shows that this effect of weight, although not regular, is progressive.

Disturbance increases considerably the general order of porpoising amplitudes, but weight changes have negligible effect on this increase (Fig. 18).

The effect of load on trim is illustrated by Fig. 17 in which the trim curves for $\eta = 0$ deg at the various loadings are compared. For each increment of load the hump trim is raised by approximately 0·4 deg and the curves maintain order up the speed range, although the degree of separation varies. It is mentioned in Chapter 4, Section 1.4., that the separations of the undisturbed lower limits are of the same order as the changes in hump trims from load to load and that at the higher speeds instability occurs at about the same elevator settings in all cases. Examination of the relevant individual stability diagrams shows this to be the case.

The load-coefficient curves (Figs. 137 to 141) are similar in form, but the point of separation moves progressively up the speed scale with increase of weight, occurring at $C_v = 5{\cdot}0$ for $C_{\Delta 0} = 2{\cdot}00$ and at $C_v = 6{\cdot}1$ for $C_{\Delta 0} = 3{\cdot}00$. These curves may be used to estimate flying speeds, but it should be noted that no allowance for ground effect was made in the computation.

2.2. **Previous Investigations.**—Results of previous investigations into the effects of load on stability for various hull forms agree very well with the present findings not only with respect to the manner of change wrought but with respect to rate of change as well.

In Fig. 17 of Ref. 16 which relates to a hull of length/beam ratio $6\frac{1}{2}$ and a starting $C_{\Delta 0}$ of 0·62, a 32 per cent increase in weight raises the lower limit, at mid-planing speeds, by just under 3 deg; the corresponding change in the present tests is 4 deg for a 50 per cent weight increase. At higher speeds the limits of Ref. 16, although still in order, run closer together. This tendency is also apparent in Fig. 16 of the current investigation, but it would probably have been more pronounced had higher speeds been reached. The characteristics of the upper limits are similar in each case; they lie close together and are disordered (The upper limits, increasing trim, should be considered in these American tests for comparison with British undisturbed limits as advocated by Gott[17]). Fig. 6 of Ref. 18 shows that for a hull with a length/beam ratio of 6·2 and a starting $C_{\Delta 0}$ of 0·89, an increase in weight of 43 per cent raises the lower limit by $3\frac{1}{2}$ deg. These limits again show the tendency to run together at higher speeds. The upper limit is also raised progressively with weight increase, but its rate of change is considerably less than that of the lower limit.

Further load effects are given in Figs. 18 and 21 of Ref. 19. With a length/beam ratio of 6·3 and an initial $C_{\Delta 0}$ of 0·74, a 57 per cent weight increase raises the lower limit at mid-planing speeds by about 4 deg and the upper limits are more or less orderly; Fig. 21 of Ref. 19 is interesting, consisting of plots of critical trim against load at several speeds. The curves of critical trim against load are approximately linear and the authors conclude that ' it should be sufficient, when a specific model is tested, to investigate only the extreme values of gross loads '.

The references quoted so far refer only to undisturbed stability; an example of load effects in the disturbed state, with a low beam loading ($C_{\Delta 0} = 1{\cdot}1$) and a length/beam ratio of 7 can be found in Ref. 20, Fig. 17. The increase in weight is only 20 per cent yet this seems to bring about the same order of deterioration in stability as does a 50 per cent weight increase in the present case (Fig. 16). This fact is also illustrated, although somewhat indirectly, in Ref. 9, Figs. 8 and 10, where, with a length/beam ratio of 6·1, a starting $C_{\Delta 0}$ of 0·78 and a 13 per cent increase in load, the deterioration in stability is seen to be of comparable order to that of Model B for a similar weight increase (by interpolation). The general order of disturbances used in the tests of Ref. 9 was, however, of 6 to 8 deg against the more severe maximum disturbance of the present tests. By arguments given in Chapter 2, Section 4.2. and Chapter 3, Section 2.1, it might well be expected that increasing the severity of disturbance to the maximum would increase the difference between the limits for the two weights.

2.3. **Discussion.**—The most general feature of the load effects on the stability characteristics of Model B is the linear nature of the changes involved; this is apparent in Figs. 16 and 17, where the stability limits and representative trim curves respectively are compared. The linear variation of lower critical trim with load in the present undisturbed case has already been mentioned (Chapter 3, Section 2.1.) and this effect of load, which it is felt will apply generally to high length/beam ratio hulls, was obtained with a design static load coefficient of 2·75.

In Ref. 19, where the tendency to linearity of the load effects is discussed and the rates of change of critical trim with load are approximately equal to those of the present investigation, the tests were made on a hull of low length/beam ratio with design static load coefficient of 0·74. As in the two cases the static load coefficients are so different and these results are substantiated by the other References, this conclusion appears to be independent of beam loading and independent of length/beam ratio. The quotation from Ref. 19 can also be modified, *viz.*, when a specific model is tested, it is only necessary to investigate any two values of gross load with a reasonable degree of separation, for the assessment of load effects on stability.

Referring to the disturbed stability limits, it was noted in the previous Section that in Ref. 20 a 20 per cent increase in weight brought about the same degree of deterioration in stability as a 50 per cent increase in weight in the present tests; equivalent results were obtained in the case of Ref. 9 where the deterioration in disturbed stability was equal to that of the present tests, but was obtained with disturbances of much smaller magnitude. One may say, therefore, that the high length/beam ratio (11) hull of Model B shows greater resistance to disturbance as weight increases, than the hulls of Ref. 20, with a length/beam ratio of 7, and Ref. 9, with a length/beam ratio of 6·1. It should be noted that the weight increases compared are not over the same absolute range.

3. **Spray.**—The effects of load on spray can be seen in Fig. 19, which shows the projections of the spray envelopes on the plane of symmetry of the model for four regular load increments. At $C_{\Delta 0} = 2{\cdot}00$ the spray formation is very good, in that spray heights relative to the hull are small, giving adequate clearance for propellers and flaps, but with increase of load there is a general deterioration. The total load change, a 50 per cent increase, causes the spray projection to be raised by about half a beam generally; this is a large change, but from the diagram it can be seen that the first load increment, from $C_{\Delta 0} = 2{\cdot}00$ to $C_{\Delta 0} = 2{\cdot}25$, accounts for half of it, with the remaining intermediate changes being of little significance when taken individually.

4. **Elevator Effectiveness.**—The effect of load on elevator effectiveness is shown directly in Fig. 20, which is a comparison of plots of mean values of $d\alpha_K/d\eta$ against C_v. In the comparison, apart from the low-speed end of the curve $C_{\Delta 0} = 2{\cdot}25$, the curves lie in order and, allowing for a reasonable degree of experimental error, the variation of effectiveness with load is approximately linear up to $C_v = 8$, an increase in load causing a decrease in elevator effectiveness. At the high-speed end, however, the curve for $C_{\Delta 0} = 2{\cdot}00$ has a tendency to flatten out. As load is increased this tendency decreases and, in the highest load case, it is just reversed (it may be noted that the summation to obtain the mean ordinate in the plots of $d\alpha_K/d\eta$ at constant C_v was made over the same constant range of elevator settings in each case, that is from $\eta = -12$ deg to $\eta = +4$ deg).

5. **Conclusions.**—The tests performed indicate that Model B has calm-water hydrodynamic properties which are very good at the lowest weight and which deteriorate to a just acceptable state at the highest.

From the investigation and discussion of load effects the following conclusions are drawn:

General Conclusions

(*a*) In the undisturbed-stability case, the rate of change of critical trim with respect to load at constant speed is both approximately linear and positive. This is independent of both beam loading and length/beam ratio.

(*b*) When testing a specific model it is only necessary, as a consequence of (*a*), to investigate two weights with a reasonable degree of separation for the assessment of load effects on longitudinal stability.

(*c*) In the disturbed stability case the high length/beam ratio hull now under consideration shows greater resistance to disturbance as weight increases, than hulls of lower length/beam ratios.

Conclusions Peculiar to This Model, but Probably Applying to Others in This Series

(*a*) The severity of disturbance effects on the stability limits increases with load.

(*b*) The hump trim increases linearly with respect to load.

(*c*) The longitudinal spray profile is unchanged in form, but the spray height at any station increases with load.

(*d*) Except at high speeds, the rate of change of elevator effectiveness with respect to load is approximately linear and negative. At high speeds the tendency for the mean $d\alpha_K/d\eta$ curve to flatten out at the lower weights decreases with increasing weight until, at the highest weight tested, it is just reversed.

CHAPTER 4

The Effects of Moment of Inertia and Radius of Gyration

1. Longitudinal Stability.—1.1. **Introduction.**—Such evidence as was available when this investigation was planned indicated that changes in the pitching moment of inertia of a flying-boat model did not in themselves, when unaccompanied by changes in mass, have any appreciable effect on the longitudinal hydrodynamic stability limits. For this reason, no particular moment of inertia was aimed at in the construction of models in the series (Table 2), nor was any attempt made to vary the moment of inertia according to any particular rule while bringing the mass of each model to the various values at which it was considered desirable to make stability tests. Extra weights were merely fixed to a lateral bar through the centre of gravity, thus keeping the moment of inertia effectively constant.

Since previous investigations of this matter did not cover the same ranges of values of the various parameters involved as are used in this programme, it was felt advisable to carry out tests on one model of the series to verify that no particular attention needed to be paid to the value of the moment of inertia. Model B was used as it permitted a more adequate range of values to be covered than other models available.

Advantage was taken of the opportunity to perform a systematic series of tests which in addition to settling the point at issue would provide general data on the effects of the parameters concerned on the longitudinal stability of high length/beam ratio hulls. Three separate sets of tests were performed, in each of which one of the three parameters, mass (m), moment of inertia (I), and radius of gyration (k), was held constant at some appropriate value, and the other two parameters were varied over a fairly large range, longitudinal hydrodynamic stability limits being obtained for each combination of values. Mass changes were, however, only considered to show their interaction with changes in the other parameters, moment of inertia and radius of gyration being the factors of direct interest, and it will be found that a number of the limits relating to changes in mass are in fact those of Chapter 3.

In addition to the limits themselves, Figures have been included showing the amplitudes of porpoising in the unstable regions. These enable the violence (or otherwise) of the instability to be judged, and comparison of them shows the effect of changes in mass, moment of inertia and radius of gyration on behaviour in these regions.

Since I, m and k are related by $I = mk^2$, the effects on the limits of changes in them are not independent. They can be related analytically by considering critical trim (*i.e.*, the trim at which longitudinal instability sets in) as a function of I, m, k and velocity and taking into account the implicit relations between the parameters. Consideration is given to this problem in Appendix III and comparisons are made of analytical and experimental results. Also, as it has been suggested that limits plotted on a draught base would show smaller sensitivity to mass and inertia changes than those on a velocity base, the theoretical analysis has been extended to indicate the relation between the two sets of limits.

1.2. **Present Investigation.**—As already stated, the tests were carried out on Model B of the series. The minimum value of $C_{\Delta 0}$ which could be achieved was 2·00, and the minimum moment of inertia 21·3 lb ft². A range of values of $C_{\Delta 0}$ was covered at this minimum moment of inertia in such a way as to change the moment of inertia by less than 1 per cent, so that it can fairly be said that the moment of inertia remained constant. A second series of tests was performed at constant radius of gyration with $C_{\Delta 0}$ varying between 2·00 and 3·00, this constant value being 1·26 ft, the only value which could be obtained at all the values of $C_{\Delta 0}$ required. Finally, with $C_{\Delta 0}$ fixed at 2·50, the centre of the range, the moment of inertia was increased by 40 per cent, almost the maximum increase obtainable at this $C_{\Delta 0}$ and one which is likely to exceed any natural increase which may arise in the manufacture of the models; moreover, the range covered was much wider than would be likely full scale. In these last two cases the chosen moment of inertia was obtained by sliding lead weights along a light bar running fore and aft inside the model.

The stability limits obtained in these tests are shown in Figs. 21 to 26, and the porpoising amplitudes in Fig. 27, the limits also being reproduced in the latter Figure for convenience.

1.3. **Previous Investigations.**—Reference has already been made to previous work relating to the effects of load or mass on longitudinal stability. Direct consideration will therefore only be given here to previous investigations into the effects of varying the pitching moment of inertia and radius of gyration, though it should be noted that a change of mass will automatically imply a change either in moment of inertia or radius of gyration.

The effect of moment of inertia on the stability of a seaplane was first considered theoretically by Perring and Glauert[21], who by treating the planing surfaces as flat plates showed that in the single-step case too small a moment of inertia would produce instability at an otherwise stable point while in the two-step case too large a moment of inertia would have this effect. Their general conclusion was that in model tests the ratio mass/moment of inertia was the most critical factor, *i.e.*, that the radius

of gyration should be given its correct scale value, and that if the model was then stable, an increase in the radius of gyration from this value would produce instability in the two-step case while a decrease would produce instability in the one-step case. No specific consideration was, however, given to which, if any, of I, m and k were to be kept constant during the changes mentioned for the conclusions to be valid.

Richards and Hutchinson[22] also considered radius of gyration to be the factor which would have most effect on stability, and mentioned that changes in mass while retaining the radius of gyration at its scale value (by altering the moment of inertia) still resulted in a movement of the stability limits. The latter point was investigated by means of the Routh discriminant, and led to the conclusion that both mass and radius of gyration should be given correct scale values in model tests. The size of the effect referred to in this report was illustrated in Ref. 7 for one particular model, the mass being increased by 15 per cent and the moment of inertia by 100 per cent; the movement of the stability limit here was very slight, being approximately one-fifth of the change produced by a 30 per cent change of mass at constant moment of inertia.

In Ref. 2, the results of fairly extensive tests on the effects of radius-of-gyration and moment-of-inertia changes were given both on critical trim and amplitudes of porpoising; the planing surface used represented the forebody only of a flying-boat hull, so that the treatment was concerned with the lower limit. The tests covered a range of values of $C_{\Delta 0}$ from 0 to 2, of C_v from 3 to 7 and of radius of gyration from 0·5 to 1·3 beams. An increase in radius of gyration at constant load was found to lower the critical trim, while an increase in load at constant radius of gyration raised it. Both these effects were fairly large, being of the order of 2 deg for 100 per cent change in the former case and 1 deg for a change from $C_{\Delta 0} = 0{\cdot}27$ to $0{\cdot}40$ in the latter. Porpoising amplitudes were found to increase markedly with decrease in radius of gyration at constant load. Further tests with a dynamic model showed that these amplitudes also increased with moment of inertia at constant radius of gyration. An analysis in this report of conventional flying boats showed them to have radii of gyration of at most 1·55 beams, associated with a $C_{\Delta 0}$ of the order of 1.

Further limited data on the subject were given by Olson and Land[16]. Little significant change was found to result from increasing the moment of inertia of a dynamic model by 25 per cent at constant load ($C_{\Delta 0} = 0{\cdot}72$). Similar results were quoted by Davidson for 100 per cent change in moment of inertia at constant $C_{\Delta 0}$ of 0·89 in Ref. 18.

The general conclusions of the various reports mentioned are substantiated in other sources but no quantitative data are given.

It will be seen that the experimental data mentioned all relate to fairly low values of $C_{\Delta 0}$. However, the general theoretical and experimental conclusions may be expected to extend to higher values of $C_{\Delta 0}$.

1.4. **Discussion.**—The results of individual tests in the present investigation are given in Fig. 27, and the stability limits are compared in Figs. 21 to 26.

Figs. 21 and 22 illustrate conditions at constant moment of inertia, and show that stability decreases markedly with increasing load, corresponding to decreasing radius of gyration. The effect holds in both the undisturbed and disturbed cases, but in the latter the limits are not so well separated in order of increasing load; indeed, there is an intersection of the lower limit for $C_{\Delta 0} = 2{\cdot}25$ with the others, so that the order is not preserved. It will be seen that the two upper limits for $C_{\Delta 0} = 3{\cdot}00$ are out of order. It is not, however, felt that any particular significance should be attached to this point since the separation of the different limits is small; in any event there is no reason to suppose that the upper limits should lie in any particular order.

With the mass held constant and the moment of inertia and radius of gyration varied (Figs. 23 and 24) almost no change in the undisturbed limits results; what difference there is can be attributed to experimental error. The disturbed limits are rather more widely separated, but the amount is still not significant. The fact that the limits are not in order here tends to confirm this view.

Finally, Figs. 25 and 26 show that with radius of gyration held constant the variation of the limits with load is of the same order as in the case of constant moment of inertia, though here there are no cases of curves being positioned out of order. The variation here can also of course be considered as a moment-of inertia effect.

It is interesting to note that in all cases the separations of the undisturbed lower limits are of the same order as the changes in hump trims from load to load and that at the higher speeds instability occurs at about the same elevator settings in all cases (Figs. 127 to 135).

Considering the three sets of limits as a whole, it seems that over the ranges of values considered the value of $C_{\Delta 0}$ is the most critical factor, and that neither changes in the radius of gyration nor in the moment of inertia will have any significant effect unless accompanied by changes in $C_{\Delta 0}$.

The effects of the various changes on the amplitudes of porpoising (Fig. 27) are in general less marked, though in all cases there is a large difference between the amplitudes at corresponding points in the undisturbed and disturbed cases. With moment of inertia constant, an increase in load and decrease in radius of gyration produces a small change in the amplitudes in the disturbed case and no discernible change in the undisturbed case. At constant load there is a small increase with increasing radius of gyration and moment of inertia in the disturbed case, and a most marked increase in the undisturbed case. In the remaining case, with radius of gyration constant, there is no evidence of change in either direction.

It is interesting to compare these results as a whole with those quoted in the preceding section as relevant to lower values of $C_{\Delta 0}$. While the general, qualitative, conclusions of those References are confirmed, the radius of gyration has not been found to have the importance it possessed at lower loadings; as already mentioned, $C_{\Delta 0}$ seems to be the only critical factor. Of course, if, as is common in model tests, the moment of inertia is held appreciably constant while the load is increased, then a change in $C_{\Delta 0}$ is accompanied by a change in radius of gyration, so that in this sense the value of the radius of gyration can be said to be critical. However, the results quoted in Ref. 2 referred to limit changes resulting from changes in radius of gyration at constant load; this effect is not noticeable in the present case, though it is possible, but unlikely, that it exists at other values of $C_{\Delta 0}$ in the range 2·00 to 3·00. It may be noted that the value of radius of gyration in the present tests ranges between 2·17 and 2·82 beams, somewhat higher values than those relevant to Ref. 2; since the radius of gyration of a full-scale version of the design now tested would be about 2·2 beams, however, this range of values is a realistic one.

1.5. **Conclusions.**—The experimental evidence obtained in this series of tests indicates that within the ranges of values of the parameters covered, only load has an appreciable effect on stability limits. When this is held constant, moment-of-inertia increases of up to 40 per cent have no appreciable effect on the limits.

Increase of the radius of gyration at constant mass has the effect of increasing the amplitude of propoising, particularly in the undisturbed case, while the amplitudes are not noticeably affected by changes of mass.

CHAPTER 5

The Effects of Slipstream

1. **Introduction.**—The tests of the main investigation were made for convenience without slipstream. Because of the importance of this parameter, however, particularly in full-scale designs, an assessment was made of its effects on the longitudinal stability and spray characteristics of the basic model and a method is suggested for relating the results to other models of the series. The tests themselves are also felt to give a general appreciation of the effects of slipstream on the longitudinal stability and spray characteristics of high length/beam ratio seaplane hulls.

Four configurations of Model A were used in the slipstream investigation, the differences between them being purely aerodynamic; the hull, tail unit and basic mainplane were identical in each case. Photographs of the four test configurations (which are described below) are given in Fig. 28 and the hull lines of the model can be seen in Fig. 41; relevant aerodynamic and hydrodynamic data are given in Tables 1 and 2 respectively.

The configurations tested may be described briefly as being:

(*a*) with take-off power
(*b*) with fairings replacing propellers
(*c*) with propellers windmilling
} and wing-tip slats

(*d*) with full-span leading-edge slats (and no propellers, fairings or nacelles).

Results of tests on the first three of these configurations, all fitted with nacelles, show the general effects of slipstream on the stability and spray characteristics of a high length/beam ratio hull, while comparison of these results with those of the last configuration (the standard test configuration) enable the slipstream characteristics to be related to the models of the main series.

2. **Details of Test Configurations.**—The following details of the test configurations are given both for convenience and to amplify the information in Chapter 2, Section 2.1, and a general view of each configuration is given in Fig. 28.

(*a*) *With Take-Off Power.*—The 1/15 scale *Sunderland* mainplane, common to all models of the series, was fitted with four turbine-propeller units; the turbines were Mk.IIb compressed-air turbines (Ref. 23) and the propellers were 0·795 ft in diameter. Leading-edge slats were fitted outboard of the outer nacelles and the turbine units were supplied with compressed air at constant pressure to give take-off thrusts of the right order for this type of hull. The resulting variations of both thrust and thrust coefficient (T_c) with speed are shown in Fig. 29. The mean thrust line was inclined upwards at 3° 9′ to the hull datum (tangent to forebody keel at step) and its distance from the c.g. measured normal to the thrust line was 0·28 ft. The pitching moment of inertia of the model in this configuration was 23·25 lb ft².

(*b*) *With Propellers Windmilling.*—This configuration was exactly the same as (*a*), except that no compressed air was supplied to the turbines.

(*c*) *With Fairings.*—In this configuration the propellers and turbines of (*a*) were removed; dummy engines (weights) were placed inside the nacelles to maintain the pitching moment of inertia at 23·25 lb ft² and fairings were fitted in place of the propellers.

(*d*) *With Full-Span Slats.*—In this case the turbines, propellers and nacelles of (*a*) were removed, the compressed-air outlets to the turbines were plugged and pared down to leave a smooth wing leading edge and full-span leading-edge slats were fitted. This wing configuration is the standard one and has been used throughout the main investigation for the routine tests on each model. The reduced pitching moment of inertia of Model A with full-span slats was 22·90 lb ft².

3. **Aerodynamic Lift.**—As the differences between the configurations are such as to affect primarily the aerodynamics of the model, the lift characteristics and the state of flow over the wing are briefly considered below. It may be remembered that the lift curves are used in the calculation of load coefficients, which in turn are used in the transposition of the stability limits to a $C_\Delta{}^{1/2}/C_v$ base, so any peculiarity in the lift characteristics will be reflected throughout the sequence. It should also be noted that the curves have been plotted on a keel attitude base so as to be directly applicable to the stability diagrams; wing incidence is 6° 9′ greater than keel attitude.

The lift curves with take-off power (Fig. 30a) show an increasing tendency to regularity as the thrust coefficient is decreased; at $T_c = 9{\cdot}4$ the points are disorderly and only the curve for $\eta = 0$ deg has been drawn, while at $T_c = 0{\cdot}4$ a clear indication of the effect of elevator is seen. As planing is not established until about $C_v = 4{\cdot}5$, however, only the curves for $T_c < 2{\cdot}0$ are significant in the present context and the transposed stability limits should be fairly accurate. The airflow past the wing will probably be mixed; at the tips it should be laminar over much of the chord, the slats preventing breakaway and delaying transition, while behind the propeller discs normal slipstream conditions will exist.

The lift curves with propellers windmilling (Fig. 30b) are peculiar in that the curve for $\eta = 0$ deg is of greater slope and reaches higher lift coefficients than do the curves for the other elevator settings. The loss of lift with elevator may be due to inefficiency of the tailplane at other than the zero elevator setting, as a result of the retarded flow through the propellers, or to elevator changes affecting the flow over the mainplane (subtraction of tailplane lift (as measured with no slipstream, Chapter 2, Section 3) for $\eta = 0$ deg at $\alpha_K = 8$ and 10 deg would give lift coefficients of 0·97 and 1·00 respectively, thereby putting the curve in place within the set. The tailplane lift curve is given in Fig. 2). It should be noted that this configuration may be considered as one with negative thrust and there may therefore be a variation of the lift characteristics with thrust coefficient for $T_c < 0$. This should be small, however, and the transposed stability limits should be reasonably correct.

The lift curves with fairings (Fig. 30c) clearly indicate transition and associated breakaway[24]. The flow over the wing is thus in a critical state and likely to be affected by small changes in Reynolds number. The associated load coefficients can therefore only be of the right order and the accuracy of the transposed stability limits will suffer accordingly.

The lift curves with full-span slats (Fig. 30d) are regular and accurate; this is the result of laminar flow being maintained with little breakaway over the whole wing span by means of the leading-edge slats and there should be little error in the corresponding transposition.

4. **Longitudinal Stability.**—The effects of slipstream on the longitudinal stability characteristics of Model A may be determined from a detailed study of the individual stability diagrams which are given in Figs. 31a to 32d, but it is more convenient to make separate comparisons of the limits and the trim curves.

Both undisturbed and disturbed stability limits are compared on a C_v base in Fig. 33. If the curves for the case with full-span slats are neglected initially, those for the other three cases (take-off power, fairings and propellers windmilling, taken in that order) constitute a set over which there is a progressive reduction of thrust, and hence thrust coefficient, from positive through zero to negative values. In the undisturbed case the effects of this reduction are to increase both the speeds and attitudes at which the limits are encountered. At low attitudes the lower limits converge and at high attitudes there is a minor exception to the foregoing rule in the case with propellers windmilling, but this is not significant. In the disturbed case the same type of pattern can be seen, although it is modified slightly because of the different limits involved (it may be remembered that the disturbed limit for the case with fairings was obtained with only 5 deg disturbance. The part of the limit drawn should only be altered slightly by the application of the maximum disturbance technique, however (Chapter 2, Section 4.2), and may thus be usefully included in this comparison). The progressive movement of the limits up the speed scale with decrease of T_c is much greater than in the undisturbed case, while the attitude changes are about the same.

By comparing individually the undisturbed and disturbed limits for each thrust case, the changes in disturbance effects following general variations in thrust coefficient can be ascertained. With positive thrust or take-off power the effects of disturbance are to double the vertical band of instability found across the take-off path without disturbance and to raise the high-speed part of the lower limit; with zero thrust or fairings the disturbance effects are greater, the vertical band being more than doubled, while in the negative-thrust case disturbance causes the onset of instability over almost the whole of the planing speed range; there is thus a rapid worsening of disturbance effects with decrease in thrust coefficient. This means that during landing an aircraft is far more susceptible to disturbance than during take-off (it is felt that this conclusion is a general one and is not peculiar to this hull form).

Considering now the limits obtained with full-span slats, it will be seen that these lie, in general, with the limits for the cases with propellers windmilling and fairings, away from those obtained with take-off power. They are better appreciated however, in relation to the other limits, when plotted on a $C_\Delta{}^{1/2}/C_v$ base (Fig. 34) which relates waterborne load to speed[25]. The probable relationship between the corresponding limits for the remaining models of the series is discussed below. As already stated, only limits for the cases with full-span slats have been determined for these models.

The hulls concerned are of the same family, differing only in the hull parameter under investigation, and differences in loading and trim are taken account of by plotting on a $C_\Delta{}^{1/2}/C_v$ base. It follows that any difference between the magnitude of the various slipstream effects for Model A (Fig. 34) and those for any other model of the series will be due entirely to the effect of the hull parameter which has been varied in going from one model to the other; in other words, to some ancillary effect. The magnitude of this effect may of course be affected by the specific values of the hull parameters which are common to the two models. Where such ancillary effects are small, therefore, the effects of slipstream and windmilling propellers may be taken to be the same as in the case of Model A. For instance, the lower undisturbed stability limits for most of the models with unwarped forebodies collapse approximately on that for Model A when plotted on a $C_\Delta{}^{1/2}/C_v$ base; the secondary effects should therefore be small and slipstream effects sensibly the same in each case*. Upper-limit changes will have to be applied with discretion and only the general nature of the effects can be considered in the disturbed case. It is felt that with a suitable

* It also appears, following the arguments of Chapter 9, Section 1.3, that if a change is made in the definition of stability, almost perfect collapse is obtained and if this fact is used in the present context a very accurate estimate of limits with slipstream for later models in the series can be obtained.

redefinition of keel attitude the foregoing will also apply with small error to the warped-forebody cases.

The plots of stability limits with elevator angles replacing keel attitudes as ordinates in Fig. 35 are given mainly for information. It may be noted, however, that in the undisturbed case the lower limits obtained with take-off power and windmilling propellers are separated from those for the full-span-slat case by negative and positive amounts of elevator respectively. This is consistent with the representation of the additional thrust moments by a change in elevator setting, but the idea cannot be taken far, without consideration of differences in elevator efficiency and in the actual stability limits.

The effects of slipstream on trim are shown in Fig. 38, where the curves for $\eta = 0$ deg, which have been taken as typical, are compared. As would be expected, they lie in order, the highest attitudes being reached on the trim curves with the lowest forward thrust, and this inverse relationship is preserved throughout the take-off speed range. The spacing of the curves is almost constant over the planing speed range, but it should be noted that while the increase in attitude with decrease in thrust is progressive, it varies with speed and is non-linear. Comparison of other trim curves shows that the inverse variation of trim with thrust coefficient is found at all elevator settings, but the spacing of the curves varies, the distribution being more even at high values of elevator angle and less so at low values.

The trim curves for the cases with fairings and full-span slats in Fig. 38 lie together, indicating that only a small amount of drag is obtained from the faired nacelles.

The load-coefficient curves, which were used for the transposition of the stability limits to a $C_\Delta{}^{1/2}/C_v$ base, are shown in Figs. 36a to 36d. From them flying speeds may be estimated, but it should be noted that no allowance was made for ground effect during the computation.

5. **Wake Formation.**—As photographs of the wake regions taken during the tests were of representative rather than specific cases they could only be compared individually in isolated instances, that is, when speeds and attitudes were approximately equal. Where this could be done, which was in the full-span-slat and windmilling-propeller cases only, there were no noticeable differences in wake characteristics.

Taken as groups, the photographs gave the same general impression in each case, there being no major differences between the configurations. With take-off power, however, the flow at the lower speeds did appear to be more broken than in the other cases, but this effect was not well defined.

No photographs were taken of flow in the wake region in the case with fairings, but it is felt that such photographs would not differ appreciably from those for the full-span-slat configuration.

6. **Spray.**—The effects of slipstream on spray are best considered by adopting the method used in the comparison of longitudinal stability limits. Neglecting initially, therefore, the full-span-slat case and considering the spray photographs for the configurations with take-off power, fairings and windmilling propellers respectively (Figs. 39a, 39b and 39c), the effects on spray of a progressive reduction in thrust coefficient can be seen at each speed.

In general, with reduction of thrust coefficient there is an increase in the height of the spray blister and, while with zero thrust there is an unbroken and apparently undisturbed blister, in the cases with positive and negative thrust the spray is, or tends to be, sucked into the propellers and broken up. These points are illustrated in the photographs for individual speeds. At $C_v = 2$ the relative heights of the spray profiles can be seen clearly together with the raising and breaking of the blister in the positive-thrust case. At $C_v = 3$ in the case with negative thrust there appears to be a suction at some distance behind the propeller plane, which distorts and raises the blister, while with positive thrust the suction occurs either in the propeller plane or just in front of it. Photographs for the higher speeds are not quite so instructive, except perhaps for the rear views at $C_v = 4$. The relative positions of the spray profiles are clearly shown here, but that for the positive-thrust case is disturbed just below the wing trailing edge and indicates depression by the slipstream.

It should be noted that as in the negative-thrust case the propeller drag is a function of the forward speed and the thrust coefficient will probably vary only a small amount, and as in the positive-thrust case the thrust coefficient varies greatly at low speeds, the separation of the three sets of photographs in terms of thrust coefficient will vary with speed, being most uneven at the lowest speed. This should be borne in mind when examining the photographs.

The projections of the envelopes of the spray profiles in Fig. 40 show the decrease in spray height with increase of thrust coefficient, except at high values of C_x where the positive-thrust curve rises across the others. This is undoubtedly due to the reduction in attitude and consequent movement forward of the spray origin which occurs at low speeds with positive thrust.

The projection for the full-span-slat case is included in this Figure and its relation to the other curves may be seen easily. At low speeds the spray heights with full-span slats are midway between those for the cases with fairings and with propellers windmilling, while at high speeds the projections for the full-span-slat and propellers-windmilling cases are virtually coincident.

Photographs of the spray obtained at individual speeds when full-span slats are fitted to Model A may be seen in Figs. 51, 52 and 53; the spray formation closely resembles that obtained in the case with fairings.

7. **Elevator Effectiveness.**—The comparison of curves of mean elevator effectiveness (Fig. 37) shows that with a progressive general increase in thrust coefficient there is an increase in mean elevator effectiveness and, except in the case with positive thrust, the effect is sensibly constant over the planing range of speeds; with positive thrust the

increase in effectiveness with speed is reduced at the higher speeds. The curve for the full-span-slat configuration lies a little above that for the case with fairings.

In considering these curves it should be noted that, at a given speed, an increase in thrust coefficient will have two main effects, namely, the load on water will be reduced, which effect by itself will produce an increase in elevator effectiveness (Chapter 3, Section 4), and the efficiency of the elevators and tailplane will be improved when they are in the accelerated flow of the slipstream. It would appear, however, from the nature of the change, that neither of these effects is the cause of the rather sudden decrease in slope of the positive-thrust curve at $C_v = 7$. It is probable that the large nose-down moment obtained with positive thrust has caused such a general reduction in trim that an effective lower limit, in the form of high opposing hydrodynamic moments, has been reached and this limit has caused a flattening of the lower trim curves with a consequent reduction in trim range for a given speed, *i.e.*, a reduction in mean elevator effectiveness. The effect can be seen in Fig. 31a, where the lower trim curves show a decrease in slope at speed coefficients greater than 7.

A comparison of the relevant load coefficients, on a basis of either constant elevator angle ($\eta = -8$ deg) or attitude ($\alpha_K = 8$ deg), shows that at the higher speeds the loads on water obtained with positive thrust are about half those obtained with negative thrust and while, as would be expected, the case with slats lies in between these two, that with fairings gives the greatest loads at all planing speeds. These high water loads with fairings are a direct result of the loss of lift with transition and associated breakaway and, as they constitute the major difference between this and the full-span-slat configuration (both are zero-thrust cases), elevator effectiveness should be slightly greater at all speeds with slats than with fairings, which in fact it is. The low values of elevator effectiveness obtained with negative thrust are lower than the corresponding decrease in load would lead one to expect; it is suggested that the further loss of effectiveness is due to the inefficiency of the elevators and tailplane mentioned in Chapter 5, Section 3.

8. **Conclusions.**—The tests made show that the application of take-off power results in a general improvement in both the stability and spray characteristics of a high length/beam ratio hull. The detailed effects of a propressive and general increase in thrust coefficient are:

(*a*) to reduce both the speeds and attitudes at which stability limits without disturbance are met

(*b*) to reduce both the speeds and attitudes at which stability limits with disturbance are met, the decrease in speed being much greater than in (*a*)

(*c*) to increase resistance to disturbance

(*d*) to reduce trim throughout the take-off range of speeds, the reduction being much greater in the planing than in the displacement range of speeds

(*e*) to lower the spray blister generally, which results in a lower spray envelope except at very low speeds and

(i) with increase in T_c from zero, to raise the blister locally near the propeller plane with the spray sheet ultimately being broken and sucked into the propellers

(ii) with increase in T_c to zero, to reduce the local distortion of the spray sheet behind the propeller plane until at $T_c = 0$ the undisturbed blister is obtained

(*f*) to increase elevator effectiveness

(*g*) to reduce the elevator setting at which lower limit, undisturbed instability is encountered.

The above conclusions can be applied to obtain a fair idea of the effects of slipstream on the stability and spray characteristics of any model of the present series. A better estimate can be made, however, in the case of stability limits only, by plotting the limits with full span slats on a $C_\Delta{}^{1/2}/C_v$ base together with those for Model A in the corresponding configuration; where a collapse is obtained the results for Model A can be applied directly with little probable error (*see* footnote to Chapter 5, Section 4). This will occur mainly in the case of the lower limit without disturbance, leaving the upper-limit-without-disturbance and the disturbed-limit cases to be interpreted in the light of the general conclusions.

CHAPTER 6

The Effects of Forebody Warp

1. **Introduction.**—In this Section the effects of forebody warp (progressive increase in angle of deadrise from main step to bow) on the hydrodynamic stability and spray characteristics of a high length/beam ratio flying boat are deduced from the results of tests on the first three models of the series. These models, A, B, and C, were identical except in respect of forebody warp and this single parameter was varied in the following manner:

Model A	0-deg forebody warp per beam (basic model)
Model B	4-deg forebody warp per beam
Model C	8-deg forebody warp per beam

The effect of this variation on the forebody planing bottom shape can be seen in Fig. 41, which is a comparison of hull lines, and the deadrise-angle distributions are compared in Fig. 42. Aerodynamic and hydrodynamic data common to the three models are given in Tables 1 and 2.

2. **Longitudinal Stability.**—2.1. **Present Tests.**—The effect of forebody warp on longitudinal stability limits at different weights for both undisturbed and disturbed cases is illustrated in Figs. 43, 44 and 45, where the various limits for Models A, B and C are compared.

In the undisturbed case, the effect on the stability limits for $C_{\Delta 0} = 2{\cdot}75$ is clearly shown in Fig. 44a. The result of increasing forebody warp from 0 deg to 8 deg per beam is to give a large increase in the stable planing region; the lower limit is everywhere lowered by at least 2 deg and the upper limit by about $\frac{1}{2}$ deg. Confirmation of this change can be obtained from Figs. 43a and 45a, which are for lower and higher loads respectively ($C_{\Delta 0} = 2{\cdot}25$ and $3{\cdot}00$).

It may be noted that the relative positions of the undisturbed upper limits are not consistent for all weights, but this discrepancy should not be given undue importance. The upper limits in general are not so accurate as the lower limits, being based on fewer points which in themselves are difficult to obtain due to the proneness of the model to become airborne in this region.

In the disturbed case, the effects of forebody warp are shown in Figs. 43b, 44b and 45b. Before discussing them, however, a few points on technique should be considered (Chapter 2, Section 4.2). In all tests the maximum possible disturbance was given to the model; as the critical disturbances in the mid-planing region were small, instability was easily induced and the limit is that for maximum disturbance, *i.e.*, there is negligible error; in the high-speed lower-limit region maximum disturbance was difficult to effect safely because either the attitude was low and the nose of the model would have been submerged or, with a disturbance, the resulting oscillation (which may have damped out) was often of such large amplitude that it was stopped by the operator before the completion of one cycle; in the upper-limit region it was difficult to disturb the model because it often reached a semi-stalled condition clear of the water with the motion becoming predominantly aerodynamic. The disturbed limits are therefore not as precise as those obtained without disturbance, but within this limitation a very good idea of the susceptibility of the models to a large external disturbance is still obtained.

Considering orders, then, rather than absolute amounts of change, the total effect of 8 deg forebody warp is to give a significant increase in the disturbed stable region, most of which accrues from the higher values of warp. The effect is not appreciably altered by changes in loading.

The effects of forebody warp on the stability limits are shown in a different light in Fig. 46 (which is for one loading, $C_{\Delta 0} = 2{\cdot}75$), where elevator angles replace keel attitudes as ordinates. In this diagram the undisturbed limits are grouped together, and the lower limits all lie more or less along the same elevator setting, a point which is made in Chapter 4, Section 1.4. Where a vertical band of instability must be crossed during take-off, as in the case of 0 deg warp, it is emphasised by this type of presentation. It can be concluded that when, in the undisturbed case, there is a completely stable take-off path for this type of hull, the application of forebody warp does not materially alter the elevator setting at which instability is encountered.

Little can be said about the disturbed case, except that an increase in the stable region with application of forebody warp is indicated.

Trim curves for $\eta = 0$ deg are compared in Fig. 47 for different weights. The effect of increasing forebody warp from 0 deg to 8 deg is to reduce trim generally. At $C_{\Delta 0} = 2{\cdot}75$ static floating trim is reduced by $1\frac{1}{2}$ deg and this order of separation continues over most of the displacement speed range. At the hump, attitude is decreased by $\frac{3}{4}$ deg and in the planing speed range by 2 deg, although, when planing, the reduction varies with speed and is altered by elevator setting (Figs. 31d, 133 and 145). The attitude changes with warp are roughly linear over the greater part of the displacement range, but when planing most of the effects are due to the first increment of warp, 0 deg to 4 deg, the trim curves for 4-deg and 8-deg warp being disorderly and lying close together from and including the hump.

These tendencies are confirmed in Figs. 47a and 47c, the differences in weight seeming to have little effect.

The effect of forebody warp on amplitudes of porpoising in both undisturbed and disturbed cases is shown for one load ($C_{\Delta 0} = 2{\cdot}75$) in Fig. 49. In the undisturbed case, there is no obvious change in the general level of porpoising amplitudes. In the disturbed case, however, with 4-deg warp (Fig. 49b) values are in general less than those for both no warp and 8-deg warp, but the difference is small. In Chapter 4, Section 1.5, it is concluded that increase of the radius of gyration at constant mass has the effect of increasing the amplitudes of porpoising, particularly in the undisturbed case. It may therefore be that the lower amplitudes obtained with 4-deg warp are directly attributable to the fact that Model B has the lowest radius of gyration. The data in the undisturbed cases of Fig. 49 are rather sparse, but in general it appears that forebody warp does not produce any significant change in the amplitudes of porpoising. Similar remarks apply in the lower load case, $C_{\Delta 0} = 2{\cdot}25$ (Fig. 48); no significant changes in the amplitudes of porpoising are produced by increasing forebody warp.

2.2. **Previous Investigations.**—Although there are numerous references to the effects of forebody warp in various reports, only two available experimental investigations are concerned directly with this subject. The first, by Carter and Weinstein[26], deals solely with forebody-warp effects on the hydrodynamic qualities of a high length/beam ratio hull and the second, by Davidson and Locke[18], treats these effects as part of a fuller investigation into the porpoising characteristics of hulls of lower length/beam ratio. As both reports are American, it may be recalled that the tank techniques used in these model tests differ from those used in the current programme. These differences in techniques are discussed in Refs. 4 and 17, whence it appears that comparisons of results should be made on the basis of steady runs; the N.A.C.A. lower limit and upper limit increasing trim then correspond to M.A.E.E. undisturbed limits, and the N.A.C.A. upper limit decreasing trim corresponds (as far as it goes) to the M.A.E.E. limit(s) with disturbance.

In Ref. 26 the hull used had a length/beam ratio of 15 and was tested at $C_{\Delta 0} = 5{\cdot}88$. The forebody, which was 8·6 beams in length, was warped at the rate of $7\frac{1}{2}$ deg per beam (this is described as extreme warping), incorporated chine flare and had a main-step deadrise of 20 deg. It differed from its basic forebody in the same general manner as that of Model C from that of Model A in the present tests. The conclusions reached are general and indicate that an appreciable increase in the stable range of trim between limits results from forebody warping, with no appreciable effect on the maximum amplitudes of porpoising. In addition the results of this Reference are quantitatively very close to those of the present work.

In the forebody-warp investigation of Ref. 18 the model used had a length/beam ratio of 6·2 and was tested at $C_{\Delta 0} = 0{\cdot}89$. The forebodies, which were 3·44 beams in length, were warped at several rates including 8·1 deg per beam. It also incorporated chine flare and had a main-step deadrise angle of 20 deg. The differences between basic and warped forebodies were obtained in the same general manner as those of the previous reference. The conclusions state that ' increasing the warping of the forebody bottom very appreciably lowers the lower limit at high speeds but only slightly at speeds just beyond the hump. The upper limit is also lowered, but to a very much less extent. Increasing the warping of the forebody lowers the free-to-trim track at high speeds '. Here again there is close quantitive agreement with the present work.

2.3. **Discussion.**—As the aim of the present investigation is to provide design information, variation of the hull parameters has been kept within practical design limits, with occasional exceptions to aid in the fuller understanding of a phenomenon, and the conclusions drawn will in general hold only within these limits. The adequacy of the variations of forebody warp tested thus deserves some comment.

The main-step deadrise angle, 25 deg, is a compromise, chosen as the optimum from experience of impact, resistance, stability and final hull shape characteristics. The range of warps tested, up to 8 deg per beam, is considered adequate. If, for instance, 12 deg per beam had been used, the section half-way along the forebody would have had a deadrise angle of 61 deg, and to obtain a forebody length of 6 beams the rate of warping forward of this section would have had to be considerably reduced, giving rise to concave buttock and water lines; this would result in small forebody stowage volume, and a possible increase in aerodynamic pressure drag. It is also known that hydrodynamic resistance is increased slightly by forebody warping [18, 26]. These criticisms of course apply in the case of 8 deg warp per beam, but the effects will be relatively small.

In each case tested, the forebody warp was uniform for three beams forward of the step and then varied to give good lines with a deadrise angle of 63 deg at the forward perpendicular. The half of the forebody planing bottom nearer the step is the important part from a stability point of view, and as the buttock lines here are approximately straight, the question of what effects a non-uniform rate of change of deadrise angle may have is raised. If non-uniform warp were applied so that the planing bottom developed a slight concave camber, the lower limit would probably be lowered (Ref. 27), thus improving stability, but aerodynamic drag would be increased; if the warp variation were such that the planing-bottom camber was convex, drag would be improved but hydrodynamic stability would probably be impaired (Ref. 28). The configurations with uniform warping are therefore considered to be good compromises.

The present investigation of forebody-warp effects on a high length/beam ratio model covers a range of warps which was tested at at least two weights and under different representative operational conditions. The investigation of Ref. 26, which is for one warp change at one weight under calm-water conditions on a model of

higher length/beam ratio, and Ref. 18, which covers a range of warps at one weight, also for calm water, on a hull of low length/beam ratio, allow the conclusions of the present investigation to be extended in scope. Taking all three investigations as a whole, these covering between them ranges of length/beam ratio from 6·2 to 15·0, forebody length from 3·44 to 8·6 beams and static load coefficient from 0·89 to 5·88, it is concluded that throughout these ranges the application of 8-deg forebody warp per beam lowers the undisturbed lower limit by about 2 deg, the rate of change being, however, non-linear. The corresponding upper limit is lowered by a considerably smaller amount. The disturbed stability limits show that a useful increase in the stable region can be obtained here by the use of 8 deg per beam forebody warp.

The changes in trim and the absence of any significant change in the amplitudes of porpoising obtained with forebody warp in the present tests are in general agreement with the results of the two References, Nos. 18 and 26.

3. **Wake Formation.**—An examination of the individual wake photographs taken during tests on Models A, B and C failed to reveal any differences in the shape of the wake which might be directly attributable to forebody warp. What minor differences there were might well have been the result of slight variations in attitude from model to model.

The position of the afterbody relative to the wake and its association with instability in each case may be summarised in the following general manner:

It seems from this Table that the question of whether the afterbody is planing or not bears little relation to stability either disturbed or undisturbed.

4. **Spray.**—4.1. **Present Tests.**—The spray characteristics of the models are summarised in Fig. 50 where projections of the spray envelopes, taken mainly over the displacement speed range, are compared. The effects of forebody warp on spray can be seen clearly at one weight ($C_{\Delta 0} = 2{\cdot}75$) in Fig. 50b. The projection for 0-deg warp is discontinuous because spray struck the model wing, while that for 4-deg warp is continuous, showing that the spray was at all times clear of the model. This is known from observation to be only just the case, however, the spray at about $C_v = 6$ barely clearing the wing trailing edge. The 8-deg warp curve is similar in form to that for 4-deg warp, but a considerable reduction in spray height is obtained where it is generally most needed, *i.e.*, where propellers are normally situated. It is clear that increasing forebody warp improves the spray characteristics. At taxying speeds, where maximum spray heights are in the region $C_z = 4$, there is little difference in spray; at the higher displacement speeds, where spray normally gives most trouble, and the highest spray is between $C = 1$ and 2, the projection is lowered by the second increment of warp by 0·3 beams. The total improvement due to 8-deg warp unfortunately cannot be measured, but it is obviously greater than this. At planing speeds the projections converge at $C_z = -2$, and beyond this the spray in every case is too high for the normal tailplane to be unaffected. With this type of hull, therefore, the tailplane must either be high on the

Attitude	Speed	Afterbody position	Stability		Remarks
			Undisturbed	Disturbed	
High	Low	Planing	Stable	Unstable	Every case A, B and C*
Low	Low	Clear	Stable	Unstable	
High	High	Planing	Stable	Stable	
Low	High	Well clear	Stable	Unstable—violent	
Mid-planing		Clear	Stable	Unstable	A and B both loadings ($C_{\Delta 0} = 2{\cdot}25$ and $2{\cdot}75$)
Mid-planing		Clear	Stable	Stable	C both loadings ($C_{\Delta 0} = 2{\cdot}25$ and $2{\cdot}75$)

* A 0-deg forebody warp per beam
B 4-deg forebody warp per beam
C 8-deg forebody warp per beam.

fin to avoid interference, or stressed to take the resulting water loads. In Figs. 50a and 50c the warp effects just considered are substantiated at $C_{\Delta 0} = 2{\cdot}25$ and $3{\cdot}00$ respectively.

An examination of the individual spray photographs taken during the tests has shown that in the displacement range at lower speeds forebody warp causes the spray to develop a sweepback, *i.e.*, it is less spread out laterally. This tendency decreases with speed until it becomes almost unnoticeable just below hump speed, where the attitude is high and only a small area of the planing bottom forward of the step is wetted. In this region differences in deadrise due to warp are very small and one would expect small or negligible differences in spray as a result. Examples showing warp effects on spray at three speeds, $C_v = 2$, 3 and 4 approximately, are given in Figs. 51, 52 and 53.

The foregoing remarks apply mainly to main spray. Velocity spray is slight in all cases at higher planing speeds, and can be neglected, while at the lower displacement speeds it is practically inseparable from the main spray. In the case with 0-deg warp the lateral distribution of the spray is sufficient to affect wing-tip floats at medium displacement speeds, when the spray origin is well forward, near the bow. This configuration, however, is not a practical one from considerations of stability and impact. With 4-deg warp, possible spray interference with floats occurs only around one speed, about $C_v = 3{\cdot}0$, and in a normal take-off the effect would be of such small duration that no damage would be expected. With 8-deg warp, floats would be clear of spray at all times.

4.2. **Previous Investigations.**—The only spray investigation available which seems to be at all comparable with the present case is that of Ref. 26 for a hull of length/beam ratio 15. The data are presented differently, spray being assessed at several loads, but the conclusions state that bow spray characteristics were substantially better for the hull with the warped forebody than for the hull with the basic forebody; in smooth water a 25 per cent increase in gross load was possible before spray in the propellers and on the flaps was equivalent to that of the basic forebody. Spray striking the tail was approximately the same with both forebodies. These results can only be compared indirectly with those of the present investigation, but it does appear that changes in spray characteristics due to 8-deg forebody warp are approximately the same in each case.

4.3. **Discussion.**—Damage caused by spray normally occurs when propellers, flaps or tailplane are struck by main spray, or when spray enters jet intakes and causes corrosion. Tailplane damage occurs mainly at low planing speeds and would be more likely with a normally positioned tailplane, on a high length/beam ratio hull; it may be overcome by placing the tailplane high on the fin, thus avoiding the high spray plume occurring at these speeds, or it may be met by stressing the tailplane to take the water loads which will certainly occur if the tailplane is in the normal position. The height of this plume relative to the hull is, for practical purposes, unaffected by forebody warp. The remaining sources of damage are found mainly in the displacement speed range. It is clear from the foregoing results that considerable benefit can be derived here from the use of forebody warp, 8 deg per beam giving the greatest reduction in spray height within the range tested.

The present results generally confirm those of Ref. 26, this being due in part to the fact that quantitative changes in attitude due to warp are the same in the two cases. It may be noted that the ratio of forebody length to forebody plus afterbody length is approximately the same in each case, namely $0{\cdot}56$. If this ratio is preserved, attitude changes should be approximately equal for hulls of length/beam ratios between 11 and 15 and the same order of improvement in spray characteristics can be expected with the application of 8-deg forebody warp. The indications of Fig. 50 of the present report are that load variations have little effect on changes due to forebody warp.

5. **Directional Stability.**—Directional stability diagrams for 0, 4 and 8-deg warp per beam are compared at one weight, $C_{\Delta 0} = 2{\cdot}75$, in Fig. 54. There are only two effects of warp which are at all noticeable and even these are of little practical significance. The first is that the separation between the stable equilibrium line and the speed axis at about $C_v = 3$ increases progressively with warp; the speed range affected is so small that the change is insignificant. The second change is found at speeds in the region $C_v = 9$ to 10, where as will be seen from the annotation on the diagram there is a progressive tendency from stable to neutral equilibrium with increase of warp. This effect would be unnoticed in a practical case.

6. **Elevator Effectiveness.**—The effects of forebody warp on elevator effectiveness are shown in Fig. 55b for $C_{\Delta 0} = 2{\cdot}75$. The first 4-deg warp has the greater effect, giving a mean increase in effectiveness of $0{\cdot}045$ approximately, while that due to the second increment is about $0{\cdot}03$. The corresponding changes in effectiveness shown in Figs. 55a and 55c for $C_{\Delta 0} = 2{\cdot}25$ and $3{\cdot}00$ are somewhat less than these, but in each case warp increases elevator effectiveness, the greatest improvement being derived from the first increment of warp.

It should be noted that in these tests the elevators were identical and the increase in effectiveness with application of forebody warp is due to a reduction in the nose-up hydrodynamic moments; for a specified decrease in attitude from a given datum attitude, less forebody volume and planing surface area will be immersed in the warped case and the resistance to an elevator moment will be correspondingly smaller. The effect will be most obvious at low attitudes when there is no afterbody immersion, *i.e.*, in the region of the lower stability limits. At high planing attitudes little or no difference will be found in elevator effectiveness as the hull will be planing on the surface just forward of the step, where differences due to warp are small and the afterbody, which is identical in each case, may also be planing.

These points are illustrated in the following table.

$C_{\Delta 0} = 2{\cdot}75$		0-deg warp		4-deg warp		8-deg warp	
C_v	α_K	η	E^*	η	E	η	E
7	8	+ 4	0·16	−5	0·23	−6	0·30
8	6	+ 5	0·20	−1	0·28	−2	0·37
9	4	+10	0·10	+2	0·24	+2	0·32
9	8	− 4	0·53	−7	0·50	−6	0·50

* E = Elevator effectiveness.

At each speed an attitude in the region of the lower limit has been chosen and at the highest speed a higher attitude included. In each warp case the elevator setting for this attitude and speed has been found, and the specific elevator effectiveness has then been obtained for that speed (Chapter 2, Section 7) (The values of elevator effectiveness in Fig. 55 are mean values for the whole attitude range at a given speed). It can be seen that for the first three attitudes (those nearer the lower stability limit) the effectiveness increases with warp, whereas at the higher attitude and speed there is little difference.

Returning to the presentation of longitudinal stability limits with elevator angles replacing keel attitudes as ordinates in Fig. 46a, it has been noted that apart from the neck of instability in the case of Model A, there is no significant change in the limits due to warp. To obtain a complete representation this diagram must be considered in conjunction with Fig. 55b, where the benefit derived from warp is shown as an increase in elevator effectiveness.

7. **Conclusions.**—The results of the present investigation show that the effects of increasing forebody warp are to improve hydrodynamic longitudinal stability and spray characteristics considerably, to impair directional stability very slightly and to increase elevator effectiveness. Of the configurations tested, that with 8-deg forebody warp per beam gives the best overall water performance, but this might be bettered, particularly from the spray point of view, in other cases when a further increase in the degree of warping were feasible.

Accepting 8-deg warp as the best value in the present case, the following detailed improvements result from its application:

(*a*) The undisturbed lower longitudinal stability limit is lowered by approximately 2 deg; this is independent of load.

(*b*) The undisturbed upper longitudinal stability limit is lowered by a small amount, which is not more than $\frac{1}{2}$ deg.

(*c*) The disturbed stable region is increased significantly.

(*d*) Trim is reduced by the order of $1\frac{1}{2}$ deg in the displacement range and by about 2 deg in the planing range, with $\eta = 0$ deg.

(*e*) Porpoising amplitudes are not significantly affected.

(*f*) The elevator setting at which instability is encountered is materially unaltered.

(*g*) At taxying speeds and at planing speeds spray is not significantly affected; at other speeds in the displacement range, however, the spray height, in the propeller plane in particular, is decreased by more than 0·3 beams. Below hump speed the spray is less spread out laterally. These effects appear to be independent of load.

(*h*) Directional stability is slightly impaired at both low and high speeds, but the changes are of such a nature as to allow them to be neglected.

(*i*) Elevator effectiveness is substantially increased.

Of the above results (*a*) to (*e*) are substantiated by either Ref. 18 or 26 or both. General agreement with (*g*) is obtained from Ref. 26.

CHAPTER 7

The Effects of Afterbody Length

1. **Introduction.**—The effects of afterbody length (the distance between the normal projections of the main-step point and the rear-step point on the hull datum), which are deduced from the results of tests on four models of the series are discussed in this Chapter. These models, A, D, E and F, were identical except in respect of afterbody length, this single parameter being varied in the following manner:

Model D	Afterbody length 4 beams
Model A	Afterbody length 5 beams (basic model)
Model E	Afterbody length 7 beams
Model F	Afterbody length 9 beams.

The effect of this variation on the hullshape generally can be seen in Fig. 56, which is a comparison of hull lines. Aerodynamic and hydrodynamic data common to the four models are given in Tables 1 and 2.

2. **Longitudinal Stability.**—2.1. **Present Tests.**—The effect of afterbody length on longitudinal stability limits at different weights for both undisturbed and disturbed cases is illustrated in Figs. 57 and 58 where the various limits for Models A, D, E and F are compared.

In the undisturbed case the effects of afterbody length on the stability limits for $C_{\Delta 0} = 2{\cdot}75$ are shown in Fig. 58a. With increasing afterbody length, maximum lower critical trim (maximum trim attained on the lower limit) is found at progressively lower attitudes and slightly higher speeds; apart from this the position of the limit is almost unchanged, The vertical band of instability, which occurs with the shorter afterbodies at this weight and extends across the take-off path, is removed at the greater lengths, while the upper limit is progressively lowered and the mean speed at which upper limit instability is encountered with the elevators used is increased. At the same time, the extent of the upper unstable region is decreased, until, with the longest afterbody, no upper limit instability is obtained.

Confirmation of these changes can be obtained from Fig. 57a, which is for a lower load, $C_{\Delta 0} = 2{\cdot}25$. Apart from the fact that, in the case of the two short afterbodies, the vertical bands of instability cutting across the take-off path have been removed with the reduction in weight, good agreement is obtained.

The reduction in maximum lower critical trim with increase in afterbody length is shown approximately for the two loadings, $C_{\Delta 0} = 2{\cdot}75$ and $2{\cdot}25$, in Fig. 67. This diagram gives an idea of the maximum attitude reached on the lower limit for a given length of afterbody in the present case; these attitudes would probably be altered by a change of afterbody angle or forebody shape. The points at $C_{\Delta 0} = 2{\cdot}75$ for the 4 and 5-beam afterbody lengths are not indicated in Fig. 67 because of the difficulty of defining maximum lower critical trim on the relevant set of stability limits (Fig. 58a). This arises from the band of instability found across the take-off path in each case.

As lower limit porpoising is a function of the forebody only and the forebodies used in these tests were identical, one might expect the lower limits to coincide. As will be seen from Figs. 57a and 58a, the limit for the 7-beam afterbody model is highest, but the remainder are disorderly and the separation of the limits is inconsistent, both with weight change and speed change. It is felt, however, that one mean limit for each loading would serve for all of the models. This matter is discussed generally in Chapter 9.

Examination of the upper limits shows that, in both weight cases, increasing afterbody length from 4 to 7 beams lowers the limit by approximately 2 deg and increases its mean speed, while, with a further increase to 9 beams, upper limit instability is apparently avoided altogether. It is possible, though, that had higher test speeds been feasible, an upper limit for the 9-beam afterbody model would have been found.

For the disturbed case the effects of afterbody length on the stability limits are shown in Figs. 57b and 58b. Before discussing them, the points on technique made in Chapter 6, Section 2.1, should be noted when it will be seen that, in the disturbed case, only orders of change are significant.

Considering orders, then, rather than absolute amounts of change, at $C_{\Delta 0} = 2{\cdot}75$ (Fig. 58b), the effect of increasing afterbody length is to reduce the area of disturbed instability until, with the longest afterbody, the disturbed stability limit differs only slightly from that obtained without disturbance. In the cases of the 4, 5 and 7-beam afterbody models respectively, the diagram shows vertical bands of instability which are decreased progressively in width and attitude since the hump limit* is found at higher speeds and lower attitudes.

During tests on each of the models A, D, E and F, it was found that the greatest amounts of disturbance used were necessary in the high-speed lower-limit region, Model F being susceptible only to very large disturbances.

All the trends mentioned so far in connection with disturbance are verified at the lower loading, $C_{\Delta 0} = 2{\cdot}25$ (Fig. 57b). Stability is generally improved by the weight decrease but, in particular, the limits for the 7-beam afterbody show that the vertical band of instability found

* Hump limit is the longitudinal stability limit found on the low-speed side of a band of instability crossing the take-off path just above the hump speed.

at the higher loading has been removed. It may be concluded, therefore, that lengthening the afterbody raises the general level of critical disturbances for the present basic model configuration, particularly in the mid-planing region.

The effects of afterbody length on the stability limits are shown in a different light in Fig. 59 (which is for one loading, $C_{\Delta 0} = 2{\cdot}75$), where elevator angles replace keel attitudes as ordinates. In this diagram the undisturbed lower limits are grouped together and, except for the vertical band of instability which must be crossed during take-off, they lie roughly along the same elevator setting. The upper limits are separated along the speed scale, instability being met at higher speeds with the longer afterbodies, but in each case the limit is found at the same maximum elevator setting. It can be concluded that when, in the undisturbed case, there is a completely stable take-off path for this type of hull, changes in afterbody length cause no significant alteration in the elevator setting at which instability is encountered. In the disturbed case, the high-speed limits are clustered round a common stable area and the movement up the speed scale with increasing afterbody length of the hump limit is marked.

Trim curves for $\eta = 0$ deg are compared in Fig. 60 for the two weights. The effects of increasing afterbody length are to reduce trim progressively, from and including the static floating condition up to speeds just past the hump, and to increase hump speed, while the trim curves tend to collapse at the higher speeds. The change in hump speed with afterbody length is almost unaffected by weight, but the reduction in hump attitude (Fig. 68) decreases with weight, *e.g.*, for an increase in afterbody length from 4 to 9 beams the decrease in hump attitude is $6\frac{1}{2}$ deg at $C_{\Delta 0} = 2{\cdot}75$ and $5\frac{1}{2}$ deg at $C_{\Delta 0} = 2{\cdot}25$.

The tendency for the trim curves to coincide at higher speeds might have been expected. As the afterbody is clear of the water, the configurations are virtually the same in each case, the only possible differences arising from aerodynamic suctions under the afterbody. These forces would tend to increase attitude and the effect would first become apparent with the longest afterbody, because of the greater effective moment arm. At $C_{\Delta 0} = 2{\cdot}75$ (Fig. 60b) the trim curves for the 4, 5 and 7-beam afterbody-length models are in order, while that for the 9 beam shows a definite tendency to rise. At the lower weight, $C_{\Delta 0} = 2{\cdot}25$ (Fig. 60a), the increase in attitude is more pronounced, as might have been expected from the decreased load on water. The longest afterbody trim curve is well raised, the 7-beam curve shows a tendency to rise and only the remaining curves are in order. This effect, however, is of little practical significance and could easily be counteracted by a small movement of the elevator.

The effect of afterbody length on amplitudes of porpoising in both undisturbed and disturbed cases is shown for the higher load, $C_{\Delta 0} = 2{\cdot}75$, in Fig. 62. In the undisturbed case, there is no obvious change in the general level of porpoising amplitudes near the lower limit, but in the upper-limit region a slight decrease is obtained with the longer afterbodies; in the disturbed case, however, the amplitudes of porpoising are reduced with increase of afterbody length.

Corresponding to these effects, in the case of the shortest afterbody, disturbance produces a considerable increase in the amplitudes of porpoising from the undisturbed case. As afterbody length is increased, this effect of disturbance is progressively reduced until, with the longest afterbody, there is no difference between the general levels of undisturbed and disturbed porpoising amplitudes. The region where the model porpoises clear of the water is found at higher speeds and lower attitudes as afterbody length is increased. It was observed during the tests that the frequency of forebody propoising was greatly reduced with the longer afterbodies.

The results are much the same at the lower loading, $C_{\Delta 0} = 2{\cdot}25$ (Fig. 61). There is no significant change in the undisturbed porpoising characteristics, while in the disturbed case there is a progressive reduction in the amplitudes with increasing afterbody length.

The tests were made at constant loadings and the radii of gyration of the 4 and 9-beam afterbody models were 0·96 and 1·48 ft respectively. By reference to Chapter 4, Section 1.5, this would lead one to expect an increase in porpoising amplitudes with increase of afterbody length. That this does not in fact appear indicates that the effect is completely offset (in the disturbed case more than offset) by a decrease in amplitude due purely to the increase in afterbody length. This indicates that use of a longer afterbody is in fact more beneficial than would appear from the above results.

2.2. **Previous Investigations.**—Although there is a fair amount of literature on afterbody-length variations, a large part of it does not isolate the effects of this parameter and only three reports will therefore be considered here. The first, by Kapryan and Clement[29], deals solely with afterbody-length effects on the hydrodynamic qualities of a high length/beam ratio model, the second, by Land and Lina[19], considers these effects, together with those of associated parameters, on a low length/beam ratio model and the third, by Davidson and Locke[18], treats afterbody-length variations as part of a complete investigation into the porpoising characteristics of low length/beam ratio hulls. It should be noted that, as the three reports are American, the techniques used in the model tests differ from those used in the current programme. These differences are mentioned in Chapter 6, Section 2.2. and have been considered in Refs. 4 and 17, whence it appears that comparison should be made on the basis of steady-speed runs; the N.A.C.A. lower limit and upper limit, increasing trim then correspond to M.A.E.E. undisturbed limits, and the N.A.C.A. upper limit, decreasing trim corresponds to part of the M.A.E.E. limit with disturbance.

In Ref. 29, the hull used had a basic length/beam ratio of 15 and was tested at $C_{\Delta 0} = 5{\cdot}88$. The forebody, which was 8·6 beams in length, had no warp, incorporated chine flare and had a main-step deadrise of 20-deg. Slipstream was used in the tests and the change

investigated was an increase in afterbody length from 6·4 beams to 9·25 beams. With this change in afterbody length, the step depth was increased from 16·5 per cent to 24 per cent beam (*i.e.*, two parameters were changed simultaneously) so as to keep the stern-post angle constant at 6·9 deg. The afterbody angle was thus approximately $5\frac{1}{2}$ deg at both lengths. The conclusions state that the stable range of trim between the upper and lower trim limits of stability was greater for the extended afterbody than for the basic afterbody at low and intermediate speeds, because of the lower hump of the lower trim limit and the virtual elimination of the upper limit at these speeds, and was slightly less for the extended afterbody at high speeds. The same conclusion is true for the present case, but a further examination of this Reference shows better agreement in that detailed tendencies are the same, although magnitudes of change are somewhat greater in the current tests. It may well be that the differences in magnitude of change are due to the increase in step depth in Ref. 29. On the assumption that afterbody ventilation is adequate, the effect of increasing step depth may be roughly likened to an increase in afterbody angle and this is known to have effects which, in general, are opposite to those of an increase in afterbody length in the undisturbed stability case. The main effects of slipstream will be to reduce trim, to reduce load on water, thereby moving the limits bodily to lower speeds, and to reduce aerodynamic static stability. This latter effect may alter the upper-limit position, but in general it is felt that the slipstream used in these tests will not greatly influence the afterbody-length effects.

In the investigation of Ref. 19, a model of basic length/beam ratio 6·4 was tested at $C_{\Delta 0} = 0{\cdot}87$ (based on maximum beam). The forebody of this model was 3·7 beams in length. It incorporated chine flare, had a main-step deadrise of 20 deg and was unwarped. No slipstream was used in these tests, the mainplane being fitted with full-span leading-edge slats. Step depth and afterbody angle were constant at 5·5 per cent beam and 5·5 deg respectively, and the range of afterbody lengths tested was from 1·61 to 3·11 beams. It is interesting to note that the emphasis here is on shortening the afterbody rather than lengthening it, the normal afterbody length being 2·61 beams. The authors conclude that ' the upper limits are raised to higher trims as the afterbody is shortened and an afterbody shorter than is conventional at the present time (1943) may therefore be expected to increase the stable trim range of a flying boat '. This conclusion could be applied to the undisturbed limits obtained in the planing region in the present tests, but only to the undisturbed limits; the existence of the neck of instability at near-hump speeds for the shorter afterbodies, however, complicates the issue. Figs. 14 and 15 of this Reference show that the lowering of the maximum lower critical trim is about the same and the lowering of the mean upper critical trim with increase in afterbody length somewhat less than that obtained for a corresponding increase in afterbody length in the current investigation.

In Ref. 18, a basic hull of length/beam ratio 6·2 was tested at $C_{\Delta 0} = 0{\cdot}89$. The forebody was unwarped but had chine flare and a 20-deg main-step deadrise angle and was 3·45 beams in length. The step depth was constant at 4·8 per cent and the afterbody angle was 5·0 deg. The range of afterbody lengths tested was from 2·25 to 3·25 beams and dynamic hull models were used, aerodynamic moments and forces being fed in synthetically. The results are summarised in the statement that ' decreasing the afterbody length raises the upper limit slightly and has only a very small effect on the lower limit at moderate speeds just past the hump; the speed range over which the free-to-trim track passes below the lower limit is lengthened slightly. The shortest afterbody tested stopped high-speed upper-limit porpoising in the present instance. The effects are generally similar to those resulting from modifying the afterbody angle '. These conclusions are similar to those of the preceding Reference and show general agreement with the present undisturbed case. Detailed changes are also in fair agreement.

The reductions in maximum lower-limit trim, mean upper-limit trim and hump trim for the foregoing References are compared in Table 121 with interpolated values for the current tests by expressing afterbody length as a percentage of forebody length. Only orders of change should be considered, the Table being intended merely as a convenient summary.

2.3. **Discussion.**—As in the forebody-warp case, the range of afterbody lengths tested was restricted to those felt to be within the practical design limits. The shortest afterbody (4 beams) is considered a good minimum. At the design loading, $C_{\Delta 0} = 2{\cdot}75$, undisturbed stability is poor and disturbed stability is bad, while the hump trim, 14 deg is high and, unless a wing of low aspect ratio were used, might well result in wing stalling with consequent loss of lift and aileron control; a further decrease in afterbody length would worsen these already poor qualities. The longest afterbody (9 beams), on the other hand, has good stability characteristics, both disturbed and undisturbed, but hump speed ($C_v = 6{\cdot}5$ or $V = 67$ knots at 150,000 lb) is high and, because of the strong afterbody, maximum attitudes are limited to 8 deg, so take-off speeds are also high (of the order of 110 knots, $C_v = 10{\cdot}6$). A further lengthening of the afterbody would increase these speeds and give even lower maximum attitudes. The best afterbody length of the four tested, from the design view-point, is therefore somewhere between 4 and 9 beams.

Considering longitudinal stability, in the undisturbed case it appears that for a practical low length/beam ratio hull configuration, upper-limit instability can be eliminated by sufficiently shortening the afterbody (Ref. 18), while in the high length/beam ratio case (Chapter 7, Section 2.1), upper-limit instability can be removed by lengthening the afterbody (These apparently contradictory methods are quite simply related. Shortening the afterbody raises the upper limit; by continuing the

process until the limit is above attitudes normally attained with elevators, upper-limit instability is, for practical purposes, rendered non-existent. Lengthening the afterbody lowers the upper limit, but also lowers maximum attitudes at a greater rate so that the upper limit is progressively shortened from the low-speed end. In each case the region of upper-limit instability is roughly a triangle enclosed by the maximum trim attainable with the elevators used, take-off speeds and the limit itself. The area of this triangle decreases to zero as the afterbody is either shortened or lengthened, giving effectively no instability). In the first instance, both hump attitude and maximum lower critical trim (the trim of a point on the lower stability limit) will be increased, hump speed will be decreased, there will be a much greater stable-attitude range available at planing speeds, and low-speed take-offs will be feasible. In the second case the effects are reversed, so that, although lower-limit instability is not met with the long afterbody until higher speeds are reached and there is little change in porpoising amplitudes with afterbody length, the shorter afterbody might appear initially to be preferable. If, however, an attempt is made to avoid upper-limit instability with the high length/beam ratio hull by shortening the afterbody, there appears to be a minimum length below which a band of instability forms across the take-off path. Of the four afterbody lengths tested, that of 7 beams is the shortest with which this band of instability can be avoided at the design loading of $C_{\Delta 0} = 2{\cdot}75$. This phenomenon is not found at the lower loading, $C_{\Delta 0} = 2{\cdot}25$, but this weight decrease is considerable. It is felt that the formation of this unstable band is not restricted to the high length/beam ratio class of hulls and that tests on low length/beam ratio hulls at higher loadings would produce similar results. There is on balance little to choose between long and short afterbodies when only the undisturbed characteristics are considered.

In the disturbed case, the short afterbody exhibits very poor qualities. It is susceptible to small disturbances (Fig. 7) and with large disturbances the unstable region tends to cover the greater part of the planing speed range, leaving only a small area stable at the higher speeds. In addition, amplitudes of porpoising show a large increase over the undisturbed case and the frequency of porpoising is fairly high. With the longer afterbody, however, small disturbances have no effect and large disturbances only raise the high-speed end of the lower limit, the region of upper-limit instability remaining either very small or zero. Porpoising amplitudes are unchanged from the undisturbed case and, as the frequency of forebody porpoising is low, the motion is relatively gentle ; a pilot could thus encounter instability and then take corrective action quite easily. It is obvious that, in the disturbed case, a configuration with a long afterbody is better.

As in undisturbed tests the conditions represented are ideal, they cannot be accepted as prevailing in the normal course of flying-boat operations and unless operating conditions are exceptional, weight must be given to the disturbed results in selecting an afterbody length ; this points towards a long afterbody. It should be noted, however, that the tests with disturbance are most rigorous and the disturbed conditions represented are worse than those likely to be met in practice, so that the afterbody length initially chosen can be reduced by an amount compatible with the operating conditions expected, so lowering the high minimum take-off speed. Of the configurations tested in the present investigation, the 7-beam afterbody appears to be the best compromise for average operating conditions (apart possibly from waves*). From stability considerations both the 7 and 9-beam afterbodies are good, while the 4 and 5-beam afterbodies are, at the best, mediocre. With the 7-beam configuration, however, maximum planing attitudes are 10 deg, as against 8 deg for the 9 beam, giving a lower possible take-off speed, and hump speed is reduced from $C_v = 6{\cdot}5$ to $C_v = 5{\cdot}6$. This means a shorter run in the displacement region at slightly higher attitudes, when damage due to spray will be less and both take-off distance and time will probably be reduced.

As the conclusion that a long afterbody is preferable is the opposite of that of Ref. 19, it may be enlightening to consider the reasons for this difference. The actual test results in Refs. 18, 19 and 29 and the present undisturbed case are in good agreement and the main bias towards a long afterbody has come from the disturbed results. In Ref. 19, however, the recommendation for a short afterbody is also based on the results of simulated landing tests, where the criterion was the number of skips made after touch-down (The greater the number of skips the poorer the landing stability). A comparison of the landing attitudes and skipping characteristics of the models of this Reference with their corresponding stability diagrams indicates that the worst skipping and possibly all skipping occurs for landings in what in the present investigation has been termed the disturbed unstable region, the landing itself evidently constituting a disturbance. The actual number of skips does not appear to be directly relevant and any comparison of the models would be best based on the appropriate disturbed limits ; these are unfortunately insufficiently complete in the Reference for reliable comparison to be made.

The foregoing considerations of afterbody-length effects on longitudinal hydrodynamic behaviour show that increasing afterbody length makes little overall difference to the undisturbed characteristics (*e.g.*, the advantages of reduced porpoising amplitudes are offset by the disadvantages of higher take-off speeds, etc.), while in the disturbed case, the longer afterbodies are nowhere near as susceptible to external disturbances as are the short ones. For normal operation the long afterbody is thus better ; little risk of trouble from instability is incurred during take-off and low speed as well as normal landings are feasible (Chapter 12).

It should be noted that all the hulls considered in this Section (including Refs. 18, 19 and 29) have unwarped forebodies and afterbody angles of the order of 6 deg,

* *See* Chapter 11, Section 1.5.

while step depths vary. If any of these parameters were radically altered it is possible that the foregoing conclusions would require some modification.

3. **Wake Formation.**—As all the models now under consideration (Models A, D, E and F) have identical forebodies, then under given conditions of attitude, speed and load, when the afterbody is clear of the water, the wake shapes will be identical. It is thus possible to determine from the combined results the effect of attitude at several speeds on the shape of the wake for the basic forebody. The wake photographs taken during the tests were difficult to assess, but at each speed it would appear that an increase in attitude results in a narrowing of the wake cross-section, although the change is small, and a fanning out of the velocity spray.

Whether the afterbody is planing or not at points which bear corresponding relations to the limits in the various cases seems, from the wake photographs, to be consistent from model to model, but little else can be said that does not follow directly from the stability diagrams.

4. **Spray.**—The effects of afterbody length on spray are shown at the higher weight ($C_{\Delta 0} = 2{\cdot}75$) in Fig. 63b*. Only in the case of the shortest afterbody is there a complete projection, indicating that little or no main spray strikes the wing; it was seen from photographs taken during the tests, however, that over a small speed range considerable velocity spray strikes the wing even in this case. As afterbody length is increased, spray qualities deteriorate. The spray projections are discontinuous, progressively more spray hitting the wing; the spray origin is moved forward, increasing the height of the bow spray at low speeds, and the spray plume at the tail is lowered. These trends are confirmed at the lower weight (Fig. 63a) and good qualitative agreement is obtained from Ref. 29.

The deterioration in spray characteristics with increasing afterbody length is due mainly to the decreased attitudes obtained. There will be minor changes in draught, but these should only have a small effect on the spray. The movement forward of the spray origin, at a given speed, with the decrease in attitude could easily be seen by comparing the individual spray photographs taken during the tests; an example is given in Fig. 64 at $C_v = 3{\cdot}0$ approximately for $C_{\Delta 0} = 2{\cdot}75$.

The good spray characteristics of the shortest afterbody model accrue only from the high attitudes associated with the short afterbody. The short afterbody in itself, however, gives rise to unacceptable disturbed stability characteristics and the use of the longer afterbodies to obtain good stability in the present tests results in unacceptable spray qualities. A similar long afterbody design must therefore incorporate forebody warp or some other modification to give acceptable spray behaviour.

5. **Directional Stability.**—Directional stability diagrams for the models with 4, 5, 7 and 9-beam afterbody lengths are compared at one weight, $C_{\Delta 0} = 2{\cdot}75$, in Fig. 65. The most obvious effect of increasing afterbody length is the progressive change in the low-speed, stable equilibrium line and the corresponding movement up the speed axis of the point of separation of the low-speed, unstable equilibrium line. The most significant result of these changes is the increase in the minimum speed at which inherent directional stability is obtained. At high speeds the effects of afterbody length are small and of no practical significance. It is interesting to note that the effects on directional stability of increasing afterbody length are very similar to those obtained by increasing forebody warp (Chapter 6, Section 5).

6. **Elevator Effectiveness.**—The effects of afterbody length on elevator effectiveness are shown in Fig. 66b for $C_{\Delta 0} = 2{\cdot}75$. The mean slopes of the curves are approximately equal and as afterbody length is increased there is a progressive reduction in effectiveness at a given speed. The same effects are shown in Fig. 66a for $C_{\Delta 0} = 2{\cdot}25$, the only significant difference between the two diagrams being the overall increase in effectiveness due to the decreased load.

The values of elevator effectiveness given in Fig. 66 are mean values for the whole attitude range; a more detailed examination of the elevator effects may therefore prove helpful. From Chapter 7, Section 2.1, at a given weight ($C_{\Delta 0} = 2{\cdot}75$) the lower stability limits collapse virtually on the same trim curve. The forebodies of the models and the elevators are identical so that in the region of the lower limit, when the afterbody is clear of the water, one can expect the value of elevator effectiveness at a given speed to be the same in each case. This point is illustrated below by specific values of effectiveness obtained for given attitudes (*see* Chapter 2, Section 7):

Model		D		A		E		F	
Afterbody length		4 beams		5 beams		7 beams		9 beams	
C_v	α_K	η	E*	η	E	η	E	η	E
7	8	+4	0·20	+4	0·16	+4	0·05	−12	0·02
8	6	+4	0·22	+5	0·20	+4	0·15	+ 5	0·37
9	5	+4	0·20	+4	0·22	+3	0·20	+ 4	0·20

* E = Elevator effectiveness.

* It may be noted that the spray photographs for the 4, 5 and 7-beam afterbody models were obtained with $\eta = -8$ deg., but those for the 9-beam afterbody model were taken with $\eta = 0$ deg. This will make no difference to attitudes in the displacement range, affecting only the high-speed result which is only representative in any case. The change was made to avoid running Model F at its maximum planing attitude, which is obtained with $\eta = -8$ deg.

In the Table, elevator effectiveness is the same at $C_v = 9$ for the four models, at $C_v = 8$ for Models D and A and at $C_v = 7$ for Model D. The other values differ because of afterbody immersion, the hump being found at higher speeds with the longer afterbodies.

With increasing attitude, the value of effectiveness found near the lower limit at $C_v = 9$ first increases and then tends to zero as the maximum attitude is approached. The effects of increasing afterbody length are to reduce the attitudes for maximum elevator effectiveness and to nullify the effect of elevator at progressively lower attitudes. This is shown in the following Table:

Model		D		A		E		F	
Afterbody length		4 beams		5 beams		7 beams		9 beams	
C_v	α_K	η	E*	η	E	η	E	η	E
9	8	− 4	0·50	− 4	0·59	− 6	0·52	−12	0·02
9	9	− 6	0·56	− 7	0·20	− 8	0·25	—	0
9	10	− 8	0·44	− 8	0·15	−14	0·08	—	0
9	11	−10	0·30	−20	0·07	—	0	—	0

* E = Elevator effectiveness.

Returning to the presentation of longitudinal stability limits in Fig. 59a, where elevator angles replace keel attitudes as ordinates, it has been noted that apart from the vertical neck of instability in the case of the shorter afterbodies there is little regular change due to afterbody length. For a complete representation this diagram should be considered in conjunction with Fig. 66b, when the effects of afterbody length are shown as a change in elevator effectiveness.

7. **Conclusions.**—The results of the present investigation show that the effects of increasing afterbody length are:—

(*a*) to reduce maximum lower critical trim and raise the speed at which it occurs

(*b*) to reduce trim generally and, in particular, to reduce both hump trim and the maximum trim obtainable with normal elevators

(*c*) to lower the upper stability limit and move the upper unstable region to higher speeds

(*d*) to increase resistance to disturbance

(*e*) to reduce disturbed amplitudes of porpoising

(*f*) to lower the frequency of forebody porpoising

(*g*) to move the spray origin forward, giving rise to poor spray characteristics (associated with (*b*))

(*h*) to worsen directional qualities at speeds just below the hump

(*i*) to reduce elevator effectiveness

(*j*) to leave materially unaltered the elevator setting at which undisturbed instability is encountered.

The after-body-length effects listed above are, except for some minor differences, independent of load. Results (*a*) to (*c*) are substantiated by Refs. 18, 19 and 29 and, as magnitudes of change are of the same order for corresponding afterbody length increases when afterbody length is expressed as a percentage of forebody length, may be said to be independent of actual length/beam ratio.

As the qualities listed are not all desirable, the choice of afterbody length must be a compromise; in the present case, of the four configurations tested, that with an afterbody length of 7 beams is the best but the application of forebody warp or some other modification is necessary to offset the corresponding poor spray characteristics.

CHAPTER 8

The Effects of Afterbody Angle

1. **Introduction.**—This Chapter deals with the effects of afterbody angle (the angle between the tangents to the forebody and afterbody keels at the main and rear steps respectively) and is based on the results of tests on three models of the series. These models, A, G and H, were identical except in respect of afterbody angle and this single parameter was varied in the following manner:

Model G	Afterbody angle 4 deg
Model A	Afterbody angle 6 deg (basic model)
Model H	Afterbody angle 8 deg

The effect of this variation on the hull shape generally can be seen in Fig. 69, which is a comparison of hull lines. Aerodynamic and hydrodynamic data common to the three models are given in Tables 1 and 2.

2. **Longitudinal Stability.**—2.1. **Present Tests.**—The effect of afterbody angle on longitudinal stability limits at different weights for both undisturbed and disturbed cases is shown in Figs. 70 and 71 where the relevant limits for Models A, G and H are compared.

In the undisturbed case the effects of afterbody angle on the stability limits for $C_{\Delta 0} = 2{\cdot}75$ are shown in Fig. 71a. With increasing afterbody angle, the available stable trim range is increased throughout the planing range of speeds. The most obvious detailed change is the considerable raising of the upper limit, while the position of the lower limit is almost unchanged at medium and high planing speeds. Maximum lower critical trim (maximum trim attained on the lower limit) is raised about 3 deg over the range of afterbody angles considered, but the change is not progressive and calls for further comment.

There is an irregularity which occurs with the afterbody angle of 6 deg and is due to the formation of a vertical neck of instability across the take-off path; there is thus no true maximum lower critical trim on this set of limits. Fig. 76 shows that, in the case of the 4 deg afterbody angle without disturbance, there is a similar neck of porpoising, which extends across the take-off path but is excluded by the limits because the amplitudes are in general less than 2 deg ; in the 8-deg afterbody-angle case there is no corresponding region of porpoising. With increasing afterbody angle, then, the porpoising initially occurring in this region is increased in amplitude to more than 2 deg, when the motion is formally classed as unstable and there is no true maximum lower critical trim, and then disappears, while the region itself is found at progressively higher attitudes.

Before seeking confirmation of these effects in Fig. 70a, which is a comparison of undisturbed longitudinal stability limits for the three models at a lower loading, $C_{\Delta 0} = 2{\cdot}25$, it is necessary to consider the effects of load separately for each model. Examination of Figs. 70a and 71a shows that for a reduction in beam loading, $C_{\Delta 0}$, by $0{\cdot}5$, the lower limits for Models A and G are lowered by similar amounts, about $1{\cdot}8$ deg, while that for Model H is lowered by about half of this amount. It follows that quantitative substantiation of the afterbody-angle effects shown in Fig. 71a cannot be obtained from Fig. 70a and that the difference in the rate of change of critical trim with load in the case of Model H is one of the results of increasing afterbody angle, *i.e.*, afterbody-angle effects on undisturbed stability characteristics are not independent of load.

Considering Fig. 70a, it will be seen that the main qualitative results are the same as for the higher loading. Increasing afterbody angle results in an increase in the available stable range of trims throughout the planing speed range and the upper limit is raised considerably. The separation of the lower limits is in keeping with the previous paragraph and while there is an ordered increase in maximum lower critical trim, the greater part of this accrues from the first 2-deg increase in afterbody angle from the lowest value. Although, due to the reduction in weight, there is no post-hump neck of instability, the large increase in maximum lower critical trim obtained with the 6-deg afterbody angle substantiates the proneness of this model to become unstable in this region.

It is convenient to say here that because of the unexpected separation of the lower limits in Fig. 70a, the limits for Models G and H at this weight, $C_{\Delta 0} = 2{\cdot}25$, were checked. Agreement with the original limits was very good, verifying the separation found in Fig. 70a.

In the disturbed case the effects of afterbody-angle variations are shown for the two loadings, $C_{\Delta 0} = 2{\cdot}75$ and $2{\cdot}25$, in Figs. 70b and 71b. Before discussing them, however, it should be noted that orders rather than absolute amounts of change should be considered because of the experimental limitations in the disturbance technique (Chapter 6, Section 2.1).

With increasing afterbody angle at $C_{\Delta 0} = 2{\cdot}75$ (Fig. 71b), the hump limit is found at lower speeds and much higher attitudes, while the high-speed stable region is increased considerably, with the lower, high-speed, extremities of the limits remaining almost coincident. The net result is an over-all improvement in disturbed stability characteristics with increasing afterbody angle with a progressive, but slight, reduction and movement to lower speeds of the speed range over which instability is encountered.

Similar general remarks apply in the lower-weight case (Fig. 70b), but here the progressive improvement in stability with increasing afterbody angle is even more

pronounced. The major difference from the higher-weight case is found in the high-speed lower-limit region. Where formerly the limits were coincident, only the lower parts of those for Models A and G now show this tendency (the turn-up on Model A limit was obtained only with the most violent disturbances and is not felt to be of immediate significance), while the limit for Model H is raised generally. This effect is similar to that obtained in the undisturbed case, so it may be said that afterbody angle-effects on stability are not independent of load in either undisturbed or disturbed cases.

The effects of afterbody angle on the stability limits are shown in a different light for the two beam loadings, $C_{\Delta 0} = 2{\cdot}75$ and $2{\cdot}25$, in Figs. 72 and 73 respectively, where elevator angles replace keel attitudes as ordinates.

In the undisturbed case (Figs. 72a and 73a) it might be expected from previous plots of this nature (Chapter 6, Section 2.1, and Chapter 7, Section 2.1) that the improvement in stability obtained with the higher afterbody angles would not be shown; in general this is the case, but the two features mentioned earlier, namely, the tendency for the 6-deg afterbody model to form a post-hump neck of instability, and the raising of the lower limit for the 8-deg afterbody model at the lower loading are emphasised. The neck of instability obtained with the 6-deg afterbody model is clearly shown in Fig. 73a and there is an obvious tendency towards the formation of a similar neck at the lower loading in Fig. 72a. The separation of the limit for Model H from those for the other models is found with this type of presentation not only in the case of the lower limit at the lower loading, but with both limits at both loadings. The lower limits are in order at both weights, those for the lowest afterbody angle being found at the greatest value of elevator setting.

In the disturbed case, at both loadings (Figs. 72b and 73b), the movement of the hump limit to lower speeds with increase of afterbody angle is seen to be obtained mainly with the first increment investigated, *i.e.*, from 4 deg to 6 deg, while the improvement in the high-speed stable region remains progressive. It may be noted that at each weight the high-speed lower limits show a separation and order which corresponds closely to that of the lower limits in the relevant undisturbed case.

Apart from the removal of the neck of instability in the undisturbed case, the main effect of the weight decrease (Figs. 72 and 73) is to move the limits bodily to lower speeds, particularly the upper limits. In the disturbed case there is a similar effect, which is accompanied by a slight general increase in the three high-speed stable areas.

Trim curves for $\eta = 0$ deg are given in Fig. 74 for all models at the two weights concerned. At $C_{\Delta 0} = 2{\cdot}75$ (Fig. 74b), the effects of increasing afterbody angle are to increase trim progressively from and including the static floating condition, up to speeds just past the hump, when the trim curves tend to run together. It is interesting to note that the increase in hump trim is approximately equal to the change in afterbody angle, which in turn is equal to twice the increase in static floating trim. These tendencies are confirmed at the lower loading in Fig. 74a, the differences in weight seeming to have little effect. As in the displacement speed range buoyancy forces predominate, the trim changes are almost independent of elevator setting, but over the planing speed range they vary, the increase in trim due to a given increase in afterbody angle being, in general, greater for the lower values of elevator angle and greater at the higher speeds.

The effect of afterbody angle on amplitudes of porpoising is shown in both undisturbed and disturbed cases for one load ($C_{\Delta 0} = 2{\cdot}75$) in Fig. 76. In the undisturbed case it appears that there is little difference between the 4-deg and 8-deg afterbody-angle models, but it should be noted that the data are rather sparse and, as the majority of the points for Model H (Fig. 76c) lie on the limits, they are, by definition, of 2-deg amplitude. The general level of porpoising amplitudes for the 6-deg afterbody-angle model (Fig. 76b) does, however, seem to be slightly higher than the others. In the disturbed case, with the change in afterbody angle from 4 deg to 6 deg, there is a large increase in the amplitudes of porpoising, while a further change in angle from 6 deg to 8 deg produces a further, but very slight increase. Raising the afterbody angle has thus no significant effect on undisturbed porpoising amplitudes, while disturbed amplitudes show first a marked increase, then a very slight increase. An examination of porpoising amplitudes at $C_{\Delta 0} = 2{\cdot}25$ in Fig. 75 shows that weight change makes little difference and that the above conclusions are unaltered.

2.2. **Previous Investigations.**—There are many References to afterbody-angle effects in various reports, but only three (Refs. 18, 19 and 30), which treat the subject directly, will be considered here. In each case, afterbody angle variations are considered as part of a much fuller investigation into the characteristics of low length/beam ratio hulls and, as the three reports are American, the techniques used in the model tests differ from those used in the current programme. These differences have been considered in Refs. 4 and 17, whence it appears that comparison should be made on the basis of steady-speed runs; the N.A.C.A. lower limit and the upper limit, increasing trim then correspond to M.A.E.E. undisturbed limits, and the N.A.C.A. upper limit, decreasing trim corresponds to part of the M.A.E.E. limit with disturbance.

In Ref. 19, the model used had a length/beam ratio of $6{\cdot}3$ and was tested at $C_{\Delta 0} = 0{\cdot}87$ (based on maximum beam). The forebody, which was $3{\cdot}7$ beams in length, had no warp, incorporated chine flare and had a main-step deadrise of 20 deg. The depth of the main step was constant at $5{\cdot}5$ per cent beam. A complete dynamic model was used in the tests, the mainplane being fitted with full-span leading-edge slats; no slipstream was used and the range of afterbody angles covered was from $5{\cdot}3$ deg to $9{\cdot}8$ deg. The authors concluded that increasing the afterbody angle produced no marked changes in the position of the lower limit and a non-linear raising of the upper limit, which was greatest for the afterbody-angle

increment from 6·8 deg to 8·3 deg. The final increment, from 8·3 deg to 9·8 deg, was critical in that little increase in the stable trim range resulted and the character of the unstable motion was entirely changed with the higher afterbody angle, consisting mainly of vertical oscillations with little change in trim. It is then stated that for a given configuration there is an optimum afterbody angle and that too great an angle may even decrease the stable range of trims or lead to a more violent type of porpoising. If all the limits of the Reference are considered, it appears that the optimum afterbody angle whose existence is suggested by the authors lies somewhere around 9 deg. If the existence of a similar critical afterbody angle be assumed in the present high length/beam ratio case, it would appear that it was either just reached or being approached, but had not been exceeded, with Model H (8-deg afterbody angle). Again, as afterbody-angle effects are not independent of loading, such a critical angle would probably vary with weight. This matter is further referred to in the next Section.

In the investigation of Ref. 18, a hull of length/beam ratio 6·2 was tested at $C_{\Delta 0} = 0{\cdot}89$. The forebody was unwarped but had chine flare and a 20-deg main-step deadrise angle and was 3·45 beams in length. The step depth was constant at 4·8 per cent beam and the range of afterbody angles tested was from 2 deg to 12 deg. Dynamic hull models were used, aerodynamic moments and forces being fed in synthetically. It was concluded that increasing the afterbody angle raised the lower limit at moderate speeds and caused it to start at a slightly lower speed, but had no appreciable effect on the lower limit at high speeds; the upper limit was raised and, with the two greatest afterbody angles ($9\frac{1}{2}$ deg and 12 deg), the upper limit was suppressed at high speeds. Here there is no evidence of an optimum afterbody angle and in fact the changes are progressive and straightforward, but the differences in the test techniques should be noted.

The tests of Ref. 30 were made on models of four different length/beam ratios (5·07, 6·19, 7·32 and 8·45) over a range of afterbody angles from 3 deg to 11 deg in each case. The basic hull form, from which the others were derived, had a length/beam ratio of 6·19 and a forebody length of 3·44 beams. It incorporated both forebody warp and chine flare and had a main-step deadrise angle of 20 deg with a step depth of 5·0 per cent beam. The conclusions, which are general and apply to each of the length/beam ratio cases, state that the longitudinal stability limits are widened with increasing afterbody angle. Increasing afterbody angle raises the upper stability limits and causes the lower stability limits to occur at higher trims and at lower speeds. The author also states, in effect, that static and hump trims are raised, twice the increase in static floating trim being equal to the increase in hump trim, which in turn is equal to the increase in afterbody angle. It should be noted that the technique used in these tests was the same as that of the previous Reference, *i.e.*, aerodynamic forces and moments were applied synthetically.

The longitudinal stability limits of the last Reference are presented on a non-dimensional base and this may obscure any difference in the effects of increasing afterbody angle following a change in load. In the comparison of afterbody-angle effects the main trends are clear. The lower limits collapse at higher speeds, except in the case of the lowest length/beam ratio models. All the upper limits are raised progressively with increase in afterbody angle, except in the 7·32 length/beam ratio case, when that for the 11-deg afterbody angle crosses and runs below the 7-deg upper limit at the high-speed end of the diagram.

2.3. **Discussion.**—As in the forebody-warp and afterbody-length cases, only a practical range of afterbody angles was covered in the investigation. The lowest afterbody angle (4 deg) is considered a reasonable minimum. At the design loading, $C_{\Delta 0} = 2{\cdot}75$, undisturbed stability is acceptable but disturbed stability is bad, the deterioration with disturbance being marked; a further decrease in afterbody angle would worsen these qualities. With the highest afterbody angle (8 deg), on the other hand, good stability characteristics are obtained and had a higher angle still been tested it might have further improved these good qualities or, in the manner of Ref. 19, it might not. It should be remembered, however, that one of the main objects in using a high length/beam ratio hull is to obtain low aerodynamic drag. It is known that the turn-up of the hull camber-line, obtained with contemporary afterbodies, can be responsible for a significant proportion of the hull drag[31], so a further increase in afterbody angle, which would in general produce a further increase in drag, is not considered advisable. It follows that, although increase in afterbody angle has been referred to above and this investigation indicates how variation of afterbody angle can improve longitudinal stability in the high length/beam ratio case, the immediate object is to find out by how much afterbody angle can be reduced, while maintaining reasonable stability characteristics.

In the undisturbed case the main effects on the longitudinal stability limits of increasing afterbody angle are to raise both the upper limit and maximum lower critical trim, thereby widening the available stable trim range. This general trend is found in all the cases which have been considered and is thus independent of length/beam ratio. In view of the detailed discrepancies, however, between loads and between models, some discussion is necessary.

At $C_{\Delta 0} = 2{\cdot}75$ (Fig. 71a) the lower limits obtained in the present investigation with the three different afterbody angles are almost coincident; with a decrease in loading to $C_{\Delta 0} = 2{\cdot}25$ they are lowered (Fig. 70a), but the amount of this lowering for the 8-deg afterbody angle is only half of that for the 6-deg and 4-deg angles, giving a separation of the limits at this weight. It is felt that this discrepancy can be accounted for by the airflow under the afterbodies and the associated suctions or by the choice of the 2-deg double amplitude stability criterion. It should be noted, however, that any suction effects which

do occur will be emphasised in the present case, as the high beam loadings result in deeper troughs, the long afterbodies allow a greater moment arm and the two low afterbody angles tested are lower than those of contemporary afterbodies,[32]. In a design case this load effect might well be significant. An immediate safeguard, however, when considering high length/beam ratio designs would be to check stability at two or more weights during model tests. Any large reduction in the stable region resulting from a last minute increase in loading would not then be unexpected.

Considering now the upper limits without disturbance, with one exception the main conclusion in every case is that increasing afterbody angle raises the upper limit. This exceptional case led to the suggestion that there was an optimum afterbody angle of approximately 9 deg for the general configuration tested. It is felt that this conclusion may be misleading in that the lowering of the upper limit is possibly due to the test techniques employed, the effect being the result of aerodynamic static instability or some similar cause.

In the disturbed case, there is a progressive improvement in stability with increase of afterbody angle which is similar at both loadings. Each set of limits shows a vertical band of instability across the take-off path and this gets wider as the afterbody angle is lowered, until, with the 4-deg afterbody angle, it covers the greater part of the planing speed range. The low-angle configuration as tested is, therefore, not a good design proposition although this situation is somewhat mitigated by the facts that the amplitudes of disturbed porpoising are considerably less than those for the 6-deg and 8-deg afterbody-angle models and, in the undisturbed case, there is effectively a clear stable take-off path at both loadings.

In a practical case, where good stability characteristics are the aim, the configuration with the highest afterbody angle would appear to be the best, but the hump attitude of 13·5 deg at $C_{\Delta 0} = 2{\cdot}75$, coupled possibly with a wing setting angle of about 2 deg, would, unless a wing of high aspect ratio were used, result in tip stalling and wing dropping. At the hump speed of $C_v = 4{\cdot}5$ ($V = 47$ knots at 150,000 lb) this could be dangerous. If, on the other hand, it were decided to use a low afterbody angle to obtain low air drag while maintaining acceptable hydrodynamic stability characteristics, the lowest angle tested could only be used under ideal operational conditions, *i.e.*, conditions represented by the undisturbed limits. Alternatively, in order to use the lowest angle under normal operational conditions (apart from waves), when disturbed limits apply, some additional modification would have to be made to the hull form.

3. **Wake Formation.**—The nature of the wake photographs taken during the tests on Models A, G and H did not allow an assessment of the wake depth or section and in this direction little is to be gleaned; what they did show, however, was whether or not the afterbody was touching the wake. In view of the discussion in the previous Section this may be important, particularly in the case of the lowest afterbody angle. It could be seen from the photographs that in the vicinity of the lower limit, the afterbody of Model G was in general clear of the wake, but there was a minor exception at $C_{\Delta 0} = 2{\cdot}25$; close to the point of maximum lower critical trim the aft step was just touching the water. This, however, was at the low-speed end of the planing range and might therefore have been expected. Results for Model A were similar, with the aft step just touching the wake at the lower weight near the point of maximum critical trim, while the afterbody of Model H was at all times clear.

4. **Spray.**—The effects of afterbody angle on spray are shown at the higher weight ($C_{\Delta 0} = 2{\cdot}75$) in Fig. 77b. In every case, the profile is discontinuous, indicating that the wing was struck by main spray; not one of these configurations, therefore, has good spray characteristics. As afterbody angle is increased, the low-speed spray is improved, most of the improvement accruing from the first increment of angle (from 4 deg to 6 deg); at higher displacement speeds, corresponding to the profiles aft of the main step, the effect is reversed, the lowest blisters being obtained with the lowest afterbody angle, but as at all times the tailplane and elevators were clear of spray this is not significant. That there is an overall improvement in spray characteristics with increasing afterbody angle is confirmed at the lower weight, $C_{\Delta 0} = 2{\cdot}25$ (Fig. 77a), but the effect is smaller at this weight. The general improvement due to the weight decrease is obvious in that the profiles are now continuous, showing that spray either cleared the model or barely touched the mainplane trailing edge.

The improvement in spray characteristics with increasing afterbody angle follows directly from the consequent increased attitudes at a given elevator setting. There will be minor changes in draught, but these should only have a small effect on spray. The movement backward of the spray origin, at a given speed, with the increase in attitude is small, but it could be seen when comparing the individual spray photographs; an example is given in Fig. 78 at $C_v = 3{\cdot}0$ approximately for $C_{\Delta 0} = 2{\cdot}75$.

As in the best case (Model H), spray characteristics are only moderate, it follows that any similar high length/beam ratio design having a low afterbody angle must incorporate forebody warp or some other modification to give good spray characteristics.

5. **Directional Stability.**—Directional stability diagrams for the models with afterbody angles of 4, 6 and 8 deg are compared at one weight, $C_{\Delta 0} = 2{\cdot}75$, in Fig. 79. The three diagrams are very similar, but with increasing afterbody angle an improvement in directional qualities is indicated; the low speed region bounded by the stable equilibrium lines and the 18-deg limit is widened in a direction parallel to the speed axis at values of yaw of about 5 deg and above, and the high-speed unstable equilibrium line is moved out normal to the speed axis. These small changes would only have significance in a practical case at $C_v = 4$ roughly, when the flying boat

was yawed past the unstable equilibrium line. With the 4-deg afterbody this would occur at $\psi = 2$ deg and the yaw would automatically continue in the absence of corrective action to $\psi = 13$ deg; with the 8-deg afterbody at this speed, the unstable equilibrium line would not be met till $\psi = 4$ deg and the yaw would be stopped at $\psi = 4\frac{1}{2}$ deg. The 6-deg afterbody-angle case lies between the 4-deg and 8-deg afterbody-angle cases, but nearer to the 8-deg. Over the narrow speed band around $C_v = 4$, then, the improvement in directional stability with increasing afterbody angle is quite considerable; elsewhere it is negligible.

6. **Elevator Effectiveness.**—The effects of afterbody angle on mean elevator effectiveness are shown in Fig. 80b for $C_{\Delta 0} = 2{\cdot}75$. The curves obtained with the 6-deg and 8-deg afterbody angles show roughly the same values of effectiveness at a given speed, while values for the lowest afterbody angle (4 deg) are much lower. With increasing afterbody angle, it appears that elevator effectiveness increases rapidly at first and then remains almost unaltered. The same effects are shown in Fig. 80a for $C_{\Delta 0} = 2{\cdot}25$, the main difference between the two diagrams being the overall increase in effectiveness due to the decreased load.

The values of elevator effectiveness given in Fig. 80 are mean values and a few remarks on them are necessary. Throughout this programme, when computing mean elevator effectiveness (Chapter 2, Section 7), the summation has been made from $\eta = -12$ deg to $+4$ deg and it was noted that, while maximum specific values of effectiveness for Models A and G are well within this range, those for Model H lie near the $\eta = -12$ deg limit. It follows that had the summation for Model H been made over the range of say $\eta = -16$ deg to 0 deg, higher mean values of elevator effectiveness would have been obtained for this model. This is not serious, however, and would make only a little difference to the conclusions drawn in the previous paragraph.

Reconsidering Figs. 72a and 73a, where the undisturbed stability limits are presented with elevator angles as ordinates in place of keel attitudes, it will be seen that while there is a movement of the limits with change of afterbody angle, there is no apparent orderly improvement in stability. For a complete understanding of the results these Figures should be considered in conjunction with the corresponding plots of elevator effectiveness.

7. **Conclusions.**—The results of the present investigation show that the effects of increasing afterbody angle are :—

(*a*) to increase maximum lower critical trim and slightly reduce the speed at which it occurs

(*b*) to increase trim generally and, in particular, to increase hump trim and the maximum trim obtainable with normal elevators

(*c*) to raise the upper undisturbed stability limit considerably and, in general, to leave the lower limit unaltered

(*d*) to increase resistance to disturbance

(*e*) to increase disturbed amplitudes of porpoising when the datum afterbody angle is low

(*f*) to move the spray origin backwards, giving rise to slightly improved spray characteristics (associated with (*b*))

(*g*) to improve directional qualities over a narrow speed band just below hump speed

(*h*) to increase elevator effectiveness when, as in (*e*), the datum afterbody angle is low

(*i*) to reduce slightly the elevator setting at which undisturbed lower-limit instability is encountered.

The afterbody-angle effects listed above show that if good stability characteristics are the prime consideration the configuration with the highest afterbody angle is the best. Results (*a*) to (*c*) are substantiated generally by Refs. 18, 19 and 30 and may be said to be independent of length/beam ratio if only the tendencies and not the magnitudes of change are considered. An important detail of the high length/beam ratio stability case is that increase in afterbody angle causes the rate of change of lower critical trim with respect to load at constant speed (Chapter 3, Section 5) to decrease, *i.e.*, afterbody-angle effects on stability are not independent of load; this applies to both undisturbed and disturbed cases. Tests at two loads, however, would remove any doubts about the rate of change of lower critical trim with respect to load being too high and should be made in any case where it is thought that some secondary effect may be present, *e.g.*, on high length/beam ratio hulls having low, unventilated afterbodies.

CHAPTER 9

The Interaction of Effects of Forebody Warp, Afterbody Length and Afterbody Angle

1. **Longitudinal Stability.**—1.1. **Introduction.**—In the earlier stages of the present investigation, the effects have been examined of varying separately the main parameters with which the investigation is concerned, namely, forebody warp, afterbody length and afterbody angle. Certain variations from the basic hull form have been found to have beneficial effects on longitudinal stability characteristics and it might therefore be assumed that the most stable hull form which could be produced within the range of investigation would be that in which all the beneficial variations were made simultaneously. This is, however, by no means certain and there is very little evidence one way or the other from previous investigations. The question is closely linked with that as to whether or not the effect of varying any one hull parameter is independent of the values of the remaining parameters (within practical limits).

Accordingly it was decided to investigate the nature and extent of the interaction between the effects of the different parameters, with a view to developing a method of predicting the longitudinal stability characteristics of any given hull form from the known effects of varying the various parameters individually. If this could be done, it would be simple to decide on the best hull form, within given ranges of the relevant parameters.

Three models were therefore tested, for each of which the values of two of the fundamental parameters were varied simultaneously from those employed on the basic model of the series, and a fourth model was tested for which all the three parameters were varied simultaneously. The results of the individual tests on these models are discussed in Appendix V and in the following Sections the results are analysed and compared with those for the appropriate earlier models of the series.

1.2. **Details of Tests.**—The tank-testing techniques employed in the various tests have already been described in detail in Chapter 2 of this report and no further reference will be made to them here. It should, however, be mentioned that the tests performed on those models specially designed to give information on interaction were more limited in extent than those on the models of the main series. Longitudinal stability was only investigated at one value of the static beam loading coefficient namely, at $C_{\Delta 0} = 2{\cdot}75$, and no directional stability tests were made. Spray photographs were taken during the longitudinal stability tests, but no analysis has been made of the interaction of spray effects, as this was not considered to be of great importance; diagrams illustrating the interaction are, however, included for reference purposes.

In selecting the variations from the basic form which were to be combined to produce the four ' interaction ' models already referred to, it was not felt desirable to use extreme values of the parameters concerned, as this could have led to a masking of the effects under consideration. Accordingly, the variations chosen were an increase of forebody warp from 0 deg to 4 deg per beam, an increase of afterbody length from 5 beams to 7 beams, and an increase in afterbody angle from 6 deg to 8 deg. Details of the geometry of the resulting models are given in the last Section of Table 2, in which Section are also included details of the basic model and the three models of the main series which show the three variations separately. These are the eight models on which the analysis of the interaction effects is based.

1.3. **Analysis of Results.**—The various models concerned fall naturally into four groups. Each of the first three groups consists of the basic model, two of the models in which only one parameter is varied in value from the basic model, and the ' interaction ' model, in which both the appropriate parameters are varied simultaneously. The fourth group consists of the four ' interaction ' models. For convenience in preparing the diagrams and ease of reading them, the results for the different groups have been plotted separately and the groups have been given index numbers, as follows;

Group I	Models A, B, E and L
Group II	Models A, H, E and M
Group III	Models A, B, H and K
Group IV	Models K, L, M and N.

An incidental consequence of the tests on Models K to N is that they make possible the observation of the effects of varying each parameter separately at different fixed values of the remaining parameters from those in the main series of tests. Thus, for instance, variations of the amount of forebody warp in the main series were carried out with a 5-beam afterbody length and 6-deg afterbody angle, but by comparing the test results from Models H and K it is possible to determine the effect of a similar variation with an 8-deg instead of a 6-deg afterbody angle and, by comparing the results for Models E and L, that with a 7-beam instead of a 5-beam afterbody; similarly, Models M and N show the effect when the values of both subsidiary parameters differ from the corresponding ones in the main series. The extent to which comparisons of this kind confirm the evidence in Chapters 6, 7 and 8 will be considered later; the divisions of the models into groups is of less value for this purpose than in the direct determination of interaction effects, but it has been found convenient to retain the groupings and to derive the comparisons from the diagrams included to demonstrate the interaction effects.

Interaction Effects

The undisturbed longitudinal stability limits for the various models on a C_v base, as obtained in the individual model tests, are plotted in Fig. 81. It will be seen that, taking the limits as they stand, there is no simple connection between the positions of the limits in each group, except at the highest speeds in some cases. It is not, for instance, true in general that at a given speed the attitude difference between the limits for the basic model and an interaction model is the sum of the differences between the limits for the basic model and the two appropriate models of the main series. It is, in fact, true to a close enough extent for design purposes, where an accuracy of $\frac{1}{2}$ deg or even 1 deg may be acceptable, but as the variations in limits encountered throughout the investigation have only been of the order of 1 deg, it is clearly impossible to accept such a low level of accuracy for the present purpose.

In connection with this point some remarks should be made on the accuracy of the limits obtained for the various models. The experimental points defining the limits were determined to an accuracy of $C_v \pm 0{\cdot}025$, $\alpha_K \pm 0{\cdot}1$ deg, and enough points were obtained to make it reasonably certain that the resulting limits reached a similar standard of accuracy. This was achieved not only by having regard to the positions of the actual test points but also by taking into consideration the amplitudes of porpoising at border-line and unstable points, and by maintaining the limits as smooth curves. Thus it should not be assumed that sparseness of test points necessarily indicates possible local inaccuracies in the limits, though it is not of course claimed that there is no room for their modification*.

It is not, however, considered that permissible modifications can be made in such a manner as to yield simple relations between the limits, particularly as systematic rather than random alterations would be needed even to achieve limited results, and it is therefore necessary either to seek some law more complex than a direct addition law or to find some other method of plotting the existing undisturbed limits so that a simple law emerges.

The corresponding disturbed limits (Fig. 82) are even further removed from being related by a simple law than are the undisturbed ones. Here not only the positions but the nature of the limits vary in an apparently unpredictable way. It is possible only to draw very general conclusions, such as that if two beneficial hull variations are combined the result is better than that obtained from either variation by itself.

As replotting of the limits appears to be the more likely of the two approaches mentioned to lead to a useful result, the limits have first been transferred from the (α_K, C_v) to the (η, C_v) plane (Figs. 83 and 84). This has been done for two reasons; firstly, because it eliminates the differences between the mean running attitudes of the models, and secondly because it was noticed earlier in these tests that the lower stability limits occurred at about the same elevator settings in different cases. Unfortunately, although there is quite good agreement between the undisturbed lower limits at the higher speeds for a number of the models when plotted in this manner (notably Group I), the agreement is not universal, even allowing a generous margin for error because of the difficulty of interpolating accurately to determine elevator settings on the limits. At the lower speeds there is neither agreement nor systematic variation. The replotting does not add anything to the understanding of the variation of the disturbed limits.

Accordingly the limits have next (Figs. 85 and 86) been plotted in the $(\alpha_K, C_\Delta^{1/2}/C_v)$ plane, on a so-called ' generalised ' base. This method has been advocated by a number of authors who assert that the undisturbed lower stability limits for a given hull at different weights will coincide or ' collapse ' when plotted in this way, since $C_\Delta^{1/2}/C_v$ is in effect the water load coefficient. Certain theoretical arguments have been put forward in support of this view, but are considered by the authors of the present report to be unsound. Nevertheless, experimental evidence shows the method to be fairly reliable in the absence of aerodynamic interference, and as the eight models which are being analysed here each have one of two forebody forms, it might be expected that the undisturbed lower limits for each forbody form would collapse onto one curve on the generalised base.

As will be seen, this does not in fact happen, there being relatively wide variations between the limits for different models. To examine the extent to which these variations can be eliminated by minor adjustments of the limits without amending the test points, the points defining the limits are plotted for the undisturbed case in Fig. 87. It will be seen that in the planing region it is possible to draw a common limit for the models with 4-deg forebody warp in Groups I and III, but that otherwise it is virtually impossible to move the points within the limits of experimental error ($C_\Delta^{1/2}/C_v \pm 0{\cdot}001$ $\alpha_K \pm 0{\cdot}1$ deg) in such a manner as to leave one distinct limit through all the points for one forebody form.

The location of points denoted ' borderline ' points, with amplitudes of porpoising between 0 deg and 2 deg, is a crucial factor here. In tank testing it is conventional to define the stability limit as lying through points at which the porpoising (double) amplitude is 2 deg. This is, however, to some extent an arbitrary definition, being based on full-scale handling requirements. If defining the limit on a purely scientific basis, one would normally classify all points at which porpoising occurred, of whatever amplitude, as unstable, and similarly exclude from the stable region points giving oscillations purely in heave. If such a definition is applied in the present case the result is as shown in Figs. 88 and 90.

* These remarks pertain more particularly to the lower than to the upper limits. Two of the interaction models possess no upper limits, within the range of investigation, and upper limits by their nature are in any event difficult to determine accurately, so that it is wiser not to draw direct conclusions from their positions, their main value being as a general guide.

It is now possible to insert a common undisturbed lower limit in the planing region (between $C_\Delta^{1/2}/C_v = 0{\cdot}10$ and $0{\cdot}20$ approximately) for each set of models with one forebody form, leaving only one or two points in each set on the wrong side of the limit; some points designated stable must be expected to be on the unstable side of the new limit as points with very small porpoising amplitudes would probably have been classed as stable during the tests, and aerodynamic interference could well account for some of the other discrepancies. The collapse is considered very good, particularly in view of the fact that the limits have had to be drawn on the basis of test data collected for another purpose. That collapse on the same basis could be obtained over an even wider range is illustrated by Fig. 89, where the test points defining the undisturbed lower limits for all the models with 4-deg forebody warp over a range of loads from $C_{\Delta 0} = 2{\cdot}00$ to $3{\cdot}00$ are plotted together, using the new definition of stability. The common limit inserted on this Figure is that used for the same models in Fig. 88. Only 4 of the 87 relevant points are further on the wrong side of the limit than would be accounted for by experimental error of the magnitude already laid down, and they are all points at which there might have been porpoising of very small amplitude in the tests, as already remarked. Taken together, the results are felt to be conclusive, as far as the present investigation is concerned, and it would be of great interest to know whether the same method would be effective with a completely different form of hull.

In the case of the undisturbed upper limits it would be possible in several instances to draw common limits for two or more models, but this would be due rather to the scarcity of test points than to any real collapse. Accordingly the upper limits have been drawn as fairly as possible between what test points are available and no attempt has been made to combine them. As with the lower limits there are probably test points classed as stable which would be unstable by the new definition, particularly those with very small oscillations in heave only, and because of these considerations and of the inaccuracies in upper limits generally, it is felt that no conclusions should be drawn from the redefined upper limits.

In the disturbed case the redefinition makes little significant difference, except that there is now a region of mid-planing instability for Model M. Again some difficulty has been experienced in inserting the redefined limits accurately, because of the sparseness of test points in appropriate regions.

The success in collapsing undisturbed lower limits on a $C_\Delta^{1/2}/C_v$ base by a redefinition of stability, leads one to consider whether a similar collapse would be possible on the original C_v base. Accordingly, the limits of Figs. 88 and 90 have been transposed to a C_v base and are plotted in Figs. 91 and 92. It will be seen that there is an almost perfect collapse of the appropriate undisturbed lower limits in the planing region and again there is no apparent systematic variation of the upper or disturbed limits. Whether the C_v or $C_\Delta^{1/2}/C_v$ base would be the more convenient in any particular series of tests where no change in wing form was involved would depend on circumstances, and in particular on whether the tests involved determining the limits for any model at more than one load. The $C_\Delta^{1/2}/C_v$ base is, however, more likely to give a collapse than the C_v base in the general case involving different sizes of hull.

Finally, the redefined limits have been plotted in Figs. 93 and 94 against elevator setting. The agreement here is, if anything, worse than with the original definition, in both the disturbed and undisturbed cases.

It appears, then, that it is only possible to predict the interaction of the effects of the parameters under consideration as far as the undisturbed lower limit is concerned. Here, if stability is defined in a strictly mathematical sense, the position of the limit is determined entirely by the amount of forebody warp and is independent of afterbody length and angle. The remainder of the undisturbed limit and the whole of the disturbed limit seem to be governed by no simple law or working rule, and while, particularly in the disturbed case, it appears that the combination of two hull variations separately beneficial gives an even better overall result; it does not necessarily follow that this is true in every case.

Range of Validity of Earlier Results

As already observed, the results collected and compared in the present report can be used to examine the effects of varying each of the parameters concerned in the investigation at different fixed values of the remaining parameters from those in the main series of tests, and in this way it can be seen whether the conclusions of Chapters 6, 7 and 8 are generally applicable within the series or are more restricted. As tests were only made on Models K, L, M and N at $C_{\Delta 0} = 2{\cdot}75$, no check on load effects is possible, but most of the other important factors can be investigated. Only the main conclusions of the earlier tests will be considered.

For each pair of models in the main series showing a particular hull variation, there are three other pairs of models, each containing at least one of the interaction models, also showing that variation, as follows:

(*a*) *Increase of Forebody Warp from 0 to 4 deg*

Models	*Afterbody length*	*Afterbody angle*
A–B	5 beams	6 deg (main series)
E–L	7 beams	6 deg
H–K	5 beams	8 deg
M–N	7 beams	8 deg

(*b*) *Increase of Afterbody Length from 5 to 7 Beams*

Models	*Forebody warp*	*Afterbody angle*
A–E	0	6 deg (main series)
B–L	4 deg per beam	6 deg
H–M	0	8 deg
K–N	4 deg per beam	8 deg

(*c*) *Increase of Afterbody Angle from 6 to 8 deg*

Models	*Forebody warp*	*Afterbody length*
A–H	0	5 beams (main series)
B–K	4 deg per beam	5 beams
E–M	0	7 beams
L–N	4 deg per beam	7 beams

The effects of increasing forebody warp from 0 to 4 deg per beam will be considered first. Those principally remarked on in Chapter 6 which can be checked here were:

(i) to lower the undisturbed lower limit on a C_v base by about 1·3 deg

(ii) to lower the undisturbed upper limit on a C_v base by half a degree

(iii) to leave the disturbed limits almost unchanged

(iv) to reduce trim generally

(v) to improve spray characteristics

(vi) to increase mean elevator effectiveness by about 0·045.

The lowering of the undisturbed lower limit is maintained with the other three relevant pairs of models (Fig. 81) but the magnitude of the change varies considerably, from over 2 deg at some speeds between Models E and L and between H and K, to 0·2 deg between M and N. Use of the redefined limits of Fig. 91 removes this discrepancy, except that the limits for Models M and N coincide near the hump. Models K and L have no undisturbed upper limits within the range of investigation, so that only M and N are available for comparison in this case. The upper limits for these models coincide, and while they separate a little when redefined, they do not do so sufficiently to reproduce the separation of the limits for Models A and B. The disturbed limits are not left unchanged in any of the three check cases, there being significant improvements in disturbed stability in all three, as can be seen clearly in Fig. 82 (A similar effect was found when increasing warp from 4 to 8 deg per beam in the main series).

The remaining three effects are in general maintained with the other pairs of models (Figs. 95 to 97), though the amounts of the changes vary appreciably from case to case. One exception is that elevator effectiveness is reduced by about 0·03 from Model M to N, though there are increases of 0·075 and 0·05 between Models E and L and between H and K respectively.

The corresponding effects of increasing afterbody length from 5 to 7 beams were found in Chapter 7 to be:

(i) to decrease maximum lower critical trim but otherwise to leave the undisturbed lower limit on a C_v base substantially unaltered

(ii) to lower the undisturbed upper limit on a C_v base and increase the mean speed at which upper limit instability is encountered, the net effect being to decrease the extent of the upper unstable region

(iii) to improve disturbed stability, principally by reducing the width of the unstable band in the mid-planing region

(iv) to reduce trim in the displacement region and increase hump speed

(v) to cause spray characteristics to deteriorate

(vi) to reduce elevator effectiveness.

Neither the decrease in maximum lower critical trim nor the invariance of the undisturbed lower limit on a C_v base are found with all the other three appropriate pairs of models. Only between Models B and L is there any significant reduction of maximum lower critical trim and between K and N there is actually an increase of 2 deg (Fig. 81). Similarly, while the lower limits for Models B and L coincide over part of their length, those for H and M are separated by about 0·7 deg and those for K and N by up to 2 deg. Here again, if the redefined limits of Fig. 91 are used, most of the lower limit discrepancies are resolved, but the limit for Model N is still considerably higher than that of Model K in the hump region.

The lowering of the undisturbed upper limit is maintained between Models H and M, the only pair which can be compared with A and E in the absence of upper limits for K and L, but there is now no increase in the mean speed at which upper limit instability is encountered (The absence of the upper limits for K and L could, in effect, mean of course that the lowest speed, and hence the mean speed, in these cases is greater than that corresponding to $C_v = 10$, but it could equally well be that the limits occur at attitudes greater than 12 deg).

The improvement in disturbed stability is found with all the additional pairs of models in this set, and is in fact greater than that found in the main series, there being no necks of instability with any of Models L, M and N using the original stability definition, though one appears for Model M on the redefined basis.

All the remaining effects are reproduced completely by all pairs of models, except that the elevator effectiveness of Model M is greater than that of Model H.

Finally, the effects of increasing afterbody angle from 6 to 8 deg may be considered. These were (Chapter 8):

(i) to raise the undisturbed upper limit on a C_v base considerably

(ii) to leave the undisturbed lower limit on a C_v base substantially unaltered

(iii) to improve disturbed stability characteristics

(iv) to increase trim in the displacement region

(v) to give an overall improvement in spray characteristics

(vi) to leave elevator effectiveness unaltered.

As in the previous cases, it is only possible to achieve consistency between the various pairs of models as regards the undisturbed lower limit by using the redefined limits of Fig. 91, as the original limits for Models E and M and for L and N are quite widely separated. Such upper limits as there are, however, confirm the tendency

found in the main series on either basis. Disturbed stability also is improved by the change for all pairs of models, though it is a little difficult to compare the limits for Models L and N because of the attitude difference between them.

Trim and spray changes are likewise of the same nature for all pairs of models. Elevator effectiveness, on the other hand, does not vary consistently, that for Model M being about twice the corresponding figure for Model E, but there is little separation between the other pairs of models.

It appears, taking all three sets of results together, that only on a broad basis are the conclusions from the main series of tests generally applicable when the primary form used as a basis for variations differs from the basic model of the main series. Quite a number of exceptions to individual conclusions can be obtained by judicious choice of values of the various parameters, and while those relating to the undisturbed lower limit can in the main be removed by the adoption of the amended definition of stability advocated earlier in this Section, enough exceptions remain elsewhere to make detailed prediction of the changes due to a particular hull variation difficult. Fortunately the exceptions are usually not contradictions of other results but merely absences of particular effects, so that most broad conclusions, for example, that disturbed stability characteristics are improved by some chosen variation, are still valid. Generally speaking, it is in connection with the undisturbed upper limit and with elevator effectiveness that the greatest care must be exercised.

1.4. **Conclusions.**—The analysis shows that it is only possible to predict at all accurately the interaction of the effects of the parameters under consideration as far as the undisturbed lower stability limit is concerned. Here, if stability is defined in a strictly mathematical sense instead of as at present, the position of the limit is determined entirely by the amount of forebody warp and is independent of afterbody length and angle. The remainder of the undisturbed limit and the whole of the disturbed limit seem to be governed by no simple law, though some overall generalisations are possible within the present investigation and in particular it seems generally advantageous to combine hull variations which have been found beneficial individually. This tendency should, however, be checked with a radically different parent form before it is taken to be generally applicable.

As a consequence of this some conclusions reached earlier in the tests as to the effects of various hull variations are subject to restrictions when applied to similar variations on different basic forms, and it is in general not possible to enumerate all the detailed effects of any such modification regardless of the parent form.

Taken in conjunction, the results indicate that generalisations can be made only on the broad effects of a particular variation as applied to different hull forms, and that detailed conclusions based on any one form can be misleading, except possibly in relation to an undisturbed lower stability limit mathematically defined. This does not, however, affect the more important general conclusions of the earlier Sections of the present report. In particular, taking into account the new evidence, it is still true to say that the application of forebody warp is beneficial, and that the use of a moderately long afterbody with a high afterbody angle makes for good stability characteristics.

The selection of an optimum hull form within a given set of variations would therefore be a matter of predicting from available test results what the best general type of hull would be, and improving on this shape by experiment.

CHAPTER 10

The Effects of a Tailored Afterbody

1. **Introduction.**—In this Section the effects of a tailored afterbody on the hydrodynamic stability and spray characteristics of a high length/beam ratio hull are deduced from comparisons of test results for Model A (the basic model of the series) with similar results for Model J. The afterbody of Model J was designed by applying the procedure (' tailoring ') laid down in Ref. 33. Briefly, this procedure consists of determining by calculation the wake shape behind the forebody for a number of representative speed-attitude combinations (high and low attitudes at low, medium and high planing speeds), selecting the case with the least afterbody-wake clearance, and choosing an afterbody deadrise angle at each station such that the vertical separation of the keel and the wake is less than that of the wake and any other point on the planing bottom at that station. The deadrise angles so obtained are then used as a basis for an afterbody with a smooth deadrise-angle distribution, that resulting for Model J being shown in Fig. 100 together with the standard afterbody deadrise-angle distribution of Model A; it is seen that large increases in deadrise result from the application of the afterbody tailoring technique.

Models A and J were identical except in respect of afterbody shape, and differences here, which were related directly to the high afterbody deadrises of Model J, can be easily seen by comparing photographs of Model J (Fig. 99) with those of Model A (Fig. 1); the differences in afterbody shape may also be seen by comparing the hull lines for Models A and J (Figs. 41 and 98 respectively). Aerodynamic and hydrodynamic data for the two models are given in Tables 1 and 2.

2. **Longitudinal Stability.**—The effects of a tailored afterbody on the longitudinal stability limits are shown in Fig. 101, where both undisturbed and disturbed limits for Models A and J are compared. In the undisturbed case at both loadings, tailoring the afterbody has resulted in a considerable increase in the available stable planing region; this improvement has been brought about in each case primarily by the reduction and movement to higher speeds and attitudes of the upper-limit unstable region. Higher attitudes are attained generally and in particular, the lower limits for Model J extend to higher attitudes; at $C_{\Delta 0} = 2{\cdot}25$, maximum lower critical trim has been raised by 2 deg, while at $C_{\Delta 0} = 2{\cdot}75$ the low-speed neck of instability is similarly raised by about 2 deg.

The effect of load change on the undisturbed limits is only modified slightly by the tailored afterbody, the general form of the limits remaining the same at each weight. The amount by which the lower limit is raised with increase of weight is reduced slightly by tailoring, and the upper limit, while being found at higher speeds as in the basic-model case, is not raised by weight increase.

In the disturbed case the results of tailoring the after body are very similar in detail to those of the undisturbed case; the improvement is much greater, however, with the available stable planing region being almost doubled. The resistance of the model to disturbance has thus been greatly increased, i.e., the general level of critical disturbances has been raised (Chapter 2, Section 4.2). Examination of Fig. 101b indicates that this effect is greatest at high attitudes, being progressively reduced with decrease of attitude, until it becomes negligible in the high-speed, lower-limit regions. The general relationships between the two sets of limits are the same from weight to weight and it is clear that the effects of load changes are unaltered by the tailored afterbody.

An explanation of disturbed instability in terms of afterbody suctions has been offered by Gott[13] and upheld by recent experience (Chapter 2, Section 4.2). Accepting this it follows that, as there is still some difference between the disturbed and undisturbed limits for the tailored afterbody model, there must remain some regions of afterbody suction, *i.e.*, the design technique is not quite correct or it has been inadequately applied. In view of the gains obtained and on general physical grounds, there is no reason for suspecting the technique, so that the application must be at fault. An obvious source of suction on Model J is in the use of a transverse vertical step, the space immediately behind which is normally a low-pressure region. If this step were streamlined or ducted and all afterbody suctions were thereby alleviated, one might expect complete elimination of instability peculiar to the disturbed case. Such modifications could hardly affect upper-limit undisturbed stability and, as with the present tailored afterbody only negligible upper-limit instability is met, the issue is in any case of secondary importance. In a practical design incorporating a tailored afterbody, therefore, streamlining or ducting of the main step may be an advantage.

The effects of a tailored afterbody on trim are illustrated in Fig. 107, where trim curves for $\eta = 0$ deg, which have been taken as typical, are compared. At both loadings there is an increase in trim in the static floating condition of $1\frac{1}{2}$ deg, which value increases over the displacement range of speeds, becoming 2 deg at the hump, and the curves tend to run just below those for the unmodified afterbody in the planing speed range. This positioning of the tailored-afterbody trim curves below those of the standard afterbody is general over the planing speed range of trims, the effect being slightly greater at the higher weight than at the lower, and is what one would expect following a relief of suctions in the tailored-afterbody case.

Amplitudes of porpoising (Figs. 191 and 192 for Model J and 48 and 49 for Model A) are not materially affected in the undisturbed case at either weight by tailoring the afterbody; in the disturbed case, however, tailoring reduces amplitudes slightly at the lower weight and increases them at the higher weight.

3. **Wake Formation.**—Photographs of flow in the wake region taken during the tests on Models A and J have been compared and two examples at each of two weights are given in Figs. 102 and 103. It may be recalled that the aim of the tailored-afterbody design technique is to ensure good afterbody ventilation, thereby eliminating, to a large extent, instability which is directly attributable to poor ventilation. For this to happen there must be adequate clearance between the afterbody chines and trough walls so that the inflowing air suffers no impedance. That this is in fact obtained with the present design can be seen by the examples given.

Two main conclusions may be drawn from the photographs as a whole. The first is that the tailored-afterbody chines are in every case well clear of the trough wall, so that ventilation from this source should be adequate, and the second is that all chine wetting is confined to the region within half a beam of the aft step, so that as far as the planing range of speeds is concerned, the chines forward of this point could be faired, thereby further improving the ventilation. It may be remarked that in the present case the chine clearance may be excessive. This will in no way affect the conclusions drawn with respect to the tailored afterbody, but in a specific design it will clearly be advantageous to keep afterbody deadrises as small as possible in order to maintain maximum afterbody volume.

4. **Spray.**—The effects of a tailored afterbody on spray are shown at both loadings in Figs. 104 and 105; in the former, photographs of the spray at one speed for Models A and J are compared, while in the latter complete projections of the spray envelopes for the speed range tested are given for both models.

At $C_{\Delta 0} = 2{\cdot}25$ the projections for both models are continuous and show that in each case the mainplanes were more or less clear of spray. At positive values of C_X, however, in which region the spray envelope corresponds to low displacement speeds, the curve for the tailored afterbody model is well below that for the basic model, indicating a useful reduction in maximum spray height in the vicinity of the propeller plane; at higher speeds there is negligible difference between the spray profiles. The peculiar afterbody spray formation of Model J, which occurs at both weights and can be seen in Fig. 104, should not be significant because of its short duration during take-off or landing. At the higher loading, $C_{\Delta 0} = 2{\cdot}75$, the improvement in low-speed spray characteristics obtained with the tailored afterbody is verified and appears to be unchanged in magnitude. The general deterioration due to the weight increase is obvious in that the profiles are now discontinuous, indicating that main spray or heavy velocity spray struck the mainplane.

The improvement in spray characteristics obtained with the tailored afterbody follows directly from the consequent increased attitudes at a given elevator setting. There will be minor changes in draught, but these should only have a small effect on spray. The movement backward of the spray origin, at a given speed, with the increase in attitude can be seen when comparing the individual spray photographs and is considerable at $C_v = 3$ and 4 at both weights.

5. **Directional Stability.**—Directional stability diagrams for the two models are compared in Fig. 106. It can be seen that tailoring the afterbody has resulted in a considerable overall improvement in directional characteristics. At high displacement speeds, where attitudes are high and a slight yaw could cause wing dropping, Model J is inherently stable and it is at these speeds that the greatest improvement over the basic model is obtained. At the higher speeds both hull forms should be easily controllable at small angles of yaw but, whereas the basic model shows a violent tendency to increase yaw when the equilibrium line is exceeded, the reverse is true of the tailored-afterbody model; the unstable equilibrium line of the basic model has been replaced by a line of weak stable equilibrium and the tailored hull in consequence should be controllable at angles of yaw in excess of 10 deg. Such a characteristic would be most useful in cross wind landings.

(*NOTE:* During the directional stability tests on Model J the elevator setting of zero deg chosen initially was changed to − 4 deg about half-way through the tests in an attempt to reduce the porpoising induced by yawing the model with the zero deg setting. Apart from the reduction of porpoising, this elevator change should have negligible effect on the directional stability characteristics of the model (Chapter 2, Section 6)).

6. **Elevator Effectiveness.**—The effects of a tailored afterbody on mean elevator effectiveness are shown in Fig. 108. At the lower loading the curve for Model J lies below that for the basic model and the separation increases with speed, though at no time is it great; at the higher loading there is little practical difference between the two models. Perhaps the most significant effect that tailoring the afterbody has on elevator effectiveness is the reduction, about one third, in the effect of load change.

7. **Conclusions.**—The results of the present investigation show that appreciable gains in hydrodynamic stability and spray characteristics are obtained by applying the tailoring design technique to the afterbody of a high length/beam ratio flying-boat hull. The detailed effects of tailoring the afterbody (without tailoring the main step) are:

(*a*) to increase maximum lower critcial trim and slightly reduce the speed at which it occurs

(*b*) to increase trim generally and, in particular, to increase hump trim and the maximum trim available with normal elevators

(*c*) to raise the upper undisturbed stability limit while at the same time reducing the extent of the upper unstable region, the lower limit remaining substantially unaltered

(*d*) to reduce slightly the effect of load on the position of the lower stability limit

(*e*) to increase resistance to disturbance

(*f*) to increase disturbed amplitudes of porpoising at high loadings and to decrease them slightly at the low loadings

(*g*) to move the spray origin backwards, giving rise to improved spray characteristics (associated with (*b*))

(*h*) to improve directional qualities considerably from high displacement speeds upwards

(*i*) to reduce the effect of load on elevator effectiveness.

The effects listed above are, except where otherwise indicated, independent of load.

The tailored afterbody design technique has been proved efficacious in the case of a high length/beam ratio hull by the present tests, but in a practical design case the application of the technique should include modifications of the main step and chines.

CHAPTER 11

Results of Tests in Waves

1. **Longitudinal Stability.**—1.1. **Introduction.**—In carrying out routine assessments of the longitudinal stability characteristics of the various models in the present investigation, tests were made both with and without disturbance to give a complete representation of calm-water stability characteristics. As it was known that the application of disturbance impaired model stability in calm water and that full-scale seaplane stability generally was adversely affected by rough seas or swells, it was thought that it might be possible to use the disturbed limits obtained in the calm-water tests to assess full-scale rough-water characteristics. In this connection consideration has been given to the significance of the disturbed limits (Chapter 2, Section 4.2) and a number of experiments have been carried out to observe model behaviour in waves. These experiments were designed to be sufficiently extensive to allow a number of detailed conclusions to be drawn with respect to the stability characteristics of high length/beam ratio hulls in waves and it is felt that these conclusions will apply to seaplane hulls in general. Details of the tests are given below together with a discussion of the results.

The subject of wave-disturbance correlation itself, while being of fundamental importance, is not specifically related to high length/beam ratio hulls and has therefore been dealt with in Appendix IV. The points made therein are based on information given in Chapter 2, Section 4.2, and in the present Section; the arguments show that there is no practical correlation between stability with disturbance and stability in waves.

1.2. **Previous Investigations.**—In 1935 it was the practice to make brief tests in waves of two lengths, the shorter being about equal to the length of the hull, and the longer three times this length; the chief object of these tests was to obtain an assessment of the general seaworthiness of the hull[7]. It was considered that tests in waves merely accentuated any porpoising tendency and were not necessary (from the stability point of view) if the normal routine tests had been made. These views seem to have been generally held, where tests on specific aircraft are concerned, up to the present day. Some thorough seaworthiness tests on the *Saunders-Roe E*6/44 were reported in 1946 (Ref. 9) and in the most recent review of tank-testing technique[1] most of the emphasis is on seaworthiness when waves are considered. A method is described, however, for recording the motion in pitch and heave of a model during a run through waves and reference is made to a series of tests on models of the *Princess* and *Shetland*[34], in which this method was used. These tests were very limited in scope, due probably to the time-taking nature of wave tests in general and, apart from the present programme, they appear to be the only tests made in the Royal Aircraft Establishment Tank with the sole object of examining aircraft stability in waves.

1.3. **Present Investigation.**—Wave tests have been made in the R.A.E. Seaplane Tank for some time and the tank apparatus seems to have undergone little, if any, modification in that time. The wave maker is of the oscillating-flap type and reproduces a deep sea wave or long swell; the wave-form is approximately sinusoidal but deteriorates (*a*) for wave length/height ratios of about 20 : 1 and below, when the waves fail to reach the far end of the tank without change of form and (*b*) when the wave-maker is operating under heavy loads, which give rise to ill-formed double-crested waves[35]. The model can only be run head on into the wavetrain, and the runs may be made with acceleration or deceleration, or at steady speeds.

Apart from the generation of waves and their effects, the general procedure for each of the present series of test runs was identical to that used in the corresponding calm-water case without disturbance. All wave tests were made with zero flap, no slipstream, one c.g. position and at one beam loading, $C_{\Delta 0} = 2{\cdot}75$; the model was towed from the wing tips on the lateral axis through the c.g. with the model free in pitch and heave, and runs were made with selected elevator settings and at constant speeds, all of which were in the planing speed range. On no occasion was the model given any manual disturbance.

Attempts were made to read the trim, as well as any change in trim, but these were not entirely successful. Sometimes the trim indicator (pointer) was steady and at other times it had a constant amplitude, high-frequency vibration superimposed on the obviously steady trim indication from the model; on these occasions the motion was classed as stable. When the model oscillated in pitch a steady oscillation of greater than 2 deg amplitude was called unstable, for consistency with the calm-water tests, but on a great number of runs the amplitude of the motion varied over the run. When this happened a certain amount of discretion was used; if, for instance, the maximum amplitude was sustained for, say, only two or three cycles and only this maximum value was greater than 2 deg, the run was classed as stable; if it was sustained for about five or six cycles the run was termed unstable. On some runs the pitching oscillations were violent and the motion was obviously unstable. At no time, when deciding whether a motion should be called stable or unstable, was any allowance made for the motion in heave, which was occasionally very pronounced, as the initial reason for doing the tests was to provide a comparison with the calm-water test results, when only the motion in pitch was considered.

Having selected a speed and elevator setting, the procedure adopted was to choose a wave length/height ratio and, starting with waves of small height, effectively increase the height while keeping the ratio constant until instability set in. It was found that by repeating this procedure for several wave length/height ratios, curves of definite form could be obtained (Fig. 113) separating regions of stable and unstable motion; similar curves were obtained for each speed-elevator combination tested.

Corresponding calm-water critical disturbances were determined when required by carrying out test runs in calm water and applying disturbances, the magnitudes of which were progressively increased until instability set in.

During most of the tests only visual observations were taken because of the time otherwise involved in analysis, but recordings of a small group of runs were made, by the methods of Chapter 2, Section 4.4, for comparison with the results of Ref. 34.

1.4. **Scope of Tests.**—Wave tests were made on Models A, B and L of the series, aerodynamic and hydrodynamic data for which are given in Tables 1 and 2 respectively. As the initial aim was to determine the extent of any wave-disturbance correlation, the points in the (η, V) plane examined at first were in the region between the undisturbed and disturbed stability limits; later, in the case of Model L only, the tests were extended to include points in that part of the stable region which was unaffected by disturbance. All of the points considered are numbered and listed in Table 99; for convenience they will be referred to henceforth by the number and letter given in this Table, *e.g.*, 4B will indicate that Model B is being considered at a speed of 32 ft/sec with elevators set at — 4 deg. The relationships between these points and the corresponding sets of stability limits are shown for each model in Fig. 109, in which presentations are made both with keel attitudes and elevator angles as ordinates.

The tests on Model A were of two kinds and all were made at point 1A in the mid-planing region. In the first case a series of runs, made through waves of fixed height but of differing length/height ratios, were recorded for comparison with similar results for the *Princess* and *Shetland*. In the second case, a curve of limiting wave heights for stability was obtained on a wave length/height ratio base. In determining the points for this curve no recordings were made, the runs being classed as stable, border-line or unstable in the manner indicated in the previous section. The nature of these tests was mainly exploratory and fuller tests were for convenience made on Model B.

These tests on Model B consisted of obtaining curves of limiting wave heights for stability at five points, 1B to 5B, and of determining the critical calm water disturbance at each point. These results made it fairly clear that no detailed wave-disturbance correlation would be forthcoming, though some useful general results were obtained with respect to the behaviour of the model in different wave systems. Further tests were made on Model L, but no critical disturbances were determined.

The tests on Model L were made to check the general results of Model B on a model having vastly different disturbed limits and, in addition, wave tests were made at points in regions of the stability diagram which were completely unaffected by disturbance. Greater coverage of the (η, V) plane was made in an effort to obtain a better understanding of stability in waves and one curve, that for point 6L, was extended as far as possible within the limitations of the wavemaking system.

1.5. **Discussion.**

Comparison of Basic Model with Princess and Shetland

Tests were made for comparison with similar tests on the *Princess* and *Shetland*[34], and test conditions had to be chosen accordingly. The full-scale design loading for Model A was taken as 150,000 lb, the load coefficient as 2·75 and the point selected for test, 1A, was in the mid-planing region. Test runs were made in waves of a height corresponding to 2·35 ft* full scale and, to cater for the differences in absolute scale in the comparison of results with the *Princess*, linear dimensions associated with Model A and the *Shetland* were scaled up in the ratios 1·28: 1 and 1·33: 1 respectively.

Six recordings were made, one for each of the wave length/height ratios 80: 1 by 10: 1 to 130: 1 and they are shown in Fig. 110. Maximum and mean pitching and heaving amplitudes and the ratios between them are given in Table 100, together with corresponding results for the *Princess* and *Shetland*, which were taken from Ref. 34, the amplitudes are plotted in Fig. 111 and their ratios in Fig. 112.

The most obvious feature of the Model A records generally is the apparent difference between the motions in the various cases. This is probably due to the motion in each case being compounded of several basic elements, the magnitude and frequency of each being proportional to different physical characteristics of the motion. In only one, that for a wave length/height ratio of 110: 1, is there a regular constant amplitude motion. The 80: 1 recording resembles a beat between two frequencies, the 90: 1 is irregular, the 100: 1 has an envelope of square wave-form, while in the 120: 1 and 130: 1 recordings a certain tendency to regularity can be observed. It is clear that any detailed analysis of such results *en masse* would have to be statistical and many more recordings would be necessary, so that only a rough picture can be obtained from the present set of curves.

The results are presented together with those for the *Princess* and *Shetland* in Table 100 where the steady speeds referred to are speeds for the hull form concerned scaled up to the full-scale design loading and the tabulated

* This figure was arrived at by scaling down the *Princess* wave height of 3 ft by the cube root of the ratio of the aircraft weights, *viz.*,

$$\text{Wave height} = 3\left(\frac{150{,}000}{310{,}000}\right)^{1/3}$$

figures are for runs through the waves of the corresponding scaled heights indicated. When the *Shetland* test results are scaled up for comparison with the *Princess* results, the test speed for the *Shetland* becomes the same as that for the *Princess*, whereas when Model A results are similarly scaled, the speed for Model A becomes 84 knots approximately, much higher than that for the *Princess*. To obtain the same scaled speed for Model A as for the *Princess* would have meant running Model A at $C_v = 5{\cdot}9$, which is in the undisturbed unstable region (Fig. 31d). The correspondence chosen, *viz.*, that each of the three points is representative of the mid-planing region, is considered reasonable, but the much higher speed of Model A should be borne in mind. These results are compared in Figs. 111 and 112.

The mean pitching and heaving amplitudes of Fig. 111 are of about the same order for the three hull forms as far as one can generalise but the maximum values for Model A are greater than those for the *Princess* and the *Shetland*, particularly in the case of the heave motions. From Fig. 112 the ratios of maximum amplitude to mean amplitude in both pitch and heave are seen to be greater for Model A than for the other two hulls. It should be noted that these ratios constitute amongst other things a measure of the irregularity of the motion, and that one large oscillation could greatly increase these values; the plots in Ref. 34 were faired by hand, there being no effective damping in the recording system, and it is possible that occasional high peaks were unwittingly smoothed out. Some interesting points do arise, however, from these limited data. Resonance* occurs for Model A at a wave length of 330 ft, for the *Princess* at 300 ft, although the curves for pitch and heave are out of phase, and for the *Shetland* at 270 ft (Fig. 112); in each case one complete oscillation of the model corresponds to its passage through two wave crests. The greatest amplitudes of oscillation in general occur at a wave length of 330 ft for Model A, at 270 ft for the *Shetland* and 270 ft for the *Princess* (Fig. 111). The values at 300 ft for the *Princess* are, however, only slightly smaller than those at 270 ft and it may be said therefore that maximum amplitudes and resonance are found at approximately the same wave lengths.

Consider now the length and maximum beam of each of these hulls scaled for comparison:

* *See* footnote to Chapter 2, Section 4.2, para. 4.

If the ratios of the resonant wave lengths to the respective hull lengths are determined from these figures they are found to be almost equal, *viz*,

$$\text{Model A} \quad \frac{330}{132{\cdot}6} = 2{\cdot}5$$

$$\textit{Princess} \quad \frac{300}{121{\cdot}0} = 2{\cdot}5$$

$$\textit{Shetland} \quad \frac{270}{113{\cdot}1} = 2{\cdot}4.$$

It would appear, therefore, that the resonant wave length is a simple multiple of the hull length and that it is independent of hull shape or length/beam ratio.

The Wave Diagram

Before the remaining tests are considered a detailed examination of the extended wave diagram which was mentioned in Chapter 11, Section 1.3, will make it easier to follow the subsequent discussion. The curve was obtained for point 6L (Table 111) and it is given in Fig. 113 as originally plotted on a wave length/height ratio base. In this form it has a shape characteristic of this type of diagram but the plot on a wave-length base in Fig. 114 is easier to appreciate, though curves plotted in this manner have rather more varied shapes. Both Figures are non-dimensional and normal stability diagram notation has been used for the stable, border-line and unstable points respectively. Maximum amplitudes of oscillation are indicated by the numbers near the relevant points; if the observed motion was regular this is indicated by the underlining of the number, otherwise the motion was irregular.

It can be seen from Fig. 114 that there is a minimum wave height of 0·05 beam below which there is no instability. It may also be seen from Fig. 113 that there is an upper limiting wave length/height ratio for instability; in this case the motion is stable above a ratio of about 850. There may also be a lower limiting value, but this cannot be decided from the diagram. The motion at the border-line points near and below the limit at the higher wave lengths in Fig. 114 is mainly oscillatory, regular and of small amplitude, while that found at the lower wave lengths is as often irregular as regular, and the transition from steady to oscillatory motion is rather sharp. It may be noted that at these wave lengths (below 25 beams),

Hull form	Beam b (ft)	Length† L (ft)	L/b	$C_{\Delta 0}$	bL (sq ft)
Model A ..	12·05	132·6	11·0	2·75	1,600
Princess ..	16·66	121·0	7·3	1·08	2,010
Shetland ..	16·66	113·1	6·8	1·08	1,885

† From forward perpendicular to aft step.

had the limit been drawn with respect to regular motions only, it would have been less severe.

In general, with ingress into the unstable region, porpoising amplitudes seem to increase at first and then reach a maximum value of the order of 8 deg; one point ($h = 0{\cdot}351$ beam, $L = 35{\cdot}10$ beams) is unmarked on Fig. 114, but it lies well into this region and still has a maximum amplitude of only 8 deg.

The existence of limiting values of wave height, length and length/height ratio for stability could have been expected. With regard to wave height, a wave of infinitesimal height could have no effect on the motion. In the case of wave length, as this is increased at constant height the water surface approaches a plane, for practical purposes, and the motion becomes as for calm water. When the wave length is decreased, it reaches a minimum value for a given wave height, below which a stable waveform cannot exist[36]; there is thus a limiting wave length/height ratio (7) for the existence of stable waves and neither of the curves in Fig. 113 or Fig. 114 would therefore touch the y-axis.

The main results are presented in the form of Fig. 114. Only the curve or limit is drawn in each case, but the points defining this curve are given in the relevant Table. Lines of constant wave length/wave height ratio are shown in each Figure to aid discussion and it may be noted that the maximum wave lengths and heights in which the general tests were made were 35 beams and $0{\cdot}5$ beam respectively. This gives a smaller coverage of the wave-length range than in the case discussed above.

Individual Model Results

(*a*) *Model* **A** *Results.*—The curve of limiting wave height for stability at different wave lengths is given for point 1A (*see* Table 99 and Fig. 109) in Fig. 115 and the points defining the curve are given in Table 101. It is of similar form to that of Fig. 114 when account is taken of the different vertical scales, and as wave length is increased there is a progressive decrease in the wave height at which instability is met. The rate of decrease is reduced as wave length increases, until a minimum wave height for instability of the order of $0{\cdot}06$ beam is indicated.

The six points marked at a wave height of $0{\cdot}25$ beam and length/height ratios of 80 to 130 respectively are the points at which the recordings shown in Fig. 110 were made. Each of these recordings illustrates the type of motion which occurs at one point in the kind of diagram now being considered. It is interesting to see that the six points all lie well within the unstable region and that if there is a tendency here to a limiting porpoising amplitude as mentioned in the previous Section, it was probably reached by each of the three models, Model A, *Princess* and *Shetland*, during the tests considered earlier in this Section.

(*b*) *Model* **B** *Results.*—The curves of limiting wave height for stability at different wave lengths are given for points 1B to 5B (*see* Table 99 and Fig. 109) in Fig. 115 and the points defining the curves are given in Tables 102 to 106; the relevant critical disturbances are also given in these Tables. The general tendency in all of these diagrams is the same as in that for Model A; as wave length is increased there is a progressive decrease in the wave height necessary to produce instability and, although the curves end rather abruptly, there is in three of the cases a definite tendency towards a minimum wave height for instability, the value of which differs from case to case. Too much attention should not be paid to the irregular shape of the curves for points 2B and 3B; the varied nature of the motions involved and the fact that their representation is only by stable or unstable points should be remembered.

An examination of the five curves shows that in a given wave system the most stable configuration, or part of the stability diagram, is that represented by point 5B and the least stable by point 3B. If the five curves are put in order of quality with the poorest first, the resulting order is 3B, 2B, 1B, 4B and 5B. 2B and 1B are at the same elevator setting (Fig. 109) and indicate an improvement in stability, *i.e.*, an increase in the wave height necessary to induce instability, with increase in speed, while 3B and 1B are at virtually the same speed and show an improvement with increase in elevator setting. Points 1B, 4B and 5B are for both progressively higher speeds and elevator settings and should, if the changes already noted are progressive and additive, show a much greater degree of improvement than the individual changes; this is in fact the case.

It may thus be tentatively concluded that stability characteristics in waves will be improved by an increase in speed, or an increase in elevator setting (*i.e.*, in nose-down pitching moment), or both.

(*c*) *Model* **L** *Results.*—The curves of limiting wave height for stability at different wave lengths are given for points 1L to 14L (*see* Table 99 and Fig. 109) in Fig. 115 and the points defining the curves are given in Tables 107 to 120. The general tendency for the wave height necessary for instability to be reduced as wave length is increased can still be seen in these Figures, but the greater coverage of the stability diagram by the test points has resulted in a diversity of curve forms.

It is convenient to consider the curves in the following groups:

(i) 6L, 3L and 7L where $\eta = -12$ deg
(ii) 2L, 1L and 8L where $\eta = -8$ deg
(iii) 10L and 4L where $\eta = -4$ deg
(iv) 12L and 13L where $\eta = 0$ deg

This allows the effect of increasing speed to be assessed at different elevator settings; a regrouping:

(v) 6L, 1L, 10L and 14L where $C_v = 6{\cdot}9$
(vi) 8L, 4L and 12L where $C_v = 8{\cdot}2$
(vii) 7L, 9L, 5L and 11L where $C_v = 9{\cdot}2$,

allows the effect of increasing elevator setting or angle to be determined at different speeds.

The curves of the first group show, with the exception of that for 2L, that with increase in speed the wave height necessary to induce instability is increased and that the elevator setting has little bearing on this change (It should

be remembered that these remarks apply to any given wave system within the range tested and they are therefore general). The exception to this rule, point 2L, shows that much higher waves can be encountered without instability resulting than is the case at the next higher speed, point 1L. Point 2L represents the lowest speed tested, however, and is just past the hump, while the remaining points are at or above low planing speeds. The conclusion that increase in speed increases the wave height necessary for instability applies therefore only at planing speeds, not at hump speeds.

The second group shows that at all speeds, as elevator angle is increased so is the wave height necessary to induce instability and as speed is increased, so is the rate of this change.

The best configuration when planing in waves therefore is one where both speed and elevator angle are high.

General

From the foregoing results three general conclusions can be drawn. They apply over the range of wave systems covered in the main tests, that is, in waves having wave length/height ratios of up to 200 : 1 or in waves of lengths which are less than that at which the minimum wave height for instability is found. The conclusions are that:

(*a*) at any point in the planing speed range the wave height necessary to induce instability decreases with increase of wave length (probably until the resonant wave length is reached, after which it increases)

(*b*) at any point in the planing speed range and at any wave length the wave height necessary to induce instability increases with increase of elevator angle

(*c*) at any point in the planing speed range and at any wave length the wave height necessary to induce instability increases with increase of speed.

Minor exceptions to these conclusions can be found, but they are not felt to be significant.

It may be noted that here and elsewhere in the discussion test points have been defined in terms of η and V, not α_K and V, i.e., elevator angle has been used in preference to keel attitude. The reason is that while both are usually known accurately in calm-water tests, this is not generally so in waves. When the model oscillates in pitch during wave tests it is difficult to obtain an attitude reading and when the model is reasonably steady the attitude is usually different to that obtained in calm water for the same speed and elevator setting. Observers were left with the impression that attitudes were increased by waves from their calm-water values and, to check this, readings were taken at seven points, 4L, 5L, 7L, 8L, 9L, 10L and 14L (Tables 110, 111, 113, 114, 115, 116 and 120). When the motion was oscillatory and of small amplitude, the mid-point between maximum and minimum readings (*see* Fig. 110, for instance) was taken as the attitude for this purpose if it was not possible to obtain a steady reading before any instability built up. The mean of the readings obtained in different wave systems for each point was then plotted against the corresponding calm-water attitude and the resulting curve, which is of definite form, is given in Fig. 117.

It can be seen that for this particular model, L, calm-water attitudes of less than 8 deg are increased by waves, while those greater than 8 deg are decreased. Maximum and minimum values of attitude apparently exist for planing in waves and in this case are 8·0 and 6·8 deg respectively; the mean working attitude range has thus been reduced to $1\frac{1}{4}$ deg for this model. The speeds and elevator settings at which each set of wave tests were made are indicated; speed alone does not appear to be significant, while elevator angle decreases more or less progressively with increase in attitude at each speed. The long afterbody of Model L (7 beams) has undoubtedly played a large part in fixing the changes quantitatively (the reduction of the attitude range, for instance, would probably not be so great with a shorter afterbody), but it is considered that in general the calm-water attitudes of all the models of this series will be similarly modified by waves.

It is interesting to examine the test results for Model L in the light of the resonant wave length found at $2\frac{1}{2}$ times the hull length with three other models. Since the hull length of Model L is 13 beams one would expect a resonant wave length of 32 beams if this ratio is to be maintained. As can be seen from Fig. 114, this is consistent with the test results if a little latitude is allowed in the drawing of the wave curve. Considering the diversity of shapes represented by the four hulls concerned the agreement between the ratios resonant wave length/hull length is remarkably good and suggests that in fact there may be a general relationship involving this factor.

In Fig. 116 a comparison is made of the wave stability characteristics of Models A, B and L. In the first diagram curves for the three models are compared at a mid-planing speed and medium elevator setting. The basic model (A) is the poorest, a large improvement results from forebody warp (B) and a further but lesser improvement is obtained with forebody warp and a long afterbody (L). This does not of course mean that for any given model an increase in afterbody length will be more effective than application of forebody warp in improving behaviour in waves, since it may well be that, in the instance quoted, most of the possible improvement was effected by the addition of forebody warp, leaving little scope for any further improvement by an increase in afterbody length or any other means. The improvements occur at wave lengths which are roughly equal to hull length, but near resonant wave length there is apparently little difference between the three hull forms.

The remaining diagrams show the effect of increasing afterbody length, at several speeds and elevator settings (*see* Table 99). The first diagram of this group is for a low planing speed and shows that here the long afterbody (L) effects an enormous improvement; the remainder are for progressively higher speeds and indicate that while

the long afterbody is slightly better in short waves it shows a progressive deterioration relative to Model B with speed at the higher wave lengths, *i.e.*, the characteristics of the short afterbody model improve at a greater rate with increase of speed than those of the long afterbody model.

Summarising briefly the main points so far made with respect to longitudinal stability in waves, there is a minimum wave height and a maximum wave length/height ratio below and above which respectively no instability is obtained. The minimum wave height appears to occur at a wave length of $2\frac{1}{2}$ times the hull length; this factor of $2\frac{1}{2}$ has been found to be significant with four hull forms at mid-planing speeds, the resonant wave length in each case being $2\frac{1}{2}$ times the hull length, and within practical limits this may well be a universal figure. In general, it appears that at a constant planing speed and elevator setting the wave height necessary to induce instability decreases monotonically with increase of wave length until the resonant wave length is reached, and then increases. Again, the wave height necessary to induce instability at a given wave length is increased by increase of speed or elevator angle or both.

These results may be used to formulate a technique for future stability tests in waves, which can be made very brief. The worst and best wave stability characteristics will be obtained at low planing speeds with low elevator angles and at high planing speeds with high elevator angles respectively, while between these extremes there is a more or less steady change. Diagrams for these points will therefore give all the information necessary on the wave stability characteristics of a given hull in the planing speed range.

It is felt that in future tests account should be taken of motion in heave as well as that in pitch, which was the only motion of direct interest in the present investigation. During the present tests it was observed that the heaving motion occurred occasionally in the complete absence of any pitching motion, so that for any absolute assessment of the motion in waves of a given hull form the simple 2-deg pitch criterion is clearly inadequate; it is necessary to take account of several factors. These will include the amplitude, frequency and degree of regularity of the motion, both in pitch and heave. A suitable form of presentation for such comprehensive tests would probably be a carpet graph of amplitudes of oscillation in pitch and heave related to wave length and wave height for each elevator-speed combination, with some allowance being made for the frequency of oscillation.

Some mention should be made of the lack of longitudinal freedom in the stability test rig used in the wave tests. This lack of longitudinal freedom has been given full theoretical consideration in the indisturbed calm-water case in Ref. 21 where it was concluded that variations of longitudinal velocity had only a slight effect on stability, and these conclusions were given an experimental check (Ref. 7) when it was found that the model behaviour was similar under the two conditions, with and without longitudinal freedom, and that when porpoising was present the period and character of the motion taking place was unaffected by the introduction of the additional degree of freedom. In the wave tests now under consideration most of the conclusions are based on curves or limits which were drawn with respect to porpoising of 2-deg amplitude. It is felt that while there will undoubtedly be an effect due to the longitudinal constraint, at these small amplitudes it will probably be negligible and at higher amplitudes it will be more quantitative than qualitative; the general conclusions of the report should in any event not be affected. The magnitude of the effect should, however, be determined if possible, together with those of the corresponding effects on the heave and forward motions, and if any of the effects is large it will obviously be necessary to arrange for longitudinal freedom in future tests.

1.6. **Conclusions.**—The main conclusions arrived at above are summarised below. They are felt to be general, but the fact that they are based on limited tests should be borne in mind.

The conclusions are that :

(*a*) at mid-planing speeds there exists a resonant wave length which is approximately two and a half times the hull length and is independent of hull shape and length/beam ratio

(*b*) at any point in the planing speed range the wave height necessary to induce instability decreases with increase of wave length (probably until the resonant wave length is reached, after which it increases)

(*c*) at any point in the planing speed range and at any wave length the wave height necessary to induce instability increases with increase of nose-down elevator angle

(*d*) at any point in the planing speed range and at any wave length the wave height necessary to induce instability increases with increase of speed

(*e*) the calm-water attitude range available during take-off is reduced by waves.

It is considered that, in future tank tests in waves, account should be taken of the amplitude, frequency and degree of regularity of the motion, both in pitch and heave.

CHAPTER 12

General Discussion and Concluding Remarks

Detailed points of interest relevant to the main parameters tested have already been discussed but there are a number of issues which, while of importance in their own right, have not so far been generally considered since they are not directly related to any individual parameter. These are considered below and some remarks are made on the application of the individual results to full-scale flying techniques. Finally, general remarks pertaining to the investigation as a whole are given; detailed conclusions have already been given at the end of each Chapter.

Of great importance are two points relating to longitudinal stability assessments generally. At present a hull is classed as longitudinally unstable only if it oscillates in pitch more than 1 deg each side of its mean, but it has been shown (Chapter 9, Section 1.3) that a much greater degree of correlation between different sets of limits can be obtained if all porpoising motion, of any amplitude, is classed as unstable; it is suggested, therefore, that in future investigations a 0-deg limit should be obtained in addition to or instead of the normal 2-deg limit. Consideration should also be given to the classification of pure heave motions as unstable. This will apply equally to routine model tests in waves and to full-scale tests designed to provide correlation with model-test results; such tests would be made in the usual manner by means of steady-speed runs. Full-scale 2-deg limits obtained by the more expedient take-off and landing technique[37] would still serve to indicate the operational characteristics of the aircraft concerned. For a complete investigation of the motion in waves of a given hull form, however, the more detailed method suggested earlier in the report should be adopted.

With respect to the scope of tests to be made in future determinations of model longitudinal stability characteristics, as there is no practical correlation between disturbed stability and stability in waves, both types of test are necessary and future longitudinal stability tests should therefore include assessments of stability characteristics without disturbance, with disturbance, and in waves.

Considering now points relating to full-scale flying techniques, some remarks will first be made concerning hulls with long afterbodies. While normal landings at fairly high speeds and low attitudes with low rates of descent would obviously be possible here, the qualities peculiar to a long afterbody hull would also enable slow landings to be made at high attitudes with high rates of descent. In this case the approach attitudes would be higher than the maximum obtainable on the water, due mainly to the restriction imposed on planing attitudes by the long afterbody, and the final approach would be made with considerable power to augment the aerodynamic lift. On closing the throttles and holding the control column full back, the aircraft would virtually drop onto the water, when the long afterbody would cause an immediate reduction in attitude, with consequent loss of lift, and keep the attitude down; this, with the initial low speed, would in general render the subsequent motion stable, upper-limit instability having been avoided (provided of course that the disturbed lower limit was not crossed other than along a trim curve). Such a landing would depend for its success on the long afterbody to keep maximum planing attitudes low, and on the low landing speed. The take-off, too, would be simple; all the pilot would need to do to guarantee avoiding trouble from instability would be to keep the stick right back.

With respect to operations in waves it is possible to use the results of Chapter 11 to suggest a general method for making full-scale take-offs in waves for all types of hull. It has been shown that greater wave heights can be encountered under conditions of maximum elevator and speed without inducing instability than under other conditions, so that the best course is to keep the control column forward and increase speed as quickly as possible. This assumes that the effect of accleration is not detrimental and is roughly constant over the (η, V) plane. In the present wave tests instability was damped out while running up to speed and, since in the calm-water case (in which acceleration is beneficial) it has not been considered worthwhile in the light of experience to check the constancy of the effects of acceleration on stability over the (η, V) plane, these points can, for the present, be neglected.

While keeping the stick forward during take-off in waves undue concern about the nose of the aircraft digging in or being sucked down need not be felt. The indication of a minimum mean attitude (Chapter 11, Section 1.5) suggests that in fact the opposite will happen; the pilot will have to hold the aircraft down and allow it to become airborne when flying speed is reached.

Perhaps the most enlightening conclusion bearing on take-offs in waves is that at mid-planing speeds the resonant wave length is $2\frac{1}{2}$ times the hull length; during take-off waves of this length should be avoided as much as possible. Waves of just less than resonant length and above may be effectively lengthened by following a take-off path as near parallel to the waves as possible, when there will be little risk of instability, but application of this technique in shorter wave lengths may cause resonance and is therefore dangerous; in short waves take-offs should be made head on into the waves. The pilot can decide on which course to follow after making

or obtaining an estimate of the wave length relative to the length of his aircraft. An analagous technique could be devised for landing and would need only a suitable allowance for deceleration effects.

The test data which have been presented in the various Sections of this report enable the detailed effects of the design parameters which have been considered to be ascertained, either alone or in combination. It is not proposed to repeat here the conclusions already reached in the appropriate Sections, except to remark that it appears generally advantageous to warp the forebody of a high length/beam ratio hull, and to employ a fairly long tailored afterbody with a suitable chosen afterbody angle.

In the tests described, revised and more soundly based test techniques were used than in the past. Nevertheless, various findings during the course of the programme suggested further modifications or extensions which could usefully be made particularly with respect to the definition of stability and to tests in waves. These results are felt to have considerable importance.

The overall result of the investigation has been to extend the range of knowledge of the stability and spray characteristics of high length/beam ratio hulls considerably, while at the same time yielding checks of earlier work on a number of standard parameters, and to bring the test techniques to a stage where they can give a comprehensive and realistic estimate of the full-scale characteristics of a hull. It is felt, therefore, that the primary aims of the investigation have been fulfilled, though there is still considerable scope for further work on most of the topics considered.

LIST OF SYMBOLS

b		Beam of model at step (maximum beam)
c		Standard mean chord (S.M.C.)
C		Critical trim
C_L		Total aerodynamic lift coefficient
	$=$	$L_a/\frac{1}{2}\varrho SV^2$
C_L'		Tailplane lift coefficient
	$=$	$L_a'/\frac{1}{2}\varrho S'V^2$
C_v		Velocity coefficient
	$=$	$V/\sqrt{gb}$
C_x		Longitudinal spray coefficient
	$=$	x/b
C_y		Lateral spray coefficient
	$=$	y/b
C_z		Vertical spray coefficient
	$=$	z/b
C_Δ		Load coefficient (beam loading)
	$=$	Δ/wb^3
$C_{\Delta 0}$		Load coefficient at $V = 0$ (static beam loading)
	$=$	Δ_0/wb^3
d		Draught
D		Propeller diameter
g		Acceleration due to gravity
h		Wave height
I		Pitching moment of inertia
k		Pitching radius of gyration
L		Wave length
L_a		Total aerodynamic lift
L_a'		Tailplane lift
m		Mass of model
S		Gross mainplane area
S'		Gross tailplane area
T		Propeller thrust
T_c		Thrust coefficient
	$=$	$T/\varrho V^2D^2$
V		Forward speed
w		Specific weight of water
x, y, z		Co-ordinates of points on spray envelope relative to axes through step point
α		Wing incidence
α_K		Forebody keel attitude
Δ		Load on water
Δ_0		Load on water at $V = 0$
ψ		Angle of yaw
ϱ		Density of air
ϱ_w		Density of water
η		Elevator angle

REFERENCES

No.	Author	Title, etc.
1	T. B. Owen, A. G. Kurn and A. G. Smith	Model testing technique employed in the R.A.E. seaplane tank. R. & M. 2976. September, 1953.
2	J. M. Benson	The porpoising characteristics of a planing surface representing the forebody of a flying-boat hull. N.A.C.A. A.R.R. Wartime Report L-479. A.R.C. 6166. May, 1942.
3	K. W. Clarke and W. D. Tye	Some measurements of ground effect in the seaplane tank. R.A.E. Report B.A. 1421. A.R.C. 3263. September, 1937.
4	A. G. Smith and H. G. White	A review of porpoising instability of seaplanes. R. & M. 2852. February, 1944.
5	F. W. S. Locke	A graphical method for interpolation of hydrodynamic characteristics of specific flying boats from collapsed results of general tests of flying-boat-hull models. N.A.C.A. Tech. Note 1259. January, 1948.
6	D. Whittley and P. Crewe	An interim report on the generalised presentation of tank tests on a seaplane hull or float. Saunders-Roe Report AH/37/T. March, 1947.
7	L. P. Coombes, W. G. A. Perring and L. Johnston	The use of dynamically similar models for determining the porpoising characteristics of seaplanes. R. & M. 1718. November, 1936.
8	J. P. Gott	Note on the technique of tank testing dynamic models of flying boats as affected by recent full-scale experience. R.A.E. Report B.A. 1572. A.R.C. 4378. December, 1939.
9	G. L. Fletcher	Tank tests on a jet propelled boat seaplane fighter (*Saunders-Roe E6/44*). R. & M. 2718. January, 1946.
10	J. Taylor and A. G. Smith	Note on damage to *Solent* N.J.201 during simulated engine failure in take-off. M.A.E.E. Report F/Res/230. A.R.C. 15,539. January, 1953.
11	J. P. Gott	Further note on the tank testing of dynamic models of flying boats with special reference to the model of the G-class boat. R.A.E. Tech. Note Aero. 962. June, 1942.
12	F. W. S. Locke and W. C. Hugli ..	A method for studying the longitudinal dynamic stability of flying-boat-hull models at high planing speeds and during landing. N.A.C.A. Wartime Report W-57. April, 1945.
13	J. P. Gott	Interference between airflow and water flow in seaplane tank testing. R.A.E. Tech. Note Aero. 1460. A.R.C. 7906. July, 1944.
14	F. R. J. Spearman	Measurement of dynamic performance of Desynn repeater. R.A.E. Tech. Note Instn. 122. August, 1948.
15	T. B. Owen	Model tests on the directional stability on the water of the *Princess* flying boat. R.A.E. Tech. Memo. Aero. 262. April, 1952.
16	R. E. Olsen and N. S. Land	Methods used in the N.A.C.A. tank for the investigation of the longitudinal stability characteristics of models of flying boats. N.A.C.A. Report 753. 1943.
17	J. P. Gott	Note on the comparison of British and American methods of tank testing dynamic models of flying-boats. R.A.E. Tech. Note Aero. 1197 (Tank). A.R.C. 6892. May, 1943.
18	K. S. M. Davidson and F. W. S. Locke	Some systematic model experiments on the porpoising characteristics of flying-boat hulls. N.A.C.A. Wartime Report W-67. June, 1943.
19	N. S. Land and L. J. Lina	Tests of a dynamic model in N.A.C.A. tank No. 1 to determine the effect of length of afterbody, angle of afterbody keel, gross load, and a pointed step on landing and planing instability. N.A.C.A. Wartime Report L-400. March, 1943.

REFERENCES—*continued*

No.	*Author*	*Title, etc.*
20	A. G. Smith, D. F. Wright and T. B. Owen	Towing-tank tests on a large six-engined flying-boat seaplane, to Specification 10/46, *Princess*. Pt. II. Porpoising stability, spray and air-drag tests, with improved step fairing, afterbody design and aerodynamic modifications. R. & M. 2834. November, 1950.
21	W. G. A. Perring and H. Glauert ..	The stability on the water of a seaplane in the planing condition. R. & M. 1493. September, 1932.
22	G. J. Richards and J. L. Hutchinson ..	Some notes on the mathematical investigation of porpoising. M.A.E.E. Report F/Res/72. A.R.C. 1259. May, 1934.
23	D. T. Llewelyn-Davies, W. D. Tye and D. C. MacPhail	The design and installation of small compressed-air turbines for testing powered dynamic models in the Royal Aircraft Establishment Seaplane Tank. R. & M. 2620. April, 1947.
24	F. W. Schmitz	*Aerodynamik des Flugmodells*. pp. 1 to 71 and 142 to 159. G. J. E. Volckmann and E. Wette. Berlin.
25	K. S. M. Davidson and F. W. S. Locke	Some analyses of systematic experiments on the resistance and porpoising characteristics of flying-boat hulls. N.A.C.A. Wartime Report W-68. September, 1943.
26	A. W. Carter and I. Weinstein ..	Effect of forebody warp on the hydrodynamic qualities of a hypothetical flying-boat having a hull length/beam ratio of 15. N.A.C.A. Tech. Note 1828. March, 1949.
27	W. Sottorf	Systematic model researches on the stability limits of the D.V.L. series of float designs. (M.A.E.E. Translation F.T.3 and N.A.C.A. Tech. Memo. 1254). *Jahrbuch der L.F.F.* 1942.
28	E. C. Stout	Development of high-speed water-based aircraft. *J. Ae. Sci.* Vol. 17. No. 8. pp. 457 to 480. August, 1950.
29	W. J. Kapryan and E. P. Clement ..	Effect of increase in afterbody length on the hydrodynamic qualities of a flying-boat hull of high length-beam ratio. N.A.C.A. Tech. Note 1853. April, 1949.
30	A. Strumpf	Model tests on a standard series of flying-boat hulls. Stevens Institute of Technology E.T.T. Report No. 325. May, 1947
31	A. G. Smith and J. E. Allen	Water and air performance of seaplane hulls as affected by fairing and fineness ratio. R. & M. 2896. August, 1950.
32	A. G. Smith and J. A. Hamilton ..	Notes on a detailed research programme on aero and hydrodynamics of hulls with high fineness ratio and full step fairings. M.A.E.E. Report F/Res/221. A.R.C. 13,877. March, 1951.
33	K. N. Tomaszewski and A. G. Smith ..	Some aspects of the flow round planing seaplane hulls or floats and improvement in step and afterbody design. M.A.E.E. Note F/TN/4. A.R.C. 14,376. September, 1954.
34	T. B. Owen and D. F. Wright ..	Comparative model tests of the *Princess* and *Shetland* flying boats in waves. R.A.E. Tech. Note Aero. 2166. A.R.C. 15,496. May, 1952.
35	C. H. E. Warren and W. D. Tye ..	Calibration of the wave-maker in the R.A.E. towing tank. R.A.E. Tech. Note Aero. 1764. A.R.C. 9770. March, 1946.
36	V. Cornish	*Ocean Waves*. p. 125. Cambridge University Press. 1934.
37	H. G. White and A. G. Smith	A method for determining the water stability of a seaplane in take-off and landing. R. & M. 2719. May, 1943.
38	—	Royal Aeronautical Society data sheets—aerodynamics.
39	E. P. Warner	*Airplane Design—Performance*. McGraw-Hill. 1936.

APPENDIX I

Effects of Static Margin on Longitudinal Stability Limits

1. **Introduction.**—It is stated in Chapter 2, Section 2.1, that the static margin of the basic model is approximately $0{\cdot}15c$ at $\alpha_K = 0$ deg. As the c.g. position is low relative to the model wing, however, it might be expected that attitude changes would have an appreciable effect on the static margin and that this in turn might affect the hydrodynamic stability characteristics of the model. The variation of static margin and its effect on hydrodynamic stability are considered below, use being made of data obtained during the present series of tests.

As the aerodynamics of each of the models were identical as far as manufacture would allow with those of the basic model, the points made below will apply generally to all models of the series.

2. **Discussion.**—The variation of static margin with attitude has been plotted in Fig. 217 for the basic model. The maximum value of $0{\cdot}33c$ is reached at approximately 8-deg keel attitude, showing an increase of $0{\cdot}19c$ over the value at $\alpha_K = 0$ deg; it then decreases with further attitude increases due to the stalling of the tailplane (it should be remembered that in the towing tank tests low Reynolds numbers prevail, correct Froude number being the main consideration, and give rise to poor lift curves when such devices as leading-edge slats are not used). As tests are made with fixed elevator, the static margins considered are stick fixed, and in computing the curve of Fig. 217, the elevator has been assumed fixed at $\eta = 0$ deg and drag has been ignored.

As the higher attitudes are normally reached with negative elevator, the static margin has been found in one such case, namely, for $\eta = -10$ deg at $\alpha_K = 8$ deg (Fig. 217); the static margin is decreased by $0{\cdot}11c$ from the zero-elevator-setting case. The destabilising effect of slipstream can also be seen in this Figure.

In assessing the effect of these changes in static margin on longitudinal stability limits three aerodynamic configurations of the basic model have been considered; they are those with take-off power, with fairings and with full-span slats respectively and are described in Chapter 5, Section 2. The moments of inertia of these configurations were all within 2 per cent of each other and the c.g. positions were identical. Lift curves are given in Figs. 30a, 30c and 30d for the take-off-power, fairings and full-span-slat cases respectively and the hydrodynamic longitudinal stability limits are compared in Figs. 33 and 34. The static margins for each case at $\alpha_K = 5$ deg and 8 deg are shown in Fig. 217. The tailplane characteristics for each configuration have been assumed identical; this may appear to be a crude approximation, but it should be remembered that the tailplane is high enough on the fin for it to be clear of the slipstream except possibly at high attitudes and draughts.

The configurations with take-off power and fairings are identical except for slipstream, the main effects of which are, from the present point of view, to increase lift and introduce a nose-down pitching moment. As the speed varies in the former case, so does the thrust coefficient T_c, and the slope of the lift curve increases with T_c. This variation, however, is not great over the planing range of speeds and the lift curve at $T_c = 0{\cdot}8$ in Fig. 30a is considered typical; this curve has been used in the calculation of the relevant static margins. When the propellers are replaced by fairings, the loss of slipstream results in a kink in the lift curve. This is shown in Fig. 30c, where the slope of the lift curve from $\alpha_K = 6$ deg to 10 deg is reversed in sign. The model is thus statically unstable in this region. To carry out the tests of the main investigation without the complications of slipstream and still have good lift characteristics, the nacelles were therefore removed and full-span slats fitted, giving rise to the lift curve ($\eta = 0$ deg) of Fig. 30d.

Undisturbed longitudinal hydrodynamic stability limits for the three configurations are shown in Fig. 33. The most obvious feature of this comparison is that the limits for the take-off-power case extend up to a keel attitude of 10 deg, while the other two sets reach about $11\frac{1}{2}$ deg. This is due to the nose-down thrust moment in the take-off-power case which prevented the higher trims being reached with the elevators used. As the test runs were made at steady speeds, the thrust moment was constant during each run and may be considered as approximately equivalent to a change in the elevator setting; it will thus have negligible effect on the position of the stability limits, although the trim curves will in general be lowered.

The major reason for the disorderly arrangement of the limits in Fig. 33 is that at a given speed the three limits are for three different loads on water. Reasonable account can be taken of this by plotting on a $C_\Delta{}^{1/2}/C_v$ base (Ref. 25) as in Fig. 34. In Fig. 5, limits for a $C_{\Delta 0}$ range of 2·00 to 3·00 show a large measure of collapse when plotted on this base (a set of limits is considered to be completely collapsed when the limits coincide). In the present case, the static beam loadings of the three configurations tested were equal at $C_{\Delta 0} = 2{\cdot}75$, so that the only differences due to load are aerodynamic. In general, and along the lower limit in particular, it is felt that if these aerodynamic load differences are the only source of discrepancy, the stability limits should collapse equally well. Within the bounds of experimental error the limits obtained with take-off power and with fairings do collapse. The slight divergence of the

upper end of the lower limit for the case with take-off power may easily be attributed to the drawing of the limit, as in this region the determined points on the stability diagram do not position the limit exactly. The upper limits are not superimposed because of attitude differences, but they appear to be continuous. With full-span slats the lower limit below $\alpha_K = 8$ deg and the upper limit are both above the other two sets; this discrepancy cannot be wholly discounted as experimental error and as the basic difference between this configuration and the others is the removal of nacelles and the introduction of full-span slats, this must be the initial cause of the discrepancy. It may be mentioned, however, that as there is little change in static margin from case to case at the lower attitudes, the discrepancy does not appear to be a static margin effect.

Estimates have been made of the static margin in each case at two attitudes with $\eta = 0$ deg, as under

α_K (deg)		With take-off power	With fairings	With full-span slats
5	Static margin	+0·16	+0·26	+0·20
	$C_\Delta^{1/2}/C_v$	+0·157	+0·152	+0·135
8	Static margin	+0·25	−1·06	+0·33
	$C_\Delta^{1/2}/C_v$	+0·192	+0·194	+0·190

At $\alpha_K = 8$ deg the stability limits are very close together and the change in static margin is 1·3; at $\alpha_K = 5$ deg, the full-span slat limit differs from the others, and the change in static margin is only 0·1. A large change in static margin, therefore, does not necessarily have a material effect on the inception of undisturbed hydrodynamic instability, assuming of course that there are no sizeable secondary effects.

The foregoing considerations apply to the effects of static margin variations on undisturbed longitudinal stability limits, where porpoising is of 2-deg amplitude only; in the case of disturbed instability, where very large amplitudes of porpoising are encountered, the effects would be complex and are commented on very briefly below.

When disturbed instability is produced in a model it usually appears in the form of a large amplitude oscillation in pitch coupled with a large oscillation in heave. The two can be taken to be roughly in phase (Fig. 3) when an upward motion in heave will be accompanied by a nose-up motion in pitch. This motion in heave will thus effectively reduce incidence at both mainplane and tailplane, while the motion in pitch will greatly increase tailplane incidence and have a direct but smaller effect on mainplane incidence; there will also be numerous second-order effects. In addition, there will be what might be called the geometric fluctuation of static margin due to attitude changes. All of these effects will depend on the period and amplitudes of the oscillations.

It is obviously difficult to say what would happen in a given case, but at the highest attitudes obtained during the porpoising cycles it is fairly certain that the tailplane will in general be stalled and the model will be statically unstable. This may well have an effect in the region of the upper limit at speeds near to take-off, when it is remembered that (in a purely aerodynamic case) as static stability changes from positive to negative, divergent instability develops in the dynamic motion[38]. If it were considered necessary, such an effect could be reduced by fitting the tailplane with leading-edge slats, when the stall would be delayed and static stability could be maintained up to higher attitudes, but model periods of oscillation will still be reduced dimensionally and nothing can be done about this.

In the general case of high-amplitude porpoising it is conceivable that static margin changes will affect the motion: an analogous motion full scale would, however, be similarly affected and with a large amplitude oscillation, note of the correct order is at present considered adequate. It may also be mentioned that the disturbed stability limits are normally treated as being less precise than those obtained without disturbance.

3. **Conclusions.**—A variation in static margin with attitude does in fact occur with the models of this series, but it has negligible effect on the position of the lower undisturbed stability limits, although it may affect the upper limits. Its effect on the disturbed stability limits is probably greater, being largest at high attitudes and speeds when draught is small. It is considered, however, that allowance for this is made implicitly in the interpretation of disturbed limits and that the c.g. position chosen is fully representative of full-scale high length/beam ratio flying boats.

APPENDIX II

Model Hull Design

1. **General.**—In the basic design reference is made to a streamline shape. This is defined[39] by:

Forward 40 per cent: $(x/L)^2 + 0{\cdot}16y^2 = 0{\cdot}16$ .. .. (1)

Aft 60 per cent: $(x/L)^2 + 0{\cdot}0679y^2 + 0{\cdot}2921y = 0{\cdot}36$, ... (2)

where y = diameter at any station

x = distance along axis to the station from point of maximum diameter

L = overall length of streamline shape.

The maximum hull beam, $b = 0{\cdot}475$ ft, maximum height $= 2b$ and step depth $= 0{\cdot}15b$.

2. **Forebody.**—The forebody is 6 beams long and is of constant beam for 3 beams forward of the step. The beam for any station in the forward half is given by equation (1) and the tumble-home is semi-circular in cross-section with the beam at that section as diameter. Forebody warp varies from model to model, but in the case of zero warp, deadrise is constant at 25 deg for the first half of the forebody forward of the step and increases in a manner giving good lines to 63 deg at the forward perpendicular. In side view the forebody keel is parallel to the hull crown, for the first 3 beams forward of the step; it is then elliptical, rising to 1 beam above the keel line at the forward perpendicular. All forebody cross-sections are parallel sided.

3. **Afterbody.**—Afterbody length and angle vary to conform to Table 2, but the plan view of the afterbody planing bottom is defined by equation (2). Afterbody deadrise is 26 deg at the main step, increasing to 30 deg in 40 per cent of afterbody length and remaining constant at 30 deg to the aft step. Cross-sections are parallel-sided up to at least the height of the aft step, but above this a fairing has been added to carry the tail unit. This has been drawn so as to give good lines and can be seen in Fig. 1. The hull crown aft of the mainstep is parallel to the forebody keel and the afterbody tumble-home is semi-circular in cross-section. The aerodynamic tail arm is constant, so that the presence and design of the counter depend on afterbody length and angle.

APPENDIX III

Theoretical Analysis of Effects of Changes in Mass, Moment of Inertia and Radius of Gyration on Longitudinal Stability Limits and Correlation with Experiment

1. **Introduction.**—Since the mass (m), moment of inertia (I) and radius of gyration (k) of a model are related by $I = mk^2$, the effects on the longitudinal stability limits of changes in them are not independent. They can be related analytically by considering critical trim (*i.e.*, the trim at which longitudinal instability sets in) as a function of I, m, k and velocity and taking into account the implicit relations between the parameters. Details of this treatment are given below and a comparison is made between analytical and experimental results using the limits obtained in the tests described in Chapters 3 and 4 of the main text. The centre of gravity has been taken to be fixed throughout the theoretical treatment to correspond with the conditions of the model tests.

2. **Theoretical Analysis.**—

Let V denote velocity

α_K keel attitude

d draught

m mass

I moment of inertia

k radius of gyration

C critical trim (*i.e.*, the trim at which longitudinal instability sets in for any particular velocity or draught).

Then families of stability limits for a given model plotted against V and α_K for ranges of values of I, m or k, of the type shown in Figs. 21 to 26 (C_v is merely a constant multiple of V), can be regarded as graphs of C as a function of V and two of I, m, and k, e.g., in Figs. 21 and 22 C is represented as a function of V, m and I, or V, k and I; in Figs. 23 and 24 of V, I and m, or V, k and m; and in Figs. 25 and 26 of V, I and k, or V, m and k.

Because of the implicit relationship $I = mk^2$, the separations of the critical trim lines on these various graphs are not all independent. These separations can be represented analytically by partial derivatives of the type $(\partial C/\partial I)_{V,k}$, where the suffixes indicate the variables taken as the independent variables other than the one with respect to which differentiation is being effected. The complete set of these derivatives in the (α_K, V) plane is:

$$\left(\frac{\partial C}{\partial V}\right)_{m,I}, \quad \left(\frac{\partial C}{\partial m}\right)_{V,I}, \quad \left(\frac{\partial C}{\partial I}\right)_{V,m}$$

$$\left(\frac{\partial C}{\partial V}\right)_{m,k}, \quad \left(\frac{\partial C}{\partial m}\right)_{V,k}, \quad \left(\frac{\partial C}{\partial k}\right)_{V,m}$$

$$\left(\frac{\partial C}{\partial V}\right)_{I,k}, \quad \left(\frac{\partial C}{\partial I}\right)_{V,k}, \quad \left(\frac{\partial C}{\partial k}\right)_{V,I}$$

For relations between them we proceed as follows:

Let $$C = f(V, m, I),$$

then $$dC = \frac{\partial f}{\partial V}dV + \frac{\partial f}{\partial m}dm + \frac{\partial f}{\partial I}dI,$$

and since $$I = mk^2 = \phi(m, k), \text{ say,}$$

$$dI = \frac{\partial \phi}{\partial m}dm + \frac{\partial \phi}{\partial k}dk$$

$$= k^2\,dm + 2mk\,dk.$$

To find $(\partial C/\partial h)_{i,j}$ where h, i and j are the three variables chosen as independent variables, dC must first be expressed in terms of dh, di and dj only. $(\partial C/\partial h)\ i,j$ is then the coefficient of dh in this expression, *e.g.*,

$$\left(\frac{\partial C}{\partial V}\right)_{m,I} = \frac{\partial f}{\partial V}, \quad \left(\frac{\partial C}{\partial I}\right)_{V,m} = \frac{\partial f}{\partial I}, \quad \left(\frac{\partial C}{\partial m}\right)_{V,I} = \frac{\partial f}{\partial m}$$

and since

$$dC = \frac{\partial f}{\partial V} dV + \frac{\partial f}{\partial m} dm + \frac{\partial f}{\partial I}(k^2\, dm + 2mk\, dk),$$

then

$$\left(\frac{\partial C}{\partial m}\right)_{V,k} = \frac{\partial f}{\partial m} + k^2 \frac{\partial f}{\partial I} = \left(\frac{\partial C}{\partial m}\right)_{V,I} + k^2 \left(\frac{\partial C}{\partial I}\right)_{V,m}, \text{ etc.}$$

Other relations are obtained by eliminating dm instead of dI. The set of relations of this kind is:

$$\left(\frac{\partial C}{\partial V}\right)_{m,I} = \left(\frac{\partial C}{\partial V}\right)_{m,k} = \left(\frac{\partial C}{\partial V}\right)_{I,k} \quad \ldots\ldots\ldots\ldots\ldots\ldots\ldots \quad (1)$$

$$\left(\frac{\partial C}{\partial m}\right)_{V,k} = \left(\frac{\partial C}{\partial m}\right)_{V,I} + k^2 \left(\frac{\partial C}{\partial I}\right)_{V,m} \quad \ldots\ldots\ldots\ldots\ldots\ldots\ldots \quad (2)$$

$$\left(\frac{\partial C}{\partial k}\right)_{V,m} = 2mk \left(\frac{\partial C}{\partial I}\right)_{V,m} \quad \ldots\ldots\ldots\ldots\ldots\ldots\ldots \quad (3)$$

$$\left(\frac{\partial C}{\partial I}\right)_{k,V} = \left(\frac{\partial C}{\partial I}\right)_{V,m} + \frac{1}{k^2} \left(\frac{\partial C}{\partial m}\right)_{V,I} \quad \ldots\ldots\ldots\ldots\ldots\ldots\ldots \quad (4)$$

$$\left(\frac{\partial C}{\partial k}\right)_{I,V} = -\frac{2m}{k} \left(\frac{\partial C}{\partial m}\right)_{V,I}. \quad \ldots\ldots\ldots\ldots\ldots\ldots\ldots \quad (5)$$

A similar argument and set of relations holds with the draught d replacing V throughout, giving

$$\left(\frac{\partial C}{\partial d}\right)_{m,I} = \left(\frac{\partial C}{\partial d}\right)_{m,k} = \left(\frac{\partial C}{\partial d}\right)_{I,k} \quad \ldots\ldots\ldots\ldots\ldots\ldots\ldots \quad (6)$$

$$\left(\frac{\partial C}{\partial m}\right)_{d,k} = \left(\frac{\partial C}{\partial m}\right)_{d,I} + k^2 \left(\frac{\partial C}{\partial I}\right)_{d,m} \quad \ldots\ldots\ldots\ldots\ldots\ldots\ldots \quad (7)$$

$$\left(\frac{\partial C}{\partial k}\right)_{d,m} = 2mk \left(\frac{\partial C}{\partial I}\right)_{d,m} \quad \ldots\ldots\ldots\ldots\ldots\ldots\ldots \quad (8)$$

$$\left(\frac{\partial C}{\partial I}\right)_{k,d} = \left(\frac{\partial C}{\partial I}\right)_{d,m} + \frac{1}{k^2} \left(\frac{\partial C}{\partial m}\right)_{d,I} \quad \ldots\ldots\ldots\ldots\ldots\ldots\ldots \quad (9)$$

$$\left(\frac{\partial C}{\partial k}\right)_{I,d} = -\frac{2m}{k} \left(\frac{\partial C}{\partial m}\right)_{d,I}. \quad \ldots\ldots\ldots\ldots\ldots\ldots\ldots \quad (10)$$

The two sets can be linked as follows. In general d is a function of V, m and η, and the trim curves give η as a function of α_K, V and m, so that d can be expressed in terms of V, m and α_K. In the transformation of stability limits from a velocity to a draught base, however, all the points considered are points on critical trim lines so that $\alpha_K = C$, and as C is already known as $f(V, m, I)$, d can be expressed as $\psi(V, m, I)$. We then have

$$\left.\begin{aligned} C &= f(V, m, I) \\ I &= mk^2 \\ d &= \psi(V, m, I) \end{aligned}\right\},$$

and a similar treatment to that already employed gives relations linking the various derivatives. We obtain

$$\left(\frac{\partial C}{\partial m}\right)_{d,I} = \left(\frac{\partial C}{\partial m}\right)_{V,I} - \frac{(\partial d/\partial m)_{I,V}}{(\partial d/\partial V)_{m,I}} \left(\frac{\partial C}{\partial V}\right)_{m,I}, \quad \ldots\ldots\ldots\ldots\ldots \quad (11)$$

$$\left(\frac{\partial C}{\partial I}\right)_{m,d} = \left(\frac{\partial C}{\partial I}\right)_{m,V} - \frac{(\partial d/\partial I)_{m,V}}{(\partial d/\partial V)_{m,I}} \left(\frac{\partial C}{\partial V}\right)_{m,I}, \quad \ldots\ldots\ldots\ldots\ldots \quad (12)$$

$$\left(\frac{\partial C}{\partial d}\right)_{I,m} = \frac{(\partial C/\partial V)_{m,I}}{(\partial d/\partial V)_{m,I}}, \quad \ldots\ldots\ldots\ldots\ldots\ldots\ldots \quad (13)$$

which with the other two sets of relations are sufficient to determine all other possible relations.

3. **Relation of Theory to Experiment.**—As already noted, the separations of the various limits plotted for comparison purposes in Figs. 21 to 26 can be related to the partial derivatives enumerated in the previous Section, as can the slopes of these limits. This is equally true of both disturbed and undisturbed limits, but consideration will only be given here to the latter, as ancillary complications occur in the correlation of the disturbed limits.

For example, consider Fig. 21. The slopes of the curves are given by $(\partial C/\partial V)_{I,m}$ and their separations normal to the velocity axis by $(\partial C/\partial m)_{V,I}$ (it it immaterial that the non-dimensional parameters C_v and $C_{\Delta 0}$ have been used in annotating the Figure itself rather than V and m; the effect is merely to change the units of measurement). That the slopes and separations are different in different sections of the diagram merely indicates that the derivatives are not constants but are themselves functions of V, I, m and k.

In similar manner $(\partial C/\partial V)_{I,m}$ and $(\partial C/\partial I)_{V,m}$ give slopes and separations on Fig. 23 and $(\partial C/\partial V)_{k,m}$ and $(\partial C/\partial m)_{V,k}$ on Fig. 25. It should perhaps be noted that in all the cases so far mentioned there is an alternative choice of independent variables, e.g., $(\partial C/\partial V)_{I,m}$ (Fig. 21) could equally well have been $(\partial C/\partial V)_{I,k}$ and $(\partial C/\partial m)_{V,I}$ have been $(\partial C/\partial k)_{V,I}$. The fact that the existence of this choice does not affect the slopes of the limits is expressed by Equation (1) of the preceding Section; this equation also takes account of the fact that the various sets of limits consist in part of the same limits collected together in different combinations.

Equations (2) to (5) give the theoretical relations between the vertical separations of the limits in Figs. 21, 23 and 25. If it is assumed that the movement of the limits in Fig. 23 is negligible, being only of the order of possible experimental error*, then we have $(\partial C/\partial I)_{V,m} = 0$ and $(\partial C/\partial k)_{V,m} = 0$ (this is self-consistent; *see* Equation (3)). Equations (2) and (4) then reduce to

$$\left(\frac{\partial C}{\partial m}\right)_{V,k} = \left(\frac{\partial C}{\partial m}\right)_{V,I}$$

and

$$k^2\left(\frac{\partial C}{\partial I}\right)_{k,V} = \left(\frac{\partial C}{\partial m}\right)_{V,I}$$

respectively.

The first of these equations is in direct accord with the evidence of Figs. 21 and 25, the vertical separation of the limits for $C_{\Delta 0} = 2{\cdot}00$ and for $C_{\Delta 0} = 3{\cdot}00$ being the same in both cases, within the limits of experimental error. Verification of the second relation is not directly possible without expressing the various derivatives as functions of I, m, k and V, but a brief calculation readily shows it to give results of the correct order of magnitude. Equation (5) is self-evident.

Since no experimental readings of draught were obtained during the tests it is not possible to verify equations (6) to (13) directly. As, however, the predictions of equations (1) to (5) have been confirmed, there is no reason to doubt them. It is important to remember in any attempted check that d in the equations denotes draught at points on critical-trim lines only.

It will be seen, then, that all the analytical predictions which it has been possible to test have been verified and therefore it seems likely that, in general, it would not be necessary to cover a complete range of all the parameters in order to ascertain the effect of varying them; this could be done by a limited series of tests together with the results derived above. In a similar manner it should be possible to predict the effects of any change of base without actually carrying out the work.

4. **Conclusions.**—Such of the general predictions of the theoretical analysis as it has been possible to check have been confirmed; this indicates that to obtain complete information on the behaviour of a model under variations of the various parameters involved, it is unnecessary to perform a large number of tests, since all the results can be forecast from a limited number of experiments. In the same way it should be possible to predict the effect of a change of base on stability limits accurately analytically.

* The order of accuracy of the limits being considered here is slightly less than that of those in the main series of tests referred to in Chapter 9, Section 1.3, as there is a smaller number of experimental points defining the limits.

APPENDIX IV

Wave-Disturbance Correlation

An attempt to correlate the effects of waves and disturbances on undisturbed calm-water stability characteristics may be made in several ways and the correlation may be detailed or general; both approaches are used in this discussion which is based on data taken from Chapter 2, Section 2, and Chapter 11, Section 1.5, for disturbance and wave tests respectively. In the detailed type of correlation the critical disturbances and wave diagrams at corresponding speeds and elevator settings are compared in an attempt to obtain a point to point correspondence over the whole (η, V)-plane; this can obviously be applied only to Model B results in the present case because of the limited test data available. In the general type of correlation an attempt is made to draw conclusions concerning whole areas of the (η, V)-plane; Model L results are most suitable for this type of treatment by virtue of the fairly good coverage of the (η, V)-plane with test points.

It should be noted that in all of the tests now under consideration the model was taken to be unstable when it oscillated in pitch with an amplitude of more than 2 deg and, because of the wave effect on attitude results are expressed in terms of elevator angle, not keel attitude.

For correlation the critical disturbance, *i.e.*, the smallest disturbance which would induce instability at any speed and elevator setting, is assumed to be equivalent to any wave system which would similarly just induce instability.

A detailed correlation may be made in the following manner. Let an x-deg disturbance limit be chosen (*see* Chapter 2, Section 4.2); the points at which the critical disturbances are greater than x deg will be stable and those at which the critical disturbances are less than x deg will be unstable. If a wave system (defined by wave height h and wave length L) can be found which, by virtue of the relevant curves of critical wave heights (*e.g.*, Fig. 115), renders the points stable and unstable in exactly the same way as does the x-deg disturbance limit and if the procedure can be repeated with disturbance limits of various values, from one which excludes to one which includes all the points, then a detailed correlation may be said to have been established. In such a correlation the converse need not necessarily be true. The aim is to interpret disturbance limits in terms of stability in waves, not *vice versa*, and in the event of a detailed correlation there may remain wave systems which have no corresponding disturbance limit.

Applying this technique to Model B and choosing initially a 3·5-deg disturbance limit, and bearing in mind the magnitudes of the critical disturbances (Tables 102 to 106), points 2B and 3B will be stable, points 1B and 4B will be unstable and point 5B will be border-line, *i.e.*, the representative point will be on or near the stability limits (Fig. 109, Table 99). Turning to Fig. 115 it can be seen that border-line stability will be obtained at point 5B in several wave systems having wave heights of the order of 0·2 beams. Selecting a wave system of wave height 0·2 beams and wave length 20 beams it can be seen that points 1B to 4B are rendered unstable thereby and this occurs with any system lying on the 5B curve. In this case, therefore, detailed correlation cannot be established. The same is true of any limit obtained with disturbance in the range 3·0 to 4·5 deg for Model B.

In attempting to make a general correlation no particular method is used; instead the wave curves and the calm-water stability limits obtained with maximum disturbance for Model L are compared and any relevant facts are considered.

The region of instability obtained with disturbance is much smaller for Model L than for Model B and, because of this, wave tests were made at points 2L, 4L, 5L and 7L to 10L, which are in the stable region which is unaffected by disturbance (Fig. 109). Even at these points wave systems were encountered which could induce instability and it is clear, therefore, that at these points there can be no wave-disturbance correlation. In the previous discussion on Model B results, limits obtained with given degrees of disturbance are considered in conjunction with critical disturbances; in the case of Model L no critical disturbances have been determined and the disturbed limit is that for maximum disturbance. This, as can be seen by analogy with Fig. 7, is probably a compound limit involving various degrees of disturbance. In a wave system which is the equivalent of this disturbed limit the previously mentioned points must be stable, points 1L, 6L, 11L, 12L and 13L must be unstable and 3L and 14L must be border-line, *i.e.*, the representative points must lie on or near the limits. Considering the curves for points 3L and 14L in Fig. 115 it can be seen that no wave system which is common to the two curves can be found. There is thus no correlation between stability characteristics in waves and the stability limit obtained with maximum disturbance.

This lack of correlation in the case of Model L is implicit in the conclusion (*c*) of Chapter 11, Section 1.6 which states in effect that as elevator angle is increased, stability characteristics in waves are improved. As some of the high

elevator-angle points (11L, 12L, 13L) lie within the disturbed unstable region (Fig. 109), where for any sort of correspondence a deterioration in model stability characteristics in waves would be expected, there can be no wave-disturbance correlation.

It would appear from fundamental considerations that if any correlation were obtained, it would be purely fortuitous. From the discussion on disturbance limits (Chapter 2, Section 4.2), it follows that there is a physical discontinuity at the limit; in going from stable to unstable regions a sudden change from steady motion to porpoising of large amplitude is obtained, whereas with the wave curves, there is a progressive increase in the amplitudes of porpoising with ingress into the unstable region and, by definition (Chapter 11, Section 1.3) porpoising on the curve is of 2-deg amplitude.

It is clear from the whole of the foregoing that disturbance limits cannot be interpreted in any way in terms of stability in waves*.

* It is interesting to note from Figs. 3 and 110 (at the wave length/height ratio of 110 : 1), that although the test conditions were the same in each case, the recording with disturbance shows no similarity to the recording with waves. The frequencies and amplitudes of oscillation, both in pitch and heave, show marked differences.

APPENDIX V

Discussion of Individual Model Results

In the main text of the report the effects of various hull-shape parameters on the stability and spray characteristics of high length/beam ratio hulls and the interaction of these effects have been determined by comparing in turn the individual hydrodynamic qualities of each of a group of models; no separate appraisal of the behaviour of each model has, however, been made. A brief account is therefore given below of the stability and spray characteristics of each model of the series and any peculiarities in behaviour which have not been considered in the main text are noted. The remarks may be taken generally as applying at the design loading of $C_{\Delta 0} = 2 \cdot 75$ and the detailed hydrodynamic characteristics of the models are illustrated in Figs. 118 to 216.

Model A.—Model A, the basic model of the series, has a simple high length/beam ratio hull with no refinements and, as may be expected, its characteristics are mediocre. Undisturbed longitudinal stability is fairly poor and deteriorates further with disturbance; spray is indifferent, but the directional stability characteristics are fairly good; trim, porpoising amplitudes and elevator effectiveness are of average values.

Model B.—Model B, with a medium amount of forebody warp, has fairly good hydrodynamic qualities. Longitudinal stability is fairly good without disturbance but it becomes very poor under disturbed conditions, and while the directional stability is indifferent, spray formation and elevator effectiveness are good.

Model C.—Model C has a highly warped forebody and is outstanding in this series because of its extremely good spray characteristics; its qualities in general are good. Longitudinal stability without disturbance is very good and with disturbance fairly good, while values of elevator effectiveness are high, but these properties are offset somewhat by rather poor directional stability.

Model D.—Model D is of short afterbody form and has poor characteristics. The initially poor longitudinal stability of this model becomes very bad with disturbance and the disturbed porpoising amplitudes are high. Spray is good, but this is associated with undesirably high hump and planing attitudes; directional stability is rather good.

Model E.—Model E has a long afterbody and, as far as one can generalise, it possesses good characteristics. Undisturbed stability is very good and disturbance has only a little effect on this, disturbed stability remaining rather good, while disturbed amplitudes of porpoising are low. Spray, however, is poor and directional stability is fairly poor while hump speed is rather high.

Model F.—Model F embodies a very long afterbody and is notable mainly for its great resistance to disturbance. This is reflected in the longitudinal stability characteristics, which are extremely good both with and without disturbance, and in the very low disturbed amplitudes of porpoising which are almost unchanged from the undisturbed case. It may also be noted that forebody porpoising when it occurs is of very low frequency. Maximum trimming angles and mean values of elevator effectiveness on the other hand are very low, spray is bad and directional stability is poor, while hump speed is high.

Model G.—Model G has a low afterbody angle and most obvious amongst its characteristics is a complete inability to resist disturbance. Undisturbed longitudinal stability is fairly good, but with disturbance this deteriorates greatly giving extremely bad disturbed characteristics. Spray and elevator effectiveness are poor, values of the latter being very low, while directional stability is fair and disturbed porpoising amplitudes are low.

Model H.—Model H is a high afterbody-angled model and it exhibits fairly good qualities. Longitudinal stability is good without disturbance but poor with disturbance, while both disturbed amplitudes of porpoising and maximum planing attitudes are high. Spray characteristics are indifferent, but directional stability is fairly good.

Model J.—Model J has a tailored afterbody and its performance is notable in two respects. Longitudinal stability is fairly good in both undisturbed and disturbed cases, illustrating an ability to resist disturbance, and directional stability is very good. The spray formation is also fairly good but disturbed porpoising amplitudes and maximum trims are very high; the undisturbed porpoising amplitudes for this model are also rather high.

Model K.—Model K* embodies a medium amount of forebody warp and a high afterbody angle and it has good hydrodynamic characteristics. Longitudinal stability is extremely good without disturbance and it remains fairly good under disturbed conditions. Spray is also good, but disturbed porpoising amplitudes and maximum trims are rather high.

* No directional stability tests were made on these models.

Model L.—Model L* has a medium amount of forebody warp and a long afterbody. It exhibits very good qualities, which include extremely good undisturbed longitudinal stability, very good disturbed stability and low disturbed amplitudes of porpoising. Spray is, however, fairly poor.

Model M.—Model M* has a high-angled and long afterbody. It has very good longitudinal stability characteristics, both undisturbed and disturbed, indicating a high resistance to disturbance, and disturbed porpoising amplitudes are low, but spray formation is mediocre.

Model N.—Model N* incorporates a medium amount of forebody warp and a long, high-angled afterbody; its properties are very good. Resistance to disturbance is high, as evidenced by very good stability both with and without, disturbance, disturbed porpoising amplitudes are fairly low and spray characteristics are good.

* No directional stability tests were made on these models.

TABLE 1

Model Aerodynamic Data

Mainplane :	
Section	Göttingen 436 (mod.)
Gross area	6·85 sq ft
Span	6·27 ft
S.M.C.	1·09 ft
Aspect ratio	5·75
Dihedral on 30 per cent spar axis	3° 0′
Sweepback on 30 per cent spar axis	4° 0′
Wing setting (root chord to hull datum)	6° 9′
Tailplane :	
Section	RAF 30 (mod.)
Gross area	1·33 sq ft
Span	2·16 ft
Total elevator area	0·72 sq ft
Tailplane setting (root chord to hull datum)	2° 0′
Fin :	
Section	RAF 30
Gross area	0·80 sq ft
Height	1·14 ft
General :	
c.g. position:*	
Distance forward of step point	0·237 ft
Distance above step point	0·731 ft
¼-chord point S.M.C.:*	
Distance forward of step point	0·277 ft
Distance above step point	1·015 ft
Tail arm (c.g. to hinge axis)*	3·1 ft
Height of tailplane root-chord leading edge above hull crown*	0·72 ft
Thrust line:	
Inclination upwards from hull datum	3° 9′
Distance from c.g. normal to thrust line	0·28 ft
Propeller diameter	0·795 ft

* These distances are measured either parallel to or normal to the hull datum as appropriate.

TABLE 2

Model Hydrodynamic Data

Data Common to All Models :

Beam at step (b)	0·475 ft
Length of forebody ($6b$)	2·850 ft
Forebody deadrise at step	25 deg
Afterbody deadrise (except for Model J)	30 deg (decreasing to 26 deg at step over forward 40 per cent of afterbody length)
Step depth (0·15b)	0·071 ft
Step form	Unfaired transverse

Other Data :

Model	Forebody warp (deg per beam)	Afterbody length (beams)	Afterbody-forebody keel angle (deg)	Moment of inertia (lb ft²)	To determine effect of
A	0	5	6	*22·9	forebody warp
B	4	5	6	†21·3	
C	8	5	6	23·7	
D	0	4	6	16·8	afterbody length
A	0	5	6	22·9	
E	0	7	6	25·0	
F	0	9	6	40·2	
G	0	5	4	23·5	afterbody angle
A	0	5	6	22·9	
H	0	5	8	23·5	
A	0	5	6	22·9	tailored afterbody
J	0	5	6	23·9	
A	0	5	6	22·9	interaction of parameters
B	4	5	6	21·3	
E	0	7	6	25·0	
H	0	5	8	23·5	
K	4	5	8	23·1	
L	4	7	6	25·5	
M	0	7	8	23·2	
N	4	7	8	23·9	

* Except at $C_{\Delta_0} = 2{\cdot}25$ in the main series of tests when the moment of inertia for Model A was 24·5 lb ft² and at $C_{\Delta_0} = 2{\cdot}75$ in the slipstream tests when the moment of inertia was 23·2 lb ft².

† Except in the moment of inertia investigation when additional moments of inertia for Model B of 26·5 and 29·8 lb ft² at $C_{\Delta_0} = 2{\cdot}50$ and of 31·7 lb ft² at $C_{\Delta_0} = 3{\cdot}00$ were used.

TABLE 3

Tests Performed on Models

Tests Performed on all Models (A to N) :

(i) Assessment of aerodynamic lift characteristics*

(ii) Assessment of hydrodynamic longitudinal stability characteristics, both with and without disturbance, at $C_{\Delta 0} = 2{\cdot}75$

(iii) Assessment of spray characteristics at $C_{\Delta 0} = 2{\cdot}75$.

Other Tests :

Model	Hydrodynamic longitudinal stability assessment at a $C_{\Delta 0}$ of	Spray Assessment at a $C_{\Delta 0}$ of	Hydrodynamic directional stability assessment at a $C_{\Delta 0}$ of
A	2·25 3·00 2·75 with take-off power 2·75 with propellers windmilling 2·75 with fairings replacing propellers	2·25 3·00 2·75 with take-off power 2·75 with propellers windmilling 2·75 with fairings replacing propellers	2·75 with no roll constraint high attitudes† 2·75 with no roll constraint low attitudes 2·75 at high attitudes 2·75 at low attitudes 2·75 at high attitudes with breaker strips
B	2·00 2·25 2·50 at three different moments of inertia 3·00 at two different moments of inertia	2·00 2·25 2·50 3·00	2·75
C	2·25	2·25	2·25 2·75
D E F G H J	2·25	2·25	2·75
A B L	2·75 Longitudinal stability tests in waves		

* The normal model configuration for all tests was with full-span slats and no propellers, fairings or nacelles.

† For the main hydrodynamic directional stability tests the model was constrained in roll and had no breaker strips, and the tests were made at low attitudes.

AERODYNAMIC LIFT CHARACTERISTICS

TABLE 4

(See also Table 8)

Model A

(With wing used for longitudinal stability tests at $C_{\Delta 0} = 2{\cdot}75$ and $3{\cdot}00$ and for directional stability tests)

Speed V (ft/sec)	Velocity coefficient C_v	Keel attitude α_K (deg)	Elevator angle η (deg)	Lift L (lb)	Lift coefficient C_L
28·0	7·16	0	−20	2·70	0·421
28·0	7·16	+ 4	−20	4·85	0·756
28·0	7·16	+ 8	−20	6·86	1·070
27·9	7·13	+12	−20	8·53	1·339
27·9	7·13	0	−10	2·98	0·468
28·0	7·16	+ 4	−10	5·28	0·824
27·8	7·08	+ 8	−10	7·09	1·120
27·8	7·08	+12	−10	8·95	1·414
20·0	5·11	0	0	1·70	0·518
27·7	7·07	0	0	3·48	0·555
20·0	5·11	+ 2	0	2·36	0·730
27·7	7·07	+ 2	0	4·52	0·721
20·0	5·11	+ 4	0	2·98	0·908
28·0	7·16	+ 4	0	5·81	0·906
20·0	5·11	+ 6	0	3·55	1·082
27·7	7·07	+ 6	0	6·65	1·061
20·0	5·11	+ 8	0	4·02	1·224
27·7	7·07	+ 8	0	7·61	1·214
20·0	5·11	+10	0	4·52	1·378
27·7	7·07	+10	0	8·45	1·348
20·0	5·11	+12	0	4·78	1·457
28·0	7·16	+12	0	9·50	1·480
27·8	7·08	0	+10	3·84	0·607
27·8	7·08	+ 4	+10	6·02	0·951
27·2	7·08	+ 8	+10	7·67	1·265
27·6	7·08	+10	+10	8·83	1·417
28·3	7·22	0	+20	4·37	0·666
28·3	7·22	+ 4	+20	6·60	1·007
28·1	7·18	+ 8	+20	8·40	1·302
27·9	7·13	+12	+20	9·89	1·550

AERODYNAMIC LIFT CHARACTERISTICS

TABLE 5

Model A

(With take-off power)

Speed V (ft/sec)	Velocity coefficient C_v	Keel attitude α_K (deg)	Elevator angle η (deg)	Lift L (lb)	Lift coefficient C_L
10·0	2·55	0	−20	1·38	1·700
20·0	5·11	0	−20	2·95	0·905
29·9	7·64	0	−20	4·87	0·670
39·5	10·10	0	−20	7·39	0·581
10·0	2·55	+ 4	−20	2·23	2·750
20·0	5·11	+ 4	−20	4·80	1·477
30·2	7·71	+ 4	−20	8·50	1·148
39·6	10·11	+ 4	−20	12·99	1·020
10·0	2·55	+ 8	−20	3·03	3·730
20·1	5·12	+ 8	−20	6·57	2·000
30·3	7·73	+ 8	−20	11·74	1·570
10·2	2·62	+12	−20	3·94	4·650
20·2	5·16	+12	−20	8·57	2·570
30·1	7·67	+12	−20	14·60	1·980
10·0	2·55	0	−10	1·33	1·640
19·9	5·09	0	−10	3·12	0·970
29·9	7·64	0	−10	5·55	0·763
39·1	10·0	0	−10	8·25	0·663
10·0	2·55	+ 4	−10	2·26	2·790
19·9	5·09	+ 4	−10	4·96	1·540
30·1	7·67	+ 4	−10	8·80	1·196
39·2	10·01	+ 4	−10	13·37	1·068
10·1	2·58	+ 8	−10	2·97	3·580
20·1	5·12	+ 8	−10	6·56	2·000
30·2	7·71	+ 8	−10	11·85	1·600
9·9	2·54	+12	−10	4·04	5·070
19·7	5·03	+12	−10	8·60	2·720
29·6	7·61	+12	−10	14·90	2·090
9·9	2·54	0	0	1·27	1·590
19·6	5·01	0	0	3·02	0·970
29·4	7·50	0	0	5·70	0·810
38·7	9·86	0	0	8·81	0·730
9·9	2·54	+ 4	0	2·37	2·970
19·6	5·01	+ 4	0	5·13	1·640
29·5	7·54	+ 4	0	9·17	1·300
39·0	9·97	+ 4	0	14·18	1·150
10·1	2·58	+ 8	0	3·26	3·930
19·6	5·01	+ 8	0	6·82	2·190
30·0	7·66	+ 8	0	12·61	1·720
39·5	10·10	+ 8	0	19·25	1·520
10·0	2·55	+12	0	4·06	4·880
20·0	5·11	+12	0	8·93	2·750
30·1	7·67	+12	0	15·35	2·080
34·7	8·87	+12	0	18·50	1·890
10·1	2·58	+14	0	4·47	5·400
20·1	5·12	+14	0	9·76	2·960
30·2	7·71	+14	0	16·25	2·190

TABLE 5—*continued*

Speed V (ft/sec)	Velocity coefficient C_v	Keel attitude α_K (deg)	Elevator angle η (deg)	Lift L (lb)	Lift coefficient C_L
10·0	2·55	0	+10	1·60	1·970
20·0	5·11	0	+10	3·70	1·135
30·1	7·67	0	+10	6·50	0·882
39·6	10·11	0	+10	10·00	0·784
10·1	2·58	+ 4	+10	2·42	2·920
20·1	5·12	+ 4	+10	5·46	1·660
30·1	7·67	+ 4	+10	9·89	1·342
39·7	10·13	+ 4	+10	15·07	1·176
10·1	2·58	+ 8	+10	3·13	3·770
20·0	5·11	+ 8	+10	7·02	2·160
30·2	7·71	+ 8	+10	12·81	1·730
10·2	2·62	+12	+10	4·14	4·890
20·2	5·16	+12	+10	9·25	2·790
30·1	7·67	+12	+10	15·90	2·160
10·1	2·58	0	+20	1·62	1·950
20·2	5·16	0	+20	3·82	1·176
30·2	7·71	0	+20	6·97	0·939
39·5	10·10	0	+20	10·76	0·848
10·1	2·58	+ 4	+20	2·44	2·930
20·1	5·12	+ 4	+20	5·48	1·665
30·2	7·71	+ 4	+20	10·28	1·386
39·7	10·13	+ 4	+20	15·57	1·215
10·2	2·62	+ 8	+20	3·32	3·930
20·3	5·19	+ 8	+20	7·22	2·160
30·2	7·71	+ 8	+20	13·30	1·790
10·1	2·58	+12	+20	4·14	4·990
20·2	5·16	+12	+20	9·50	2·860
30·2	7·71	+12	+20	16·20	2·180

AERODYNAMIC LIFT CHARACTERISTICS

TABLE 6

Model A

(With propellers windmilling)

Speed V (ft/sec)	Velocity coefficient C_v	Keel attitude α_K (deg)	Elevator angle η (deg)	Lift L (lb)	Lift coefficient C_L
24·1	6·16	− 2	−20	0·92	0·194
23·8	6·09	+ 2	−20	2·44	0·520
23·8	6·09	+ 6	−20	3·65	0·793
24·0	6·14	+10	−20	4·40	0·936
24·0	6·14	− 2	−10	1·53	0·326
23·8	6·09	+ 2	−10	2·60	0·565
23·9	6·11	+ 6	−10	3·87	0·832
24·0	6·14	+10	−10	4·30	0·960
19·8	5·06	− 2	0	1·16	0·364
27·6	7·06	− 2	0	2·21	0·357
19·8	5·06	0	0	1·68	0·525
27·8	7·08	0	0	3·31	0·526
20·0	5·11	+ 2	0	2·20	0·675
27·8	7·08	+ 2	0	4·14	0·658
20·0	5·11	+ 4	0	2·61	0·803
27·9	7·13	+ 4	0	5·25	0·828
20·0	5·11	+ 6	0	3·13	0·960
28·0	7·16	+ 6	0	6·28	0·980
20·0	5·11	+ 8	0	3·45	1·030
28·1	7·18	+ 8	0	6·79	1·060
20·1	5·14	+10	0	3·62	1·100
28·1	7·18	+10	0	6·90	1·075
20·0	5·11	+12	0	3·45	1·060
27·4	7·01	+12	0	6·51	1·070
24·0	6·14	− 2	+10	1·94	0·414
23·9	6·11	+ 2	+10	3·28	0·705
24·0	6·14	+ 6	+10	4·45	0·950
23·9	6·11	+10	+10	4·70	1·010
24·0	6·14	− 2	+20	2·27	0·485
23·9	6·11	+ 2	+20	3·58	0·770
23·9	6·11	+ 6	+20	4·70	1·010
23·9	6·11	+10	+20	4·87	1·046

AERODYNAMIC LIFT CHARACTERISTICS

TABLE 7

Model A

(With fairings)

Speed V (ft/sec)	Velocity coefficient C_v	Keel attitude α_K (deg)	Elevator angle η (deg)	Lift L (lb)	Lift coefficient C_L
24·3	6·21	− 2	−20	1·32	0·272
24·3	6·21	0	−20	2·22	0·460
24·2	6·18	+ 4	−20	3·60	0·754
24·4	6·24	+ 6	−20	4·39	0·905
24·3	6·21	+ 7	−20	4·60	0·953
24·2	6·19	+ 8	−20	4·78	0·994
24·2	6·18	+ 9	−20	4·37	0·914
24·2	6·18	+10	−20	4·34	0·908
24·4	6·24	+ 2	−10	3·15	0·649
23·7	6·06	+ 4	−10	3·55	0·774
24·4	6·24	+ 6	−10	4·40	0·906
24·0	6·14	+ 7	−10	4·70	0·950
23·5	6·01	+ 8	−10	4·05	0·900
23·6	6·03	+ 9	−10	4·01	0·882
23·7	6·06	+10	−10	4·11	0·895
20·2	5·15	− 2	0	1·20	0·360
28·3	7·24	− 2	0	2·34	0·358
20·0	5·11	0	0	1·83	0·560
28·3	7·22	0	0	3·57	0·546
19·4	4·95	+ 2	0	2·21	0·718
27·3	6·97	+ 2	0	4·44	0·729
19·9	5·09	+ 4	0	2·37	0·733
20·0	5·11	+ 4	0	2·37	0·725
23·5	5·99	+ 4	0	3·84	0·852
27·6	7·04	+ 4	0	5·21	0·824
28·2	7·19	+ 4	0	5·61	0·887
19·9	5·09	+ 6	0	3·19	0·987
27·8	7·09	+ 6	0	6·13	0·975
20·2	5·16	+ 8	0	3·13	0·939
27·8	7·09	+ 8	0	6·00	0·954
20·4	5·21	+10	0	3·06	0·900
28·0	7·16	+10	0	6·41	1·013
28·2	7·21	+10	0	6·27	0·991
28·3	7·23	+10	0	6·72	1·062
20·3	5·19	+12	0	3·32	0·985
28·2	7·21	+12	0	6·56	1·010
24·4	6·23	+ 2	+10	3·83	0·789
23·8	6·07	+ 4	+10	4·21	0·909
24·4	6·23	+ 6	+10	5·01	1·032
24·0	6·14	+ 8	+10	5·23	1·113
24·3	6·21	+ 8	+10	5·33	1·104
24·4	6·23	+ 8	+10	5·45	1·122
24·2	6·18	+ 9	+10	4·85	1·013
24·3	6·21	+ 9	+10	5·21	1·079
24·3	6·21	+10	+10	4·72	0·977
24·1	6·16	− 2	+20	2·31	0·488
24·2	6·18	+ 2	+20	3·81	0·797
24·2	6·18	+ 4	+20	4·66	0·964
24·3	6·21	+ 6	+20	5·20	1·077
24·3	6·21	+ 8	+20	5·45	1·130
24·3	6·21	+ 9	+20	5·21	1·078
23·5	6·00	+10	+20	4·69	0·996
24·2	6·17	+12	+20	4·94	1·032

AERODYNAMIC LIFT CHARACTERISTICS

TABLE 8

(*See also Table* 1)

Model A

(With wing used for longitudinal stability tests at $C_{A0} = 2{\cdot}25$)

Speed V (ft/sec)	Velocity coefficient C_v	Keel attitude α_K (deg)	Elevator angle η (deg)	Lift L (lb)	Lift coefficient C_L
26·7	6·83	0	−20	2·49	0·428
27·6	7·06	+ 6	−20	6·37	1·022
27·8	7·11	+12	−20	8·95	1·420
27·7	7·08	0	−10	3·07	0·490
27·5	7·03	+ 6	−10	6·46	1·045
27·8	7·11	+12	−10	9·20	1·460
27·5	7·03	0	0	3·54	0·573
28·0	7·16	+ 2	0	4·66	0·726
27·4	7·01	+ 4	0	5·64	0·920
27·5	7·03	+ 6	0	6·84	1·107
27·7	7·08	+ 8	0	7·98	1·273
27·7	7·08	+10	0	8·90	1·420
27·8	7·11	+12	0	9·64	1·530
27·5	7·03	0	+10	4·03	0·653
27·6	7·06	+ 6	+10	7·32	1·176
27·8	7·11	+12	+10	9·96	1·580
27·6	7·06	0	+20	4·26	0·686
27·7	7·08	+ 6	+20	7·63	1·218
27·8	7·11	+12	+20	10·09	1·600

AERODYNAMIC LIFT CHARACTERISTICS

TABLE 9

Model B

Speed V (ft/sec)	Velocity coefficient C_v	Keel attitude α_K (deg)	Elevator angle η (deg)	Lift L (lb)	Lift coefficient C_L
23·9	6·12	+ 4	−20	3·65	0·780
23·9	6·12	+ 6	−20	4·50	0·962
23·9	6·12	+ 4	−10	4·05	0·864
23·6	6·03	+ 6	−10	4·74	1·043
23·7	6·06	0	0	2·62	0·571
23·7	6·07	+ 2	0	3·40	0·738
23·8	6·09	+ 4	0	4·21	0·909
23·9	6·11	+ 6	0	4·95	1·062
24·0	6·14	+ 8	0	5·92	1·260
23·9	6·12	+10	0	6·45	1·379
23·9	6·12	+12	0	6·97	1·490
23·8	6·10	+ 4	+10	4·60	0·988
23·7	6·07	+ 6	+10	5·42	1·175
23·8	6·09	+ 4	+20	4·92	1·062
23·8	6·09	+ 6	+20	5·68	1·226

AERODYNAMIC LIFT CHARACTERISTICS

TABLE 10

Model C

Speed V (ft/sec)	Velocity coefficient C_v	Keel attitude α_K (deg)	Elevator angle η (deg)	Lift L (lb)	Lift coefficient C_L
23·4	5·98	0	−20	1·88	0·420
23·8	6·09	+ 6	−20	4·53	0·980
24·2	6·18	+12	−20	6·42	1·341
23·1	5·91	0	−10	2·08	0·478
23·8	6·09	+ 6	−10	4·64	1·002
24·2	6·18	+12	−10	6·64	1·389
20·2	5·16	0	0	1·96	0·590
20·2	5·16	+ 6	0	3·71	1·110
28·1	7·18	+ 6	0	7·16	1·110
28·2	7·21	+12	0	9·80	1·510
20·2	5·16	+12	0	4·90	1·470
23·8	6·09	0	+10	2·93	0·632
23·8	6·09	+ 6	+10	5·21	1·127
24·2	6·18	+12	+10	7·18	1·501
23·8	6·09	0	+20	3·13	0·676
23·8	6·09	+ 6	+20	5·38	1·160
24·2	6·18	+12	+20	7·31	1·530

AERODYNAMIC LIFT CHARACTERISTICS

TABLE 11

Model D

Speed V (ft/sec)	Velocity coefficient C_v	Keel attitude α_K (deg)	Elevator angle η (deg)	Lift L (lb)	Lift coefficient C_L
24·5	6·27	0	−20	2·34	0·478
24·6	6·29	+ 8	−20	5·70	1·155
24·6	6·29	+14	−20	7·40	1·500
24·6	6·29	0	−10	2·62	0·530
24·6	6·29	+ 8	−10	6·00	1·215
24·6	6·29	+14	−10	7·62	1·540
28·1	7·18	0	0	3·86	0·598
27·3	6·98	+ 8	0	7·57	1·246
24.4	6.24	0	+10	3.32	0.682
24·4	6·24	+ 8	+10	6·50	1·337
24·3	6·22	+14	+10	7·81	1·622
24·5	6·27	0	+20	3·58	0·730
24·5	6·27	+ 8	+20	6·82	1·391
24·5	6·27	+14	+20	8·15	1·665

AERODYNAMIC LIFT CHARACTERISTICS

TABLE 12

Model E

Speed V (ft/sec)	Velocity coefficient C_v	Keel attitude α_K (deg)	Elevator angle η (beg)	Lift L (lb)	Lift coefficient C_L
28·1	7·18	+ 4	−20	4·87	0·756
28·6	7·32	+ 8	−20	7·38	1·105
28·6	7·32	+12	−20	9·24	1·384
28·1	7·18	+ 2	−10	4·25	0·643
28·1	7·18	+ 6	−10	6·51	1·008
28·9	7·39	+10	−10	8·89	1·300
27·7	7·08	0	0	3·17	0·510
28·8	7·36	+ 2	0	4·88	0·720
27·9	7·13	+ 4	0	5·39	0·848
28·7	7·34	+ 6	0	7·23	1·076
27·9	7·13	+ 8	0	7·73	1·218
28·0	7·16	+12	0	9·38	1·467
28·2	7·21	+ 2	+10	4·98	0·766
28·6	7·32	+ 6	+10	7·52	1·128
28·0	7·16	+10	+10	8·95	1·400
28·2	7·21	0	+20	4·00	0·632
28·8	7·36	+ 4	+20	6·75	0·998
28·8	7·36	+ 8	+20	8·75	1·283
28·8	7·36	+12	+20	10·51	1·552

AERODYNAMIC LIFT CHARACTERISTICS

TABLE 13

Model F

Speed V (ft/sec)	Velocity coefficient C_v	Keel attitude α_K (deg)	Elevator angle η (deg)	Lift L (lb)	Lift coefficient C_L
27·1	6·92	0	−20	3·00	0·500
27·5	7·02	+ 4	−20	5·25	0·850
27·6	7·05	+ 8	−20	7·13	1·150
27·7	7·07	+12	−20	8·81	1·410
27·3	6·98	0	−10	3·50	0·576
27·6	7·05	+ 4	−10	5·60	0·900
27·6	7·05	+ 8	−10	7·64	1·230
27·6	7·05	+12	−10	9·21	1·480
19·7	5·03	0	0	1·93	0·610
27·2	6·95	0	0	3·85	0·637
19·3	4·93	+ 4	0	2·95	0·973
27·4	7·00	+ 4	0	6·07	0·990
19·5	4·98	+ 8	0	4·01	1·287
26·1	6·68	+ 8	0	7·17	1·283
26·8	6·86	+12	0	8·91	1·520
27·3	6·98	0	+10	4·25	0·697
27·4	7·00	+ 4	+10	6·36	1·040
27·3	6·98	+ 8	+10	8·15	1·340
27·6	7·05	+12	+10	9·85	1·580
27·3	6·98	0	+20	4·61	0·756
27·3	6·98	+ 4	+20	6·73	1·100
27·3	6·98	+ 8	+20	8·45	1·390
27·6	7·05	+12	+20	10·15	1·630

AERODYNAMIC LIFT CHARACTERISTICS

TABLE 14

Model G

Speed V (ft/sec)	Velocity coefficient C_v	Keel attitude α_K (deg)	Elevator angle η (deg)	Lift L (lb)	Lift coefficient C_L
27·5	7·02	0	−20	2·58	0·417
27·5	7·02	+ 4	−20	4·78	0·773
27·0	6·90	+ 8	−20	6·50	1·093
27·0	6·90	+12	−20	7·92	1·331
27·5	7·02	0	−10	2·97	0·480
27·5	7·02	+ 4	−10	5·08	0·820
27·0	6·90	+ 8	−10	6·85	1·154
26·9	6·87	+12	−10	8·21	1·390
26·6	6·79	0	0	3·16	0·547
26·9	6·87	+ 4	0	5·21	0·882
27·0	6·90	+ 8	0	7·14	1·198
27·2	6·96	+12	0	8·72	1·445
27·6	7·06	0	+10	3·80	0·611
27·4	7·00	+ 4	+10	5·86	0·957
27·0	6·90	+ 8	+10	7·53	1·285
26·8	6·85	+12	+10	8·76	1·492
27·7	7·08	0	+20	4·09	0·653
27·3	6·98	+ 4	+20	6·15	1·010
27·3	6·98	+ 8	+20	7·98	1·310

AERODYNAMIC LIFT CHARACTERISTICS

TABLE 15

Model H

Speed V (ft/sec)	Velocity coefficient C_v	Keel attitude α_K (deg)	Elevator angle η (deg)	Lift L (lb)	Lift coefficient C_L
26·5	6·77	0	−20	2·28	0·399
27·9	7·13	+ 4	−20	4·91	0·773
27·4	7·00	+ 8	−20	6·75	1·102
27·7	7·08	+10	−20	7·95	1·275
27·5	7·03	+12	−20	8·65	1·405
27·5	7·03	+14	−20	9·50	1·540
27·0	6·90	0	−10	2·83	0·476
27·9	7·13	+ 4	−10	5·31	0·838
27·4	7·00	+ 8	−10	7·15	1·168
27·5	7·03	+10	−10	8·20	1·330
27·7	7·08	+10	−10	8·40	1·343
27·5	7·03	+12	−10	9·15	1·484
27·4	7·00	+14	−10	9·69	1·581
27·0	6·90	0	0	3·28	0·551
27·0	6·90	+ 4	0	5·32	0·897
27·2	6·95	+ 8	0	7·50	1·230
27·3	6·98	+12	0	9·44	1·557
27·1	6·92	0	+10	3·63	0·607
27·8	7·11	+ 4	+10	6·10	0·969
27·5	7·03	+ 8	+10	8·00	1·300
27·8	7·11	+10	+10	9·10	1·444
27·8	7·11	+12	+10	9·89	1·573
27·3	6·98	0	+20	3·94	0·647
27·8	7·11	+ 4	+20	6·40	1·016
27·5	7·03	+ 8	+20	8·25	1·342
27·6	7·06	+10	+20	9·15	1·475
35·1	8·96	+10	+20	14·66	1·462

AERODYNAMIC LIFT CHARACTERISTICS

TABLE 16

Model J

Speed V (ft/sec)	Velocity coefficient C_v	Keel attitude α_K (deg)	Elevator angle η (deg)	Lift L (lb)	Lift coefficient C_L
26·9	6·88	0	−30	2·85	0·482
27·6	7·06	+ 4	−30	5·17	0·830
27·8	7·11	+ 8	−30	7·15	1·134
27·2	6·95	+12	−30	8·41	1·393
27·7	7·08	+16	−30	8·10	1·293
26·6	6·80	0	−20	2·85	0·493
27·5	7·03	+ 4	−20	5·17	0·836
27·8	7·11	+ 8	−20	7·24	1·147
27·1	6·93	+12	−20	8·41	1·404
27·7	7·08	+16	−20	8·28	1·323
25·8	6·59	0	−10	2·99	0·550
27·5	7·03	+ 4	−10	5·65	0·915
27·7	7·08	+ 8	−10	7·62	1·217
27·8	7·11	+12	−10	9·26	1·465
27·7	7·08	+16	−10	8·42	1·345
26·9	6·88	0	0	3·55	0·600
27·2	6·95	+ 2	0	4·55	0·754
27·3	6·98	+ 4	0	5·82	0·957
27·4	7·00	+ 6	0	6·91	1·130
27·7	7·08	+ 8	0	7·90	1·262
27·8	7·11	+10	0	8·71	1·380
27·6	7·06	+12	0	9·41	1·513
27·7	7·08	+14	0	10·16	1·620
28·0	7·16	+15	0	10·03	1·570
27·4	7·00	+16	0	8·56	1·400
27·1	6·93	0	+10	4·07	0·680
27·2	6·95	+ 4	+10	6·10	1·001
27·8	7·11	+ 8	+10	8·38	1·325
27·4	7·00	+12	+10	9·50	1·553
27·8	7·11	+16	+10	9·27	1·470
27·2	6·95	0	+20	4·48	0·740
27·2	6·95	+ 4	+20	6·48	1·073
27·8	7·11	+ 8	+20	8·47	1·342
27·5	7·03	+12	+20	9·65	1·562
27·8	7·16	+16	+20	9·36	1·482
27·3	6·98	0	+30	4·45	0·735
27·4	7·00	+ 4	+30	6·68	1·090
27·8	7·11	+ 8	+30	8·42	1·337
28·0	7·16	+16	+30	9·41	1·472

AERODYNAMIC LIFT CHARACTERISTICS

TABLE 17

Model K

Speed V (ft/sec)	Velocity coefficient C_v	Keel attitude α_K (deg)	Elevator angle η (deg)	Lift L (lb)	Lift coefficient C_L
27·7	7·08	0	−20	2·71	0·430
27·7	7·08	+ 6	−20	6·10	0·970
27·3	6·98	+12	−20	8·51	1·400
27·6	7·05	0	−10	3·13	0·500
27·6	7·05	+ 6	−10	6·56	1·060
27·5	7·03	+12	−10	8·92	1·440
27·0	6·90	0	0	3·32	0·560
27·1	6·92	+ 4	0	5·45	0·910
27·3	6·98	+ 4	0	5·75	0·950
27·4	7·00	+ 8	0	7·70	1·260
27·4	7·00	+12	0	9·12	1·490
27·5	7·03	+14	0	9·84	1·590
27·7	7·08	0	+10	4·00	0·640
27·5	7·03	+ 6	+10	7·18	1·160
27·5	7·03	+12	+10	9·63	1·560
27·8	7·11	0	+20	4·21	0·670
27·3	6·98	+ 6	+20	7·38	1·210
27·5	7·03	+12	+20	9·86	1·590
27·6	7·06	+12	+20	9·89	1·590

AERODYNAMIC LIFT CHARACTERISTICS

TABLE 18

Model L

Speed V (ft/sec)	Velocity coefficient C_v	Keel attitude α_K (deg)	Elevator angle η (deg)	Lift L (lb)	Lift coefficient C_L
27·1	6·92	0	−20	2·45	0·410
27·8	7·11	+ 6	−20	6·01	0·950
27·8	7·11	+12	−20	8·67	1·380
27·0	6·90	0	−10	2·86	0·480
27·8	7·11	+ 6	−10	6·42	1·020
27·5	7·03	+12	−10	8·83	1·430
26·9	6·87	0	0	3·28	0·560
27·1	6·92	+ 4	0	5·55	0·930
27·2	6·95	+ 8	0	7·50	1·240
27·3	6·98	+12	0	9·02	1·480
26·3	6·73	0	+10	3·48	0·620
27·9	7·13	+ 6	+10	7·35	1·160
27·3	6·98	+12	+10	9·33	1·530
26·0	6·65	0	+20	3·68	0·670
27·9	7·13	+ 6	+20	7·66	1·210
27·4	7·00	+12	+20	9·48	1·550

AERODYNAMIC LIFT CHARACTERISTICS

TABLE 19

Model M

Speed V (ft/sec)	Velocity coefficient C_v	Keel attitude α_K (deg)	Elevator angle η (deg)	Lift L (lb)	Lift coefficient C_L
27·7	7·08	0	−20	2·57	0·411
27·8	7·11	+ 4	−20	4·72	0·750
27·8	7·11	+ 8	−20	6·71	1·070
27·5	7·05	+12	−20	8·30	1·350
27·4	7·00	0	−10	2·95	0·482
27·8	7·11	+ 4	−10	5·26	0·836
27·8	7·11	+ 8	−10	7·12	1·135
27·4	7·00	+12	−10	8·54	1·400
27·8	7·11	0	0	3·48	0·551
27·8	7·11	+ 2	0	4·54	0·720
27·8	7·11	+ 4	0	5·60	0·890
27·8	7·11	+ 6	0	6·61	1·055
27·8	7·11	+ 8	0	7·56	1·200
26·7	6·83	+10	0	7·73	1·336
27·2	6·96	+12	0	8·59	1·425
27·3	6·98	0	+10	3·72	0·613
27·8	7·11	+ 4	+10	6·08	0·967
27·8	7·11	+ 8	+10	8·04	1·280
26·9	6·88	+10	+10	8·30	1·410
27·3	6·98	+12	+10	9·05	1·493
27·4	7·00	0	+20	4·05	0·661
27·8	7·11	+ 4	+20	6·41	1·020
27·9	7·13	+ 8	+20	8·23	1·310
27·8	7·11	+ 8	+20	8·30	1·310
27·4	7·00	+12	+20	9·23	1·512

AERODYNAMIC LIFT CHARACTERISTICS

TABLE 20

Model N

Speed V (ft/sec)	Velocity coefficient C_v	Keel attitude α_K (deg)	Elevator angle η (deg)	Lift L (lb)	Lift coefficient C_L
28·0	7·16	0	−20	2·51	0·392
28·0	7·16	+ 4	−20	4·70	0·739
28·3	7·23	+ 8	−20	6·90	1·060
28·3	7·23	+12	−20	8·50	1·305
28·3	7·23	+12	−20	8·70	1·330
28·0	7·16	0	−10	2·80	0·440
27·8	7·11	+ 4	−10	5·10	0·812
28·4	7·26	+ 8	−10	7·46	1·140
27·9	7·12	+12	−10	8·54	1·350
28·0	7·16	0	0	3·30	0·518
28·2	7·21	0	0	3·46	0·532
28·3	7·24	+ 2	0	4·64	0·711
28·2	7·21	+ 4	0	5·65	0·872
27·7	7·08	+ 6	0	6·50	1·040
27·6	7·06	+ 6	0	6·49	1·050
27·9	7·14	+ 8	0	7·51	1·186
27·9	7·14	+10	0	8·21	1·300
28·3	7·24	+12	0	9·17	1·405
28·0	7·16	0	+10	3·84	0·602
28·0	7·16	+ 4	+10	5·90	0·927
28·2	7·21	+ 8	+10	8·00	1·240
28·4	7·26	+12	+10	9·54	1·455
28·1	7·17	0	+20	4·05	0·630
27·6	7·06	+ 4	+20	6·14	0·992
28·2	7·21	+ 8	+20	8·31	1·284
28·4	7·26	+12	+20	9·63	1·470

UNDISTURBED HYDRODYNAMIC LONGITUDINÁL STABILITY CHARACTERISTICS

TABLE 21

Model A

($C_{\Delta 0} = 2{\cdot}25$; $I = 24{\cdot}46$ lb ft^2)

Speed V (ft/sec)	Velocity coefficient C_v	Keel attitude α_K (deg)	Elevator angle η (deg)	Stable (S) Unstable (US) Border-line (B) Skipping (Sk)	Amplitude of porpoising if any (deg)	Limits of porpoising (deg)
20·5	5·24	10·5	−16	S	—	—
23·6	6·03	10·3	−16	S	—	—
27·8	7·11	10·3	−16	B Sk	1½	—
29·7	7·60	10·3	−16	US Sk	3	—
21·7	5·55	10·2	−12	S	—	—
25·5	6·52	10·2	−12	S	—	—
29·5	7·55	10·2	−12	S	—	—
33·5	8·57	10·1	−12	US Sk	3	—
0	0	3·2	− 8	S	—	—
4·0	1·02	3·1	− 8	S	—	—
7·8	1·99	5·2	− 8	S	—	—
12·0	3·07	6·0	− 8	S	—	—
14·0	3·58	7·4	− 8	S	—	—
16·0	4·09	10·2	− 8	S	—	—
17·8	4·56	10·6	− 8	S	—	—
19·5	4·98	10·4	− 8	S	—	—
21·0	5·37	10·2	− 8	B	1	—
23·7	6·06	9·8	− 8	S	—	—
27·4	7·01	9·7	− 8	S	—	—
31·4	8·03	9·6	− 8	S	—	—
34·6	8·85	9·2	− 8	S	—	—
22·8	5·83	9·7	− 6	S	—	—
25·1	6·42	9·3	− 6	S	—	—
27·6	7·06	9·0	− 6	S	—	—
31·5	8·06	8·3	− 6	S	—	—
35·3	9·03	8·2	− 6	S	—	—
19·7	5·04	10·2	− 4	S	—	—
20·8	5·32	10·0	− 4	US	4½	—
21·8	5·58	9·8	− 4	US	5	—
22·9	5·86	9·4	− 4	S	—	—
25·5	6·52	8·5	− 4	S	—	—
29·9	7·65	7·2	− 4	S	—	—
33·0	8·44	6·8	− 4	S	—	—
37·0	9·46	6·9	− 4	S	—	—
27·5	7·03	7·2	− 2	S	—	—
28·9	7·39	6·9	− 2	S	—	—
30·1	7·70	6·2	− 2	S	—	—
31·2	7·98	6·2	− 2	S	—	—
33·0	8·44	5·4	− 2	S	—	—
37·0	9·46	4·3	− 2	S	—	—

TABLE 21—*continued*

Speed V (ft/sec)	Velocity coefficient C_v	Keel attitude α_K (deg)	Elevator angle η (deg)	Stable (S) Unstable (US) Border-line (B) Skipping (Sk)	Amplitude of porpoising if any (deg)	Limits of porpoising (deg)
20·4	5·22	9·8	0	US	$3\frac{1}{2}$	—
23·8	6·09	8·3	0	S	—	—
27·8	7·11	6·8	0	S	—	—
29·9	7·65	5·8	0	S	—	—
33·8	8·65	4·3	0	S	—	—
38·0	9·72	3·2	0	S	—	—
22·4	5·73	8·7	+ 4	US	$2\frac{1}{2}$	—
23·6	6·03	7·7	+ 4	US	>2	—
24·8	6·34	7·0	+ 4	B	$1\frac{1}{2}$	—
27·2	6·96	5·8	+ 4	B	$1\frac{1}{2}$	—
29·5	7·55	4·9	+ 4	S	—	—
33·0	8·44	3·8	+ 4	S	—	—
36·8	9·41	3·0	+ 4	S	—	—
23·7	6·06	7·2	+ 6	US	$4\frac{1}{2}$	—
24·7	6·32	6·7	+ 6	US	4	—
27·5	7·03	5·3	+ 6	US	8	—
31·5	8·06	4·0	+ 6	US	$3\frac{1}{2}$	—
35·0	8·95	3·0	+ 6	US	4	—

UNDISTURBED HYDRODYNAMIC LONGITUDINAL STABILITY CHARACTERISTICS

TABLE 22

Model A

($C_{\Delta 0} = 2{\cdot}75$; $I = 22{\cdot}90$ lb ft^2)

Speed V (ft/sec)	Velocity coefficient C_v	Keel attitude α_K (deg)	Elevator angle η (deg)	Stable (S) Unstable (US) Border-line (B) Skipping (Sk)	Amplitude of porpoising if any (deg)	Limits of porpoising (deg)
20·0	5·11	11·8	−20	S	—	—
21·1	5·39	11·7	−20	S	—	—
22·3	5·70	11·4	−20	US	2½	—
25·0	6·39	11·2	−20	B	1	—
28·1	7·17	11·2	−20	S	—	—
31·0	7·91	11·1	−20	B	1	—
33·0	8·44	11·1	−20	US	10	—
34·6	8·85	11·2	−20	US	4	—
33·9	8·66	11·0	—	US	3	—
36·0	9·21	11·0	—	US	4	—
24·0	6·13	10·9	−12	US	10	—
25·6	6·54	10·6	−12	S	—	—
33·0	8·43	10·6	−12	S	—	—
34·4	8·79	10·6	−12	S	—	—
36·0	9·20	10·7	−12	B	2	—
38·1	9·74	10·6	−12	US	2½	—
0	0	3·4	− 8	S	—	—
3·9	1·00	3·5	− 8	S	—	—
8·2	2·10	5·9	− 8	S	—	—
12·1	3·10	6·9	− 8	S	—	—
16·4	4·19	11·4	− 8	S	—	—
18·0	4·60	11·7	− 8	S	—	—
20·1	5·13	11·4	− 8	S	—	—
25·1	6·42	10·4	− 8	B	2	8 to 10
26·1	6·67	10·3	− 8	S	—	—
32·0	8·18	9·9	− 8	S	—	—
35·5	9·08	9·9	− 8	S	—	—
39·4	10·09	9·4	− 8	S	—	—
27·8	7·10	9·3	− 4	S	—	—
29·0	7·41	9·0	− 4	S	—	—
30·0	7·66	8·8	− 4	S	—	—
32·0	8·18	8·4	− 4	S	—	—
33·8	8·65	8·2	− 4	S	—	—
20·1	5·14	11·4	0	S	—	—
21·0	5·36	11·0	0	S	—	—
21·4	5·47	11·0	0	US	4	8 to 12

TABLE 22—*continued*

Speed V (ft/sec)	Velocity coefficient C_v	Keel attitude α_K (deg)	Elevator angle η (deg)	Stable (S) Unstable (US) Border-line (B) Skipping (Sk)	Amplitude of porpoising if any (deg)	Limits of porpoising (deg)
22·1	5·65	10·9	0	US	6	—
24·1	6·16	10·4	0	US	—	—
24·3	6·21	10·3	0	B	2	8 to 10
26·1	6·67	9·2	0	B	$1\frac{1}{2}$	12 to $13\frac{1}{2}$
28·0	7·15	8·3	0	S	—	—
29·9	7·64	7·8	0	S	—	—
31·7	8·10	7·2	0	S	—	—
33·7	8·61	6·6	0	S	—	—
34·7	8·86	6·2	0	S	—	—
35·5	9·08	6·0	0	S	—	—
37·5	9·59	5·4	0	S	—	—
25·8	6·59	8·7	+ 4	B	2	—
27·2	6·96	7·8	+ 4	B	1	—
28·2	7·21	7·4	+ 4	B	$1\frac{1}{2}$	—
29·4	7·52	6·8	+ 4	B	1	—
30·3	7·74	6·6	+ 4	S	—	—
34·1	8·71	5·4	+ 4	S	—	—
37·0	9·45	4·5	+ 4	S	—	—
39·7	10·16	3·9	+ 4	S	—	—
21·1	5·39	10·8	+ 6	US	4	8 to 12
23·6	6·03	9·7	+ 6	US	6	—
26·0	6·65	8·4	+ 6	US	5	5 to 10
27·0	6·89	7·4	+ 6	US	$3\frac{1}{2}$	6 to $9\frac{1}{2}$
30·0	7·66	6·5	+ 6	US	3	4 to 7
31·0	7·93	5·9	+ 6	B	$1\frac{1}{2}$	$4\frac{1}{2}$ to 6
35·5	9·09	4·4	+ 6	US	—	—
39·4	10·09	3·4	+ 6	S	—	—
28·1	7·19	6·9	+ 8	US	7	4 to 11
24·3	6·21	9·2	+10	US	—	—
25·4	6·48	8·6	+10	US	—	—
26·4	6·74	7·7	+10	US	—	—
30·3	7·74	5·9	+10	US	—	—
31·5	8·06	5·3	+10	US	—	—
34·2	8·75	4·8	+10	US	—	—
37·9	9·69	3·1	+10	US	—	—

UNDISTURBED HYDRODYNAMIC LINGITUDINAL STABILITY CHARACTERISTICS

TABLE 23

Model A

($C_{\Delta 0} = 3{\cdot}00$; $I = 22{\cdot}90$ lb ft^2)

Speed V (ft/sec)	Velocity coefficient C_v	Keel attitude α_K (deg)	Elevator angle η (deg)	Stable (S) Unstable (US) Border-line (B) Skipping (Sk)	Amplitude of porpoising if any (deg)	Limits of porpoising (deg)
22·2	5·67	12·1	−20	S	—	—
25·7	6·56	11·4	−20	US	—	—
29·8	7·61	11·3	−20	S	—	—
33·5	8·56	11·4	−20	US	2½	—
37·5	9·59	11·3	−20	US	—	—
26·2	6·69	10·8	−12	S	—	—
29·9	7·64	10·7	−12	S	—	—
33·5	8·56	10·8	−12	S	—	—
37·6	9·61	10·8	−12	US	3	—
0	0	3·4	− 8	S	—	—
4·0	1·02	3·5	− 8	S	—	—
8·1	2·07	5·9	− 8	S	—	—
12·0	3·07	7·3	− 8	S	—	—
16·1	4·12	11·9	− 8	S	—	—
19·8	5·06	12·0	− 8	S	—	—
23·7	6·06	11·7	− 8	US	6	6 to 12
27·9	7·14	10·6	− 8	S	—	—
31·6	8·07	10·6	− 8	S	—	—
35·4	9·05	10·3	− 8	S	—	—
39·2	10·02	10·0	− 8	S	—	—
22·0	5·62	11·8	− 4	US	6	—
26·0	6·64	10·7	− 4	US	4	—
29·9	7·64	9·8	− 4	S	—	—
33·7	8·61	9·4	− 4	S	—	—
37·6	9·61	9·3	− 4	S	—	—
34·6	8·84	8·1	− 2	S	—	—
36·1	9·24	7·8	− 2	S	—	—
38·1	9·74	7·5	− 2	S	—	—
39·2	10·02	7·3	− 2	S	—	—
21·3	5·44	11·4	0	S	—	—
23·7	6·06	11·1	0	US	10	—
27·9	7·14	8·9	0	S	—	—
31·5	8·05	7·9	0	S	—	—
35·4	9·05	6·9	0	S	—	—
39·0	9·96	6·4	0	S	—	—
20·2	5·16	11·6	+ 4	S	—	—
24·3	6·21	10·7	+ 4	US	10	—
28·0	7·16	8·1	+ 4	B	1½	—
31·8	8·12	7·0	+ 4	B	½	—
35·6	9·10	5·6	+ 4	S	—	—
39·7	10·16	4·7	+ 4	S	—	—
20·2	5·17	11·4	+ 8	S	—	—
21·1	5·39	10·9	+ 8	B	1	—
22·0	5·62	10·9	+ 8	US	7	—
25·5	6·52	9·6	+ 8	US	—	—
29·8	7·62	7·1	+ 8	US	—	—
33·5	8·56	5·7	+ 8	US	4	—
37·5	9·59	3·9	+ 8	US	4	—

UNDISTURBED HYDRODYNAMIC LONGITUDINAL STABILITY CHARACTERISTICS

TABLE 24

Model A

(With take-off power)

($C_{\Delta 0} = 2{\cdot}75$; $I = 23{\cdot}25$ lb ft^2)

Speed V (ft/sec)	Velocity coefficient C_v	Keel attitude α_K (deg)	Elevator angle η (deg)	Stable (S) Unstable (US) Border-line (B) Skipping (Sk)	Amplitude of porpoising if any (deg)	Limits of porpoising (deg)
19·2	4·91	9·9	−24	S	—	—
22·1	5·65	9·6	−24	US	—	—
24·1	6·15	9·5	−24	S	—	—
28·1	7·19	9·8	−24	S	—	—
30·2	7·72	9·9	−24	S	—	—
31·2	7·98	9·9	−24	US	—	—
19·1	4·88	9·8	−16	S	—	—
19·9	5·08	9·8	−16	US	4½	—
22·2	5·68	9·4	−16	US	—	—
24·1	6·16	9·2	−16	S	—	—
26·1	6·67	9·3	−16	S	—	—
28·0	7·16	9·3	−16	S	—	—
30·1	7·70	9·2	−16	S	—	—
32·0	8·18	9·2	−16	S	—	—
33·8	8·65	9·0	−16	US	—	—
35·5	9·08	8·6	−16	US	—	—
24·9	6·37	8·5	−12	S	—	—
26·0	6·65	8·1	−12	S	—	—
27·5	7·04	8·3	−12	S	—	—
29·9	7·65	8·3	−12	S	—	—
31·8	8·14	8·2	−12	S	—	—
32·7	8·36	8·2	−12	S	—	—
35·5	9·08	8·0	−12	S	—	—
0	0	2·8	− 8	S	—	—
3·8	0·97	2·7	− 8	S	—	—
8·1	2·07	5·0	− 8	S	—	—
12·0	3·07	6·0	− 8	S	—	—
16·1	4·12	9·6	− 8	S	—	—
18·1	4·63	9·7	− 8	S	—	—
20·2	5·17	9·5	− 8	US	5	—
24·0	6·14	8·3	− 8	S	—	—
26·0	6·64	7·4	− 8	S	—	—
28·0	7·16	6·8	− 8	S	—	—
31·8	8·14	7·1	− 8	S	—	—
35·5	9·08	7·4	− 8	S	—	—
38·5	9·85	7·7	− 8	S	—	—
22·1	5·65	8·8	− 4	US	—	—
24·0	6·13	7·9	− 4	US	—	—
27·8	7·10	5·8	− 4	S	—	—
31·8	8·14	5·2	− 4	S	—	—
39·5	10·11	5·3	− 4	S	—	—
25·0	6·39	6·8	0	US	—	—
27·6	7·06	5·2	0	S	—	—
31·4	8·04	4·4	0	S	—	—
35·4	9·05	3·8	0	S	—	—
39·1	10·00	3·4	0	S	—	—
18·0	4·61	9·3	+ 4	S	—	—
18·9	4·84	9·0	+ 4	B	2	—
19·7	5·04	8·6	+ 4	US	—	—
28·0	7·16	4·5	+ 4	US	—	—
32·0	8·18	3·8	+ 4	US	—	—
35·9	9·18	3·0	+ 4	US	—	—
39·4	10·09	3·0	+ 4	US	—	—

UNDISTURBED HYDRODYNAMIC LONGITUDINAL STABILITY CHARACTERISTICS

TABLE 25

Model A

(With propellers windmilling)

($C_{\Delta 0} = 2{\cdot}75$; $I = 23{\cdot}25$ lb ft^2)

Speed V (ft/sec)	Velocity coefficient C_v	Keel attitude α_K (deg)	Elevator angle η (deg)	Stable (S) Unstable (US) Border-line (B) Skipping (Sk)	Amplitude of porpoising if any (deg)	Limits of porpoising (deg)
21·0	5·37	11·9	−16	S	—	—
24·0	6·14	11·4	−16	B	1½	—
29·4	7·52	11·1	−16	S	—	—
35·4	9·05	11·0	−16	S	—	—
36·4	9·31	10·9	−16	B	1	—
37·3	9·55	10·9	−16	US	2	—
23·5	6·01	11·3	−12	US	—	—
24·5	6·26	11·1	−12	B	1½	—
27·3	6·98	10·9	−12	S	—	—
31·4	8·03	10·9	−12	S	—	—
35·2	9·00	10·9	−12	S	—	—
38·5	9·85	10·7	−12	US	>2	—
0	0	3·5	− 8	S	—	—
4·0	1·02	3·5	− 8	S	—	—
7·8	1·99	5·9	− 8	S	—	—
11·7	2·99	6·9	− 8	S	—	—
15·9	4·07	11·2	− 8	S	—	—
19·4	4·95	12·1	− 8	S	—	—
27·0	6·90	10·7	− 8	S	—	—
31·0	7·92	10·4	− 8	S	—	—
34·8	8·90	10·1	− 8	S	—	—
38·9	9·95	10·3	− 8	S	—	—
21·8	5·57	11·8	− 4	S	—	—
25·5	6·52	11·0	− 4	B	1	—
29·2	7·46	10·2	− 4	S	—	—
33·0	8·44	9·4	− 4	S	—	—
37·0	9·46	8·4	− 4	S	—	—
22·6	5·78	11·4	0	S	—	—
27·3	6·98	9·9	0	S	—	—
31·0	7·93	8·4	0	S	—	—
33·5	8·56	7·8	0	S	—	—
37·5	9·59	6·4	0	S	—	—
21·5	5·50	11·2	+ 4	S	—	—
25·1	6·42	10·3	+ 4	US	—	—
29·3	7·49	8·4	+ 4	S	—	—
32·7	8·36	7·3	+ 4	S	—	—
36·5	9·34	5·8	+ 4	S	—	—
22·0	5·63	11·1	+ 8	S	—	—
25·2	6·44	10·0	+ 8	US	—	—
27·4	7·00	8·9	+ 8	B	1	—
29·4	7·52	7·9	+ 8	B	1	—
33·0	8·44	5·8	+ 8	B	1½	—
36·8	9·41	4·2	+ 8	S	—	—
23·0	5·88	10·6	+12	US	—	—
27·3	6·98	8·3	+12	US	4	—
31·2	7·98	5·7	+12	US	3	—
34·6	8·85	4·3	+12	US	6	—

UNDISTURBED HYDRODYNAMIC LONGITUDINAL STABILITY CHARACTERISTICS

TABLE 26

Model A

(With fairings)

($C_{\Delta 0} = 2{\cdot}75$; $I = 23{\cdot}25$ lb ft²)

Speed V (ft/sec)	Velocity coefficient C_v	Keel attitude α_K (deg)	Elevator angle η (deg)	Stable (S) Unstable (US) Border-line (B) Skipping (Sk)	Amplitude of porpoising if any (deg)	Limits of porpoising (deg)
25·1	6·41	11·6	−24	US	—	—
27·0	6·91	11·1	−24	[S]	—	—
29·1	7·44	11·1	−24	[S]	—	—
32·0	8·18	11·1	−24	S	—	—
33·9	8·66	11·1	−24	S	—	—
34·8	8·90	11·1	−24	US	—	—
20·0	5·11	11·7	−16	S	—	—
21·1	5·40	11·6	−16	S	—	—
22·1	5·65	11·4	−16	B	1½	—
23·5	6·01	11·2	−16	US	—	—
25·5	6·52	10·9	−16	B	1½	—
27·5	7·04	10·6	−16	S	—	—
29·6	7·56	10·6	−16	S	—	—
33·8	8·65	10·7	−16	S	—	—
35·5	9·08	10·8	−16	B	1½	—
0	0	3·2	− 8	S	—	—
4·0	1·02	3·6	− 8	S	—	—
8·1	2·07	5·6	− 8	S	—	—
11·8	3·02	6·6	− 8	S	—	—
16·0	4·09	10·2	− 8	S	—	—
19·7	5·03	10·9	− 8	S	—	—
20·8	5·32	11·2	− 8	S	—	—
23·5	6·01	10·9	− 8	S	—	—
27·5	7·04	10·1	− 8	US	—	—
31·8	8·13	9·7	− 8	S	—	—
35·5	9·08	10·1	− 8	S	—	—
37·8	9·66	10·1	− 8	S	—	—
39·6	10·12	10·0	− 8	S	—	—
20·7	5·30	11·0	− 4	S	—	—
23·5	6·01	10·7	− 4	US	—	—
27·5	7·04	9·5	− 4	S	—	—
31·9	8·15	8·7	− 4	S	—	—
35·7	9·13	8·2	− 4	S	—	—
38·6	9·86	8·3	− 4	S	—	—
21·5	5·50	10·9	0	S	—	—
25·9	6·62	9·8	0	B	1½	—
30·0	7·66	7·7	0	S	—	—
33·7	8·62	6·3	0	S	—	—
37·6	9·61	5·3	0	S	—	—
23·0	5·88	10·5	+ 4	US	—	—
26·9	6·88	8·1	+ 4	B	2	—
31·0	7·93	6·3	+ 4	S	—	—
34·7	8·87	5·1	+ 4	S	—	—
38·6	9·88	4·0	+ 4	S	—	—
22·0	5·63	10·7	+ 8	S	—	—
26·1	6·67	8·4	+ 8	US	—	—
28·0	7·16	7·0	+ 8	US	—	—
30·1	7·70	5·9	+ 8	B	1	—
33·9	8·67	4·5	+ 8	B	1	—
37·8	9·67	3·4	+ 8	B	1	—
30·0	7·67	5·0	+12	US	4	4 to 8
34·0	8·70	3·8	+12	US	—	—

UNDISTURBED HYDRODYNAMIC LONGITUDINAL STABILITY CHARACTERISTICS

TABLE 27

Model B

($C_{\Delta 0} = 2{\cdot}00$; $I = 21{\cdot}30$ lb ft^2)

Speed V (ft/sec)	Velocity coefficient C_v	Keel attitude α_K (deg)	Elevator angle η (deg)	Stable (S) Unstable (US) Border-line (B) Skipping (Sk)	Amplitude of porpoising if any (deg)	Limits of porpoising (deg)
20·0	5·11	9·8	−16	S	—	—
25·9	6·62	10·0	−16	S	—	—
28·8	7·36	10·0	−16	B	1½	—
31·9	8·16	9·6	−16	US	3	—
29·9	7·65	9·8	−12	B	1	—
33·5	8·57	9·1	−12	US	3	—
33·5	8·57	8·9	—	S	—	—
0	0	2·7	− 8	S	—	—
4·0	1·02	2·6	− 8	S	—	—
8·3	2·12	4·6	− 8	S	—	—
12·3	3·15	5·2	− 8	S	—	—
16·7	4·27	9·4	− 8	S	—	—
20·5	5·24	9·2	− 8	S	—	—
23·5	6·01	8·3	− 8	S	—	—
27·6	7·06	8·3	− 8	S	—	—
31·5	8·05	8·3	− 8	S	—	—
35·5	9·08	7·8	− 8	S	—	—
19·9	5·09	9·0	0	S	—	—
23·8	6·09	6·6	0	S	—	—
27·7	7·08	5·0	0	S	—	—
32·1	8·21	3·9	0	S	—	—
35·6	9·10	3·1	0	S	—	—
39·1	10·00	2·5	0	S	—	—
25·7	6·57	4·9	+ 4	S	—	—
29·5	7·54	3·2	+ 4	S	—	—
33·0	8·44	2·3	+ 4	S	—	—
37·0	9·46	1·3	+ 4	S	—	—
20·0	5·11	8·5	+ 8	S	—	—
23·5	6·01	5·5	+ 8	B	1	—
27·5	7·03	3·4	+ 8	B	2	—
31·5	8·05	2·2	+ 8	B	1½	—
35·2	9·00	1·1	+ 8	US	4	—
19·0	4·86	8·6	+12	S	—	—
20·0	5·11	7·8	+12	S	—	—
20·6	5·27	7·3	+12	S	—	—
21·0	5·37	7·1	+12	S	—	—
22·0	5·63	6·3	+12	S	—	—
23·2	5·93	5·5	+12	US	3	—
24·0	6·14	4·9	+12	US	3	—
25·9	6·62	4·0	+12	US	4	—
29·9	7·65	2·3	+12	US	4	—

UNDISTURBED HYDRODYNAMIC LONGITUDINAL STABILITY CHARACTERISTICS

TABLE 28

Model B

($C_{\Delta 0} = 2{\cdot}25$; $I = 21{\cdot}30$ lb ft^2)

Speed V (ft/sec)	Velocity coefficient C_v	Keel attitude α_K (deg)	Elevator angle η (deg)	Stable (S) Unstable (US) Border-line (B) Skipping (Sk)	Amplitude of porpoising if any (deg)	Limits of porpoising (deg)
21·5	5·50	10·0	−16	S	—	—
26·4	6·75	10·0	−16	S	—	—
30·4	7·77	10·0	−16	B	2	—
32·4	8·28	9·8	−16	B	2	—
34·3	8·77	8·9	−12	B Sk	2	—
27·4	7·01	9·5	−10	S	—	—
32·3	8·26	9·1	−10	S	—	—
36·2	9·26	8·4	−10	S	—	—
0	0	2·8	− 8	S	—	—
4·0	1·02	2·8	− 8	S	—	—
8·2	2·10	4·7	− 8	S	—	—
12·2	3·12	5·2	− 8	S	—	—
16·1	4·12	9·7	− 8	S	—	—
20·0	5·11	9·9	− 8	S	—	—
23·8	6·08	9·5	− 8	S	—	—
25·6	6·55	9·0	− 8	S	—	—
26·6	6·80	8·9	− 8	S	—	—
28·2	7·22	8·9	− 8	S	—	—
32·2	8·24	8·8	− 8	S	—	—
36·0	9·21	8·2	− 8	S	—	—
22·5	5·76	8·2	0	S	—	—
26·3	6·73	6·2	0	S	—	—
30·5	7·80	4·7	0	S	—	—
34·3	8·77	3·8	0	S	—	—
38·3	9·80	2·8	0	S	—	—
20·3	5·19	9·0	+ 4	S	—	—
22·0	5·62	7·9	+ 4	S	—	—
23·4	5·98	6·6	+ 4	US	3	—
27·5	7·03	4·7	+ 4	B	2	—
31·5	8·06	3·4	+ 4	B	1	—
35·0	8·95	2·2	+ 4	B	½	—
39·0	9·97	1·2	+ 4	US	2	—
19·0	4·86	9·3	+ 8	S	—	—
29·9	7·65	2·9	+ 8	US	4	—
33·5	8·57	1·7	+ 8	US	4	—

UNDISTURBED HYDRODYNAMIC LONGITUDINAL STABILITY CHARACTERISTICS

TABLE 29

Model B

($C_{\Delta 0} = 2{\cdot}50$; $I = 21{\cdot}30$ lb ft^2)

Speed V (ft/sec)	Velocity coefficient C_v	Keel attitude α_K (deg)	Elevator angle η (deg)	Stable (S) Unstable (US) Border-line (B) Skipping (Sk)	Amplitude of porpoising if any (deg)	Limits of porpoising (deg)
22·1	5·65	10·2	−16	S	—	—
25·7	6·57	10·1	−16	S	—	—
27·7	7·08	10·2	−16	S	—	—
29·7	7·60	10·1	−16	S	—	—
33·5	8·56	10·2	−16	US	4	—
35·4	9·06	9·7	−16	US	3	—
27·8	7·11	9·9	−12	S	—	—
34·5	8·82	9·7	−12	B	1½	—
35·5	9·08	9·6	−12	B	1½	—
37·5	9·59	9·0	−12	B	2	—
28·5	7·29	9·6	−10	S	—	—
34·1	8·72	9·1	−10	S	—	—
36·1	9·24	8·8	−10	S	—	—
39·1	10·00	8·4	−10	B Sk	1	—
0	0	2·7	− 8	S	—	—
4·0	1·02	2·7	− 8	S	—	—
8·0	2·04	4·8	− 8	S	—	—
12·0	3·07	5·3	− 8	S	—	—
16·0	4·09	10·0	− 8	S	—	—
19·8	5·06	10·3	− 8	S	—	—
24·0	6·14	9·3	− 8	S	—	—
27·5	7·03	8·6	− 8	S	—	—
31·5	8·06	8·0	− 8	S	—	—
35·4	9·05	8·3	− 8	S	—	—
39·2	10·03	7·9	− 8	S	—	—
21·6	5·52	9·8	− 4	S	—	—
25·5	6·52	7·8	− 4	S	—	—
29·6	7·57	6·8	− 4	S	—	—
33·5	8·56	6·8	− 4	S	—	—
37·5	9·59	6·4	− 4	S	—	—
20·0	5·12	10·0	0	S	—	—
23·8	6·08	8·1	0	S	—	—
27·8	7·11	6·2	0	S	—	—
31·6	8·08	5·1	0	S	—	—
34·8	8·90	4·2	0	S	—	—
39·0	9·97	3·3	0	S	—	—
21·8	5·58	9·1	+ 4	S	—	—
25·7	6·57	6·3	+ 4	B	2	—
29·7	7·60	5·0	+ 4	B	1	—
33·5	8·56	3·3	+ 4	B	1½	—
37·4	9·56	2·5	+ 4	S	—	—
20·2	5·16	9·6	+ 8	S	—	—
22·7	5·80	7·8	+ 8	B	1	—
24·0	6·14	7·0	+ 8	US	5	—
27·8	7·11	5·3	+ 8	US	4	—
31·7	8·11	3·3	+ 8	US	3	—
35·4	9·06	2·3	+ 8	US	3	—
39·6	10·13	1·6	+ 8	US	—	—

UNDISTURBED HYDRODYNAMIC LONGITUDINAL STABILITY CHARACTERISTICS

TABLE 30

Model B

($C_{\Delta 0} = 2{\cdot}75$; $I = 21{\cdot}30$ lb ft^2)

Speed V (ft/sec)	Velocity coefficient C_v	Keel attitude α_K (deg)	Elevator angle η (deg)	Stable (S) Unstable (US) Border-line (B) Skipping (Sk)	Amplitude of porpoising if any (deg)	Limits of porpoising (deg)
21·8	5·58	10·8	−20	S	—	—
25·8	6·60	10·5	−20	S	—	—
29·6	7·57	10·5	−20	B	1	—
33·5	8·57	10·6	−20	US	4	—
19·3	4·94	11·0	−16	S	—	—
23·3	5·96	10·6	−16	S	—	—
27·5	7·04	10·4	−16	S	—	—
31·3	8·00	10·4	−16	S	—	—
35·1	8·98	10·5	−16	US Sk	4	—
39·1	10·00	10·6	−16	US Sk	—	—
21·9	5·60	10·5	−12	S	—	—
26·3	6·72	10·1	−12	S	—	—
30·2	7·72	10·1	−12	S	—	—
34·0	8·70	10·1	−12	S	—	—
37·8	9·67	10·0	−12	B	1	—
0	0	2·8	− 8	S	—	—
3·8	0·97	2·8	− 8	S	—	—
5·0	1·28	3·5	− 8	S	—	—
8·3	2·22	5·0	− 8	S	—	—
12·1	3·09	5·5	− 8	S	—	—
14·2	3·63	7·0	− 8	S	—	—
16·0	4·09	10·4	− 8	S	—	—
18·0	4·60	10·6	− 8	S	—	—
19·6	5·01	10·6	− 8	S	—	—
23·5	6·01	10·1	− 8	S	—	—
27·5	7·04	8·8	− 8	S	—	—
31·5	8·06	8·6	− 8	S	—	—
35·2	9·00	8·6	− 8	S	—	—
39·0	9·98	8·0	− 8	S	—	—
22·1	5·65	10·2	− 4	S	—	—
25·7	6·58	8·3	− 4	S	—	—
29·9	7·64	7·0	− 4	S	—	—
33·6	8·59	6·6	− 4	S	—	—
24·0	6·13	8·9	0	S	—	—
27·9	7·13	6·9	0	S	—	—
31·6	8·08	5·4	0	S	—	—
35·4	9·05	4·4	0	S	—	—
39·1	10·00	3·5	0	S	—	—
18·0	4·60	10·4	+ 4	S	—	—
20·9	5·34	10·0	+ 4	S	—	—
22·0	5·63	9·7	+ 4	S	—	—
25·8	6·60	7·4	+ 4	US	4	—
29·6	7·56	5·4	+ 4	B	1½	—
33·5	8·56	4·0	+ 4	B	—	—
37·4	9·56	2·9	+ 4	S	—	—
19·7	5·04	10·2	+ 8	S	—	—
21·8	5·58	9·6	+ 8	S	—	—
23·0	5·88	8·8	+ 8	US	—	—
23·7	6·06	8·4	+ 8	US	5	—
27·7	7·08	5·9	+ 8	US	4	—
31·6	8·08	4·3	+ 8	US	3	—
35·4	9·05	2·6	+ 8	US	3	—
39·5	10·11	1·6	+ 8	US	—	—

UNDISTURBED HYDRODYNAMIC LONGITUDINAL STABILITY CHARACTERISTICS

TABLE 31

Model B

($C_{\Delta 0} = 3{\cdot}00$; $I = 21{\cdot}30$ lb ft^2)

Speed V (ft/sec)	Velocity coefficient C_v	Keel attitude α_K (deg)	Elevator angle η (deg)	Stable (S) Unstable (US) Border-line (B) Skipping (Sk)	Amplitude of porpoising if any (deg)	Limits of porpoising (deg)
22·2	5·68	11·0	−20	S	—	—
24·1	6·16	10·6	−20	US	2½	—
25·1	6·42	10·7	−20	US	5	—
27·8	7·11	10·7	−20	B	½	—
29·4	7·52	10·6	−20	S	—	—
33·7	8·62	10·5	−20	US	6	—
22·2	5·68	10·7	−16	S	—	—
25·0	6·39	10·3	−16	B	2	—
26·0	6·65	10·2	−16	B	½	—
27·8	7·11	10·3	−16	S	—	—
31·8	8·13	10·2	−16	S	—	—
34·2	8·75	10·2	−16	B	2	—
35·6	9·10	10·2	−16	US	4	—
39·5	10·11	10·2	−16	US	4	—
32·2	8·24	9·6	−10	S	—	—
34·2	8·75	9·6	−10	S	—	—
38·2	9·77	9·6	−10	S	—	—
40·0	10·23	9·6	−10	S	—	—
0	0	2·8	− 8	S	—	—
4·0	1·02	2·8	− 8	S	—	—
8·2	2·10	5·0	− 8	S	—	—
12·0	3·07	5·4	− 8	S	—	—
16·0	4·09	10·5	− 8	S	—	—
19·7	5·04	11·1	− 8	S	—	—
23·9	6·11	10·3	− 8	US	4	—
24·0	6·14	10·1	− 8	B	1	—
27·5	7·03	9·0	− 8	S	—	—
31·2	7·98	8·5	− 8	S	—	—
35·2	9·00	8·7	− 8	S	—	—
39·1	10·00	8·2	− 8	S	—	—
21·9	5·61	10·5	− 4	S	—	—
33·5	8·57	6·7	− 4	S	—	—
38·0	9·72	6·1	− 4	S	—	—
23·5	6·01	10·0	—	US	3	—
24·3	6·22	9·7	—	US	6	—
19·9	5·09	10·7	0	S	—	—
23·3	5·96	10·0	0	US	5	—
27·5	7·03	7·3	0	B	2	—
31·5	8·06	5·5	0	S	—	—
35·1	8·98	5·0	0	S	—	—
39·2	10·02	4·1	0	S	—	—
21·1	5·39	10·3	+ 4	S	—	—
22·1	5·65	10·1	+ 4	S	—	—
29·5	7·55	5·9	+ 4	US	3	—
33·2	8·49	4·5	+ 4	B	1½	—
37·2	9·52	3·2	+ 4	B	1	—
39·5	10·11	2·5	+ 4	US	3	—
31·7	8·11	3·9	+ 8	US	5	—
35·6	9·10	2·8	+ 8	US	4	—

UNDISTURBED HYDRODYNAMIC LONGITUDINAL STABILITY CHARACTERISTICS

TABLE 32

Model B

($C_{\Delta 0} = 2{\cdot}50$; $I = 26{\cdot}50$ lb ft^2)

Speed V (ft/sec)	Velocity coefficient C_v	Keel attitude α_K (deg)	Elevator angle η (deg)	Stable (S) Unstable (US) Border-line (B) Skipping (Sk)	Amplitude of porpoising if any (deg)	Limits of porpoising (deg)
31·6	8·08	10·3	−20	S	—	—
31·9	8·16	10·3	−20	S	—	—
32·9	8·42	10·3	−20	US	2½	—
31·7	8·11	10·1	−18	S	—	—
32·6	8·34	10·1	−18	B	2	—
31·4	8·03	10·0	−16	S	—	—
32·5	8·32	10·0	−16	S	—	—
20·2	5·17	10·3	−12	S	—	—
21·7	5·55	10·2	−12	S	—	—
28·5	7·29	9·9	−12	S	—	—
29·7	7·60	9·7	−12	S	—	—
28·6	7·32	8·5	− 6	S	—	—
29·9	7·65	7·6	− 6	S	—	—
30·9	7·91	7·0	− 6	S	—	—
33·8	8·65	6·9	− 6	S	—	—
36·9	9·44	7·0	− 6	S	—	—
20·1	5·14	10·1	− 4	S	—	—
21·2	5·43	9·8	− 4	S	—	—
28·8	7·37	6·9	− 4	S	—	—
31·8	8·13	6·6	− 4	S	—	—
34·8	8·90	5·7	− 4	S	—	—
23·7	6·06	7·7	+ 6	S	—	—
25·6	6·55	6·8	+ 6	B	2	—
28·9	7·39	4·9	+ 6	B	2	—
32·4	8·29	3·4	+ 6	S	—	—
35·0	8·95	2·8	+ 6	S	—	—
37·6	9·62	2·6	+ 6	S	—	—
19·8	5·06	9·7	+ 8	S	—	—
21·1	5·40	9·5	+ 8	B	1	—
24·0	6·14	7·5	+ 8	US	5	—
27·2	6·96	5·9	+ 8	US	3	—
31·0	7·93	3·7	+ 8	US	3	—
37·8	9·67	2·4	+ 8	US	3	—

UNDISTURBED HYDRODYNAMIC LONGITUDINAL STABILITY CHARACTERISTICS

Table 33

Model B

($C_{\Delta 0} = 2{\cdot}50$; $I = 29{\cdot}82$ lb ft²)

Speed V (ft/sec)	Velocity coefficient C_v	Keel attitude α_K (deg)	Elevator angle η (deg)	Stable (S) Unstable (US) Border-line (B) Skipping (Sk)	Amplitude of porpoising if any (deg)	Limits of porpoising (deg)
32·4	8·29	10·1	−20	S	—	—
33·2	8·49	10·0	−20	B	2	—
34·9	8·93	9·9	−20	US	3½	—
35·9	9·19	9·7	−20	US	3	7 to 10
33·4	8·54	9·8	−18	B	1½	—
28·1	7·18	10·1	−16	S	—	—
29·5	7·55	9·9	−16	S	—	—
35·9	9·18	9·0	−16	S	—	—
21·1	5·40	10·1	−12	S	—	—
21·8	5·58	10·0	−12	S	—	—
22·4	5·73	10·1	−12	S	—	—
28·2	7·22	9·5	−12	S	—	—
29·1	7·44	9·6	−12	S	—	—
37·1	9·49	8·8	−12	S	—	—
37·8	9·67	8·7	−12	S	—	—
0	0	2·5	− 8	S	—	—
4·0	1·02	2·5	− 8	S	—	—
8·0	2·04	4·7	− 8	S	—	—
12·2	3·12	5·2	− 8	S	—	—
18·4	4·71	10·1	− 8	S	—	—
20·5	5·24	9·9	− 8	S	—	—
24·5	6·27	9·0	− 8	S	—	—
27·0	6·91	8·3	− 8	S	—	—
28·5	7·29	8·3	− 8	S	—	—
32·5	8·31	8·2	− 8	S	—	—
35·8	9·16	8·2	− 8	S	—	—
27·8	7·11	7·8	− 6	S	—	—
29·0	7·41	7·4	− 6	S	—	—
30·6	7·82	6·9	− 6	S	—	—
34·1	8·72	6·8	− 6	S	—	—
37·7	9·64	6·9	− 6	S	—	—
19·2	4·91	9·7	0	S	—	—
20·7	5·29	9·6	0	S	—	—
21·5	5·50	9·4	0	S	—	—
22·8	5·83	8·6	0	S	—	—
29·8	7·62	4·7	0	S	—	—
30·8	7·87	5·1	0	S	—	—
31·7	8·10	4·8	0	S	—	—
32·0	8·18	4·5	0	S	—	—
35·6	9·10	3·6	0	S	—	—
40·0	10·23	2·7	0	S	—	—
24·5	6·26	7·3	+ 4	S	—	—
28·5	7·29	5·1	+ 4	S	—	—
32·5	8·31	3·8	+ 4	S	—	—
35·7	9·13	2·7	+ 4	S	—	—
38·6	9·87	2·0	+ 4	S	—	—
22·0	5·62	8·3	+ 8	S	—	—
26·4	6·75	5·8	+ 8	B	1	—
30·5	7·80	4·0	+ 8	B	2	—
34·0	8·69	2·6	+ 8	B	2	—
37·6	9·62	1·7	+ 8	US	2½	—
24·6	6·29	6·4	+12	US	12	3 to 15
28·5	7·28	4·5	+12	US	12	—

UNDISTURBED HYDRODYNAMIC LONGITUDINAL STABILITY CHARACTERISTICS

TABLE 34

Model B

($C_{\Delta 0} = 3{\cdot}00$; $I = 31{\cdot}70$ lb ft^2)

Speed V (ft/sec)	Velocity coefficient C_v	Keel attitude α_K (deg)	Elevator angle η (deg)	Stable (S) Unstable (US) Border-line (B) Skipping (Sk)	Amplitude of porpoising if any (deg)	Limits of porpoising (deg)
20·8	5·32	11·0	−20	S	—	—
25·8	6·59	10·2	−20	S	—	—
34·3	8·77	10·3	−20	S	—	—
35·4	9·05	10·5	−20	B	2	—
21·3	5·45	10·7	−16	S	—	—
22·6	5·78	10·5	−16	S	—	—
23·6	6·03	10·5	−16	S	—	—
24·2	6·18	10·3	−16	US	—	—
25·6	6·54	10·1	−16	S	—	—
26·7	6·83	10·1	−16	S	—	—
27·6	7·06	10·1	−16	S	—	—
32·5	8·31	10·1	−16	S		—
33·5	8·56	10·2	−16	S	—	—
35·0	8·95	9·7	−16	S	—	—
36·5	9·33	9·7	−16	US	5	—
31·9	8·16	9·4	−12	S	—	—
32·5	8·31	9·7	−12	S	—	—
33·0	8·44	9·5	−12	S	—	—
36·2	9·26	9·5	−12	S	—	—
37·5	9·59	9·4	−12	B	1	—
38·5	9·84	9·1	−12	B	½	—
20·6	5·27	10·5	0	S	—	—
23·6	6·03	9·9	0	US	—	—
24·6	6·30	8·9	0	B	1½	—
24·8	6·34	9·1	0	S	—	—
25·6	6·54	8·8	0	B	1½	—
28·5	7·28	6·9	0	S	—	—
31·5	8·05	5·7	0	S	—	—
20·6	5·27	10·4	+ 4	S	—	—
21·6	5·52	10·1	+ 4	S	—	—
22·8	5·83	10·0	+ 4	US	12	—
32·5	8·31	4·7	+ 4	S	—	—
35·8	9·16	3·8	+ 4	S	—	—
38·6	9·87	3·1	+ 4	S	—	—
24·0	6·13	9·2	+ 6	US	12	—
25·9	6·62	7·5	+ 6	US	—	—
30·3	7·75	5·1	+ 6	US	—	—
33·5	8·56	4·0	+ 6	US	2½	—
38·7	9·90	2·6	+ 6	US	—	—

UNDISTURBED HYDRODYNAMIC LONGITUDINAL STABILITY CHARACTERISTICS

TABLE 35

Model C

($C_{\Delta 0} = 2{\cdot}25$; $I = 23{\cdot}75$ lb ft²)

Speed V (ft/sec)	Velocity coefficient C_v	Keel attitude α_K (deg)	Elevator angle η (deg)	Stable (S) Unstable (US) Border-line (B) Skipping (Sk)	Amplitude of porpoising if any (deg)	Limits of porpoising (deg)
21·0	5·37	10·3	−16	S	—	—
24·0	6·14	10·3	−16	S	—	—
28·2	7·21	10·3	−16	S	—	—
31·9	8·16	10·3	−16	B	2	8½ to 10½
24·0	6·14	9·9	−12	S	—	—
25·3	6·47	9·9	−12	S	—	—
34·0	8·70	9·9	−12	B	2	8 to 10
0	0	2·0	− 8	S	—	—
4·2	1·07	2·0	− 8	S	—	—
8·4	2·15	4·1	− 8	S	—	—
12·2	3·12	4·7	− 8	S	—	—
14·2	3·63	8·0	− 8	S	—	—
16·7	4·27	10·1	− 8	S	—	—
20·0	5·11	10·0	− 8	S	—	—
24·1	6·16	8·7	− 8	S	—	—
28·0	7·16	8·5	− 8	S		—
32·0	8·18	9·3	− 8	S	—	—
35·8	9·16	8·7	− 8	S	—	—
21·8	5·58	9·3	− 4	S	—	—
23·8	6·09	8·0	− 4	S	—	—
28·3	7·24	6·7	− 4	S	—	—
32·0	8·18	6·6	− 4	S	—	—
35·7	9·13	7·2	− 4	S	—	—
38·5	9·85	6·4	− 4	S	—	—
20·2	5·16	9·6	0	S	—	—
24·2	6·19	6·9	0	S	—	—
28·0	7·16	5·3	0	S	—	—
32·1	8·21	4·6	0	S	—	—
36·2	9·26	3·6	0	S	—	—
39·9	10·20	4·0	0	S	—	—
19·3	4·94	9·4	+ 8	S	—	—
20·5	5·24	8·5	+ 8	S	—	—
21·3	5·45	7·9	+ 8	S	—	—
22·4	5·73	7·0	+ 8	S	—	—
25·3	6·47	4·7	+ 8	B	2	5 to 7
30·1	7·70	3·1	+ 8	S	—	—
34·0	8·70	2·0	+ 8	B	½	1½ to 2
38·0	9·72	1·1	+ 8	US	3	0 to 3
22·6	5·78	6·3	+12	US	4	6 to 10
23·0	5·88	5·8	+12	US	—	—
27·5	7·04	3·6	+12	US	—	—
31·8	8·13	2·0	+12	US	3	1 to 4

UNDISTURBED HYDRODYNAMIC LONGITUDINAL STABILITY CHARACTERISTICS

TABLE 36

Model C

($C_{\Delta 0} = 2{\cdot}75$; $I = 23{\cdot}75$ lb ft²)

Speed V (ft/sec)	Velocity coefficient C_v	Keel attitude α_K (deg)	Elevator angle η (deg)	Stable (S) Unstable (US) Border-line (B) Skipping (Sk)	Amplitude of porpoising if any (deg)	Limits of porpoising (deg)
21·1	5·40	10·9	−16	S	—	—
22·5	5·76	10·6	−16	S	—	—
27·3	6·98	10·3	−16	S	—	—
29·0	7·42	10·4	−16	S	—	—
32·2	8·24	10·4	−16	B	1½	9½ to 11
35·2	9·01	10·4	−16	US	3	8 to 11
24·3	6·22	10·1	−12	S	—	—
28·2	7·21	10·0	−12	S	—	—
30·4	7·78	10·1	−12	S	—	—
32·2	8·24	10·1	−12	S	—	—
36·0	9·20	10·1	−12	B	2	8½ to 10½
38·0	9·72	9·3	—	S	—	—
0	0	2·0	− 8	S	—	—
4·1	1·05	2·0	− 8	S	—	—
8·4	2·15	4·2	− 8	S	—	—
12·2	3·12	4·7	− 8	S	—	—
14·1	3·61	7·0	− 8	S	—	—
16·8	4·29	10·9	− 8	S	—	—
20·1	5·14	10·6	− 8	S	—	—
24·2	6·18	9·6	− 8	S	—	—
27·4	7·01	8·6	− 8	S	—	—
28·5	7·28	8·6	− 8	S	—	—
31·2	7·98	8·5	− 8	S	—	—
35·0	8·95	9·3	− 8	S	—	—
39·1	10·00	8·6	− 8	S	—	—
24·4	6·24	9·0	− 4	S	—	—
28·5	7·28	7·0	− 4	S	—	—
32·2	8·23	6·8	− 4	S	—	—
35·0	8·95	7·0	− 4	S	—	—
39·0	9·97	7·2	− 4	S	—	—
20·5	5·24	10·3	0	S	—	—
24·2	6·18	8·3	0	S	—	—
27·8	7·11	6·4	0	S	—	—
30·0	7·67	5·7	0	S	—	—
32·0	8·18	5·0	0	S	—	—
35·9	9·18	4·5	0	S	—	—
22·2	5·68	9·1	+ 4	S	—	—
23·8	6·08	7·9	+ 4	US	—	—
26·2	6·70	6·6	+ 4	B	1	—
30·4	7·77	4·5	+ 4	S	—	—
34·0	8·70	3·4	+ 4	S	—	—
38·1	9·75	2·6	+ 4	S	—	—
19·6	5·02	10·3	+ 8	S	—	—
21·3	5·45	9·7	+ 8	S	—	—
22·2	5·68	8·9	+ 8	S	—	—
23·0	5·88	8·1	+ 8	US	—	—
24·5	6·27	7·3	+ 8	US	5	5 to 10
28·2	7·21	4·9	+ 8	US	4½	2½ to 7
31·9	8·16	3·5	+ 8	US	3½	2½ to 6
35·6	9·11	2·2	+ 8	B	1½	1½ to 3
35·9	9·18	2·0	+ 8	B	2	1 to 3
40·0	10·23	1·4	+ 8	US	3	1 to 4

UNDISTURBED HYDRODYNAMIC LONGITUDINAL STABILITY CHARACTERISTICS

TABLE 37

Model D

($C_{\Delta 0} = .2 \cdot 25$; $I = 16 \cdot 81$ lb ft²)

Speed V (ft/sec)	Velocity coefficient C_v	Keel attitude α_K (deg)	Elevator angle η (deg)	Stable (S) Unstable (US) Border-line (B) Skipping (Sk)	Amplitude of porpoising if any (deg)	Limits of porpoising (deg)
19·2	4·91	12·6	−20	S	—	—
24·4	6·24	11·8	−20	S	—	—
27·5	7·01	11·9	−20	S	—	—
28·4	7·26	11·9	−20	US	—	—
28·4	7·26	11·2	−12	S	—	—
30·5	7·80	11·1	−12	B	1	10½ to 11½
30·5	7·80	10·9	−10	S	—	—
34·4	8·80	10·0	−10	S	—	—
0	0	4·3	− 8	S	—	—
4·0	1·02	4·7	− 8	S	—	—
8·4	2·15	7·4	− 8	S	—	—
12·2	3·12	10·5	− 8	S	—	—
16·5	4·22	12·8	− 8	S	—	—
20·1	5·14	11·7	− 8	B	1	—
24·5	6·27	10·9	− 8	S	—	—
28·2	7·22	11·0	− 8	S	—	—
31·2	7·98	10·0	− 8	S	—	—
36·0	9·21	9·5	− 8	S	—	—
19·3	4·94	11·7	− 2	S	—	—
20·5	5·24	11·2	− 2	S	—	—
21·1	5·40	10·8	− 2	S	—	—
26·5	6·78	8·4	− 2	S	—	—
28·5	7·29	7·7	− 2	S	—	—
32·5	8·32	6·4	− 2	S	—	—
34·5	8·83	6·1	− 2	S	—	—
20·2	5·17	10·9	+ 2	US	6	8 to 14
22·4	5·73	9·7	+ 2	S	—	—
26·4	6·75	7·2	+ 2	S	—	—
30·4	7·78	5·9	+ 2	S	—	—
34·3	8·78	4·6	+ 2	S	—	—
24·6	6·29	7·8	+ 6	B	1½	7 to 8½
32·1	8·21	4·4	+ 6	S	—	—
36·0	9·21	3·3	+ 6	S	—	—
18·2	4·66	12·0	+ 8	S	—	—
22·4	5·73	9·3	+ 8	US	2½	—
26·3	6·73	6·5	+ 8	B	½	—
29·9	7·65	4·9	+ 8	S	—	—
34·0	8·70	3·5	+ 8	US	2½	3 to 5½
20·1	5·14	10·4	+10	US	7	7 to 14
24·2	6·19	7·0	+10	US	—	—
26·2	6·70	6·0	+10	US	3	4 to 7
28·1	7·18	5·1	+10	US	4	4 to 8
32·1	8·21	3·4	+10	US	8	1 to 9

UNDISTURBED HYDRODYNAMIC LONGITUDINAL STABILITY CHARACTERISTICS

TABLE 38

Model D

($C_{\Delta 0} = 2{\cdot}75$; $I = 16{\cdot}81$ lb ft^2)

Speed V (ft/sec)	Velocity coefficient C_v	Keel attitude α_K (deg)	Elevator angle η (deg)	Stable (S) Unstable (US) Border-line (B) Skipping (Sk)	Amplitude of porpoising if any (deg)	Limits of porpoising (deg)
18·9	4·84	14·0	−20	S	—	—
19·9	5·08	13·5	−20	S	—	—
21·5	5·50	13·1	−20	US	14	5 to 19
23·6	6·04	12·4	−20	US	2½	—
25·5	6·52	12·2	−20	S	—	—
30·2	7·72	12·0	−20	S	—	—
32·2	8·24	12·0	−20	US	5	8 to 13
20·5	5·24	13·1	−16	S	—	—
24·5	6·26	12·0	−16	B	1	—
28·6	7·31	11·9	−16	S	—	—
34·5	8·82	11·7	−16	US	4	8 to 12
18·5	4·73	13·7	−12	S	—	—
22·5	5·76	12·1	−12	US	12	6 to 18
26·1	6·68	11·3	−12	S	—	—
30·6	7·82	11·3	−12	S	—	—
34·5	8·82	11·4	−12	B	1	—
0	0	4·8	− 8	S	—	—
4·0	1·02	5·1	− 8	S	—	—
8·2	2·10	8·0	− 8	S	—	—
12·0	3·07	11·1	− 8	S	—	—
16·3	4·17	14·2	− 8	S	—	—
20·5	5·24	12·7	− 8	S	—	—
24·2	6·19	11·3	− 8	S	—	—
28·5	7·29	10·5	− 8	S	—	—
36·0	9·20	10·2	− 8	S	—	—
40·0	10·23	9·2	− 8	S	—	—
18·5	4·73	13·5	− 4	S	—	—
22·5	5·76	11·7	− 4	US	—	—
26·5	6·78	10·0	− 4	S	—	—
30·5	7·80	9·0	− 4	S	—	—
34·3	8·77	8·1	− 4	S	—	—
38·2	9·77	8·0	− 4	S	—	—
18·9	4·84	13·2	0	S	—	—
21·0	5·37	12·0	0	S	—	—
24·5	6·26	10·2	0	S	—	—
28·5	7·28	8·3	0	S	—	—
32·5	8·31	7·0	0	S	—	—
36·2	9·26	6·0	0	S	—	—
23·3	5·96	10·4	+ 4	US	2½	—
26·6	6·80	8·4	+ 4	B	½	—
30·5	7·80	6·4	+ 4	S	—	—
34·3	8·77	5·3	+ 4	S	—	—
38·3	9·80	4·4	+ 4	S	—	—
21·5	5·50	11·0	+ 8	US	—	—
25·0	6·28	8·4	+ 8	US	3½	7 to 10½
28·5	7·28	6·7	+ 8	B	2	6 to 8
32·3	8·26	5·4	+ 8	B	2	—
36·0	9·20	4·3	+ 8	B	2	3 to 5
30·3	7·75	5·2	—	US	—	—

UNDISTURBED HYDRODYNAMIC LONGITUDINAL STABILITY CHARACTERISTICS

TABLE 39

Model E

($C_{\Delta 0} = 2{\cdot}25$; $I = 25{\cdot}02$ lb ft^2)

Speed V (ft/sec)	Velocity coefficient C_v	Keel attitude α_K (deg)	Elevator angle η (deg)	Stable (S) Unstable (US) Border-line (B) Skipping (Sk)	Amplitude of porpoising if any (deg)	Limits of porpoising (deg)
24·5	6·26	9·4	−16	S	—	—
28·1	7·18	9·5	−16	S	—	—
32·4	8·28	9·6	−16	B Sk	2	—
35·8	9·16	9·6	−16	B Sk	2	—
26·5	6·78	9·2	−12	S	—	—
30·6	7·82	9·4	−12	B	1	—
34·0	8·70	9·4	−12	S	—	—
35·2	9·00	9·4	−12	B Sk	2	7½ to 9½
0	0	3·3	− 8	S	—	—
4·1	1·05	3·1	− 8	S	—	—
8·3	2·12	4·6	− 8	S	—	—
12·4	3·17	4·8	− 8	S	—	—
16·6	4·24	6·3	− 8	S	—	—
18·7	4·78	8·4	− 8	S	—	—
20·2	5·16	9·0	− 8	S	—	—
24·4	6·24	9·1	− 8	S	—	—
28·0	7·16	9·0	− 8	S	—	—
32·0	8·18	8·9	− 8	S	—	—
35·5	9·08	8·3	− 8	S	—	—
22·8	5·83	9·0	− 4	S	—	—
26·5	6·78	8·2	− 4	S	—	—
30·5	7·80	7·0	− 4	S	—	—
34·0	8·70	6·6	− 4	S	—	—
37·9	9·69	6·3	− 4	S	—	—
24·7	6·31	8·3	0	S	—	—
28·6	7·31	6·9	0	S	—	—
32·2	8·24	5·2	0	S	—	—
35·8	9·16	4·5	0	S	—	—
39·5	10·11	3·5	0	S	—	—
22·8	5·68	8·6	+ 4	S	—	—
26·7	6·83	7·5	+ 4	B	1	—
28·8	7·36	6·0	+ 4	B	½	—
30·5	7·80	5·2	+ 4	S	—	—
33·7	8·62	4·4	+ 4	S	—	—
38·0	9·72	3·3	+ 4	S	—	—
24·7	6·31	7·7	+ 6	US	2½	6½ to 9
26·7	6·83	6·4	+ 6	B	2	—
28·9	7·39	5·5	+ 6	B	2	—
32·5	8·31	4·4	+ 6	B	1½	—
36·0	9·20	3·3	+ 6	US	2½	—
40·0	10·23	2·5	+ 6	US	—	—
32·5	8·31	4·1	—	US	3½	3 to 6½

UNDISTURBED HYDRODYNAMIC LONGITUDINAL STABILITY CHARACTERISTICS

TABLE 40

Model E

($C_{\Delta 0} = 2{\cdot}75$; $I = 25{\cdot}02$ lb ft^2)

Speed V (ft/sec)	Velocity coefficient C_v	Keel attitude α_K (deg)	Elevator angle η (deg)	Stable (S) Unstable (US) Border-line (B) Skipping (Sk)	Amplitude of porpoising if any (deg)	Limits of porpoising (deg)
25·9	6·62	9·7	−12	S	—	—
27·0	6·90	9·8	−12	S	—	—
30·0	7·66	9·6	−12	S	—	—
33·6	8·59	9·7	−12	S	—	—
37·7	9·64	9·7	−12	B	1	8½ to 9½
39·5	10·11	9·1	−12	US Sk	2½	7½ to 10
0	0	3·1	− 8	S	—	—
4·0	1·02	2·9	− 8	S	—	—
8·4	2·14	4·5	− 8	S	—	—
12·1	3·10	4·7	− 8	S	—	—
16·8	4·29	6·6	− 8	S	—	—
18·5	4·72	8·8	− 8	S	—	—
20·9	5·34	9·7	− 8	S	—	—
24·0	6·14	9·7	− 8	S	—	—
28·5	7·28	9·5	− 8	S	—	—
32·5	8·31	8·9	− 8	S	—	—
36·3	9·28	9·4	− 8	S	—	—
40·0	10·23	8·4	− 8	S	—	—
27·0	6·90	9·4	− 4	S	—	—
30·7	7·85	8·3	− 4	S	—	—
34·0	8·70	7·4	− 4	S	—	—
38·0	9·72	6·8	− 4	S	—	—
25·1	6·42	9·4	0	S	—	—
26·5	6·78	8·9	0	S	—	—
27·5	7·03	8·5	0	S	—	—
29·0	7·41	7·8	0	S	—	—
32·0	8·18	6·7	0	S	—	—
36·0	9·20	5·5	0	S	—	—
39·7	10·16	4·5	0	S	—	—
27·1	6·93	8·3	+ 4	B	2	7 to 9
28·1	7·18	7·7	+ 4	US	3	—
30·7	7·85	6·5	+ 4	B	1	6 to 7
34·2	8·74	5·2	+ 4	S	—	—
39·5	10·11	3·6	+ 4	B	1	3½ to 4½
32·1	8·21	5·6	+ 6	US	3	—
36·0	9·20	4·2	+ 6	US	2½	—
39·8	10·18	3·2	+ 6	US	4	—
30·7	7·85	5·2	+ 8	US	3½	4½ to 8

UNDISTURBED HYDRODYNAMIC LONGITUDINAL STABILITY CHARACTERISTICS

TABLE 41

Model F

($C_{\Delta 0} = 2{\cdot}25$; $I = 40{\cdot}25$ lb ft^2)

Speed V (ft/sec)	Velocity coefficient C_v	Keel attitude α_K (deg)	Elevator angle η (deg)	Stable (S) Unstable (US) Border-line (B) Skipping (Sk)	Amplitude of porpoising if any (deg)	Limits of porpoising (deg)
0	0	2·6	− 8	S	—	—
4·0	1·02	2·5	− 8	S	—	—
7·9	2·02	3·3	− 8	S	—	—
10·9	2·79	3·8	− 8	S	—	—
17·0	4·34	4·4	− 8	S	—	—
20·5	5·24	6·3	− 8	S	—	—
23·2	5·93	7·2	− 8	S	—	—
27·0	6·90	7·3	− 8	S	—	—
30·7	7·84	7·5	− 8	S	—	—
34·6	8·84	7·4	− 8	B Sk	1½	—
38·0	9·71	7·4	− 8	B Sk	1½	—
29·5	7·54	7·3	− 4	S	—	—
33·2	8·48	7·4	− 4	S	—	—
27·3	6·98	7·1	0	S	—	—
31·0	7·92	6·5	0	S	—	—
35·0	8·94	5·9	0	S	—	—
38·5	9·84	5·8	0	S	—	—
25·4	6·49	7·0	+ 4	S	—	—
29·5	7·54	5·8	+ 4	S	—	—
31·5	8·05	5·2	+ 4	S	—	—
35·5	9·08	4·1	+ 4	S	—	—
38·5	9·84	3·2	+ 4	S	—	—
29·5	7·54	5·7	+ 6	S	—	—
33·0	8·44	4·5	+ 6	S	—	—
37·0	9·46	3·5	+ 6	S	—	—
27·5	7·02	6·1	+ 8	S	—	—
30·7	7·84	4·9	+ 8	S	—	—
34·5	8·82	3·8	+ 8	S	—	—
38·5	9·84	2·8	+ 8	B	1½	—
25·2	6·44	6·8	+10	S	—	—
26·3	6·73	6·2	+10	B	2	—
27·5	7·02	5·7	+10	US	5½	—
29·5	7·54	5·0	+10	B	2	—
30·6	7·81	4·4	+10	B	2	—
32·0	8·17	4·0	+10	S	—	—
33·1	8·46	3·5	+10	US	6	—
30·2	7·71	4·3	+12	US	5½	—
32·0	8·17	3·4	+12	US	5	—

UNDISTURBED HYDRODYNAMIC LONGITUDINAL STABILITY CHARACTERISTICS

TABLE 42

Model F

($C_{\Delta 0} = 2{\cdot}75$; $I = 40{\cdot}25$ lb ft^2)

Speed V (ft/sec)	Velocity coefficient C_v	Keel attitude α_K (deg)	Elevator angle η (deg)	Stable (S) Unstable (US) Border-line (B) Skipping (Sk)	Amplitude of porpoising if any (deg)	Limits of porpoising (deg)
29·0	7·41	7·9	−12	S	—	—
34·7	8·88	7·9	−12	S	—	—
37·0	9·45	7·6	−12	B Sk	1½	—
38·1	9·75	7·7	−12	B Sk	1½	—
0	0	2·6	− 8	S	—	—
4·0	1·02	2·4	− 8	S	—	—
7·9	2·02	3·2	− 8	S	—	—
11·8	3·02	3·4	− 8	S	—	—
17·0	4·34	4·5	− 8	S	—	—
19·4	4·96	5·3	− 8	S	—	—
23·2	5·93	7·5	− 8	S	—	—
27·3	6·98	7·8	− 8	S	—	—
31·0	7·92	7·8	− 8	S	—	—
34·5	8·82	7·8	− 8	S	—	—
38·7	9·89	7·6	− 8	B	1½	—
25·5	6·52	7·6	− 4	S	—	—
29·5	7·54	7·6	− 4	S	—	—
31·8	8·12	7·6	− 4	S	—	—
36·0	9·20	7·6	− 4	S	—	—
31·2	7·98	7·1	− 2	S	—	—
34·9	8·92	7·0	− 2	S	—	—
38·5	9·85	7·0	− 2	S	—	—
26·8	6·85	7·6	0	S	—	—
31·0	7·92	7·1	0	S	—	—
34·5	8·82	6·1	0	S	—	—
38·5	9·85	5·3	0	S	—	—
25·5	6·52	7·4	+ 4	S	—	—
29·5	7·54	6·9	+ 4	S	—	—
33·0	8·43	5·9	+ 4	S	—	—
36·8	9·40	4·8	+ 4	S	—	—
27·0	6·91	7·2	+ 6	B	1	—
31·0	7·92	5·9	+ 6	S	—	—
35·2	9·00	4·6	+ 6	S	—	—
39·0	9·97	3·9	+ 6	S	—	—
29·5	7·55	6·1	+ 8	US	2½	—
33·2	8·48	4·9	+ 8	US	4½	—
37·5	9·59	3·6	+ 8	US	3	—

UNDISTURBED HYDRODYNAMIC LONGITUDINAL STABILITY CHARACTERISTICS

TABLE 43

Model G

($C_{\Delta 0} = 2{\cdot}25$; $I = 23{\cdot}50$ lb ft^2)

Speed V (ft/sec)	Velocity coefficient C_v	Keel attitude α_K (deg)	Elevator angle η (deg)	Stable (S) Unstable (US) Border-line (B) Skipping (Sk)	Amplitude of porpoising if any (deg)	Limits of porpoising (deg)
21·0	5·37	8·5	−12	S	—	—
25·2	6·44	8·2	−12	S	—	—
29·2	7·46	8·2	−12	S	—	—
31·2	7·97	8·2	−12	B	2	
0	0	2·3	− 8	S	—	—
4·0	1·02	2·4	− 8	S	—	—
7·6	1·94	4·0	− 8	S	—	—
11·5	2·94	4·4	− 8	S	—	—
15·5	3·96	5·7	− 8	S	—	—
17·5	4·47	7·4	− 8	S	—	—
19·3	4·93	8·4	− 8	S	—	—
23·3	5·95	8·2	− 8	S	—	—
27·0	6·90	7·9	− 8	S	—	—
31·0	7·92	7·9	− 8	S	—	—
32·5	8·30	7·7	− 8	S	—	—
23·5	6·00	8·1	− 4	S	—	—
25·5	6·52	7·9	− 4	S	—	—
27·5	7·02	7·7	− 4	S	—	—
31·4	8·03	7·5	− 4	S	—	—
32·8	8·39	7·2	− 4	S	—	—
34·2	8·75	6·9	− 4	S	—	—
35·0	8·94	6·4	− 4	S	—	—
36·5	9·34	6·2	− 4	S	—	—
21·6	5·52	8·2	0	S	—	—
25·5	6·52	7·4	0	S	—	—
29·5	7·54	6·4	0	S	—	—
32·9	8·40	5·8	0	S	—	—
37·0	9·46	4·7	0	S	—	—
23·5	6·00	7·7	+ 4	S	—	—
24·5	6·27	7·4	+ 4	S	—	—
27·5	7·02	5·9	+ 4	S	—	—
31·5	8·06	5·1	+ 4	S	—	—
35·1	8·96	3·9	+ 4	S	—	—
20·8	5·31	8·1	+ 8	S	—	—
23·2	5·93	7·4	+ 8	S	—	—
24·5	6·27	6·9	+ 8	US	4	—
26·1	6·66	6·2	+ 8	B	2	
29·2	7·46	4·7	+ 8	US	3	—
33·0	8·44	3·7	+ 8	US	3	—
37·5	9·59	2·6	+ 8	US	—	—

UNDISTURBED HYDRODYNAMIC LONGITUDINAL STABILITY CHARACTERISTICS

TABLE 44

Model G

($C_{\Delta 0} = 2{\cdot}75$; $I = 23{\cdot}50$ lb ft^2)

Speed V (ft/sec)	Velocity coefficient C_v	Keel attitude α_K (deg)	Elevator angle η (deg)	Stable (S) Unstable (US) Border-line (B) Skipping (Sk)	Amplitude of porpoising if any (deg)	Limits of porpoising (deg)
28·5	7·28	8·6	−16	S	—	—
32·2	8·22	8·6	−16	B	1	—
35·0	8·94	8·6	−16	US	5	—
20·5	5·24	9·4	−12	S	—	—
24·2	6·18	9·0	−12	S	—	—
25·3	6·46	8·8	−12	B	2	—
26·5	6·77	8·7	−12	B	2	—
28·5	7·27	8·5	−12	S	—	—
32·7	8·35	8·4	−12	B	1	—
0	0	2·3	− 8	S	—	—
4·0	1·02	2·4	− 8	S	—	—
8·0	2·04	4·4	− 8	S	—	—
12·0	3·07	5·2	− 8	S	—	—
16·0	4·08	8·5	− 8	S	—	—
18·0	4·60	9·3	− 8	S	—	—
19·8	5·06	9·4	− 8	S	—	—
23·8	6·08	8·9	− 8	S	—	—
27·5	7·02	8·5	− 8	S	—	—
32·2	8·22	8·3	− 8	S	—	—
33·5	8·65	8·3	− 8	S	—	—
35·2	8·99	8·3	− 8	S	—	—
38·6	9·86	7·6	− 8	B Sk	1	—
19·5	4·98	9·3	− 4	S	—	—
23·4	5·98	9·0	− 4	S	—	—
25·2	6·44	8·6	− 4	B	2	—
27·4	7·00	8·3	− 4	B	1½	—
28·8	7·35	8·1	− 4	S	—	—
31·1	7·95	7·8	− 4	S	—	—
34·8	8·89	7·5	− 4	S	—	—
39·0	9·96	7·3	− 4	S	—	—
21·7	5·54	9·1	0	S	—	—
25·5	6·51	8·4	0	B	1	—
29·7	7·58	7·5	0	S	—	—
33·6	8·58	6·5	0	S	—	—
37·0	9·46	5·5	0	S	—	—
23·6	6·03	8·6	+ 4	S	—	—
26·3	6·72	8·1	+ 4	B	½	—
27·6	7·05	7·6	+ 4	B	1	—
29·7	7·60	7·1	+ 4	S	—	—
31·6	8·07	6·5	+ 4	S	—	—
35·2	8·99	5·3	+ 4	S	—	—
38·6	9·85	4·3	+ 4	S	—	—
35·5	9·06	4·5	+ 6	B	2	—
38·8	9·92	3·4	+ 6	US	3	—
24·2	6·18	8·4	+ 8	S	—	—
25·8	6·60	7·8	+ 8	B	1½	—
26·6	6·79	7·5	+ 8	US	3	—
28·5	7·27	6·8	+ 8	US	4	—
32·0	8·18	5·5	+ 8	US	2½	—
36·0	9·20	3·5	+ 8	US	3½	—

UNDISTURBED HYDRODYNAMIC LONGITUDINAL STABILITY CHARACTERISTICS

TABLE 45

Model H

($C_{\Delta 0} = 2{\cdot}25$; $I = 23{\cdot}50$ lb ft^2)

Speed V (ft/sec)	Velocity coefficient C_v	Keel attitude α_K (deg)	Elevator angle η (deg)	Stable (S) Unstable (US) Border-line (B) Skipping (Sk)	Amplitude of porpoising if any (deg)	Limits of porpoising (deg)
20·5	5·24	12·8	−20	S	—	—
24·7	6·31	12·5	−20	S	—	—
27·1	6·92	12·5	−20	S	—	—
28·8	7·36	12·6	−20	S	—	—
30·5	7·79	12·6	−20	B Sk	1½	—
31·0	7·92	12·7	−20	B Sk	2	—
32·0	8·17	12·7	−20	B Sk	2	—
33·1	8·46	12·7	−20	US Sk	3	—
19·8	5·06	12·9	−16	S	—	—
23·8	6·08	12·0	−16	S	—	—
27·6	7·05	11·3	−16	S	—	—
31·5	8·05	11·9	−16	B	1	—
33·5	8·56	11·8	−16	B Sk	2	—
33·5	8·56	11·4	−14	S	—	—
35·3	9·02	11·0	−14	S	—	—
21·8	5·57	12·0	−12	S	—	—
25·7	6·57	10·9	−12	S	—	—
29·6	7·56	9·9	−12	S	—	—
33·2	8·49	10·7	−12	S	—	—
37·0	9·46	10·4	−12	S	—	—
0	0	4·5	− 8	S	—	—
4·0	1·02	4·6	− 8	S	—	—
7·8	1·99	6·8	− 8	S	—	—
11·8	3·02	8·0	− 8	S	—	—
16·0	4·08	11·3	− 8	S	—	—
17·8	4·55	12·9	− 8	S	—	—
19·5	4·98	12·4	− 8	S	—	—
23·5	6·01	10·5	− 8	S	—	—
27·5	7·03	8·9	− 8	S	—	—
31·3	8·00	7·9	− 8	S	—	—
35·0	8·95	8·4	− 8	S	—	—
39·0	9·96	8·0	− 8	S	—	—
19·8	5·06	12·3	− 4	S	—	—
21·8	5·57	10·9	− 4	S	—	—
25·5	6·52	8·6	− 4	S	—	—
27·5	7·03	7·9	− 4	S	—	—
28·6	7·31	7·4	− 4	S	—	—
29·5	7·54	7·1	− 4	S	—	—
33·1	8·46	6·1	− 4	S	—	—
37·3	9·53	5·3	− 4	S	—	—
22·0	5·62	10·2	0	S	—	—
24·0	6·13	8·9	0	S	—	—
25·7	6·57	7·9	0	S	—	—
29·0	7·41	6·3	0	S	—	—
32·5	8·30	5·3	0	S	—	—
36·3	9·27	4·1	0	S	—	—

TABLE 45—*continued*

Speed V (ft/sec)	Velocity coefficient C_v	Keel attitude α_K (deg)	Elevator angle η (deg)	Stable (S) Unstable (US) Border-line (B) Skipping (Sk)	Amplitude of porpoising if any (deg)	Limits of porpoising (deg)
24·5	6·26	8·2	—	S	—	—
25·2	6·44	7·9	—	B	2	—
26·6	6·79	7·1	—	B	1	—
20·0	5·11	11·8	+ 4	S	—	—
22·0	5·62	9·9	+ 4	S	—	—
23·8	6·08	8·7	+ 4	B	1	—
25·5	6·52	7·5	+ 4	US	3	—
27·6	7·06	6·2	+ 4	US	$2\frac{1}{2}$	—
31·5	8·05	4·9	+ 4	US	$2\frac{1}{2}$	—
35·0	8·95	3·8	+ 4	US	$2\frac{1}{2}$	—
22·0	5·62	9·5	+ 8	B	1	—
24·0	6·13	8·1	+ 8	US	9	—
21·1	5·39	9·9	+12	US	$2\frac{1}{2}$	—
22·2	5·68	8·9	+12	US	9	—

UNDISTURBED HYDRODYNAMIC LONGITUDINAL STABILITY CHARACTERISTICS

TABLE 46

Model H

($C_{\Delta 0} = 2{\cdot}75$; $I = 23{\cdot}50$ lb ft^2)

Speed V (ft/sec)	Velocity coefficient C_v	Keel attitude α_K (deg)	Elevator angle η (deg)	Stable (S) Unstable (US) Border-line (B) Skipping (Sk)	Amplitude of porpoising if any (deg)	Limits of porpoising (deg)
21·0	5·36	13·4	−20	S	—	—
23·8	6·08	12·8	−20	S	—	—
27·8	7·10	12·5	−20	S	—	—
29·8	7·61	12·4	−20	S	—	—
31·7	8·11	12·6	−20	S	—	—
33·5	8·56	12·2	−20	B Sk	1	—
19·7	5·04	13·7	−16	S	—	—
23·8	6·08	12·5	−16	S	—	—
27·6	7·05	12·2	−16	S	—	—
31·7	8·11	12·3	−16	S	—	—
35·2	8·99	11·6	−16	B Sk	1	—
38·0	9·72	11·3	−16	B Sk	2	—
22·0	5·62	12·9	−12	S	—	—
25·7	6·57	11·2	−12	S	—	—
27·3	6·98	10·5	−12	S	—	—
28·5	7·28	10·7	−12	S	—	—
30·0	7·66	10·5	−12	S	—	—
32·0	8·18	10·0	−12	S	—	—
33·2	8·48	10·2	−12	S	—	—
35·9	9·17	10·5	−12	S	—	—
37·8	9·66	10·3	−12	S	—	—
0	0	4·3	− 8	S	—	—
4·0	1·02	4·4	− 8	S	—	—
7·8	1·99	6·7	− 8	S	—	—
11·8	3·10	8·1	− 8	S	—	—
14·0	3·58	9·7	− 8	S	—	—
16·0	4·08	13·3	− 8	S	—	—
16·8	4·29	13·7	− 8	S	—	—
19·5	4·98	13·5	− 8	S	—	—
19·9	5·09	13·3	− 8	S	—	—
24·0	6·13	11·5	− 8	S	—	—
24·8	6·34	11·0	− 8	S	—	—
25·8	6·59	10·2	− 8	S	—	—
27·5	7·03	9·4	− 8	S	—	—
31·5	8·05	8·3	− 8	S	—	—
35·3	9·02	7·7	− 8	S	—	—
39·0	9·96	8·1	− 8	S	—	—
20·8	5·31	13·0	− 4	S	—	—
27·8	7·11	8·4	—	S	—	—
29·0	7·41	8·1	− 4	S	—	—
32·5	8·30	6·9	− 4	S	—	—
36·5	9·33	6·0	− 4	S	—	—

TABLE 46—*continued*

Speed V (ft/sec)	Velocity coefficient C_v	Keel attitude α_K (deg)	Elevator angle η (deg)	Stable (S) Unstable (US) Border-line (B) Skipping (Sk)	Amplitude of porpoising if any (deg)	Limits of porpoising (deg)
22·6	5·78	11·6	0	S	—	—
24·0	6·13	10·8	0	B	½	—
24·5	6·26	10·4	0	S	—	—
25·9	6·62	9·5	0	B	2	—
27·8	7·10	8·0	0	B	1	—
31·6	8·07	6·4	0	S	—	—
31·7	8·10	6·2	—	S	—	—
35·2	9·00	5·1	—	S	—	—
35·6	9·10	5·3	0	S	—	—
38·9	9·94	4·8	0	S	—	—
22·3	5·70	11·9	+ 2	S	—	—
24·1	6·16	10·4	+ 2	B	2	—
27·8	7·10	7·7	+ 2	US	2½	—
31·7	8·10	5·8	+ 2	B	2	—
35·4	9·04	4·7	+ 2	B	2	—
38·5	9·84	3·9	+ 2	B	2	—

UNDISTURBED HYDRODYNAMIC LONGITUDINAL STABILITY CHARACTERISTICS

TABLE 47

Model J

($C_{\Delta 0} = 2{\cdot}25$; $I = 23{\cdot}90$ lb ft^2)

Speed V (ft/sec)	Velocity coefficient C_v	Keel attitude α_K (deg)	Elevator angle η (deg)	Stable (S) Unstable (US) Border-line (B) Skipping (Sk)	Amplitude of porpoising if any (deg)	Limits of porpoising (deg)
18·8	4·80	12·7	−28	B	½	—
22·2	5·67	11·4	−28	S	—	—
25·7	6·56	11·4	−28	S	—	—
30·0	7·67	11·7	−28	S	—	—
33·8	8·64	11·6	−28	US Sk	4	—
16·0	4·08	13·5	−24	S	—	—
20·0	5·11	12·0	−24	B	½	—
24·1	6·16	11·3	−24	S	—	—
28·2	7·21	11·6	−24	S	—	—
32·2	8·24	11·6	−24	B	1	—
34·2	8·75	11·6	−24	US Sk	4	—
17·5	4·47	13·1	−20	B	¼	—
20·5	5·24	11·8	−20	B	½	—
24·4	6·24	11·1	−20	S	—	—
28·5	7·29	11·3	−20	S	—	—
32·2	8·24	11·2	−20	S	—	—
18·7	4·78	12·5	−16	B	¼	—
19·0	4·86	12·0	−16	US	5	—
24·3	6·21	10·5	−16	S	—	—
28·3	7·24	10·7	−16	S	—	—
32·2	8·24	10·6	−16	S	—	—
17·2	4·40	12·8	−12	B	½	—
19·5	4·99	11·6	−12	US	>3	—
21·1	5·40	10·8	−12	B	1	—
22·2	5·67	10·4	−12	S	—	—
25·8	6·60	9·9	−12	S	—	—
30·0	7·66	9·9	−12	S	—	—
33·5	8·56	9·9	−12	S	—	—
0	0	4·7	− 8	S	—	—
4·0	1·02	4·7	− 8	S	—	—
8·0	2·04	7·0	− 8	S	—	—
12·1	3·09	8·7	− 8	S	—	—
14·5	3·71	12·3	− 8	S	—	—
16·1	4·11	12·8	− 8	S	—	—
18·5	4·73	12·0	− 8	US	4	—
20·2	5·16	10·9	− 8	US	>5	—
24·3	6·21	9·6	− 8	S	—	—
28·4	7·26	8·7	− 8	S	—	—
32·2	8·24	8·5	− 8	S	—	—
36·0	9·20	9·3	− 8	S	—	—

TABLE 47—*continued*

Speed V (ft/sec)	Velocity coefficient C_v	Keel attitude α_K (deg)	Elevator angle η (deg)	Stable (S) Unstable (US) Border-line (B) Skipping (Sk)	Amplitude of porpoising if any (deg)	Limits of porpoising (deg)
18·5	4·73	11·8	− 4	US	6	—
22·5	5·75	9·5	− 4	S	—	—
26·0	6·65	7·7	− 4	S	—	—
30·2	7·72	6·6	− 4	S	—	—
34·6	8·85	6·2	− 4	S	—	—
37·8	9·66	5·7	− 4	S	—	—
16·5	4·22	12·5	0	S	—	—
19·4	4·96	11·0	0	US	$6\frac{1}{2}$	—
21·9	5·60	9·5	0	US	5	—
23·5	6·01	8·5	0	B	2	—
28·0	7·16	6·3	0	S	—	—
31·8	8·13	5·0	0	S	—	—
35·6	9·10	4·2	0	S	—	—
17·5	4·47	11·9	+ 4	B	$1\frac{1}{2}$	—
22·2	5·67	8·4	+ 4	US	7	—
26·1	6·67	6·4	+ 4	B	2	—
30·3	7·75	4·9	+ 4	B	2	—
34·0	8·69	3·5	+ 4	US	>2	—
38·0	9·71	2·7	+ 4	US	3	—

UNDISTURBED HYDRODYNAMIC LONGITUDINAL STABILITY CHARACTERISTICS

TABLE 48

Model J

($C_{\Delta 0} = 2{\cdot}75$; $I = 23{\cdot}90$ lb ft^2)

Speed V (ft/sec)	Velocity coefficient C_v	Keel attitude α_K (deg)	Elevator angle η (deg)	Stable (S) Unstable (US) Border-line (B) Skipping (Sk)	Amplitude of porpoising if any (deg)	Limits of porpoising (deg)
17·5	4·47	14·7	−28	S	—	—
18·5	4·72	14·5	−28	S	—	—
20·0	5·11	13·6	−28	US	8	—
23·8	6·08	11·9	−28	B	½	—
27·5	7·03	11·7	−28	S	—	—
31·8	8·13	11·8	−28	S	—	—
35·2	9·00	11·8	−28	S	—	—
39·0	9·97	10·9	−28	US Sk	4	—
22·0	5·62	12·5	−24	B	½	—
25·5	6·52	11·7	−24	S	—	—
29·5	7·54	11·7	−24	S	—	—
33·5	8·56	11·7	−24	S	—	—
36·8	9·40	11·7	−24	S	—	—
19·8	5·06	13·4	−20	US	6	—
23·0	5·87	11·7	−20	B	¼	—
27·0	6·90	11·2	−20	S	—	—
31·0	7·92	11·4	−20	S	—	—
34·8	8·89	11·5	−20	S	—	—
37·8	9·66	11·3	−20	US Sk	3½	—
19·6	5·01	13·7	−16	US	8	—
21·9	5·60	12·4	−16	B	2	—
25·0	6·39	10·8	−16	S	—	—
29·7	7·59	10·8	−16	S	—	—
33·1	8·46	10·8	−16	S	—	—
36·5	9·33	10·7	−16	S	—	—
18·7	4·78	14·2	−12	US	5	—
22·2	5·67	11·7	−12	US	6	—
25·5	6·52	10·3	−12	S	—	—
29·5	7·54	10·1	−12	S	—	—
33·5	8·56	10·2	−12	S	—	—
37·6	9·61	10·0	−12	S	—	—
0	0	4·8	− 8	S	—	—
4·0	1·02	4·7	− 8	S	—	—
7·9	2·02	7·3	− 8	S	—	—
11·9	3·04	9·0	− 8	S	—	—
14·0	3·58	11·8	− 8	S	—	—
16·0	4·08	14·0	− 8	S	—	—
18·0	4·60	14·0	− 8	S	—	—
19·5	4·98	13·4	− 8	US	9	—
23·5	6·01	10·7	− 8	US	6	—
27·1	6·93	9·2	− 8	S	—	—
31·0	7·92	8·9	− 8	S	—	—
34·6	8·84	8·4	− 8	S	—	—
39·0	9·96	9·3	− 8	S	—	—

TABLE 48—*continued*

Speed V (ft/sec)	Velocity coefficient C_v	Keel attitude α_K (deg)	Elevator angle η (deg)	Stable (S) Unstable (US) Border-line (B) Skipping (Sk)	Amplitude of porpoising if any (deg)	Limits of porpoising (deg)
18·7	4·78	13·5	− 4	S	—	—
21·8	5·57	11·6	− 4	US	9	—
25·5	6·51	9·5	− 4	S	—	—
29·0	7·41	8·0	− 4	S	—	—
32·5	8·30	7·0	− 4	S	—	—
36·8	9·40	6·5	− 4	S	—	—
19·8	5·06	12·4	0	US	10	—
23·8	6·08	9·7	0	US	6	—
27·7	7·08	7·8	0	S	—	—
31·3	8·00	6·5	0	S	—	—
35·0	8·95	5·4	0	S	—	—
39·0	9·97	4·7	0	S	—	—
25·8	6·59	8·3	+ 4	US	>4	—
29·9	7·65	6·1	+ 4	B	$1\frac{1}{2}$	—
33·5	8·56	5·0	+ 4	B	$\frac{1}{2}$	—
36·9	9·44	3·9	+ 4	B	$\frac{1}{2}$	—
27·8	7·11	6·4	+ 8	US	10	—
31·8	8·13	5·0	+ 8	US	8	—
35·3	9·02	4·0	+ 8	US	4	—

UNDISTURBED HYDRODYNAMIC LONGITUDINAL STABILITY CHARACTERISTICS

TABLE 49

Model K

($C_{\Delta 0} = 2{\cdot}75$; $I = 23{\cdot}10$ lb ft²)

Speed V (ft/sec)	Velocity coefficient C_v	Keel attitude α_K (deg)	Elevator angle η (deg)	Stable (S) Unstable (US) Border-line (B) Skipping (Sk)	Amplitude of porpoising if any (deg)	Limits of porpoising (deg)
20·8	5·32	12·8	−20	S	—	—
22·0	5·62	12·6	−20	S	—	—
25·7	6·56	12·3	−20	S	—	—
29·7	7·59	12·3	−20	S	—	—
19·7	5·04	12·8	−16	S	—	—
23·6	6·03	12·2	−16	S	—	—
27·5	7·03	12·2	−16	S	—	—
31·2	7·97	12·2	−16	S	—	—
35·1	8·97	11·5	−16	B	½	—
38·2	9·76	10·9	−16	B	1	—
21·8	5·57	12·2	−12	S	—	—
25·5	6·51	10·2	−12	S	—	—
29·6	7·56	10·1	−12	S	—	—
33·0	8·44	10·0	−12	S	—	—
36·0	9·21	10·2	−12	S	—	—
0	0	3·6	− 8	S	—	—
4·0	1·02	3·7	− 8	S	—	—
7·9	2·02	5·9	− 8	S	—	—
11·8	3·02	6·8	− 8	S	—	—
16·0	4·08	12·3	− 8	S	—	—
17·8	4·55	12·7	− 8	S	—	—
19·2	4·91	12·5	− 8	S	—	—
23·4	5·98	10·5	− 8	S	—	—
27·0	6·90	8·4	− 8	S	—	—
31·3	7·99	8·0	− 8	S	—	—
34·3	8·82	7·8	− 8	S	—	—
38·0	9·72	8·3	− 8	S	—	—
20·8	5·32	12·2	− 4	S	—	—
22·0	5·62	11·0	− 4	S	—	—
25·6	6·55	8·5	− 4	S	—	—
28·0	7·16	7·2	− 4	S	—	—
32·0	8·18	6·7	− 4	S	—	—
35·5	9·08	6·0	− 4	S	—	—
19·5	4·98	12·3	0	S	—	—
23·5	6·01	9·4	0	S	—	—
27·6	7·06	6·9	0	S	—	—
31·2	7·98	5·6	0	S	—	—
35·0	8·95	4·6	0	S	—	—
38·0	9·72	3·8	0	S	—	—
22·0	5·62	10·1	+ 4	S	—	—
24·5	6·26	8·0	+ 4	B	½	—
29·2	7·46	5·6	+ 4	B	1	—
33·2	8·48	3·9	+ 4	B	1½	—
37·0	9·45	3·2	+ 4	B	1	—

TABLE 49—*continued*

Speed V (ft/sec)	Velocity coefficient C_v	Keel attitude α_K (deg)	Elevator angle η (deg)	Stable (S) Unstable (US) Border-line (B) Skipping (Sk)	Amplitude of porpoising if any (deg)	Limits of porpoising (deg)
23·8	6·08	8·3	+ 6	S	—	—
27·5	7·03	5·6	+ 6	US	$2\frac{1}{2}$	—
31·3	8·00	4·3	+ 6	US	$2\frac{1}{2}$	—
35·0	8·94	3·0	+ 6	US	$2\frac{1}{2}$	—
38·6	9·86	2·2	+ 6	US	$3\frac{1}{2}$	—
22·5	5·75	9·2	+ 8	S	—	—
25·0	6·39	7·1	+ 8	B	2	—
21·7	5·54	9·6	+12	S	—	—
23·3	5·96	8·0	+12	US	5	—

UNDISTURBED HYDRODYNAMIC LONGITUDINAL STABILITY CHARACTERISTICS

TABLE 50

Model L

($C_{\Delta 0} = 2{\cdot}75$; $I = 25{\cdot}50$ lb ft^2)

Speed V (ft/sec)	Velocity coefficient C_v	Keel attitude α_K (deg)	Elevator angle η (deg)	Stable (S) Unstable (US) Border-line (B) Skipping (Sk)	Amplitude of porpoising if any (deg)	Limits of porpoising (deg)
24·0	6·14	9·4	−16	S	—	—
27·8	7·11	9·4	−16	S	—	
31·0	7·93	9·4	−16	S	—	—
25·5	6·51	9·2	−12	S	—	—
29·7	7·59	9·2	−12	S	—	—
33·5	8·56	9·1	−12	S	—	—
36·5	9·32	9·0	−12	B Sk	1	—
0	0	2·2	− 8	S	—	—
4·0	1·02	2·2	− 8	S	—	—
7·8	1·99	3·4	− 8	S	—	—
12·0	3·07	3·7	− 8	S	—	—
16·0	4·08	5·0	− 8	S	—	—
16·0	4·08	5·0	− 8	S	—	—
17·9	4·57	7·4	− 8	S	—	—
19·6	5·01	8·8	− 8	S	—	—
23·4	5·98	9·1	− 8	S	—	—
26·0	6·64	8·8	− 8	S	—	—
27·9	7·13	8·6	− 8	S	—	—
31·2	7·98	8·3	− 8	S	—	—
35·0	8·95	8·4	− 8	S	—	—
38·1	9·75	8·1	− 8	S	—	—
25·3	6·46	8·5	− 4	S	—	—
27·8	7·11	7·3	− 4	S	—	—
29·7	7·60	7·0	− 4	S	—	—
33·0	8·44	6·4	− 4	S	—	—
37·0	9·45	5·7	− 4	S	—	—
23·8	6·08	8·8	0	S	—	—
25·5	6·51	8·0	0	S	—	—
26·8	6·85	7·2	0	S	—	—
27·5	7·03	6·8	0	S	—	—
30·8	7·86	5·4	0	S	—	—
31·3	8·00	5·1	0	S	—	—
35·0	8·94	4·3	0	S	—	—
38·2	9·77	3·3	0	S	—	—
23·8	6·08	8·4	+ 4	S	—	—
24·8	6·33	8·0	+ 4	B	1	—
25·5	6·51	7·6	+ 4	US	2½	—
26·2	6·69	6·9	+ 4	US	—	—
27·6	7·05	6·1	+ 4	B	1½	—
30·0	7·66	4·8	+ 4	B	½	—
32·3	8·25	4·2	+ 4	S	—	—
35·0	8·94	3·5	+ 4	S	—	—
38·5	9·84	2·7	+ 4	S	—	—
28·2	7·21	5·1	+ 8	US	3	—
31·3	8·00	4·1	+ 8	US	3½	—
35·2	8·99	2·8	+ 8	US	4	—
38·5	9·84	1·8	+ 8	US	3	—

UNDISTURBED HYDRODYNAMIC LONGITUDINAL STABILITY CHARACTERISTICS

TABLE 51

Model M

($C_{\Delta 0} = 2{\cdot}75$; $I = 23{\cdot}20$ lb ft^2)

Speed V (ft/sec)	Velocity coefficient C_v	Keel attitude α_K (deg)	Elevator angle η (deg)	Stable (S) Unstable (US) Border-line (B) Skipping (Sk)	Amplitude of porpoising if any (deg)	Limits of porpoising (deg)
23·2	5·93	11·1	−16	S	—	—
27·0	6·90	11·1	−16	S	—	—
29·0	7·42	11·1	−16	S	—	—
34·6	8·85	11·2	−16	B	1½	—
36·5	9·34	11·2	−16	US	3	—
22·0	5·62	11·0	−12	S	—	—
23·8	6·09	11·0	−12	S	—	—
25·7	6·57	10·8	−12	S	—	—
27·6	7·05	11·0	−12	S	—	—
29·9	7·66	11·0	−12	S	—	—
33·3	8·51	11·0	−12	S	—	—
36·1	9·23	11·0	−12	B	1½	—
37·8	9·69	11·0	−12	US	3	—
37·5	9·60	10·8	−10	S	—	—
39·0	9·98	10·8	−10	US	2½	—
0	0	4·0	− 8	S	—	—
3·9	1·00	4·0	− 8	S	—	—
7·8	1·99	5·3	− 8	S	—	—
11·9	3·04	5·7	− 8	S	—	—
16·4	4·19	7·6	− 8	S	—	—
19·5	4·99	10·9	− 8	S	—	—
23·5	6·01	10·7	− 8	B	1½	—
26·0	6·65	10·4	− 8	S	—	—
27·8	7·11	9·8	− 8	S	—	—
31·7	8·11	9·6	− 8	S	—	—
35·4	9·05	9·9	—	S	—	—
35·5	9·08	9·7	− 8	S	—	—
38·9	9·95	9·3	− 8	S	—	—
22·1	5·65	10·7	− 4	S	—	—
23·3	5·97	10·5	− 4	B	1½	—
24·0	6·14	10·2	− 4	S	—	—
26·0	6·64	9·1	− 4	S	—	—
30·0	7·67	8·0	− 4	S	—	—
33·5	8·56	7·2	− 4	S	—	—
37·0	9·46	6·6	− 4	S	—	—
20·0	5·12	10·7	0	S	—	—
24·0	6·13	9·9	0	US	4	—
25·5	6·52	8·8	0	B	1	—
27·3	6·98	8·0	0	S	—	—
31·5	8·06	6·6	0	S	—	—
35·5	9·09	5·0	0	S	—	—
39·0	9·99	3·9	0	S	—	—
22·2	5·68	10·5	+ 4	US	3½	—
24·3	6·23	9·0	+ 4	US	4	—
26·1	6·68	7·8	+ 4	US	4½	—
30·0	7·68	6·0	+ 4	B	1	—
34·0	8·70	4·7	+ 4	B	1½	—
37·5	9·61	3·5	+ 4	US	>2	—
21·5	5·50	10·5	+ 6	S	—	—
28·2	7·23	6·5	+ 6	US	3½	—
32·0	8·17	4·9	+ 6	US	3	—

UNDISTURBED HYDRODYNAMIC LONGITUDINAL STABILITY CHARACTERISTICS

TABLE 52

Model N

($C_{\Delta 0} = 2{\cdot}75$; $I = 23{\cdot}90$ lb ft^2)

Speed V (ft/sec)	Velocity coefficient C_v	Keel attitude α_K (deg)	Elevator angle η (deg)	Stable (S) Unstable (US) Border-line (B) Skipping (Sk)	Amplitude of porpoising if any (deg)	Limits of porpoising (deg)
23·6	6·04	11·2	−20	S		
28·0	7·16	11·3	−20	S		
32·0	8·18	11·4	−20	B	1½	
34·0	8·70	11·5	−20	US	2	
22·1	5·66	11·1	−16	S		
25·0	6·40	10·8	−16	S		
26·1	6·66	10·7	−16	S		
30·0	7·67	10·8	−16	S		
33·0	8·42	10·9	−16	S		
34·0	8·70	11·0	−16	S		
35·0	8·95	11·3	−16	B	1	
38·0	9·72	10·9	−16	B	1½	
23·0	5·87	10·9	−12	S		
25·0	6·40	10·1	−12	S		
27·1	6·92	9·9	−12	S		
31·0	7·93	9·7	−12	S		
34·3	8·76	10·2	−12	S		
37·8	9·66	9·8	−12	S		
0	0	3·5	− 8	S		
4·0	1·02	3·3	− 8	S		
8·0	2·04	4·7	− 8	S		
12·0	3·07	5·1	− 8	S		
16·6	4·24	7·4	− 8	S		
19·7	5·04	11·0	− 8	S		
23·3	5·96	10·7	− 8	B	1½	
23·5	6·01	10·5	− 8	B	1	
27·2	6·95	8·5	− 8	S		
31·1	7·96	8·2	− 8	S		
35·0	8·95	8·4	− 8	S		
38·9	9·95	8·9	− 8	S		
21·7	5·55	10·7	− 4	S		
23·8	6·07	9·7	− 4	B	1	
25·5	6·52	8·4	− 4	B	1	
29·5	7·55	6·6	− 4	S		
33·0	8·44	5·8	− 4	S		
36·1	9·23	5·4	− 4	S		
20·0	5·11	10·7	0	S		
22·0	5·63	10·5	0	B	2	
23·1	5·91	10·0	0	US	4	
23·8	6·07	9·7	0	US	2½	
25·5	6·52	8·1	0	US	3	
28·0	7·16	6·7	0	B	1	
30·3	7·75	5·7	0	S		
34·6	8·85	4·3	0	S		
39·0	9·98	3·2	0	S		
29·8	7·62	5·5	+ 4	US	2½	
33·7	8·62	4·2	+ 4	B	2	
37·2	9·51	3·0	+ 4	B	1	

DISTURBED HYDRODYNAMIC LONGITUDINAL STABILITY CHARACTERISTICS

TABLE 53

Model A

($C_{\Delta 0} = 2{\cdot}25$; $I = 24{\cdot}46$ lb ft^2)

Speed V (ft/sec)	Velocity coefficient C_v	Keel attitude α_K (deg)	Elevator angle η (deg)	Stable (S) Unstable (US) Border-line (B) Skipping (Sk) before disturbance	Stable (S) Unstable (US) Border-line (B) Skipping (Sk) after disturbance	Disturbance nose-down (deg)	Amplitude of porpoising, if any, after disturbance (deg)	Limits of porpoising after disturbance (deg)
20·5	5·24	10·5	—16	S	US	8	2½	—
23·6	6·03	10·3	—16	S	US	11	9	—
27·8	7·11	10·3	—16	B Sk	US	11	7	—
29·7	7·60	10·3	—16	US Sk	US Sk	11	3	—
21·7	5·55	10·2	—12	S	US	10	10	—
25·5	6·52	10·2	—12	S	US	11	9	—
29·5	7·55	10·2	—12	S	S	10	—	—
33·5	8·57	10·1	—12	US Sk	US Sk	—	—	—
0	0	3·2	— 8	S	S	—	—	—
4·0	1·02	3·1	— 8	S	S	—	—	—
7·8	1·99	5·2	— 8	S	S	—	—	—
12·0	3·07	6·0	— 8	S	S	—	—	—
14·0	3·58	7·4	— 8	S	S	—	—	—
16·0	4·09	10·2	— 8	S	S	—	—	—
17·8	4·56	10·6	— 8	S	S	—	—	—
19·5	4·98	10·4	— 8	S	S	11	—	—
21·0	5·37	10·2	— 8	B	US	—	—	—
23·7	6·06	9·8	— 8	S	US	10	9	—
27·4	7·01	9·7	— 8	S	US	10	9	—
31·4	8·03	9·6	— 8	S	S	11	—	—
34·6	8·85	9·2	— 8	S	S	11	—	—
22·8	5·83	9·7	— 6	S	US	—	—	—
25·1	6·42	9·3	— 6	S	US	11	10	—
26·8	6·86	9·2	— 6	S	US	11	8	—
27·8	7·11	9·0	— 6	S	S	9½	—	—
31·5	8·06	8·3	— 6	S	S	10	—	—
35·3	9·03	8·2	— 6	S	S	—	—	—
19·7	5·04	10·2	— 4	S	S	11	—	—
20·8	5·32	10·0	— 4	US	US	11	8	—
21·8	5·58	9·8	— 4	US	US	10	10	—
22·9	5·86	9·4	— 4	S	US	—	—	—
25·5	6·52	8·5	— 4	S	US	10	10	—
29·9	7·65	7·2	— 4	S	S	10	—	—
33·0	8·44	6·8	— 4	S	S	9	—	—
37·0	9·46	6·9	— 4	S	S	6	—	—
31·7	8·11	6·3	—	S	S	6	—	—
33·4	8·54	6·2	—	S	S	7	—	—
34·5	8·82	5·7	—	S	S	7	—	—
35·0	8·95	5·3	—	S	US	7	—	—
36·3	9·29	5·3	—	S	US	—	—	—
36·3	9·29	6·0	—	S	US	—	—	—
37·0	9·46	6·0	—	S	US	7½	—	—

TABLE 53—*continued*

Speed V (ft/sec)	Velocity coefficient C_v	Keel attitude α_K (deg)	Elevator angle η (deg)	Stable (S) Unstable (US) Border-line (B) Skipping (Sk) before disturbance	Stable (S) Unstable (US) Border-line (B) Skipping (Sk) after disturbance	Disturbance nose-down (deg)	Amplitude of porpoising, if any, after disturbance (deg)	Limits of porpoising after disturbance (deg)
27·5	7·03	7·2	— 2	S	US	8	—	—
28·9	7·39	6·9	— 2	S	S	8	—	—
30·1	7·70	6·2	— 2	S	S	7	—	—
31·2	7·98	6·2	— 2	S	US	7	—	—
33·0	8·44	5·4	— 2	S	US	7	—	—
37·0	9·46	4·3	— 2	S	US	—	—	—
20·4	5·22	9·8	0	US	US	—	—	—
23·8	6·09	8·3	0	S	US	12	11	—
27·8	7·11	6·8	0	S	US	9	—	—
29·9	7·65	5·8	0	S	US	8	—	—
33·8	8·65	4·3	0	S	US	7	—	—
38·0	9·72	3·2	0	S	US	—	—	—

DISTURBED HYDRODYNAMIC LONGITUDINAL STABILITY CHARACTERISTICS

TABLE 54

Model A

($C_{\Delta 0} = 2{\cdot}75$; $I = 22{\cdot}90$ lb ft²)

Speed V (ft/sec)	Velocity coefficient C_v	Keel attitude α_K (deg)	Elevator angle η (deg)	Stable (S) Unstable (US) Border-line (B) Skipping (Sk) before disturbance	Stable (S) Unstable (US) Border-line (B) Skipping (Sk) after disturbance	Disturbance nose-down (deg)	Amplitude of porpoising, if any, after disturbance (deg)	Limits of porpoising after disturbance (deg)
20·0	5·11	11·8	−20	S	S	—	—	—
21·1	5·39	11·7	−20	S	B	—	2	—
22·3	5·70	11·4	−20	US	US	—	6	—
25·0	6·38	11·2	−20	B	US	—	10	—
26·1	6·66	11·0	−20	S	US	—	10	—
28·1	7·18	11·2	−20	S	US	—	10	—
31·0	7·91	11·1	−20	S	US	7	9	—
33·0	8·44	11·1	−20	US	US	—	10	—
34·6	8·84	11·2	−20	US	US	—	—	—
29·0	7·42	11·1	—	S	US	—	9	—
30·0	7·67	11·0	—	S	US	5	8	—
36·0	9·20	11·0	—	US	US	—	4	—
21·1	5·39	11·3	−12	S	US	2	3	—
24·0	6·14	10·9	−12	US	US	6	10	9 to 19
25·6	6·54	10·6	−12	S	US	5	11	9 to 20
33·0	8·44	10·6	−12	S	US	5	10	5 to 15
34·4	8·79	10·6	−12	S	S	7	—	—
36·0	9·20	10·7	−12	B	US	—	—	—
38·1	9·74	10·6	−12	US	US	—	—	—
0	0	3·4	− 8	S	S	—	—	—
3·9	1·00	3·5	− 8	S	S	—	—	—
8·2	2·09	5·9	− 8	S	S	—	—	—
12·1	3·10	6·9	− 8	S	S	—	—	—
16·0	4·08	11·4	− 8	S	S	—	—	—
18·0	4·60	11·7	− 8	S	S	—	—	—
20·1	5·14	11·4	− 8	S	S	—	—	—
25·1	6·41	10·4	− 8	US	US	—	10	5 to 15
26·1	6·67	10·3	− 8	S	US	5	10	5 to 15
27·9	7·14	10·4	− 8	S	US	—	8	—
31·8	8·14	10·4	− 8	S	US	5	8	—
32·0	8·18	9·9	− 8	S	US	—	$7\frac{1}{2}$	5 to $12\frac{1}{2}$
35·5	9·08	9·9	− 8	S	S	—	—	—
39·4	10·09	9·4	− 8	S	S	—	—	—
27·0	6·91	9·9	− 6	S	US	—	—	—
29·9	7·64	9·5	− 6	S	US	—	8	5 to 13
31·7	8·11	9·1	− 6	S	S	—	—	—
33·6	8·58	8·7	− 6	S	S	—	—	—
31·0	7·91	9·0	—	S	US	6	7	10 to 17

TABLE 54—*continued*

Speed V (ft/sec)	Velocity coefficient C_v	Keel attitude α_K (deg)	Elevator angle η (deg)	Stable (S) Unstable (US) Border-line (B) Skipping (Sk) before disturbance	Stable (S) Unstable (US) Border-line (B) Skipping (Sk) after disturbance	Disturbance nose-down (deg)	Amplitude of porpoising, if any, after disturbance (deg)	Limits of porpoising after disturbance (deg)
27·8	7·10	9·3	− 4	S	US	—	10	9 to 19
29·0	7·41	9·0	− 4	S	US	—	10	9 to 19
30·0	7·66	8·8	− 4	S	US	—	10	9 to 19
32·0	8·18	8·4	− 4	S	US	7	9	9 to 18
32·6	8·34	7·2	—	S	US	9	$8\frac{1}{2}$	—
33·8	8·65	8·2	− 4	S	S	—	—	—
34·7	8·88	6·9	—	S	US	9	—	—
36·7	9·39	6·7	—	S	S	8	—	—
28·0	7·16	8·9	—	S	US	—	10	5 to 15
36·0	9·20	7·0	—	S	S	—	—	—
38·2	9·77	5·7	—	S	US	6	—	—
20·1	5·14	11·4	0	S	S	—	—	—
21·0	5·36	11·0	0	S	US	—	4	—
22·1	5·66	10·9	0	US	US	—	6	—
26·1	6·67	9·2	0	B	US	—	—	—
29·9	7·64	7·8	0	S	US	—	11	—
31·7	8·10	7·2	0	S	US	—	11	—
33·7	8·61	6·6	0	S	US	—	11	—
34·7	8·86	6·2	0	S	US	7	—	—
35·5	9·06	6·0	0	S	US	—	—	—
37·5	9·59	5·4	0	S	US	—	—	—
25·8	6·59	8·7	+ 4	B	US	—	—	—
27·2	6·96	7·8	+ 4	B	US	—	—	—
28·2	7·23	7·4	+ 4	B	US	—	—	—
29·4	7·52	6·8	+ 4	B	US	—	—	—
30·3	7·74	6·6	+ 4	S	US	—	—	—
34·1	8·71	5·4	+ 4	S	US	—	—	—
37·0	9·45	4·5	+ 4	S	US	—	—	—
39·7	10·16	3·9	+ 4	S	US	—	—	—
21·1	5·39	10·8	+ 6	US	US	—	—	—
23·6	6·03	9·7	+ 6	US	US	—	11	—
26·0	6·65	8·4	+ 6	US	US	7	12	8 to 20
27·0	6·89	7·4	+ 6	US	US	—	—	—
31·0	7·93	5·9	+ 6	B	US	—	—	—
35·6	9·10	4·4	+ 6	US	US	—	—	—
39·4	10·09	3·4	+ 6	S	US	—	—	—
20·0	5·11	11·2	+ 8	S	S	—	—	—

DISTURBED HYDRODYNAMIC LONGITUDINAL STABILITY CHARACTERISTICS

TABLE 55

Model A

($C_{\Delta 0} = 3{\cdot}00$; $I = 22{\cdot}90$ lb ft^2)

Speed V (ft/sec)	Velocity coefficient C_v	Keel attitude α_K (deg)	Elevator angle η (deg)	Stable (S) Unstable (US) Border-line (B) Skipping (Sk) before disturbance	Stable (S) Unstable (US) Border-line (B) Skipping (Sk) after disturbance	Disturbance nose-down (deg)	Amplitude of porpoising, if any, after disturbance (deg)	Limits of porpoising after disturbance (deg)
22·2	5·67	12·1	−20	S	US	4	6	—
25·7	6·56	11·4	−20	US	US	—	—	—
29·8	7·61	11·3	−20	S	US	—	8	—
33·5	8·56	11·4	−20	US	US	—	—	—
37·5	9·59	11·3	−20	US	US	—	—	—
26·2	6·69	10·8	−12	S	US	6	10	—
29·9	7·64	10·7	−12	B	US	8	9	—
33·5	8·56	10·8	−12	S	US	—	—	—
37·6	9·61	10·8	−12	US	US	—	—	—
0	0	3·4	− 8	S	S	—	—	—
4·0	1·02	3·5	− 8	S	S	—	—	—
8·1	2·07	5·9	− 8	S	S	—	—	—
12·0	3·07	7·3	− 8	S	S	—	—	—
16·1	4·12	11·9	− 8	S	S	—	—	—
19·8	5·06	12·0	− 8	S	S	—	—	—
23·7	6·06	11·7	− 8	US	US	—	—	—
27·9	7·14	10·6	− 8	S	US	—	—	—
35·4	9·05	10·3	− 8	S	S	10	—	—
39·2	10·02	10·0	− 8	S	S	—	—	—
22·0	5·62	11·8	− 4	US	US	—	—	—
26·0	6·64	10·7	− 4	US	US	5	10	—
29·9	7·64	9·8	− 4	US	S	4	10	—
33·7	8·61	9·4	− 4	S	US	6	10	—
37·6	9·61	9·3	− 4	S	S	—	—	—
34·6	8·84	8·1	− 2	S	US	—	—	—
36·1	9·24	7·8	− 2	S	S	—	—	—
38·1	9·74	7·5	− 2	S	S	—	—	—
39·2	10·02	7·3	− 2	S	S	—	—	—
21·3	5·44	11·4	0	S	S	—	—	—
23·7	6·06	11·1	0	US	US	—	10	—
27·9	7·14	8·9	0	S	US	—	—	—
31·5	8·05	7·9	0	S	US	—	—	—
35·4	9·05	6·9	0	S	US	—	—	—
39·0	9·96	6·4	0	S	US	—	—	—
20·2	5·16	11·6	+ 4	S	S	—	—	—
24·3	6·21	10·7	+ 4	US	US	—	10	—
28·0	7·16	8·1	+ 4	B	US	5	—	—
31·8	8·12	7·0	+ 4	S	US	—	—	—
35·6	9·10	5·6	+ 4	S	US	3	—	—
39·7	10·16	4·7	+ 4	S	US	2	—	—
20·2	5·17	11·4	+ 8	S	S	—	—	—
21·1	5·39	10·9	+ 8	B	B	—	1	—
22·0	5·62	10·9	+ 8	US	US	—	—	—
25·5	6·52	9·6	+ 8	US	US	—	—	—
29·8	7·62	7·1	+ 8	US	US	—	—	—
33·5	8·56	5·7	+ 8	US	US	—	—	—
37·5	9·59	3·9	+ 8	US	US	—	—	—

DISTURBED HYDRODYNAMIC LONGITUDINAL STABILITY CHARACTERISTICS

TABLE 56

Model A

(With take-off power)

($C_{\Delta 0} = 2{\cdot}75$; $I = 23{\cdot}25$ lb ft^2)

Speed V (ft/sec)	Velocity coefficient C_v	Keel attitude α_K (deg)	Elevator angle η (deg)	Stable (S) Unstable (US) Border-line (B) Skipping (Sk) before disturbance	Stable (S) Unstable (US) Border-line (B) Skipping (Sk) after disturbance	Disturbance nose-down (deg)	Amplitude of porpoising, if any, after disturbance (deg)	Limits of porpoising after disturbance (deg)
19·2	4·91	9·9	−24	S	S	—	—	—
22·1	5·65	9·6	−24	US	US	—	—	—
24·1	6·16	9·5	−24	S	US	—	—	—
28·1	7·19	9·8	−24	S	S	—	—	—
30·2	7·72	9·9	−24	S	S	—	—	—
31·2	7·98	9·9	−24	US	US	—	—	—
19·1	4·88	9·8	−16	S	S	—	—	—
19·9	5·08	9·8	−16	US	US	—	—	—
22·2	5·68	9·4	−16	US	US	—	—	—
24·1	6·16	9·2	−16	S	US	—	—	—
26·1	6·67	9·3	−16	S	US	—	—	—
28·0	7·16	9·3	−16	S	S	—	—	—
30·1	7·70	9·2	−16	S	S	—	—	—
32·0	8·18	9·2	−16	S	S	—	—	—
33·8	8·65	9·0	−16	US	US	—	—	—
35·5	9·08	8·6	−16	US	US	—	—	—
24·9	6·37	8·5	−12	S	US	—	—	—
26·0	6·65	8·1	−12	S	US	—	—	—
27·5	7·04	8·3	−12	S	S	—	—	—
29·9	7·65	8·3	−12	S	S	—	—	—
31·8	8·14	8·2	−12	S	S	—	—	—
35·6	9·10	8·0	−12	S	S	—	—	—
0	0	2·8	− 8	S	S	—	—	—
3·8	0·97	2·7	− 8	S	S	—	—	—
8·1	2·07	5·0	− 8	S	S	—	—	—
12·0	3·07	6·0	− 8	S	S	—	—	—
16·1	4·12	9·6	− 8	S	S	—	—	—
18·1	4·63	9·7	− 8	S	S	—	—	—
20·2	5·17	9·5	− 8	US	US	—	—	—
24·0	6·14	8·3	− 8	S	US	—	9	—
26·0	6·65	7·4	− 8	S	US	—	—	—
28·0	7·16	6·8	− 8	S	S	—	—	—
31·8	8·14	7·1	− 8	S	S	—	—	—
35·5	9·08	7·4	− 8	S	S	—	—	—
38·5	9·85	7·7	− 8	S	S	—	—	—
22·1	5·65	8·8	− 4	US	US	—	—	—
24·0	6·13	7·9	− 4	US	US	—	—	—
27·8	7·10	5·8	− 4	S	US	—	—	—
31·4	8·03	5·8	—	S	US	—	—	—
31·8	8·14	5·2	− 4	S	US	—	—	—
34·6	8·85	5·5	—	S	US	—	—	—

TABLE 56—*continued*

Speed V (ft/sec)	Velocity coefficient C_v	Keel attitude α_π (deg)	Elevator angle η (deg)	Stable (S) Unstable (US) Border-line (B) Skipping (Sk) before disturbance	Stable (S) Unstable (US) Border-line (B) Skipping (Sk) after disturbance	Disturbance nose-down (deg)	Amplitude of porpoising, if any, after disturbance (deg)	Limits of porpoising after disturbance (deg)
25·0	6·39	6·8	0	US	US	—	—	—
27·6	7·06	5·2	0	S	US	—	—	—
31·4	8·04	4·4	0	S	US	—	—	—
35·4	9·05	3·8	0	S	US	—	11½	½ to 12
39·1	10·00	3·4	0	S	US	—	—	—
18·0	4·61	9·3	+ 4	S	S	—	—	—
18·9	4·84	9·0	+ 4	B	B	—	2	—
19·7	5·04	8·6	+ 4	US	US	—	—	—
28·0	7·16	4·5	+ 4	US	US	—	—	—
32·0	8·18	3·8	+ 4	US	US	—	—	—
35·9	9·18	3·0	+ 4	US	US	—	—	—
39·4	10·09	3·0	+ 4	US	US	—	—	—

DISTURBED HYDRODYNAMIC LONGITUDINAL STABILITY CHARACTERISTICS

TABLE 57

Model A

(With propellers windmilling)

($C_{\Delta 0} = 2{\cdot}75$; $I = 23{\cdot}25$ lb ft^2)

Speed V (ft/sec)	Velocity coefficient C_v	Keel attitude α_K (deg)	Elevator angle η (deg)	Stable (S) Unstable (US) Border-line (B) Skipping (Sk) before disturbance	Stable (S) Unstable (US) Border-line (B) Skipping (Sk) after disturbance	Disturbance nose-down (deg)	Amplitude of porpoising, if any, after disturbance (deg)	Limits of porpoising after disturbance (deg)
21·0	5·37	11·9	−16	S	S	—	—	—
24·0	6·14	11·4	−16	B	US	—	10	—
29·4	7·52	11·1	−16	S	US	7	9	—
35·4	9·05	11·0	−16	S	US	—	—	—
36·4	9·31	10·9	−16	B	US	—	4	—
23·5	6·01	11·3	−12	US	US	—	10	—
24·5	6·26	11·1	−12	B	US	—	10	—
27·3	6·98	10·9	−12	S	US	—	10	—
31·4	8·03	10·9	−12	S	US	—	9	—
35·2	9·00	10·9	−12	S	US	—	5	—
38·5	9·85	10·7	−12	US	US	—	—	—
0	0	3·5	− 8	S	S	—	—	—
4·0	1·02	3·5	− 8	S	S	—	—	—
7·8	1·99	5·9	− 8	S	S	—	—	—
11·7	2·99	6·9	− 8	S	S	—	—	—
15·9	4·07	11·2	− 8	S	S	—	—	—
19·4	4·96	12·1	− 8	S	S	7	—	—
27·0	6·90	10·7	− 8	S	US	7	10	—
31·0	7·92	10·4	− 8	S	US	7	9	—
34·8	8·90	10·1	− 8	S	US	6	7	—
37·0	9·46	10·3	− 8	S	S	—	—	—
38·9	9·95	10·3	− 8	S	S	6	—	—
21·8	5·57	11·8	− 4	S	US	6	4	—
25·5	6·52	11·0	− 4	B	US	6	10	—
29·2	7·46	10·2	− 4	S	US	4	10	—
33·0	8·44	9·4	− 4	S	US	6	9	—
35·2	9·00	8·8	− 4	S	US	—	5	—
37·0	9·46	8·4	− 4	S	S	—	—	—
36·1	9·23	7·7	− 2	S	US	—	8	—
38·1	9·75	7·3	− 2	S	S	8	—	—
22·6	5·78	11·4	0	S	US	—	10	—
27·3	6·98	9·9	0	S	US	8	11	—
31·0	7·93	8·4	0	S	US	—	12	—
33·5	8·56	7·8	0	S	US	—	13	—
35·2	9·00	7·2	0	S	US	—	—	—
37·5	9·59	6·4	0	S	US	7	12	—
21·5	5·50	11·2	+ 4	S	S	—	—	—
25·1	6·42	10·3	+ 4	US	US	—	—	—
29·3	7·49	8·4	+ 4	S	US	8	11	—
32·7	8·36	7·3	+ 4	S	US	9	16	—
36·5	9·34	5·8	+ 4	S	US	9	14	—
22·0	5·63	11·1	+ 8	S	US	8	5	—

DISTURBED HYDRODYNAMIC LONGITUDINAL STABILITY CHARACTERISTICS

TABLE 58

Model A

(With fairings)

($C_{\Delta 0} = 2{\cdot}75$; $I = 23{\cdot}25$ lb ft^2)

Speed V (ft/sec)	Velocity coefficient C_v	Keel attitude α_K (deg)	Elevator angle η (deg)	Stable (S) Unstable (US) Border-line (B) Skipping (Sk) before disturbance	Stable (S) Unstable (US) Border-line (B) Skipping (Sk) after disturbance	Disturbance nose-down (deg)	Amplitude of porpoising, if any, after disturbance (deg)	Limits of porpoising after disturbance (deg)
25·1	6·41	11·6	−24	US	US	—	—	—
27·0	6·91	11·1	−24	S	US	—	—	—
29·1	7·43	11·1	−24	S	US	—	—	—
32·0	8·18	11·1	−24	S	S	—	—	—
33·9	8·66	11·1	−24	S	S	—	—	—
34·8	8·90	11·1	−24	US	US	—	—	—
20·0	5·11	11·7	−16	S	S	—	—	—
21·1	5·40	11·6	−16	S	S	—	—	—
22·1	5·65	11·4	−16	B	US	—	—	—
23·5	6·01	11·2	−16	US	US	—	—	—
25·5	6·52	10·9	−16	B	US	—	—	—
27·5	7·04	10·6	−16	S	US	—	—	—
29·6	7·56	10·6	−16	S	S	—	—	—
33·8	8·65	10·7	−16	S	S	—	—	—
35·5	9·08	10·8	−16	B	US	—	—	—
0	0	3·2	− 8	S	S	—	—	—
4·0	1·02	3·6	− 8	S	S	—	—	—
8·1	2·07	5·6	− 8	S	S	—	—	—
11·8	3·02	6·6	− 8	S	S	—	—	—
16·0	4·09	10·2	− 8	S	S	—	—	—
19·7	5·03	10·9	− 8	S	S	—	—	—
20·8	5·32	11·2	− 8	S	S	—	—	—
23·5	6·01	10·9	− 8	US	US	—	—	—
27·5	7·04	10·1	− 8	S	US	—	—	—
31·8	8·13	9·7	− 8	S	S	—	—	—
35·5	9·08	10·1	− 8	S	S	—	—	—
37·8	9·66	10·1	− 8	S	S	—	—	—
39·6	10·12	10·0	− 8	S	S	—	—	—
20·7	5·30	11·0	− 4	S	S	—	—	—
23·5	6·01	10·7	− 4	US	US	—	—	—
27·5	7·04	9·5	− 4	S	US	—	—	—
30·1	7·69	9·3	− 4	S	US	—	—	—
31·9	8·15	8·7	− 4	S	S	—	—	—
35·6	9·10	8·2	− 4	S	S	—	—	—
38·6	9·86	8·3	− 4	S	S	—	—	—
21·5	5·50	10·9	0	S	S	—	—	—
25·9	6·62	9·8	0	B	US	—	—	—
30·0	7·66	7·7	0	S	US	—	—	—
33·7	8·62	6·3	0	S	S	—	—	—
37·6	9·61	5·3	0	S	S	—	—	—

TABLE 58—*continued*

Speed V (ft/sec)	Velocity coefficient C_v	Keel attitude α_K (deg)	Elevator angle η (deg)	Stable (S) Unstable (US) Border-line (B) Skipping (Sk) before disturbance	Stable (S) Unstable (US) Border-line (B) Skipping (Sk) after disturbance	Disturbance nose-down (deg)	Amplitude of porpoising, if any, after disturbance (deg)	Limits of porpoising after disturbance (deg)
23·0	5·88	10·5	+ 4	US	US	—	—	—
26·9	6·88	8·1	+ 4	B	US	—	—	—
31·0	7·93	6·3	+ 4	S	US	—	—	—
34·7	8·87	5·1	+ 4	S	S	—	—	—
38·6	9·88	4·0	+ 4	S	S	—	—	—
22·0	5·63	10·7	+ 8	S	US	—	—	—
26·1	6·67	8·4	+ 8	US	US	—	—	—
28·0	7·16	7·0	+ 8	US	US	—	—	—
30·1	7·70	5·9	+ 8	B	US	—	—	—
33·9	8·67	4·5	+ 8	B	B	—	—	—
37·8	9·67	3·4	+ 8	B	B	—	—	—
30·0	7·67	5·0	+12	US	US	—	—	—
34·0	8·70	3·8	+12	US	US	—	—	—

DISTURBED HYDRODYNAMIC LONGITUDINAL STABILITY CHARACTERISTICS

TABLE 59

Model B

($C_{\Delta 0} = 2{\cdot}00$; $I = 21{\cdot}30$ lb ft²)

Speed V (ft/sec)	Velocity coefficient C_v	Keel attitude α_K (deg)	Elevator angle η (deg)	Stable (S) Unstable (US) Border-line (B) Skipping (Sk) before disturbance	Stable (S) Unstable (US) Border-line (B) Skipping (Sk) after disturbance	Disturbance nose-down (deg)	Amplitude of porpoising, if any, after disturbance (deg)	Limits of porpoising after disturbance (deg)
20·0	5·12	9·8	−16	S	S	6	—	—
24·8	6·34	9·6	—	S	US	10	8	—
25·8	6·60	9·7	—	S	S	10	—	—
25·9	6·62	10·0	−16	S	S	5	—	—
28·8	7·37	10·0	−16	B	B	—	1½	—
31·9	8·16	9·6	−16	US	US	—	—	—
29·9	7·65	9·8	−12	B	B	—	1	—
33·5	8·57	9·1	−12	US	US	—	—	—
24·7	6·32	8·9	—	S	US	9½	8	—
25·8	6·60	8·7	—	S	S	11	—	—
33·5	8·57	8·9	—	S	S	—	—	—
0	0	2·7	− 8	S	S	—	—	—
4·0	1·02	2·6	− 8	S	S	—	—	—
8·3	2·12	4·6	− 8	S	S	—	—	—
12·3	3·15	5·2	− 8	S	S	—	—	—
16·7	4·27	9·4	− 8	S	S	—	—	—
20·5	5·24	9·2	− 8	S	S	—	—	—
27·6	7·06	8·3	− 8	S	S	10	—	—
31·5	8·06	8·3	− 8	S	S	—	—	—
35·5	9·08	7·8	− 8	S	S	—	—	—
21·2	5·42	9·1	− 6	S	US	6	8	—
22·2	5·68	8·8	− 6	S	US	6	9	—
25·0	6·39	7·8	− 6	S	US	10	—	—
26·1	6·68	7·7	− 6	S	S	8½	—	—
33·8	8·64	6·6	− 6	S	S	10	—	—
35·8	9·16	6·6	− 6	S	S	8	—	—
19·3	4·94	9·2	− 4	S	S	15	—	—
20·5	5·24	9·1	− 4	S	S	6½	—	—
22·1	5·65	8·7	− 4	S	US	6	10	—
24·0	6·14	7·5	− 4	S	US	9	9	—
26·5	6·78	6·5	− 4	S	S	9	—	—
31·0	7·93	5·8	− 4	S	S	7	—	—
35·7	9·13	5·3	− 4	S	US	6	—	—
24·5	6·27	6·9	− 2	S	US	—	8	4 to 12
28·0	7·16	5·7	− 2	S	S	7	—	—
31·8	8·13	4·9	− 2	S	US	8	—	—
19·9	5·09	9·0	0	S	S	—	—	—
20·8	5·32	8·7	0	S	S	—	—	—
21·8	5·58	8·5	0	S	US	—	8	—
24·0	6·14	6·7	0	S	US	—	8	—
24·8	6·34	6·5	0	S	US	—	—	—
26·0	6·65	5·8	0	S	S	—	—	—
26·8	6·86	5·4	0	S	S	—	—	—
27·7	7·08	5·0	0	S	US	—	—	—
25·8	6·60	5·6	+ 2	S	US	7	11	—
26·6	6·80	5·0	+ 2	S	US	7	11	—

DISTURBED HYDRODYNAMIC LONGITUDINAL STABILITY CHARACTERISTICS

TABLE 60

Model B

($C_{\Delta 0} = 2{\cdot}25$; $I = 21{\cdot}30$ lb ft²)

Speed V (ft/sec)	Velocity coefficient C_v	Keel attitude α_K (deg)	Elevator angle η (deg)	Stable (S) Unstable (US) Border-line (B) Skipping (Sk) before disturbance	Stable (S) Unstable (US) Border-line (B) Skipping (Sk) after disturbance	Disturbance nose-down (deg)	Amplitude of porpoising, if any, after disturbance (deg)	Limits of porpoising after disturbance (deg)
21·5	5·50	10·0	−16	S	US	9	9	—
26·4	6·75	10·0	−16	S	US	5	7	—
27·7	7·08	10·0	−16	S	B	6	½	—
30·4	7·77	10·0	−16	B	B	7	2	—
32·4	8·28	9·8	−16	B	B	8	2	—
34·3	8·77	8·9	−12	B Sk	B Sk	—	2	—
27·4	7·01	9·5	−10	S	S	7	—	—
32·3	8·26	9·1	−10	S	S	7	—	—
36·2	9·26	8·4	−10	S	S	—	—	—
0	0	2·8	− 8	S	S	—	—	—
4·0	1·02	2·8	− 8	S	S	—	—	—
8·2	2·10	4·7	− 8	S	S	—	—	—
12·2	3·12	5·2	− 8	S	S	—	—	—
16·1	4·12	9·7	− 8	S	S	—	—	—
20·0	5·11	9·9	− 8	S	S	—	—	—
23·8	6·08	9·5	− 8	S	US	7	9	—
25·6	6·55	9·0	− 8	S	US	7	9	—
28·2	7·22	8·9	− 8	S	S	7	—	—
32·2	8·24	8·8	− 8	S	S	6	—	—
36·0	9·21	8·2	− 8	S	S	6	—	—
26·2	6·70	8·7	—	S	US	11	8	—
27·3	6·98	8·5	—	S	US	6	9	—
28·5	7·29	8·5	—	S	S	8½	—	—
24·5	6·26	8·3	− 6	S	US	7	9	—
25·5	6·52	8·0	− 6	S	US	9	8	—
27·6	7·06	7·5	− 6	S	US	9½	7	—
29·3	7·49	7·5	—	S	S	8½	—	—
31·2	7·98	7·0	− 6	S	S	9	—	—
33·2	8·49	7·0	− 6	S	S	7½	—	—
34·0	8·70	7·0	− 6	S	S	7½	—	—
36·0	9·21	7·2	—	S	S	8	—	—
38·0	9·72	7·0	− 6	S	US	7½	—	—
38·5	9·85	7·3	—	S	S	8	—	—
24·5	6·27	7·7	− 4	S	US	6	9	—
29·2	7·46	6·5	− 4	S	US	8½	12	—
31·2	7·98	6·2	− 4	S	US	8	—	—
34·0	8·70	6·0	− 4	S	US	7	—	—
38·5	9·85	5·8	− 4	S	US	6	—	—
31·0	7·93	5·8	− 2	S	US	9	—	—
35·0	8·95	5·2	− 2	S	US	7	—	—
38·5	9·85	4·5	− 2	S	US	6	—	—
20·3	5·19	9·0	+ 4	S	US	7	2½	—
19·0	4·86	9·3	+ 8	S	S	—	—	—

DISTURBED HYDRODYNAMIC LONGITUDINAL STABILITY CHARACTERISTICS

TABLE 61

Model B

($C_{\Delta 0} = 2{\cdot}50$; $I = 21{\cdot}30$ lb ft^2)

Speed V (ft/sec)	Velocity coefficient C_v	Keel attitude α_K (deg)	Elevator angle η (deg)	Stable (S) Unstable (US) Border-line (B) Skipping (Sk) before disturbance	Stable (S) Unstable (US) Border-line (B) Skipping (Sk) after disturbance	Disturbance nose-down (deg)	Amplitude of porpoising, if any, after disturbance (deg)	Limits of porpoising after disturbance (deg)
22·1	5·65	10·2	−16	S	US	—	8	—
27·7	7·08	10·2	−16	S	US	—	8	—
29·7	7·60	10·1	−16	S	S	—	—	—
33·5	8·56	10·2	−16	US	US	—	—	—
35·4	9·06	9·7	−16	US	US	—	—	—
27·8	7·11	9·9	−12	S	US	—	—	—
34·5	8·82	9·7	−12	B	B	—	—	—
35·5	9·08	9·6	−12	B	B	—	—	—
37·5	9·59	9·0	−12	B	B	—	—	—
28·5	7·29	9·6	−10	S	S	—	—	—
34·1	8·72	9·1	−10	S	S	—	—	—
36·1	9·24	8·8	−10	S	S	—	—	—
39·1	10·00	8·4	−10	S	S	—	—	—
0	0	2·7	− 8	S	S	—	—	—
4·0	1·02	2·7	− 8	S	S	—	—	—
8·0	2·04	4·8	− 8	S	S	—	—	—
12·0	3·07	5·3	− 8	S	S	—	—	—
16·0	4·09	10·0	− 8	S	S	—	—	—
19·8	5·06	10·3	− 8	S	S	—	—	—
24·0	6·14	9·3	− 8	S	US	—	12	—
27·5	7·03	8·6	− 8	S	US	5	8	—
31·5	8·06	8·0	− 8	S	S	5	—	—
35·4	9·05	8·3	− 8	S	S	—	—	—
39·2	10·03	7·9	− 8	S	S	—	—	—
28·6	7·32	7·2	—	S	US	9	9	—
21·6	5·52	9·8	− 4	S	S	—	—	—
25·5	6·52	7·8	− 4	S	US	—	10	—
29·6	7·57	6·8	− 4	S	S	—	—	—
30·6	7·83	6·3	—	S	US	6	—	—
30·8	7·88	6·9	− 4	S	S	8	—	—
33·5	8·56	6·8	− 4	S	S	—	—	—
33·9	8·66	5·5	—	S	US	6	—	—
35·5	9·08	6·2	—	S	S	8	—	—
37·5	9·59	6·4	− 4	S	S	—	—	—
30·0	7·67	6·0	− 2	S	US	7	—	—
31·8	8·13	5·5	− 2	S	US	5	—	—
35·8	9·16	4·7	− 2	S	US	6	—	—
20·0	5·12	10·0	0	S	S	—	—	—
23·8	6·08	8·1	0	S	US	6	10	—
27·8	7·11	6·2	0	S	US	7	14	—
31·6	8·08	5·1	0	S	US	6	9	—
34·8	8·90	4·2	0	S	US	—	—	—
39·0	9·97	3·3	0	S	S	—	—	—
21·8	5·58	9·1	+ 4	S	US	—	3	—
25·7	6·57	6·3	+ 4	B	US	—	—	—
29·7	7·60	5·0	+ 4	B	US	—	—	—
33·5	8·56	3·3	+ 4	B	US	—	—	—
20·2	5·16	9·6	+ 8	S	S	—	—	—

DISTURBED HYDRODYNAMIC LONGITUDINAL STABILITY CHARACTERISTICS

TABLE 62

Model B

($C_{\Delta 0} = 2\ 75$; $I = 21 \cdot 30$ lb ft^2)

Speed V (ft/sec)	Velocity coefficient C_v	Keel attitude α_K (deg)	Elevator angle η (deg)	Stable (S) Unstable (US) Border-line (B) Skipping (Sk) before disturbance	Stable (S) Unstable (US) Border-line (B) Skipping (Sk) after disturbance	Disturbance nose-down (deg)	Amplitude of porpoising, if any, after disturbance (deg)	Limits of porpoising after disturbance (deg)
21·8	5·58	10·8	−20	S	S	—	—	—
25 8	6·60	10·5	−20	S	US	—	10	—
29·6	7·57	10·5	−20	S	US	—	7	—
33·5	8·57	10 6	−20	US	US	—	4	—
19·3	4·94	11·0	−16	S	S	—	—	—
23·3	5·96	10·6	−16	S	US	—	9	—
27·5	7·04	10·4	−16	S	US	—	7	—
35·1	8·98	10·5	−16	US Sk	US Sk	—	—	—
39·1	10·00	10·6	−16	US Sk	US Sk	—	—	—
21·9	5·60	10·5	−12	S	S	—	—	—
26·3	6·72	10·1	−12	S	US	—	9	—
30·2	7·72	10 1	−12	S	US	—	7	—
34·0	8·70	10·1	−12	S	S	—	—	—
37·8	9·67	10·0	−12	B	B	—	—	—
31·5	8·06	9·8	—	S	US	7	6½	—
32·5	8·31	9·8	—	S	S	9	—	—
32·5	8·31	8·5	—	S	S	8½	—	—
0	0	2·8	− 8	S	S	—	—	—
3·8	0·97	2·8	− 8	S	S	—	—	—
5·0	1·28	3·5	− 8	S	S	—	—	—
8·3	2·22	5·0	− 8	S	S	—	—	—
12·1	3·09	5·5	− 8	S	S	—	—	—
14·2	3·63	7·0	− 8	S	S	—	—	—
16·0	4·09	10·4	− 8	S	S	—	—	—
18·0	4·60	10·6	− 8	S	S	—	—	—
19·6	5·01	10·6	− 8	S	S	—	—	—
23·5	6·01	10·1	− 8	S	US	—	9	—
27·5	7·04	8·8	− 8	S	US	—	9	—
29·7	7·60	8·7	− 8	S	US	—	—	—
31·5	8·06	8·6	− 8	S	US	—	—	—
33·0	8·43	8·0	—	S	US	9	8	—
35·0	8·95	7·8	—	S	S	8	—	—
35·2	9·00	8·6	− 8	S	S	—	—	—
39·0	9·98	8·0	− 8	S	S	—	—	—
34·7	8·88	7·2	—	S	US	8½	—	—
36·7	9·39	6·8	—	S	S	7	—	—
38·6	9·87	6·8	—	S	S	8	—	—
22·1	5·65	10·2	− 4	S	S	—	—	—
25·7	6·58	8·3	− 4	S	US	—	11	—
29·9	7·64	7·0	− 4	S	US	—	9	—
34·5	8·82	6·2	− 4	S	US	—	8	—
39·0	9·97	5·7	− 4	S	US	—	8	—
18·0	4·60	10·4	+ 4	S	S	—	—	—
20·9	5·34	10·0	+ 4	S	S	—	—	—
22·0	5·63	9·7	+ 4	S	US	—	2½	—

DISTURBED HYDRODYNAMIC LONGITUDINAL STABILITY CHARACTERISTICS

TABLE 63

Model B

($C_{\Delta 0} = 3{\cdot}00$; $I = 21{\cdot}30$ lb ft^2)

Speed V (ft/sec)	Velocity coefficient C_v	Keel attitude α_K (deg)	Elevator angle η (deg)	Stable (S) Unstable (US) Border-line (B) Skipping (Sk) before disturbance	Stable (S) Unstable (US) Border-line (B) Skipping (Sk) after disturbance	Disturbance nose-down (deg)	Amplitude of porpoising, if any, after disturbance (deg)	Limits of porpoising after disturbance (deg)
24·1	6·16	10·6	−20	US	US	—	>2	—
22·2	5·68	10·7	−16	S	S	7	—	—
26·0	6·65	10·2	−16	B	US	—	—	—
27·8	7·12	10·3	−16	S	US	—	—	—
31·8	8·14	10·2	−16	S	US	—	—	—
34·2	8·75	10·2	−16	B	B	—	2	—
35·6	9·11	10·2	−16	US Sk	US Sk	—	—	—
39·5	10·11	10·2	−16	US Sk	US Sk	—	—	—
32·2	8·24	9·8	—	S	US	8	8	—
33·5	8·57	9·8	—	S	US	8	5½	—
34·5	8·83	9·8	—	S	S	8	—	—
32·0	8·18	9·0	—	S	US	7½	8	—
32·2	8·24	9·6	−10	S	US	9	7	—
33·0	8·44	9·3	—	S	US	8	5	—
34·0	8·70	8·5	—	S	S	9½	—	—
34·2	8·75	9·6	−10	S	S	7	—	—
34·2	8·75	9·3	—	S	S	7	—	—
38·2	9·77	9·6	−10	S	S	7	—	—
40·0	10·23	9·6	−10	S	S	6	—	—
0	0	2·8	− 8	S	S	—	—	—
4·0	1·02	2·8	− 8	S	S	—	—	—
8·2	2·10	5·0	− 8	S	S	—	—	—
12·0	3·07	5·4	− 8	S	S	—	—	—
16·0	4·09	10·5	− 8	S	S	—	—	—
19·7	5·04	11·1	− 8	S	S	—	—	—
23·7	6·06	10·2	− 8	S	US	6	10	—
27·5	7·04	9·0	− 8	S	US	6	10	—
31·2	7·98	8·5	− 8	S	US	—	9	—
34·0	8·70	7·8	—	S	US	7	8	—
35·2	9·01	8·7	− 8	S	S	6	—	—
35·9	9·19	7·8	—	S	S	8	—	—
39·1	10·00	8·2	− 8	S	S	6	—	—
33·8	8·65	7·5	—	S	US	7	10	—
35·9	9·18	7·3	—	S	US	9	—	—
21·9	5·61	10·5	− 4	S	S	8	—	—
33·5	8·57	6·7	− 4	S	US	6	—	—
37·5	9·60	5·8	− 4	S	US	6½	—	—
23·5	6·01	10·0	− 2	US	US	—	—	—
24·3	6·22	9·7	− 2	US	US	—	—	—
19·9	5·09	10·7	0	S	S	10	—	—
23·3	5·96	10·0	0	US	US	—	—	—
27·5	7·04	7·3	0	B	US	—	—	—
21·1	5·40	10·3	—	S	B	—	2	—

DISTURBED HYDRODYNAMIC LONGITUDINAL STABILITY CHARACTERISTICS

TABLE 64

Model B

($C_{\Delta 0} = 2{\cdot}50$; $I = 26{\cdot}50$ lb ft²)

Speed V (ft/sec)	Velocity coefficient C_v	Keel attitude α_K (deg)	Elevator angle η (deg)	Stable (S) Unstable (US) Border-line (B) Skipping (Sk) before disturbance	Stable (S) Unstable (US) Border-line (B) Skipping (Sk) after disturbance	Disturbance nose-down (deg)	Amplitude of porpoising, if any, after disturbance (deg)	Limits of porpoising after disturbance (deg)
31·6	8·08	10·3	−20	S	S	—	—	—
31·9	8·16	10·3	−20	S	US	—	—	—
32·9	8·42	10·3	−20	US	US	—	—	—
31·7	8·11	10·1	−18	S	S	—	—	—
32·6	8·34	10·1	−18	B	B	—	—	—
31·4	8·03	10·0	−16	S	S	—	—	—
32·5	8·32	10·0	−16	S	S	—	—	—
20·2	5·17	10·3	−12	S	S	11	—	—
21·7	5·55	10·2	−12	S	US	10	9	—
28·5	7·29	9·9	−12	S	US	6	8	—
29·7	7·60	9·7	−12	S	S	10	—	—
28·6	7·32	8·5	− 6	S	US	6	9	—
29·9	7·65	7·6	− 6	S	US	10	10	—
30·9	7·91	7·0	− 6	S	US	10	10	—
33·8	8·65	6·9	− 6	S	S	9	—	—
36·9	9·44	7·0	− 6	S	S	12	—	—
20·1	5·14	10·1	− 4	S	S	10	—	—
21·2	5·43	9·8	− 4	S	US	10	4	—
28·8	7·37	6·9	− 4	S	US	9	—	—
31·8	8·13	6·6	− 4	S	US	7	—	—
34·8	8·90	5·7	− 4	S	US	9	—	—

DISTURBED HYDRODYNAMIC LONGITUDINAL STABILITY CHARACTERISTICS

TABLE 65

Model B

($C_{\Delta 0} = 2{\cdot}50$; $I = 29{\cdot}82$ lb ft²)

Speed V (ft/sec)	Velocity coefficient C_v	Keel attitude α_K (deg)	Elevator angle η (deg)	Stable (S) Unstable (US) Border-line (B) Skipping (Sk) before disturbance	Stable (S) Unstable (US) Border-line (B) Skipping (Sk) after disturbance	Disturbance nose-down (deg)	Amplitude of porpoising, if any, after disturbance (deg)	Limits of porpoising after disturbance (deg)
32·4	8·29	10·1	−20	S	S	10	—	—
33·2	8·49	10·0	−20	B	B	—	2	—
34·9	8·93	9·9	−20	US	US	—	—	—
35·9	9·19	9·7	−20	US	US	—	—	—
33·4	8·54	9·8	−18	S	S	8	—	—
28·1	7·18	10·1	−16	S	US	10	10	4½ to 14½
29·5	7·55	9·9	−16	S	S	11	—	—
35·9	9·18	9·0	−16	S	S	6	—	—
21·1	5·40	10·1	−12	S	US	9	9	5 to 14
21·8	5·58	10·0	−12	S	US	6	10	5 to 15
22.4	5·73	10·1	−12	S	US	10	9	4 to 13
28·2	7·22	9·5	−12	S	US	5	10	4½ to 14½
29·1	7·44	9·6	−12	S	S	10	—	—
37·1	9·49	8·8	−12	S	S	5	—	—
37·8	9·67	8·7	−12	S	S	3	—	—
0	0	2·5	− 8	S	S	—	—	—
4·0	1·02	2·5	− 8	S	S	—	—	—
8·0	2·04	4·7	− 8	S	S	—	—	—
12·2	3.12	5·2	− 8	S	S	—	—	—
18·4	4·71	10·1	− 8	S	S	—	—	—
20·5	5·24	9·9	− 8	S	S	5½	—	—
24·5	6·27	9·0	− 8	S	US	6	10	5 to 15
27·0	6·91	8·3	− 8	S	US	6	9	5½ to 14½
28·5	7·29	8·3	− 8	S	S	5½	—	—
32·5	8·31	8·2	− 8	S	S	7	—	—
35·8	9·16	8·2	− 8	S	S	6½	—	—
27·8	7·11	7·8	− 6	S	US	6	8	4 to 12
29·0	7·41	7·4	− 6	S	S	5	—	—
30·6	7·82	6·9	− 6	S	S	11	—	—
34·1	8·72	6·8	− 6	S	S	8	—	—
37·7	9·64	6·9	− 6	S	S	8	—	—
28·5	7.29	6·6	− 4	S	US	5½	7	4½ to 11½
31·0	7·92	6·2	− 4	S	US	7	—	—
34·2	8·74	5·5	− 4	S	US	7½	—	—
36·0	9·21	5·5	− 4	S	US	6½	—	—
38·0	9·72	5·4	− 4	S	US	6½	—	—
30·2	7·72	5·7	− 2	S	US	6	10	5 to 15
32·2	8·23	5·5	− 2	S	US	7	—	—
35·4	9·05	4·7	− 2	S	US	5½	—	—
37·6	9·61	4·6	− 2	S	US	5½	—	—

TABLE 65—*continued*

Speed V (ft/sec)	Velocity coefficient C_v	Keel attitude α_K (deg)	Elevator angle η (deg)	Stable (S) Unstable (US) Border-line (B) Skipping (Sk) before disturbance	Stable (S) Unstable (US) Border-line (B) Skipping (Sk) after disturbance	Disturbance nose-down (deg)	Amplitude of porpoising, if any, after disturbance (deg)	Limits of porpoising after disturbance (deg)
19·2	4·91	9·7	0	S	S	7	—	—
20·7	5·29	9·6	0	S	US	8	5	$6\frac{1}{2}$ to $11\frac{1}{2}$
21·5	5·50	9·4	0	S	US	—	10	$3\frac{1}{2}$ to $13\frac{1}{2}$
22·8	5·83	8·6	0	S	US	5	9	6 to 15
29·8	7·62	4·7	0	S	US	4	11	4 to 15
30·8	7·87	5·1	0	S	S	3	—	—
31·7	8·10	4·8	0	S	S	4	—	—
32·0	8·18	4·5	0	S	US	4	—	—
35·6	9·10	3·6	0	S	US	4	—	—
40·0	10·23	2·7	0	S	US	3	—	—
24·5	6·26	7·3	+ 4	S	US	—	10	—
28·5	7·29	5·1	+ 4	S	US	6	$16\frac{1}{2}$	$1\frac{1}{2}$ to 18
32·5	8·31	3·8	+ 4	S	US	$4\frac{1}{2}$	—	—
35·7	9·13	2·7	+ 4	S	US	3	—	—
38·6	9·87	2·0	+ 4	S	US	$1\frac{1}{2}$	—	—
22·0	5·62	8·3	+ 8	S	US	5	9	$3\frac{1}{2}$ to $12\frac{1}{2}$

DISTURBED HYDRODYNAMIC LONGITUDINAL STABILITY CHARACTERISTICS

TABLE 66

Model B

($C_{\Delta 0} = 3{\cdot}00$; $I = 31{\cdot}70$ lb ft²)

Speed V (ft/sec)	Velocity coefficient C_v	Keel attitude α_K (deg)	Elevator angle η (deg)	Stable (S) Unstable (US) Border-line (B) Skipping (Sk) before disturbance	Stable (S) Unstable (US) Border-line (B) Skipping (Sk) after disturbance	Disturbance nose-down (deg)	Amplitude of porpoising, if any, after disturbance (deg)	Limits of porpoising after disturbance (deg)
20·8	5·32	11·0	−20	S	S	8	—	—
25·8	6·59	10·2	−20	S	S	—	—	—
34·3	8·77	10·3	−20	S	S	—	—	—
35·4	9·05	10·5	−20	B	B	—	2	—
21·3	5·45	10·7	−16	S	US	10	4	—
22·6	5·78	10·5	−16	S	US	7	11	—
23·6	6·03	10·5	−16	S	US	—	11	4 to 15
24·2	6·18	10·3	−16	US	US	—	—	—
25·6	6·54	10·1	−16	S	US	—	—	—
26·7	6·83	10·1	−16	S	US	6	10	—
27·6	7·06	10·1	−16	S	US	6	10	—
32·5	8·31	10·1	−16	S	US	6	6	—
33·5	8·56	10·2	−16	S	S	11	—	—
35·0	8·95	9·7	−16	S	S	6	—	—
36·5	9·33	9·7	−16	US	US	—	—	—
31·9	8·16	9·4	−12	S	US	—	5	—
32·5	8·31	9·7	−12	S	US	—	—	—
33·0	8·44	9·5	−12	S	S	—	—	—
36·2	9·26	9·5	−12	S	S	8	—	—
37·5	9·59	9·4	−12	B	B	5	1	—
38·5	9·84	9·1	−12	B	B	6	½	—
40·0	10·23	8·0	−10	S	S	6	—	—
32·8	8·38	7·6	− 8	S	US	8	10	—
34·5	8·82	7·3	− 8	S	S	7½	—	—
36·5	9·33	7·1	− 8	S	S	7½	—	—
39·5	10·10	7·4	− 8	S	S	7½	—	—
34·5	8·82	6·5	− 6	S	US	5½	—	—
38·0	9·72	6·5	− 6	S	US	7	—	—
36·0	9·20	5·7	− 4	S	US	8	—	—
39·5	10·10	5·3	− 4	S	US	6	—	—
20·6	5·27	10·5	0	S	S	—	—	—
23·6	6·03	9·9	0	US	US	—	—	—
24·8	6·34	9·1	0	S	US	—	—	—
25·6	6·54	8·8	0	S	US	—	—	—
28·5	7·28	6·9	0	S	US	6	13	—
31·5	8·05	5·7	0	S	US	5	—	—
20·6	5·27	10·4	+ 4	S	S	—	—	—
21·6	5·52	10·1	+ 4	S	US	6	8	—
22·8	5·83	10·0	+ 4	US	US	—	—	—
32·5	8·31	4·7	+ 4	S	US	6	—	—

DISTURBED HYDRODYNAMIC LONGITUDINAL STABILITY CHARACTERISTICS

TABLE 67

Model C

($C_{\Delta 0} = 2{\cdot}25$; $I = 23{\cdot}75$ lb ft²)

Speed V (ft/sec)	Velocity coefficient C_v	Keel attitude α_K (deg)	Elevator angle η (deg)	Stable (S) Unstable (US) Border-line (B) Skipping (Sk) before disturbance	Stable (S) Unstable (US) Border-line (B) Skipping (Sk) after disturbance	Disturbance nose-down (deg)	Amplitude of porpoising, if any, after disturbance (deg)	Limits of porpoising after disturbance (deg)
21·0	5·37	10·3	−16	S	B	5	—	—
24·0	6·14	10·3	−16	S	US	9	9	5 to 14
28·2	7·21	10·3	−16	S	S	9	—	—
31·9	8·16	10·3	−16	B	B	—	—	—
24·0	6·14	9·9	−12	S	US	8	8½	5 to 13½
25·3	6·47	9·9	−12	S	S	11	—	—
34·0	8·70	9·9	−12	B	B	—	—	—
0	0	2·0	− 8	S	S	—	—	—
4·2	1·07	2·0	− 8	S	S	—	—	—
8·4	2·15	4·1	− 8	S	S	—	—	—
12·2	3·12	4·7	− 8	S	S	—	—	—
14·2	3·63	8·0	− 8	S	S	—	—	—
16·7	4·27	10·1	− 8	S	S	—	—	—
20·0	5·11	10·0	− 8	S	S	6	—	—
28·0	7·16	8·5	− 8	S	S	5½	—	—
32·0	8·18	9·3	− 8	S	S	5	—	—
35·8	9·16	8·7	− 8	S	S	6	—	—
24·0	6·14	8·3	− 6	S	US	9½	10	—
25·5	6·52	7·6	− 6	S	S	9½	—	—
27·0	6·90	7·3	− 6	S	S	10½	—	—
31·0	7·93	6·9	− 6	S	S	9½	—	—
35·0	8·95	7·2	− 6	S	S	8½	—	—
21·8	5·58	9·3	− 4	S	US	6½	6	7 to 13
23·7	6·06	7·9	− 4	S	US	10	10	—
25·6	6·54	7·0	− 4	S	S	10	—	—
27·5	7·03	6·5	− 4	S	S	9	—	—
31·5	8·05	6·0	− 4	S	S	8	—	—
33·0	8·44	6·0	− 4	S	S	8	—	—
35·0	8·95	5·9	− 4	S	US	7½	—	—
24·5	6·26	7·2	− 2	S	US	9	10	—
25·0	6·39	7·0	− 2	S	B	10½	—	—
27·7	7·08	5·9	− 2	S	US	9	—	—
31·5	8·05	5·3	− 2	S	US	9½	—	—
20·2	5·16	9·6	0	S	S	10	—	—
24·2	6·19	6·9	0	S	US	7	10	3 to 13
28·0	7·16	5·3	0	S	US	6½	—	—
32·1	8·21	4·6	0	S	US	5½	—	—
36·2	9·26	3·6	0	S	US	—	—	—
39·9	10·20	4·0	0	S	US	—	—	—
25·6	6·55	5·5	+ 4	S	US	6	8	3 to 11
19·3	4·94	9·4	—	S	S	10	—	—
20·5	5·24	8·5	—	S	US	9	4½	6½ to 11
21·3	5·45	7·9	+ 8	S	US	6	10	3 to 13
22·4	5·73	7·0	+ 8	S	US	5½	10	3 to 13

DISTURBED HYDRODYNAMIC LONGITUDINAL STABILITY CHARACTERISTICS

TABLE 68

Model C

($C_{\Delta 0} = 2{\cdot}75$; $I = 23{\cdot}75$ lb ft^2)

Speed V (ft/sec)	Velocity coefficient C_v	Keel attitude α_K (deg)	Elevator angle η (deg)	Stable (S) Unstable (US) Border-line (B) Skipping (Sk) before disturbance	Stable (S) Unstable (US) Border-line (B) Skipping (Sk) after disturbance	Disturbance nose-down (deg)	Amplitude of porpoising, if any, after disturbance (deg)	Limits of porpoising after disturbance (deg)
21·1	5·40	10·9	−16	S	US	6	3	9 to 12
22·5	5·76	10·6	−16	S	US	7	10	5 to 15
27·3	6·98	10·3	−16	S	US	5	9	5 to 14
29·0	7·42	10·4	−16	S	US	7	10	4 to 14
32·2	8·24	10·4	−16	B	B	7	1½	9½ to 11
35·2	9·01	10·4	−16	US	US	—	—	—
24·3	6·22	10·1	−12	S	US	7	11	5 to 16
28·2	7·21	10·0	−12	S	US	10	9	5 to 14
28·5	7·29	9·5	—	S	US	11½	9½	—
29·6	7·57	9·2	—	S	S	10	—	—
30·4	7·78	10·1	−12	S	S	7	—	—
32·2	8·24	10·1	−12	S	S	6	—	—
36·0	9·20	10·1	−12	B	B	10	—	—
0	0	2·0	− 8	S	S	—	—	—
4·1	1·05	2·0	− 8	S	S	—	—	—
8·4	2·15	4·2	− 8	S	S	—	—	—
12·2	3·12	4·7	− 8	S	S	—	—	—
14·1	3·61	7·0	− 8	S	S	—	—	—
16·8	4·29	10·9	− 8	S	S	—	—	—
20·1	5·14	10·6	− 8	S	S	—	—	—
24·2	6·18	9·6	− 8	S	US	4	11	4 to 15
27·4	7·01	8·6	− 8	S	US	5	10	4 to 14
28·7	7·34	8·3	—	S	US	10	9½	—
29·6	7·56	8·0	—	S	S	9½	—	—
31·2	7·98	8·5	− 8	S	S	4½	—	—
35·0	8·95	9·3	− 8	S	S	5	—	—
39·1	10·00	8·6	− 8	S	S	4½	—	—
29·3	7·49	7·3	− 6	S	US	8½	9	—
31·3	8·00	7·3	− 6	S	S	9½	—	—
33·0	8·44	6·6	—	S	US	6½	—	—
24·4	6·24	9·0	− 4	S	US	8½	13	3 to 16
38·0	9·72	6·1	—	S	B	7	—	—
20·5	5·24	10·3	0	S	S	6	—	—
24·2	6·18	8·3	0	S	US	5½	12	3 to 15
27·8	7·11	6·4	0	S	US	8½	14	2 to 16
30·0	7·67	5·7	0	S	US	5	—	—
32·0	8·18	5·0	0	S	US	4½	—	—
35·9	9·18	4·5	0	S	US	3	—	—
39·9	10·20	4·0	0	S	US	3	—	—
22·2	5·68	9·1	+ 4	S	US	10	10	4 to 14
21·3	5·45	9·7	+ 8	S	US	9	8	5 to 13
22·5	5·76	8·9	+ 8	S	US	5	12	3 to 15

DISTURBED HYDRODYNAMIC LONGITUDINAL STABILITY CHARACTERISTICS

TABLE 69

Model D

($C_{\Delta 0} = 2{\cdot}25$; $I = 16{\cdot}81$ lb ft^2)

Speed V (ft/sec)	Velocity coefficient C_v	Keel attitude α_K (deg)	Elevator angle η (deg)	Stable (S) Unstable (US) Border-line (B) Skipping (Sk) before disturbance	Stable (S) Unstable (US) Border-line (B) Skipping (Sk) after disturbance	Disturbance nose-down (deg)	Amplitude of porpoising, if any, after disturbance (deg)	Limits of porpoising after disturbance (deg)
18·2	4·66	12·7	−20	S	S	8	—	—
19·2	4·91	12·6	−20	S	US	5	6	9 to 15
24·4	6·24	11·8	−20	S	US	6	7	8 to 15
27·5	7·03	11·9	−20	S	US	5	8	7 to 15
28·4	7·26	11·9	−20	US	US	—	—	—
28·4	7·26	11·2	−12	S	S	5	—	—
30·5	7·80	11·1	−12	B	B	$6\frac{1}{2}$	1	$10\frac{1}{2}$ to $11\frac{1}{2}$
30·5	7·80	10·9	−10	S	S	$6\frac{1}{2}$	—	—
34·4	8·80	10·0	−10	S	S	7	—	—
0	0	4·3	− 8	S	S	—	—	—
4·0	1·02	4·7	− 8	S	S	—	—	—
8·4	2·15	7·4	− 8	S	S	—	—	—
12·2	3·12	10·5	− 8	S	S	—	—	—
16·5	4·22	12·8	− 8	S	S	—	—	—
20·1	5·14	11·7	− 8	S	US	6	12	5 to 17
24·5	6·27	10·9	− 8	S	US	6	11	6 to 17
26·0	6·65	10·4	—	S	US	$8\frac{1}{2}$	9	—
27·8	7·11	10·2	—	S	S	$11\frac{1}{2}$	—	—
28·2	7·22	11·0	− 8	S	S	7	—	—
31·2	7·98	10·0	− 8	S	S	5	—	—
36·0	9·21	9·5	− 8	S	S	3	—	—
26·2	6·70	9·8	− 6	S	US	8	9	6 to 15
26·7	6·83	9·7	− 6	S	US	$5\frac{1}{2}$	7	6 to 13
19·3	4·94	11·7	− 2	S	US	5	5	9 to 14
20·5	5·24	11·2	− 2	S	US	—	—	—
21·1	5·40	10·8	− 2	S	US	—	—	—
26·5	6·78	8·4	− 2	S	US	6	9	6 to 15
26·8	6·86	8·2	− 2	S	US	$10\frac{1}{2}$	9	—
27·5	7·03	7·6	—	S	B	$9\frac{1}{2}$	—	—
28·5	7·29	7·7	− 2	S	S	6	—	—
32·5	8·32	6·4	− 2	S	S	6	—	—
35·3	9·03	6·2	—	S	B	8	—	—
31·5	8·06	5·8	—	S	US	8	—	—
20·2	5·17	10·9	+ 2	US	US	—	—	—
22·4	5·73	9·7	+ 2	S	US	7	11	6 to 17
26·4	6·75	7·2	+ 2	S	US	$3\frac{1}{2}$	13	5 to 18
30·4	7·78	5·9	+ 2	S	US	5	—	—
34·3	8·78	4·6	+ 2	S	US	5	—	—
18·2	4·66	12·0	+ 8	S	S	8	—	—
22·4	5·73	9·3	+ 8	US	US	$4\frac{1}{2}$	12	5 to 17
26·3	6·73	6·5	+ 8	B	B	$3\frac{1}{2}$	$\frac{1}{2}$	—
29·9	7·65	4·9	+ 8	S	US	5	—	—
34·0	8·70	3·5	+ 8	US	US	—	—	—

DISTURBED HYDRODYNAMIC LONGITUDINAL STABILITY CHARACTERISTICS

TABLE 70

Model D

($C_{\Delta 0} = 2{\cdot}75$; $I = 16{\cdot}81$ lb ft^2)

Speed V (ft/sec)	Velocity coefficient C_v	Keel attitude α_K (deg)	Elevator angle η (deg)	Stable (S) Unstable (US) Border-line (B) Skipping (Sk) before disturbance	Stable (S) Unstable (US) Border-line (B) Skipping (Sk) after disturbance	Disturbance nose-down (deg)	Amplitude of porpoising, if any, after disturbance (deg)	Limits of porpoising after disturbance (deg)
18·9	4·84	14·0	−20	S	S	7	—	—
19·9	5·08	13·5	−20	S	US	4	6	10 to 16
21·5	5·50	13·1	−20	US	US	—	—	—
25·5	6·52	12·2	−20	S	US	3½	11	7 to 18
30·2	7·72	12·0	−20	S	US	4½	8	7 to 15
20·5	5·24	13·1	−16	S	US	6	12	6 to 18
24·5	6·26	12·0	−16	B	US	6	11	6 to 17
28·6	7·31	11·9	−16	S	US	5	9	7 to 16
34·5	8·82	11·7	−16	US	US	—	—	—
18·5	4·73	13·7	−12	S	S	—	—	—
22·5	5·76	12·1	−12	US	US	—	—	—
26·1	6·68	11·3	−12	S	US	6	11	7 to 18
30·6	7·82	11·3	−12	S	US	6	7	7 to 14
32·5	8·31	11·4	−12	S	US	5	5	7 to 12
34·5	8·82	11·4	−12	B	B	3	1	—
0	0	4·8	− 8	S	S	—	—	—
4·0	1·02	5·1	− 8	S	S			
8·2	2·10	8·0	− 8	S	S	—	—	—
12·0	3·07	11·1	− 8	S	S	—	—	—
16·3	4·17	14·2	− 8	S	S	—	—	—
20·5	5·24	12·7	− 8	S	US	—	12	6 to 18
24·2	6·19	11·3	− 8	S	US	6	12	6 to 18
28·5	7·29	10·5	− 8	S	US	6	9	6 to 15
31·5	8·06	10·8	—	S	US	9½	7	—
32·4	8·14	10·5	− 8	S	S	6	—	—
33·5	8·57	10·7	—	S	S	10½	—	—
36·0	9·20	10·2	− 8	S	S	3	—	—
31·2	7·98	9·6	—	S	US	9½	6	—
33·5	8·57	9·6	—	S	S	9½	—	—
18·5	4·73	13·5	− 4	S	S	—	—	—
22·5	5·76	11·7	− 4	US	US	—	—	—
26·5	6·78	10·0	− 4	S	US	6½	10	7 to 17
30·5	7·80	9·0	− 4	S	US	—	9	7 to 16
31·2	7·98	8·6	—	S	US	9½	9	—
32·3	8·26	8·5	− 4	S	S	8½	—	—
34·3	8·77	8·1	− 4	S	S	5	—	—
38·2	9·77	8·0	− 4	S	S	4½	—	—
38·3	9·80	7·5	—	S	S	8½	—	—
31·2	7·98	7·7	− 2	S	US	9½	—	—
34·7	8·88	6·9	− 2	S	US	7½	—	—
38·0	9·72	6·3	− 2	S	US	5½	—	—

TABLE 70—*continued*

Speed V (ft/sec)	Velocity coefficient C_v	Keel attitude α_K (deg)	Elevator angle η (deg)	Stable (S) Unstable (US) Border-line (B) Skipping (Sk) before disturbance	Stable (S) Unstable (US) Border-line (B) Skipping (Sk) after disturbance	Disturbance nose-down (deg)	Amplitude of porpoising, if any, after disturbance (deg)	Limits of porpoising after disturbance (deg)
18·9	4·84	13·2	0	S	S	6	—	—
19·5	4·99	12·9	0	S	US	—	4	—
21·0	5·37	12·0	0	S	US	—	—	—
24·5	6·26	10·2	0	S	US	6	11	6 to 17
28·5	7·28	8·3	0	S	US	4	11	6 to 17
32·5	8·31	7·0	0	S	US	6	—	—
36·2	9·26	6·0	0	S	US	5	—	—
23·3	5·96	10·4	+ 4	US	US	—	—	—
26·6	6·80	8·4	+ 4	B	US	—	—	—
30·5	7·80	6·4	+ 4	S	US	3	—	—
34·3	8·77	5·3	+ 4	S	US	3	—	—
38·3	9·80	4·4	+ 4	S	US	4	—	—

DISTURBED HYDRODYNAMIC LONGITUDINAL STABILITY CHARACTERISTICS

TABLE 71

Model E

($C_{\Delta 0} = 2{\cdot}25$; $I = 25{\cdot}02$ lb ft²)

Speed V (ft/sec)	Velocity coefficient C_v	Keel attitude α_K (deg)	Elevator angle η (deg)	Stable (S) Unstable (US) Border-line (B) Skipping (Sk) before disturbance	Stable (S) Unstable (US) Border-line (B) Skipping (Sk) after disturbance	Disturbance nose-down (deg)	Amplitude of porpoising, if any, after disturbance (deg)	Limits of porpoising after disturbance (deg)
24·5	6·26	9·4	−16	S	S	—	—	—
28·1	7·18	9·5	−16	S	S	7½	—	—
32·4	8·28	9·6	−16	B Sk	B	—	—	—
35·8	9·16	9·6	−16	B Sk	B	—	—	—
26·5	6·78	9·2	−12	S	S	4	—	—
30·6	7·82	9·4	−12	S	S	6	—	—
34·0	8·70	9·4	−12	S	B Sk	4½	—	—
35·2	9·00	9·4	−12	B Sk	B Sk	—	—	—
0	0	3·3	− 8	S	S	—	—	—
4·1	1·05	3·1	− 8	S	S	—	—	—
8·3	2·12	4·6	− 8	S	S	—	—	—
12·4	3·17	4·8	− 8	S	S	—	—	—
16·6	4·24	6·3	− 8	S	S	—	—	—
18·7	4·78	8·4	− 8	S	S	—	—	—
20·2	5·16	9·0	− 8	S	S	7	—	—
24·4	6·24	9·1	− 8	S	S	6	—	—
28·0	7·15	9·0	− 8	S	S	5	—	
32·0	8·18	8·9	− 8	S	S	6	—	—
35·5	9·08	8·3	− 8	S	S	7	—	—
22·8	5·83	9·0	− 4	S	S	—	—	—
26·5	6·78	8·2	− 4	S	S	7	—	—
30·5	7·80	7·0	− 4	S	S	5	—	—
34·0	8·70	6·6	− 4	S	S	6	—	—
37·9	9·69	6·3	− 4	S	S	2	—	—
33·4	8·54	5·8	− 2	S	S	5	—	—
37·8	9·66	5·5	− 2	S	S	5	—	—
24·7	6·31	8·3	0	S	S	6	—	—
28·6	7·31	6·9	0	S	S	6	—	—
31·5	8·06	5·7	0	S	S	7	—	—
33·0	8·44	5·4	—	S	US	6½	—	—
35·8	9·16	4·5	0	S	S	4½	—	—
27·1	6·93	6·6	—	S	S	7½	—	—
22·8	5·83	8·6	+ 4	S	S	8	—	—
26·7	6·83	7·5	+ 4	B	B	5	1	—
28·8	7·36	6·0	+ 4	S	S	5	—	—
29·6	7·57	5·6	+ 4	S	US	10½	7	—
30·5	7·80	5·2	+ 4	S	US	3	10	3 to 13
33·7	8·62	4·4	+ 4	S	US	3	—	—
24·7	6·31	7·7	—	US	US	—	—	—
26·7	6·83	6·4	—	B	US	5	5	5 to 10
27·5	7·04	6·2	—	S	US	6	3	—

DISTURBED HYDRODYNAMIC LONGITUDINAL STABILITY CHARACTERISTICS

TABLE 72

Model E

($C_{\Delta 0} = 2{\cdot}75$; $I = 25{\cdot}02$ lb ft^2)

Speed V (ft/sec)	Velocity coefficient C_v	Keel attitude α_K (deg)	Elevator angle η (deg)	Stable (S) Unstable (US) Border-line (B) Skipping (Sk) before disturbance	Stable (S) Unstable (US) Border-line (B) Skipping (Sk) after disturbance	Disturbance nose-down (deg)	Amplitude of porpoising, if any, after disturbance (deg)	Limits of porpoising after disturbance (deg)
25·9	6·62	9·7	−12	S	S	7	—	—
27·0	6·90	9·8	−12	S	S	9½	—	—
30·0	7·66	9·6	−12	S	US	7	6	6 to 12
32·5	8·31	9·7	−12	S	US	7	5	6 to 11
33·5	8·56	9·3	—	S	S	9	—	—
33·6	8·59	9·7	−12	S	S	7	—	—
37·7	9·64	9·7	−12	B	B Sk	—	1	8½ to 9½
39·5	10·11	9·1	−12	US Sk	US Sk	—	—	—
0	0	3·1	− 8	S	S	—	—	—
4·0	1·02	2·9	− 8	S	S	—	—	—
8·4	2·14	4·5	− 8	S	S	—	—	—
12·1	3·10	4·7	− 8	S	S	—	—	—
16·8	4·29	6·6	− 8	S	S	—	—	—
18·5	4·72	8·8	− 8	S	S	—	—	—
20·9	5·34	9·7	− 8	S	S	—	—	—
24·0	6·14	9·7	− 8	S	S	9	—	—
28·5	7·28	9·5	− 8	S	US	8	5	6 to 11
32·5	8·31	8·9	− 8	S	US	6	6	6 to 12
36·3	9·28	9·4	− 8	S	S	7	—	—
40·0	10·23	8·4	− 8	S	US Sk	4½	3	7 to 10
36·0	9·20	7·9	− 6	S	S	7½	—	—
40·0	10·23	7·5	− 6	S	S	5	—	—
27·0	6·90	9·4	− 4	S	S	8	—	—
30·7	7·85	8·3	− 4	S	US	7	6	6 to 12
34·0	8·70	7·4	− 4	S	US	6	5	7 to 12
34·5	8·82	7·3	− 4	S	S	7½	—	—
36·0	9·20	7·0	− 4	S	S	6	—	—
38·0	9·72	6·8	− 4	S	S	6	—	—
36·0	9·20	6·4	− 2	S	US	4	—	—
37·5	9·59	6·4	− 2	S	S	7½	—	—
39·7	10·16	5·9	− 2	S	US	4	8	4 to 12
25·1	6·42	9·4	0	S	S	7	—	—
26·5	6·78	8·9	0	S	S	6½	—	—
27·5	7·03	8·5	0	S	S	6	—	—
29·0	7·41	7·8	0	S	US	5	6	5 to 11
32·0	8·18	6·7	0	S	US	7	6	6 to 12
36·0	9·20	5·5	0	S	US	4	—	—
39·7	10·16	4·5	0	S	US	5	—	—
27·1	6·93	8·3	—	B	B	—	—	—

DISTURBED HYDRODYNAMIC LONGITUDINAL STABILITY CHARACTERISTICS

TABLE 73

Model F

($C_{\Delta 0} = 2{\cdot}25$; $I = 40{\cdot}25$ lb ft²)

Speed V (ft/sec)	Velocity coefficient C_v	Keel attitude α_K (deg)	Elevator angle η (deg)	Stable (S) Unstable (US) Border-line (B) Skipping (Sk) before disturbance	Stable (S) Unstable (US) Border-line (B) Skipping (Sk) after disturbance	Disturbance nose-down (deg)	Amplitude of porpoising, if any, after disturbance (deg)	Limits of porpoising after disturbance (deg)
0	0	2·6	− 8	S	S	—	—	—
4	1·02	2·5	− 8	S	S	—	—	—
7·9	2·02	3·3	− 8	S	S	—	—	—
10·9	2·79	3·8	− 8	S	S	—	—	—
17·0	4·34	4·4	− 8	S	S	—	—	—
20·5	5·24	6·3	− 8	S	S	—	—	—
23·2	5·93	7·2	− 8	S	S	7	—	—
27·0	6·90	7·3	− 8	S	S	8½	—	—
30·7	7·84	7·5	− 8	S	S	7	—	—
34·6	8·84	7·4	− 8	B Sk	B Sk	8	1½	—
33·2	8·48	7·4	—	S	S	—	—	—
29·6	7·56	7·2	− 1	S	S	—	—	—
33·0	8·43	6·6	− 1	S	S	—	—	—
37·0	9·45	6·1	− 1	S	S	—	—	—
38·8	9·92	6·1	− 1	S	S	—	—	—
27·3	6·98	7·1	0	S	S	9	—	—
31·0	7·92	6·5	0	S	S	7½	—	—
35·0	8·94	5·9	0	S	S	7	—	—
38·5	9·84	5·8	0	S	S	5	—	—
35·5	9·08	5·1	+ 1	S	S	6½	—	—
36·6	9·36	4·8	+ 1	S	S	5½	—	—
38·0	9·72	4·7	+ 1	S	S	5½	—	—
29·5	7·54	6·3	+ 2	S	S	7½	—	—
31·8	8·13	5·8	+ 2	S	S	6½	—	—
35·0	8·94	4·9	+ 2	S	S	5½	—	—
35·7	9·12	4·8	+ 2	S	US	6	—	—
37·0	9·46	4·4	+ 2	S	US	5	—	—
38·3	9·79	4·3	+ 2	S	US	5	—	—
25·4	6·49	7·0	+ 4	S	S	8	—	—
29·5	7·54	5·8	+ 4	S	S	6½	—	—
31·5	8·05	5·2	+ 4	S	S	6	—	—
32·7	8·36	4·9	+ 4	S	S	5	—	—
34·5	8·82	4·4	+ 4	S	US	4	10	—
35·5	9·08	4·1	+ 4	S	US	4	10	—
29·5	7·54	5·7	—	S	US	7	3	—
33·0	8·43	4·5	—	S	S	5½	—	—
27·5	7·02	6·1	+ 8	S	B	6	1½	—
29·2	7·47	5·3	+ 8	S	US	6½	5	—
30·7	7·84	4·9	+ 8	S	US	6	2½	—
32·0	8·17	4·3	+ 8	S	US	6	4	—
34·5	8·82	3·8	+ 8	S	US	5	—	—
33·0	8·43	4·2	+ 8	S	S	7½	—	—
33·0	8·43	3·9	—	S	US	5	5	—

DISTURBED HYDRODYNAMIC LONGITUDINAL STABILITY CHARACTERISTICS

TABLE 74

Model F

($C_{\Delta 0} = 2{\cdot}75$; $I = 40{\cdot}25$ lb ft^2)

Speed V (ft/sec)	Velocity coefficient C_v	Keel attitude α_K (deg)	Elevator angle η (deg)	Stable (S) Unstable (US) Border-line (B) Skipping (Sk) before disturbance	Stable (S) Unstable (US) Border-line (B) Skipping (Sk) after disturbance	Disturbance nose-down (deg)	Amplitude of porpoising, if any, after disturbance (deg)	Limits of porpoising after disturbance (deg)
29·0	7·41	7·9	−12	S	S	8	—	—
34·7	8·88	7·9	−12	S	S	8	—	—
37·0	9·45	7·6	−12	B Sk	B Sk	4	1½	—
38·1	9·75	7·7	−12	B Sk	B Sk	7½	1½	—
0	0	2·6	− 8	S	S	—	—	—
4·0	1·02	2·4	− 8	S	S	—	—	—
7·9	2·02	3·2	− 8	S	S	—	—	—
11·8	3·02	3·4	− 8	S	S	—	—	—
17·0	4·34	4·5	− 8	S	S	—	—	—
19·4	4·96	5·3	− 8	S	S	—	—	—
23·2	5·93	7·5	− 8	S	S	7	—	—
27·3	6·98	7·8	− 8	S	S	6½	—	—
31·0	7·92	7·8	− 8	S	S	5	—	—
34·5	8·82	7·8	− 8	S	S	6	—	—
38·7	9·89	7·6	− 8	B Sk	B Sk	6	1½	—
37·2	9·52	6·3	—	S	S	6½	—	—
38·5	9·85	6·4	—	S	S	5½	—	—
37·0	9·46	6·0	—	S	S	6	—	—
38·5	9·85	5·7	—	S	US	5½	—	—
25·5	6·52	7·6	− 4	S	S	8½	—	—
29·5	7·54	7·6	− 4	S	S	8	—	—
31·8	8·12	7·6	− 4	S	S	8	—	—
36·0	9·20	7·6	− 4	S	S	8	—	—
37·2	9·52	5·7	—	S	US	5	—	—
35·8	9·16	5·8	—	S	S	10	—	—
37·0	9·45	5·4	—	S	US	5½	—	—
36·0	9·20	5·5	—	S	US	7½	—	—
26·8	6·85	7·6	0	S	S	8	—	—
31·0	7·92	7·1	0	S	S	7½	—	—
34·5	8·82	6·1	0	S	S	7½	—	—
36·0	9·20	5·2	—	S	US	5½	—	—
38·5	9·85	5·3	0	S	S	6	—	—
37·5	9·59	5·1	+ 2	S	US	6½	—	—
25·5	6·52	7·4	+ 4	S	S	7	—	—
29·5	7·54	6·9	+ 4	S	S	7½	—	—
32·0	8·18	6·2	+ 4	S	S	6½	—	—
33·0	8·43	5·9	+ 4	S	S	6½	—	—
34·5	8·82	5·6	+ 4	S	S	5	—	—
35·5	9·08	5·1	+ 4	S	US	5	9	—
36·8	9·40	4·8	+ 4	S	US	6	10	—
27·0	6·91	7·2	+ 6	B	B	6½	1	—
28·8	7·35	6·8	+ 6	B	B	6½	1½	—
31·0	7·92	5·9	+ 6	S	US	6½	3½	—
32·0	8·18	5·6	+ 6	S	US	5	2½	—
33·0	8·44	5·5	+ 6	S	US	6	2½	—
34·0	8·70	5·1	+ 6	S	US	6	2½	—
35·2	9·00	4·6	+ 6	S	US	5	—	—

DISTURBED HYDRODYNAMIC LONGITUDINAL STABILITY CHARACTERISTICS

TABLE 75

Model G

($C_{\Delta 0} = 2{\cdot}25$; $I = 23{\cdot}50$ lb ft^2)

Speed V (ft/sec)	Velocity coefficient C_v	Keel attitude α_K (deg)	Elevator angle η (deg)	Stable (S) Unstable (US) Border-line (B) Skipping (Sk) before disturbance	Stable (S) Unstable (US) Border-line (B) Skipping (Sk) after disturbance	Disturbance nose-down (deg)	Amplitude of porpoising, if any, after disturbance (deg)	Limits of porpoising after disturbance (deg)
21·0	5·37	8·5	−12	S	S	11	—	—
25·2	6·44	8·2	−12	S	US	8	7	—
29·2	7·46	8·2	−12	S	US	8	6½	—
0	0	2·3	− 8	S	S	—	—	—
4·0	1·02	2·4	− 8	S	S	—	—	—
7·6	1·94	4·0	− 8	S	S	—	—	—
11·5	2·94	4·4	− 8	S	S	—	—	—
15·5	3·96	5·7	− 8	S	S	—	—	—
17·5	4·47	7·4	− 8	S	S	—	—	—
19·3	4·93	8·4	− 8	S	S	10	—	—
23·3	5·95	8·2	− 8	S	S	10	—	—
27·0	6·90	7·9	− 8	S	US	9½	7	—
31·0	7·92	7·9	− 8	S	US	8½	6	—
32·5	8·30	7·7	− 8	S	US	9	3	—
23·5	6·00	8·1	− 4	S	S	10½	—	—
25·5	6·52	7·9	− 4	S	US	—	6	—
27·5	7·02	7·7	− 4	S	US	10½	7½	—
31·4	8·03	7·5	− 4	S	US	9	6½	—
32·8	8·39	7·2	− 4	S	US	7	5	—
34·2	8·75	6·9	− 4	S	S	6½	—	—
35·0	8·94	6·4	− 4	S	S	—	—	—
36·5	9·34	6·2	− 4	S	S	7	—	—
31·5	8·06	6·5	− 2	S	US	7	8	—
33·5	8·55	6·1	− 2	S	S	7½	—	—
35·0	8·94	5·7	− 2	S	S	6	—	—
37·0	9·46	5·3	− 2	S	S	6	—	—
21·6	5·52	8·2	0	S	S	9	—	—
25·5	6·52	7·4	0	S	US	8½	6	—
29·5	7·54	6·4	0	S	US	6	8	—
32·9	8·40	5·8	0	S	US	7	—	—
35·0	8·94	5·1	0	S	US	6½	—	—
37·0	9·46	4·7	0	S	US	6	—	—
23·5	6·00	7·7	+ 4	S	S	8	—	—
24·5	6·27	7·4	+ 4	S	US	7	5½	—
27·5	7·02	5·9	+ 4	S	US	6½	8	—
31·5	8·06	5·1	+ 4	S	US	5½	—	—
35·1	8·96	3·9	+ 4	S	US	—	—	—

DISTURBED HYDRODYNAMIC LONGITUDINAL STABILITY CHARACTERISTICS

TABLE 76

Model G

($C_{\Delta 0} = 2{\cdot}75$; $I = 23{\cdot}50$ lb ft^2)

Speed V (ft/sec)	Velocity coefficient C_v	Keel attitude α_K (deg)	Elevator angle η (deg)	Stable (S) Unstable (US) Border-line (B) Skipping (Sk) before disturbance	Stable (S) Unstable (US) Border-line (B) Skipping (Sk) after disturbance	Disturbance nose-down (deg)	Amplitude of porpoising, if any, after disturbance (deg)	Limits of porpoising after disturbance (deg)
20·5	5·24	9·4	−12	S	S	9	—	—
24·2	6·18	9·0	−12	S	S	8½	—	—
28·5	7·27	8·5	−12	S	US	7	8	—
0	0	2·3	− 8	S	S	—	—	—
4·0	1·02	2·4	− 8	S	S	—	—	—
8·0	2·04	4·4	− 8	S	S	—	—	—
12·0	3·07	5·2	− 8	S	S	—	—	—
16·0	4·08	8·5	− 8	S	S	—	—	—
18·0	4·60	9·3	− 8	S	S	—	—	—
19·8	5·06	9·4	− 8	S	S	10	—	—
23·8	6·08	8·9	− 8	S	S	9½	—	—
25·3	6·46	8·7	− 8	S	US	7	5	—
27·5	7·02	8·5	− 8	S	US	9	7	—
31·5	8·05	8·4	− 8	S	US	8	7	—
35·2	8·99	8·3	− 8	S	US	8	5	—
38·6	9·86	7·6	− 8	B Sk	US	7	3	—
19·5	4·98	9·3	− 4	S	S	—	—	—
23·4	5·98	9·0	− 4	S	S	10½	—	—
27·4	7·00	8·3	− 4	B	US	8	7	—
31·1	7·95	7·8	− 4	S	US	9½	8	—
34·8	8·89	7·5	− 4	S	US	7½	7	—
36·7	9·37	7·4	− 4	S	US	8	7	—
37·6	9·61	7·2	− 4	S	US	6½	—	—
38·5	9·84	7·0	− 4	S	S	7½	—	—
39·0	9·96	7·3	− 4	S	S	7	—	—
37·5	9·58	6·6	− 3	S	US	7	—	—
38·5	9·84	6·5	− 3	S	S	6	—	—
38·2	9·76	6·0	− 2	S	US	5½	—	—
21·7	5·54	9·1	0	S	S	9	—	—
25·5	6·51	8·4	0	B	US	9	6	—
29·7	7·58	7·5	0	S	US	7½	6	—
33·6	8·58	6·5	0	S	US	6	—	—
37·0	9·46	5·5	0	S	US	5	—	—
38·2	9·77	5·3	0	S	US	4	—	—
23·6	6·03	8·6	+ 4	S	S	8	—	—
27·6	7·05	7·6	+ 4	B	US	—	7	—
31·6	8·07	6·5	+ 4	S	US	4	—	—
35·2	8·99	5·3	+ 4	S	US	5½	—	—
38·6	9·85	4·3	+ 4	S	US	4½	—	—
24·2	6·18	8·4	+ 8	S	S	9	—	—
28·5	7·27	6·8	+ 8	US	US	—	—	—
32·0	8·18	5·5	+ 8	US	US	—	—	—

DISTURBED HYDRODYNAMIC LONGITUDINAL STABILITY CHARACTERISTICS

TABLE 77

Model H

($C_{\Delta 0} = 2{\cdot}25$; $I = 23{\cdot}50$ lb ft^2)

Speed V (ft/sec)	Velocity coefficient C_v	Keel attitude α_K (deg)	Elevator angle η (deg)	Stable (S) Unstable (US) Border-line (B) Skipping (Sk) before disturbance	Stable (S) Unstable (US) Border-line (B) Skipping (Sk) after disturbance	Disturbance nose-down (deg)	Amplitude of porpoising, if any, after disturbance (deg)	Limits of porpoising after disturbance (deg)
20·5	5·24	12·8	−20	S	US	11	10	—
24·7	6·31	12·5	−20	S	US	12	9	—
26·3	6·72	12·6	−20	S	S	12½	—	—
27·1	6·92	12·5	−20	S	S	10½	—	—
28·8	7·36	12·6	−20	S	S	8½	—	—
31·0	7·92	12·7	−20	B Sk	B Sk	—	2	—
32·0	8·17	12·7	−20	B Sk	B Sk	—	2	—
33·1	8·46	12·7	−20	US Sk	US Sk	—	3	—
19·8	5·06	12·9	−16	S	S	13	—	—
23·8	6·08	12·0	−16	S	US	11	11	—
27·6	7·05	11·3	−16	S	S	10½	—	—
31·5	8·05	11·9	−16	B	B	7½	1	—
33·5	8·56	11·8	−16	B Sk	B Sk	—	2	—
33·5	8·56	11·4	−14	S	S	7	—	—
35·3	9·02	11·0	−14	S	S	—	—	—
21·8	5·51	12·0	−12	S	US	10	11	—
24·8	6·34	11·3	−12	S	US	11	9	—
25·7	6·57	10·9	−12	S	S	10½	—	—
29·6	7·56	9·9	−12	S	S	10	—	—
33·2	8·49	10·7	−12	S	S	7	—	—
37·0	9·46	10·4	−12	S	S	—	—	—
0	0	4·5	− 8	S	S	—	—	—
4·0	1·02	4·6	− 8	S	S	—	—	—
7·8	1·99	6·8	− 8	S	S	—	—	—
11·8	3·02	8·0	− 8	S	S	—	—	—
16·0	4·08	11·3	− 8	S	S	—	—	—
17·8	4·55	12·9	− 8	S	S	—	—	—
19·5	4·98	12·4	− 8	S	S	10	—	—
23·5	6·01	10·5	− 8	S	US	10	10	—
27·5	7·03	8·9	− 8	S	S	9	—	—
31·3	8·00	7·9	− 8	S	S	9	—	—
35·0	8·95	8·4	− 8	S	S	7½	—	—
31·5	8·05	7·4	− 6	S	S	7½	—	—
35·3	9·02	7·6	− 6	S	S	6½	—	—
19·8	5·06	12·3	− 4	S	US	12	4	—
21·8	5·57	10·9	− 4	S	US	10	11	—
23·8	6·08	9·7	− 4	S	US	9	12	—
24·7	6·32	8·9	− 4	S	US	8	11	—
25·5	6·52	8·6	− 4	S	S	9½	—	—
27·5	7·03	7·9	− 4	S	S	6½	—	—
28·6	7·31	7·4	− 4	S	S	8½	—	—
29·5	7·54	7·1	− 4	S	US	8	—	—
33·1	8·46	6·1	− 4	S	US	5½	—	—
37·3	9·53	5·3	− 4	S	US	—	—	—

TABLE 77—*continued*

Speed V (ft/sec)	Velocity coefficient C_v	Keel attitude α_K (deg)	Elevator angle η (deg)	Stable (S) Unstable (US) Border-line (B) Skipping (Sk) before disturbance	Stable (S) Unstable (US) Border-line (B) Skipping (Sk) after disturbance	Disturbance nose-down (deg)	Amplitude of porpoising, if any, after disturbance (deg)	Limits of porpoising after disturbance (deg)
22·0	5·62	10·2	0	S	US	7	9	—
24·0	6·13	8·9	0	S	US	8	11	—
24·8	6·34	8·2	0	S	S	$7\frac{1}{2}$	—	—
25·7	6·57	7·9	0	S	S	7	—	—
26·7	6·83	7·4	0	S	US	$6\frac{1}{2}$	—	—
32·5	8·30	5·3	0	S	US	$5\frac{1}{2}$	—	—
24·5	6·26	8·2	+ 2	S	US	8	11	—
25·2	6·44	7·9	+ 2	B	US	8	—	—

DISTURBED HYDRODYNAMIC LONGITUDINAL STABILITY CHARACTERISTICS

TABLE 78

Model H

($C_{\Delta 0} = 2{\cdot}75$; $I = 23{\cdot}50$ lb ft²)

Speed V (ft/sec)	Velocity coefficient C_v	Keel attitude α_K (deg)	Elevator angle η (deg)	Stable (S) Unstable (US) Border-line (B) Skipping (Sk) before disturbance	Stable (S) Unstable (US) Border-line (B) Skipping (Sk) after disturbance	Disturbance nose-down (deg)	Amplitude of porpoising, if any, after disturbance (deg)	Limits of porpoising after disturbance (deg)
21·0	5·36	13·4	−20	S	US	14	10	—
23·8	6·08	12·8	−20	S	US	12	12	—
27·8	7·10	12·5	−20	S	US	9	9	—
29·8	7·61	12·4	−20	S	US	12	9	—
31·7	8·11	12·6	−20	S	S	9	—	—
33·5	8·56	12·2	−20	B Sk	B Sk	10	1	—
19·7	5·04	13·7	−16	S	S	11	—	—
23·8	6·08	12·5	−16	S	US	12	11	—
27·6	7·05	12·2	−16	S	US	12½	9	—
31·7	8·11	12·3	−16	S	S	8½	—	—
35·2	8·99	11·6	−16	B Sk	B Sk	8	1	—
38·0	9·72	11·3	−16	B Sk	B Sk	—	2	—
22·0	5·62	12·9	−12	S	US	10	10	—
25·7	6·57	11·2	−12	S	US	7½	11	—
27·3	6·98	10·5	−12	S	US	10	9	—
28·5	7·28	10·7	−12	S	US	10	8	—
30·0	7·66	10·5	−12	S	S	11	—	—
32·0	8·18	10·0	−12	S	S	8½	—	—
33·2	8·48	10·2	−12	S	S	11	—	—
35·9	9·17	10·5	−12	S	S	7	—	—
37·8	9·66	10·3	−12	S	S	11	—	—
0	0	4·3	− 8	S	S	—	—	—
4·0	1·02	4·4	− 8	S	S	—	—	—
7·8	1·99	6·7	− 8	S	S	—	—	—
11·8	3·10	8·1	− 8	S	S	—	—	—
14·0	3·58	9·7	− 8	S	S	—	—	—
16·0	4·08	13·3	− 8	S	S	—	—	—
16·8	4·29	13·7	− 8	S	S	—	—	—
19·5	4·98	13·5	− 8	S	S	9	—	—
19·9	5·09	13·3	− 8	S	S	—	—	—
24·0	6·13	11·5	− 8	S	US	—	11	—
24·8	6·34	11·0	− 8	S	US	7	11	—
25·8	6·59	10·2	− 8	S	US	9	10	—
27·5	7·03	9·4	− 8	S	US	8	10	—
28·6	7·31	9·0	− 8	S	US	8½	9	—
28·8	7·36	9·3	—	S	US	6½	8	—
29·6	7·56	9·1	—	S	S	9½	—	—
30·0	7·66	8·8	− 8	S	S	8½	—	—
31·5	8·05	8·3	− 8	S	S	—	—	—
35·3	9·02	7·7	− 8	S	S	5	—	—
39·0	9·96	8·1	− 8	S	S	—	—	—
29·8	7·61	8·4	− 6	S	US	8	10	—
33·2	8·49	7·7	− 6	S	S	8	—	—
37·3	9·54	7·0	− 6	S	S	7½	—	—
20·8	5·31	13·0	− 4	S	US	13½	6	—
24·5	6·26	10·4	− 4	S	US	10	12	—
29·0	7·41	8·1	− 4	S	US	8½	—	—
32·5	8·30	6·9	− 4	S	US	6½	—	—
36·5	9·33	6·0	− 4	S	US	6	—	—

DISTURBED HYDRODYNAMIC LONGITUDINAL STABILITY CHARACTERISTICS

TABLE 79

Model J

($C_{\Delta 0} = 2{\cdot}25$; $I = 23{\cdot}90$ lb ft²)

Speed V (ft/sec)	Velocity coefficient C_v	Keel attitude α_K (deg)	Elevator angle η (deg)	Stable (S) Unstable (US) Border-line (B) Skipping (Sk) before disturbance	Stable (S) Unstable (US) Border-line (B) Skipping (Sk) after disturbance	Disturbance nose-down (deg)	Amplitude of porpoising, if any, after disturbance (deg)	Limits of porpoising after disturbance (deg)
18·8	4·80	12·7	−28	B	US	14	6	—
22·2	5·67	11·4	−28	S	S	12	—	—
25·7	6·56	11·4	−28	S	S	9	—	—
30·0	7·67	11·7	−28	S	S	8	—	—
33·8	8·64	11·6	−28	US Sk	US Sk	—	—	—
16·0	4·08	13·5	−24	S	S	11	—	—
20·0	5·11	12·0	−24	B	US	11	3½	—
24·1	6·16	11·3	−24	S	S	10	—	—
28·2	7·21	11·6	−24	S	S	10	—	—
32·3	8·24	11·6	−24	B	B	7	1	—
34·2	8·75	11·6	−24	US Sk	US Sk	—	—	—
17·5	4·47	13·1	−20	B	US	11	3½	—
20·5	5·24	11·8	−20	B	US	11	4	—
24·4	6·24	11·1	−20	S	S	11	—	—
28·5	7·29	11·3	−20	S	S	9	—	—
32·2	8·24	11·2	−20	S	S	11	—	—
18·7	4·78	12·5	−16	B	US	13	6	—
19·0	4·86	12·0	−16	US	US	—	—	—
24·3	6·21	10·5	−16	S	S	10	—	—
28·3	7·24	10·7	−16	S	S	11	—	—
32·2	8·24	10·6	−16	S	S	11	—	—
17·2	4·40	12·8	−12	B	US	14	—	—
19·5	4·99	11·6	−12	US	US	—	—	—
21·1	5·40	10·8	−12	B	US	—	—	—
22·2	5·67	10·4	−12	S	US	—	—	—
25·8	6·60	9·9	−12	S	S	10	—	—
30·0	7·66	9·9	−12	S	S	10	—	—
33·5	8·56	9·9	−12	S	S	11	—	—
0	0	4·7	− 8	S	S	—	—	—
4·0	1·02	4·7	− 8	S	S	—	—	—
8·0	2·04	7·0	− 8	S	S	—	—	—
12·1	3·09	8·7	− 8	S	S	—	—	—
14·5	3·71	12·3	− 8	S	S	—	—	—
16·1	4·11	12·8	− 8	S	S	12	—	—
18·5	4·73	12·0	− 8	US	US	—	—	—
20·2	5·16	10·9	− 8	US	US	—	—	—
24·3	6·21	9·6	− 8	S	S	10	—	—
28·4	7·26	8·7	− 8	S	S	—	—	—
32·2	8·24	8·5	− 8	S	S	7	—	—
36·0	9·20	9·3	− 8	S	S	5	—	—

TABLE 79—*continued*

Speed V (ft/sec)	Velocity coefficient C_v	Keel attitude α_K (deg)	Elevator angle η (deg)	Stable (S) Unstable (US) Border-line (B) Skipping (Sk) before disturbance	Stable (S) Unstable (US) Border-line (B) Skipping (Sk) after disturbance	Disturbance nose-down (deg)	Amplitude of porpoising, if any, after disturbance (deg)	Limits of porpoising after disturbance (deg)
18·5	4·73	11·8	− 4	US	US	—	—	—
22·5	5·75	9·5	− 4	S	US	9½	7½	—
26·0	6·65	7·7	− 4	S	S	8	—	—
30·2	7·72	6·6	− 4	S	S	7	—	—
34·6	8·85	6·2	− 4	S	S	6½	—	—
30·0	7·67	6·1	− 2	S	US	6½	—	—
34·0	8·69	5·4	− 2	S	US	5½	—	—
16·5	4·22	12·5	0	S	US	12	2½	—
19·4	4·96	11·0	0	US	US	—	—	—
21·9	5·60	9·5	0	US	US	—	—	—
23·5	6·01	8·5	0	B	US	9	9	—
24·8	6·34	7·7	0	US	US	9	9	—
28·0	7·16	6·3	0	S	S	7	—	—
31·8	8·13	5·0	0	S	US	5½	—	—
35·6	9·10	4·2	0	S	US	—	—	—
17·5	4·47	11·9	+ 4	B	US	12	6	—
22·2	5·67	8·4	+ 4	US	US	—	—	—
26·1	6·67	6·4	+ 4	B	US	7	11	—
30·3	7·75	4·9	+ 4	B	US	—	—	—
34·0	8·69	3·5	+ 4	US	US	—	—	—

DISTURBED HYDRODYNAMIC LONGITUDINAL STABILITY CHARACTERISTICS

TABLE 80

Model J

($C_{\Delta 0} = 2{\cdot}75$; $I = 23{\cdot}90$ lb ft²)

Speed V (ft/sec)	Velocity coefficient C_v	Keel attitude α_K (deg)	Elevator angle η (deg)	Stable (S) Unstable (US) Border-line (B) Skipping (Sk) before disturbance	Stable (S) Unstable (US) Border-line (B) Skipping (Sk) after disturbance	Disturbance nose-down (deg)	Amplitude of porpoising, if any, after disturbance (deg)	Limits of porpoising after disturbance (deg)
17·5	4·47	14·7	−28	S	S	5	—	—
18·5	4·72	14·5	−28	S	US	13	5	—
20·0	5·11	13·6	−28	US	US	—	—	—
23·8	6·08	11·9	−28	B	US	—	—	—
27·5	7·03	11·7	−28	S	S	10	—	—
31·8	8·13	11·8	−28	S	S	11½	—	—
35·2	9·00	11·8	−28	S	S	7	—	—
39·0	9·97	10·9	−28	US Sk	US Sk	—	—	—
22·0	5·62	12·5	−24	B	US	12	9	—
25·5	6·52	11·7	−24	S	US	10	12	—
29·5	7·54	11·7	−24	S	S	10	—	—
33·5	8·56	11·7	−24	S	S	9	—	—
36·8	9·40	11·7	−24	S	US Sk	—	4	—
19·8	5·06	13·4	−20	US	US	—	—	—
23·0	5·87	11·7	−20	B	US	—	—	—
27·0	6·90	11·2	−20	S	US	10½	12	—
31·0	7·92	11·4	−20	S	S	8	—	—
34·8	8·89	11·5	−20	S	S	8	—	—
37·8	9·66	11·3	−20	US Sk	US Sk	—	—	—
19·6	5·01	13·7	−16	US	US	—	—	—
21·9	5·60	12·4	−16	B	US	9	12½	—
25·0	6·39	10·8	−16	S	S	7	14	—
29·7	7·59	10·8	−16	S	S	9	—	—
33·1	8·46	10·8	−16	S	S	7	—	—
36·5	9·33	10·7	−16	S	S	8	—	—
18·7	4·78	14·2	−12	US	US	—	—	—
22·2	5·67	11·7	−12	US	US	—	—	—
25·5	6·52	10·3	−12	S	US	10	13	—
29·5	7·54	10·1	−12	S	S	10	—	—
33·5	8·56	10·2	−12	S	S	8½	—	—
37·6	9·61	10·0	−12	S	S	7	—	—
0	0	4·8	− 8	S	S	—	—	—
4·0	1·02	4·7	− 8	S	S	—	—	—
7·9	2·02	7·3	− 8	S	S	—	—	—
11·9	3·04	9·0	− 8	S	S	—	—	—
14·0	3·58	11·8	− 8	S	S	—	—	—
16·0	4·08	14·0	− 8	S	S	11	—	—
18·0	4·60	14·0	− 8	S	S	11	—	—
19·5	4·98	13·4	− 8	US	US	—	—	—
23·5	6·01	10·7	− 8	US	US	—	—	—
27·1	6·93	9·2	− 8	S	US	10	12	—
29·8	7·62	9·1	− 8	S	S	8½	—	—
31·0	7·92	8·9	− 8	S	S	8	—	—
34·6	8·84	8·4	− 8	S	S	7½	—	—
39·0	9·96	9·3	− 8	S	S	6	—	—

TABLE 80—*continued*

Speed V (ft/sec)	Velocity coefficient C_v	Keel attitude α_K (deg)	Elevator angle η (deg)	Stable (S) Unstable (US) Border-line (B) Skipping (Sk) before disturbance	Stable (S) Unstable (US) Border-line (B) Skipping (Sk) after disturbance	Disturbance nose-down (deg)	Amplitude of porpoising, if any, after disturbance (deg)	Limits of porpoising after disturbance (deg)
18·7	4·78	13·5	— 4	S	US	14	8	—
21·8	5·57	11·6	— 4	US	US	—	—	—
25·5	6·51	9·5	— 4	S	US	—	—	—
29·0	7·41	8·0	— 4	S	US	$8\frac{1}{2}$	12	—
31·0	7·93	7·5	— 4	S	S	8	—	—
32·5	8·30	7·0	— 4	S	S	8	—	—
36·8	9·40	6·5	— 4	S	S	7	—	—
19·8	5·06	12·4	0	US	US	10	10	—
23·8	6·08	9·7	0	US	US	$11\frac{1}{2}$	15	—
27·7	7·08	7·8	0	S	US	8	14	—
31·3	8·00	6·5	0	S	US	7	—	—
35·0	8·95	5·4	0	S	US	6	—	—

DISTURBED HYDRODYNAMIC LONGITUDINAL STABILITY CHARACTERISTICS

TABLE 81

Model K

($C_{\Delta 0} = 2{\cdot}75$; $I = 23{\cdot}10$ lb ft^2)

Speed V (ft/sec)	Velocity coefficient C_v	Keel attitude α_K (deg)	Elevator angle η (deg)	Stable (S) Unstable (US) Border-line (B) Skipping (Sk) before disturbance	Stable (S) Unstable (US) Border-line (B) Skipping (Sk) after disturbance	Disturbance nose-down (deg)	Amplitude of porpoising, if any, after disturbance (deg)	Limits of porpoising after disturbance (deg)
20·8	5·32	12·8	—20	S	US	12	11	—
22·0	5·62	12·6	—20	S	US	14	11	—
25·7	6·56	12·3	—20	S	US	14½	11	—
29·7	7·59	12·3	—20	S	S	12	—	—
19·7	5·04	12·8	—16	S	S	13	—	—
23·6	6·03	12·2	—16	US	US	12	10	—
27·5	7·03	12·2	—16	S	S	11½	—	—
31·2	7·97	12·2	—16	S	S	1	—	—
35·1	8·97	11·5	—16	B	B	9	½	—
38·2	9·76	10·9	—16	B	B	9	—	—
21·8	5·57	12·2	—12	S	US	—	11	—
25·5	6·51	10·2	—12	S	US	11	10	—
26·8	6·85	10·1	—12	S	S	11½	—	—
29·6	7·56	10·1	—12	S	S	11	—	—
33·0	8·44	10·0	—12	S	S	11	—	—
36·0	9·21	10·2	—12	S	S	8	—	—
0	0	3·6	— 8	S	S	—	—	—
4·0	1·02	3·7	— 8	S	S	—	—	—
7·9	2·02	5·9	— 8	S	S	—	—	—
11·8	3·02	6·8	— 8	S	S	—	—	—
16·0	4·08	12·3	— 8	S	S	—	—	—
17·8	4·55	12·7	— 8	S	S	—	—	—
19·2	4·91	12·5	— 8	S	S	12	—	—
23·4	5·98	10·5	— 8	S	US	8	11	—
27·0	6·90	8·4	— 8	S	S	13	—	—
31·3	7·99	8·0	— 8	S	S	7	—	—
34·5	8·82	7·8	— 8	S	S	9	—	—
38·0	9·72	8·3	— 8	S	S	—	—	—
34·8	8·90	7·1	— 6	S	S	8	—	—
38·3	9·80	7·1	— 6	S	S	7½	—	—
37·0	9·46	6·6	—	S	US	9½	—	—
20·8	5·32	12·2	— 4	S	US	11	11	—
22·0	5·62	11·0	— 4	S	US	10	13	—
25·6	6·55	8·5	— 4	S	US	7½	11	—
28·0	7·16	7·2	— 4	S	S	10	—	—
32·0	8·18	6·7	— 4	S	S	6½	—	—
33·2	8·48	6·4	— 4	S	S	7½	—	—
35·5	9·08	6·0	— 4	S	US	5	—	—
29·7	7·59	6·6	— 2	S	S	8½	—	—
31·2	7·97	6·2	— 2	S	US	7	—	—
19·5	4·88	12·3	0	S	S	11½	—	—
23·5	6·01	9·4	0	S	US	10½	11	—
27·6	7·06	6·9	0	S	US	10	11	—
29·7	7·60	6·0	0	S	US	8	—	—
31·2	7·98	5·6	0	S	US	7½	—	—

DISTURBED HYDRODYNAMIC LONGITUDINAL STABILITY CHARACTERISTICS

TABLE 82

Model L

($C_{\Delta 0} = 2{\cdot}75$; $I = 25{\cdot}50$ lb ft^2)

Speed V (ft/sec)	Velocity coefficient C_v	Keel attitude α_K (deg)	Elevator angle η (deg)	Stable (S) Unstable (US) Border-line (B) Skipping (Sk) before disturbance	Stable (S) Unstable (US) Border-line (B) Skipping (Sk) after disturbance	Disturbance nose-down (deg)	Amplitude of porpoising, if any, after disturbance (deg)	Limits of porpoising after disturbance (deg)
24·0	6·14	9·4	−16	S	S	11	—	—
27·8	7·11	9·4	−16	S	US	8	5½	—
31·0	7·93	9·4	−16	S	S	6	—	—
25·5	6·51	9·2	−12	S	S	11	—	—
26·5	6·77	9·2	−12	S	US	11	5½	—
28·8	7·36	9·2	−12	S	US	9	5	—
29·7	7·59	9·2	−12	S	S	10	—	—
33·5	8·56	9·1	−12	S	S	10	—	—
36·5	9·32	9·0	−12	B Sk	B Sk	4	1	—
27·8	7·11	8·9	−10	S	US	9½	7	—
28·9	7·39	8·9	−10	S	S	7	—	—
0	0	2·2	− 8	S	S	—	—	—
4·0	1·02	2·2	− 8	S	S	—	—	—
7·8	1·99	3·4	− 8	S	S	—	—	—
12·0	3·07	3·7	− 8	S	S	—	—	—
16·0	4·08	5·0	− 8	S	S	—	—	—
17·9	4·57	7·4	− 8	S	S	—	—	—
19·6	5·01	8·8	− 8	S	S	6½	—	—
23·4	5·98	9·1	− 8	S	S	11	—	—
26·0	6·64	8·8	− 8	S	S	5½	—	—
27·0	6·90	8·5	− 8	S	S	9	—	—
27·3	6·98	8·6	− 8	S	US	8½	7	—
27·9	7·13	8·6	− 8	S	S	7½	—	—
31·2	9·98	8·3	− 8	S	S	8½	—	—
35·0	8·95	8·4	− 8	S	S	8½	—	—
38·1	9·75	8·1	− 8	S	S	7	—	—
25·3	6·46	8·5	− 4	S	S	8	—	—
27·8	7·11	7·3	− 4	S	S	8	—	—
29·7	7·60	7·0	− 4	S	S	7	—	—
33·0	8·44	6·4	− 4	S	S	6½	—	—
37·0	9·45	5·7	− 4	S	S	5½	—	—
30·0	7·67	6·4	− 2	S	S	—	—	—
31·8	8·13	6·1	− 2	S	S	6	—	—
33·8	8·64	5·6	− 2	S	S	4½	—	—
34·8	8·90	5·5	− 2	S	S	6	—	—
37·0	9·46	5·0	− 2	S	S	6½	—	—
38·5	9·84	4·8	− 2	S	S	7½	—	—
30·1	7·69	6·1	− 1	S	S	—	—	—
31·8	8·13	5·8	− 1	S	S	7½	—	—
33·5	8·56	5·5	− 1	S	S	4½	—	—
34·2	8·75	5·2	− 1	S	US	5	—	—
35·5	9·07	5·1	− 1	S	US	5	—	—
36·5	9·32	5·0	− 1	S	US	7	—	—
38·7	9·89	4·6	− 1	S	US	6	—	—

TABLE 82—*continued*

Speed V (ft/sec)	Velocity coefficient C_v	Keel attitude α_K (deg)	Elevator angle η (deg)	Stable (S) Unstable (US) Border-line (B) Skipping (Sk) before disturbance	Stable (S) Unstable (US) Border-line (B) Skipping (Sk) after disturbance	Disturbance nose-down (deg)	Amplitude of porpoising, if any, after disturbance (deg)	Limits of porpoising after disturbance (deg)
23·8	6·08	8·8	0	S	S	9½	—	—
25·5	6·51	8·0	0	S	S	8	—	—
26·8	6·85	7·2	0	S	S	8	—	—
27·5	7·03	6·8	0	S	S	6	—	—
30·8	7·86	5·4	0	S	S	7	—	—
31·3	8·00	5·1	0	S	US	6	6	—
35·0	8·94	4·3	0	S	US	3	—	—
38·2	9·75	3·3	0	S	US	2	—	—
23·8	6·08	8·4	+ 4	S	S	8	—	—
24·8	6·33	8·0	+ 4	B	B	—	1	—
25·5	6·51	7·6	+ 4	US	US	7	2½	—
26·2	6·69	6·9	+ 4	US	US	—	—	—
27·6	7·05	6·1	+ 4	B	B	6	1½	—
28·9	7·38	5·3	+ 4	S	B	7	1	—
30·0	7·66	4·8	+ 4	B	B	5	½	—
30·9	7·90	4·5	+ 4	S	US	6	—	—
26·5	6·77	6·0	+ 8	US	US	6	2½	—
28·0	7·16	5·2	+ 8	US	US	7	3	—
30·1	7·69	4·4	+ 8	US	US	4	—	—

DISTURBED HYDRODYNAMIC LONGITUDINAL STABILITY CHARACTERISTICS

TABLE 83

Model M

($C_{\Delta 0} = 2{\cdot}75$; $I = 23{\cdot}20$ lb ft²)

Speed V (ft/sec)	Velocity coefficient C_v	Keel attitude α_K (deg)	Elevator angle η (deg)	Stable (S) Unstable (US) Border-line (B) Skipping (Sk) before disturbance	Stable (S) Unstable (US) Border-line (B) Skipping (Sk) after disturbance	Disturbance nose-down (deg)	Amplitude of porpoising, if any, after disturbance (deg)	Limits of porpoising after disturbance (deg)
23·2	5·93	11·1	−16	S	B	14	1½	—
27·0	6·90	11·1	−16	S	US	9	8	—
29·0	7·42	11·1	−16	S	S	12	—	—
34·6	8·85	11·2	−16	B	B	—	1½	—
36·5	9·34	11·2	−16	US	US	—	—	—
22·0	5·62	11·0	−12	S	S	10	—	—
23·8	6·09	11·0	−12	S	B	12	1½	—
25·7	6·57	10·8	−12	S	US	11	8	—
27·6	7·05	11·0	−12	S	US	11	8	—
29·9	7·66	11·0	−12	S	S	11	—	—
33·3	8·51	11·0	−12	S	B	10	2	—
34·5	8·83	11·0	−12	S	B	8	2	—
36·1	9·23	11·0	−12	B	B	11	1½	—
37·8	9·69	11·0	−12	US	US	—	3	—
27·9	7·14	10·7	−10	S	S	10	—	—
37·5	9·60	10·8	−10	S	B	6	2	—
39·0	9·98	10·8	−10	US	US	—	2½	—
0	0	4·0	− 8	S	S	—	—	—
3·9	1·00	4·0	− 8	S	S	—	—	—
7·8	1·99	5·3	− 8	S	S	—	—	—
11·9	3·04	5·7	− 8	S	S	—	—	—
16·4	4·19	7·6	− 8	S	S	—	—	—
19·5	4·99	10·9	− 8	S	S	—	—	—
23·5	6·01	10·7	− 8	B	B	11	—	—
25·1	6·42	10·5	− 8	S	S	11	—	—
26·0	6·65	10·4	− 8	S	US	10	7	—
27·8	7·11	9·8	− 8	S	S	9	—	—
31·7	8·11	9·6	− 8	S	S	—	—	—
35·4	9·05	9·9	—	S	S	—	—	—
35·5	9·08	9·7	− 8	S	S	—	—	—
38·9	9·95	9·3	− 8	S	US Sk	8	—	—
25·8	6·59	10·0	—	S	S	10	—	—
22·1	5·65	10·7	− 4	S	B	10	1	—
23·3	5·97	10·4	− 4	B	B	10	1½	—
24·0	6·14	10·2	− 4	S	B	11	1	—
26·0	6·64	9·1	− 4	S	S	9	—	—
30·0	7·67	8·0	− 4	S	S	—	—	—
33·5	8·56	7·2	− 4	S	S	6	—	—
35·0	8·98	6·6	− 4	S	S	8	—	—
37·0	9·46	6·6	− 4	S	S	—	—	—
28·5	7·28	8·0	− 2	S	S	9	—	—
32·0	8·20	7·0	− 2	S	S	9	—	—
33·9	8·67	6·1	− 2	S	US	8	—	—
34·9	8·93	6·1	− 2	S	S	6	—	—
36·9	9·43	5·9	− 2	S	S	5	—	—

TABLE 83—*continued*

Speed V (ft/sec)	Velocity coefficient C_v	Keel attitude α_K (deg)	Elevator angle η (deg)	Stable (S) Unstable (US) Border-line (B) Skipping (Sk) before disturbance	Stable (S) Unstable (US) Border-line (B) Skipping (Sk) after disturbance	Disturbance nose-down (deg)	Amplitude of porpoising, if any, after disturbance (deg)	Limits of porpoising after disturbance (deg)
20·0	5·12	10·7	0	S	S	—	—	—
24·0	6·13	9·9	0	US	US	—	4	—
25·5	6·52	8·8	0	B	B	9	1	—
27·3	6·98	8·0	0	S	US	9	7	—
31·5	8·06	6·6	0	S	US	9	12	—
35·5	9·08	5·0	0	S	US	6	—	—
22·2	5·68	10·5	+ 4	US	US	13	$3\frac{1}{2}$	—
24·3	6·23	9·0	+ 4	US	US	8	4	—
26·1	6·68	7·8	+ 4	US	US	—	$4\frac{1}{2}$	—
30·0	7·68	6·0	+ 4	B	US	—	14	—
21·5	5·50	10·5	—	S	S	10	—	—

DISTURBED HYDRODYNAMIC LONGITUDINAL STABILITY CHARACTERISTICS

TABLE 84

Model N

($C_{\Delta 0} = 2{\cdot}75$; $I = 23{\cdot}90$ lb ft^2)

Speed V (ft/sec)	Velocity coefficient C_v	Keel attitude α_K (deg)	Elevator angle η (deg)	Stable (S) Unstable (US) Border-line (B) Skipping (Sk) before disturbance	Stable (S) Unstable (US) Border-line (B) Skipping (Sk) after disturbance	Disturbance nose-down (deg)	Amplitude of porpoising, if any, after disturbance (deg)	Limits of porpoising after disturbance (deg)
23·6	6·04	11·2	−20	S	S	9	—	—
28·0	7·16	11·3	−20	S	S	11	—	—
32·0	8·18	11·4	−20	B	B	—	1½	—
24·0	8·70	11·5	−20	US	B	—	2	—
22·1	5·65	11·1	−16	S	S	10	—	—
25·0	6·40	10·8	−16	S	S	11	—	—
26·1	6·66	10·7	−16	S	S	11	—	—
30·0	7·67	10·8	−16	S	S	10	—	—
33·0	8·44	10·9	−16	S	S	10	—	—
35·0	8·95	11·3	−16	B	B	8	1	—
38·0	9·72	10·9	−16	B	B	—	—	—
23·0	5·87	10·9	−12	S	B	11	1	—
25·0	6·40	10·1	−12	S	S	10	—	—
27·1	6·92	9·9	−12	S	S	—	—	—
31·0	7·93	9·7	−12	S	S	—	—	—
34·3	8·76	10·2	−12	S	S	8	—	—
37·8	9·67	9·8	−12	S	B	7	1½	—
0	0	3·5	− 8	S	S	—	—	—
4·0	1·02	3·3	− 8	S	S	—	—	—
8·0	2·04	4·7	− 8	S	S	—	—	—
12·0	3·07	5·1	− 8	S	S	—	—	—
16·6	4·25	7·4	− 8	S	S	—	—	—
19·7	5·04	11·0	− 8	S	S	11	—	—
23·3	5·96	10·7	− 8	B	B	10	1½	—
23·5	6·01	10·5	− 8	B	B	—	—	—
27·1	6·95	8·5	− 8	S	S	10	—	—
31·1	7·96	8·2	− 8	S	S	7	—	—
35·0	8·95	8·4	− 8	S	S	9	—	—
38·9	9·95	8·9	− 8	S	S	7	—	—
21·7	5·54	10·7	− 4	S	S	13	—	—
23·8	6·07	9·7	− 4	B	B	10	1	—
25·5	6·52	8·4	− 4	B	B	8	2	—
29·5	7·55	6·6	− 4	S	S	6	—	—
33·0	8·44	5·8	− 4	S	S	5½	—	—
36·1	9·23	5·4	− 4	S	US	6	—	—
20·0	5·11	10·7	0	S	S	11	—	—
22·0	5·63	10·5	0	B	B	9	2	—
23·1	5·91	10·0	0	US	US	—	4	—
23·8	6·09	9·7	0	US	US	2½	—	—
25·5	6·52	8·1	0	US	US	7	—	—
28·0	7·16	6·7	0	B	US	11	6	—
30·3	7·75	5·7	0	S	US	6	12	—
34·6	8·85	4·3	0	S	US	4	—	—

HYDRODYNAMIC DIRECTIONAL STABILITY CHARACTERISTICS

TABLE 85

Model A

(Not constrained in roll)

($C_{\Delta 0} = 2{\cdot}75$; $\eta = +2$ deg)

Speed (ft/sec)	Velocity coefficient C_v	Stable (S) Unstable (US) at zero yaw	First stable yaw angle (deg)	First unstable yaw angle (deg)	Second stable yaw angle (deg)	Second unstable yaw angle (deg)	Limit of test (deg)	Remarks
4·0	1·02	US	—	0	—	—	18	—
8·0	2·10	US	12·7	0	—	—	18	—
10·0	2·56	US	5·5	0	—	—	18	—
12·0	3·07	S	0	—	—	—	18	—
14·0	3·58	US	3	0	—	—	18	—
16·0	4·09	US	6·2	0	—	—	18	—
18·0	4·61	S	0	5·5	13·5	—	18	—
20·0	5·12	S	0	6·0	—	—	18	—
28·0	7·16	S	0	8·0	—	—	10	—
32·0	8·18	S	0	9·0	—	—	10	—
36·0	9·20	S	0	8·5	—	—	10	—
40·0	10·23	S	0	7·0	—	—	10	—

HYDRODYNAMIC DIRECTIONAL STABILITY CHARACTERISTICS

TABLE 86

Model A

($C_{\Delta 0} = 2{\cdot}75$; $\eta = +2$ deg)

Speed (ft/sec)	Velocity coefficient C_v	Stable (S) Unstable (US) at zero yaw	First stable yaw angle (deg)	First unstable yaw angle (deg)	Second stable yaw angle (deg)	Second unstable yaw angle (deg)	Limit of test (deg)	Remarks
7·1	1·82	US	18·5	0	—	—	18	—
8·2	2·10	US	13·2	0	—	—	18	—
11·0	2·82	US	1·3	0	—	—	8	—
12·1	3·10	S	0	—	—	—	18	—
14·0	3·58	US	2·2	0	—	—	18	—
15·1	3·86	S	0	4·0	5·5	—	10	—
16·3	4·17	S	0	5·5	7·5	—	14	—
17·0	4·35	S	0	6·0	8·5	—	18	—
17·9	4·58	S	0	6·0	9·5	10·5	18	14-deg third stable yaw angle.
19·0	4·86	S	0	6·0	17·0	—	18	—
19·7	5·04	S	0	6·0	17·9	—	18	—
28·8	7·36	S	0	6·5	—	—	—	—
32·0	8·18	S	0	6·5	—	—	—	—
36·0	9·21	S	0	8·5	—	—	—	—
40·0	10·23	S	0	6·3	—	8·0	—	—

HYDRODYNAMIC DIRECTIONAL STABILITY CHARACTERISTICS

TABLE 87

Model A

(Not constrained in roll)

($C_{\Delta 0} = 2{\cdot}75$; $\eta = -10$ deg)

Speed (ft/sec)	Velocity coefficient C_v	Stable (S) Unstable (US) at zero yaw	First stable yaw angle (deg)	First unstable yaw angle (deg)	Second stable yaw angle (deg)	Second unstable yaw angle (deg)	Limit of test (deg)	Remarks
8·0	2·10	US	12·7	0	—	—	—	—
10·0	2·56	US	5·5	0	—	—	18	—
12·0	3·07	S	0	—	—	—	18	—
14·0	3·58	US	3·0	0	—	—	18	—
16·0	4·09	US	6·2	0	—	—	18	—
18·0	4·61	S	0	5·5	13·5	—	18	—
20·0	5·12	S	0	6·0	—	—	18	—
32·0	8·18	S	0	7·0	—	—	10	—
36·0	9·20	S	0	9·0	—	—	10	—

HYDRODYNAMIC DIRECTIONAL STABILITY CHARACTERISTICS

TABLE 88

Model A

($C_{\Delta 0} = 2{\cdot}75$; $\eta = -10$ deg)

Speed (ft/sec)	Velocity coefficient C_v	Stable (S) Unstable (US) at zero yaw	First stable yaw angle (deg)	First unstable yaw angle (deg)	Second stable yaw angle (deg)	Second unstable yaw angle (deg)	Limit of test (deg)	Remarks
7·0	1·79	US	17·8	0	—	—	—	—
8·0	2·10	US	12·0	0	—	—	—	—
11·0	2·82	US	1·3	0	—	—	8	—
12·1	3·10	S	0	—	—	—	18	—
14·0	3·58	US	2·2	0	—	—	18	—
15·1	3·86	S	0	4·0	5·5	—	10	—
16·3	4·17	S	0	5·5	7·5	—	14	—
18·1	4·63	S	0	6·0	9·5	11·0	—	13-deg third stable yaw angle.
19·0	4·86	S	0	6·0	17·0	—	18	—
19·7	5·04	S	0	6·0	17·9	—	18	—
29·3	7·50	S	0	8·6	—	—	—	—
32·2	8·23	S	0	10·0	—	—	—	—
36·0	9·20	S	0	8·7	—	—	—	—
40·0	10·23	S	0	7·0	—	—	—	—

HYDRODYNAMIC DIRECTIONAL STABILITY CHARACTERISTICS

TABLE 89

Model A

(With breaker strips)

($C_{\Delta 0} = 2{\cdot}75$; $\eta = -10$ deg)

Speed (ft/sec)	Velocity coefficient C_v	Stable (S) Unstable (US) at zero yaw	First stable yaw angle (deg)	First unstable yaw angle (deg)	Second stable yaw angle (deg)	Second unstable yaw angle (deg)	Limit of test (deg)	Remarks
7·0	1·79	US	16·5	0	—	—	—	—
8·2	2·10	US	11·4	0	—	—	—	—
12·0	3·07	S	0	—	—	—	—	—
16·0	4·09	S	0	—	—	—	—	—
18·4	4·71	S	0	—	—	—	—	—
20·2	5·17	S	0	—	—	—	—	—
28·0	7·16	S	0	—	—	—	—	—
32·0	8·18	S	0	—	—	—	—	—
36·0	9·20	S	0	—	—	—	—	—

HYDRODYNAMIC DIRECTIONAL STABILITY CHARACTERISTICS

TABLE 90

Model B

($C_{\Delta 0} = 2{\cdot}75$; $\eta = 0$ deg)

Speed (ft/sec)	Velocity coefficient C_v	Stable (S) Unstable (US) at zero yaw	First stable yaw angle (deg)	First unstable yaw angle (deg)	Second stable yaw angle (deg)	Second unstable yaw angle (deg)	Limit of test (deg)	Remarks
4·0	1·02	US	18+	0	—	—	18	—
8·2	2·10	US	15	0	—	—	18	—
12·2	3·12	US	3·5	0	—	—	15	—
13·0	3·32	US	4·0	0	—	—	14	—
14·2	3·63	US	5·0	0	—	—	7	—
15·5	3·96	S	0	3·0	8·5	—	14	—
16·7	4·27	S	0	3·0	9·2	—	18	—
18·2	4·66	S	0	3·5	5·0	6·7	18	—
20·0	5·12	S	0	8·0	—	—	10	—
30·0	7·66	S	0	8·5	—	—	—	—
34·0	8·70	S	0	9·5	—	—	—	—

HYDRODYNAMIC DIRECTIONAL STABILITY CHARACTERISTICS

TABLE 91

Model C

($C_{\Delta 0} = 2{\cdot}25$; $\eta = 0$ deg)

Speed (ft/sec)	Velocity coefficient C_v	Stable (S) Unstable (US) at zero yaw	First stable yaw angle (deg)	First unstable yaw angle (deg)	Second stable yaw angle (deg)	Second unstable yaw angle (deg)	Limit of test (deg)	Remarks
4·0	1·02	US	18+	0	—	—	20	—
8·4	2·15	US	18+	0	—	—	20	—
10·5	2·68	US	11·0	0	—	—	13	—
12·5	3·20	US	7·2	0	—	—	13	—
14·6	3·74	US	8·2	0	15·0	—	15	—
15·2	3·89	US	9·0	0	16·0	—	—	—
15·8	4·04	US	—	0	—	—	—	—
16·9	4·32	S	0	2·5	—	—	—	—
17·5	4·48	S	0	2·7	6·0	6·5	—	—
19·2	4·91	US	0	4·2	—	—	—	—
19·6	5·01	US	4·0	0	6·0	—	—	—
29·5	7·54	S	0	6·0	—	—	—	—
34·0	8·70	S	0	6·0	—	—	—	—

HYDRODYNAMIC DIRECTIONAL STABILITY CHARACTERISTICS

TABLE 92

Model C

($C_{\Delta 0} = 2{\cdot}75$; $\eta = 0$ deg)

Speed (ft/sec)	Velocity coefficient C_v	Stable (S) Unstable (US) at zero yaw	First stable yaw angle (deg)	First unstable yaw angle (deg)	Second stable yaw angle (deg)	Second unstable yaw angle (deg)	Limit of test (deg)	Remarks
4·0	1·02	US	—	0	—	—	20	—
8·3	2·12	US	19·0	0	—	—	20	—
12·2	3·12	US	8·1	0	—	—	14	—
13·4	3·43	US	6·7	0	—	—	—	—
14·2	3·63	US	7·2	0	—	—	10	—
15·2	3·89	S	0	2·5	9·0	—	9	—
15·5	3·96	S	0	10·0	9·6	15·0	—	—
15·8	4·04	S	0	—	16·0	—	—	—
16·7	4·27	S	0	4·0	—	—	—	—
18·2	4·66	S	0	6·5	—	—	9	—
20·0	5·11	S	0	7·0	—	—	13	—
30·0	7·67	S	0	7·0	—	—	—	—
34·0	8·70	S	0	8·0	—	—	11	

HYDRODYNAMIC DIRECTIONAL STABILITY CHARACTERISTICS

TABLE 93

Model D

($C_{\Delta 0} = 2{\cdot}75$; $\eta = 0$ deg)

Speed (ft/sec)	Velocity coefficient C_v	Stable (S) Unstable (US) at zero yaw	First stable yaw angle (deg)	First unstable yaw angle (deg)	Second stable yaw angle (deg)	Second unstable yaw angle (deg)	Limit of test (deg)	Remarks
4·0	1·02	US	18+	0	—	—	—	—
5·9	1·51	US	18+	0	—	—	—	—
8·2	2·10	US	6·5	0	—	—	12	—
9·2	2·35	S	0	—	—	—	—	—
10·2	2·61	S	0	—	—	—	15	—
11·6	2·97	S	0	—	—	—	—	—
12·2	3·12	US	4·0	0	—	—	—	—
13·2	3·38	S	0	5·0	5·5	—	—	—
14·6	3·74	S	0	7·5	8·0	—	10	—
15·5	3·97	S	0	—	—	—	13	—
17·0	4·35	S	0	12·5	—	—	—	—
18·0	4·61	S	0	12·5	—	—	—	—
20·0	5·12	S	0	9·5	10·3	12·0	—	—
30·5	7·80	S	0	—	—	—	10	—
34·0	8·70	S	0	—	—	—	10	—
38·0	9·72	S	0	—	—	—	10	—

HYDRODYNAMIC DIRECTIONAL STABILITY CHARACTERISTICS

TABLE 94

Model E

($C_{\Delta 0} = 2{\cdot}75$; $\eta = 0$ deg)

Speed (ft/sec)	Velocity coefficient C_v	Stable (S) Unstable (US) at zero yaw	First stable yaw angle (deg)	First unstable yaw angle (deg)	Second stable yaw angle (deg)	Second unstable yaw angle (deg)	Remarks
4·0	1·02	US	—	0	—	—	—
7·6	1·94	US	—	0	—	—	—
9·7	2·48	US	12·3	0	—	—	—
11·3	2·89	US	7·0	0	—	—	Spray over port wing.
14·0	3·58	US	4·0	0	—	—	—
16·2	4·14	US	3·5	0	—	—	—
18·0	4·61	—	2·5	0 to 2	3·5	3·0	Nearly neutral stability from 0 to 2 deg.
19·4	4·96	—	3·0	0 to 3	5·2	4·5	Neutral stability from 0 to 3 deg.
21·7	5·55	S	0	5·0	6·8	9·5	—
23·9	6·11	S	0	8·0	—	—	—
25·8	6·60	S	0	8·5	—	—	—
30·0	7·67	S	0	7·5	—	—	—
34·0	8·69	S	0	7·0	—	—	—

HYDRODYNAMIC DIRECTIONAL STABILITY CHARACTERISTICS

TABLE 95

Model F

($C_{\Delta 0} = 2{\cdot}75$; $\eta = 0$ deg)

Speed (ft/sec)	Velocity coefficient C_v	Stable (S) Unstable (US) at zero yaw	First stable yaw angle (deg)	First unstable yaw angle (deg)	Second stable yaw angle (deg)	Second unstable yaw angle (deg)	Remarks
4·0	1·02	US	—	0	—	—	—
7·8	1·99	US	—	0	—	—	Large displacement force.
9·9	2·53	US	14·0	0	—	—	Spray well over wing due to low attitude.
12·0	3·07	US	9·2	0	—	—	Spray hitting wing leading edge quite solidly, a_K small.
13·8	3·53	US	5·8	0	—	—	—
16·0	4·09	US	4·2	0	—	—	Spray very bad over wing tip.
18·0	4·60	US	3·9	0	—	—	—
19·6	5·01	S	0	3·5	4·0	—	Very strong restoring forces from 4 to 10 deg. yaw.
21·8	5·58	S	0	4·0	4·5	—	Large restoring forces beyond 4·5 deg.
23·9	6·11	S	0	4·5	5·5	9·0	—
25·8	6·60	S	0	4·5	—	—	—
29·7	7·60	S	0	6·6	—	—	—
33·0	8·44	S	0	6·6	—	—	Strong displacement force at 9 deg.
37·0	9·46	S	0	—	—	—	When afterbody reaches trough side, it rises up on spray blister, due to trough being very shallow; no water flow over chine.

HYDRODYNAMIC DIRECTIONAL STABILITY CHARACTERISTICS

TABLE 96

Model G

($C_{\Delta 0} = 2{\cdot}75$; $\eta = 0$ deg)

Speed (ft/sec)	Velocity coefficient C_v	Stable (S) Unstable (US) at zero yaw	First stable yaw angle (deg)	First unstable yaw angle (deg)	Second stable yaw angle (deg)	Second unstable yaw angle (deg)	Limit of test (deg)	Remarks
4·0	1·02	US	—	0	—	—	18	—
7·8	1·99	US	15·5	0	—	—	18	—
9·7	2·48	US	9·0	0	—	—	18	—
10·9	2·79	S	0	—	—	—	18	—
11·9	3·04	S	0	—	—	—	18	—
13·9	3·56	S	0	—	—	—	18	—
15·0	3·84	US	3·8	0	10·2	9·5	15	—
16·0	4·09	S	0	2·5	15·0	—	15	—
17·9	4·58	S	0	4·0	—	—	12	—
20·6	5·27	S	0	7·0	—	—	10	—
23·7	6·06	S	0	6·7	—	—	10	—
27·5	7·03	S	0	8·0	—	—	10	—
31·4	8·03	S	0	8·5	—	—	10	—
35·0	8·95	S	0	7·5	—	—	10	—

HYDRODYNAMIC DIRECTIONAL STABILITY CHARACTERISTICS

TABLE 97

Model H

($C_{\Delta 0} = 2{\cdot}75$; $\eta = 0$ deg)

Speed (ft/sec)	Velocity coefficient C_v	Stable (S) Unstable (US) at zero yaw	First stable yaw angle (deg)	First unstable yaw angle (deg)	Second stable yaw angle (deg)	Second unstable yaw angle (deg)	Limit of test (deg)	Remarks
4·0	1·02	US	—	0	—	—	18	—
6·0	2·56	US	—	0	—	—	18	—
7·8	1·99	US	13·6	0	—	—	18	—
9·9	2·53	US	7·0	0	—	—	12	—
11·0	2·82	US	2·5	0	—	—	10	—
11·8	3·02	S	0	—	—	—	10	—
13·0	3·33	S	0	—	—	—	15	—
14·0	3·58	US	3·0	0	—	—	13	—
15·5	3·96	S	0	4·0	4·5	—	12	—
16·8	4·30	S	0	5·2	5·7	—	12	—
17·8	4·56	S	0	6·9	8·0	—	15	—
18·5	4·73	S	0	8·0	14·1	—	15	—
19·5	4·98	S	0	8·0	—	—	10	—
21·1	5·40	S	0	7·5	—	—	10	—
23·8	6·08	S	0	9·7	—	—	10	—
28·2	7·22	S	0	10·0	—	—	10	—
33·5	8·57	S	0	—	—	—	10	—
37·0	9·46	S	0	9·8	—	—	10	—

TABLE 98

Model J

($C_{\Delta 0} = 2{\cdot}75$; $\eta = 0$ and -4 deg)

Speed (ft/sec)	Velocity coefficient C_v	Stable (S) Unstable (US) at zero yaw	First stable yaw angle (deg)	First unstable yaw angle (deg)	Second stable yaw angle (deg)	Second unstable yaw angle (deg)	Remarks
	Elevator setting $\eta = 0$ *deg*						
3·9	1·00	US	—	0	—	—	$\psi = 18$ deg
7·8	1·99	US	7·5	0	—	—	—
11·7	2·99	US	3·0	0	—	—	$\psi = 0$ deg → 3 deg quite gentle. $\psi = 3$ deg → 18 deg very strong. At about $\psi = 13$ deg flow level with hull crown all the way aft from under wing. Solid water hitting port wing underside. Spray plume upwards about half-way along afterbody on starboard side.
12·8	3·28	—	2·0	—	—	—	$\psi = 18$ deg
14·0	3·58	S	0	—	—	—	On release from $\psi = 18$ deg model returned to $\psi = 0$ deg smoothly and positively. Spray over tail and wing.
16·0	4·09	S	0	10·0	—	—	Vertical spray plume about halfway along afterbody port side grew with yaw until at about $\psi = 4$ deg it hit tailplane. Tending so far to reduce yaw; at some ψ about 10 deg flow changed into continuous smooth plume from under wing all the way back, at same ψ tendency to increase yaw felt.
16·0	4·09	S	0	—	—	—	$\psi = 18$ deg +. On repeat run yaw increased rather suddenly at $\psi = 18$ deg +. The spray plume was then coming over the crown and hitting fin.
19·1	4·88	—	—	—	—	—	$\psi = 18$ deg. At $\psi = 8$ deg vertical port spray plume started. Throughout, moderate tendency to decrease yaw, no intermediate stage.
23·3	5·96	—	—	—	—	—	Seemed to wander out to $\psi = 2$ deg. Motion not positive but $\psi = 2$ deg always reached going out.
23·5	6·01	—	—	—	—	—	Wandered out to $\psi = 5$ deg. From $\psi = 0$ deg to 5 deg model would move either way with the tiniest applied moment.
23·5	6·01	—	—	—	—	—	There seemed to be a 'weak' stable equilibrium point at $\psi = 7$ deg. Yawing further to check this resulted in longitudinal instability.
23·5	6·01	—	—	—	—	—	Confirm $\psi = 7$ deg stable equilibrium point.

TABLE 98—*continued*

Speed (ft/sec)	Velocity coefficient C_v	Stable (S) Unstable (US) at zero yaw	First stable yaw angle (deg)	First unstable yaw angle (deg)	Second stable yaw angle (deg)	Second unstable yaw angle (deg)	Remarks
	Elevator setting $\eta = 0$ deg—continued						
27·2	6·96	—	9·0	—	—	—	Equilibrium appears neutral near $\psi = 0$ deg. Main spray blister not yet attaching to hull side.
27·5	7·03	—	—	—	—	—	$\psi = 5$ deg. At this yaw model tended to return to $\psi = 0$ deg when started, but there was nothing positive about the motion.
31·5	8·06	—	—	—	—	—	Longitudinal instability set in at this speed before the model was yawed; running too near the lower limit.
	Elevator setting reduced to $\eta = -4$ deg						
5·6	1·43	US	—	0	—	—	Model free; yaw increased steadily and slowly to the limit.
6·0	1·53	US	17·0	0	—	—	Yaw continued up to about $\psi = 17$ deg and then continued in a peculiar manner. From $\psi = 17$ deg to 20 deg equilibrium neutral is a good enough approximation.
6·2	1·59	US	14·0	0	—	—	Model free. It yawed out to $\psi = 14$ deg and from $\psi = 14$ deg to 20 deg it stayed where it was put.
7·2	1·84	US	10·5	0	—	—	—
9·0	2·30	US	4·0	0	—	—	$\psi = 4$ deg stable equilibrium point. Just past this the model at first appeared neutrally stable, but returned quite positively to $\psi = 4$ deg when released from $\psi = 18$ deg to 20 deg.
10·0	2·56	US	2·0	0	—	—	Positive return to $\psi = 2$ deg from greater angles of yaw.
11·2	2·87	S	0	1·5	—	—	Model free-oscillated in yaw from $\psi = \frac{1}{2}$ deg to $2\frac{1}{2}$ deg. Unstable point at say $1\frac{1}{2}$ deg.
11·4	2·92	—	—	—	—	—	Unstable point confirmed stable point at $\psi = 3$ deg.
12·3	3·15	—	—	—	—	—	Stable equilibrium point at $\psi = 2\frac{1}{2}$ deg. Bit vague below this, but positive instability.
25·8	6·60	—	—	—	—	—	When released from $\psi = 11$ deg, model tended to $\psi = 0$ deg, but at about $\psi = 9$ deg longitudinal instability set in.
26·0	6·65	—	—	—	—	—	Yawing outwards from $\psi = 0$ deg. Motion vague initially, then yaw increased automatically and at the same time longitudinal instability set in.
29·2	7·47	—	—	—	—	—	From $\psi = 2$ deg to 7 deg region of neutral equilibrium.
30·5	7·80	—	—	—	—	—	Yawed up to $\psi = 8$ deg. Equilibrium neutral.

TABLE 98—*continued*

Speed (ft/sec)	Velocity coefficient C_v	Stable (S) Unstable (US) at zero yaw	First stable yaw angle (deg)	First unstable yaw angle (deg)	Second stable yaw angle (deg)	Second unstable yaw angle (deg)	Remarks
	Elevator setting reduced to $\eta = -4$ deg—continued						
34·2	8·75	—	—	—	—	—	Neutral up to $\psi = 9$ deg.
34·5	8·83	—	—	—	—	—	When yawed up to $\psi = 10$ deg model positively stayed there. Up to $\psi = 10$ deg moments are very small or balanced out. There appears to be a stable equilibrium point at $\psi = 10$ deg.
38·3	9·80	—	—	—	—	—	Point of stable equilibrium at $\psi = 9$ deg. Below about $\psi = 6$ deg equilibrium is neutral.

TABLE 99

Test Points for Wave Tests

Point	Model	Speed (ft/sec)	C_v	Elevator setting (deg)
1	A, B, L	28*	7·2	− 8
2	B, L	24	6·1	− 8
3	B, L	29	7·4	−12
4	B, L	32	8·2	− 4
5	B, L	36	9·2	− 2
6	L	27	6·9	−12
7	L	36	9·2	−12
8	L	32	8·2	− 8
9	L	36	9·2	− 6
10	L	27	6·9	− 4
11	L	36	9·2	− 1
12	L	33	8·4	0
13	L	37	9·5	0
14	L	27	6·9	+ 4

* This speed should be 27 ft/sec for Model L.

Note : The point number and model letter are used to identify the test points, *e.g.* 3L will indicate Model L at 29 ft/sec with elevators set at −12 deg.

TABLE 100

Test Data for Recorded Steady-Speed Runs

Wave Length/Height ratio	Maximum pitching amplitude (deg)	Mean pitching amplitude (deg)	Maximum amplitude in Heave (ft)	Mean amplitude in Heave (ft)	$\frac{\text{Max. pitch}}{\text{Mean pitch}}$	$\frac{\text{Max. heave}}{\text{Mean heave}}$
Model A: Steady speed 74 kt. Wave height 2·35 ft.						
80 : 1	12·0	5·5	13·0	5·0	2·18	2·60
90 : 1	15·0	9·0	17·0	10·0	1·66	1·70
100 : 1	14·0	8·0	15·0	8·5	1·75	1·76
110 : 1	14·0	12·0	15·5	13·0	1·17	1·20
120 : 1	12·0	8·5	11·0	7·0	1·41	1·57
130 : 1	7·5	4·5	5·5	3·0	1·67	1·83
Princess : Steady speed 69 kt. Wave height 3·0 ft.						
80 : 1	11·1	8·3	12·8	9·4	1·34	1·36
90 : 1	12·6	9·3	16·3	12·3	1·35	1·33
100 : 1	10·7	8·5	16·1	11·1	1·26	1·45
110 : 1	10·0	7·2	17·3	10·4	1·39	1·66
130 : 1	12·1	8·3	20·8	12·8	1·45	1·63
Shetland : Steady speed 59 kt. Wave height 2·25 ft.						
80 : 1	12·5	11·5	9·7	9·0	1·09	1·08
90 : 1	14·8	13·6	12·8	11·8	1·09	1·08
100 : 1	6·6	4·0	5·2	2·9	1·64	1·79
110 : 1	7·6	5·7	4·7	3·2	1·34	1·47
120 : 1	7·9	6·5	5·4	4·1	1·22	1·31
130 : 1	10·1	6·7	7·0	5·1	1·49	1·38

	Assumed design loading	$C_{\Delta 0}$
Model A	150,000 lb	2·75
Princess	310,000 lb	1·08
Shetland	131,000 lb	1·08

TABLE 101

Wave Test Data for Model A

(Point 1A. $C_{\Delta 0} = 2{\cdot}75$, $C_v = 7{\cdot}2$, $\eta = -8$ deg)

h (ft)	L (ft)	h/b	L/b	L/h	Period of waves (sec)	Stability S/US/B	Max. amp. (deg)	Remarks
0·033	11·66	0·070	24·50	350	1·53	US		
0·008	1·67	0·019	3·50	200	0·56	S		
0·017	3·33	0·035	7·01	200	0·80	S		
0·025	5·00	0·053	10·53	200	0·98	S		A judder corresponding to impact on each wave front was noticeable.
0·033	6·66	0·070	14·02	200	1·14	S		Slight oscillation in height similar to previous run, but the model appeared to cut through the waves.
0·042	8·34	0·087	17·58	200	1·28	US		Constant amplitude about 9 deg. Run not quite long enough to check.
0·033	5·00	0·070	10·53	150	0·99	S		No change in attitude whatsoever; just rode the waves.
0·042	6·25	0·087	13·17	150	1·10	US	3	
0·042	6·25	0·087	13·17	150	1·10			Repeat run. Amplitude built up slowly at first, then at increasing speed reaching 12 deg approximately at the end of the run.
0·033	3·33	0·070	7·01	100	0·80	S		No change in height or attitude; cut through the waves.
0·042	4·17	0·087	8·78	100	0·90	B		Just becoming unstable at end of run; took a very long time to build up.
0·042	4·17	0·087	8·78	100	0·90	B		Repeat run. Model just became disturbed at end of run, although put in early. The motion was somewhat irregular reaching an amplitude of about 3 deg before carriage stopped.
0·050	5·00	0·105	10·53	100	0·99	US		Still not a quick build-up. An amplitude of about 10 deg reached at the end of the run.
0·042	2·09	0·087	4·39	50	0·62	S		No sign of change in height or attitude. Cut through the waves.
0·050	2·50	0·105	5·26	50	0·69	S		No height or attitude change. Boat cutting through waves.
0·058	2·92	0·123	6·14	50	0·74	S		No sign of change in attitude or height.
0·067	3·33	0·140	7·01	50	0·80	S		No change in height or attitude.
0·075	3·75	0·158	7·89	50	0·85	US		Reached an amplitude of 12 to 13 deg.
0·058	4·09	0·123	8·62	70	0·89	B	2	Damped out in middle of run and started again.
0·067	4·67	0·140	9·83	70	0·95	US		Reaching 10 deg amplitude at end of run; still taking whole run to build up.
0·092	2·75	0·193	5·79	30	0·72	S		No change in height or attitude.
0·100	3·00	0·210	6·31	30	0·76	B	2·5	Damped out and built up again at end of run; confused.
0·108	3·25	0·228	6·84	30	0·78	US		Wave system slightly irregular. Amplitude about 10 deg at end of run.

TABLE 102

Wave Test Data for Model B

(Point 1B. $C_{\Delta 0} = 2{\cdot}75$, $C_v = 7{\cdot}2$, $\eta = -8$ deg. Critical disturbance = 3·0 deg)

h (ft)	L (ft)	h/b	L/b	L/h	Period of waves (sec)	Stability S/US/B	Max. amp. (deg)	Remarks
0·033	6·67	0·070	14·04	200	1·14	S	—	—
0·042	8·34	0·087	17·54	200	1·28	US	—	—
0·042	6·25	0·087	13·15	150	1·10	B	—	Just under 2-deg amplitude
0·050	7·50	0·105	15·80	125	1·21	US	—	—
0·062	5·00	0·132	10·50	80	1·00	B	—	Just under 2-deg amplitude
0·092	4·58	0·193	9·65	50	0·94	US	—	—
0·083	4·17	0·175	8·77	50	0·90	US	—	—
0·075	3·75	0·158	7·90	50	0·85	B	—	—
0·083	2·50	0·175	5·26	30	0·68	B	—	Just under 2-deg amplitude
0·083	2·75	0·175	5·79	33	0·72	S	—	—
0·092	3·00	0·193	6·31	33	0·75	S	—	—
0·100	3·00	0·211	6·31	30	0·75	US	—	—

TABLE 103

Wave Test Data for Model B

(Point 2B. $C_{\Delta 0} = 2{\cdot}75$, $C_v = 6{\cdot}1$, $\eta = -8$ deg. Critical disturbance = 4·0 deg)

h (ft)	L (ft)	h/b	L/b	L/h	Period of waves (sec)	Stability S/US/B	Max. amp. (deg)	Remarks
0·033	6·67	0·070	14·04	200	1·14	S	—	—
0·042	8·34	0·087	17·54	200	1·28	US	—	—
0·042	6·25	0·087	13·15	150	1·10	US	—	—
0·100	3·00	0·211	6·31	30	0·75	US	—	—
0·083	2·50	0·175	5·26	30	0·68	B	—	—
0·075	2·25	0·158	4·74	30	0·65	S	—	—
0·062	3·33	0·132	7·01	53	0·80	S	—	—
0·067	3·33	0·140	7·01	50	0·80	B	—	Just under 2-deg amplitude
0·075	3·75	0·158	7·90	50	0·85	B	—	—
0·058	4·08	0·123	8·60	70	0·89	S	—	—
0·062	4·67	0·132	9·83	75	0·95	S	—	—
0·071	4·96	0·149	10·43	70	0·98	US	—	—
0·058	5·00	0·123	10·50	86	0·99	S	—	—
0·058	5·83	0·123	12·27	100	0·99	US	—	—
0·044	5·21	0·092	10·96	119	1·01	B	—	Just under 2-deg amplitude

TABLE 104

Wave Test Data for Model B

(Point 3B. $C_{\Delta 0} = 2{\cdot}75$, $C_v = 7{\cdot}4$, $\eta = -12$ deg. Critical disturbance = 4·5 deg)

h (ft)	L (ft)	h/b	L/b	L/h	Period of waves (sec)	Stability S/US/B	Max. amp. (deg)	Remarks
0·025	5·00	0·053	10·50	200	0·98	S	—	—
0·033	6·67	0·070	14·04	200	1·14	US	—	—
0·042	8·34	0·087	17·54	200	1·28	US	—	—
0·050	10·00	0·105	21·05	200	1·42	US	—	—
0·033	5·00	0·070	10·50	150	0·99	S	—	—
0·042	6·25	0·087	13·15	150	1·10	US	—	—
0·100	3·00	0·211	6·31	30	0·75	US	—	—
0·083	2·50	0·175	5·26	30	0·68	B	—	—
0·075	2·25	0·158	4·74	30	0·65	S	—	—
0·062	3·33	0·132	7·01	53	0·80	B	—	—
0·058	2·91	0·123	6·13	50	0·74	S	—	—
0·058	5·00	0·123	10·50	86	0·99	B	—	—
0·050	5·00	0·105	10·50	100	0·99	S	—	—

TABLE 105

Wave Test Data for Model B

(Point 4B. $C_{\Delta 0} = 2{\cdot}75$, $C_v = 8{\cdot}2$, $\eta = -4$ deg. Critical disturbance = 3·0 deg)

h (ft)	L (ft)	h/b	L/b	L/h	Period of waves (sec)	Stability S/US/B	Max. amp. (deg)	Remarks
0·042	8·34	0·087	17·54	200	1·28	S	—	—
0·050	10·00	0·105	21·05	200	1·42	S	—	—
0·058	11·66	0·123	24·55	200	1·53	US	—	—
0·058	8·75	0·123	18·42	150	1·32	B	—	—
0·100	3·00	0·211	6·31	30	0·75	S	—	—
0·108	3·25	0·228	6·84	30	0·78	S	—	—
0·117	3·50	0·246	7·36	30	0·82	S	—	—
0·142	3·75	0·298	7·90	26	0·85	S	—	—
0·100	5·00	0·211	10·50	50	0·98	S	—	—
0·117	5·83	0·246	12·27	50	1·07	US	—	—
0·100	7·00	0·211	14·73	70	1·17	US	—	—
0·092	6·41	0·193	13·50	70	1·12	S	—	—
0·075	7·50	0·158	15·80	100	1·21	US	—	—
0·067	6·67	0·140	14·04	100	1·14	S	—	—
0·108	5·41	0·228	11·39	50	1·03	S	—	—

TABLE 106

Wave Test Data for Model B

(Point 5B. $C_{\Delta 0} = 2{\cdot}75$, $C_v = 9{\cdot}2$, $\eta = -2$ deg. Critical disturbance = 3·5 deg)

h (ft)	L (ft)	h/b	L/b	L/h	Period of waves (sec)	Stability S/US/B	Max. amp. (deg)	Remarks
0·042	8·34	0·087	17·54	200	1·28	S	—	—
0·050	10·00	0·105	21·05	200	1·42	S	—	—
0·058	11·66	0·123	24·55	200	1·53	S	—	—
0·100	17·50	0·211	36·80	175	1·98	US	—	—
0·108	13·60	0·228	28·65	125	1·68	US	—	—
0·100	12·50	0·211	26·30	125	1·60	US	—	—
0·092	6·67	0·193	14·04	73	1·14	S	—	—
0·108	7·59	0·228	16·00	70	1·22	US	—	—
0·092	5·00	0·193	10·50	55	1·00	S	—	—
0·100	5·00	0·211	10·50	50	1·00	S	—	—
0·108	5·40	0·228	11·36	50	1·03	S	—	—
0·100	9·00	0·211	18·95	90	1·34	S	—	—
0·096	14·40	0·202	30·30	150	1·74	US	—	—
0·092	18·33	0·193	38·60	200	2·05	US	—	Just over 2-deg amplitude
0·083	15·00	0·175	31·60	180	1·78	S	—	
0·092	11·45	0·193	24·10	125	1·52	B	—	Just below 2-deg amplitude
0·108	3·50	0·228	7·36	32	0·83	S	—	—
0·125	3·50	0·263	7·36	28	0·83	S	—	—
0·117	5·83	0·246	12·27	50	1·07	S	—	—
0·125	6·25	0·263	13·15	50	1·10	S	—	—

TABLE 107

Wave Test Data for Model L

(Point 1L. $C_{\Delta 0} = 2{\cdot}75$, $C_v = 6{\cdot}9$, $\eta = -8$ deg)

h (ft)	L (ft)	h/b	L/b	L/h	Period of waves (sec)	Stability S/US/B	Max. amp. (deg)	Remarks
0·033	5·00	0·070	10·50	150	0·99	S	—	—
0·058	7·50	0·123	15·80	129	1·22	US	4·5	Not periodic.
0·050	7·50	0·105	15·80	150	1·22	US	4	Irregular
0·042	6·25	0·087	13·15	150	1·10	B	1	Irregular
0·071	5·00	0·149	10·51	71	0·99	B	—	Nearer a periodic oscillation of 1·5 deg
0·112	5·85	0·237	12·30	52	1·07	US	7	Periodic
0·079	5·85	0·167	12·30	74	1·07	US	7	Two step porpoising
0·087	4·80	0·184	10·10	55	0·97	US	4	Nearly regular
0·067	3·85	0·140	8·10	58	0·86	S	—	—
0·067	5·00	0·140	10·51	75	0·99	S	—	—
0·050	5·00	0·105	10·51	100	0·99	S	—	—
0·067	6·66	0·140	14·00	100	1·14	US	2·5	Periodic, ' jerky ' type of motion
0·117	4·65	0·246	9·79	40	0·95	US	5	Periodic
0·092	4·00	0·193	8·41	44	0·88	US	4	Periodic
0·083	3·35	0·175	7·05	40	0·80	US	2·5	Periodic
0·067	2·65	0·140	5·58	40	0·70	S	—	
0·100	3·00	0·211	6·31	30	0·75	US	2	Steady, interspersed with 3 deg
0·033	6·65	0·070	14·00	200	1·14	S	—	—
0·033	8·35	0·070	17·57	250	1·28	S	—	Steady except for one swing of 1·5 deg
0·042	8·30	0·087	17·47	200	1·28	B	—	Steady except for occasional ' flicker ' of 1 deg
0·046	10·00	0·097	21·05	218	1·42	US	4·5	—
0·042	10·40	0·087	21·90	250	1·45	US	—	Periodic ' kicks ' of 5 deg

TABLE 108

Wave Test Data for Model L

(Point 2L. $C_{\Delta 0} = 2{\cdot}75$, $C_v = 6{\cdot}1$, $\eta = -8$ deg)

h (ft)	L (ft)	h/b	L/b	L/h	Period of waves (sec)	Stability S/US/B	Max. amp. (deg)	Remarks
0·067	13·35	0·140	28·10	200	1·66	US	4	Follows wave frequency.
0·108	8·00	0·228	16·83	74	1·25	US	2·5	Divergent—convergent.
0·033	8·00	0·070	16·83	240	1·25	B	1·5	Periodic.
0·058	8·35	0·123	17·57	143	1·28	S	1	Built up erratically to 1·8 deg then down to 1·5 deg.
0·042	8·35	0·087	17·57	200	1·28	S	1·2	Erratic motion, amplitude 0·9 deg.
0·092	8·35	0·193	17·57	91	1·28	US	6·5	Steady. Before porpoising built up, wake cross-sections just off step widened and narrowed alternately; apparently at same frequency as waves met hull. When unstable, afterbody was wetted for a max. of 1b and then completely clear.
0·071	6·65	0·149	14·00	94	1·14	S	—	Steady except for slight oscillation. Wake section fluctuation, almost allowed wake to touch afterbody above chine.
0·054	10·70	0·114	22·50	197	1·47	S	1·5	Erratic. Wetting of afterbody from 1·5b to 0 but rarely completely clear.
0·075	12·00	0·158	25·26	160	1·56	US	2·7	Fairly steady. Wake nearly touched afterbody wall, and afterbody alternately clear and wetted up to max. 1·5b, mean 1b.
0·075	9·00	0·158	18·95	120	1·34	S	6·7 to 8	At start fairly steady, built up erratically. Afterbody wetting initially between 1·0 and 0·1b; finally between 1·5b and clear.
0·083	6·65	0·175	14·00	80	1·14	S	—	Steady afterbody planing area starting at 1·5b and running off end; in phase with similar movement on forebody; obviously of same period as waves.
0·130	7·50	0·272	15·80	58	1·22	S	<0·4	Steady. Motion as for previous run. Heavy vertical oscillation.
0·240	7·35	0·509	15·46	30	1·20	S	—	Steady in pitch. Large oscillation in heave.
0·175	9·70	0·368	20·40	55	1·39	US	2·2	Large oscillation in heave.
0·225	9·70	0·474	20·40	43	1·39	US	5	Fairly large oscillation in heave.
0·208	8·80	0·439	18·50	42	1·32	US	5·5	Originally stable and built up slowly.
0·175	7·70	0·368	16·20	44	1·23	S	—	Ragged movement in pitch over 1 deg. Fairly large oscillation in heave.
0·240	8·70	0·509	18·30	36	1·32	US	3·5	Motion in general seems to start with oscillation in heave while pitching motion builds up slowly, starting from zero.
0·058	14·00	0·123	29·46	240	1·71	US	4·0	

TABLE 109

Wave Test Data for Model L

(Point 3L. $C_{\Delta 0} = 2{\cdot}75$, $C_v = 7{\cdot}4$, $\eta = -12$ deg)

h (ft)	L (ft)	h/b	L/b	L/h	Period of waves (sec)	Stability S/US/B	Max. amp. (deg)	Remarks
0·033	5·00	0·070	10·50	150	0·99	S	—	—
0·058	7·50	0·123	15·80	130	1·22	US	5	Not periodic.
0·050	7·50	0·105	15·80	150	1·22	US	3·5	Irregular.
0·042	6·25	0·087	13·15	150	1·10	US	5	Irregular.
0·071	5·00	0·149	10·51	70	0·99	B	2	Irregular.
0·113	5·85	0·237	12·30	52	1·07	US	—	Approaching periodic oscillation of 6 deg.
0·079	5·85	0·167	12·30	74	1·07	US	—	Approaching periodic motion of 4·5 deg.
0·087	4·80	0·184	10·10	55	0·97	US	5·5	Steady. Two-step porpoising.
0·067	3·85	0·140	8·10	57	0·86	US	4·5	Nearly steady.
0·058	4·10	0·123	8·63	70	0·89	US	2·5	Erratic.
0·050	5·00	0·105	10·51	100	0·99	B	0·4	Slight oscillation.
0·067	6·66	0·140	14·00	100	1·14	US	3·5	Irregular.
0·058	2·75	0·123	5·79	47	0·72	S	—	—
0·071	3·75	0·149	7·90	53	0·85	B	1·5	Steady.
0·046	2·90	0·097	6·10	63	0·74	S	—	—
0·042	5·00	0·087	10·51	120	0·98	S	—	—
0·058	5·00	0·123	10·51	86	0·98	US	—	Repeatedly built up to 2·5 deg then damped out.
0·050	3·80	0·105	8·00	76	0·85	S	—	—
0·058	4·45	0·123	9·36	76	0·92	US	2·5	Periodic.
0·117	4·65	0·246	9·79	40	0·95	US	9	Two step porpoising.
0·092	4·00	0·193	8·41	43	0·88	US	4	Periodic.
0·083	3·35	0·175	7·05	40	0·80	US	4	—
0·067	2·65	0·140	5·58	40	0·70	S	—	—
0·083	2·50	0·175	5·26	30	0·69	B	1	Steady.
0·100	3·00	0·211	6·31	30	0·75	US	4	Steady.
0·033	6·65	0·070	14·00	200	1·14	B	—	Small. Periodic increase to 1·5 deg.
0·033	8·35	0·070	17·57	250	1·28	US	3	Steady.
0·042	8·30	0·087	17·47	200	1·28	US	2·5	Steady.
0·025	6·25	0·053	13·15	250	1·10	S	—	—

TABLE 110

Wave Test Data for Model L

(Point 4L. $C_{\Delta 0} = 2{\cdot}75$, $C_v = 8{\cdot}2$, $\eta = -4$ deg)

h (ft)	L (ft)	h/b	L/b	L/h	Period of waves (sec)	Stability S/US/B	Attitude (deg)	Max. amp. (deg)	Remarks
0·033	8·00	0·070	16·83	240	1·25	US	—	—	Fairly steady with occasional 'flicks' $\geqslant$ 2 deg.
0·167	6·25	0·351	13·15	38	1·10	US	7·9	—	Large heave. Pitching motion gradually built up to about 6 deg; divergent.
0·071	6·65	0·149	14·00	94	1·14	US	7·6	2·5	—
0·108	6·00	0·228	12·62	55	1·08	S	7·3	0·8	Large oscillation in heave.
0·046	6·65	0·096	14·00	145	1·14	S	6·4	—	—
0·017	4·00	0·035	8·41	240	0·88	S	6·2	—	—
0·050	6·25	0·105	13·15	125	1·10	S	7·3	—	—
0·067	6·00	0·140	12·61	90	1·08	B	7·5	0·4	Steady
0·058	8·15	0·123	17·15	140	1·27	US	7·0	—	Oscillation building up. 3-deg amplitude at end of run
0·117	6·50	0·246	13·68	56	1·13	US	7·5	4	Steady
0·175	5·65	0·368	11·90	32	1·05	US	7·8	3·5	Steady
0·142	5·65	0·298	11·90	40	1·05	S	5·8	—	—

TABLE 111

Wave Test Data for Model L

(Point 5L. $C_{\Delta 0} = 2{\cdot}75$, $C_v = 9{\cdot}2$, $\eta = -2$ deg)

h (ft)	L (ft)	h/b	L/b	L/h	Period of waves (sec)	Stability S/US/B	Attitude (deg)	Max. amp. (deg)	Remarks
0·033	8·00	0·070	16·83	240	1·25	S	—	—	—
0·046	6·65	0·097	14·00	145	1·14	S	5·5	—	—
0·050	12·00	0·105	25·26	240	1·56	US	6·5	3	Steady
0·067	8·15	0·140	17·15	125	1·26	S	7·3	—	—
0·083	10·40	0·176	21·90	125	1·44	B	6·5	1	Steady
0·096	12·50	0·202	26·65	130	1·60	US	8·0	—	Erratic motion. Divergent oscillation with model leaving water with increasing jumps until maximum of 5-deg oscillation reached, then damped out. Motion repeated
0·100	9·00	0·211	18·94	90	1·34	US	7·4	—	Occasional kicks of 4-deg amplitude
0·083	7·50	0·176	15·80	90	1·22	S	7·1	—	Occasional rapid flick of 2 deg
0·117	6·50	0·246	13·68	56	1·13	B	6·5	2	Intermittent, steady. Model periodically leaving water and steady at 6·5 deg whilst in air
0·096	6·00	0·202	12·61	62	1·08	S	6·5	—	—
0·125	7·50	0·263	15·80	60	1·22	US	—	—	Erratic oscillation. Model leaving water occasionally
0·175	5·65	0·368	11·90	32	1·05	S	6·5	—	—
0·142	5·65	0·298	11·90	40	1·05	S	6·9	—	—
0·158	6·35	0·333	13·36	40	1·12	S	6·9	—	—
0·167	7·00	0·351	14·72	42	1·17	US	—	—	Model thrown well clear of water
0·208	6·25	0·439	13·15	30	1·10	US	6·5	—	Oscillation possibly building up. 6-deg amplitude at end of run

TABLE 112

Wave Test Data for Model L

(Point 6L. $C_{\Delta 0} = 2{\cdot}75$, $C_v = 6{\cdot}9$, $\eta = -12$ deg)

h (ft)	L (ft)	h/b	L/b	L/h	Period of waves (sec)	Stability S/US/B	Max. amp. (deg)	Remarks
0·033	5·00	0·070	10·50	150	0·99	S	—	—
0·058	7·50	0·123	15·80	130	1·22	US	4	Not periodic
0·050	7·50	0·105	15·80	150	1·22	B	2	Irregular
0·042	6·25	0·087	13·15	150	1·10	US	5	Irregular
0·071	5·00	0·149	10·51	70	0·99	US	—	Nearer a periodic oscillation of 3 deg
0·058	4·10	0·123	8·63	70	0·89	S	—	—
0·113	5·85	0·237	12·30	52	1·07	US	—	Approaching periodic oscillation of 6 deg
0·087	4·80	0·184	10·10	55	0·97	US	—	Nearly steady oscillation of 5 deg
0·067	3·85	0·140	8·10	57	0·86	B	—	Nearly steady oscillation of 1·5 deg
0·050	5·00	0·105	10·51	100	0·99	B	—	Small irregular oscillations of about 0·8 deg
0·067	6·66	0·140	14·00	100	1·14	US	6·5	Two-step porpoising
0·117	4·65	0·246	9·79	40	0·95	US	5	Periodic
0·092	4·00	0·193	8·41	43	0·88	US	5·5	Periodic
0·083	3·35	0·175	7·05	40	0·80	US	3	Occasional kicks of 6 deg
0·067	2·65	0·140	5·58	40	0·70	S	—	—
0·083	2·50	0·175	5·26	30	0·69	B	0·5	Steady
0·100	3·00	0·211	6·31	30	0·75	US	—	Steady, diverging to 3-deg amplitude at end of run
0·033	6·65	0·070	14·00	200	1·14	S	0·2	Slight oscillation
0·033	8·35	0·070	17·57	250	1·28	US	—	Periodic diverging oscillation of 4 deg. Damping out
0·042	8·30	0·087	17·47	200	1·28	B	2	Steady
0·046	10·00	0·097	21·05	217	1·42	US	—	Periodic, 6 deg and 3 deg alternating
0·025	6·25	0·053	13·15	250	1·10	S	—	—
0·025	25·00	0·053	52·60	1000	2·58	B	1·5	Slow
0·033	33·30	0·070	70·00	1000	3·27	B	0·7	Slow
0·042	41·60	0·087	87·50	1000	3·95	S	—	—
0·017	16·65	0·035	35·10	1000	1·92	B	1	—
0·008	8·35	0·017	17·57	1000	1·28	S	—	—
0·025	15·00	0·053	31·60	600	1·79	B	1·5	Periodic
0·033	20·00	0·070	42·10	600	2·18	US	7	Steady
0·025	20·00	0·053	42·10	800	2·18	US	2·75	Steady
0·017	13·30	0·035	28·00	800	1·66	B	1	Steady
0·050	40·00	0·105	84·20	800	3·82	B	1	Steady
0·042	33·35	0·087	70·30	800	3·27	B	1	Steady
0·042	26·65	0·087	56·10	640	2·71	B	1·5	Steady
0·033	26·65	0·070	56·10	800	2·71	B	1	Occasional amplitude of 2 deg
0·058	35·00	0·123	73·70	600	3·41	B	1	Low frequency oscillation
0·050	20·00	0·105	42·10	400	2·18	US	8	Two step porpoising
0·121	33·35	0·254	70·30	280	3·27	US	2	Occasional 2·5 deg
0·092	33·35	0·193	70·30	360	3·27	B	<2	Very low frequency. One sudden kick of 4 deg; damped out.
0·100	33·35	0·210	70·30	330	3·27	US	2	Occasional kick of 4 deg
0·062	33·35	0·132	70·30	530	3·27	B	1	—
0·071	37·50	0·149	79·00	530	3·62	B	1	—
0·058	28·00	0·123	59·00	480	2·83	B	2	Steady
0·050	24·00	0·105	50·50	480	2·50	US	3	Steady
0·067	32·00	0·140	67·30	480	3·16	B	1	Steady
0·117	25·00	0·246	52·60	210	2·58	US	7	Irregular
0·167	16·65	0·351	35·10	100	1·91	US	8	Irregular
0·025	10·00	0·053	21·04	400	1·42	US	4	Irregular
0·017	6·65	0·035	14·00	400	1·14	S	—	—
0·067	16·65	0·140	35·00	250	1·92	US	6	Steady

TABLE 113

Wave Test Data for Model L

(Point 7L. $C_{\Delta 0} = 2{\cdot}75$, $C_v = 9{\cdot}2$, $\eta = -12$ deg)

h (ft)	L (ft)	h/b	L/b	L/h	Period of waves (sec)	Stability S/US/B	Attitude (deg)	Max. amp. (deg)	Remarks
0·033	8·00	0·070	16·83	240	1·25	US	—	4	Irregular
0·046	6·65	0·096	14·00	145	1·14	B	7·3	—	Alternate 1 and 2 deg
0·017	4·00	0·035	8·41	240	0·88	B	8·7	1·9	—
0·067	8·15	0·140	17·15	125	1·26	US	8·0	3	Steady
0·050	6·25	0·105	13·15	125	1·10	B	7·8	1·5	Steady
0·087	6·75	0·184	14·20	77	1·15	B	8·0	1	Steady
0·100	9·00	0·211	18·94	90	1·34	US	—	6·5	Very erratic, with model leaving water occasionally
0·083	7·50	0·176	15·80	90	1·22	B	8·0	1	Steady
0·117	6·50	0·246	13·68	56	1·13	B	8·0	1	Steady
0·142	8·00	0·298	16·82	56	1·26	US	7·5	—	Model thrown nose up clear of water
0·125	7·50	0·263	15·80	60	1·22	US	—	—	Erratic. Model leaving water occasionally
0·175	5·65	0·368	11·90	32	1·05	US	8·0	5	Irregular
0·142	5·65	0·298	11·90	40	1·05	S	8·2	—	—

TABLE 114

Wave Test Data for Model L

(Point 8L. $C_{\Delta 0} = 2{\cdot}75$, $C_v = 8{\cdot}2$, $\eta = -8$ deg)

h (ft)	L (ft)	h/b	L/b	L/h	Period of waves (sec)	Stability S/US/B	Attitude (deg)	Max. amp. (deg)	Remarks
0·033	8·00	0·070	16·83	240	1·25	US	—	—	Fairly steady with amplitude building up
0·046	6·65	0·096	14·00	145	1·14	US	8·0	1	Occasional kicks down to 5·5 deg
0·017	4·00	0·035	8·41	240	0·88	S	8·1	—	—
0·050	6·25	0·105	13·15	125	1·10	US	7·4	2·2	Steady
0·033	4·15	0·070	8·74	125	0·89	S	8·0	—	—
0·087	6·75	0·184	14·20	77	1·15	B	7·5	2	Steady
0·067	6·00	0·140	12·62	90	1·08	B	7·9	1·8	Steady
0·100	9·00	0·211	18·94	90	1·34	US	9·0	7	Steady
0·029	5·35	0·061	11·26	183	1·02	S	8·1	—	—
0·117	6·50	0·246	13·68	56	1·13	US	8·0	3	Steady
0·096	6·00	0·202	12·61	62	1·08	S	7·6	—	—
0·175	5·65	0·368	11·90	32	1·05	S	8·0	—	—
0·142	5·65	0·298	11·90	40	1·05	B	7·5	1	Steady. Occasional kick of 2 deg
0·158	6·35	0·333	13·36	40	1·12	US	8·0	9	Steady
0·208	6·25	0·439	13·15	30	1·10	S	8·2	—	—
0·225	6·75	0·474	14·20	30	1·15	US	—	—	Very erratic motion

TABLE 115

Wave Test Data for Model L

(Point 9L. $C_{\Delta 0} = 2{\cdot}75$, $C_v = 9{\cdot}2$, $\eta = -6$ deg)

h (ft)	L (ft)	h/b	L/b	L/h	Period of waves (sec)	Stability S/US/B	Attitude (deg)	Max. amp. (deg)	Remarks
0·046	6·65	0·097	14·00	145	1·14	S	7·0	—	—
0·033	8·00	0·070	16·82	240	1·25	S	7·3	—	Bouncing at constant attitude on every third or fourth wave crest.
0·050	12·00	0·105	25·26	240	1·56	US	7·0	3	Steady.
0·067	8·15	0·140	17·15	125	1·26	S	7·4	—	—
0·083	10·40	0·176	21·90	125	1·44	US	7·5	7	Erratic. Nose of model thrown up by waves causing model to leave water frequently.
0·100	9·00	0·211	18·94	90	1·34	US	7·0	3	Steady.
0·083	7·50	0·176	15·80	90	1·22	US	8·8	4·5	Steady.
0·096	6·00	0·202	12·61	62	1·08	B	7·5	1	Steady.
0·117	6·50	0·246	13·68	56	1·13	B	7·3	1·5	Steady.
0·067	6·00	0·140	12·61	90	1·08	B	8·1	1·2	Steady.
0·125	7·50	0·263	15·80	60	1·22	US	—	—	Erratic. Model leaving water occasionally.
0·175	5·65	0·368	11·90	32	1·05	US	7·0	3	Steady.
0·142	5·65	0·298	11·90	40	1·05	S	7·7	—	—

TABLE 116

Wave Test Data for Model L

(Point 10L. $C_{\Delta 0} = 2{\cdot}75$, $C_v = 6{\cdot}9$, $\eta = -4$ deg)

h (ft)	L (ft)	h/b	L/b	L/h	Period of waves (sec)	Stability S/US/B	Attitude (deg)	Max. amp. (deg)	Remarks
0·033	8·00	0·070	16·83	240	1·25	B	—	—	Fairly steady. Occasional 'flick' of 2 deg.
0·046	6·65	0·096	14·00	145	1·14	B	8·0	1	—
0·046	6·65	0·096	14·00	145	1·14	B	7·5	1	Steady.
0·033	8·00	0·070	16·83	240	1·25	S	8·0	—	—
0·050	12·00	0·105	25·26	240	1·56	US	6·0	4	Spasmodic.
0·067	8·15	0·140	17·15	125	1·26	US	7·6	2·7	Erratic.
0·050	6·25	0·105	13·15	125	1·10	S	8·2	—	—
0·087	6·75	0·184	14·20	77	1·15	US	7·8	4·5	Steady.
0·067	6·00	0·140	12·62	90	1·08	S	8·3	—	—
0·117	6·50	0·246	13·68	56	1·13	US	8·3	6·5	Steady.
0·096	6·00	0·202	12·61	62	1·08	US	8·0	7	Steady.
0·083	5·00	0·176	10·52	60	0·99	B	7·0	1·5	Steady.
0·175	5·65	0·368	11·90	32	1·05	US	8·0	7	Steady.
0·142	5·65	0·298	11·90	40	1·05	US	9·0	10	Steady.
0·125	5·00	0·263	10·52	40	0·99	US	7·8	5·5	Steady.
0·103	4·35	0·228	9·16	40	0·92	US	8·5	8	Steady.
0·092	3·65	0·193	7·69	40	0·84	US	7·5	4	Steady.
0·079	3·35	0·167	7·05	42	0·80	S	8·0	—	—
0·083	2·50	0·176	5·26	30	0·68	B	8·0	1	Steady.
0·100	3·00	0·210	6·31	30	0·75	S	8·3	—	—
0·117	3·50	0·246	7·36	30	0·82	US	7·5	—	Oscillation building up; 6 deg at end of run.

TABLE 117

Wave Test Data for Model L

(Point 11L. $C_{\Delta 0} = 2{\cdot}75$, $C_v = 9{\cdot}2$, $\eta = -1$ deg)

h (ft)	L (ft)	h/b	L/b	L/h	Period of waves (sec)	Stability S/US/B	Max. amp. (deg)	Remarks
0·033	5·00	0·070	10·50	150	0·99	S	—	—
0·058	7·50	0·123	15·80	129	1·22	S	—	—
0·071	11·25	0·149	23·70	159	1·51	S	—	—
0·087	11·65	0·184	24·55	133	1·54	S	—	—
0·096	13·00	0·202	27·40	125	1·64	—	—	Small erratic oscillations with occasional skips of 6 deg
0·108	10·00	0·228	21·05	92	1·42	US	—	Occasional skips of 9-deg amplitude
0·087	9·20	0·184	19·37	105	1·35	S	—	—
0·150	9·95	0·316	20·90	66	1·41	US	—	Thrown well clear of water
0·142	9·35	0·298	19·70	66	1·37	US	—	An occasional nose up ' flick ' of 4 deg
0·129	7·50	0·272	15·80	58	1·22	S	—	—
0·192	6·65	0·403	14·00	35	1·14	B	1·5	Steady
0·208	7·30	0·439	15·37	35	1·20	US	—	Bouncing clear of water
0·092	16·50	0·193	34·70	180	1·90	US	5	Bouncing from wave crest to wave crest with erratic pitching movement
0·063	13·50	0·132	28·40	216	1·68	B	2	Bouncing from wave crest to wave crest
0·075	13·50	0·158	28·40	180	1·68	S	—	—
0·067	16·50	0·140	34·70	248	1·90	US	5	Steady. Bouncing from wave crest to wave crest
0·071	16·50	0·149	34·70	233	1·90	US	4	Bouncing. Irregular oscillations
0·050	11·00	0·105	23·18	220	1·49	B	0·8	Very low frequency oscillations
0·050	12·50	0·105	26·30	250	1·60	S	—	—

TABLE 118

Wave Test Data for Model L

(Point 12L. $C_{\Delta 0} = 2{\cdot}75$, $C_v = 8{\cdot}4$, $\eta = 0$ deg)

h (ft)	L (ft)	h/b	L/b	L/h	Period of waves (sec)	Stability S/US/B	Max. amp. (deg)	Remarks
0·033	5·00	0·070	10·50	150	0·99	S	—	—
0·058	7·50	0·123	15·80	129	1·22	B	1·5	Irregular
0·071	11·25	0·149	23·70	159	1·51	US	8	Irregular. Tendency to leave water
0·067	10·00	0·140	21·02	150	1·42	S	—	—
0·108	10·00	0·228	21·05	92	1·42	US	—	Small skips of 4 deg interspersed with skips of 8 deg
0·087	9·20	0·184	19·37	105	1·35	S	—	—
0·150	9·95	0·316	20·90	66	1·41	US	—	Occasional bounces clear of water
0·142	9·35	0·298	19·70	66	1·37	US	6	Erratic
0·129	7·50	0·272	15·80	58	1·22	US	—	Model bouncing well clear of water
0·117	7·00	0·246	14·72	60	1·17	US	—	Divergent, 5 deg at end of run
0·104	6·00	0·219	12·63	58	1·07	S	—	—
0·133	6·00	0·281	12·63	45	1·07	S	—	—
0·150	6·00	0·316	12·63	40	1·07	B	2	Periodic
0·192	6·65	0·403	14·00	35	1·14	US	—	Erratic motion. Model leaving water
0·175	6·15	0·368	12·95	35	1·09	B	1·5	Oscillating
0·242	6·25	0·509	13·15	26	1·10	US	—	Erratic bouncing. Wave system poor
0·062	13·50	0·132	28·40	216	1·68	US	—	Erratic pitching movement
0·050	11·00	0·105	23·18	220	1·49	S	—	—
0·050	12·50	0·105	26·30	250	1·60	US	6·5	Irregular
0·042	10·40	0·087	21·90	250	1·44	S	—	—

TABLE 119

Wave Test Data for Model L

(Point 13L. $C_{\Delta 0} = 2{\cdot}75$, $C_v = 9{\cdot}5$, $\eta = 0$ deg)

h (ft)	L (ft)	h/b	L/b	L/h	Period of waves (sec)	Stability S/US/B	Max. amp. (deg)	Remarks
0·033	5·00	0·070	10·50	150	0·99	S	—	—
0·058	7·50	0·123	15·80	129	1·22	S	—	—
0·071	11·25	0·149	23·70	159	1·51	S	—	—
0·087	11·65	0·184	24·55	133	1·54	US	2 to 3	Occasional bounces. One of 7 deg leaving water
0·108	10·00	0·228	21·05	92	1·42	US	—	Model bouncing well clear of water
0·087	9·20	0·184	19·37	105	1·35	S	—	—
0·150	9·95	0·316	20·90	66	1·41	US	—	Bouncing well clear of water
0·142	9·35	0·298	19·70	66	1·37	US	—	Steady except for one ' hop ' of 7 deg amplitude
0·129	7·50	0·272	15·80	58	1·22	S	—	—
0·192	6·65	0·403	14·00	35	1·14	S	—	—
0·208	7·30	0·439	15·37	35	1·20	US	—	Steady except for one skip of 6-deg amplitude
0·062	13·50	0·132	28·40	216	1·68	S	—	—
0·075	13·50	0·158	28·40	180	1·68	B	1	Steady
0·092	16·50	0·193	34·70	180	1·90	US	6	Erratic. Bouncing from wave crest to wave crest

TABLE 120

Wave Test Data for Model L

(Point 14L. $C_{\Delta 0} = 2{\cdot}75$, $C_v = 6{\cdot}9$, $\eta = +4$ deg)

h (ft)	L (ft)	h/b	L/b	L/h	Period of waves (sec)	Stability S/US/B	Attitude (deg)	Max. amp. (deg)	Remarks
0·033	8·00	0·070	16·82	240	1·25	B	6·5	1	—
0·050	12·00	0·105	25·26	240	1·56	US	7·5	7·5	Alternating.
0·067	8·15	0·140	17·15	125	1·26	B	7·0	1·4	—
0·083	10·40	0·176	21·90	125	1·44	US	7·0	8	Steady.
0·100	9·00	0·211	18·94	90	1·34	US	7·0	9	Steady.
0·083	7·50	0·176	15·80	90	1·22	US	7·0	3·5	Steady.
0·096	6·00	0·202	12·61	62	1·08	US	7·5	8	Steady.
0·067	6·00	0·140	12·61	90	1·08	B	6·8	1·4	Steady.
0·083	5·00	0·176	10·52	60	0·99	B	7·1	0·5	Steady.
0·175	5·65	0·368	11·90	32	1·05	US	7·5	8	Steady.
0·142	5·65	0·298	11·90	40	1·05	US	7·5	8	Steady.
0·125	5·00	0·263	10·52	40	0·99	US	8·5	—	Divergent. Reached 6-deg amplitude at end of run.
0·108	4·35	0·228	9·16	40	0·92	US	7·5	—	Oscillating, possibly building up to 4-deg amplitude at end of run.
0·092	3·65	0·193	7·69	40	0·84	S	6·8	—	—
0·100	3·00	0·210	6·31	30	0·75	S	7·3	—	—
0·083	2·50	0·176	5·26	30	0·68	S	6·3	—	—
0·117	3·50	0·246	7·36	30	0·82	S	6·8	—	—
0·133	4·00	0·281	8·41	30	0·88	US	7·0	—	Oscillation building up. 5-deg amplitude at end of run.

TABLE 121

Comparison of Main Afterbody-Length Effects

Case	Load coefficient $C_{\Delta 0}$	Basic length beam ratio L/b	Forebody length (beams)	Afterbody-length increase (beams)	Reduction in maximum lower critical trim (deg)	Lowering of upper stability limit (deg)	Reduction in hump trim (deg)	Remarks
Ref. 11 ..	5·88	15	8·6	6·4 to 9·25	1½	1	2	With slipstream
Present tests* ..	2·25	11	6·0	same percentage increase	2	1½	2	No slipstream, but with full span leading-edge slats
Ref. 12 ..	0·87	6·4	3·7	2·11 to 3·11	2	1½	—	No slipstream, but with full-span leading-edge slats
Present tests* ..	2·25	11	6·0	same percentage increase	2	2	—	
Ref 13 ..	0·89	6·2	3·45	2·25 to 3·25	2½	1½	2	Aerodynamic forces and moments fed in synthetically
Present tests* ..	2·25	11	6·0	same percentage increase	2	1½	3	No slipstream, but with full-span leading-edge slats

* ' Present tests ' refers here to the undisturbed case. The lower loading, $C_{\Delta 0} = 2 \cdot 25$, was used for comparison as the limits concerned are all of the same form, *i.e.*, there is no vertical band of instability right across the diagram, and the loading in general has only small effect on the changes due to afterbody length. The ' same percentage increase ' is based on forebody length.

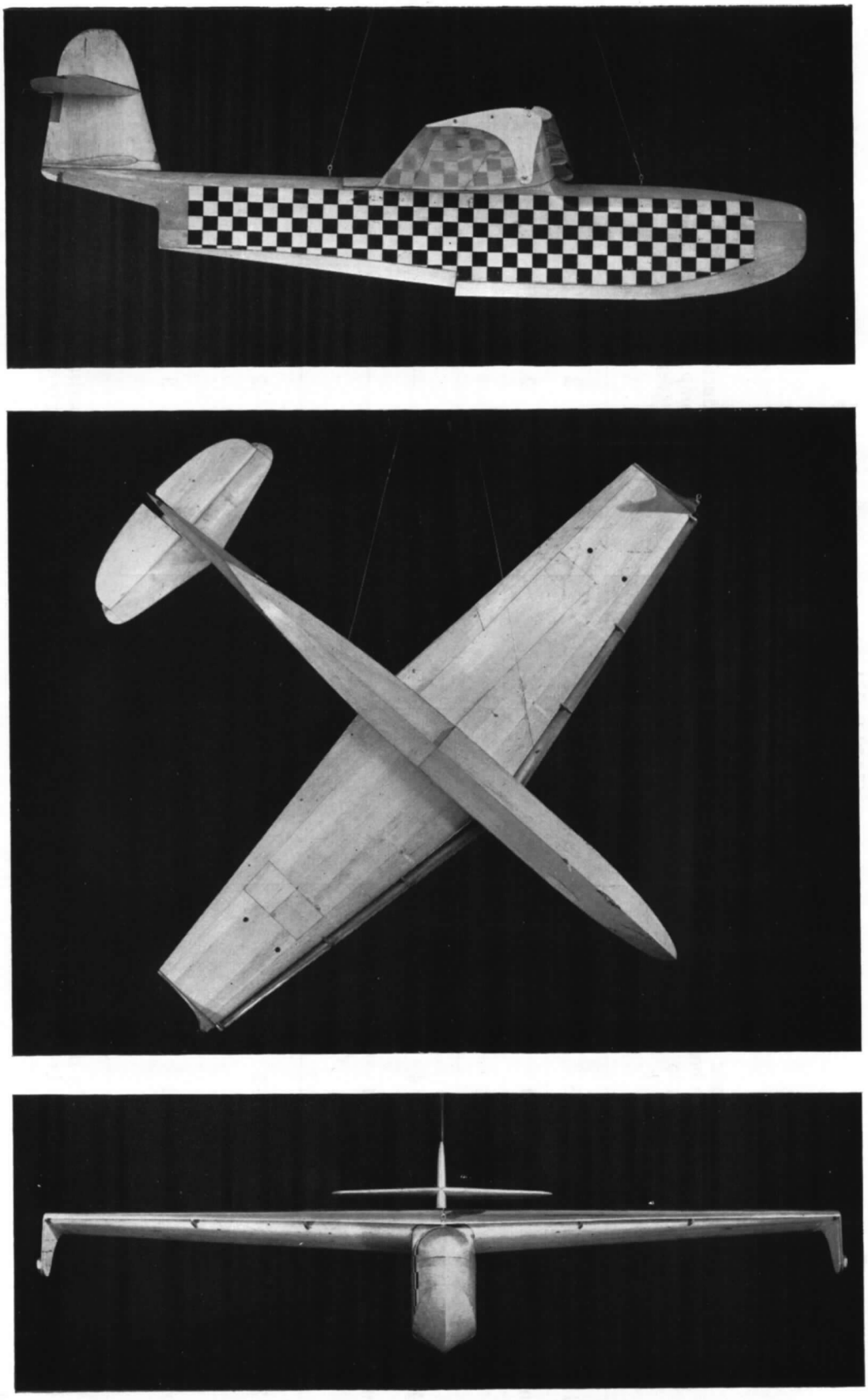

FIG. 1. Photographs of basic model (Model A).

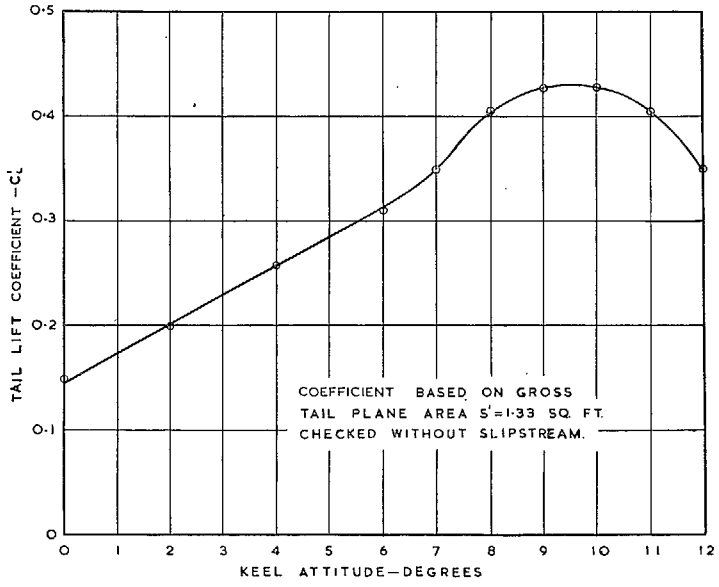

FIG. 2. Tailplane lift curve.

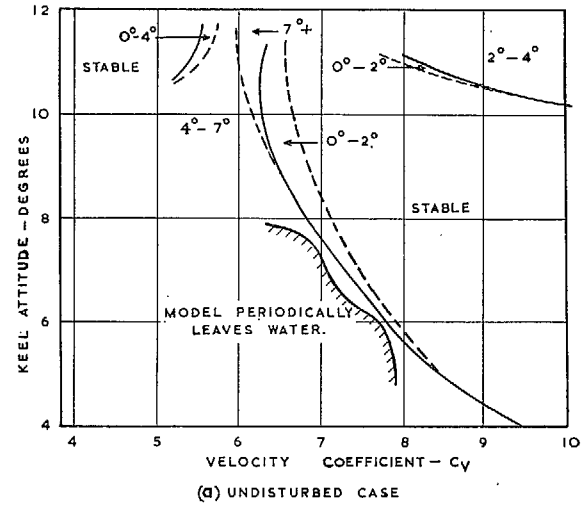

FIGURES INDICATE
AMPLITUDES OF
PORPOISING IN DEGREES

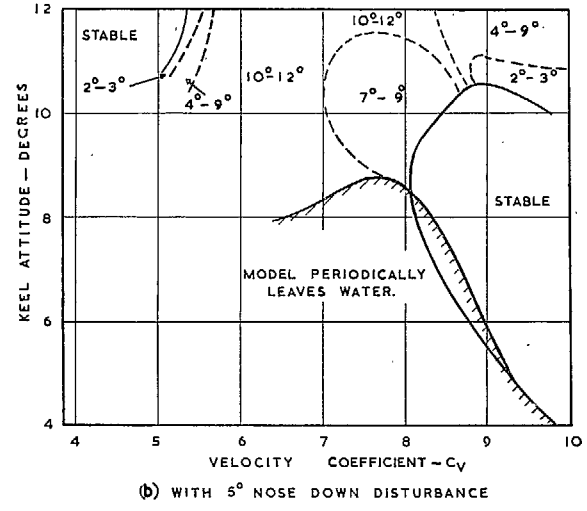

FIGS. 4a and 4b. Division of unstable region into regions of equal steady oscillations.

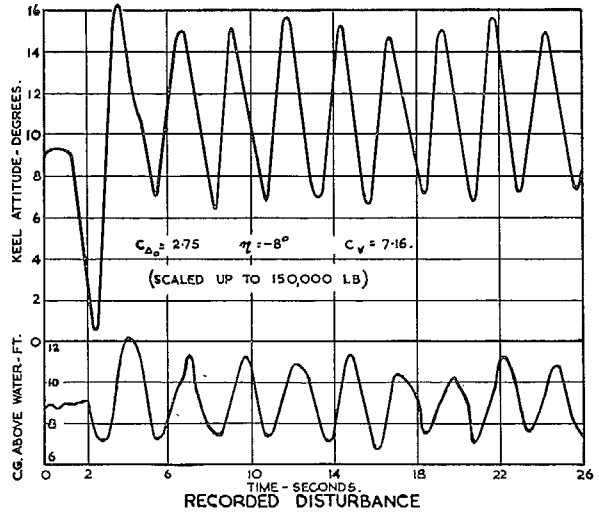

FIG. 3. Recording of disturbance.

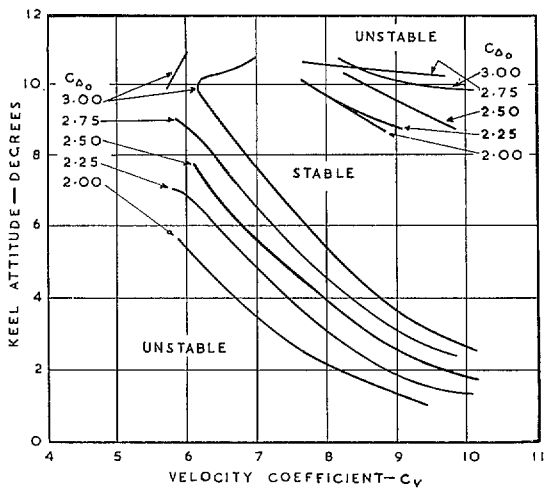

(a) ON A NON-DIMENSIONAL SPEED BASE

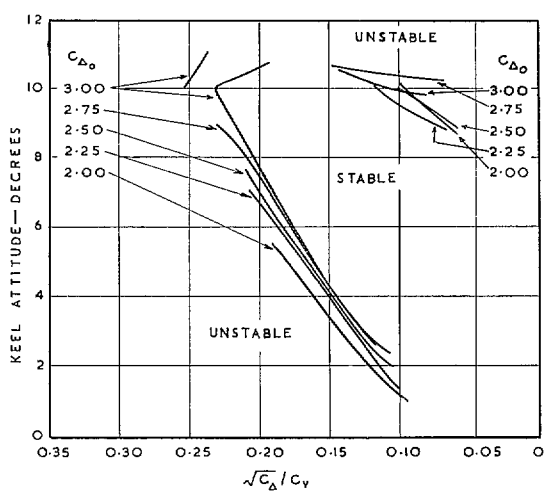

(b) ON A NON DIMENSIONAL $\sqrt{C_\Delta}/C_V$ BASE

FIGS. 5a and 5b. Longitudinal stability limits at different weights.

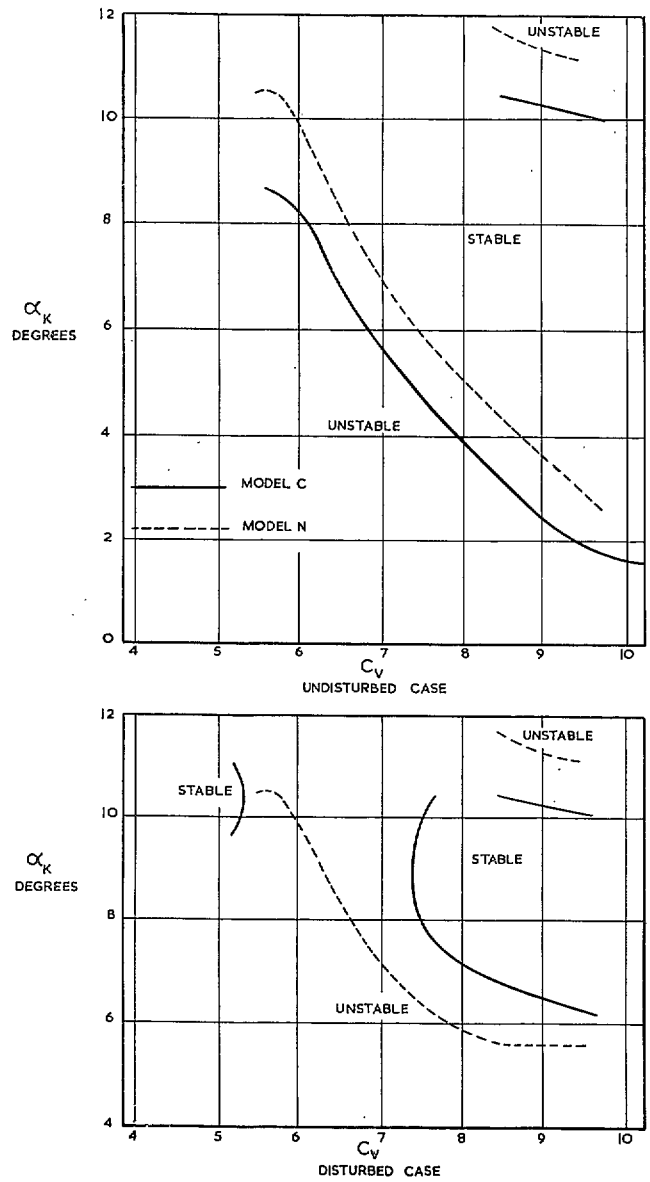

FIG. 6. Comparison of longitudinal stability limits for Models C and N.

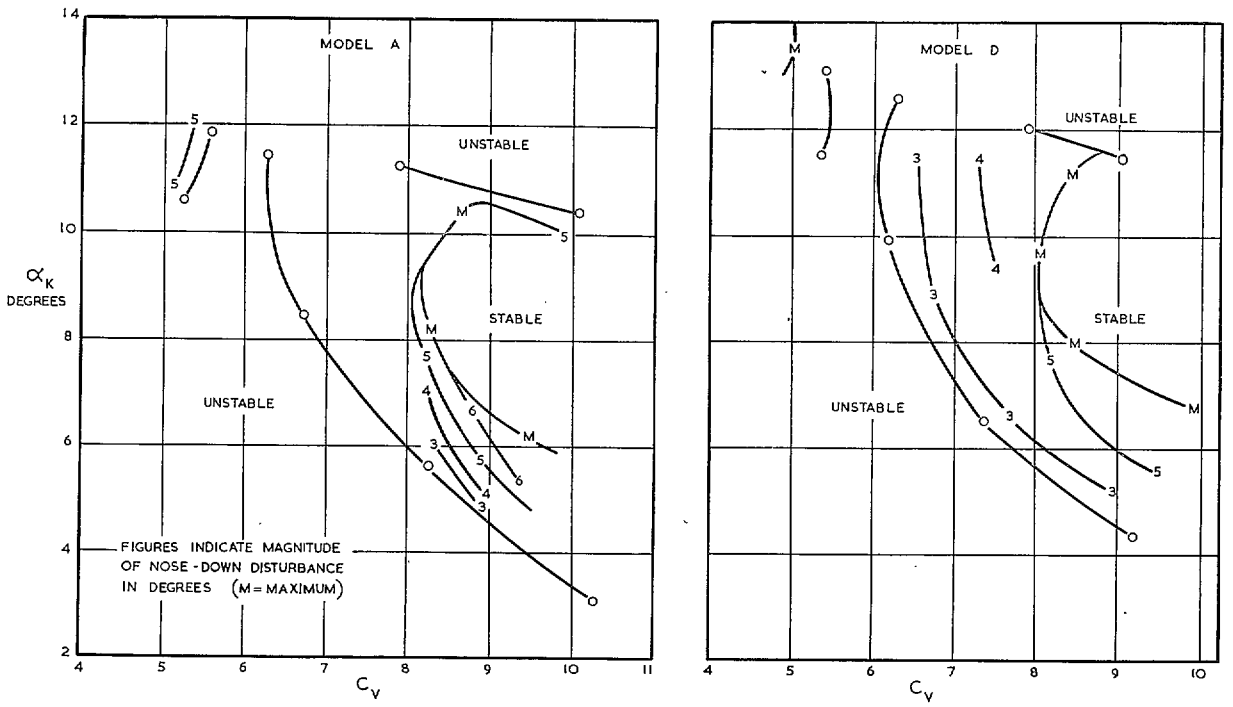

FIG. 7. Longitudinal stability limits for various degrees of disturbance.

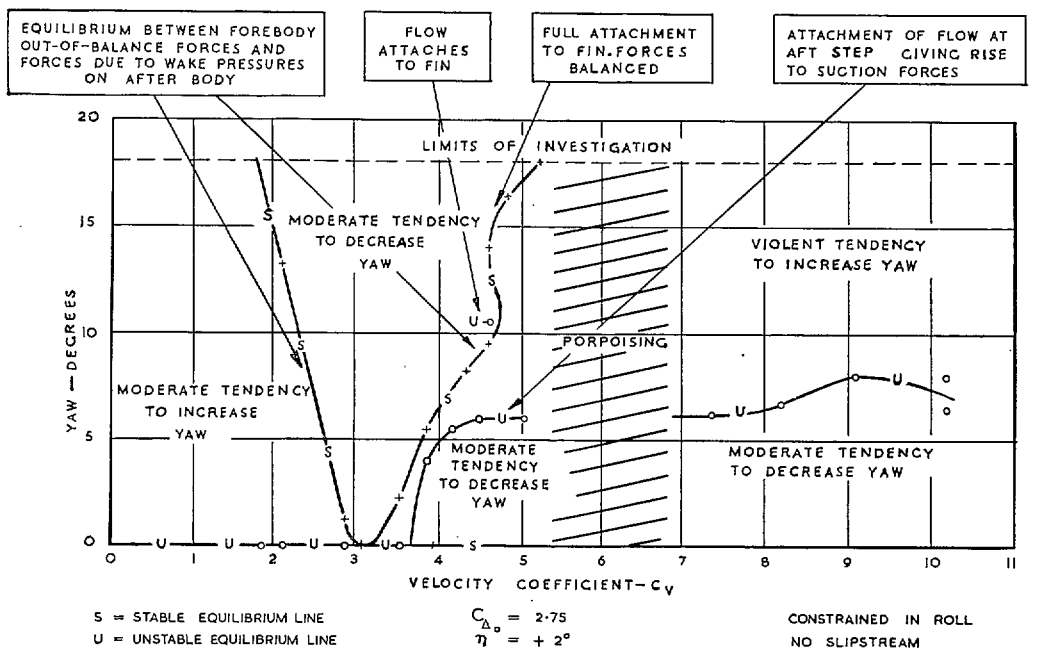

FIG. 8. Typical directional-stability diagram.

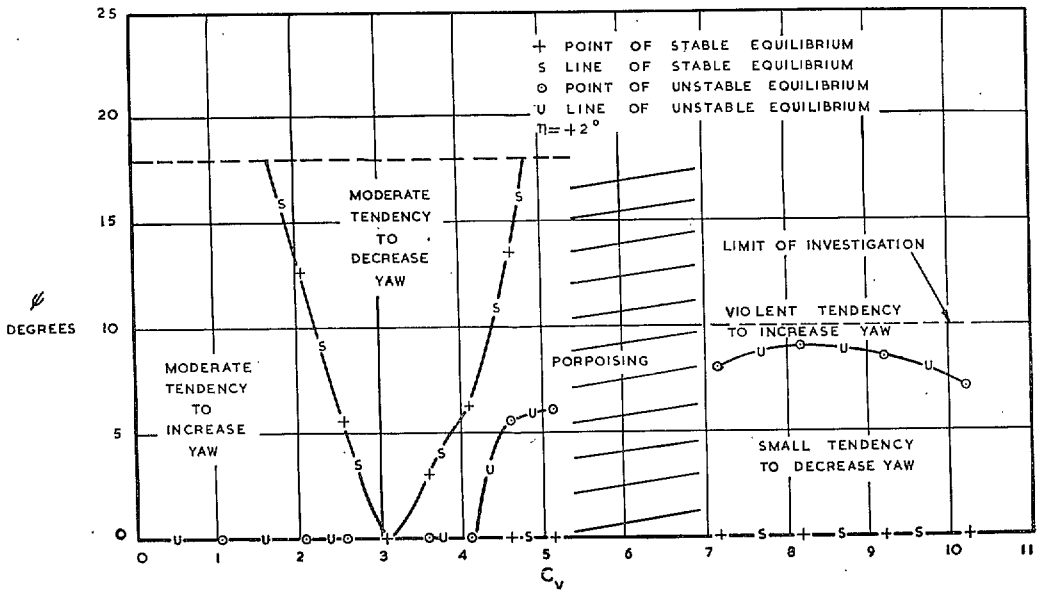

FIG. 9. Model A directional stability without roll constraint at low attitudes.

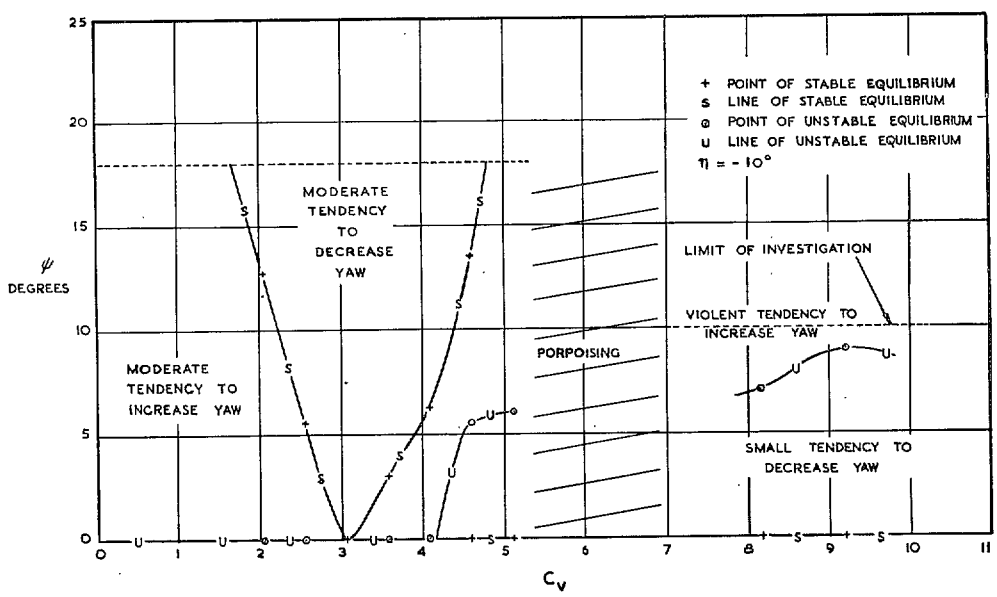

FIG. 10. Model A directional stability without roll constraint at high attitudes.

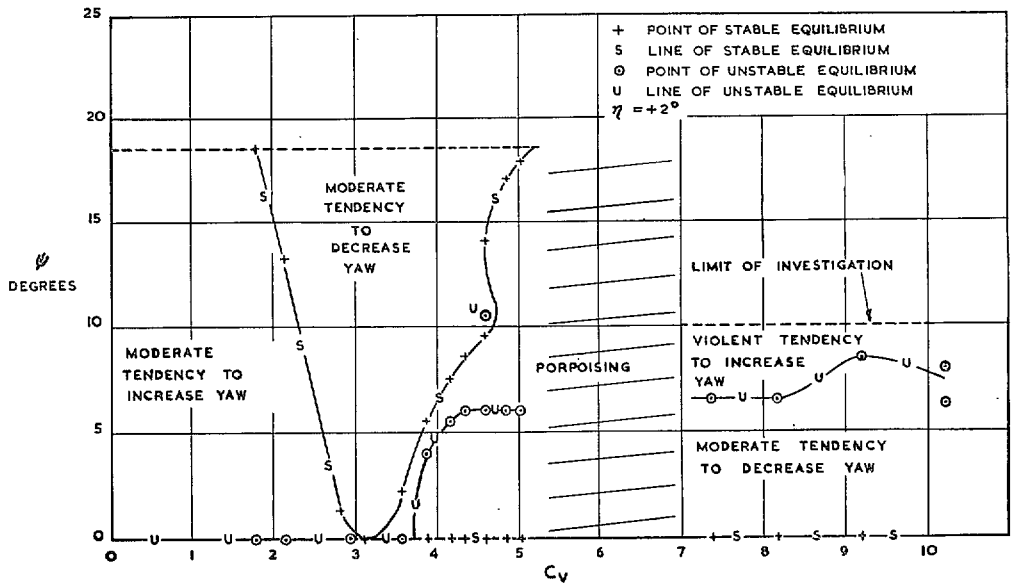

FIG. 11. Model A directional stability with roll constraint at low attitudes.

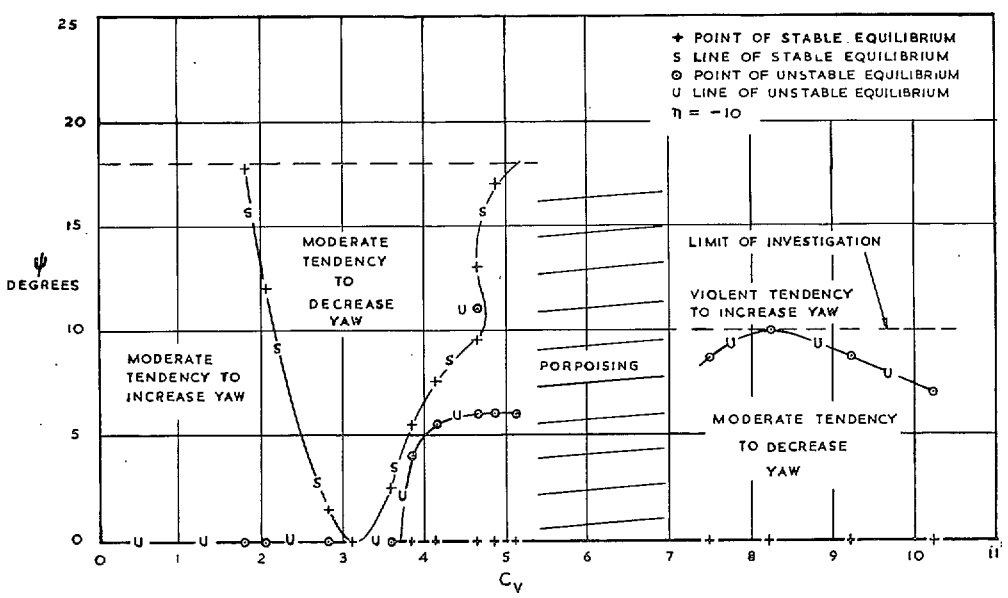

FIG. 12. Model A directional stability with roll constraint at high attitudes.

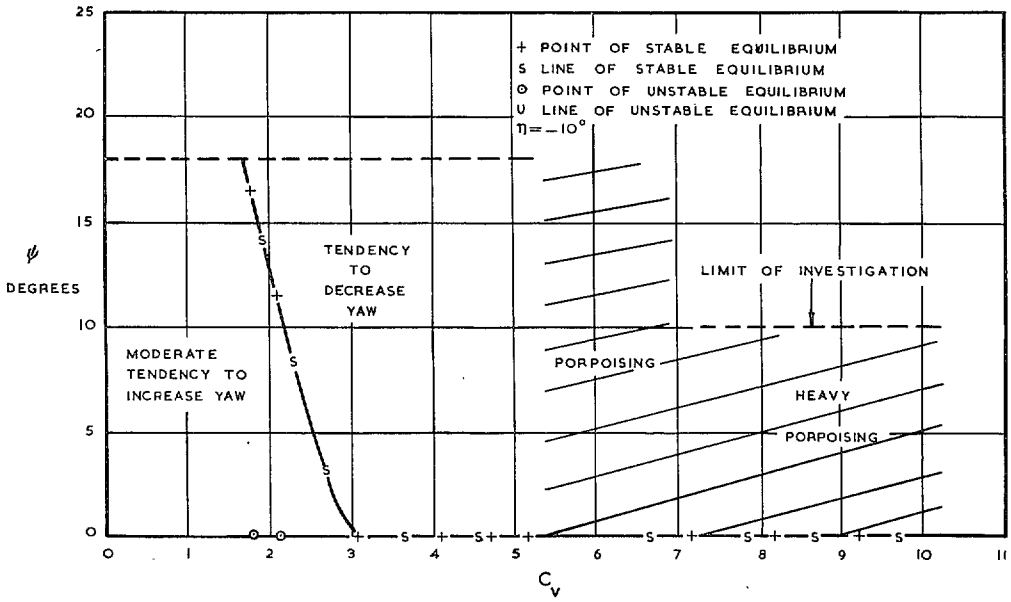

FIG. 13. Model A directional stability with roll constraint with breaker strips.

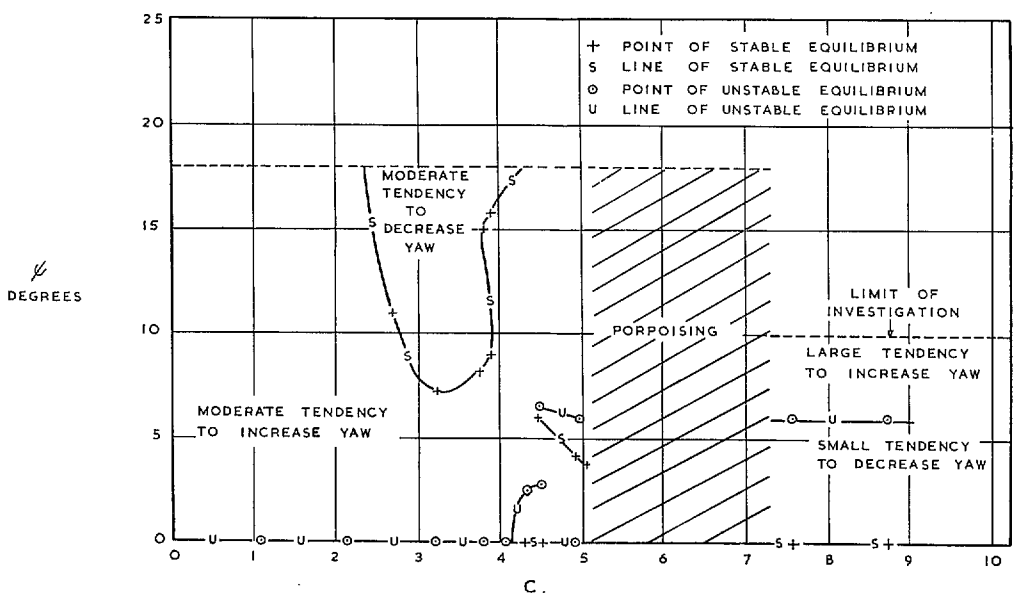

FIG. 14. Model C directional stability at low loading.

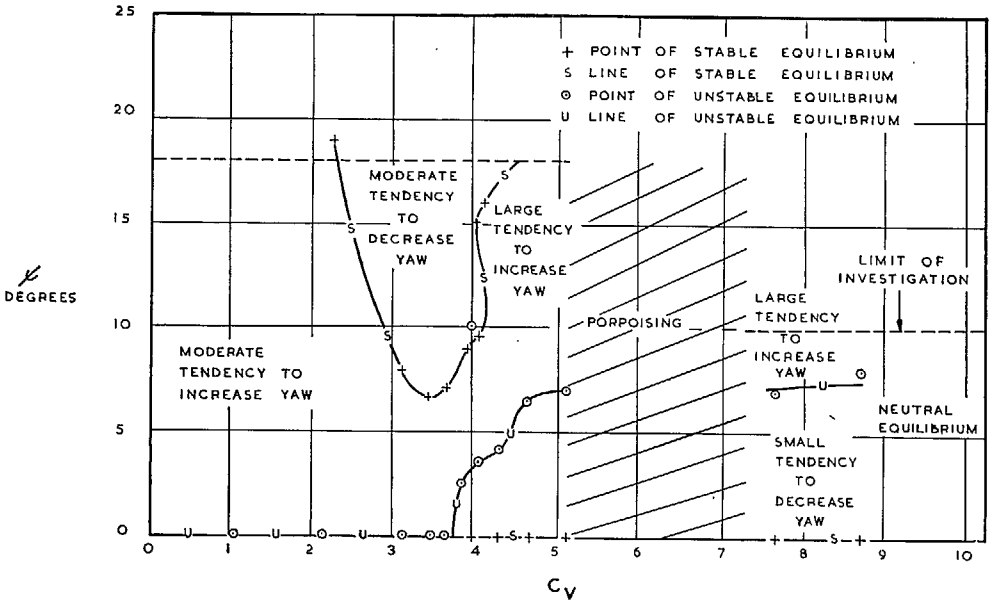

FIG. 15. Model C directional stability at high loading.

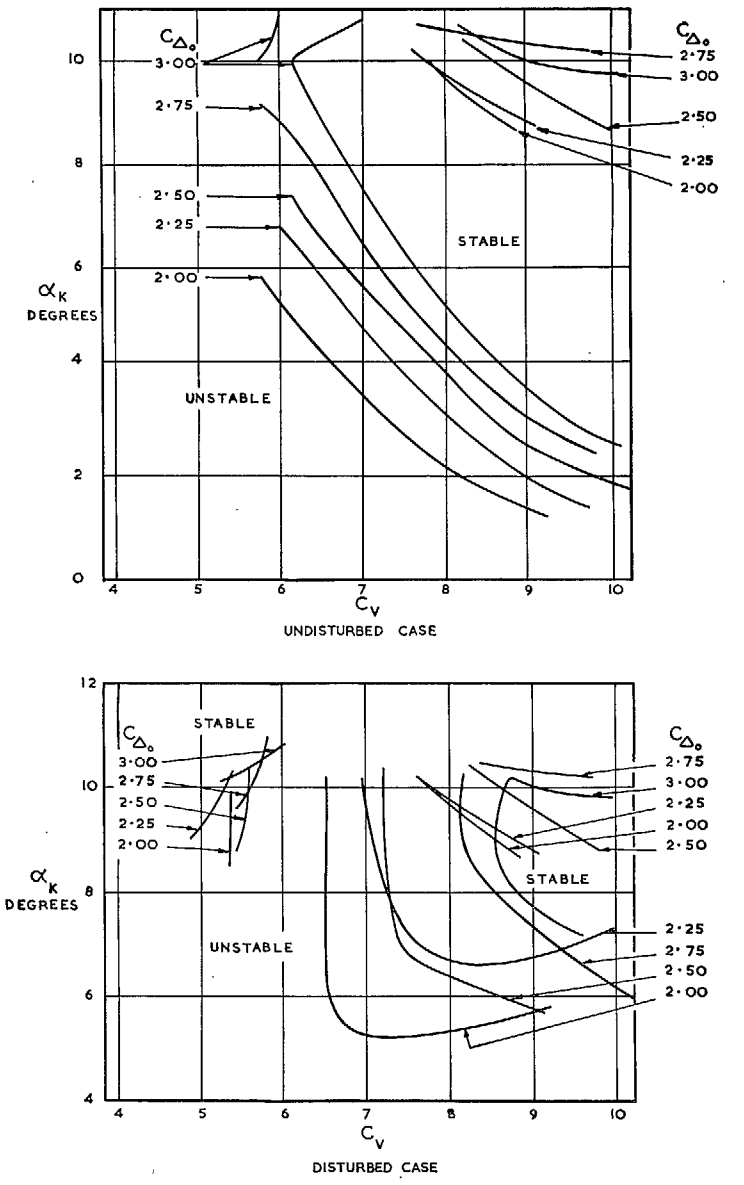

FIG. 16. Effect of load on longitudinal stability limits.

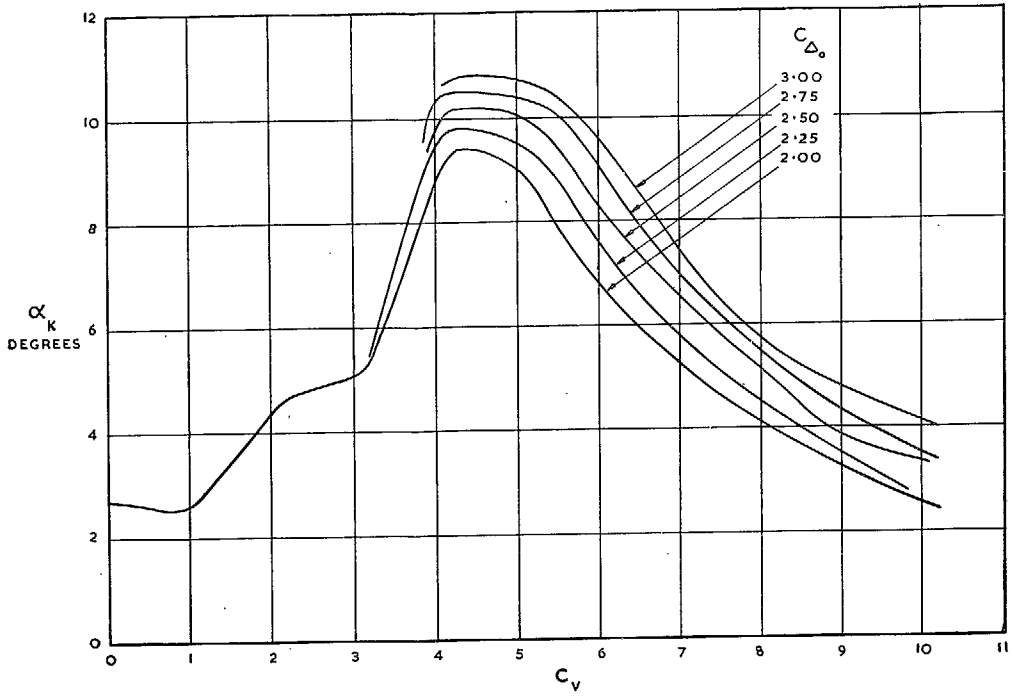

FIG. 17. Effect of load on trim curves ($\eta = 0$ deg.).

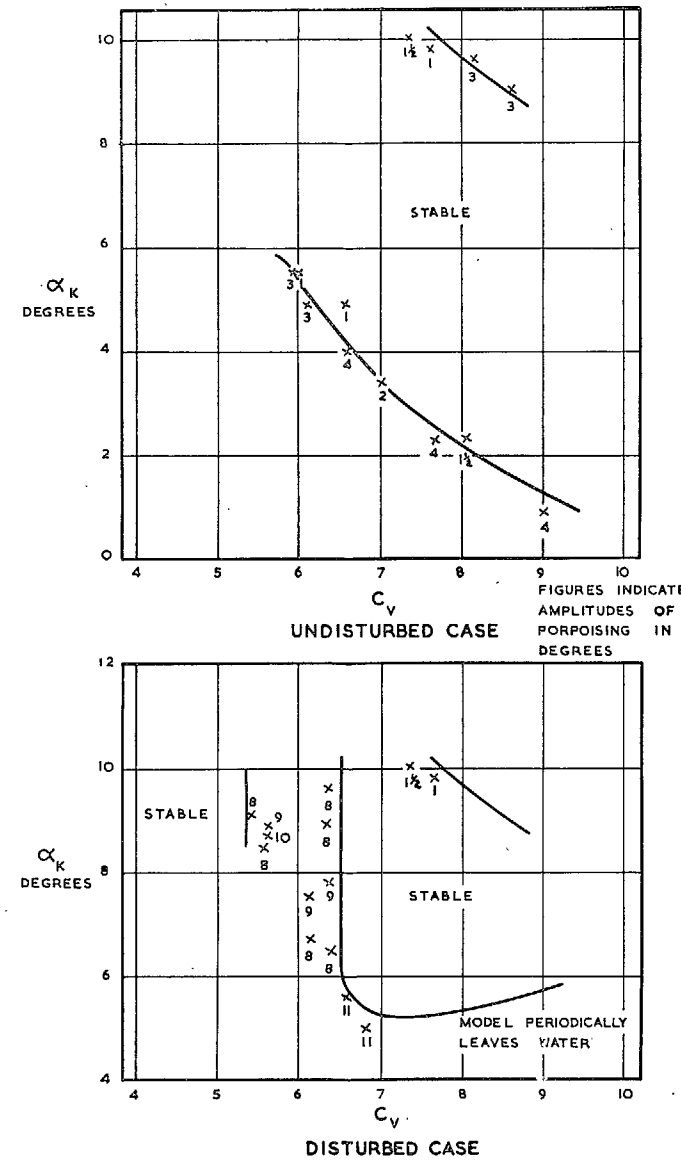

FIG. 18 (1). Effect of load on amplitudes of porpoising ($C_{\Delta 0} = 2{\cdot}00$).

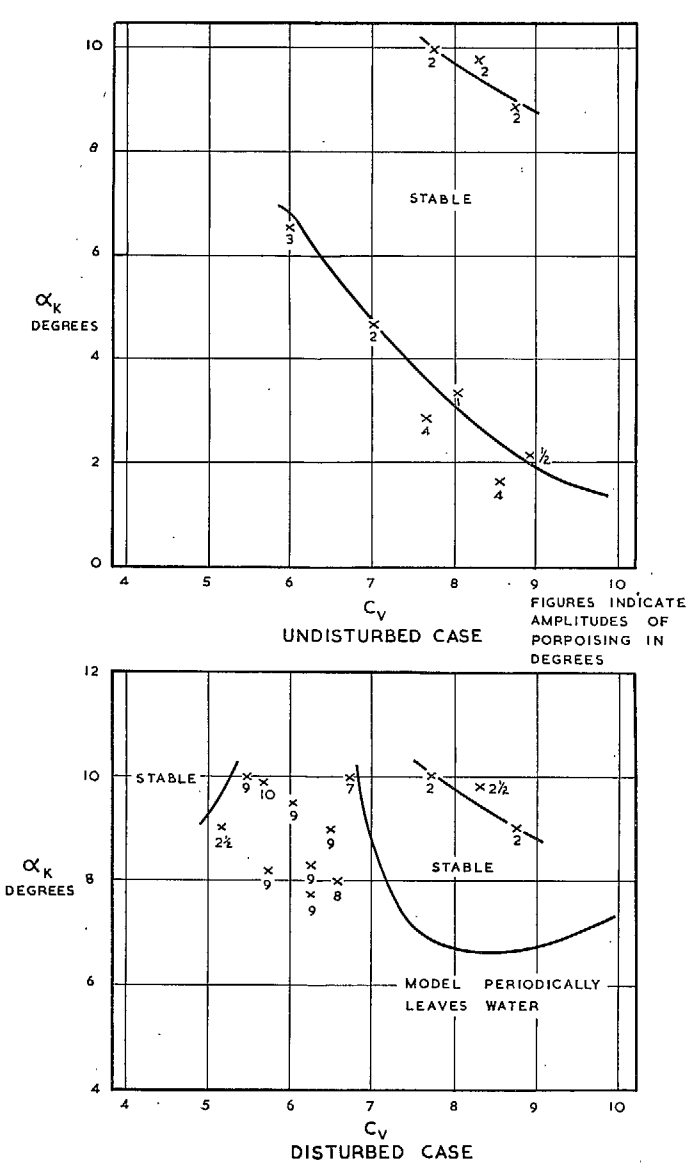

FIG. 18 (2). Effect of load on amplitudes of porpoising ($C_{\Delta 0} = 2{\cdot}25$).

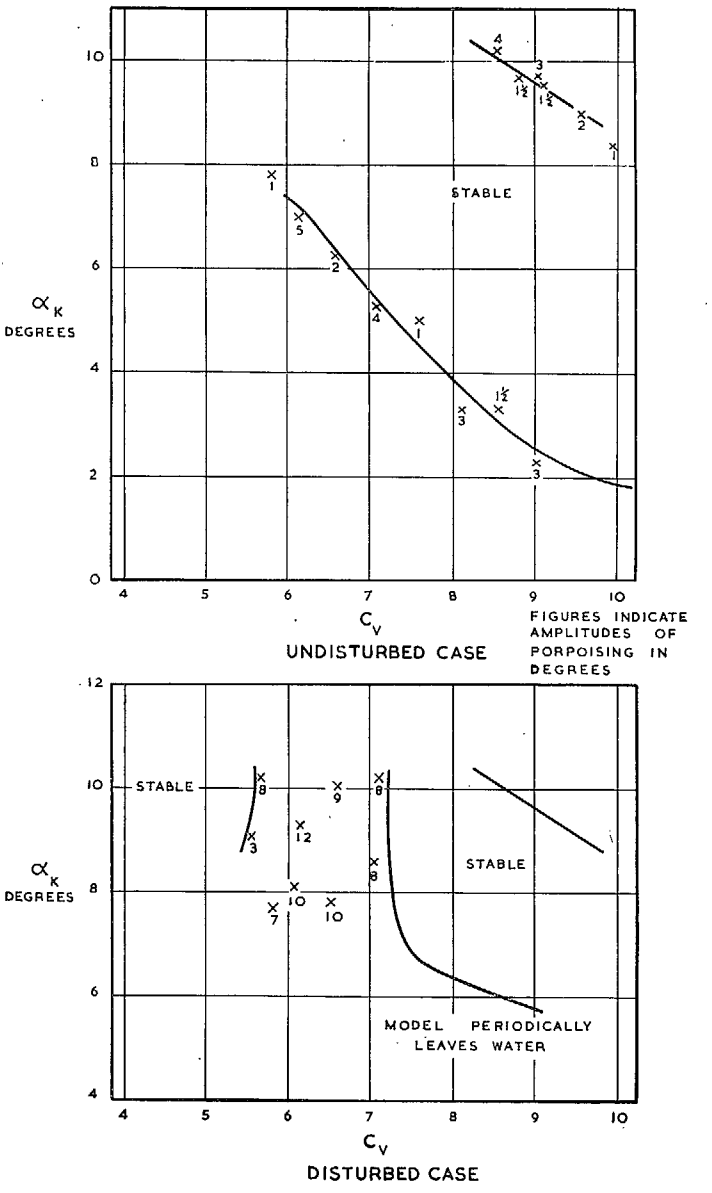

FIG. 18 (3). Effect of load on amplitudes of porpoising ($C_{\Delta 0} = 2{\cdot}50$).

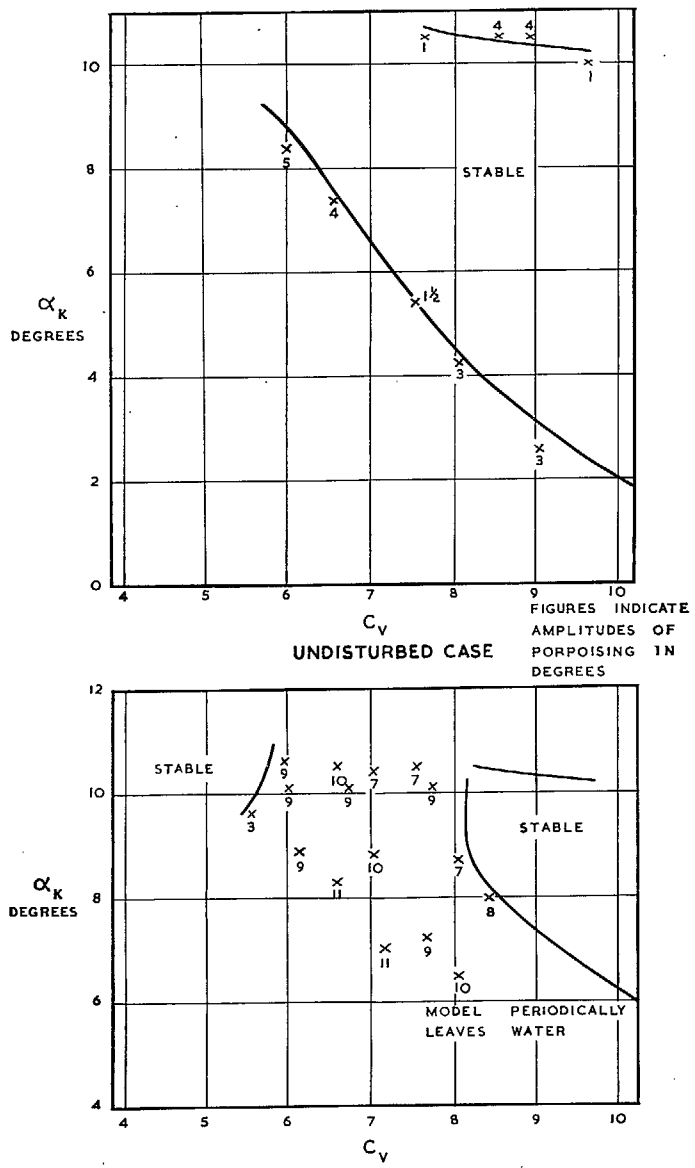

FIG. 18 (4). Effect of load on amplitudes of porpoising ($C_{\Delta 0} = 2{\cdot}75$).

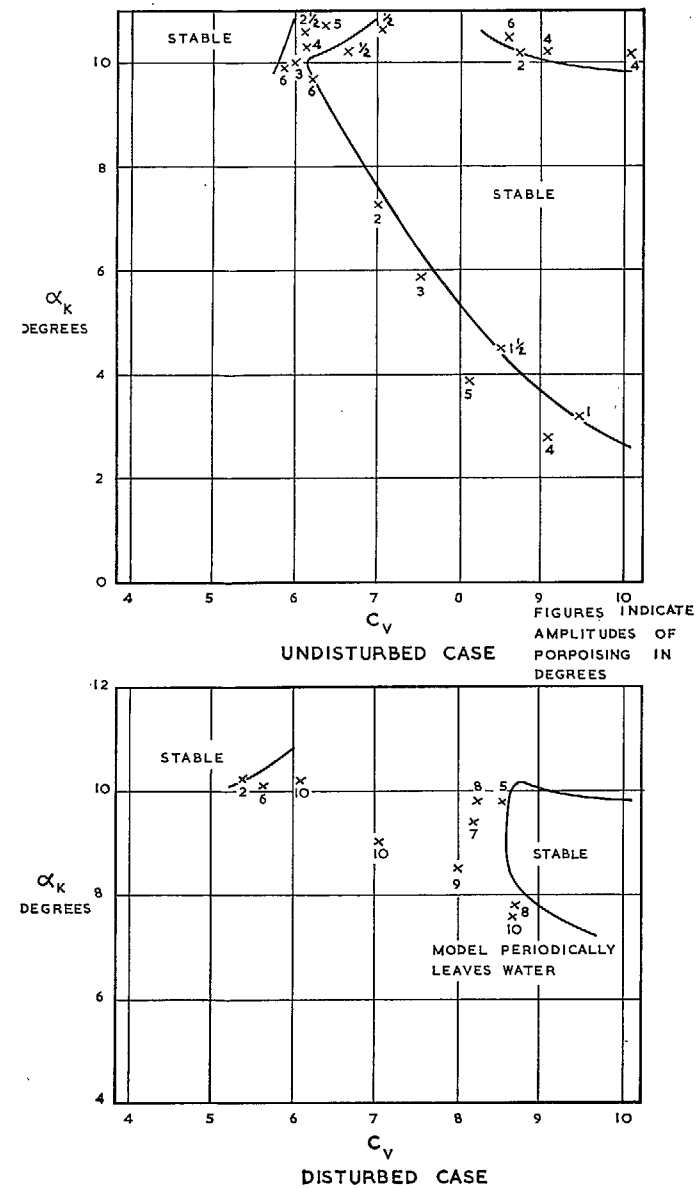

FIG. 18 (5). Effect of load on amplitudes of porpoising ($C_{\Delta 0} = 3{\cdot}00$).

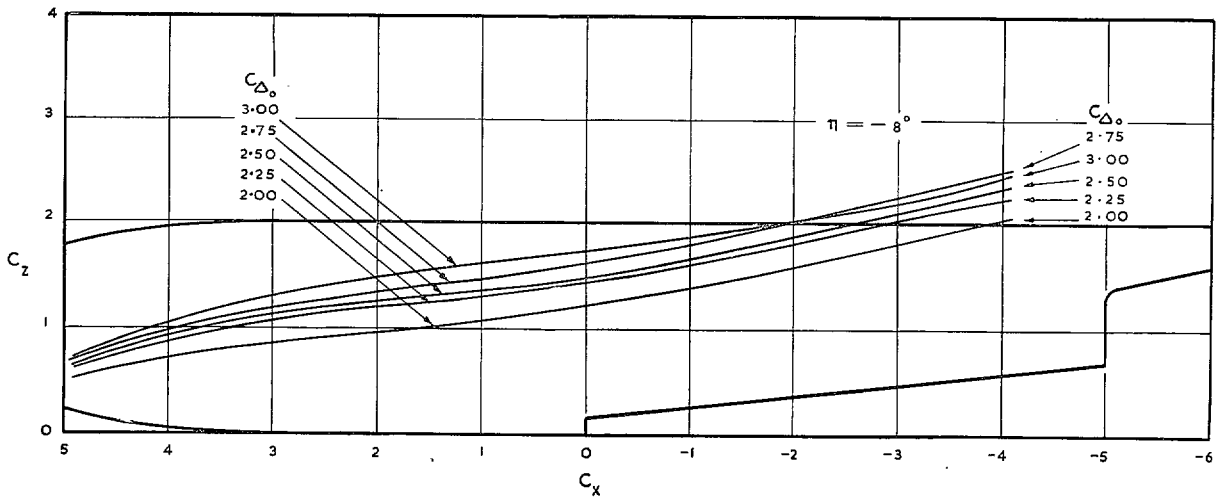

FIG. 19. Effect of load on spray projections.

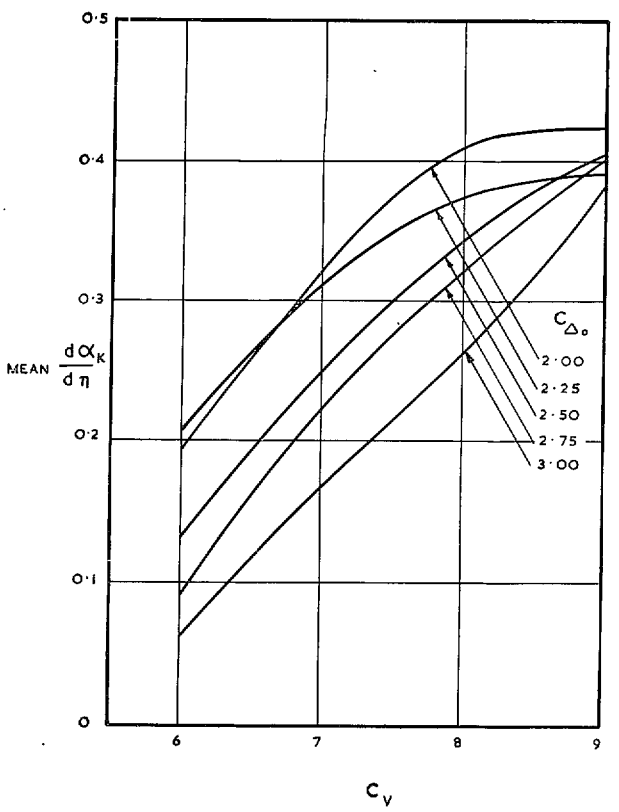

FIG. 20. Effect of load on elevator effectiveness.

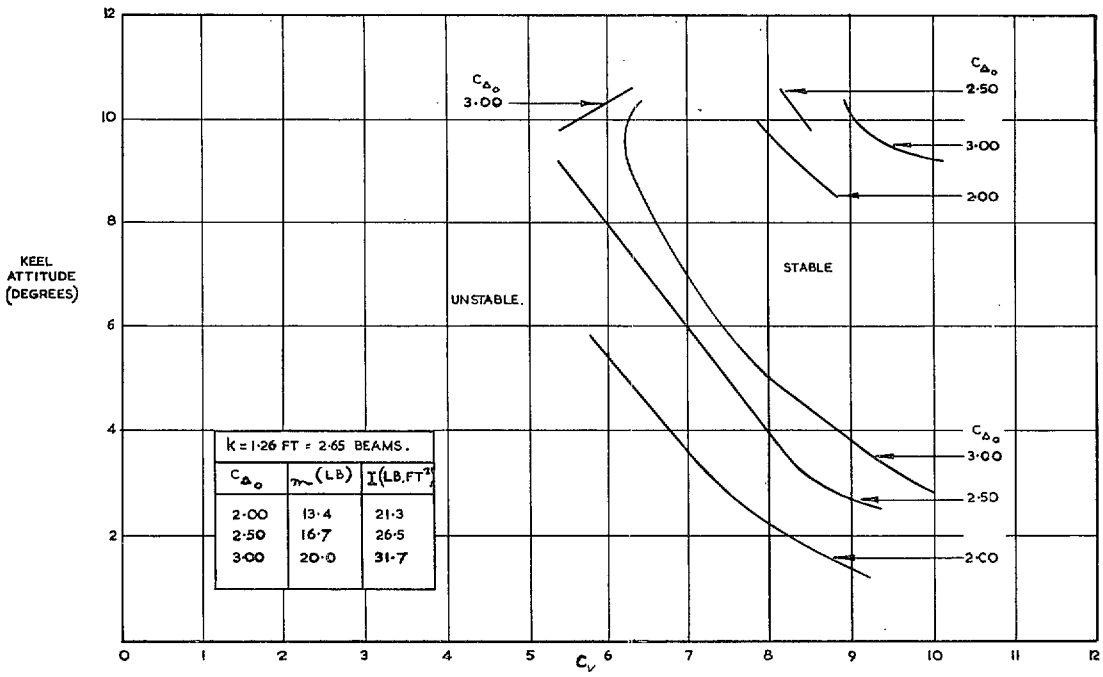

FIG. 25. Comparison of undisturbed longitudinal stability limits at constant radius of gyration.

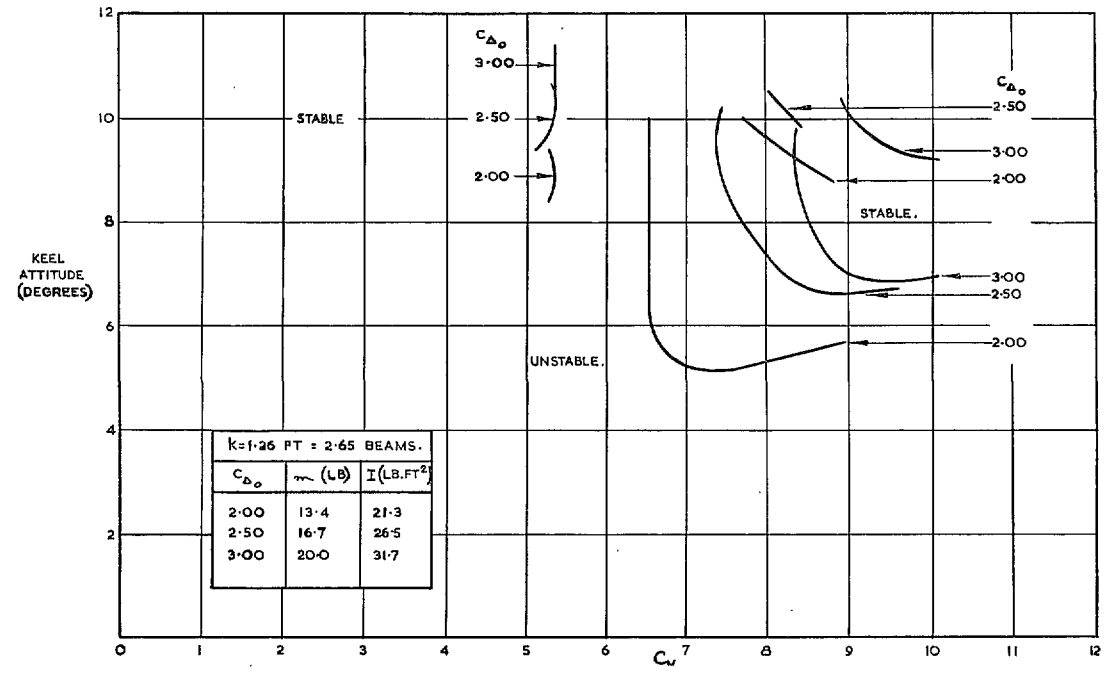

FIG. 26. Comparison of disturbed longitudinal stability limits at constant radius of gyration.

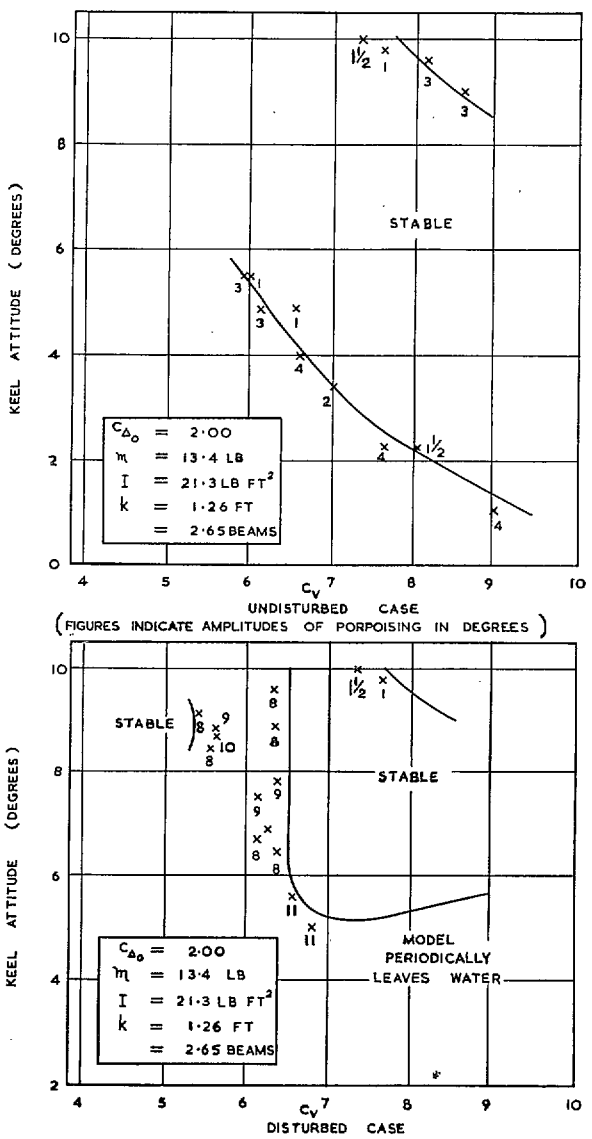

FIG. 27 (1). Porpoising amplitudes and longitudinal stability limits for moment-of-inertia investigation.

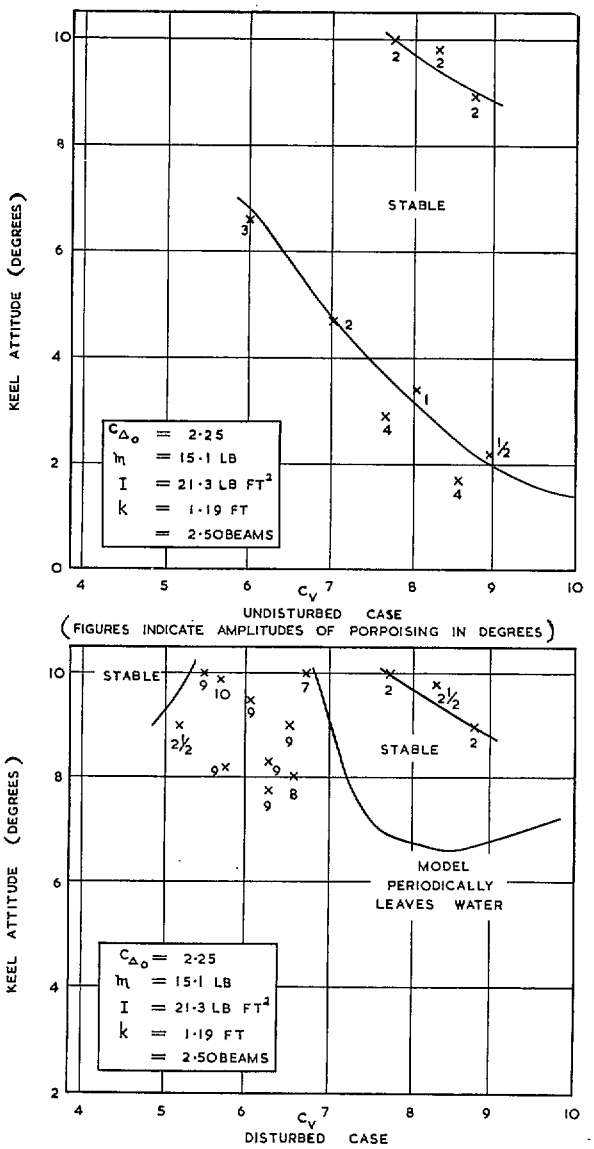

FIG. 27 (2). Porpoising amplitudes and longitudinal stability limits for moment-of-inertia investigation.

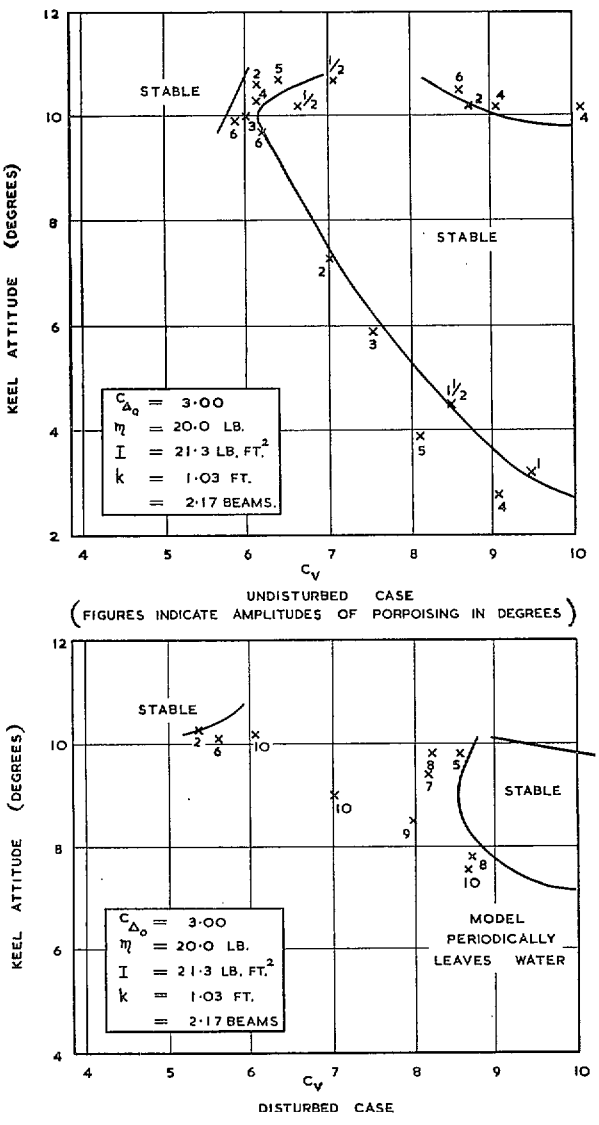

FIG. 27 (7). Porpoising amplitudes and longitudinal stability limits for moment-of-inertia investigation.

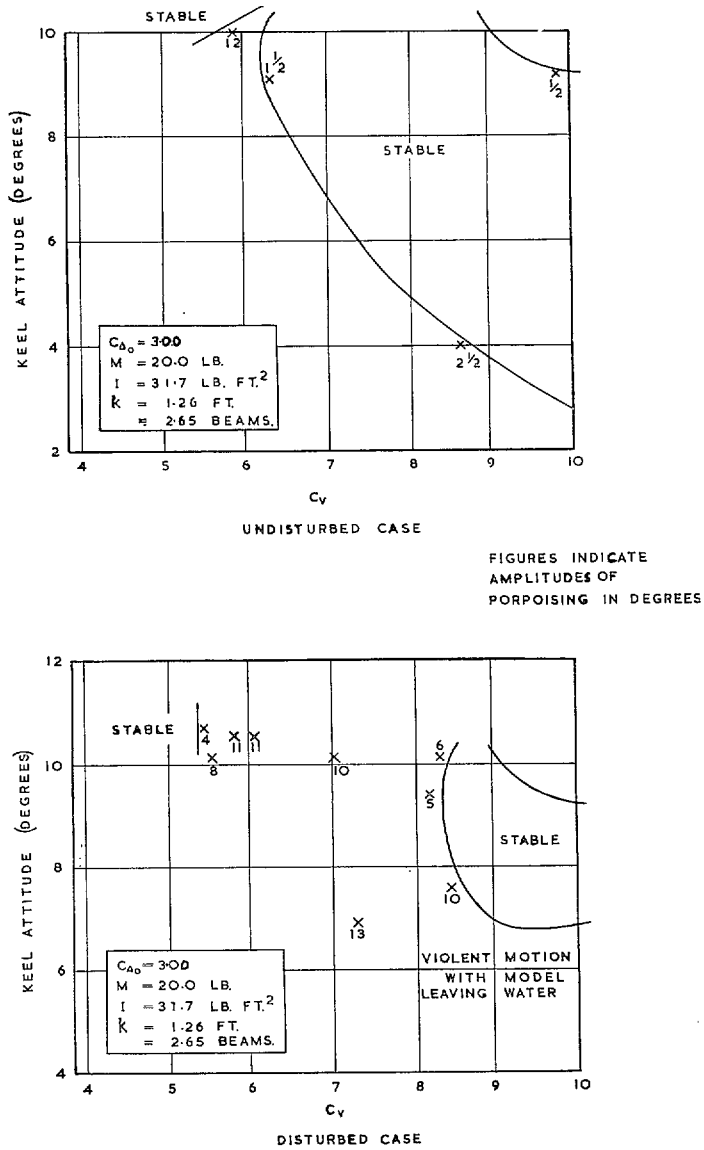

FIG. 27 (8). Porpoising amplitudes and longitudinal stability limits for moment-of-inertia investigation.

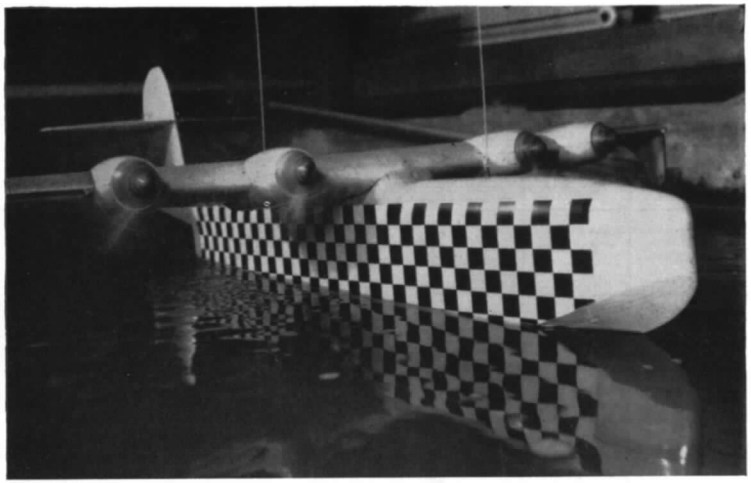

WITH TAKE-OFF POWER

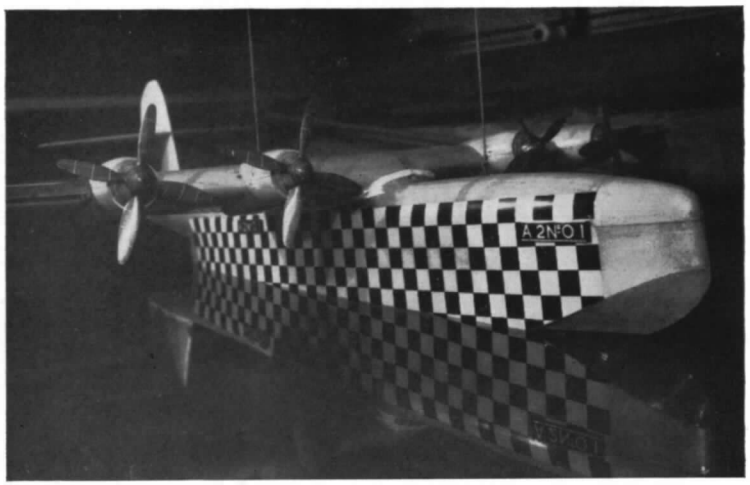

WITH PROPELLERS WINDMILLING

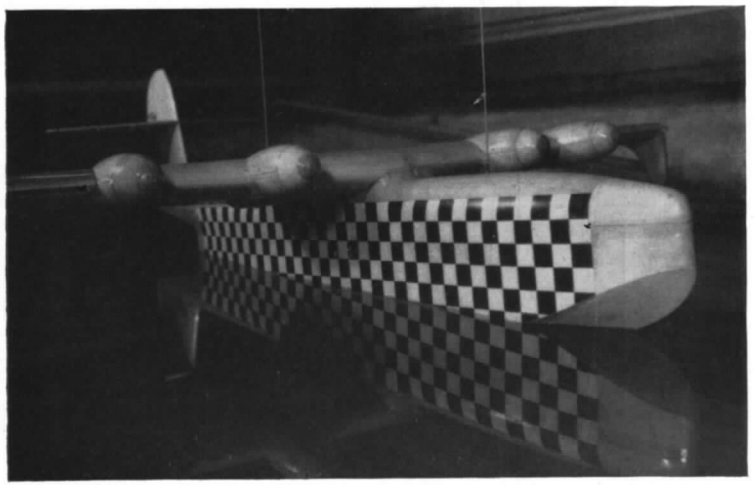

WITH FAIRINGS

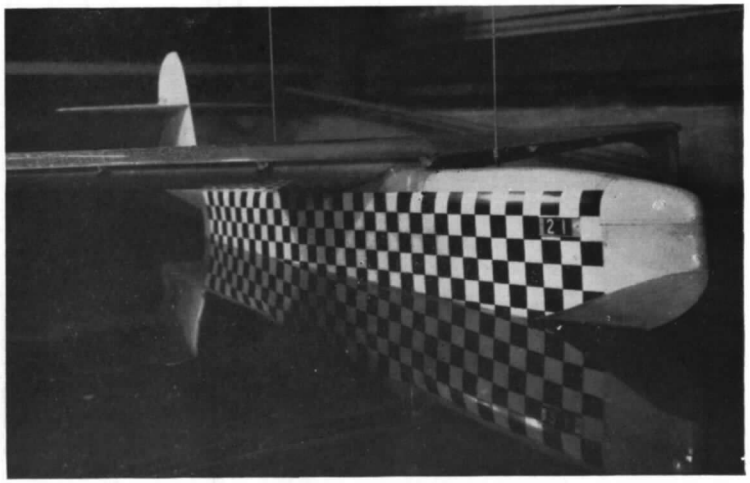

WITH FULL SPAN SLATS

FIG. 28. Photographs of slipstream test configurations.

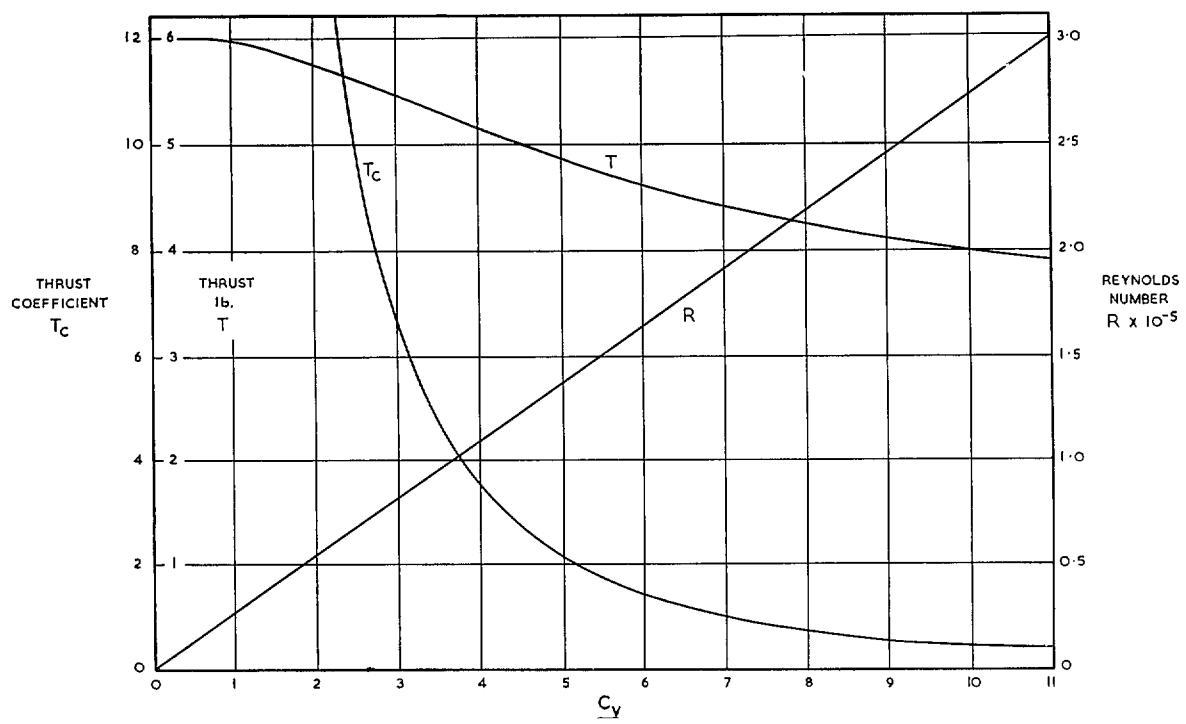

FIG. 29. Variation of thrust and Reynolds number with velocity coefficient.

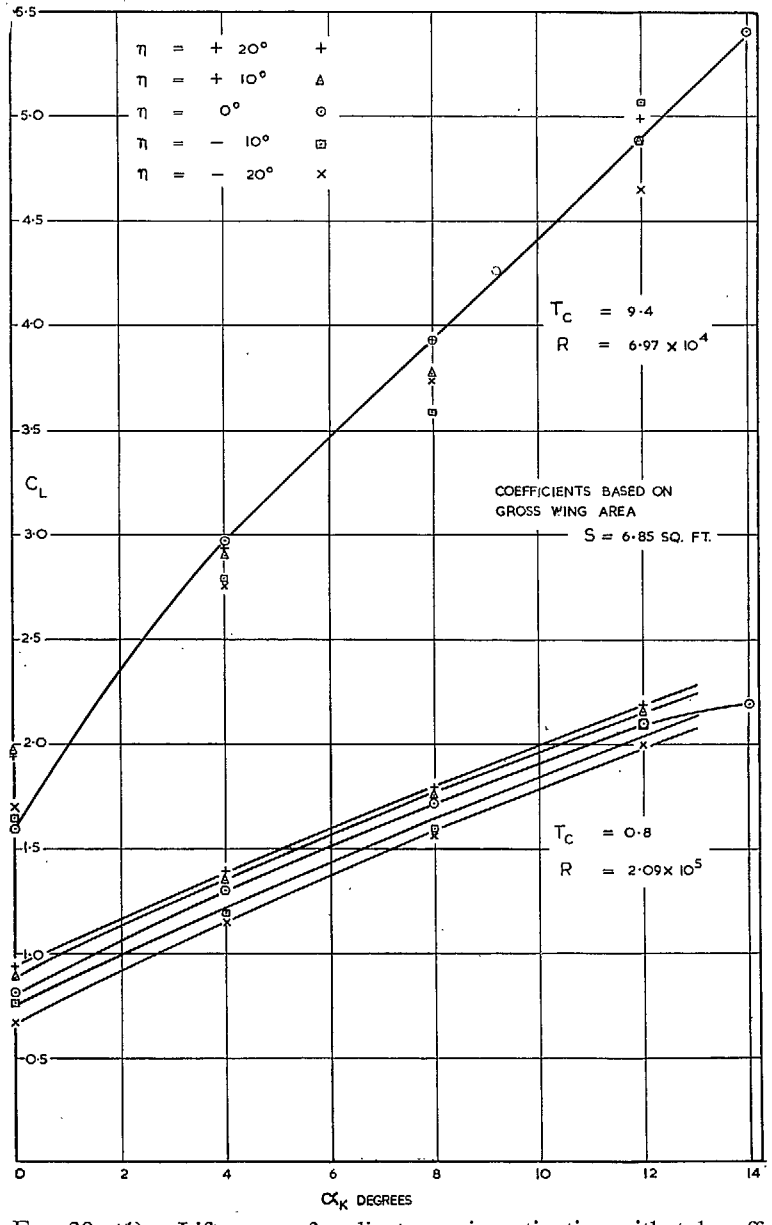

FIG. 30a (1). Lift curves for slipstream investigation with take-off power.

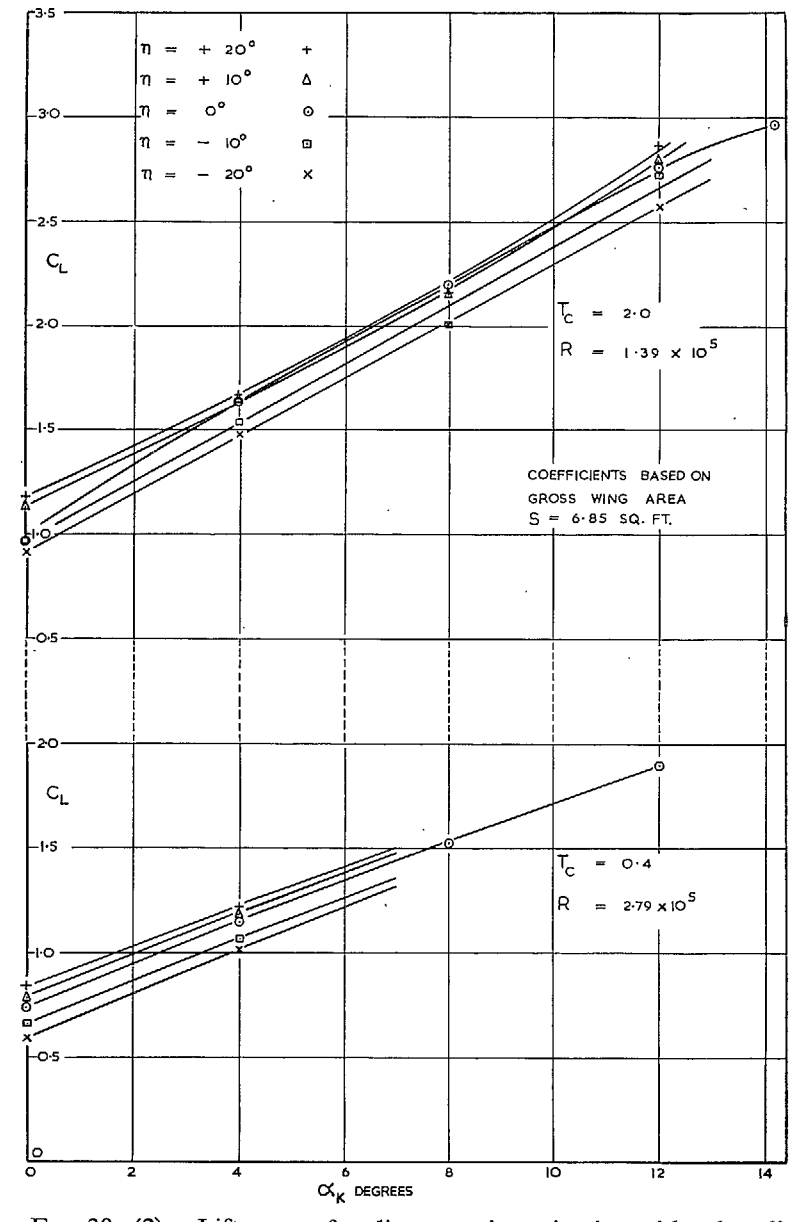

FIG. 30a (2). Lift curves for slipstream investigation with take-off power.

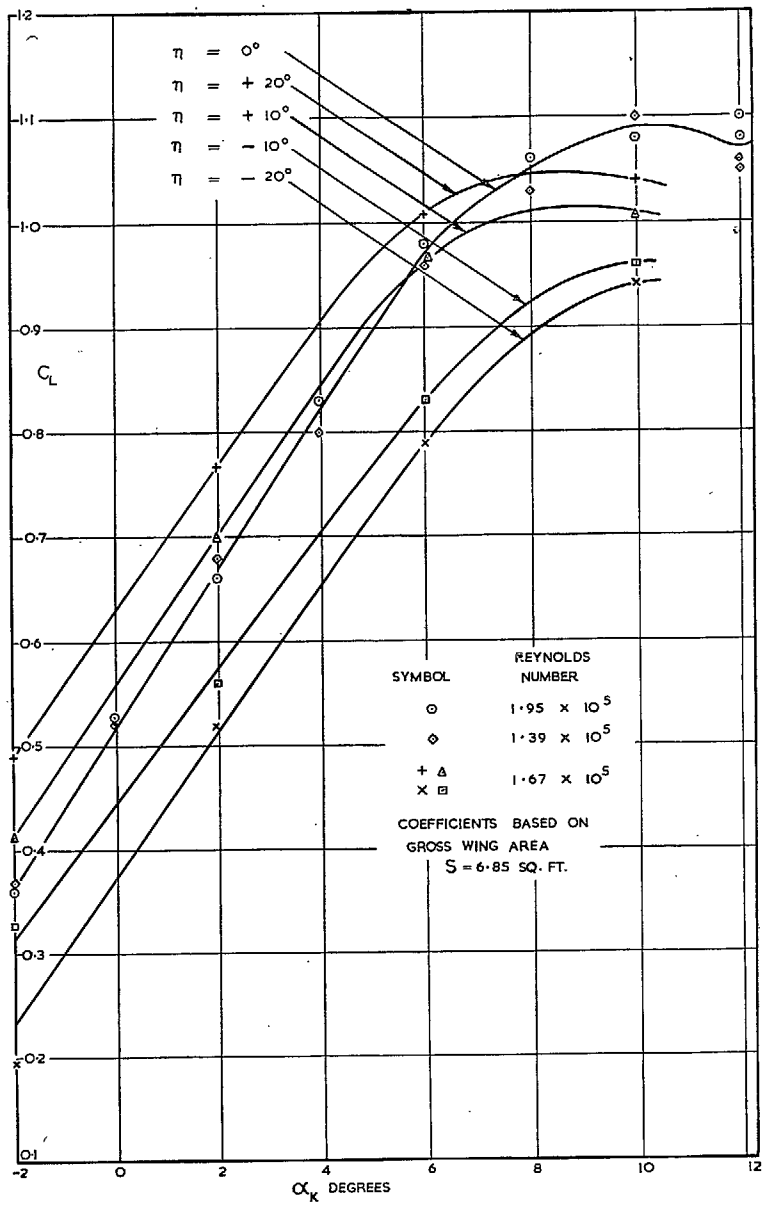

FIG. 30b. Lift curves for slipstream investigation with propellers windmilling.

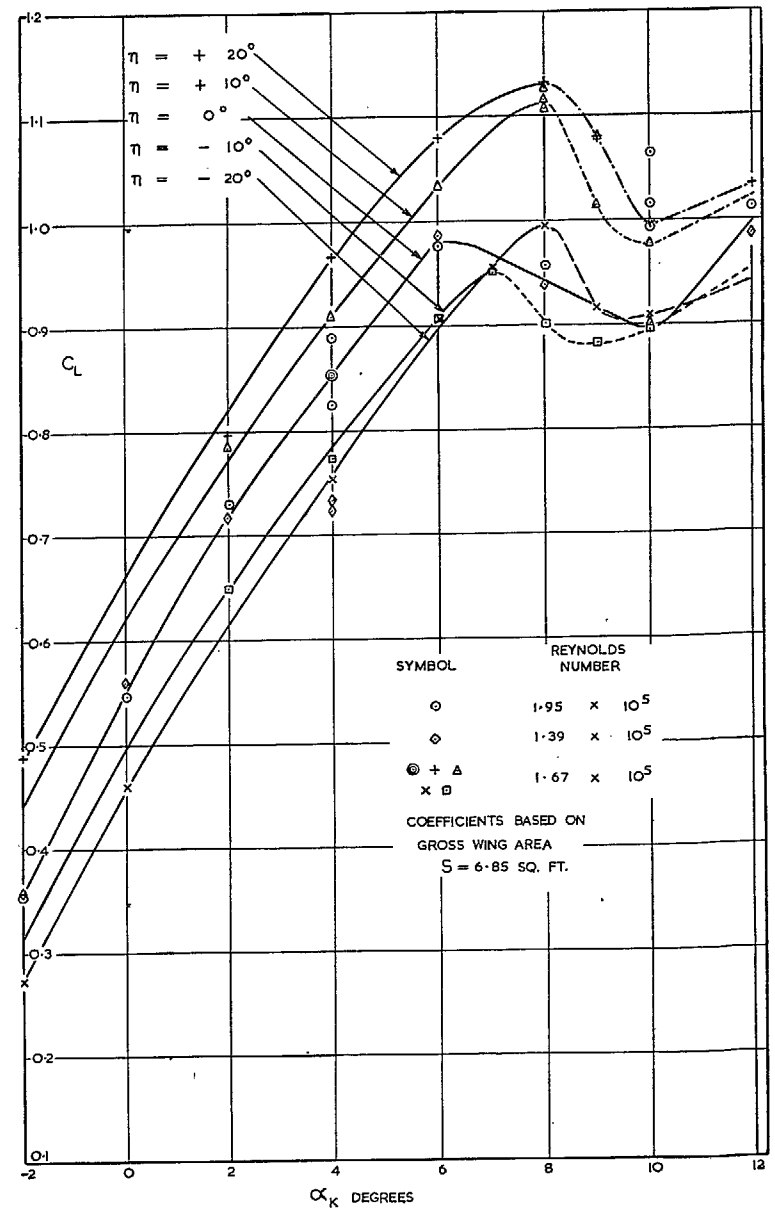

FIG. 30c. Lift curves for slipstream investigation with fairings.

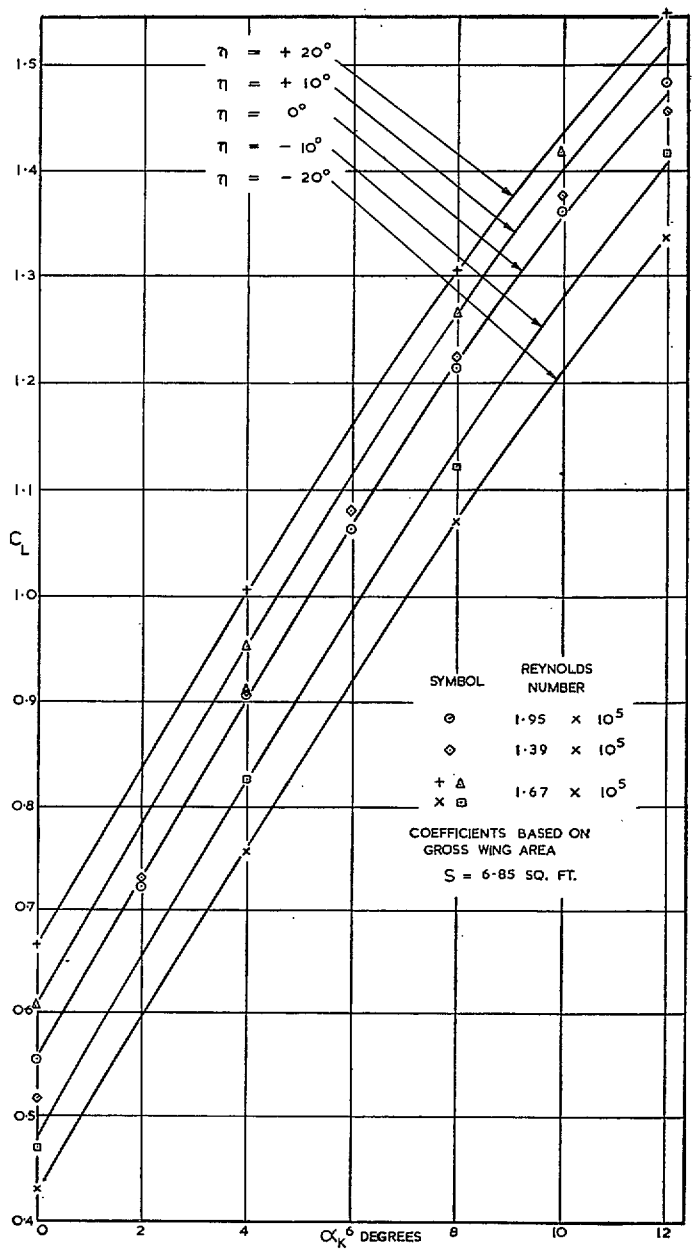

FIG. 30d. Lift curves for slipstream investigation with full-span slats.

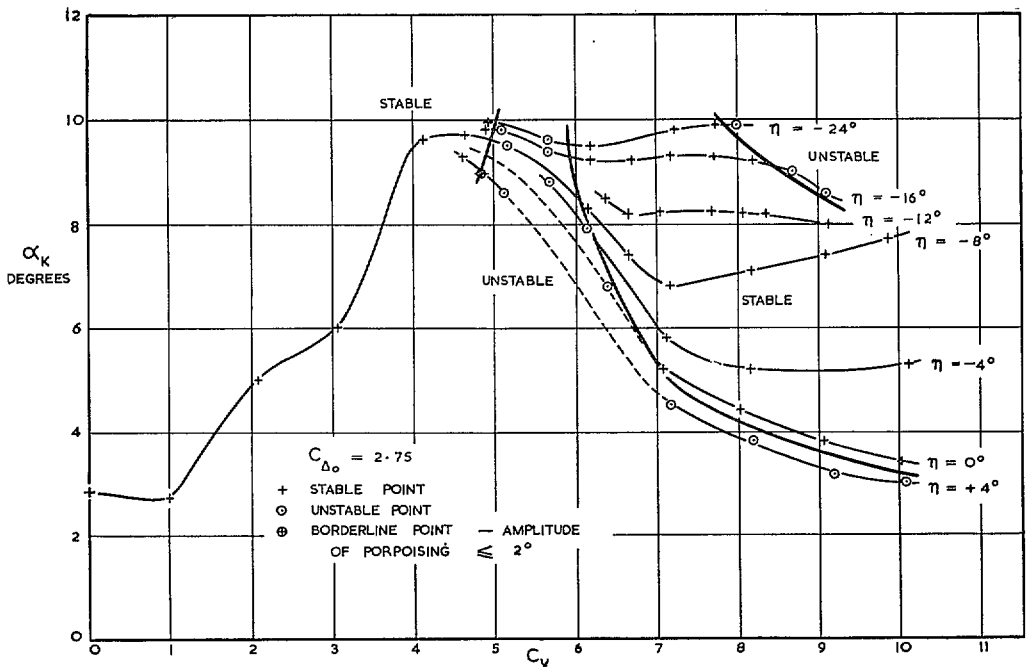

FIG. 31a. Longitudinal stability without disturbance for slipstream investigation with take-off power (Model A).

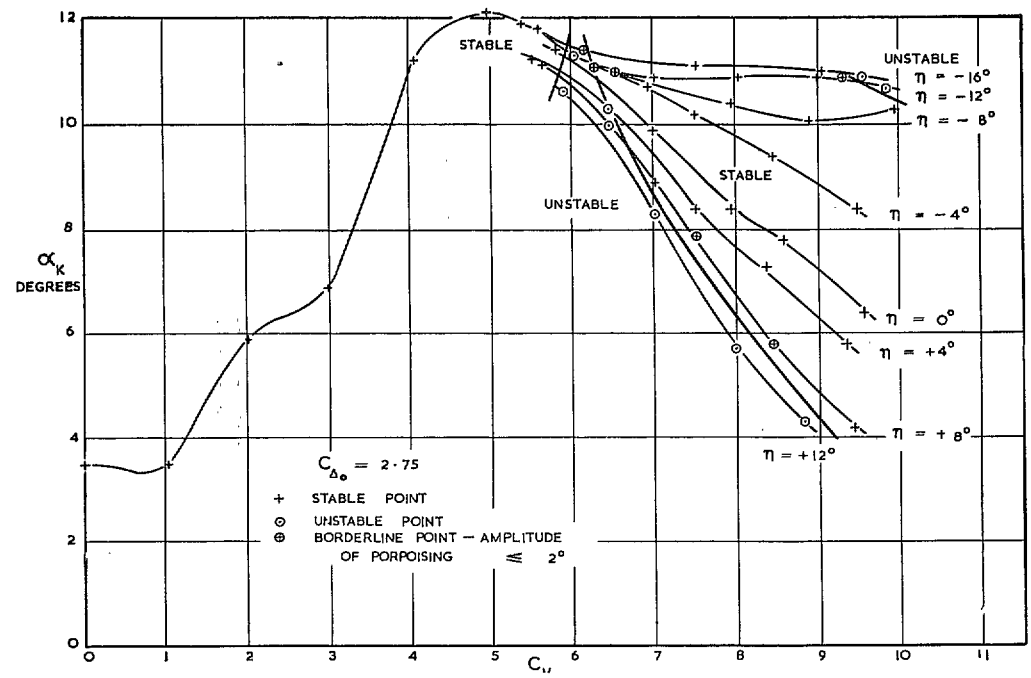

FIG. 31b. Longitudinal stability without disturbance for slipstream investigation with propellers windmilling (Model A).

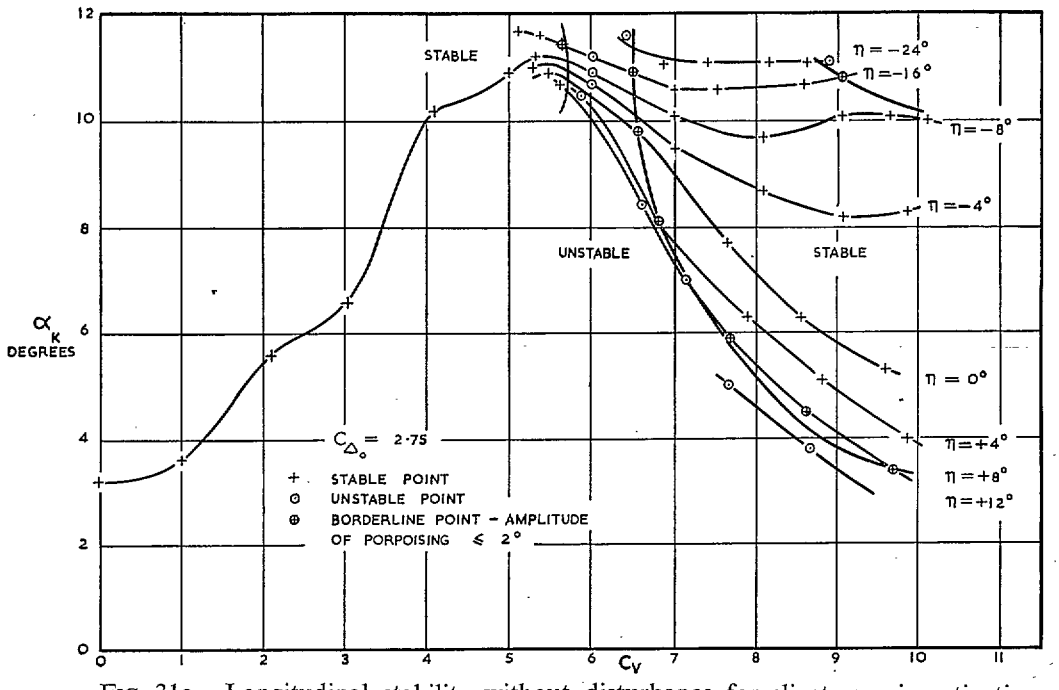

FIG. 31c. Longitudinal stability without disturbance for slipstream investigation with fairings (Model A).

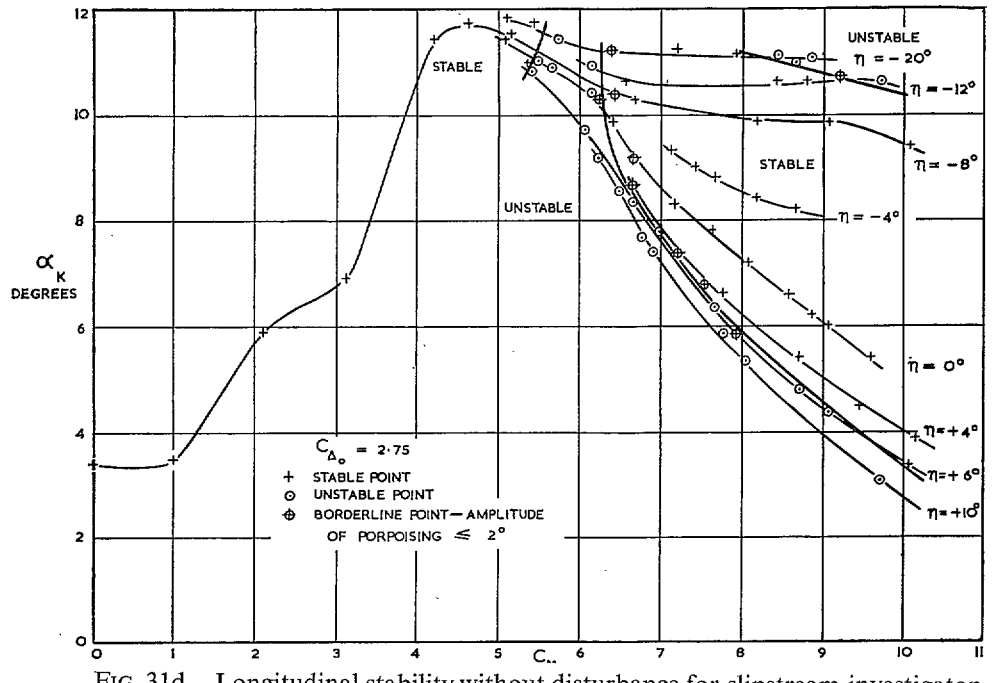

FIG. 31d. Longitudinal stability without disturbance for slipstream investigaton with full-span slats (Model A).

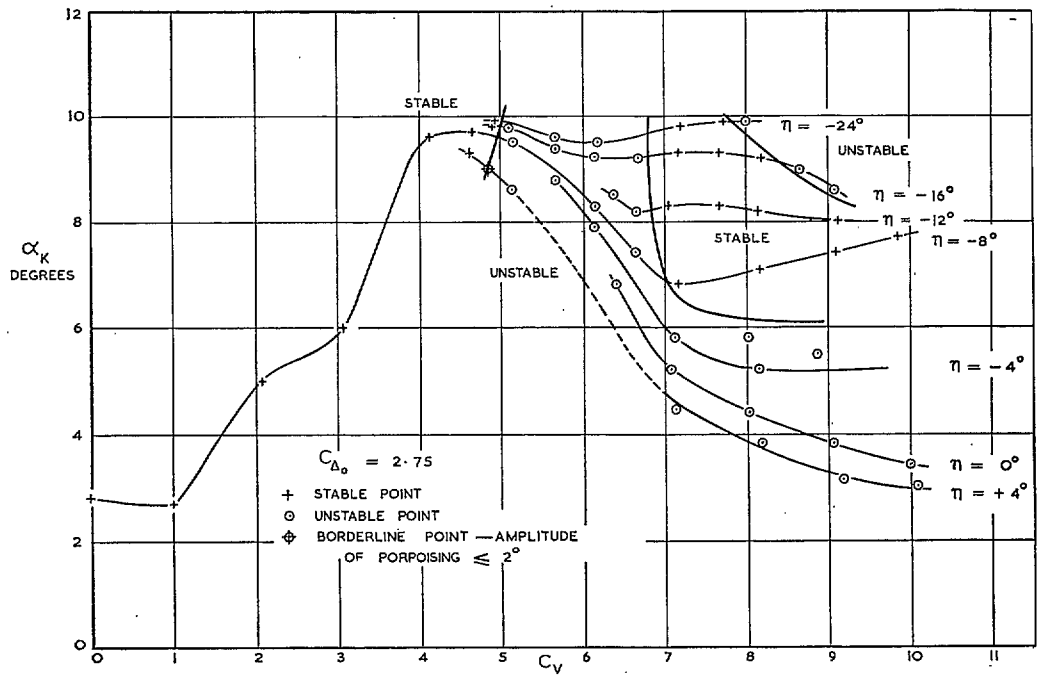

FIG. 32a. Longitudinal stability with disturbance for slipstream investigation with take-off power (Model A).

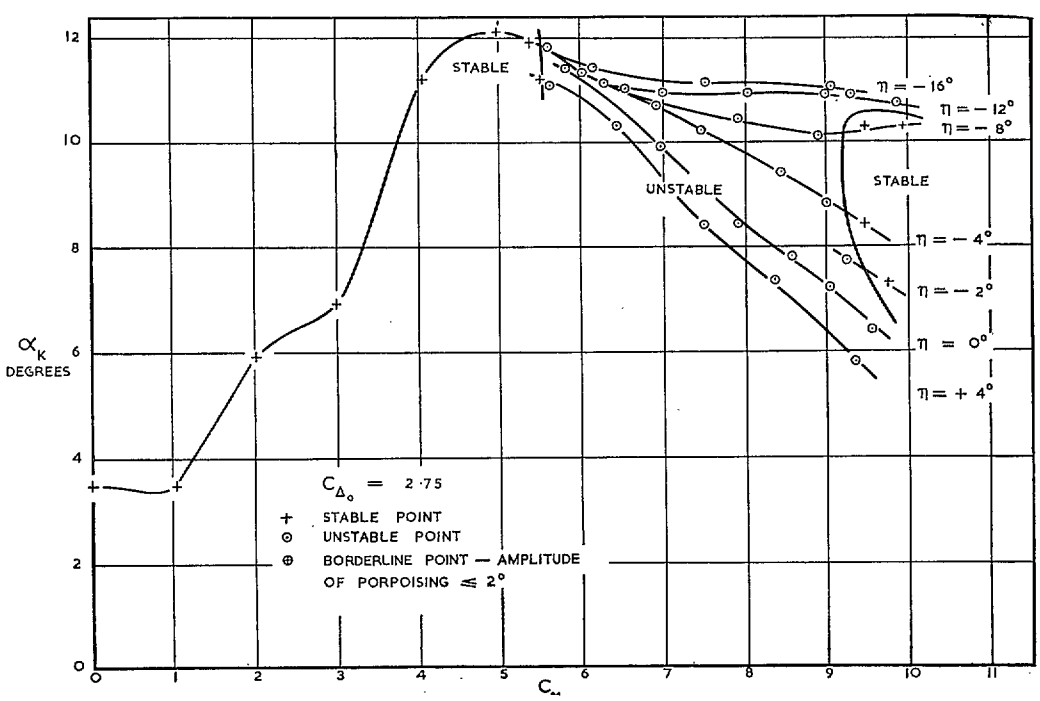

FIG. 32b. Longitudinal stability with disturbance for slipstream investigation with propellers windmilling (Model A).

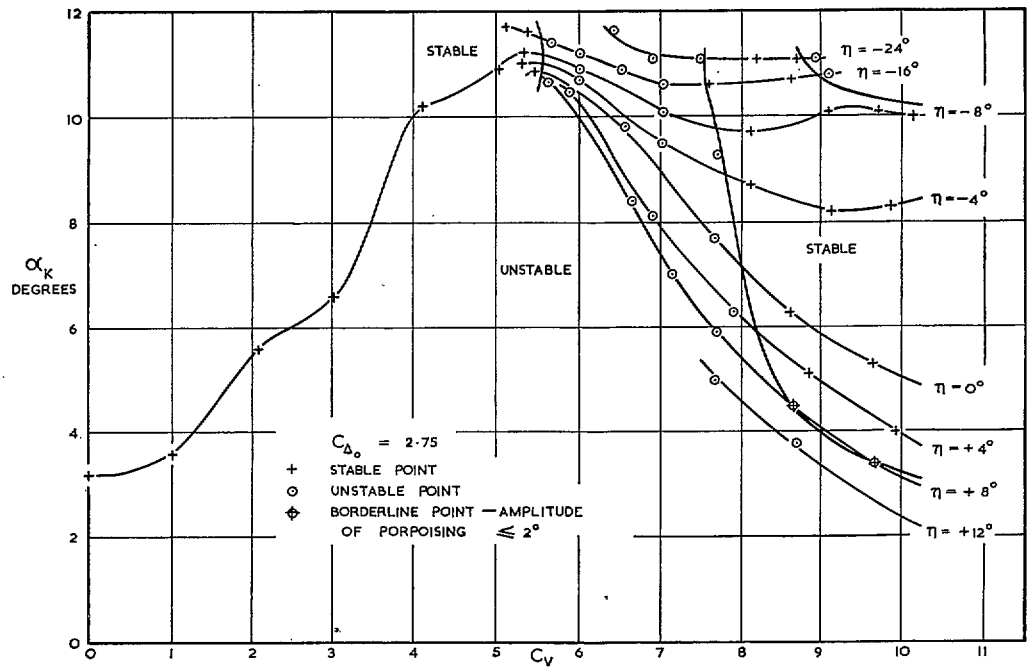

FIG. 32c. Longitudinal stability with disturbance (5-deg disturbance only) for slipstream investigation with fairings (Model A).

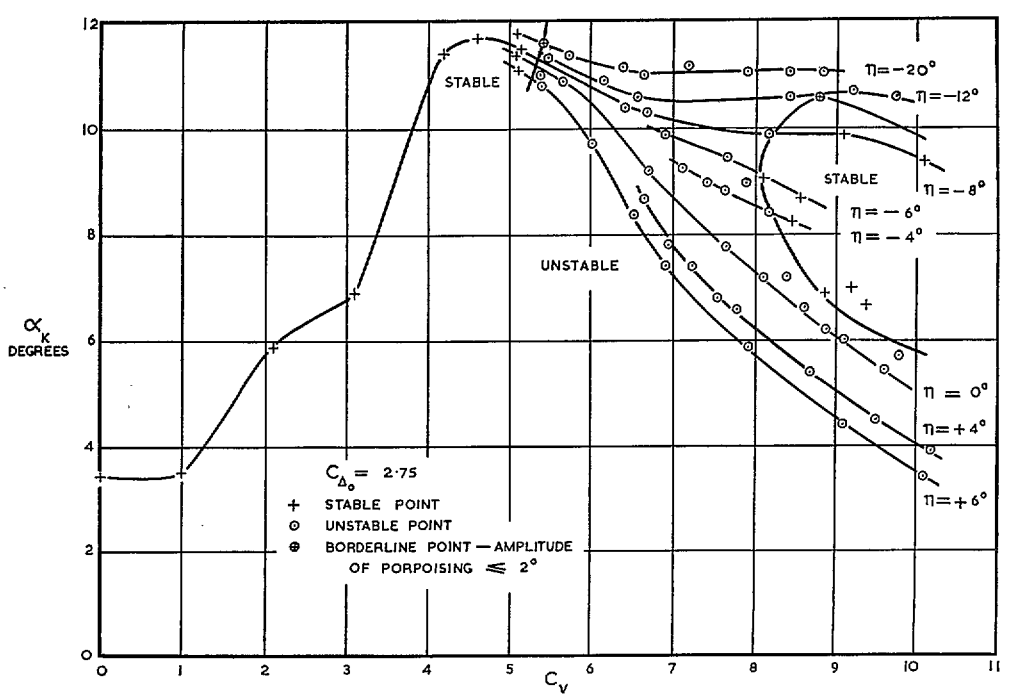

FIG. 32d. Longitudinal stability with disturbance for slipstream investigation with full-span slats (Model A).

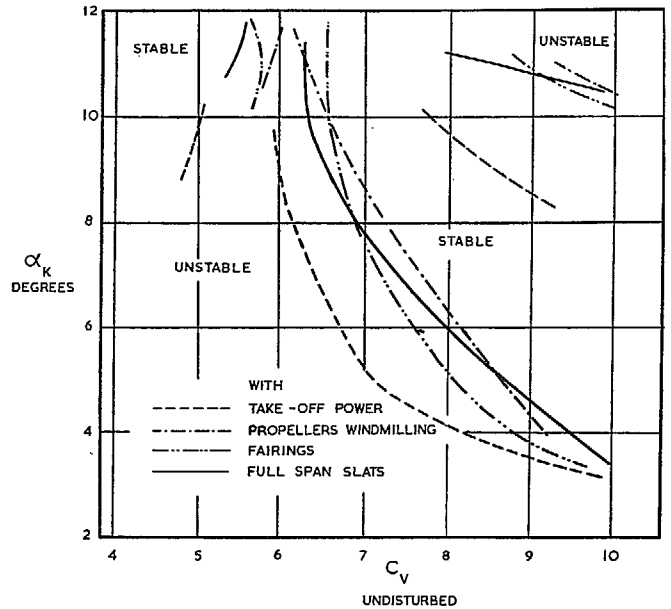

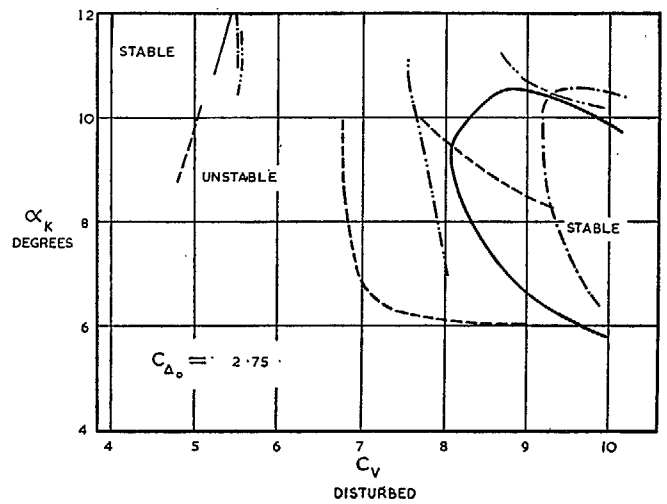

FIG. 33. Comparison of longitudinal stability limits on a C_v base for slipstream investigation (Model A).

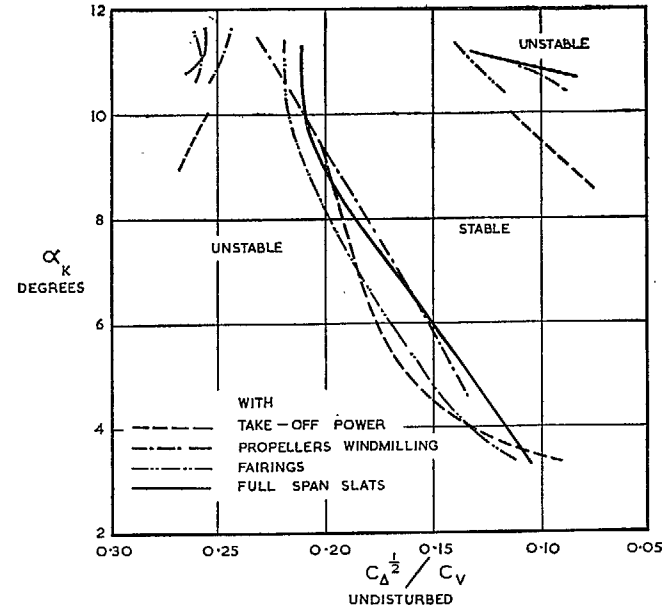

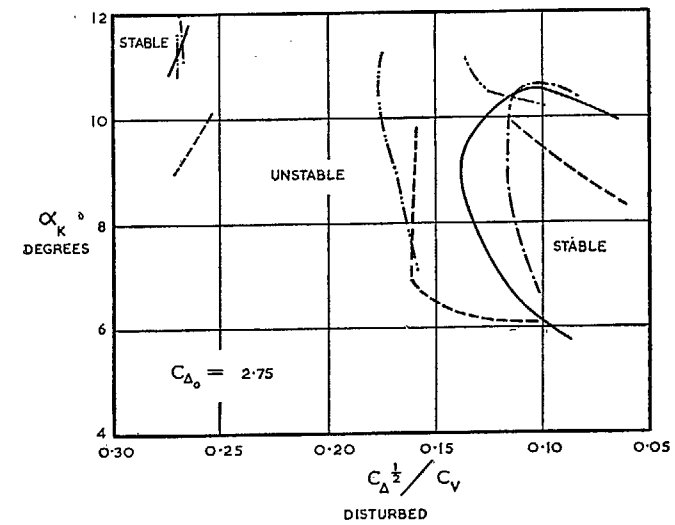

FIG. 34. Comparison of longitudinal stability limits on a $C_\Delta^{1/2}/C_v$ base for slipstream investigation (Model A).

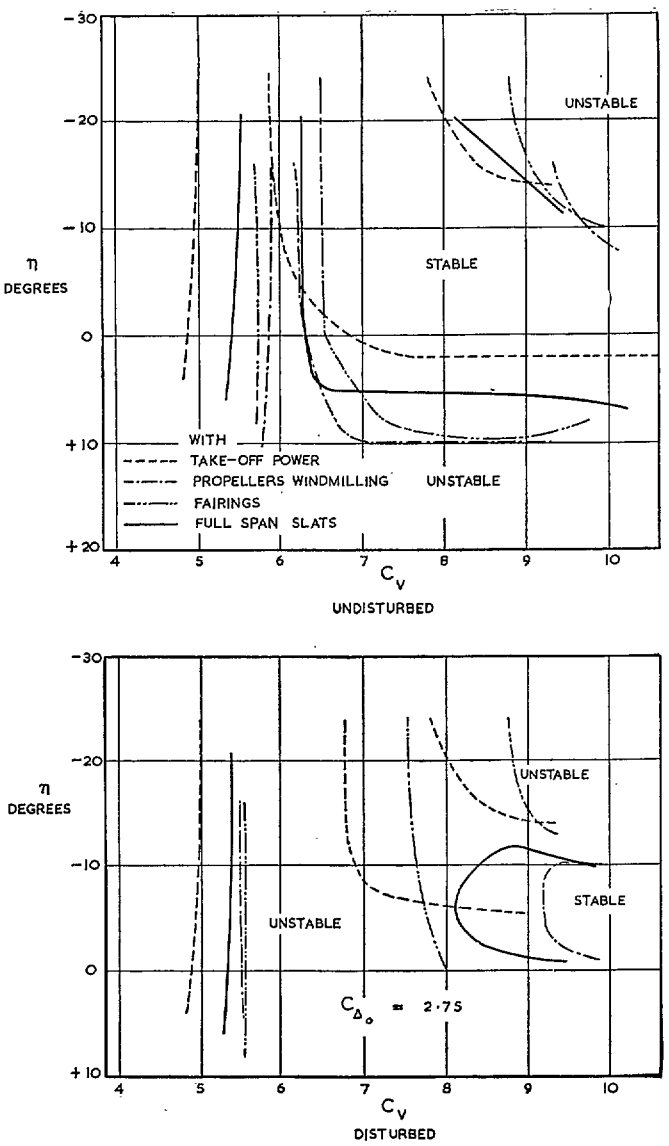

FIG. 35. Relation between elevator settings and longitudinal stability limits for slipstream investigation.

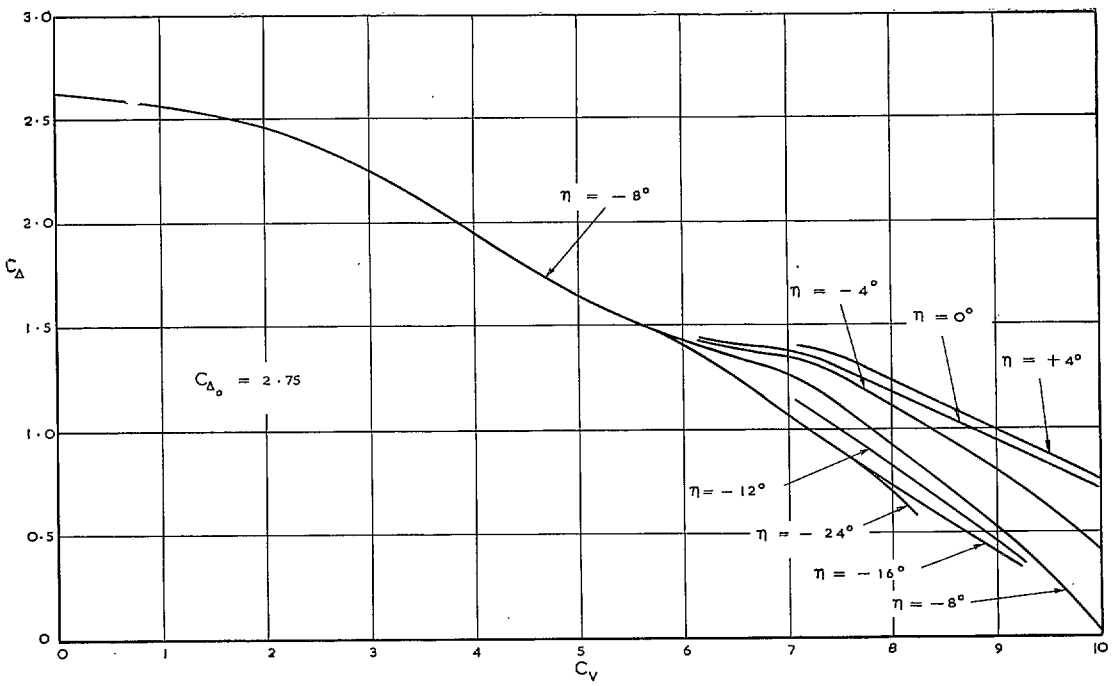

FIG. 36a. Load-coefficient curves for slipstream investigation with take-off power (Model A).

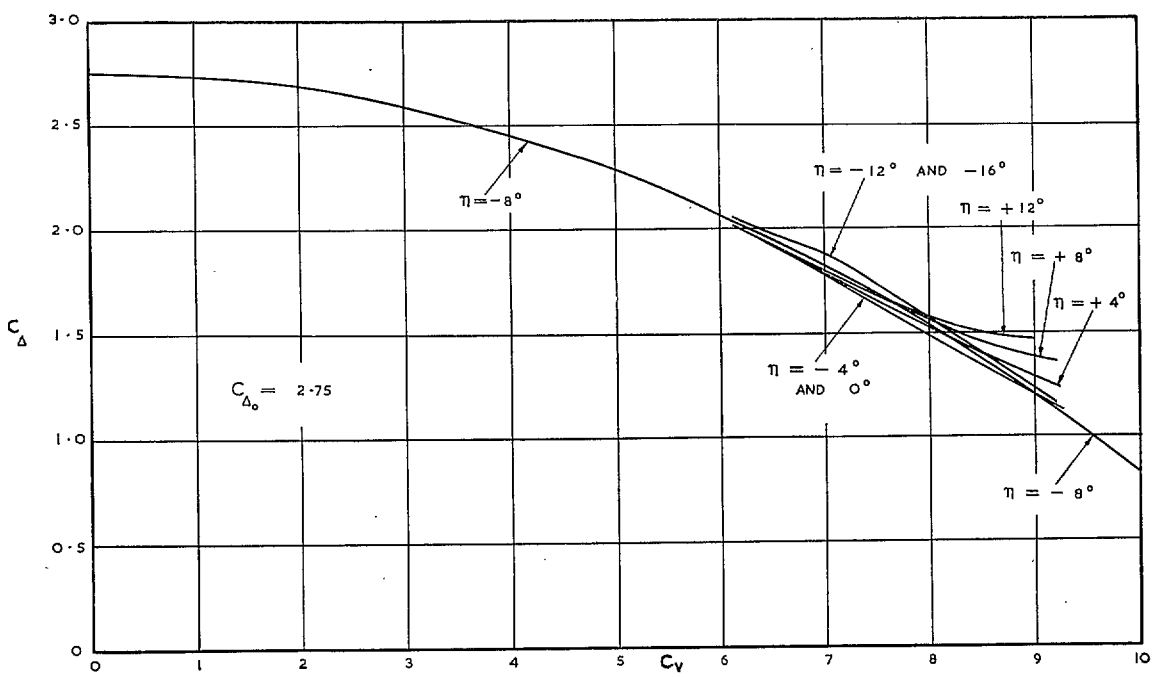

FIG. 36b. Load-coefficient curves for slipstream investigation with propellers windmilling (Model A).

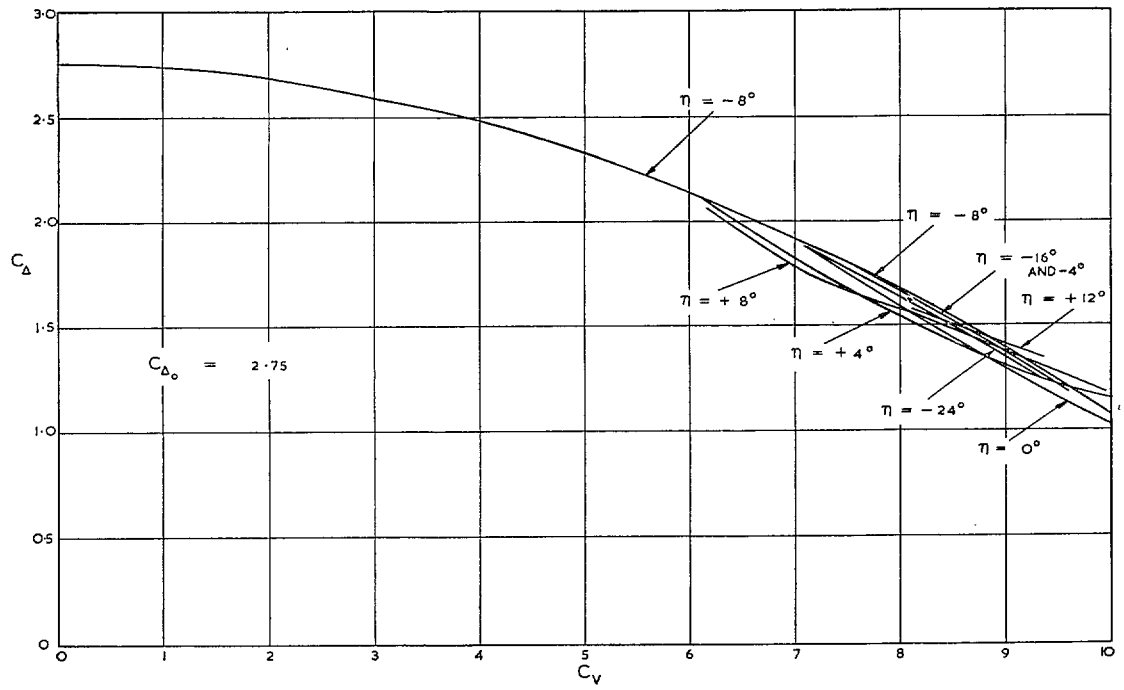

FIG. 36c. Load-coefficient curves for slipstream investigation with fairings (Model A).

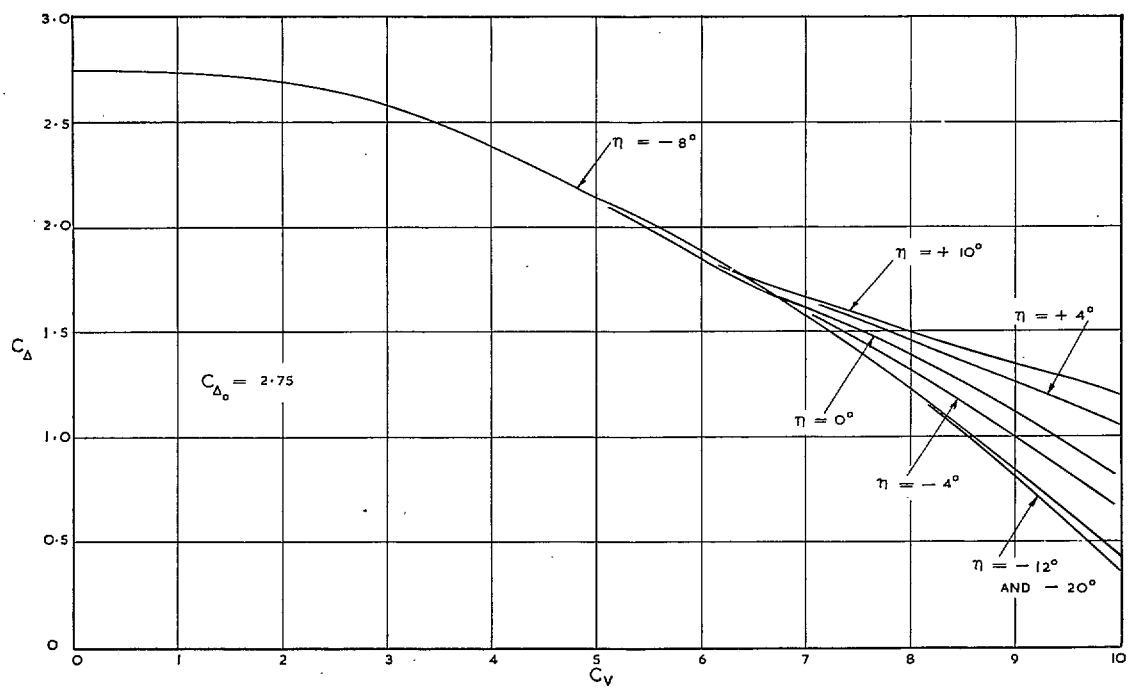

FIG. 36d. Load-coefficient curves for slipstream investigation with full-span slats (Model A).

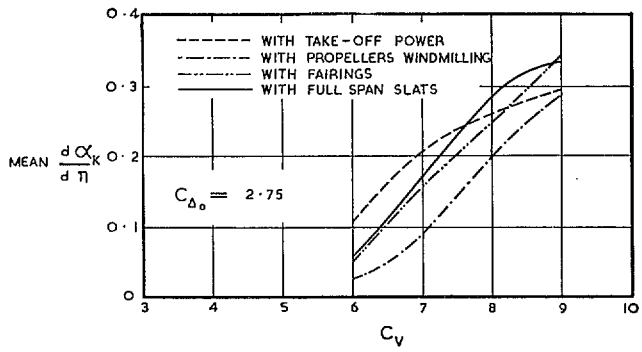

FIG. 37. Comparison of elevator effectiveness for slipstream investigation.

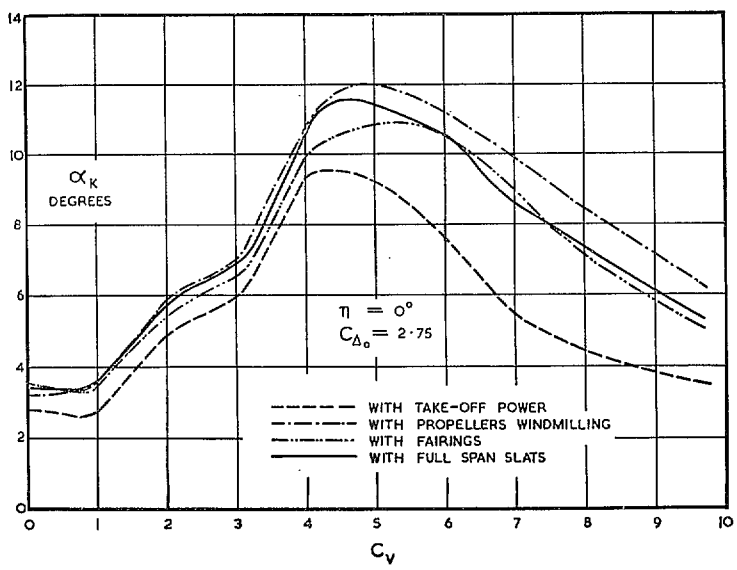

FIG. 38. Comparison of trim curves for slipstream investigation.

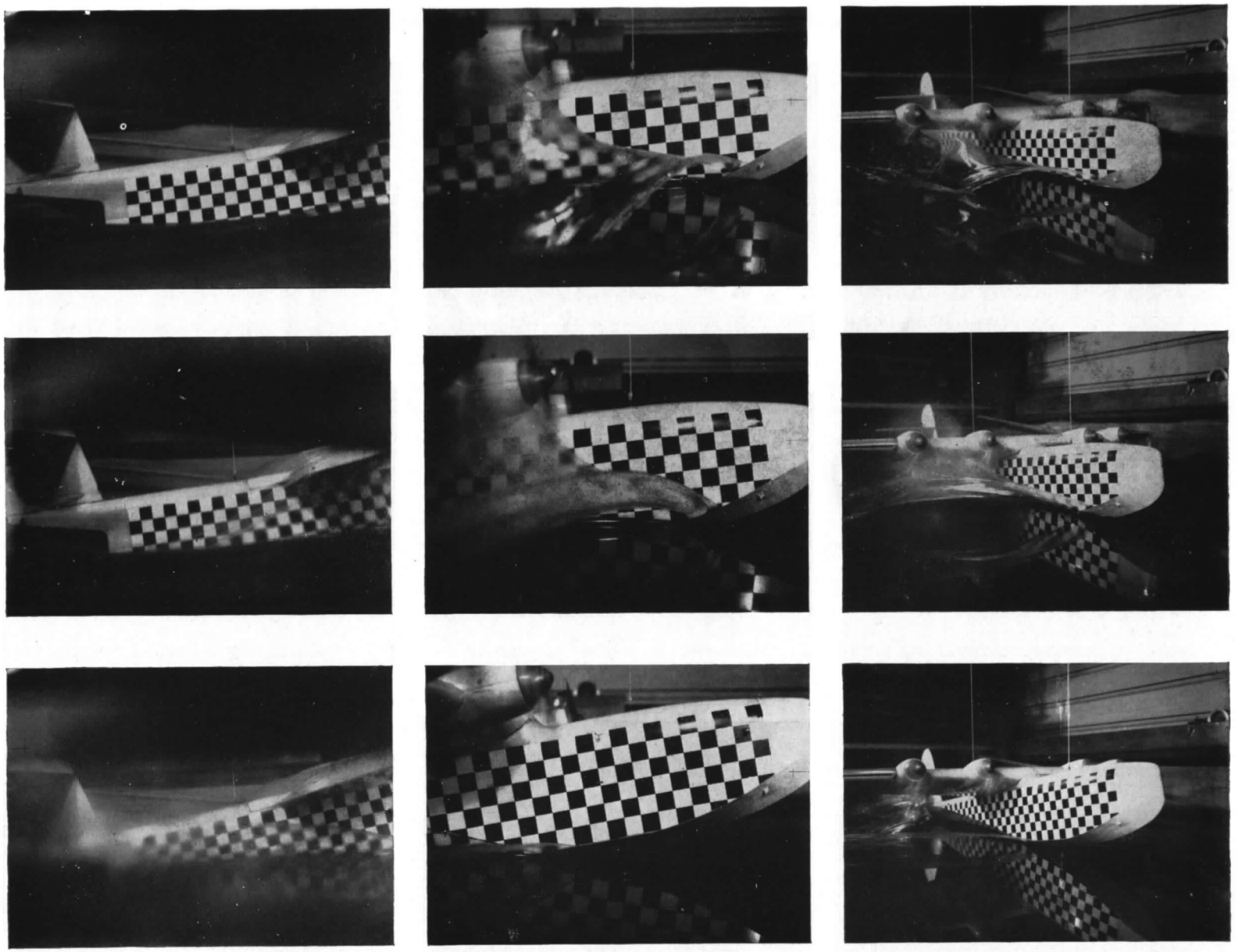

FIG. 39a. Spray photographs for slipstream investigation with take-off power.

π = −8°
C_v = 1·99
α_x = 5·9°

π = −8°
C_v = 3·02
α_x = 7·1°

π = −8°
C_v = 4·09
α_x = 11·3°

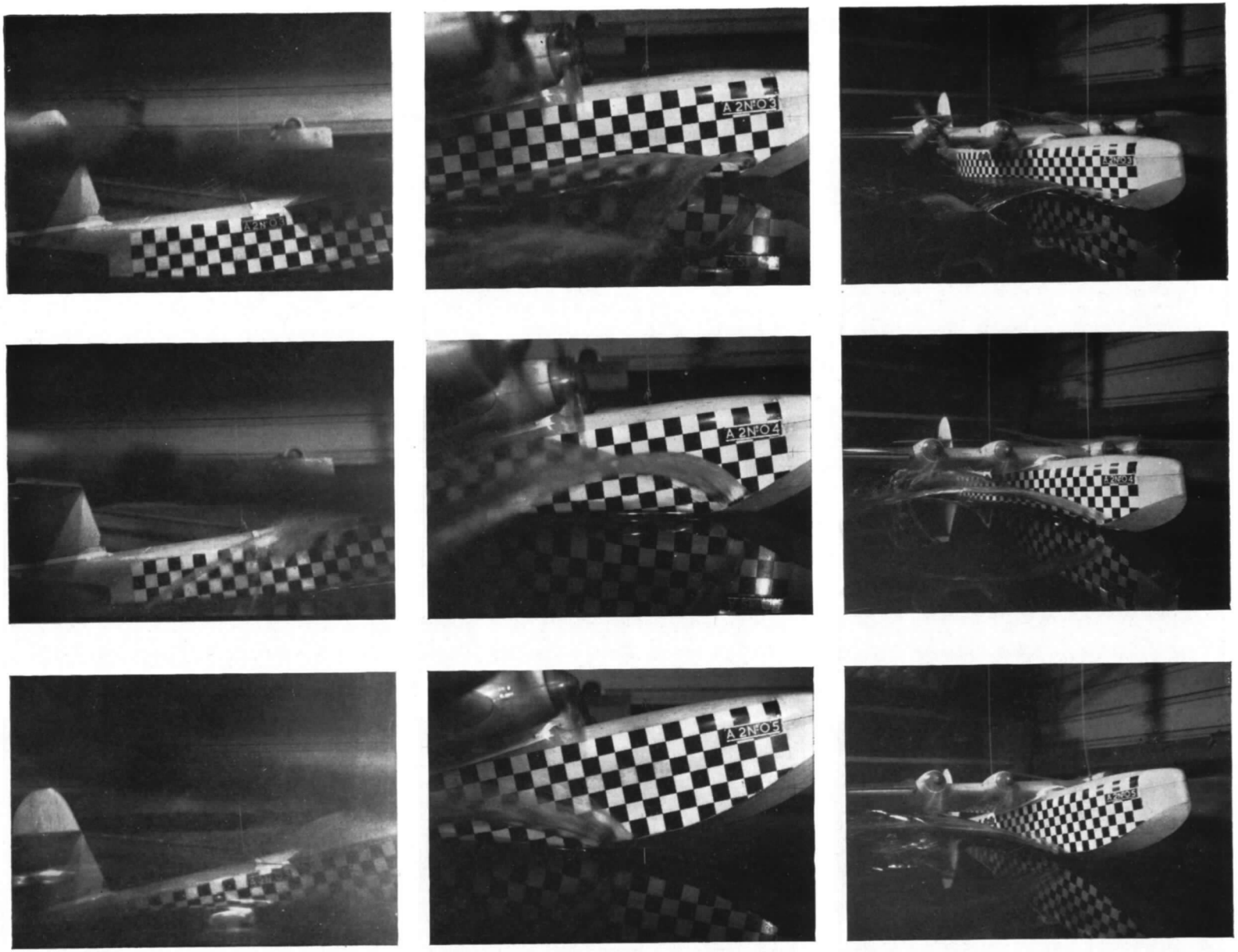

FIG. 39b. Spray photographs for slipstream investigation with propellers windmilling.

$\eta = -8°$
$C_v = 2{\cdot}05$
$\alpha_K = 5{\cdot}5°$

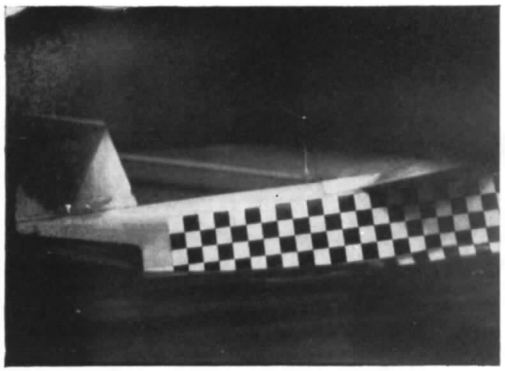

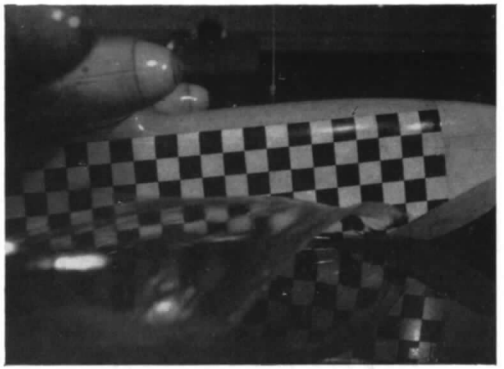

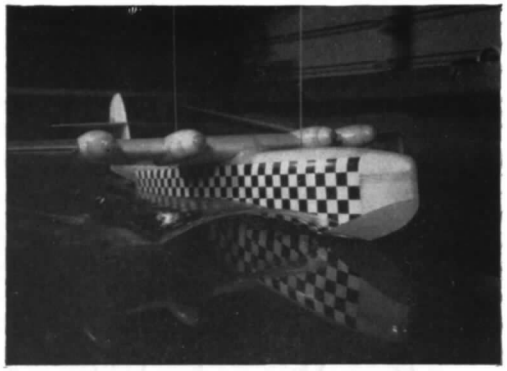

$\eta = -8°$
$C_v = 3{\cdot}07$
$\alpha_K = 6{\cdot}7°$

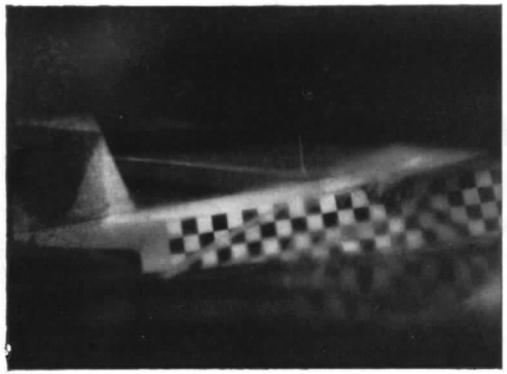

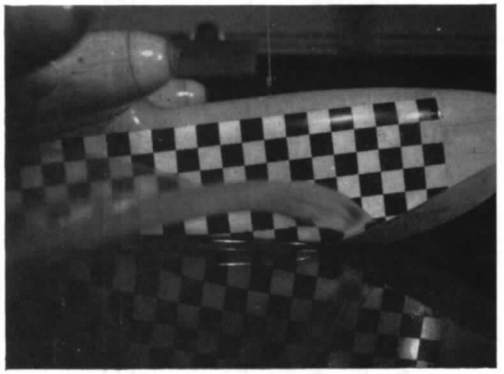

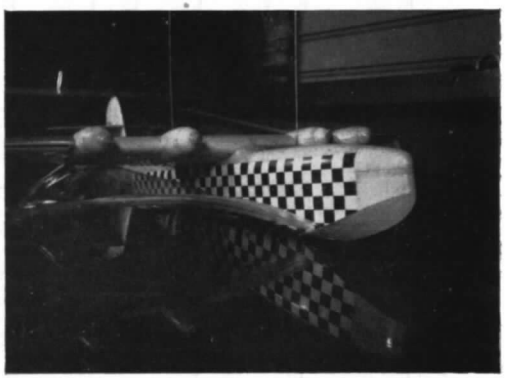

$\eta = -8°$
$C_v = 4{\cdot}09$
$\alpha_K = 10{\cdot}2°$

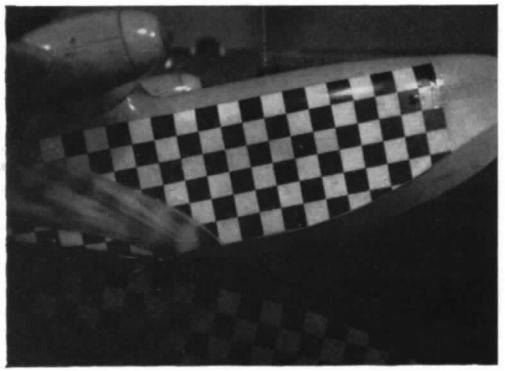

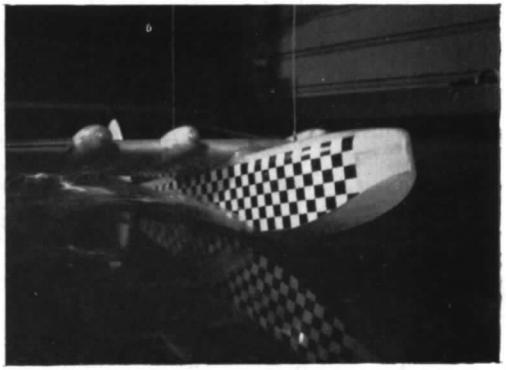

FIG. 39c. Spray photographs for slipstream investigation with fairings.

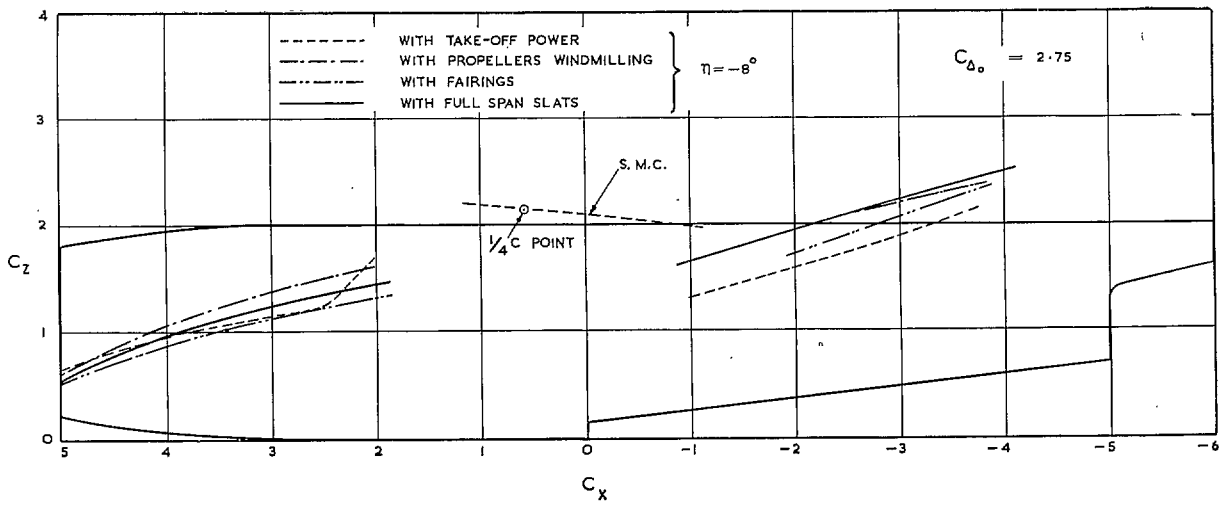

FIG. 40. Projections of spray envelopes on plane of symmetry of model (Model A).

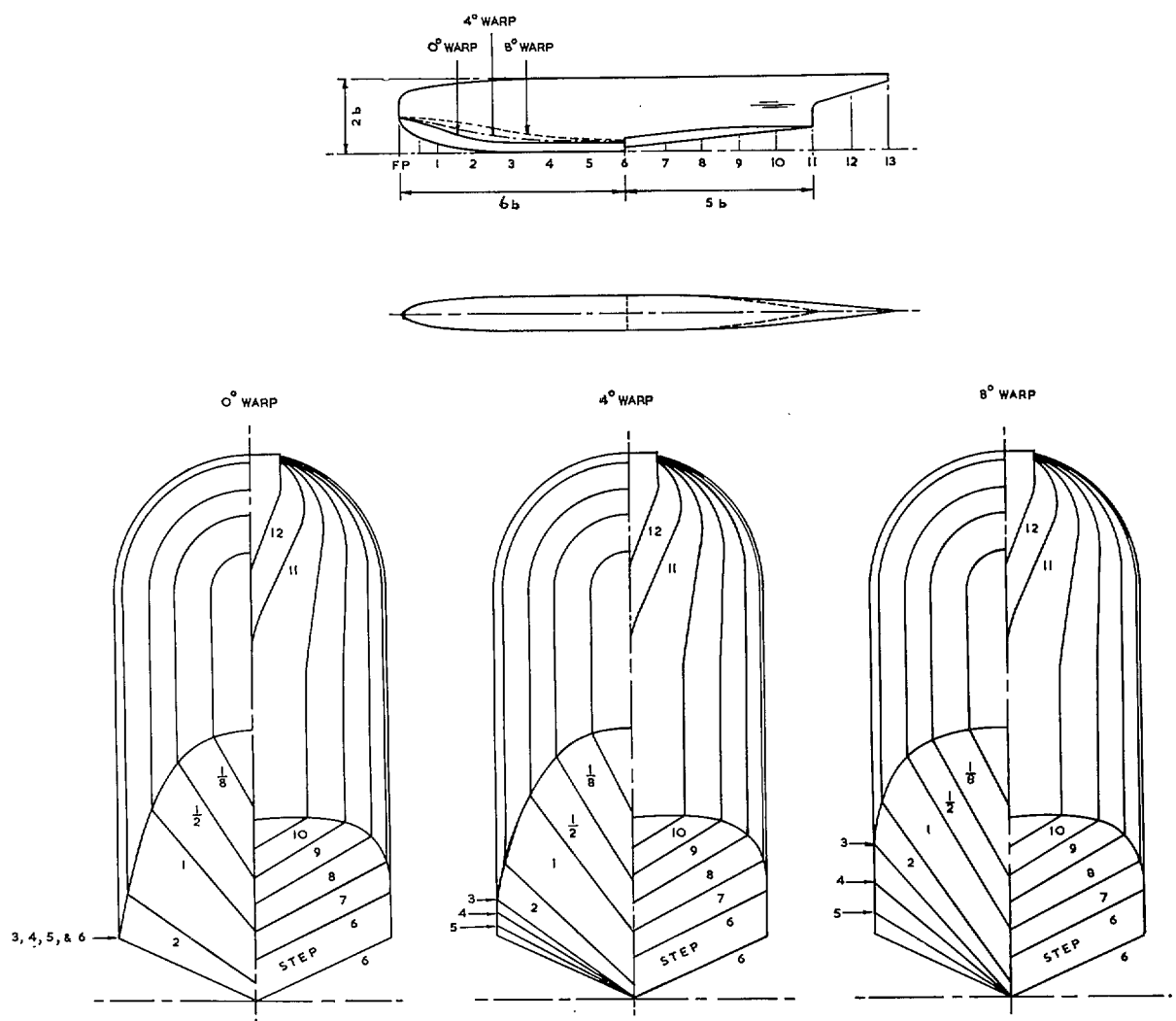

FIG. 41. Comparison of hull lines of Models A, B and C.

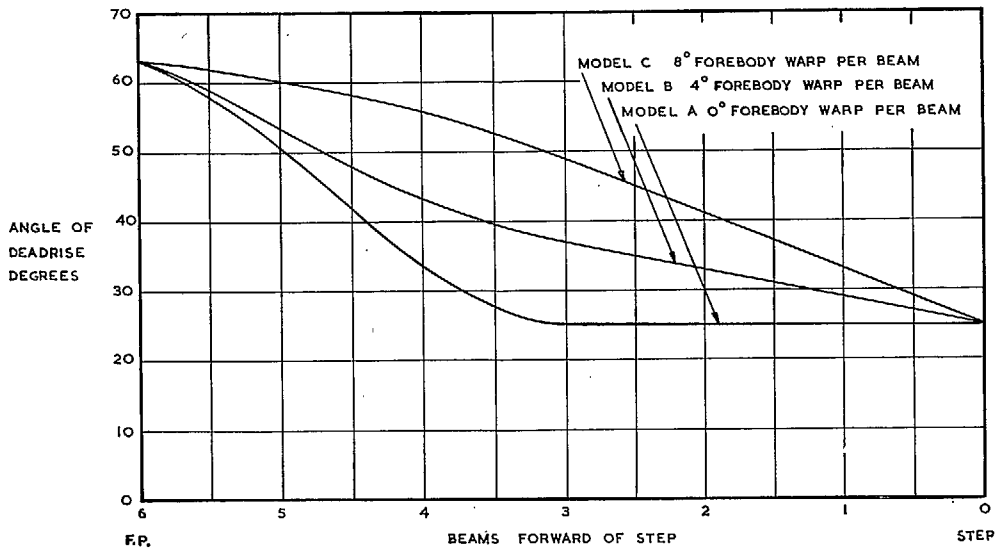

FIG. 42. Comparison of deadrise angle distributions for Models A, B and C.

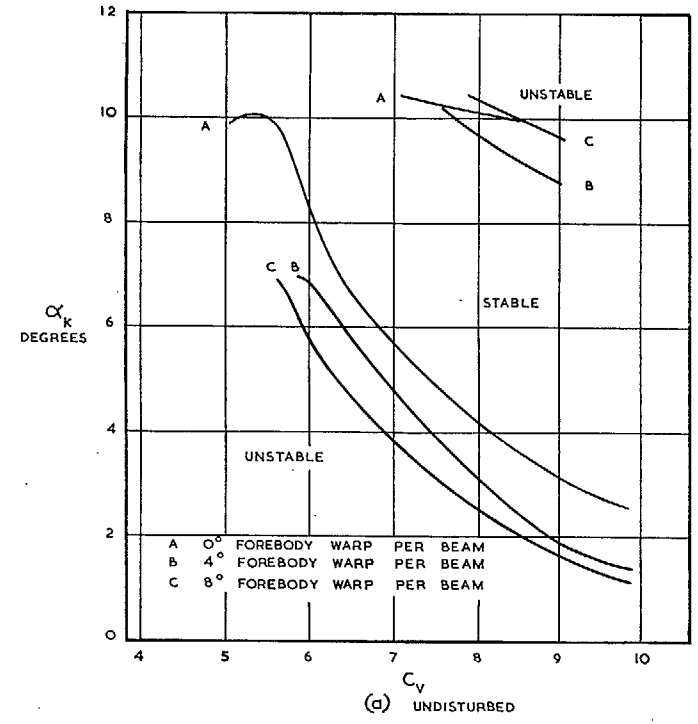

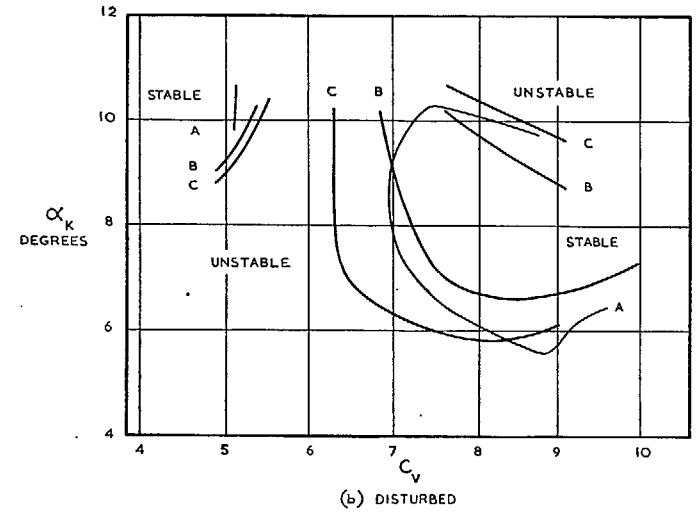

FIGS. 43a and 43b. Effect of forebody warp on longitudinal stability limits ($C_{\Delta 0} = 2{\cdot}25$).

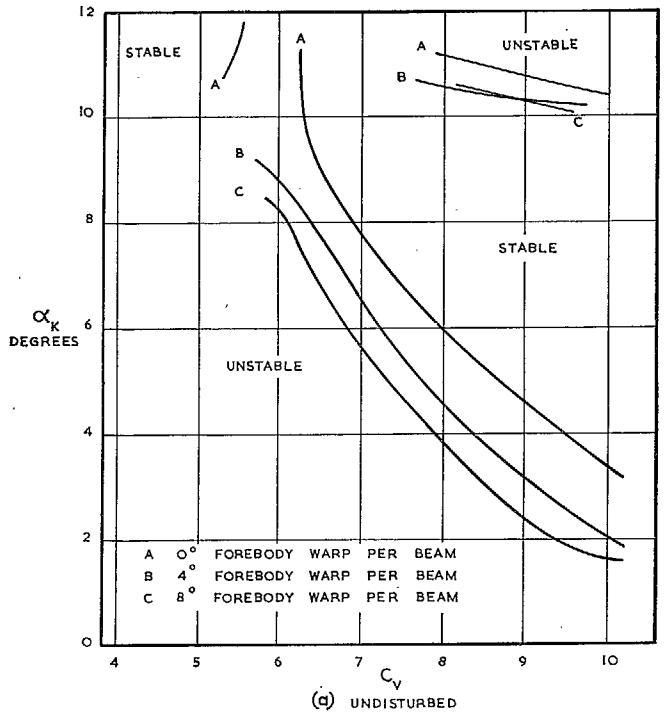

FIGS. 44a and 44b. Effect of forebody warp on longitudinal stability limits ($C_{\Delta 0} = 2{\cdot}75$).

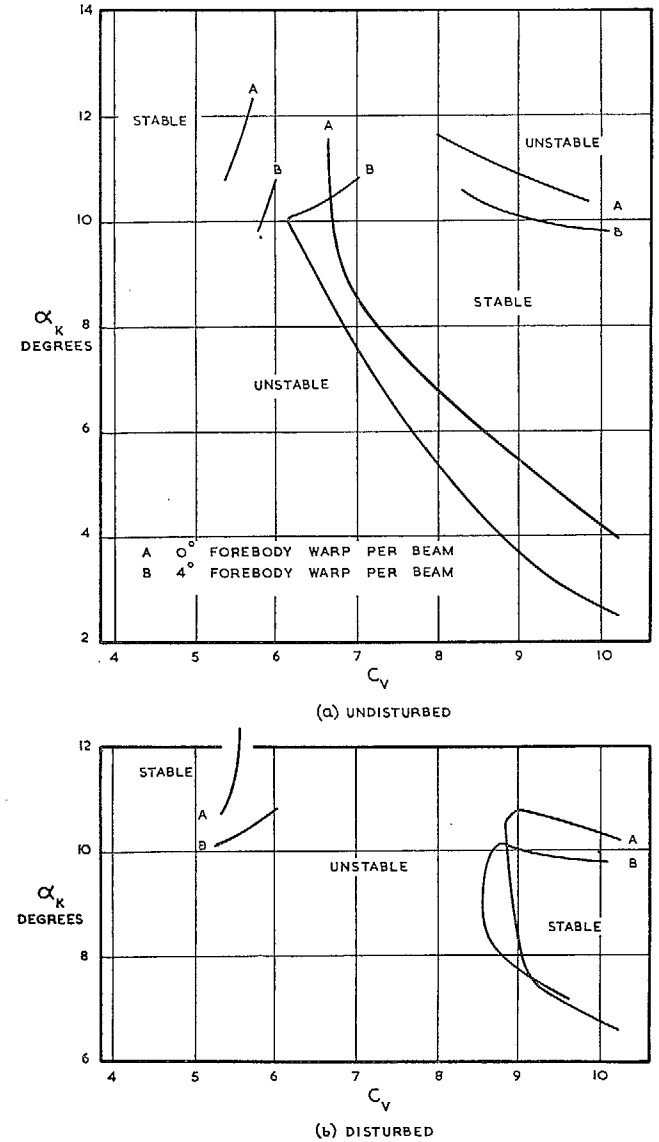

FIGS. 45a and 45b. Effect of forebody warp on longitudinal stability limits ($C_{\Delta 0} = 3{\cdot}00$).

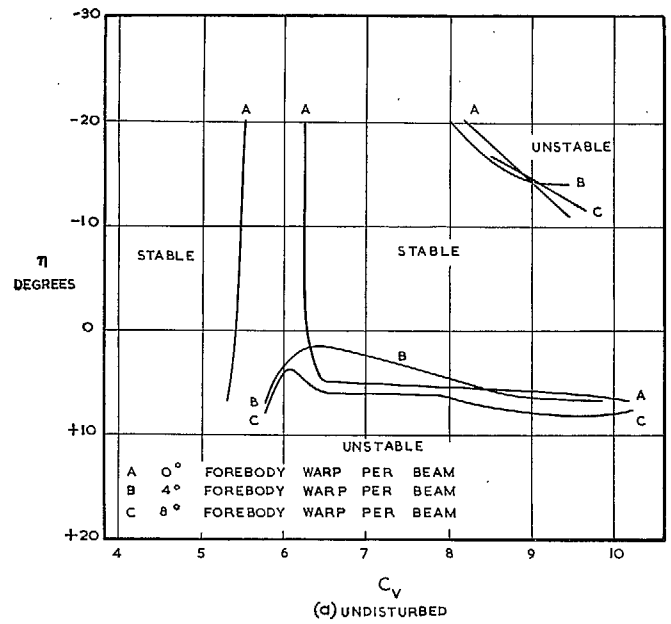

FIGS. 46a and 46b. Relation between elevator settings and longitudinal stability limits for Models A, B and C ($C_{\Delta 0} = 2{\cdot}75$).

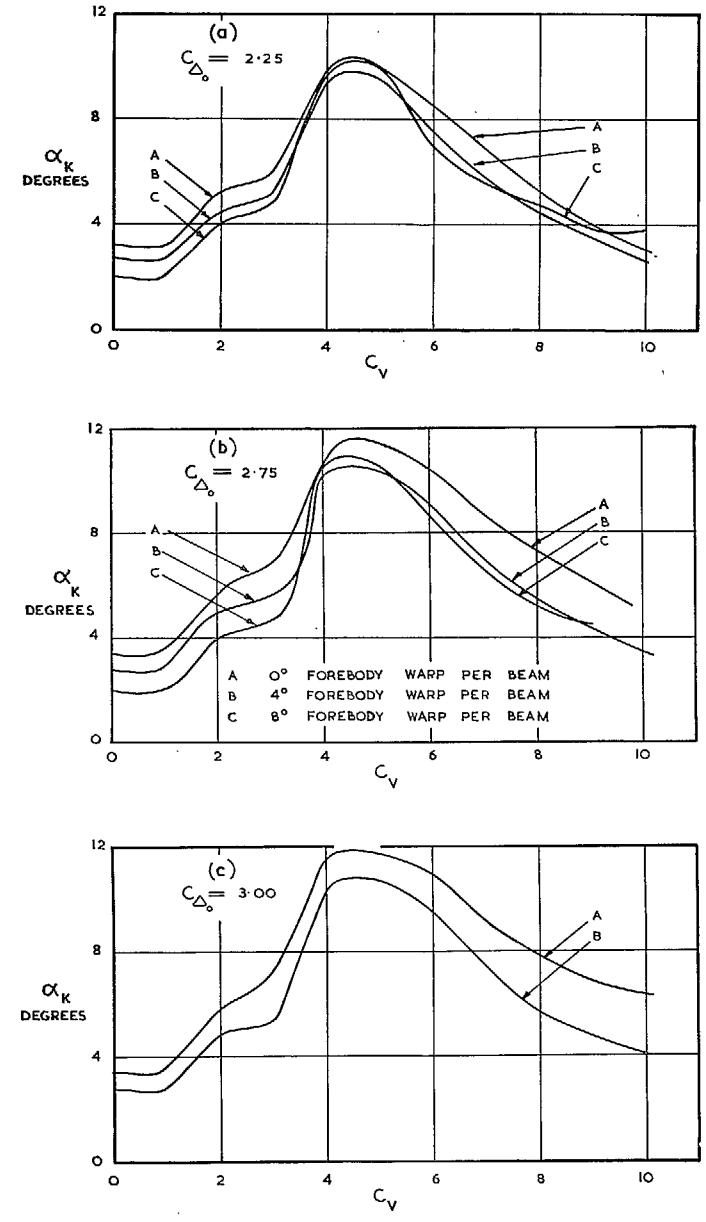

FIGS. 47a to 47c. Effect of forebody warp on trim curves ($\eta = 0$ deg.).

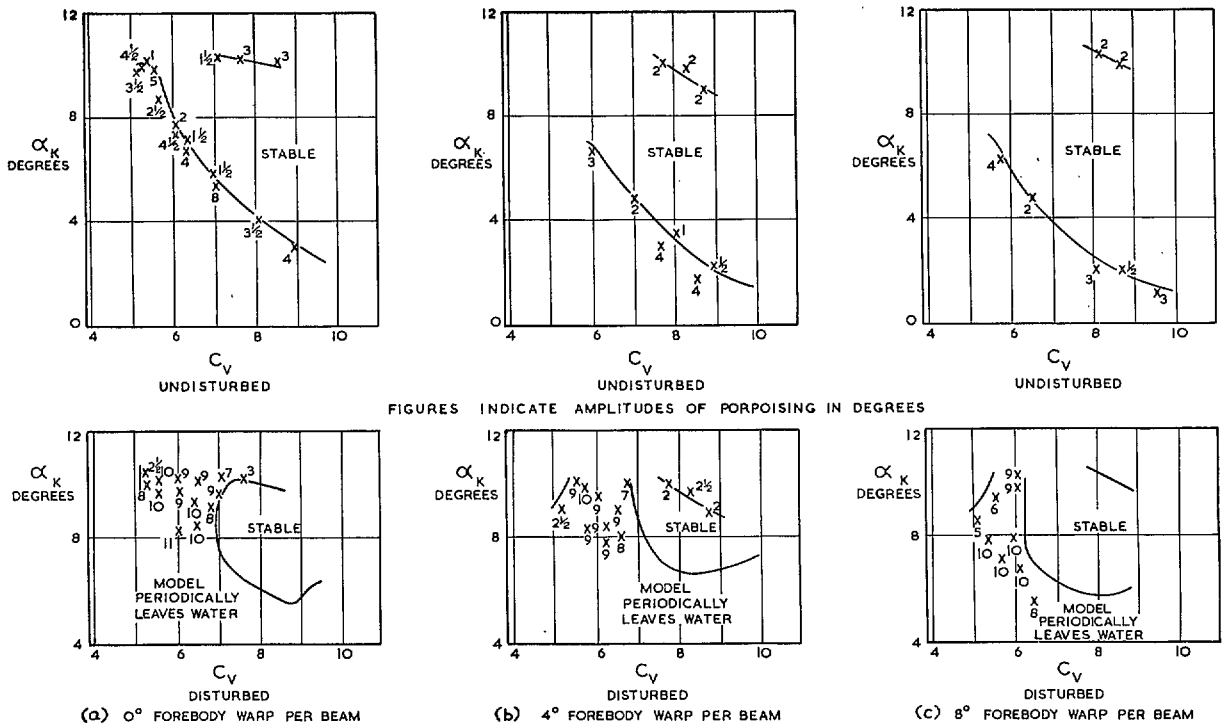

FIGS. 48a to 48c. Effect of forebody warp on amplitudes of porpoising ($C_{\Delta 0} = 2{\cdot}25$).

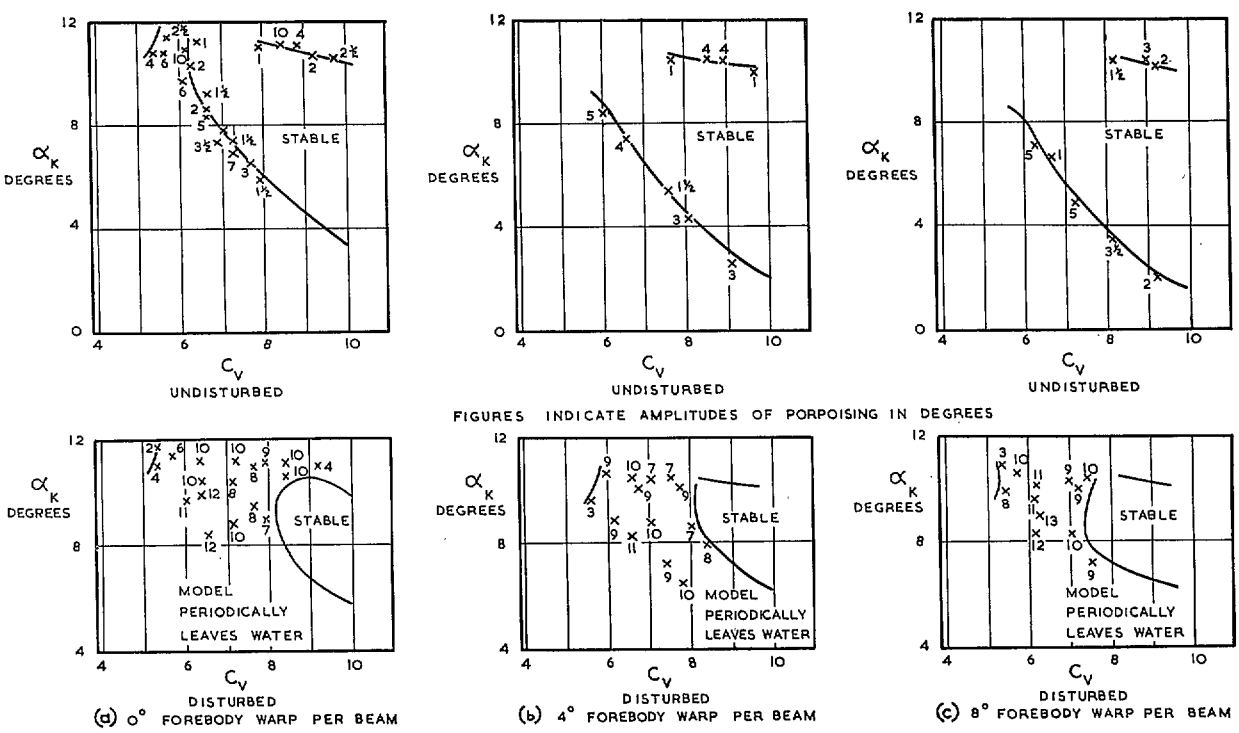

FIGS. 49a to 49c. Effect of forebody warp on amplitudes of porpoising ($C_{\Delta 0} = 2{\cdot}75$).

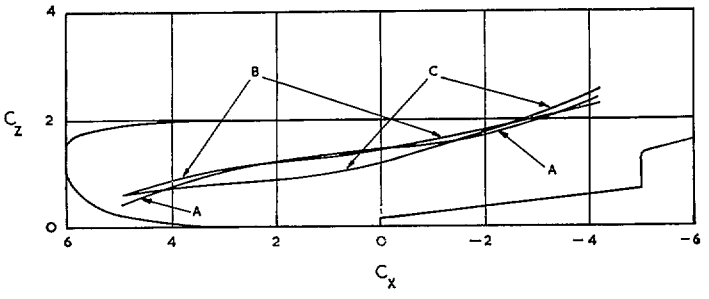

(a) $C_{\Delta_0} = 2{\cdot}25$

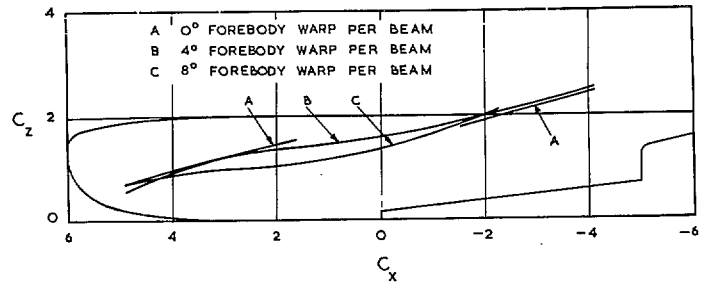

(b) $C_{\Delta_0} = 2{\cdot}75$

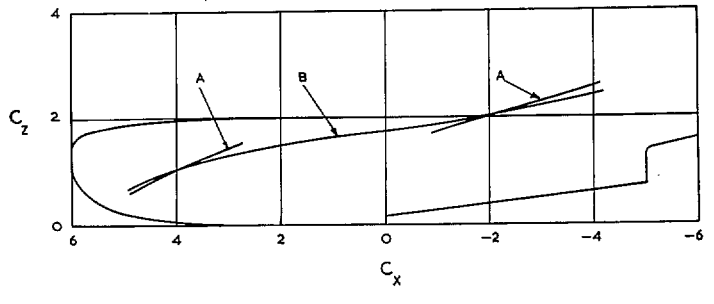

(c) $C_{\Delta_0} = 3{\cdot}00$

FIGS. 50a to 50c. Effect of forebody warp on spray projections.

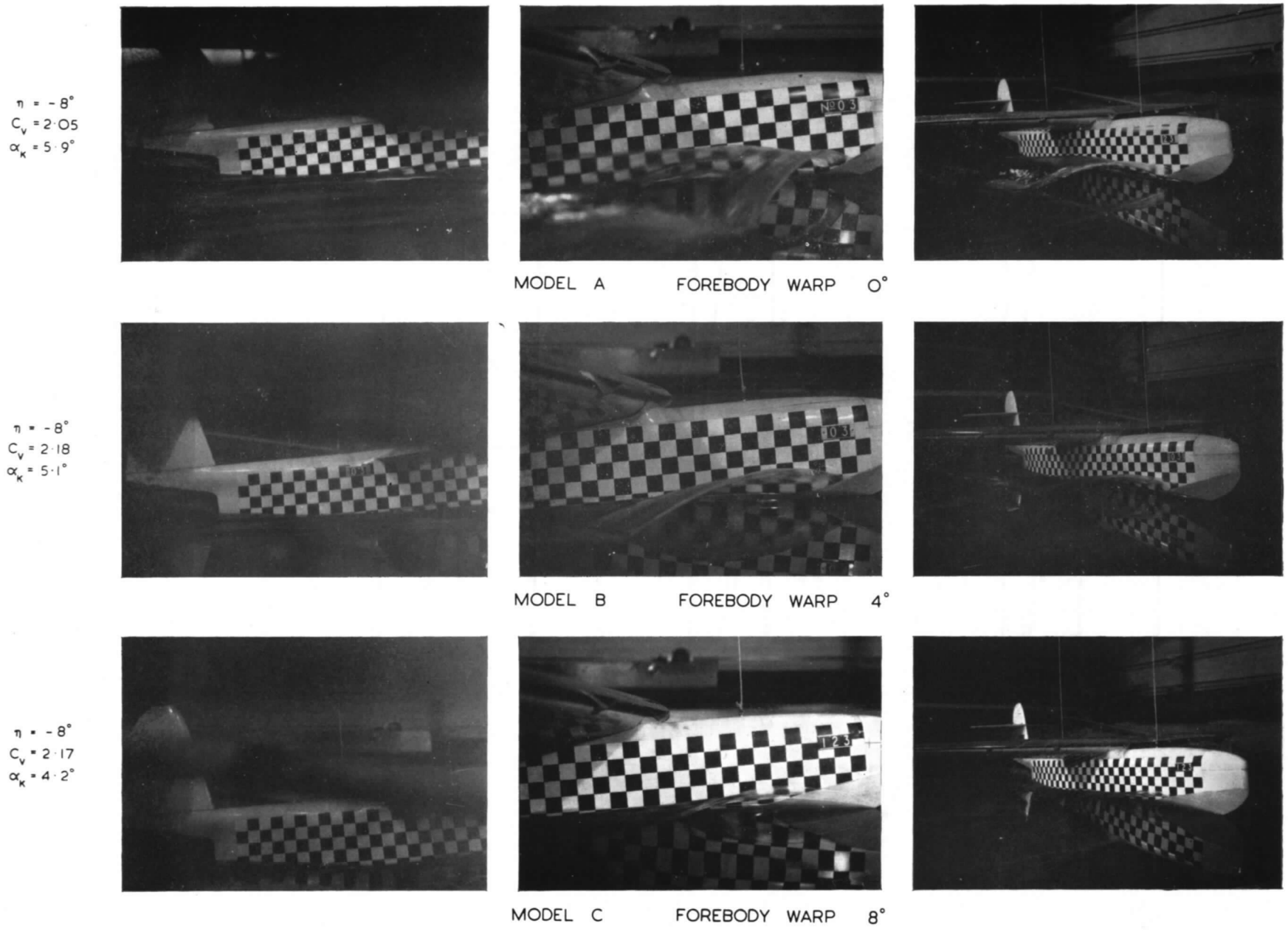

FIG. 51. Effect of forebody warp on spray ($C_{\Delta 0} = 2{\cdot}75$; $C_v = 2$).

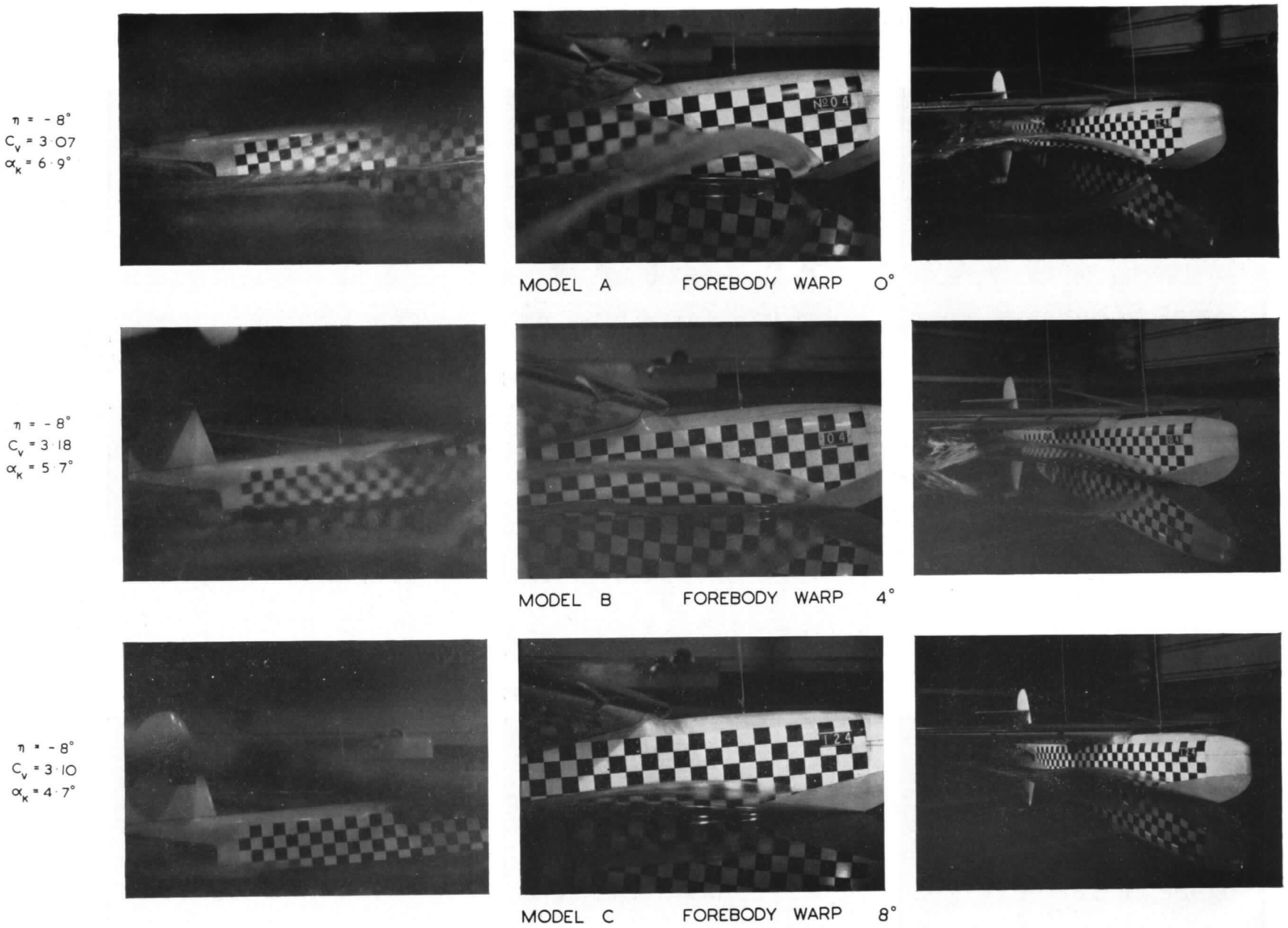

FIG. 52. Effect of forebody warp on spray ($C_{L0} = 2{\cdot}75$; $C_v = 3$).

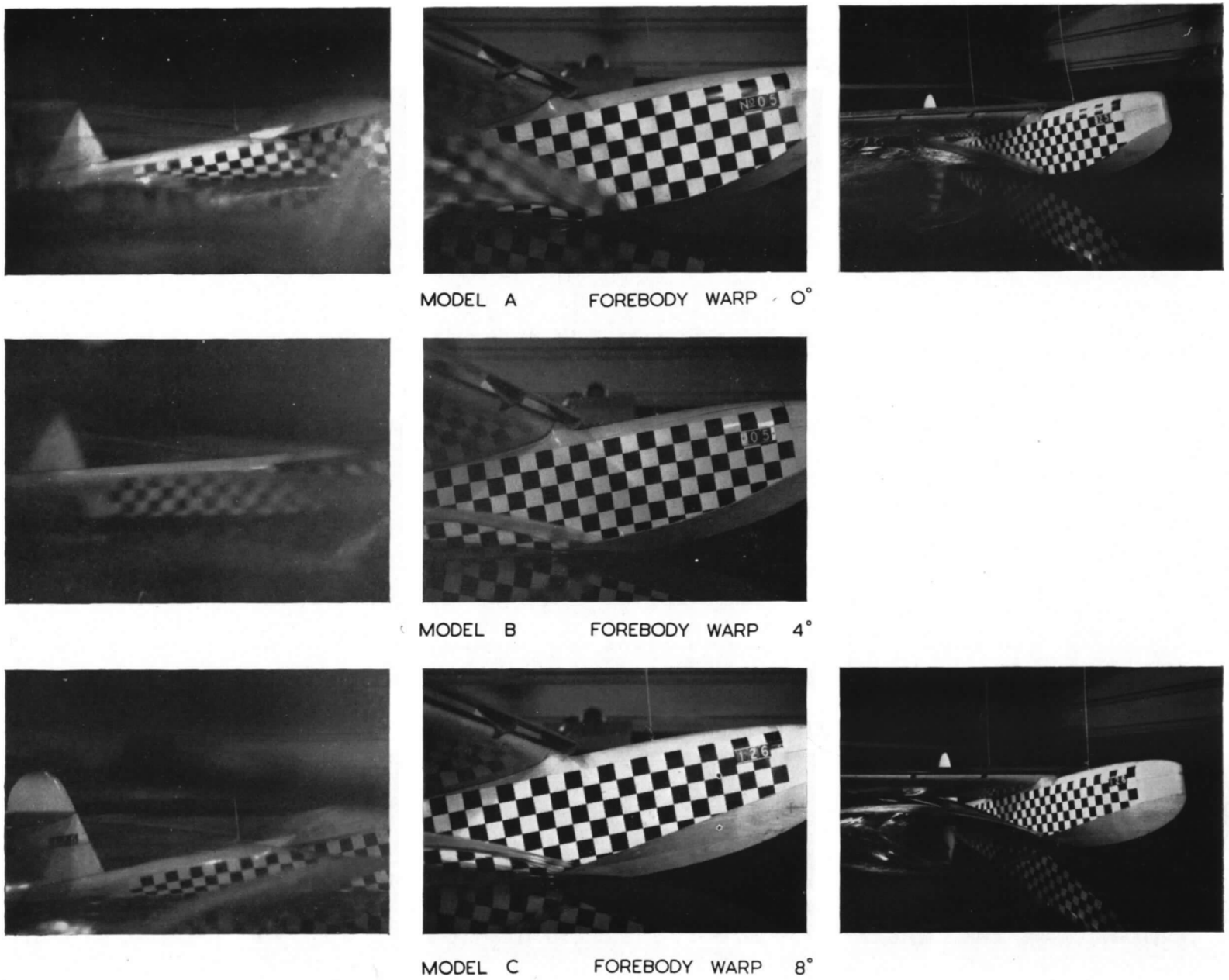

FIG. 53. Effect of forebody warp on spray ($C_{\Delta 0} = 2{\cdot}75$; $C_v = 4$).

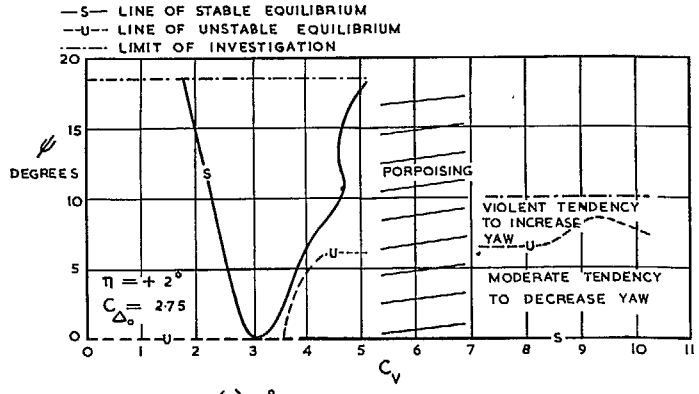

(a) 0° FOREBODY WARP PER BEAM

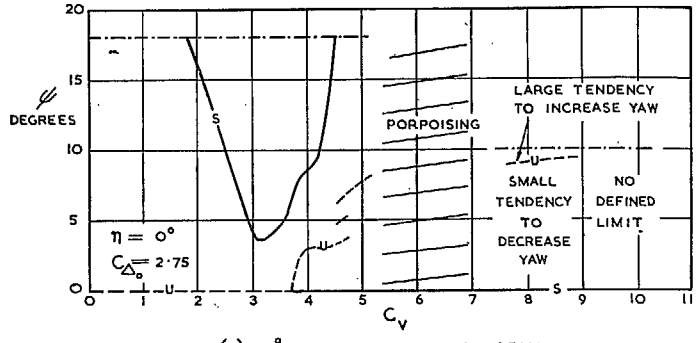

(b) 4° FOREBODY WARP PER BEAM

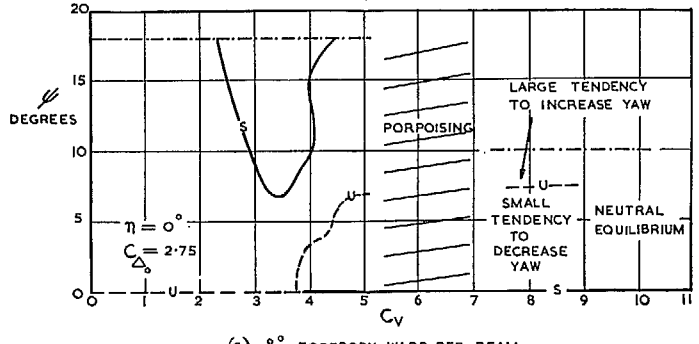

(c) 8° FOREBODY WARP PER BEAM

FIGS. 54a to 54c. Effect of forebody warp on directional stability ($C_{\Delta 0} = 2{\cdot}75$).

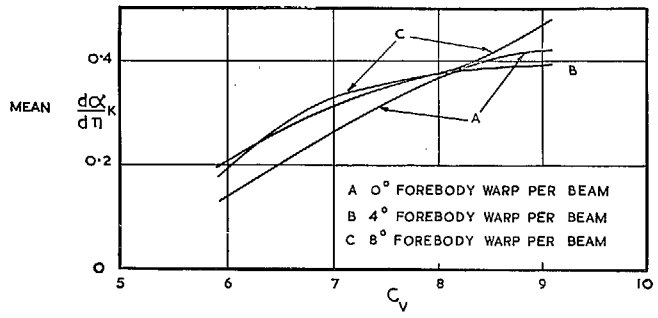

(a) $C_{\Delta_0} = 2{\cdot}25$

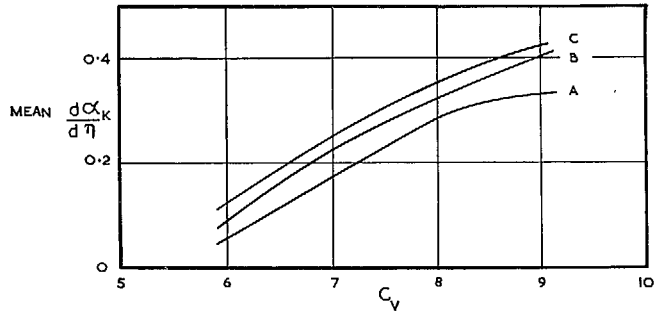

(b) $C_{\Delta_0} = 2{\cdot}75$

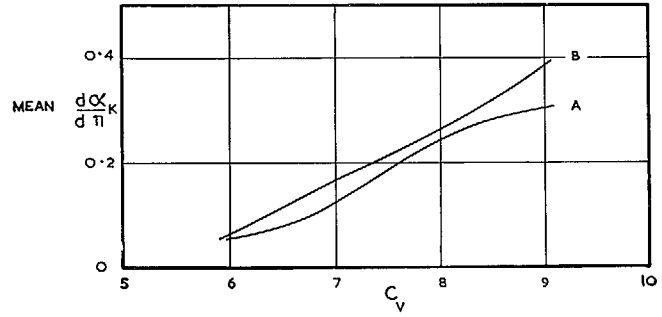

(c) $C_{\Delta_0} = 3{\cdot}00$

FIGS. 55a to 55c. Effect of forebody warp on elevator effectiveness

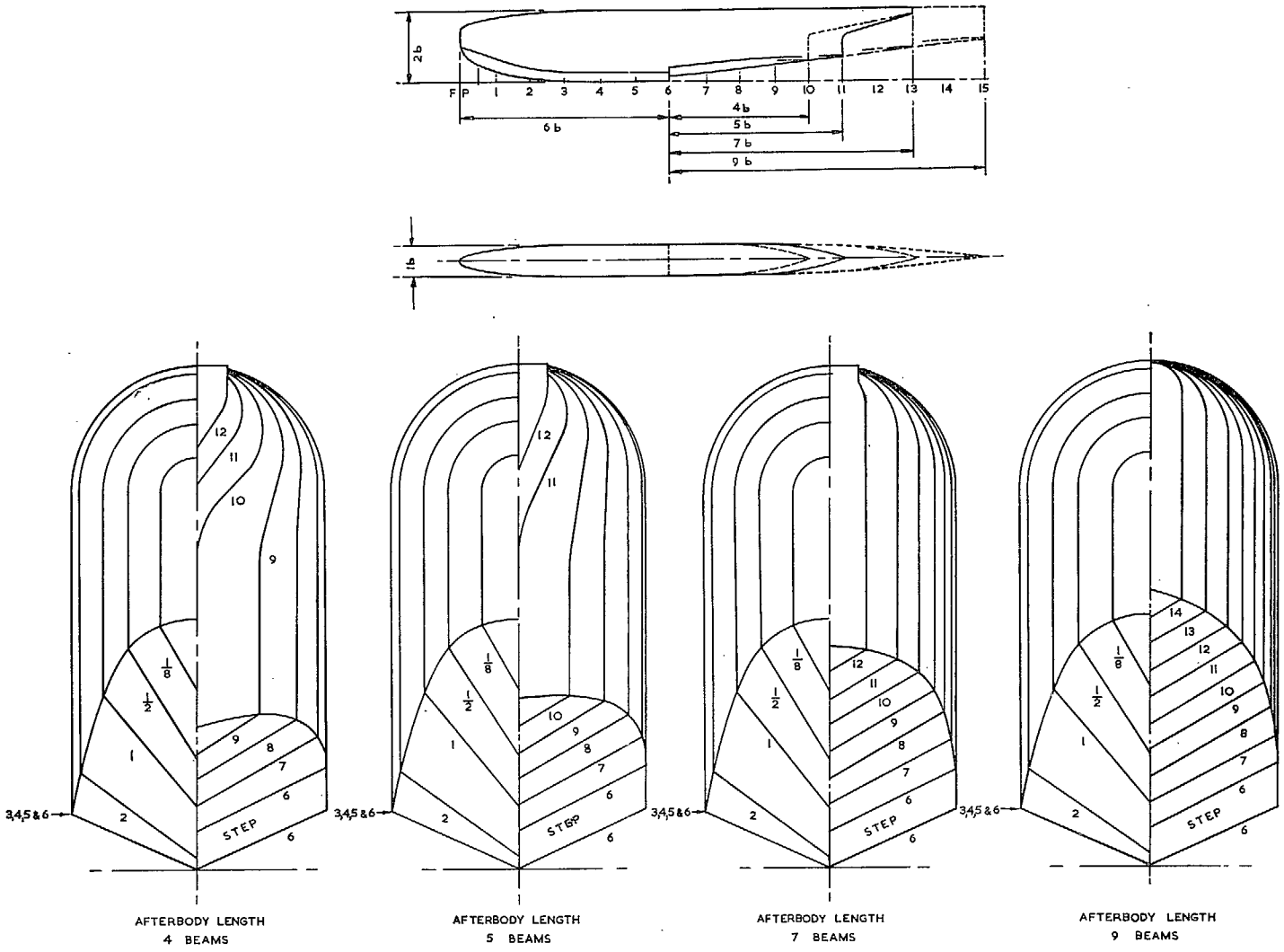

FIG. 56. Comparison of hull lines of Models A, D, E and F.

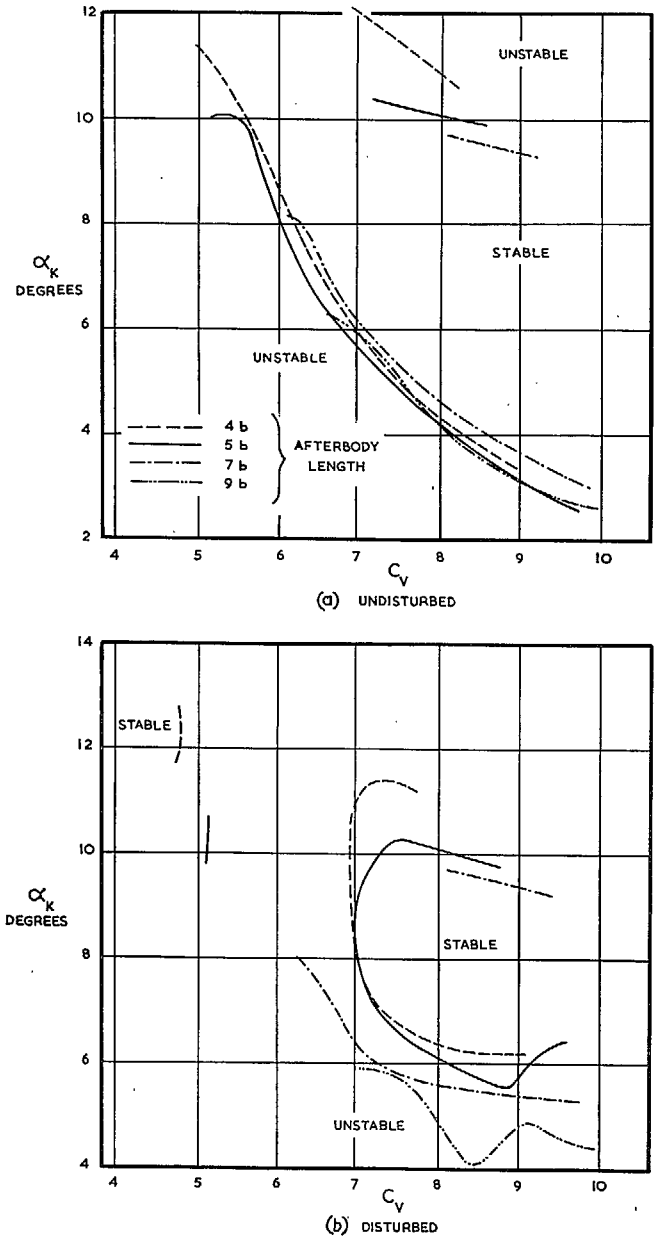

FIGS. 57a and 57b. Effect of afterbody length on longitudinal stability limits ($C_{\Delta 0} = 2{\cdot}25$).

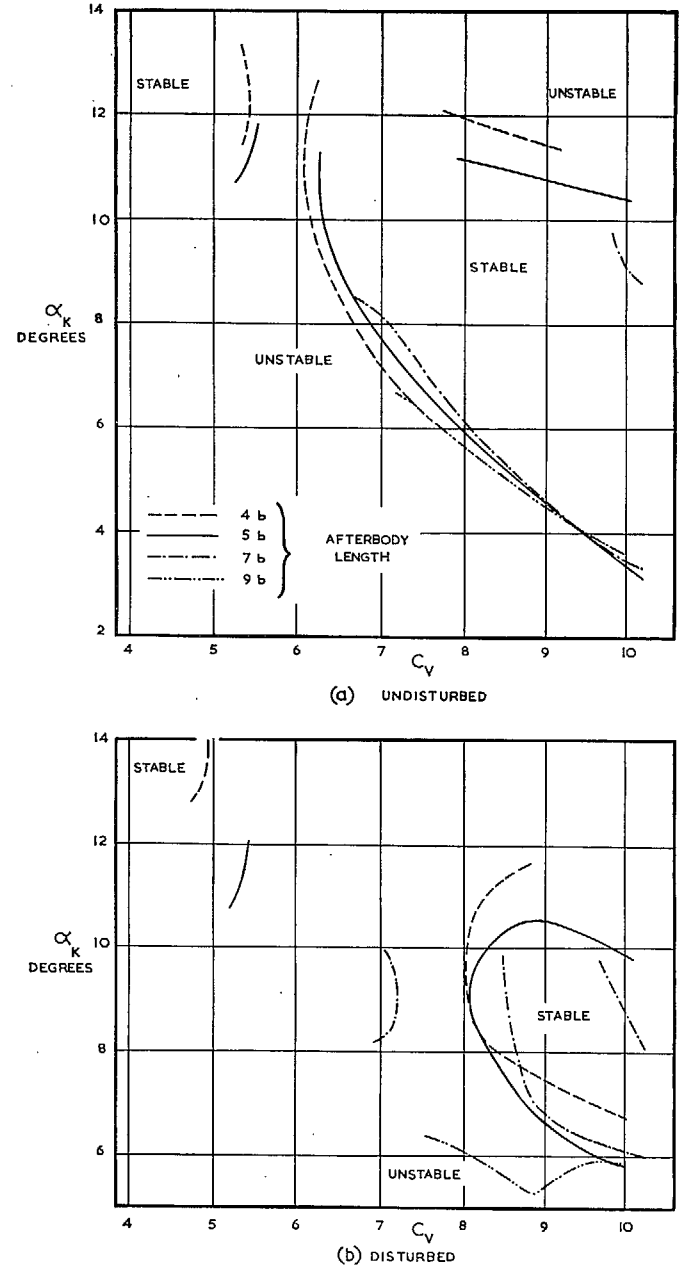

FIGS. 58a and 58b. Effect of afterbody length on longitudinal stability limits ($C_{\Delta 0} = 2{\cdot}75$).

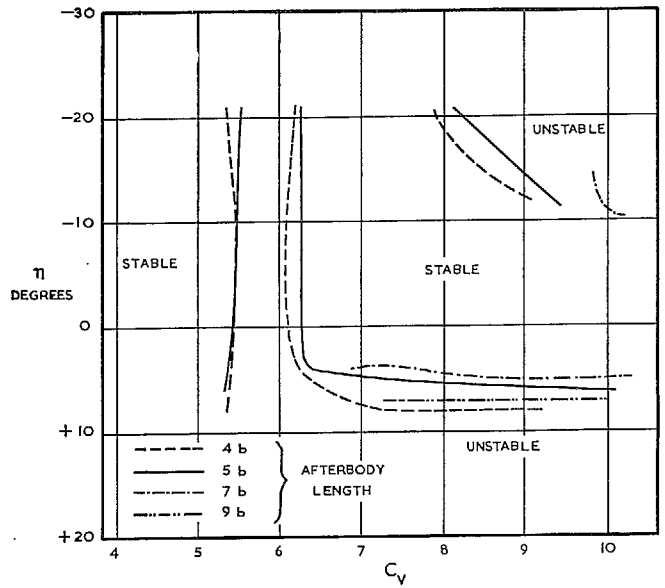

(a) UNDISTURBED

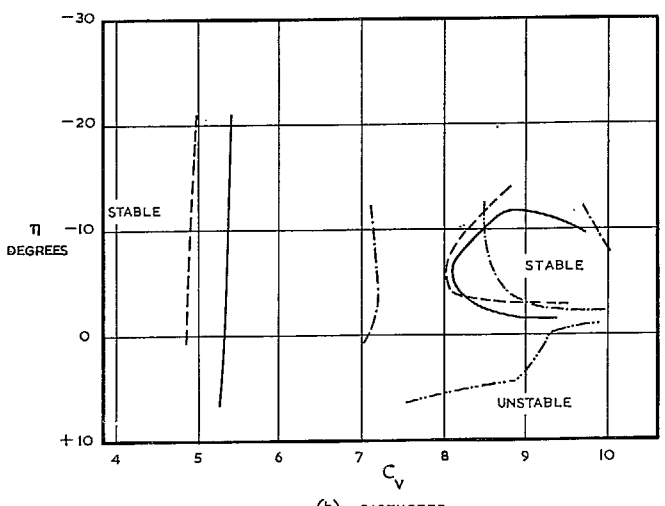

(b) DISTURBED

FIGS. 59a and 59b. Relation between elevator settings and longitudinal stability limits for Models A, D, E and F ($C_{\Delta 0} = 2{\cdot}75$).

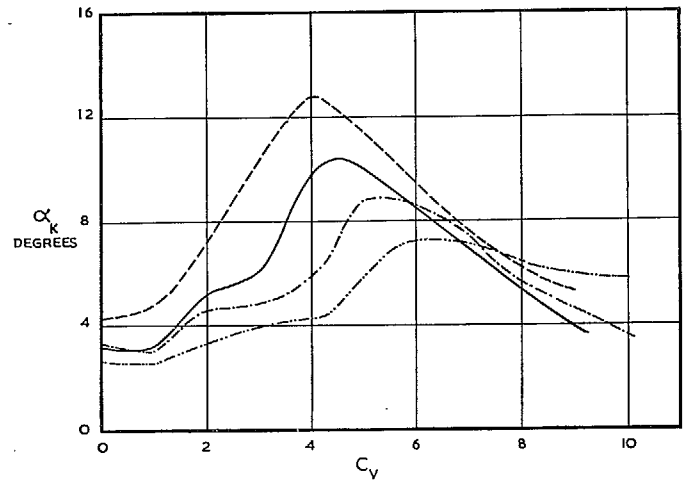

(a) $C_{\Delta_0} = 2{\cdot}25$

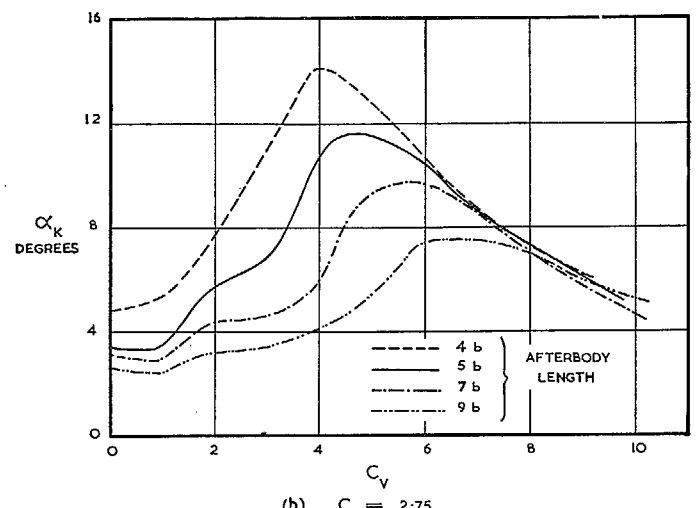

(b) $C_{\Delta_0} = 2{\cdot}75$

FIGS. 60a and 60b. Effect of afterbody length on trim curves ($\eta = 0$ deg.).

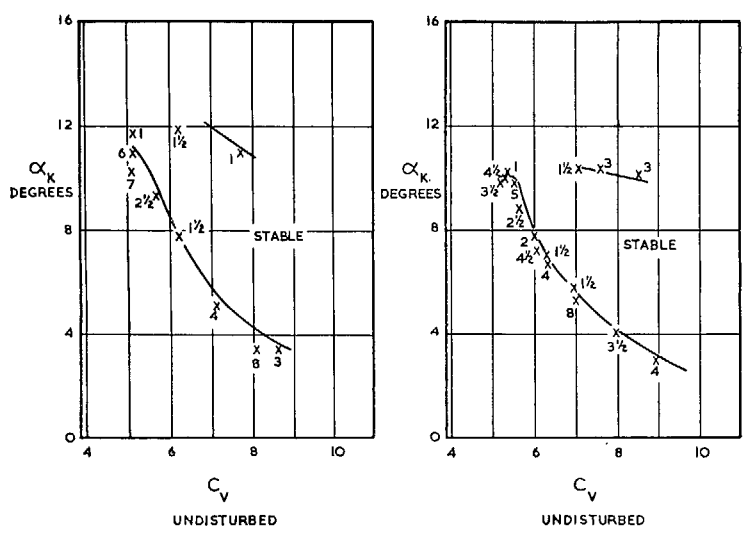

FIGURES INDICATE AMPLITUDES OF PORPOISING IN DEGREES

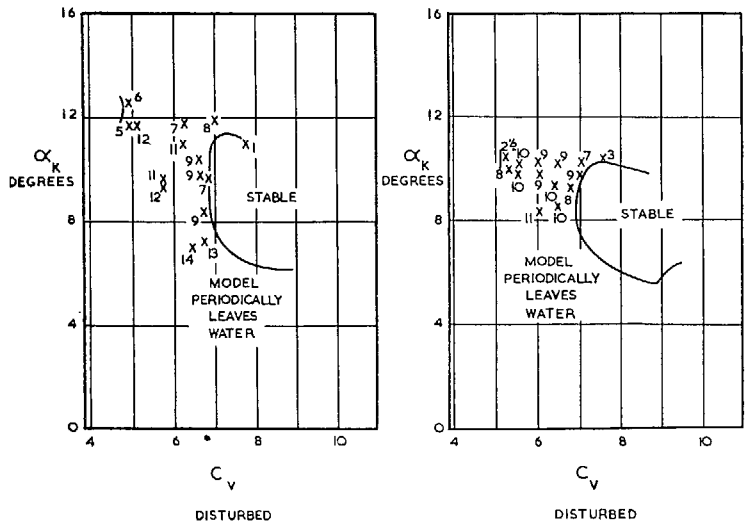

(a) AFTERBODY LENGTH 4 b (b) AFTERBODY LENGTH 5 b

FIG. 61 (1). Effect of afterbody length on amplitudes of porpoising ($C_{\Delta 0} = 2{\cdot}25$).

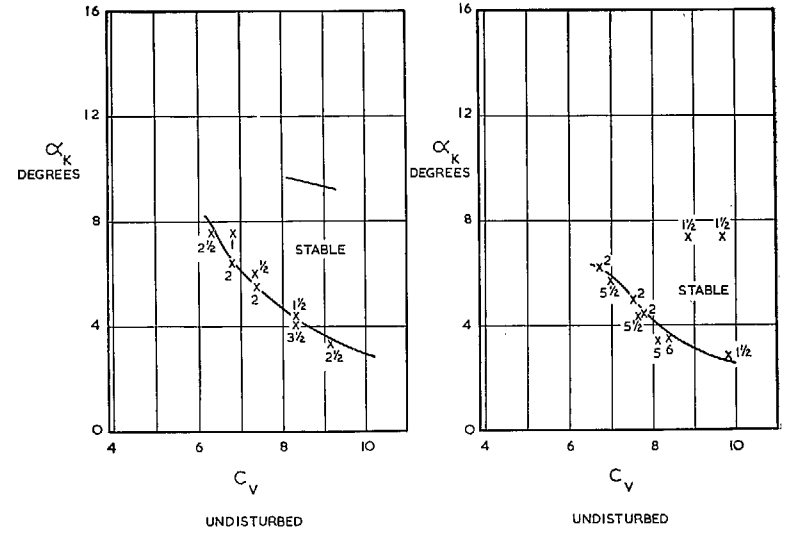

FIGURES INDICATE AMPLITUDES OF PORPOISING IN DEGREES

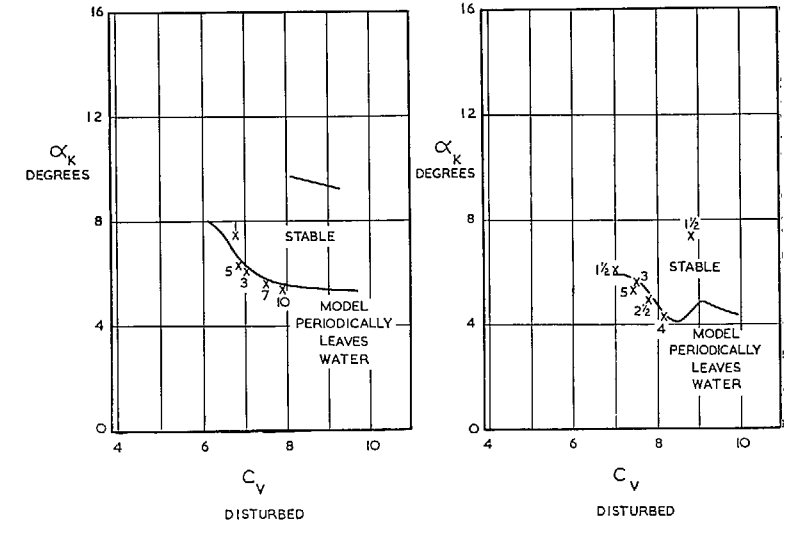

(c) AFTERBODY LENGTH 7 b (d) AFTERBODY LENGTH 9 b

FIG. 61 (2). Effect of afterbody length on amplitudes of porpoising ($C_{\Delta 0} = 2{\cdot}25$).

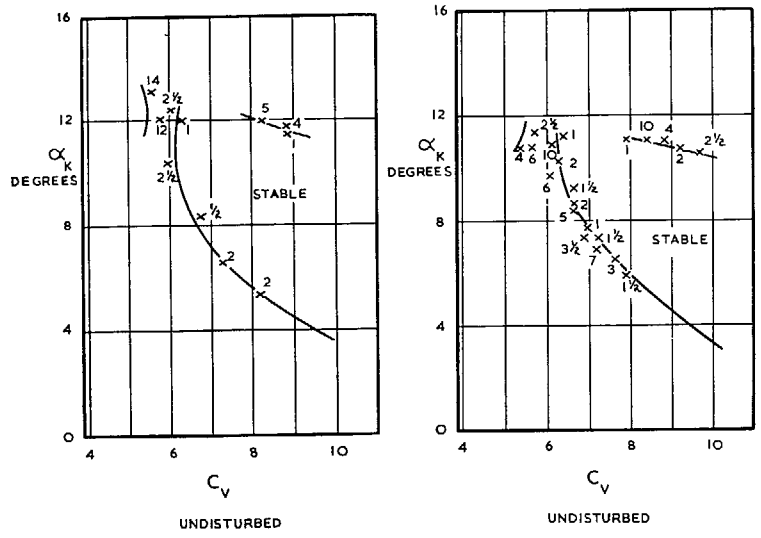

FIGURES INDICATE AMPLITUDES OF PORPOISING IN DEGREES

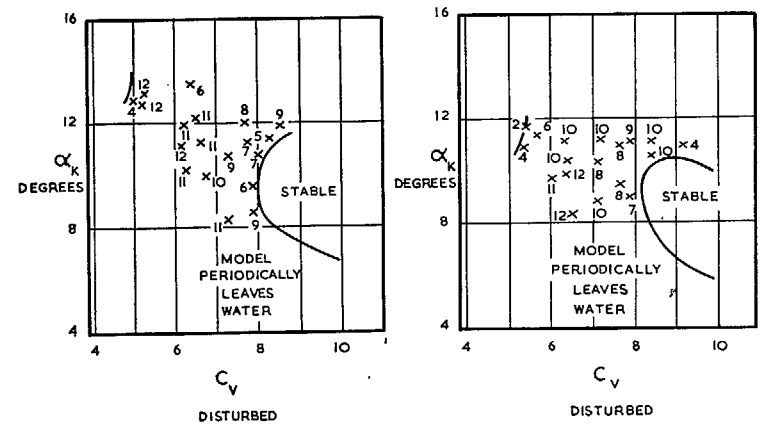

(a) AFTERBODY LENGTH 4 b (b) AFTERBODY LENGTH 5 b

FIG. 62 (1). Effect of afterbody length on amplitudes of porpoising ($C_{\Delta 0} = 2 \cdot 75$).

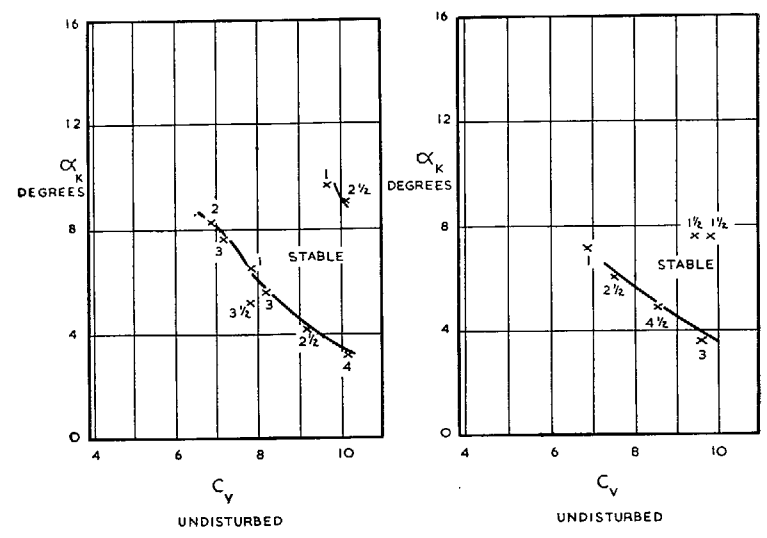

FIGURES INDICATE AMPLITUDES OF PORPOISING IN DEGREES

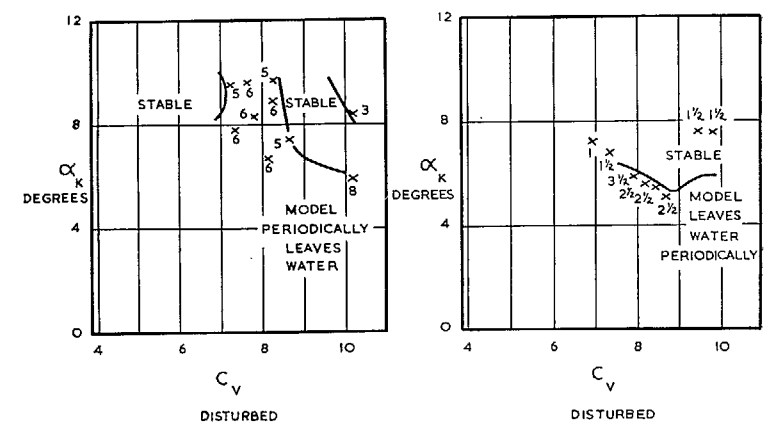

(c) AFTERBODY LENGTH 7 b (d) AFTERBODY LENGTH 9 b

FIG. 62 (2). Effect of afterbody length on amplitudes of porpoising ($C_{\Delta 0} = 2 \cdot 75$).

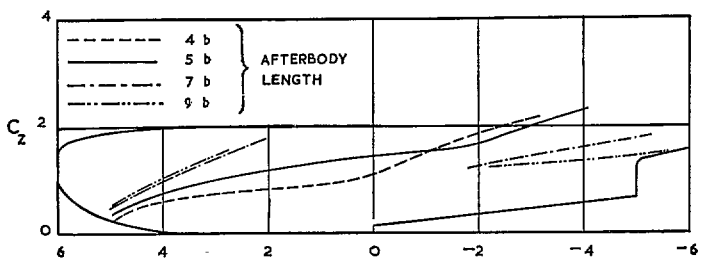

(a) $C_{\Delta_o} = 2{\cdot}25$

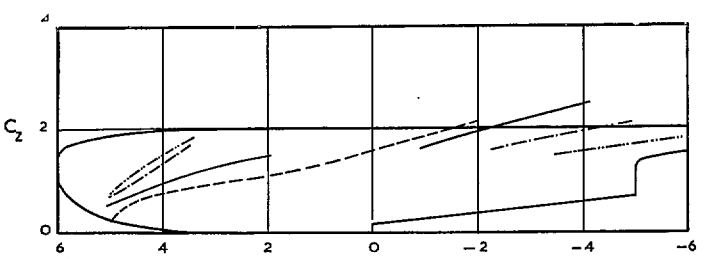

(b) $C_{\Delta_o} = 2{\cdot}75$

FIGS. 63a and 63b. Effect of afterbody length on spray projections.

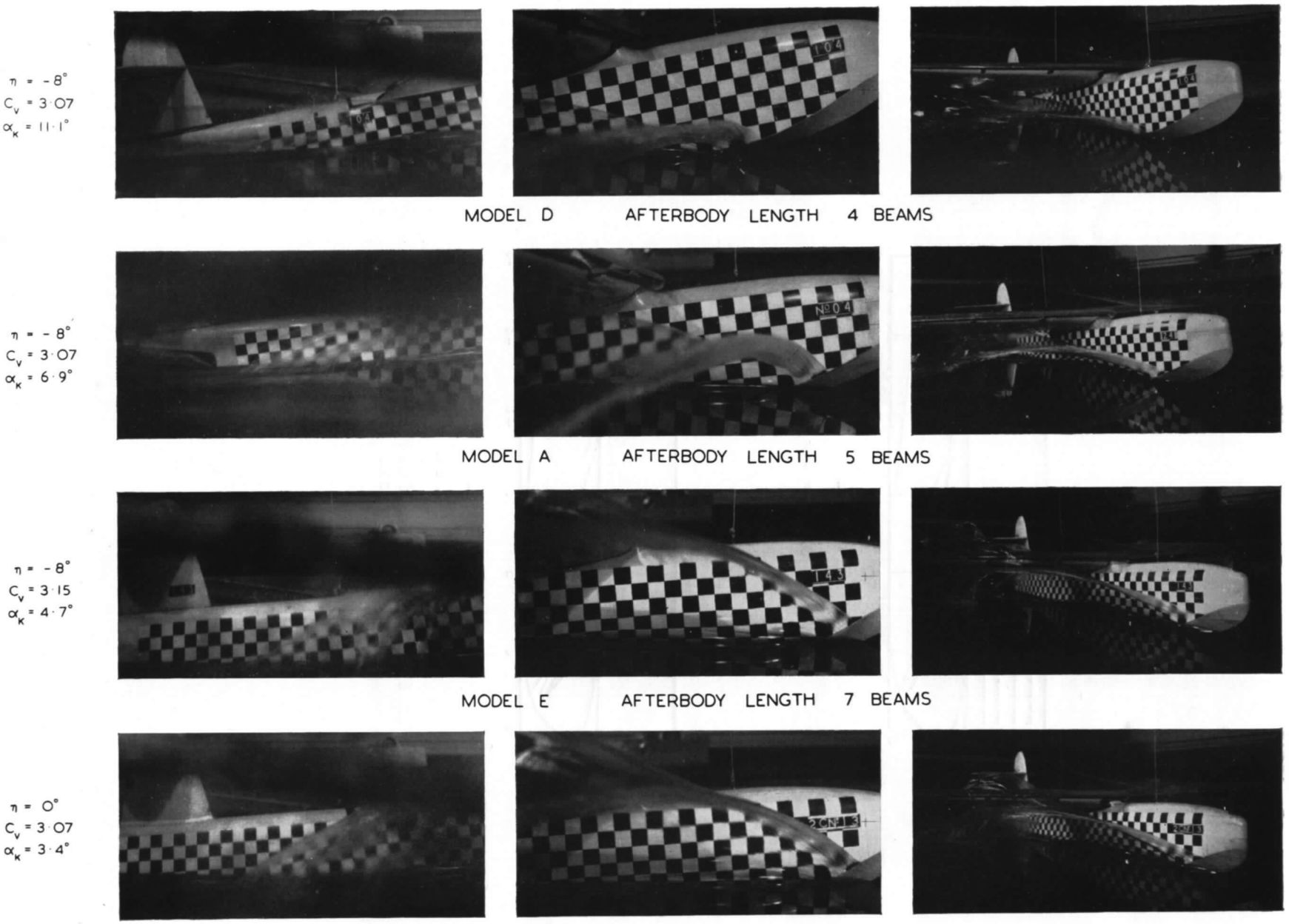

FIG. 64. Effect of afterbody length on spray ($C_{\Delta 0} = 2{\cdot}75$; $C_v = 3$).

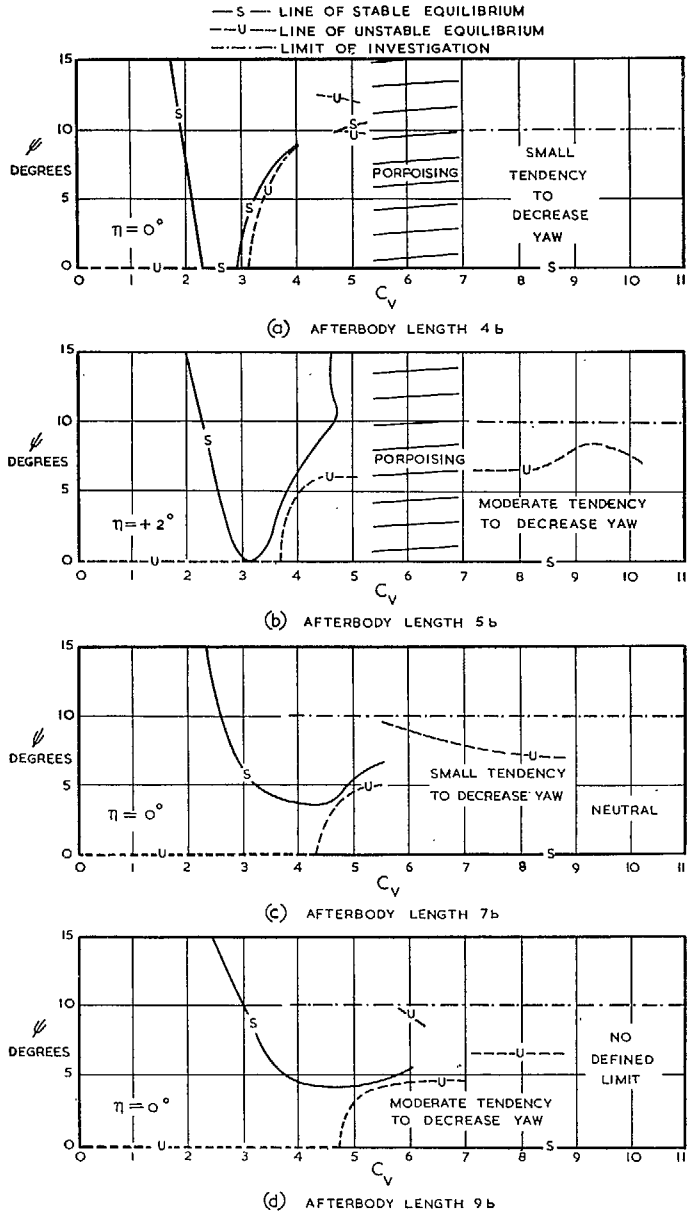

FIGS. 65a to 65d. Effect of afterbody length on directional stability ($C_{\Delta 0} = 2{\cdot}75$).

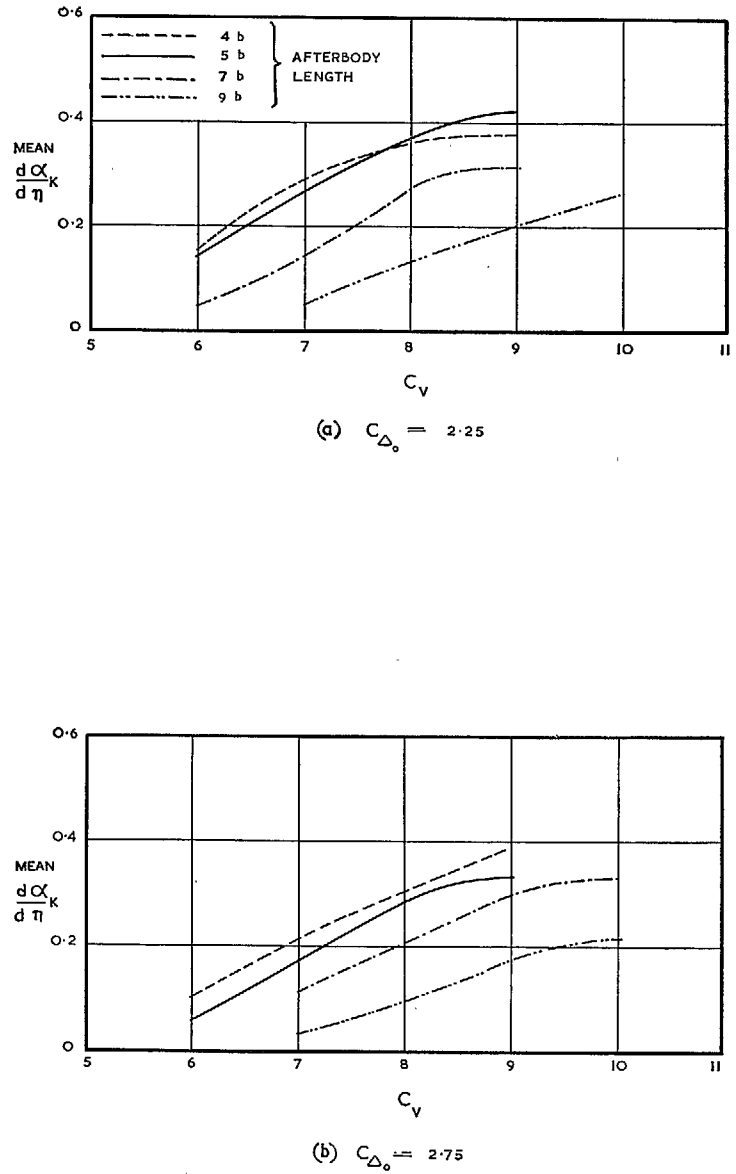

FIGS. 66a and 66b. Effect of afterbody length on elevator effectiveness.

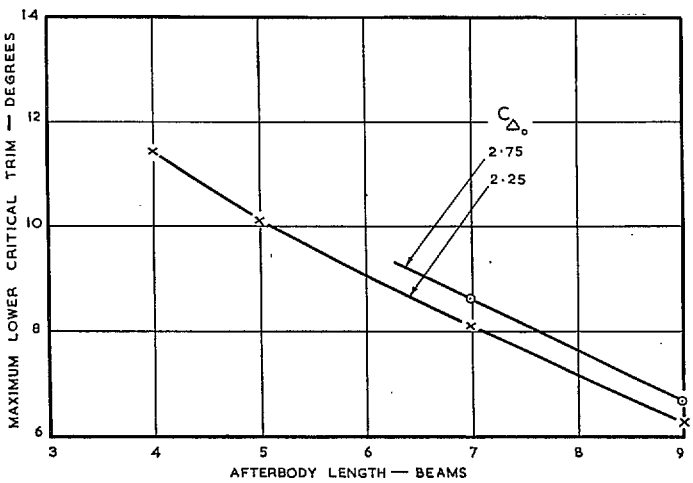

FIG. 67 Effect of afterbody length on maximum lower critical trim.

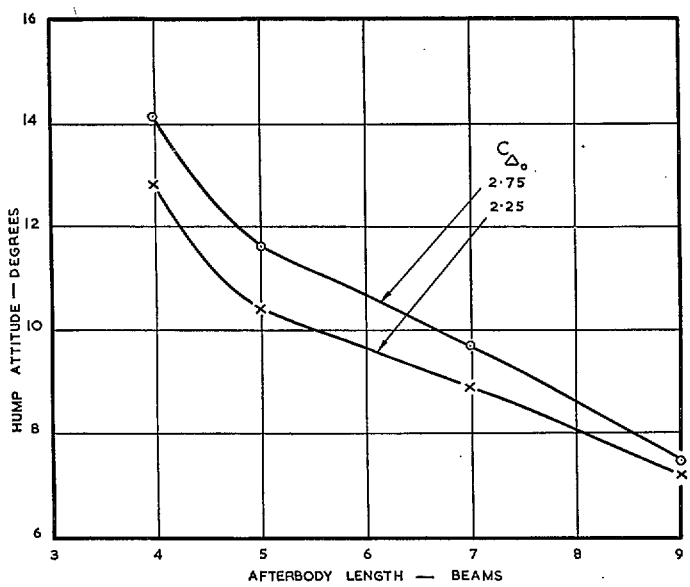

FIG. 68. Effect of afterbody length on hump attitude.

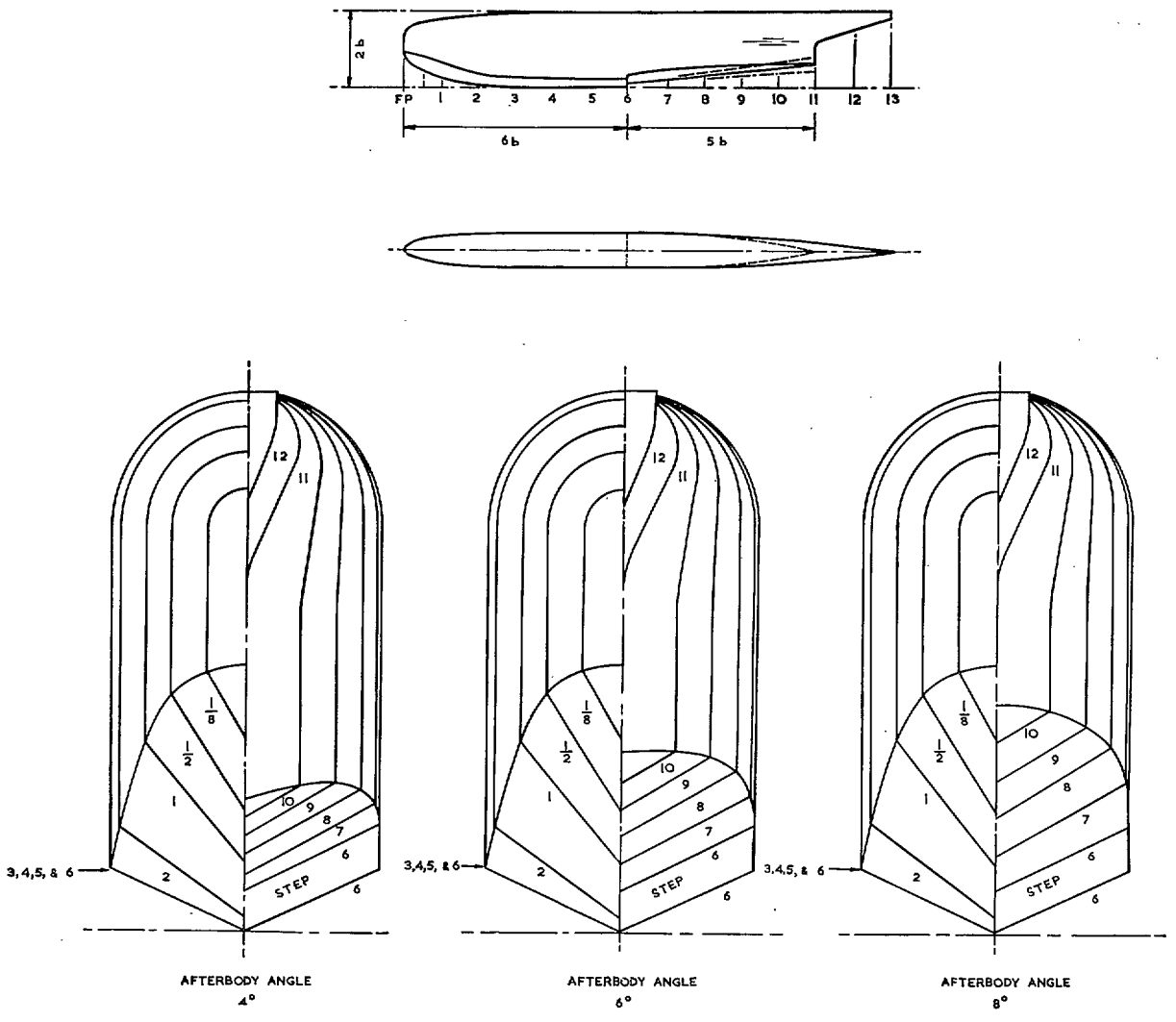

FIG. 69. Comparison of hull lines of Models A, G and H.

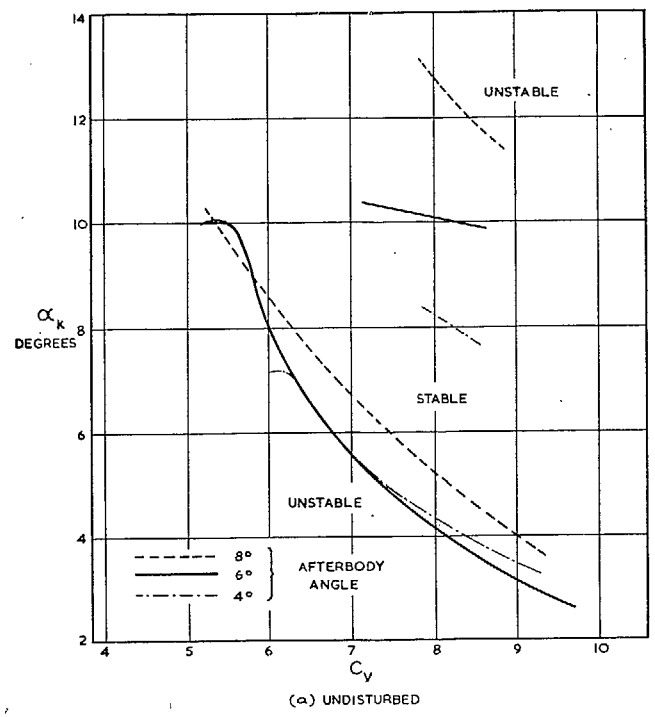

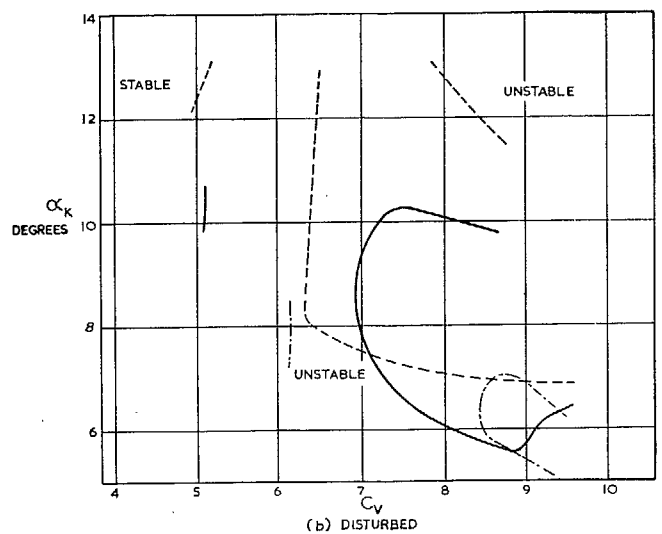

FIGS. 70a and 70b. Effect of afterbody angle on longitudinal stability limits ($C_{\Delta 0} = 2{\cdot}25$).

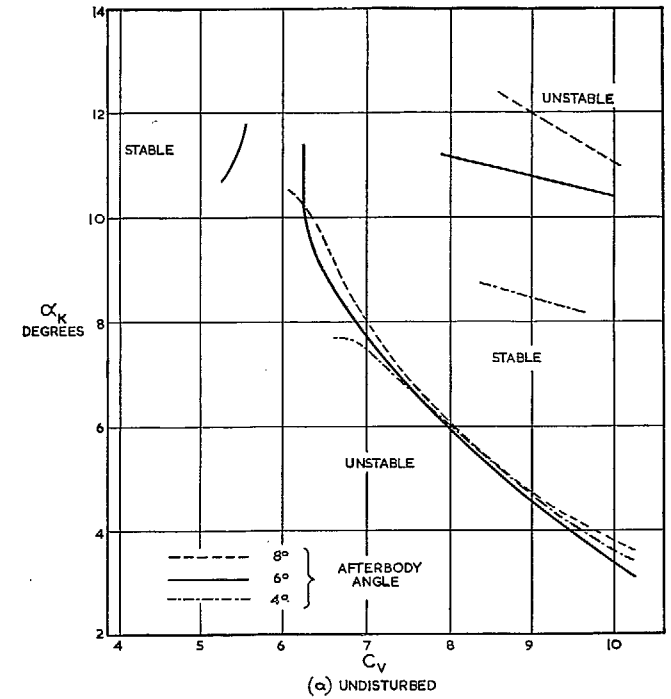

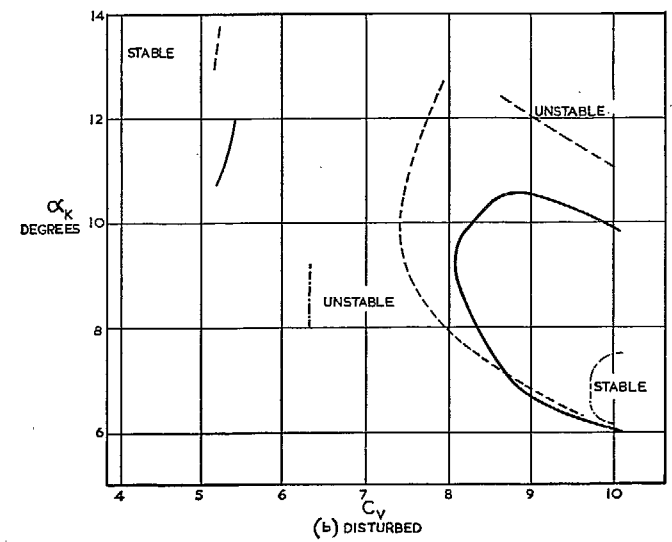

FIGS. 71a and 71b. Effect of afterbody angle on longitudinal stability limits ($C_{\Delta 0} = 2{\cdot}75$).

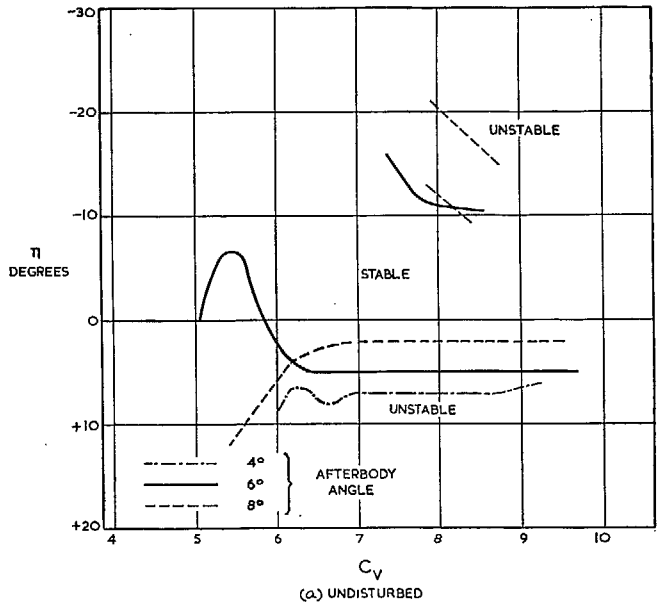

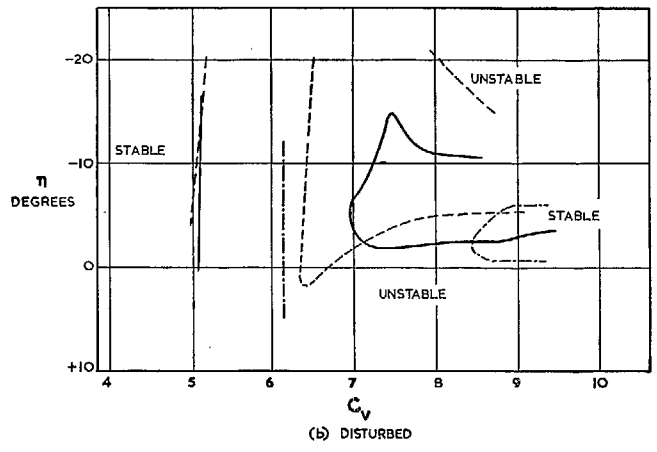

FIGS. 72a and 72b. Relation between elevator settings and longitudinal stability limits for Models A, G and H ($C_{\Delta 0} = 2{\cdot}25$).

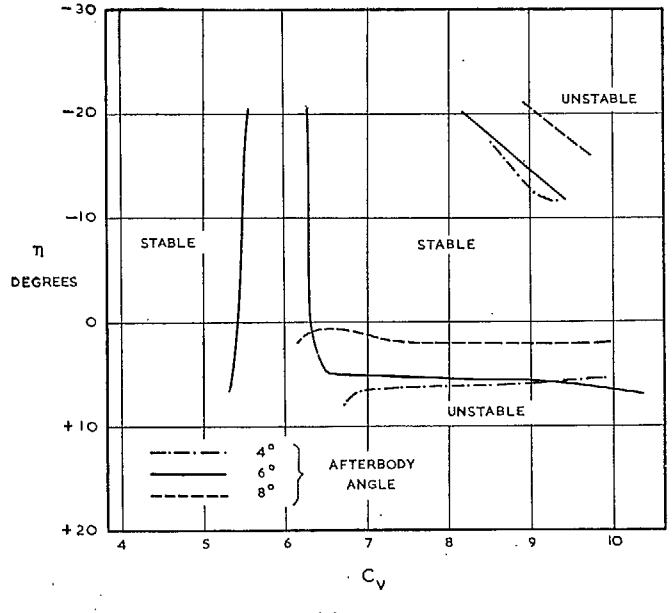

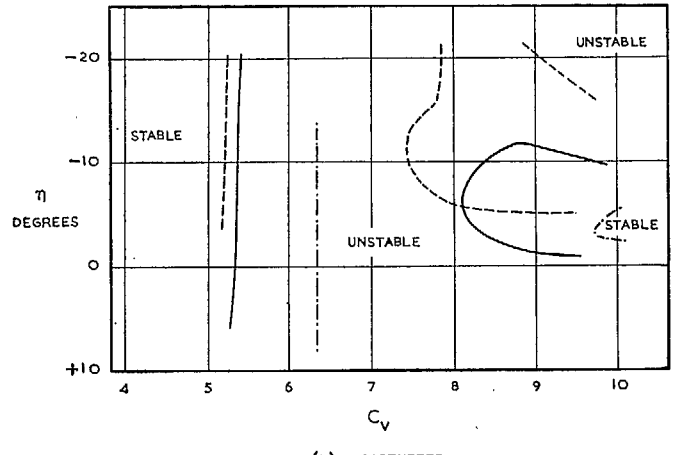

FIGS. 73a and 73b. Relation between elevator settings and longitudinal stability limits for Models A, G and H ($C_{\Delta 0} = 2{\cdot}75$).

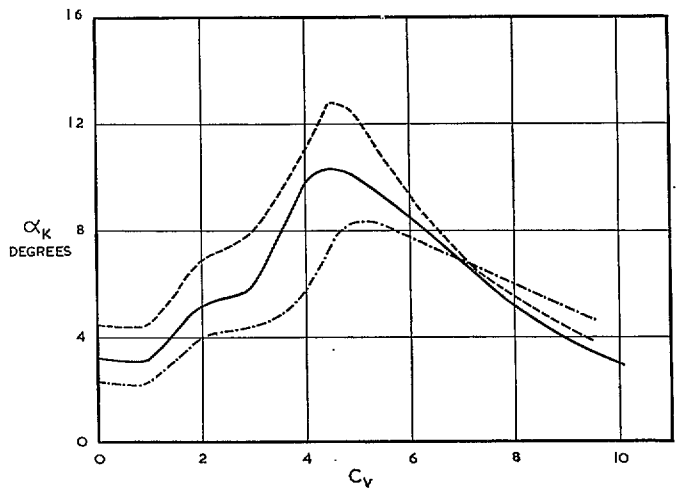

(a) $C_{\Delta_0} = 2{\cdot}25$

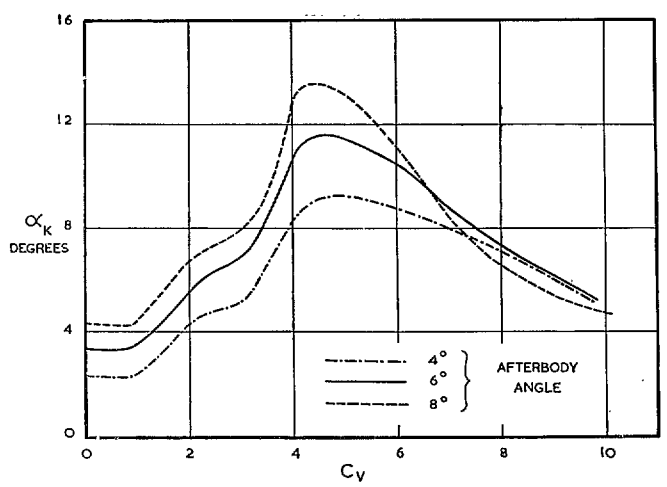

(b) $C_{\Delta_0} = 2{\cdot}75$

FIGS. 74a and 74b. Effect of afterbody angle on trim curves ($\eta = 0$ deg.).

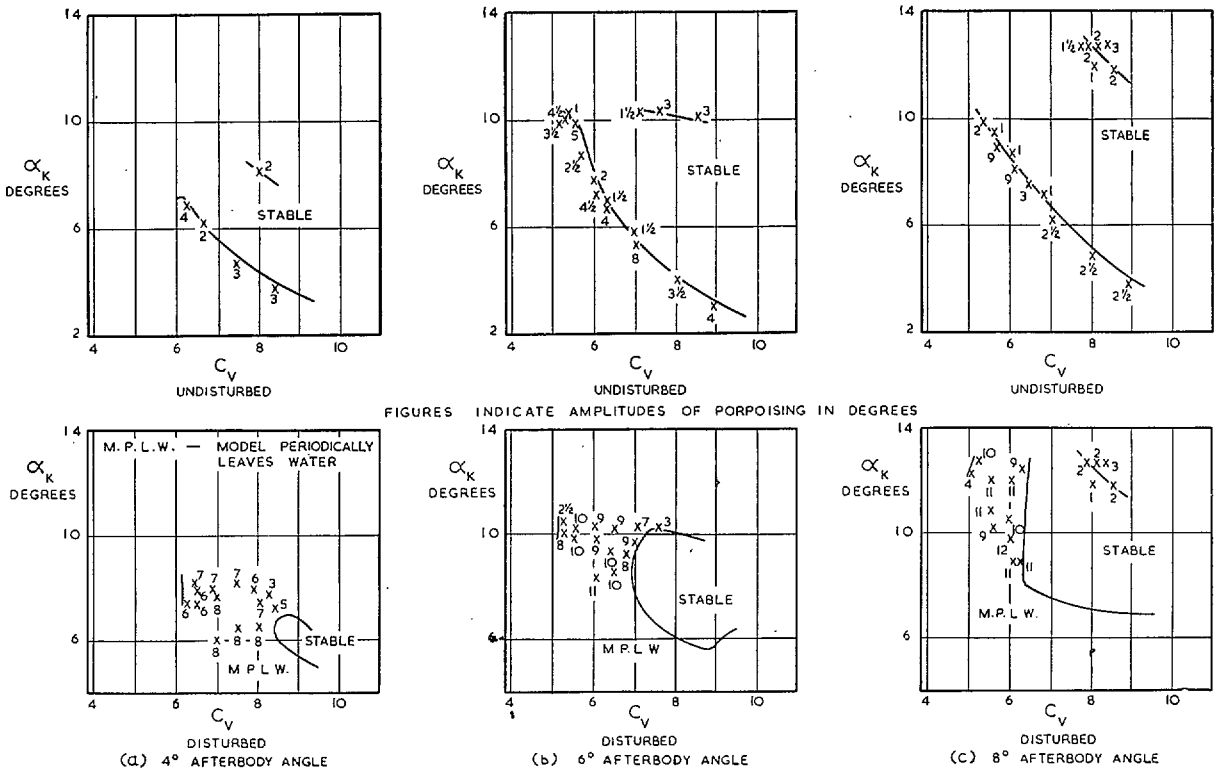

FIGS. 75a to 75c. Effect of afterbody angle on amplitudes of porpoising ($C_{\Delta 0} = 2{\cdot}25$).

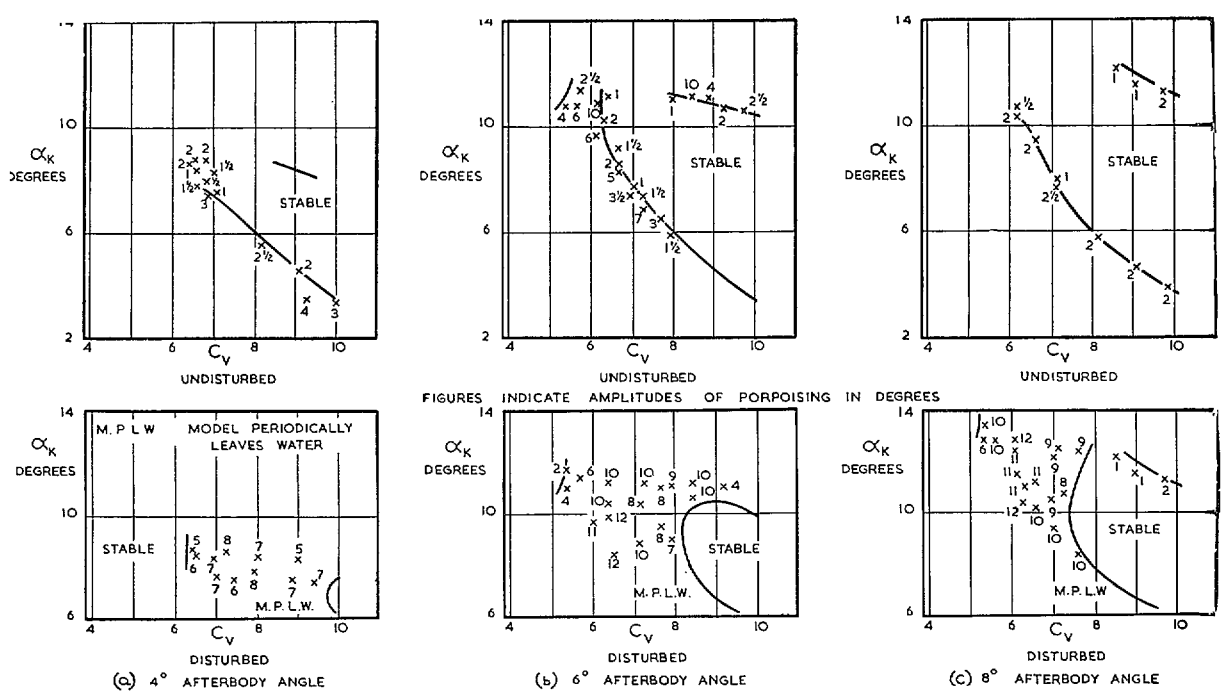

FIGS. 76a to 76c. Effect of afterbody angle on amplitudes of porpoising ($C_{\Delta 0} = 2{\cdot}75$).

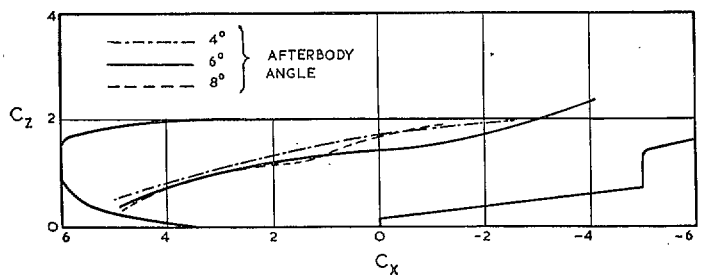

(a) $C_{\Delta_o} = 2{\cdot}25$

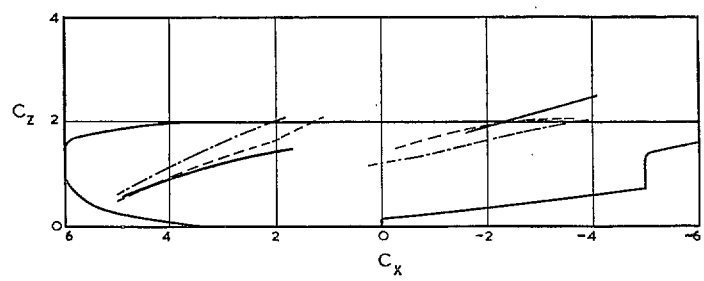

(b) $C_{\Delta_o} = 2{\cdot}75$

FIGS. 77a and 77b. Effect of afterbody angle on spray projections.

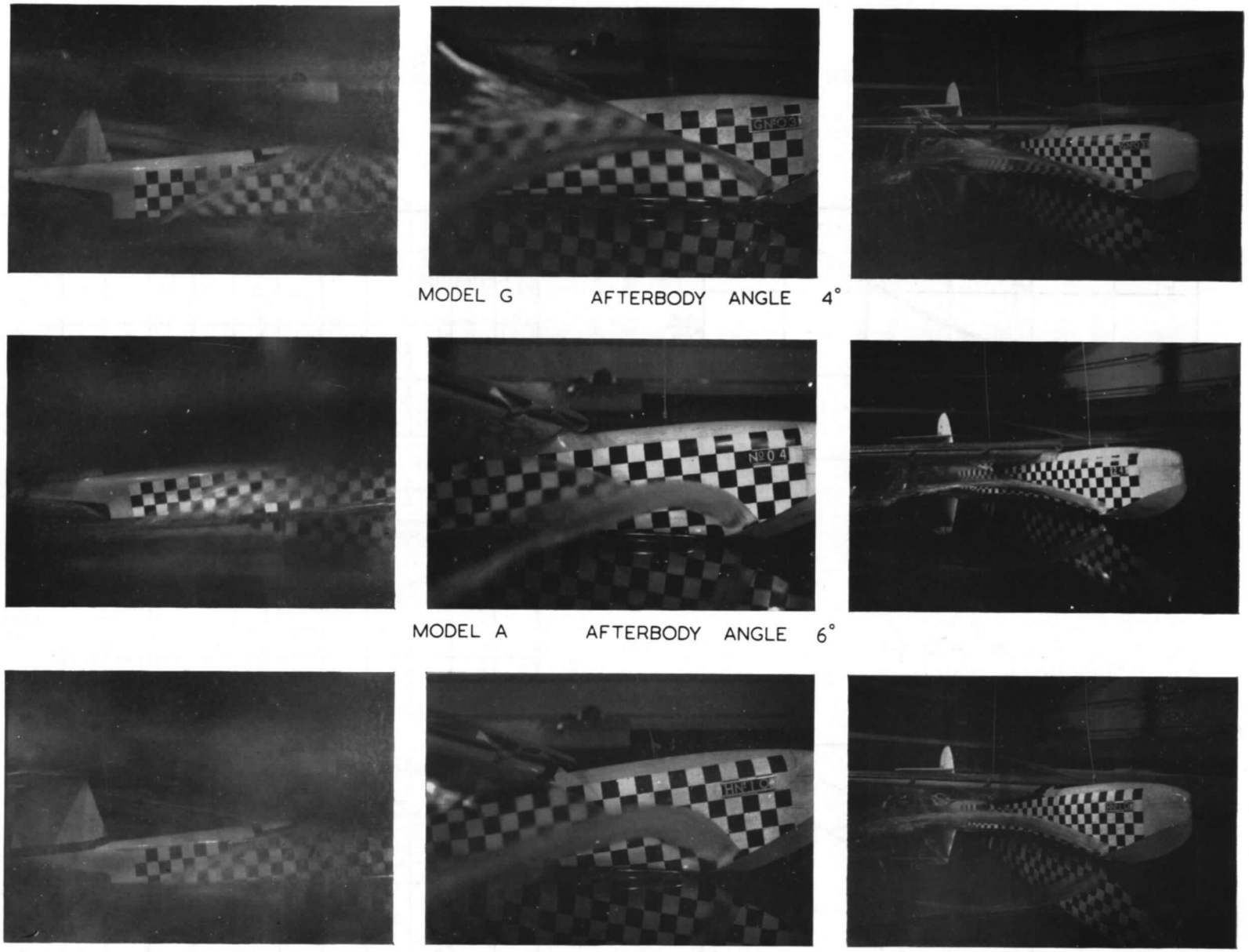

FIG. 78. Effect of afterbody angle on spray ($C_{\Delta 0} = 2{\cdot}75$; $C_v = 3$).

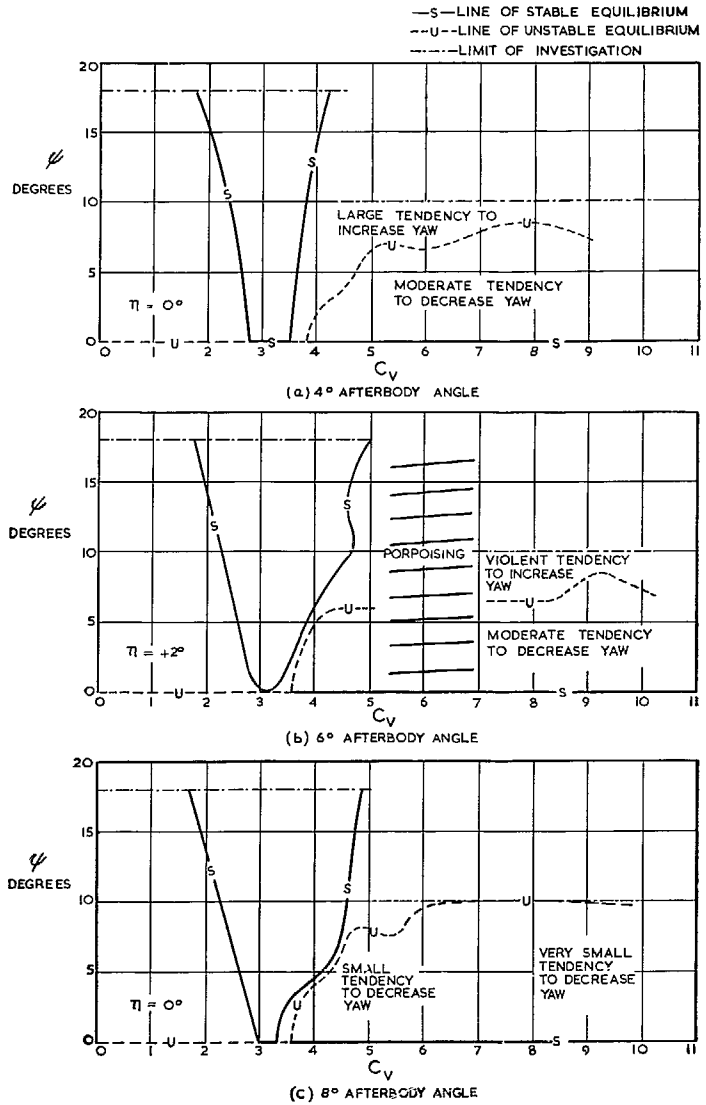

FIGS. 79a to 79c. Effect of afterbody angle on directional stability ($C_{\Delta 0} = 2{\cdot}75$).

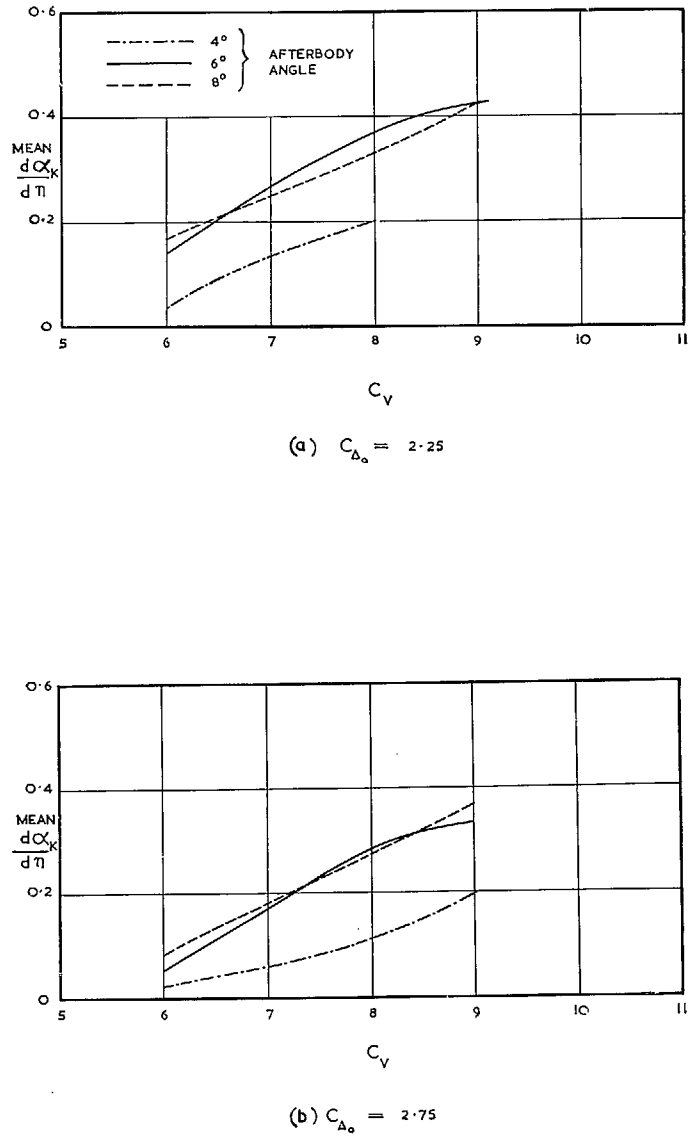

FIGS. 80a and 80b. Effect of afterbody angle on elevator effectiveness.

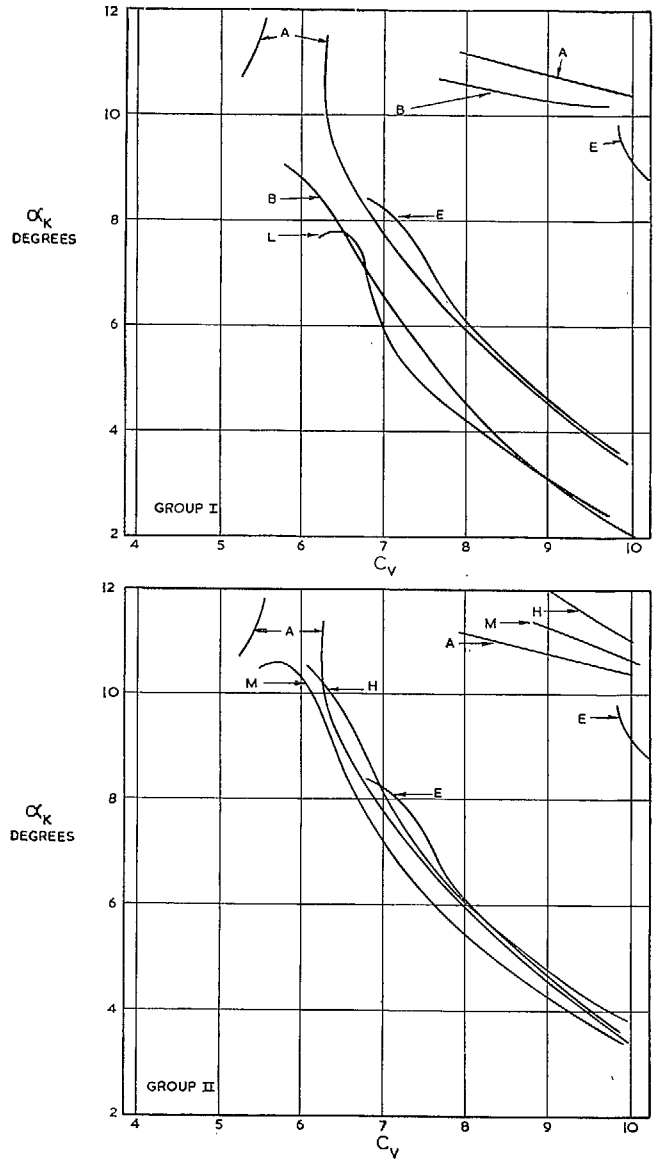

FIG. 81 (1). Longitudinal stability limits for interaction investigation on a C_v base, undisturbed case ($C_{\Delta 0} = 2{\cdot}75$).

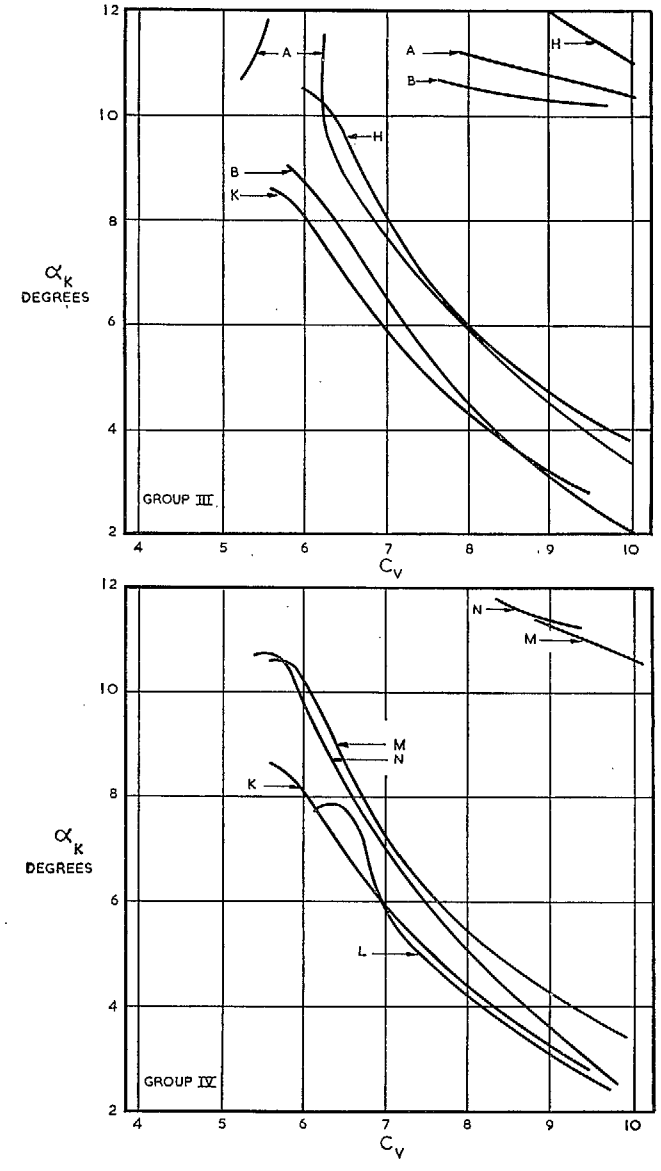

FIG. 81 (2). Longitudinal stability limits for interaction investigation on a C_v base, undisturbed case ($C_{\Delta 0} = 2{\cdot}75$).

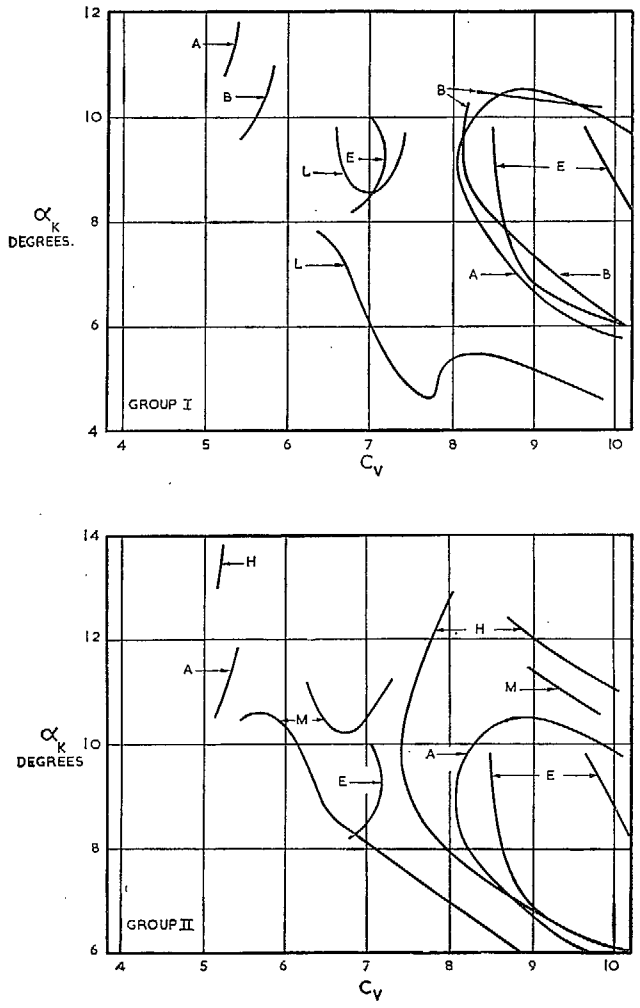

FIG. 82 (1). Longitudinal stability limits for interaction investigation on a C_v base, disturbed case ($C_{\Delta 0} = 2{\cdot}75$).

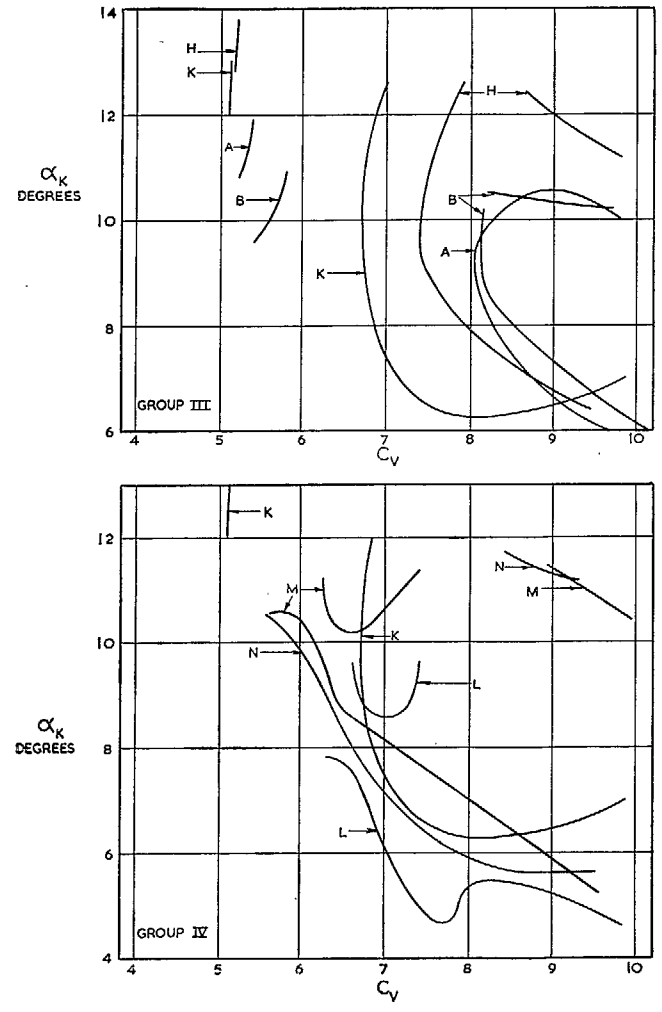

FIG. 82 (2). Longitudinal stability limits for interaction investigation on a C_v base, disturbed case ($C_{\Delta 0} = 2{\cdot}75$).

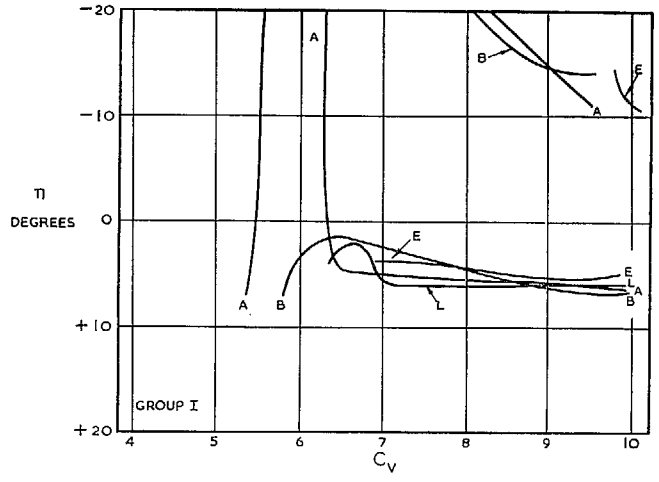

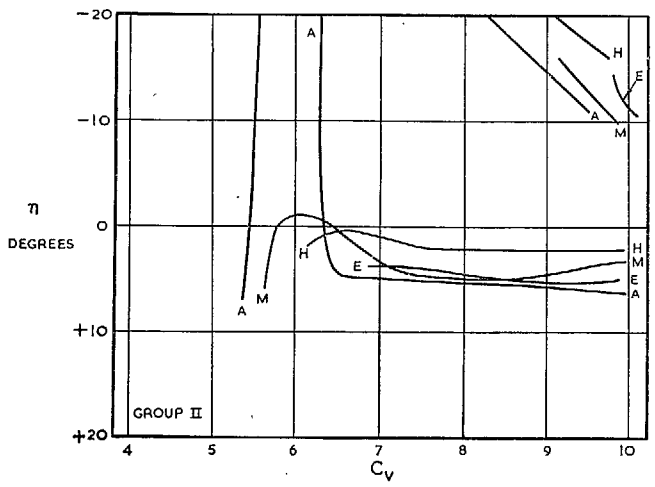

FIG. 83 (1). Relation between elevator settings and longitudinal stability limits for interaction investigation, undisturbed case ($C_{\Delta 0} = 2{\cdot}75$).

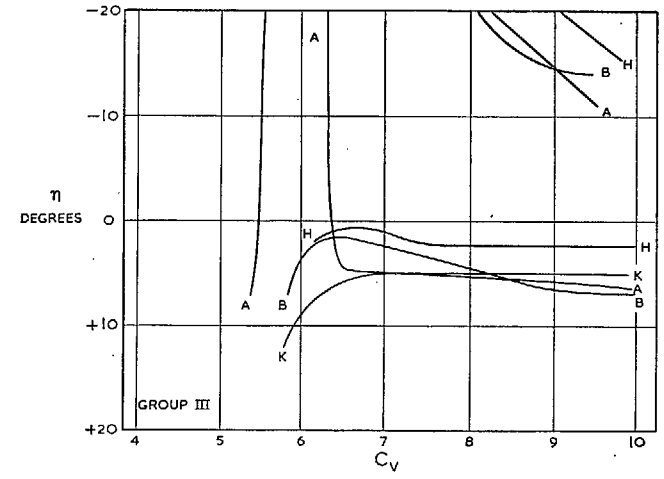

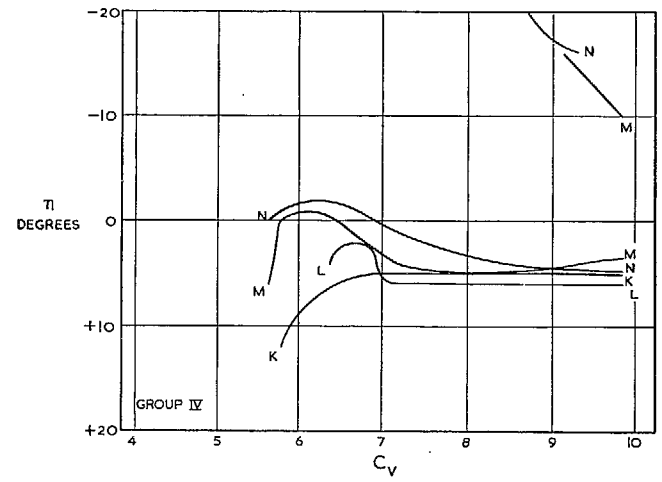

FIG. 83 (2). Relation between elevator settings and longitudinal stability limits for interaction investigation, undisturbed case ($C_{\Delta 0} = 2{\cdot}75$).

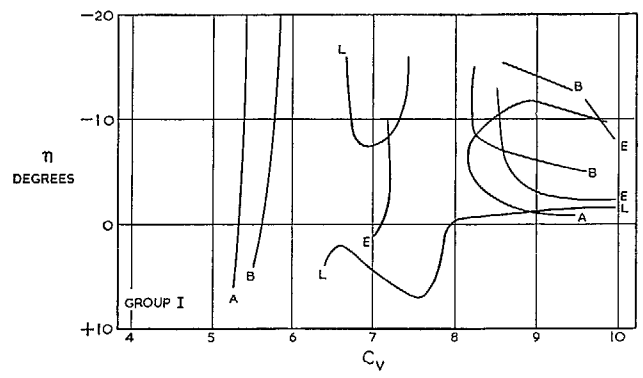

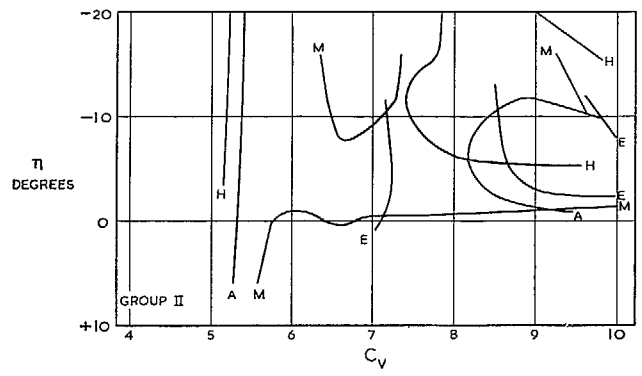

FIG. 84 (1). Relation between elevator settings and longitudinal stability limits for interaction investigation, disturbed case ($C_{\Delta 0} = 2{\cdot}75$).

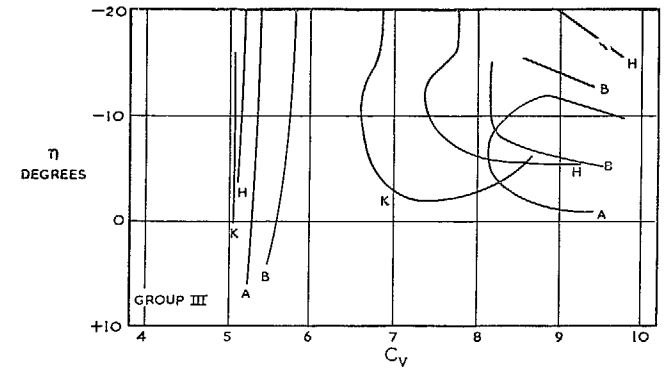

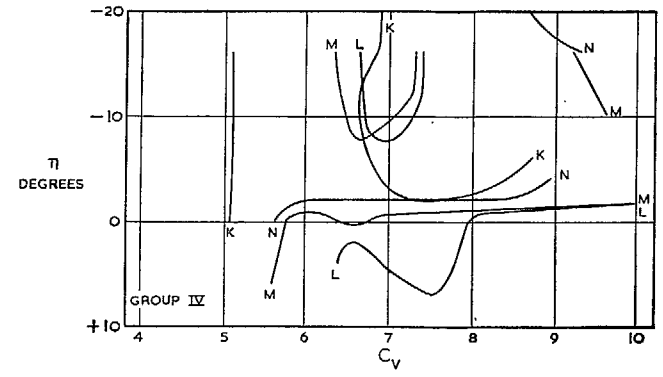

FIG. 84 (2). Relation between elevator settings and longitudinal stability limits for interaction investigation, disturbed case ($C_{\Delta 0} = 2{\cdot}75$).

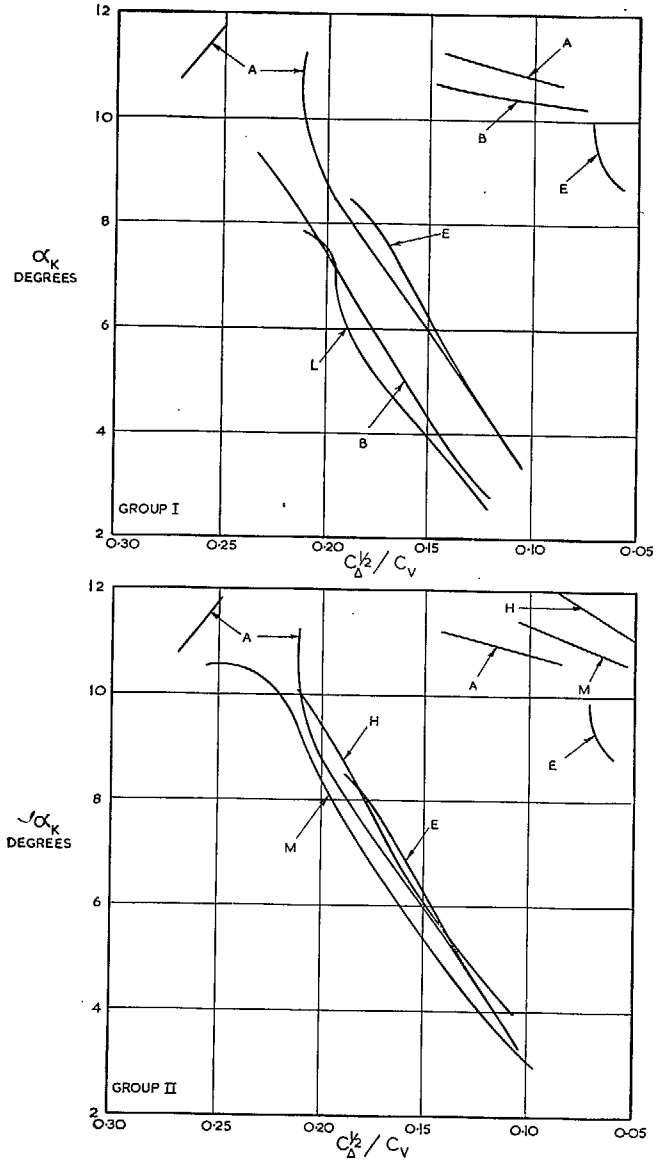

FIG. 85 (1). Longitudinal stability limits for interaction investigation on a $C_\Delta{}^{1/2}/C_v$ base, undisturbed case ($C_{\Delta 0} = 2{\cdot}75$).

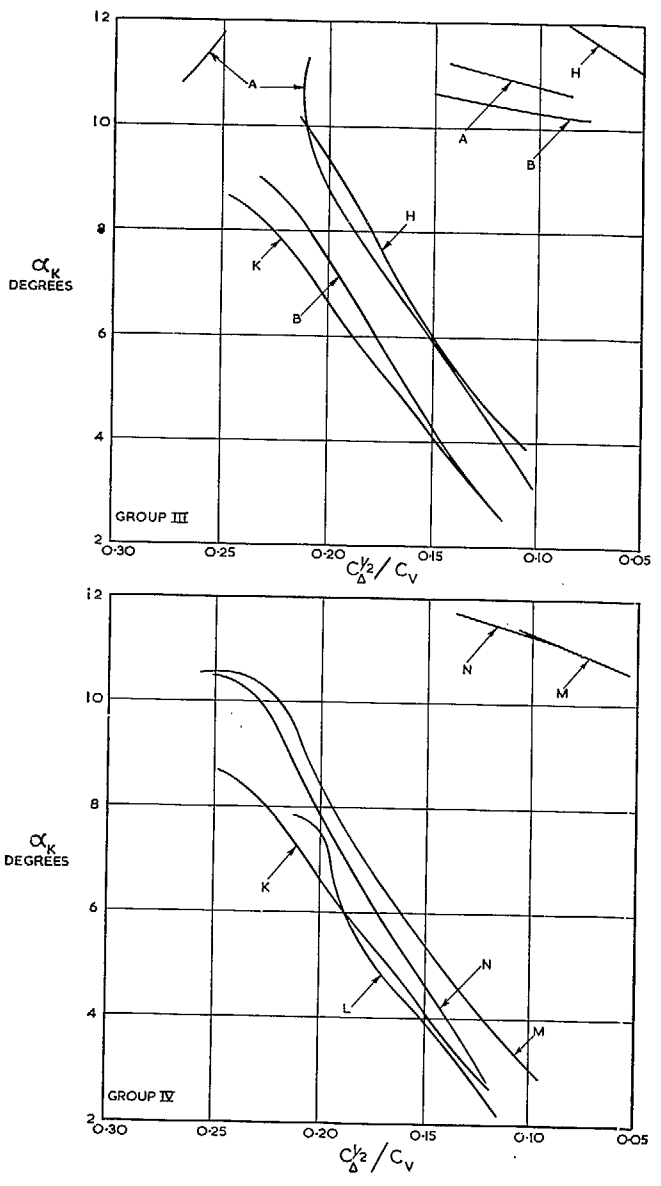

FIG. 85 (2). Longitudinal stability limits for interaction investigation on a $C_\Delta{}^{1/2}/C_v$ base, undisturbed case ($C_{\Delta 0} = 2{\cdot}75$).

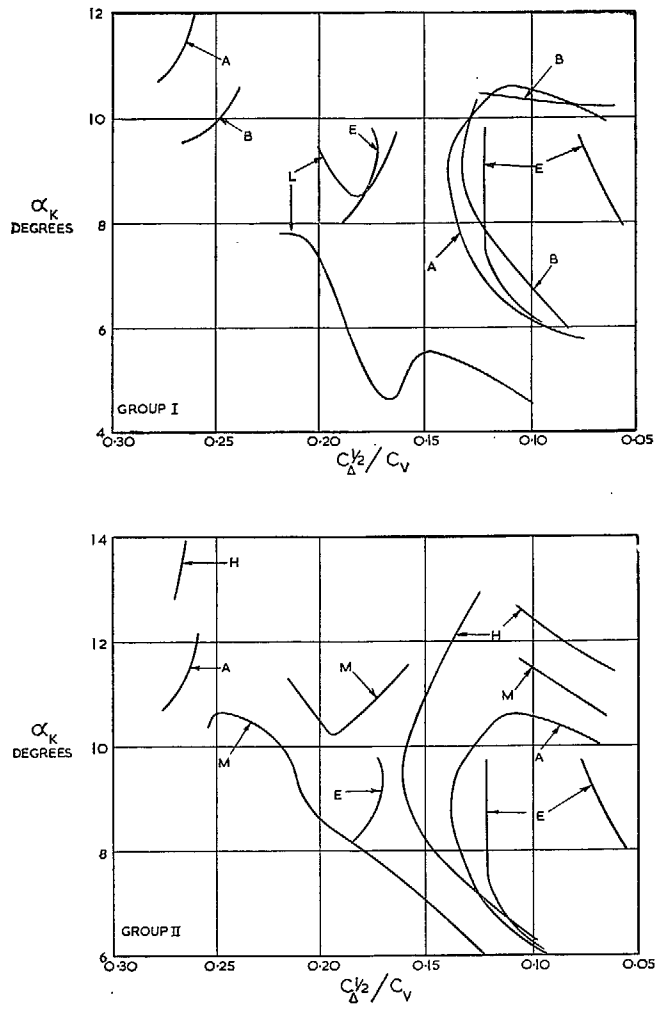

FIG. 86 (1). Longitudinal stability limits for interaction investigation on a $C_\Delta^{1/2}/C_v$ base, disturbed case ($C_{\Delta 0} = 2{\cdot}75$).

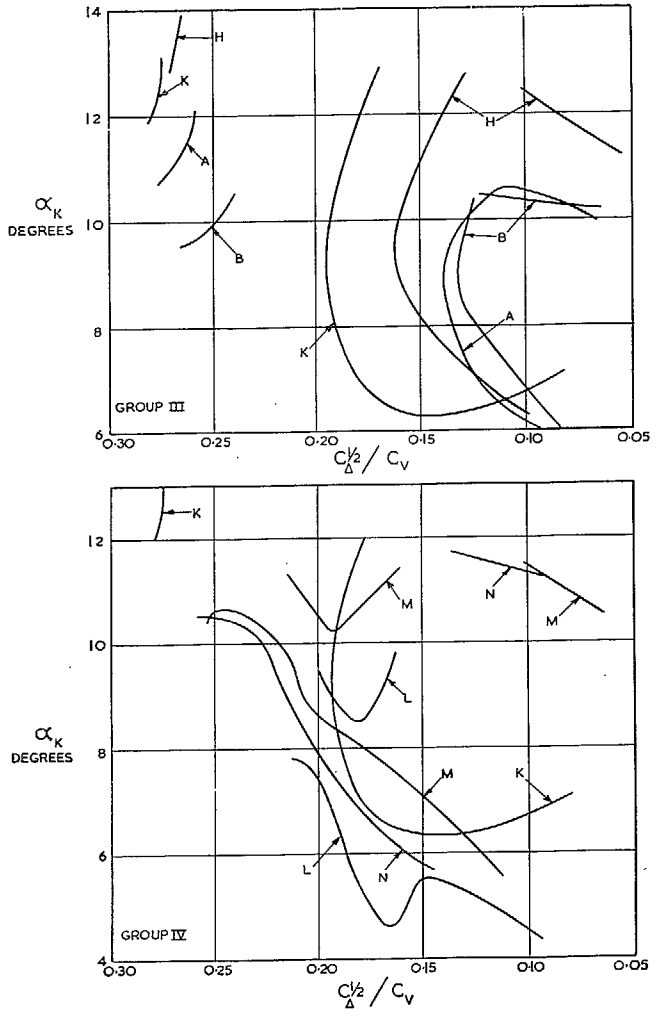

FIG. 86 (2). Longitudinal stability limits for interaction investigation on a $C_\Delta^{1/2}/C_v$ base, disturbed case ($C_{\Delta 0} = 2{\cdot}75$).

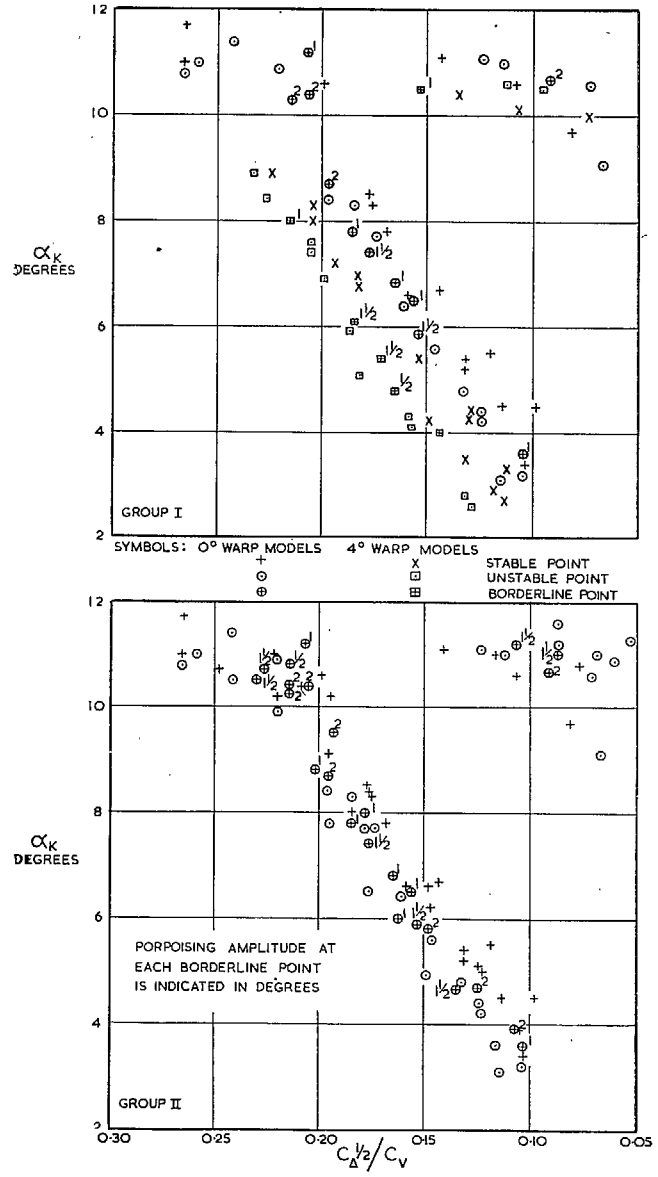

FIG. 87 (1). Points defining longitudinal stability limits for interaction investigation on a $C_{\Delta}{}^{1/2}/C_v$ base, undisturbed case ($C_{\Delta 0} = 2{\cdot}75$).

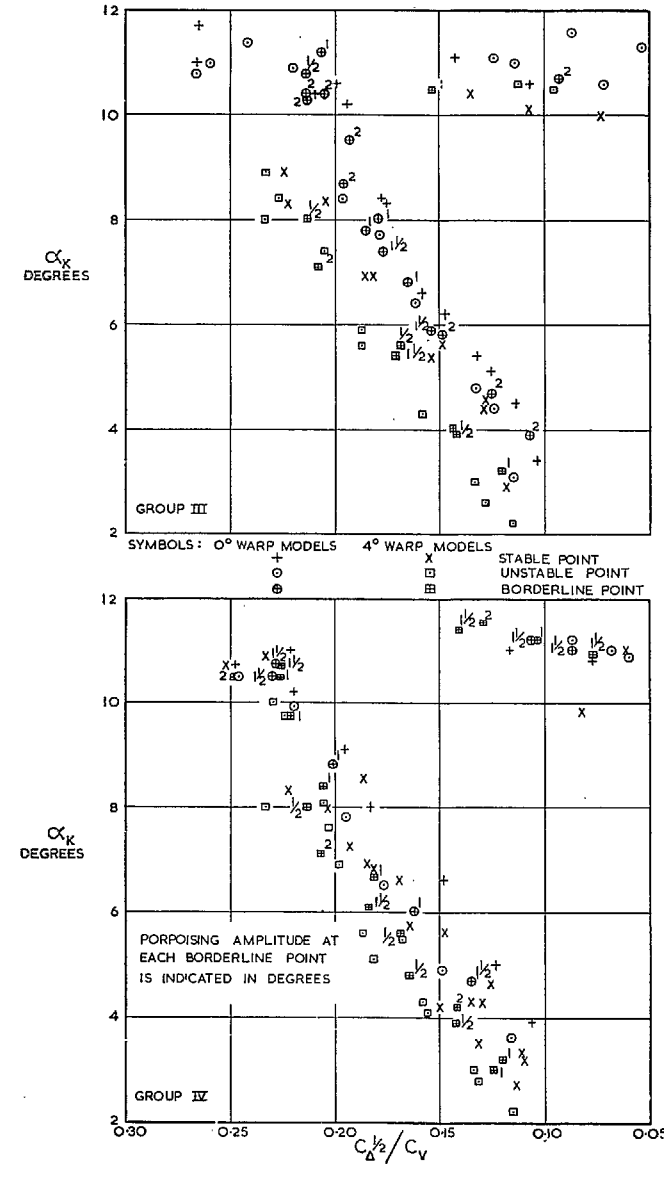

FIG. 87 (2). Points defining longitudinal stability limits for interaction investigation on a $C_{\Delta}{}^{1/2}/C_v$ base, undisturbed case ($C_{\Delta 0} = 2{\cdot}75$).

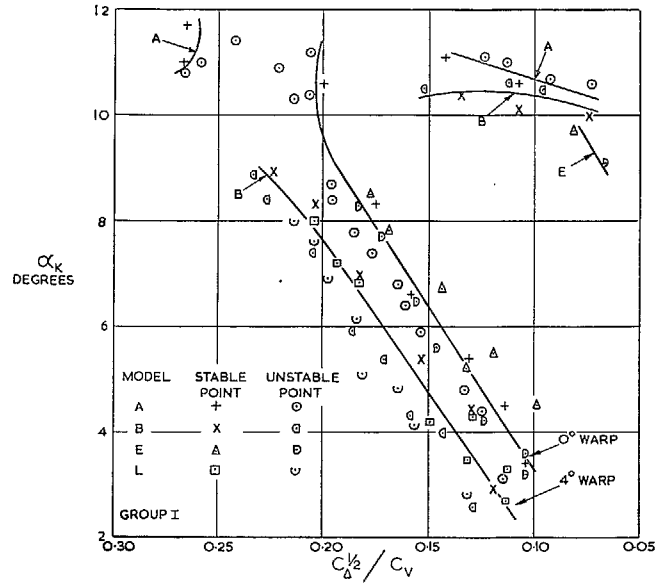

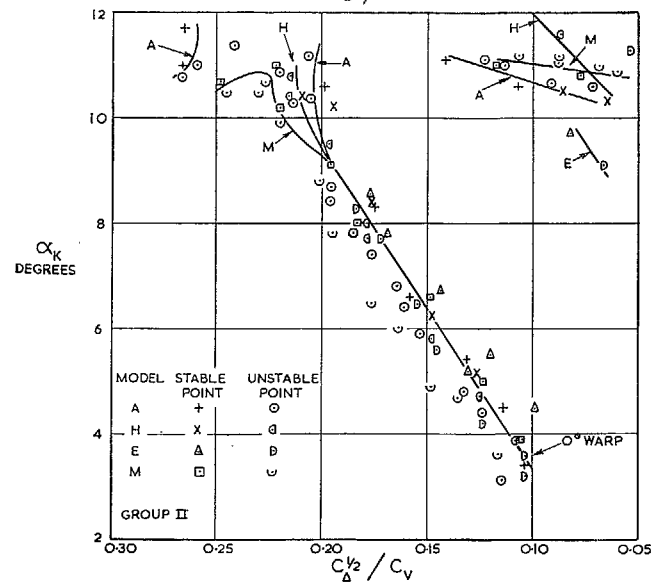

FIG. 88 (1). Redefined longitudinal stability limits for interaction investigation on a $C_{\Delta}{}^{1/2}/C_v$ base, undisturbed case ($C_{\Delta 0} = 2{\cdot}75$).

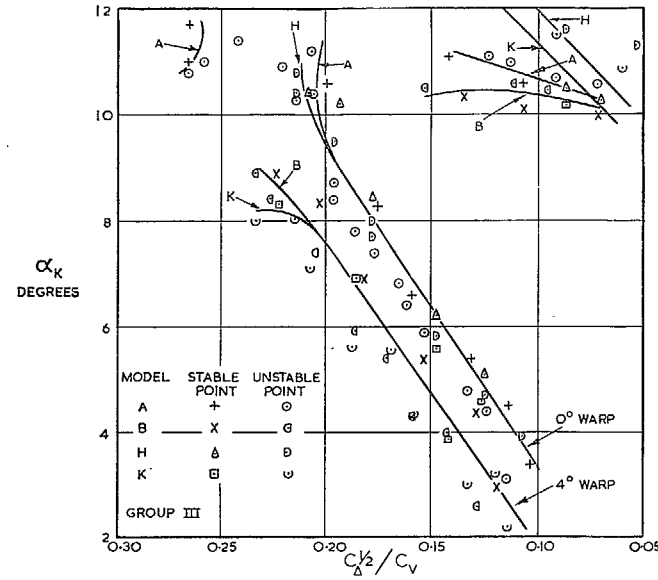

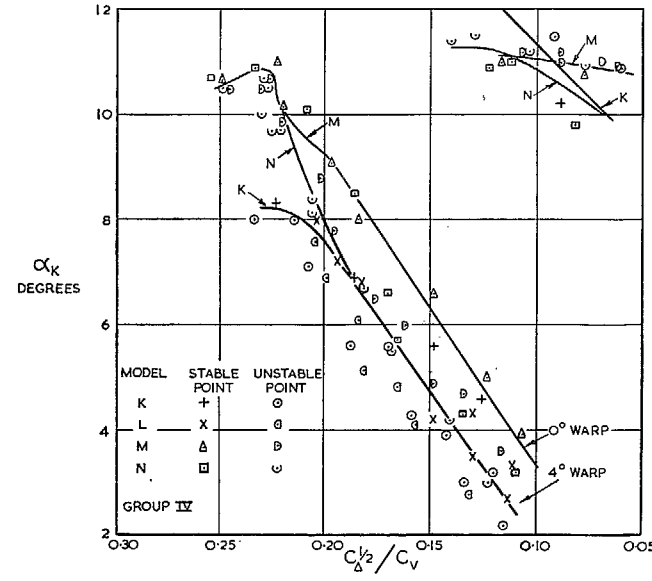

FIG. 88 (2). Redefined longitudinal stability limits for interaction investigation on a $C_{\Delta}{}^{1/2}/C_v$ base, undisturbed case ($C_{\Delta 0} = 2{\cdot}75$).

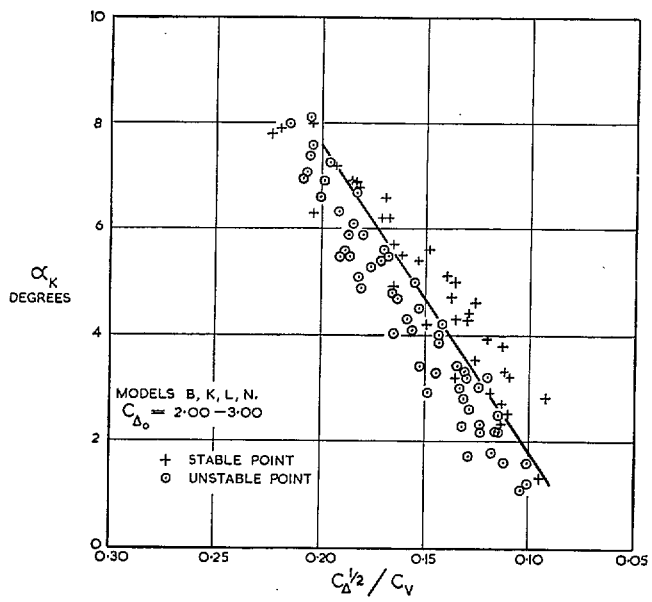

FIG. 89. Redefined lower longitudinal stability limit on a $C_\Delta{}^{1/2}/C_v$ base for warped forebody models over a range of $C_{\Delta 0}$, undisturbed case.

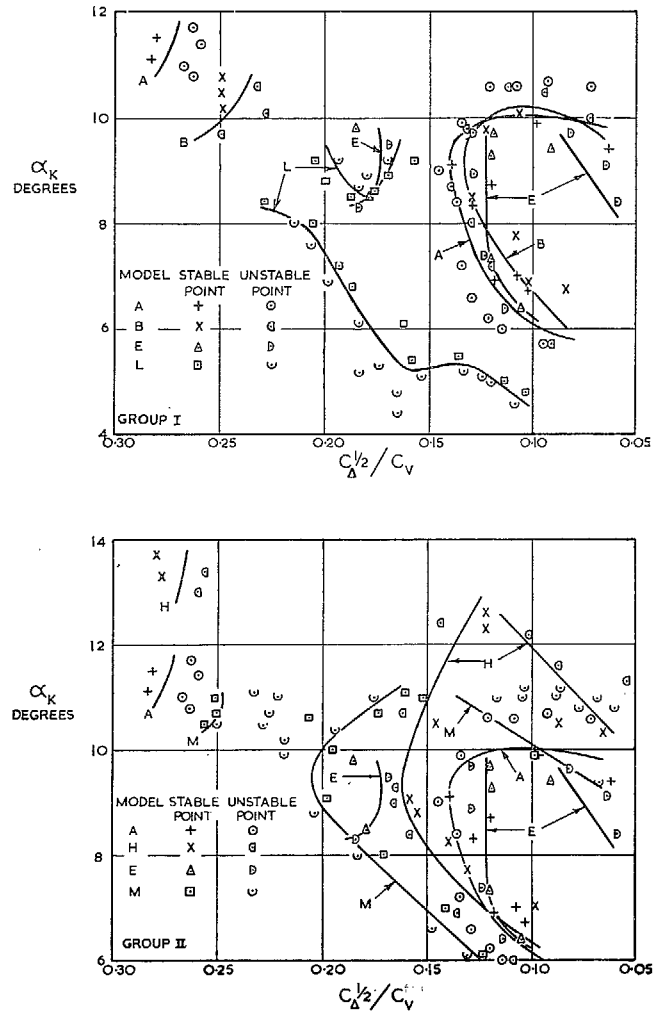

FIG. 90 (1). Redefined longitudinal stability limits for interaction investigation on a $C_{\Delta}{}^{1/2}/C_v$ base, disturbed case ($C_{\Delta 0} = 2{\cdot}75$).

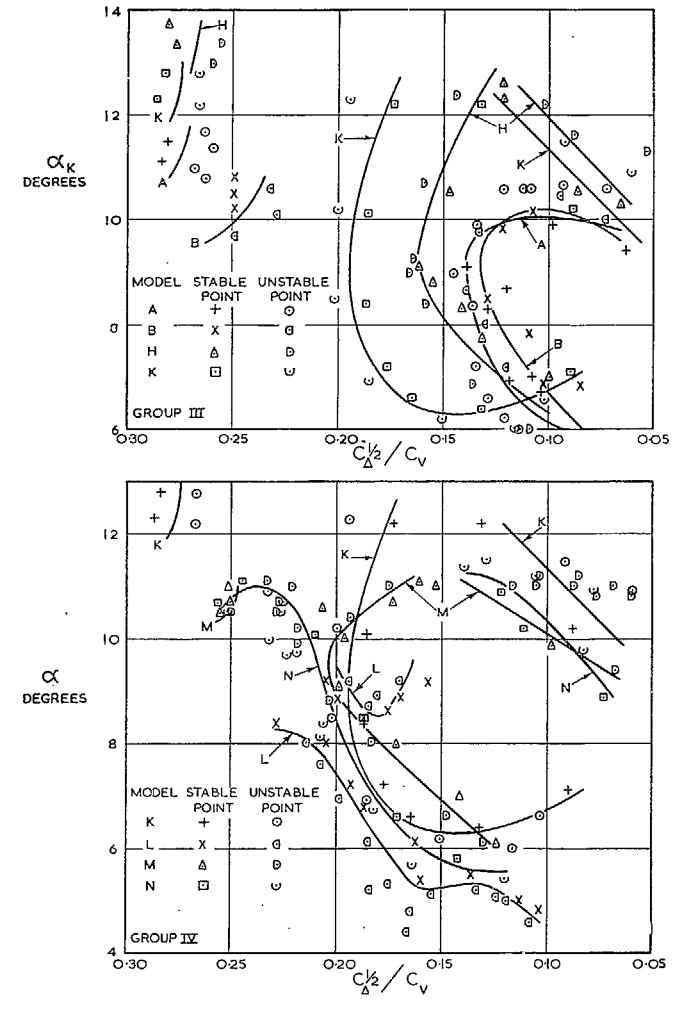

FIG. 90 (2). Redefined longitudinal stability limits for interaction investigation on a $C_{\Delta}{}^{1/2}/C_v$ base, disturbed case ($C_{\Delta 0} = 2{\cdot}75$).

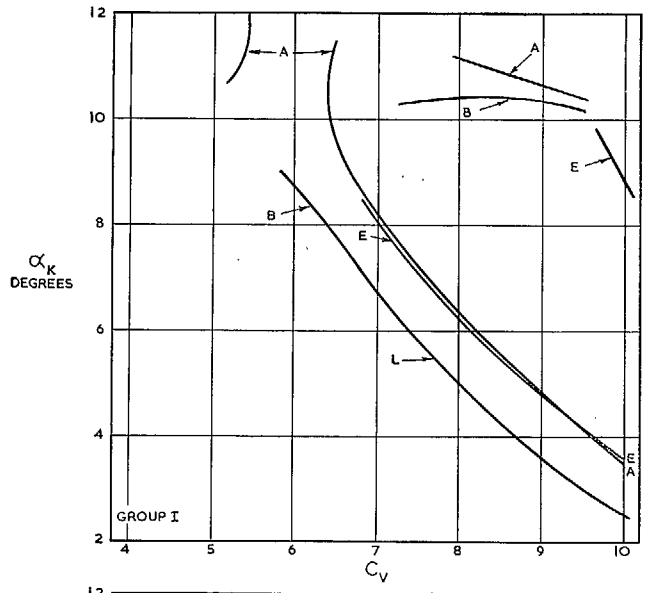

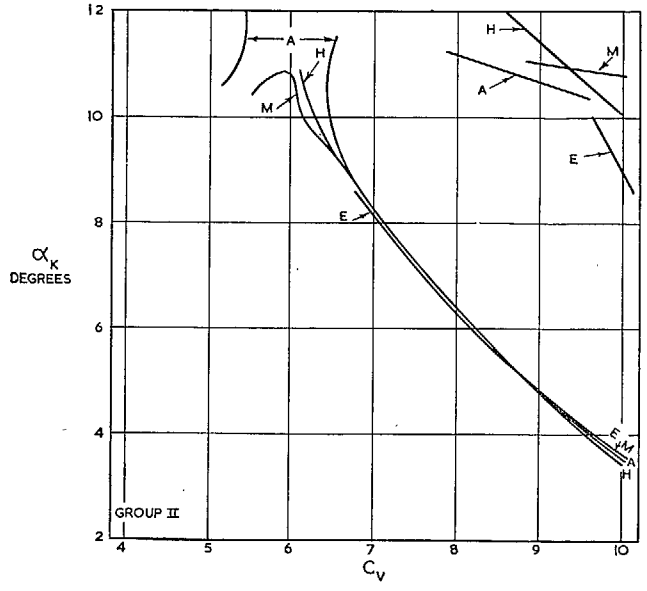

FIG. 91 (1). Redefined longitudinal stability limits for interaction investigation on a C_v base, undisturbed case ($C_{\Delta 0} = 2{\cdot}75$).

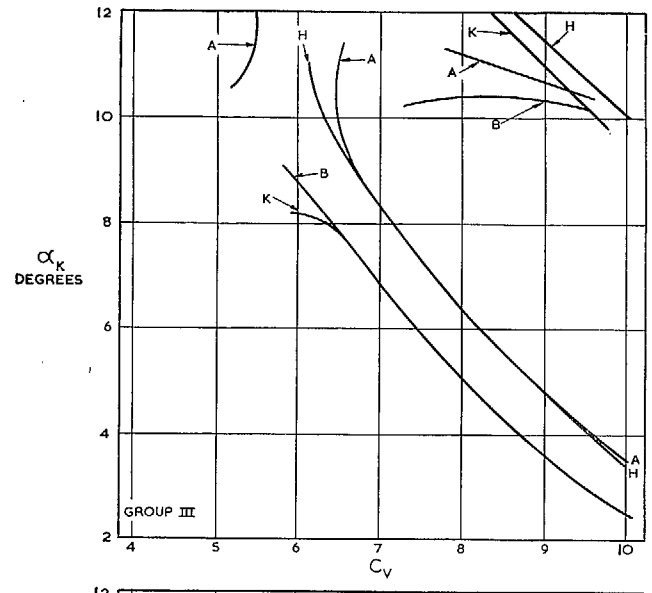

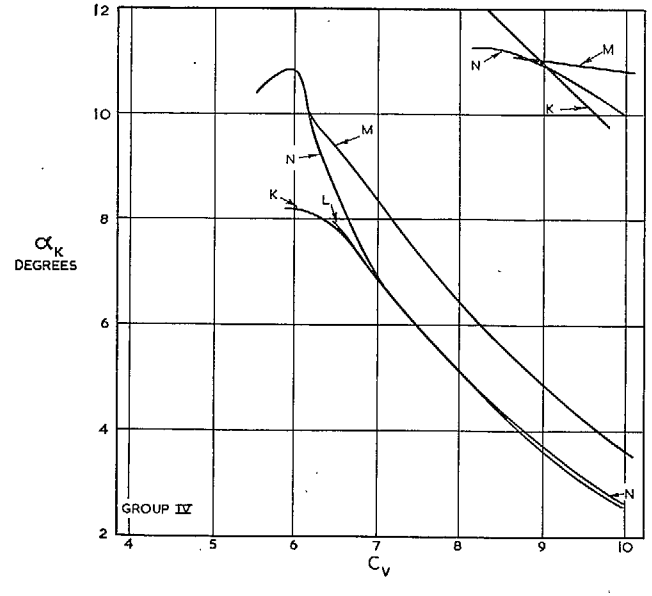

FIG. 91 (2). Redefined longitudinal stability limits for interaction investigation on a C_v base, undisturbed case ($C_{\Delta 0} = 2{\cdot}75$).

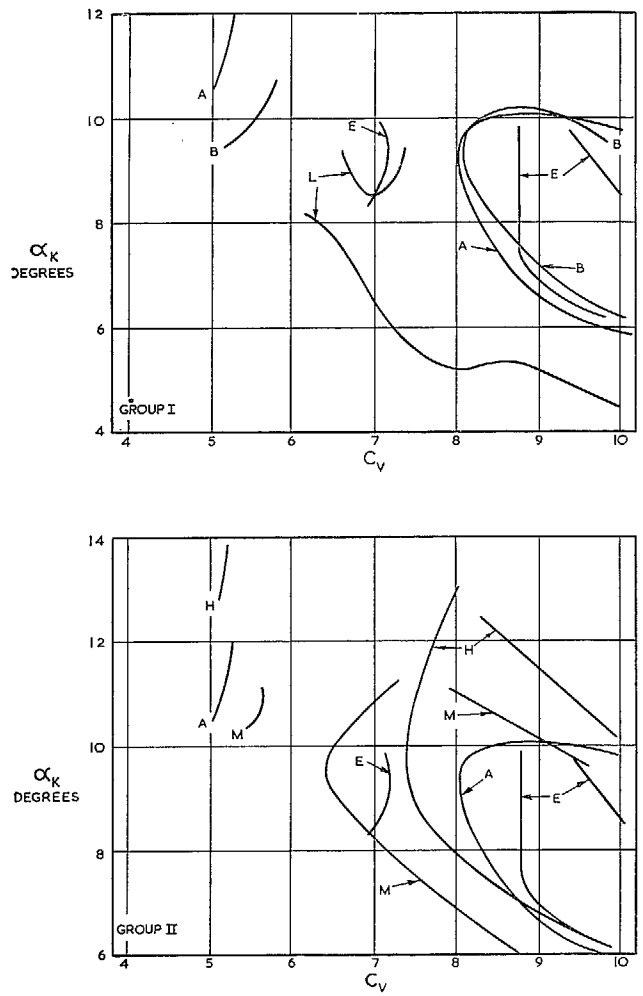

FIG. 92 (1). Redefined longitudinal stability limits for interaction investigation on a C_v base, disturbed case ($C_{\Delta 0} = 2{\cdot}75$).

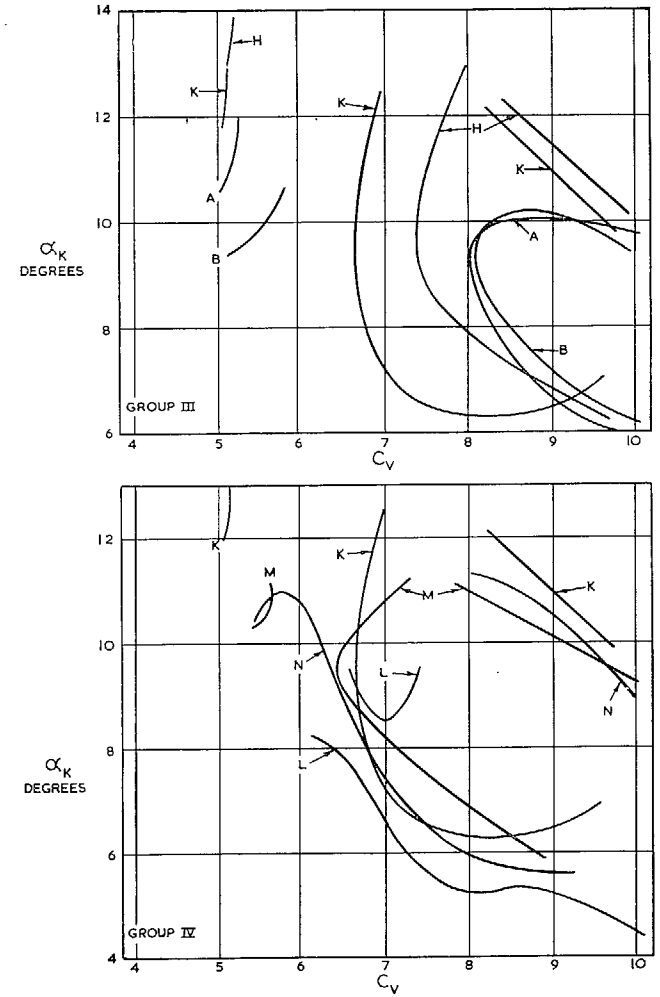

FIG. 92 (2). Redefined longitudinal stability limits for interaction investigation on a C_v base, disturbed case ($C_{\Delta 0} = 2{\cdot}75$).

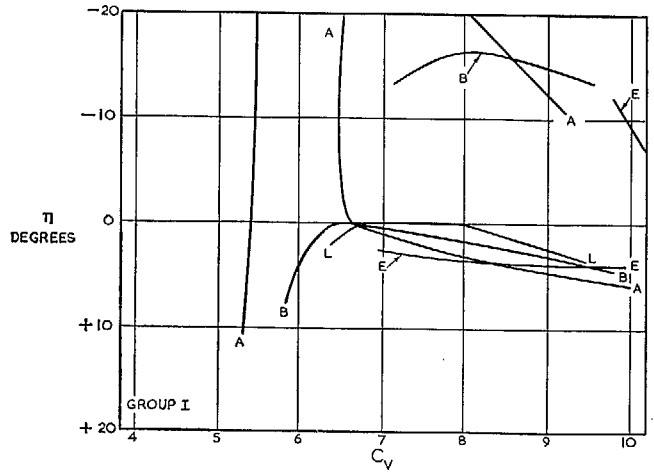

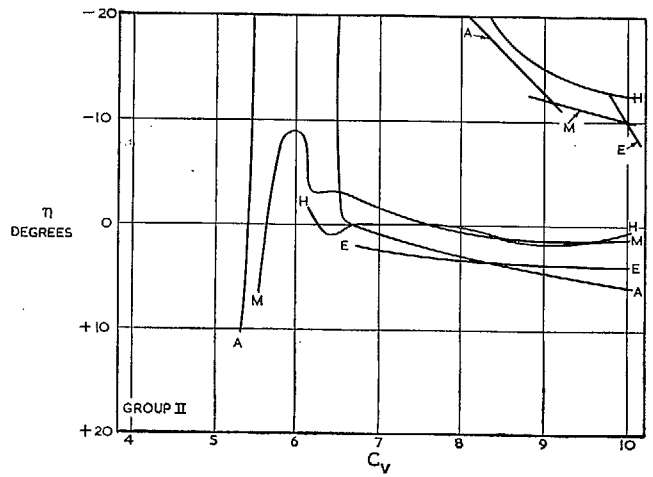

FIG. 93 (1). Relation between elevator settings and redefined longitudinal stability limits for interaction investigation, undisturbed case ($C_{\Delta 0} = 2{\cdot}75$).

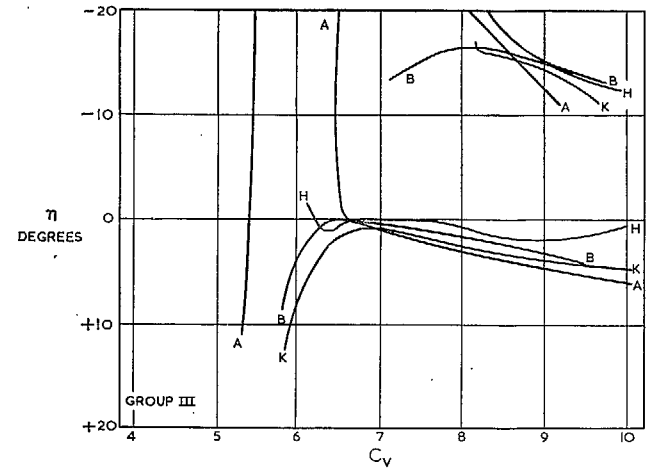

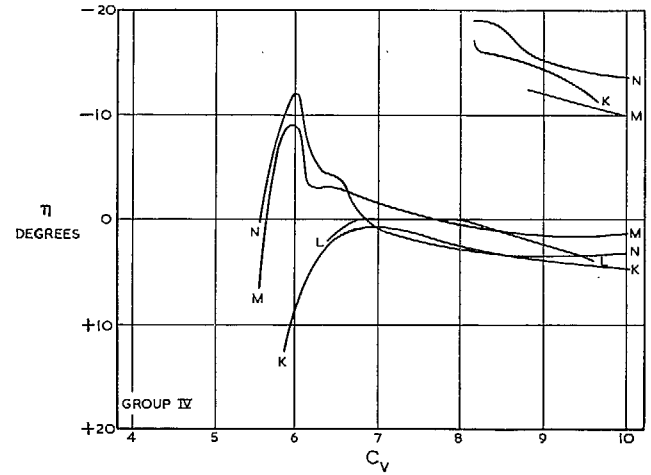

FIG. 93 (2). Relation between elevator settings and redefined longitudinal stability limits for interaction investigation, undisturbed case ($C_{\Delta 0} = 2.75$).

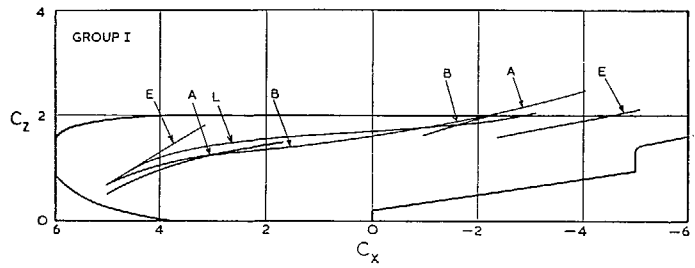

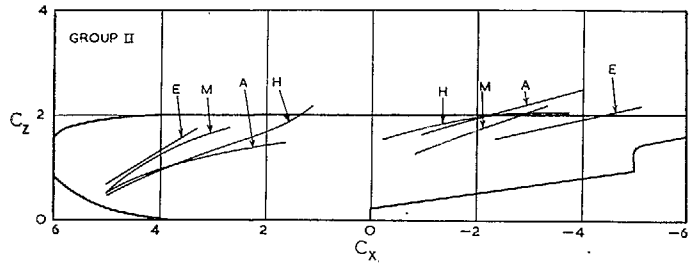

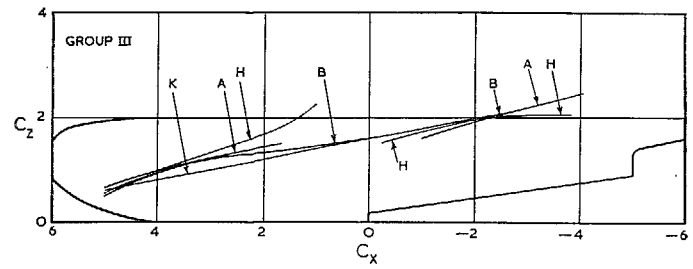

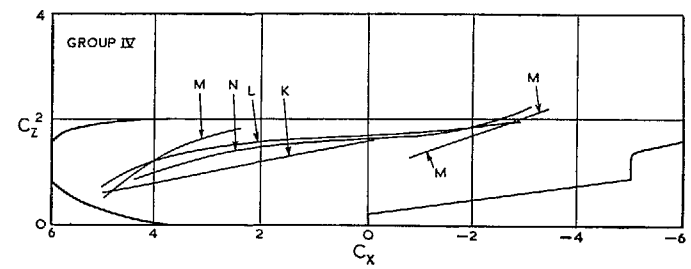

FIG. 96. Comparison of spray envelopes for interaction investigation ($C_{\Delta 0} = 2{\cdot}75$).

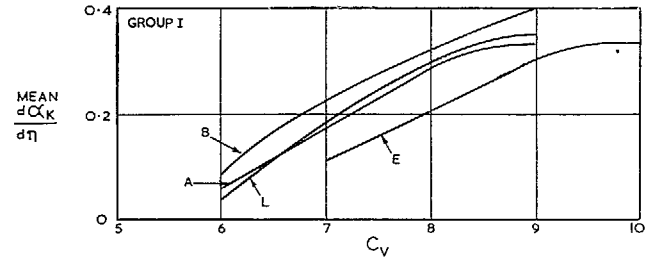

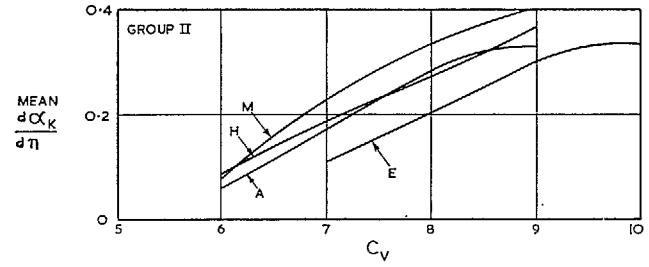

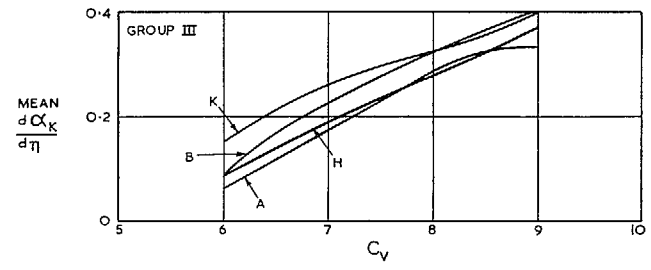

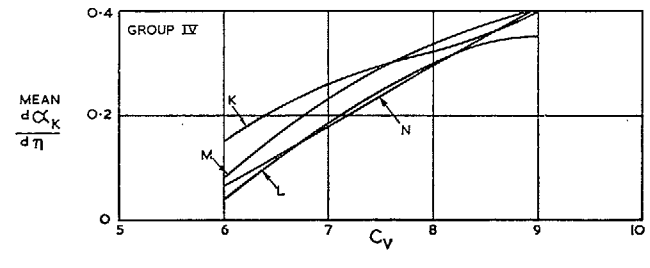

FIG. 97. Comparison of elevator effectiveness for interaction investigation ($C_{\Delta 0} = 2{\cdot}75$).

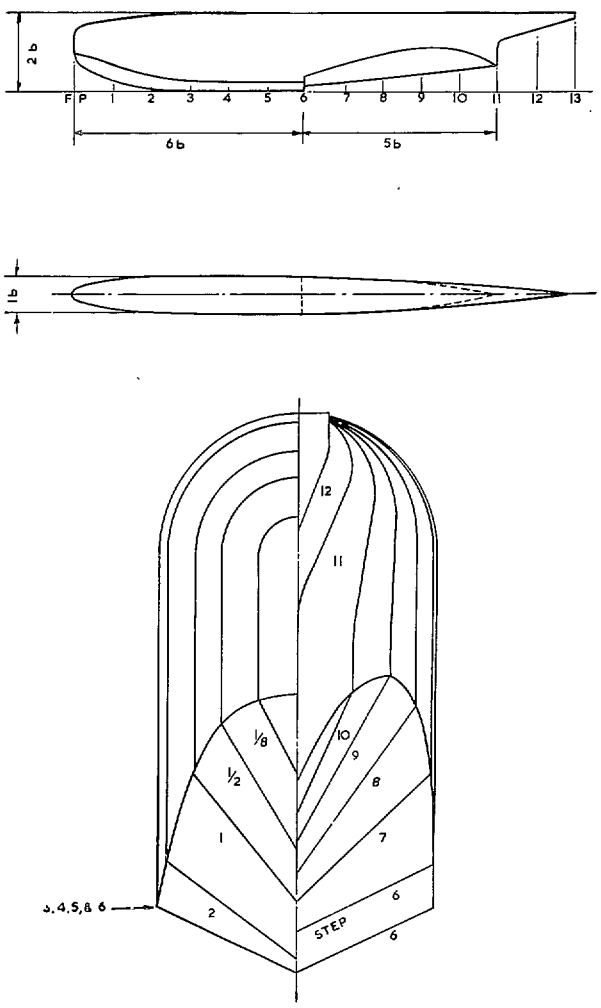

FIG. 98. Model J hull lines.

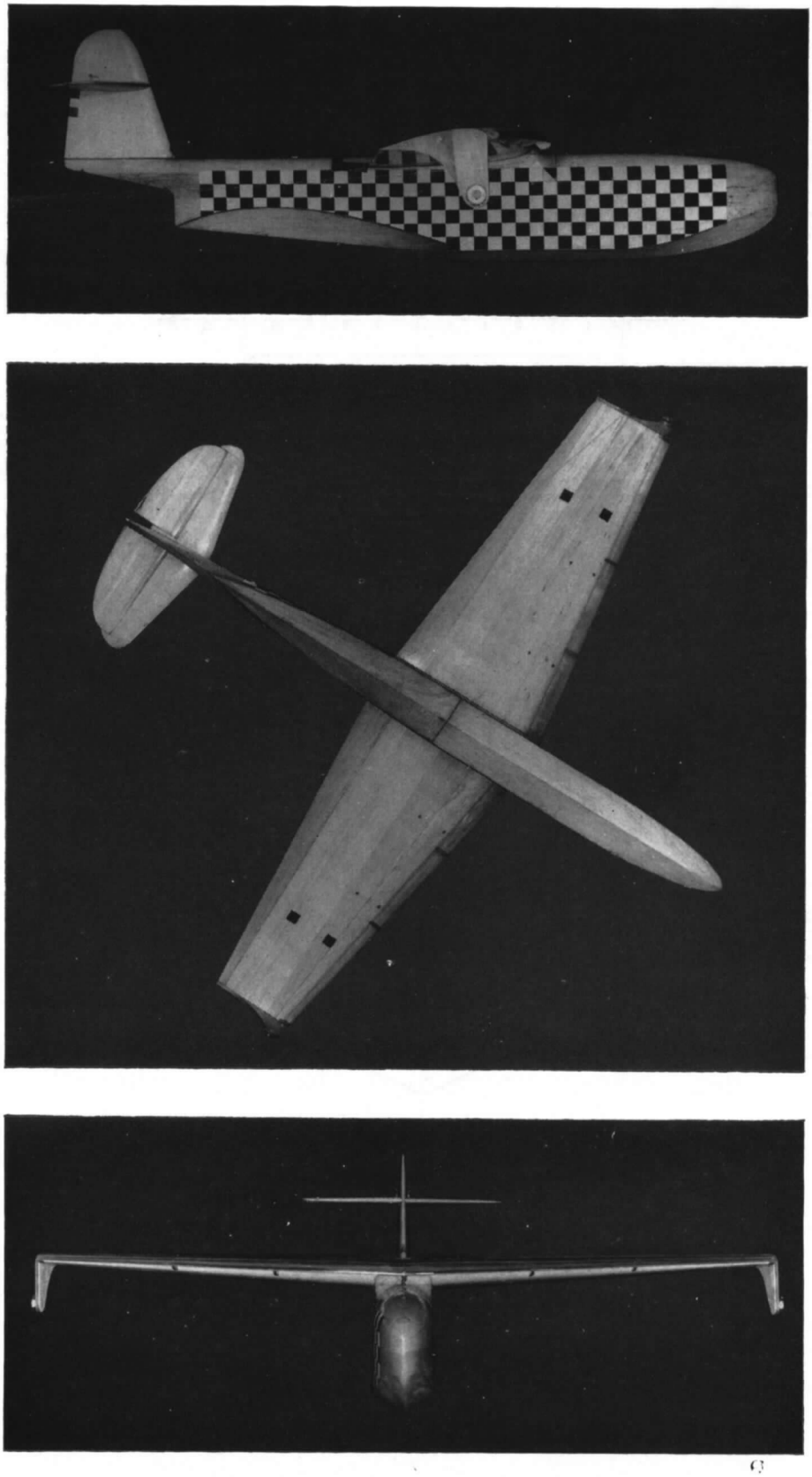

FIG. 99. Photographs of Model J.

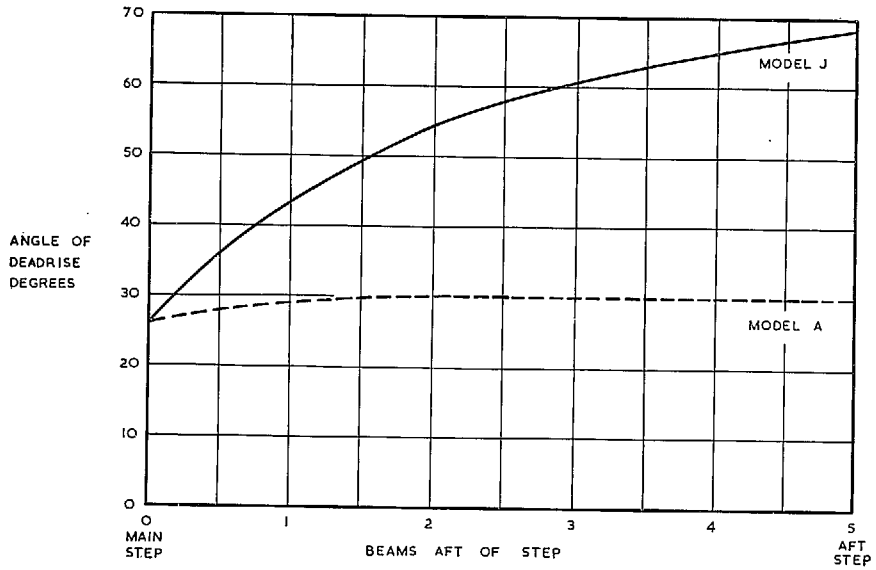

FIG. 100. Afterbody deadrise-angle distributions for Models A and J.

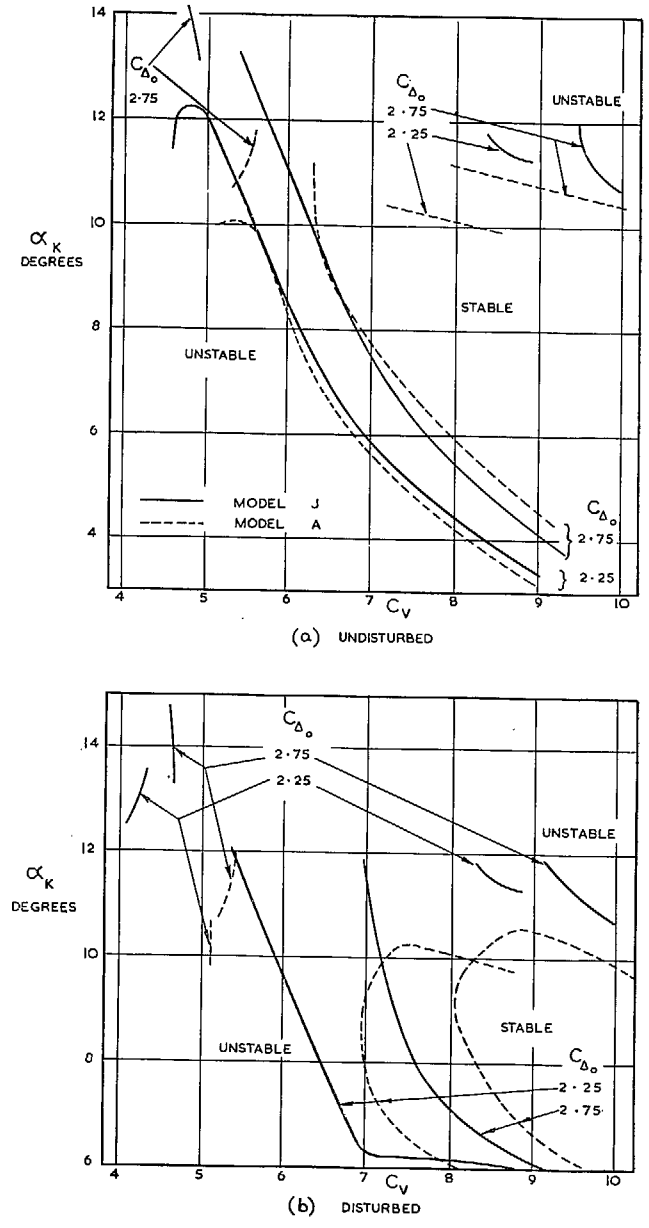

FIGS. 101a and 101b. Effect of a tailored afterbody on longitudinal stability limits.

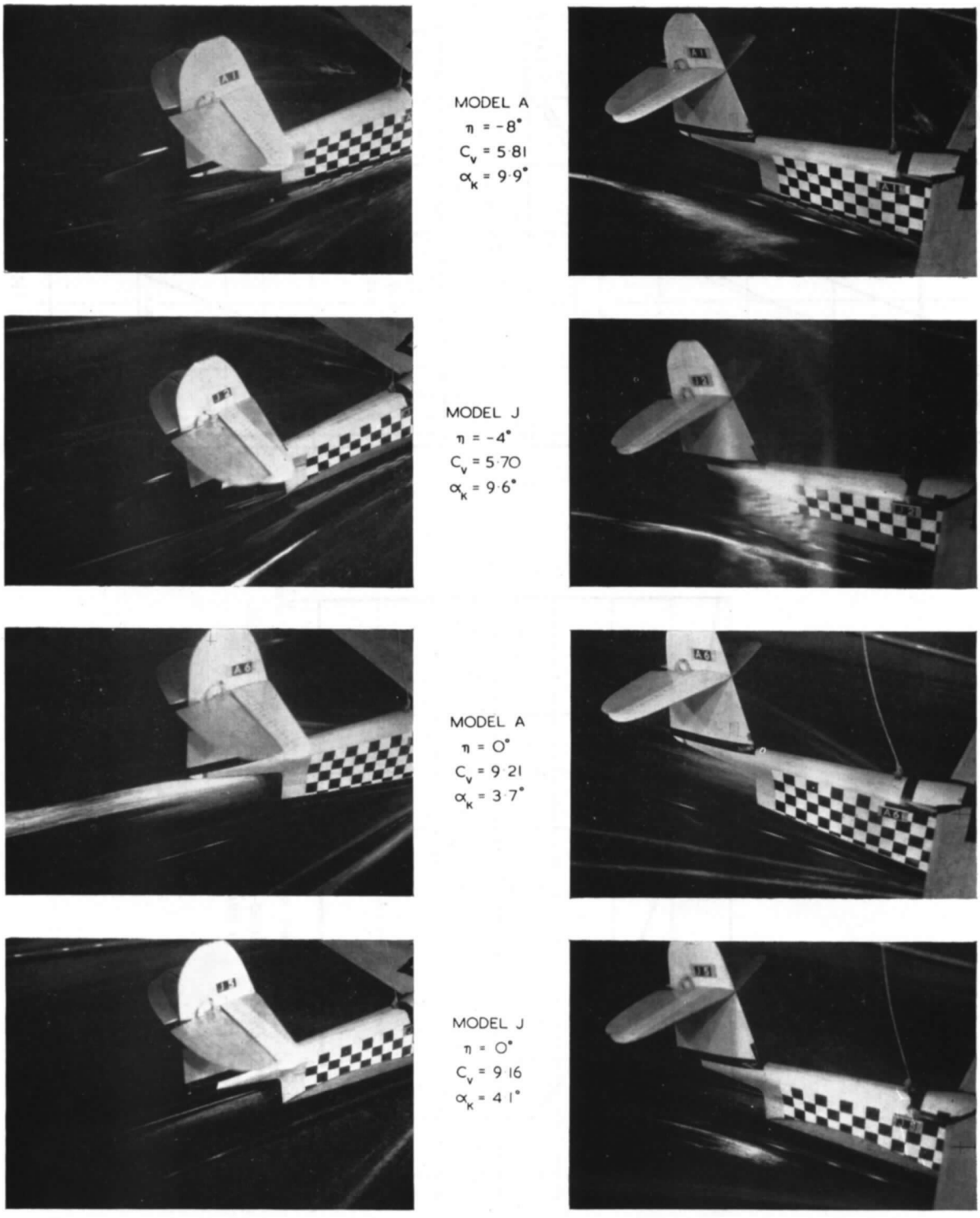

FIG. 102. Wake photographs for Models A and J ($C_{\Delta 0} = 2{\cdot}25$).

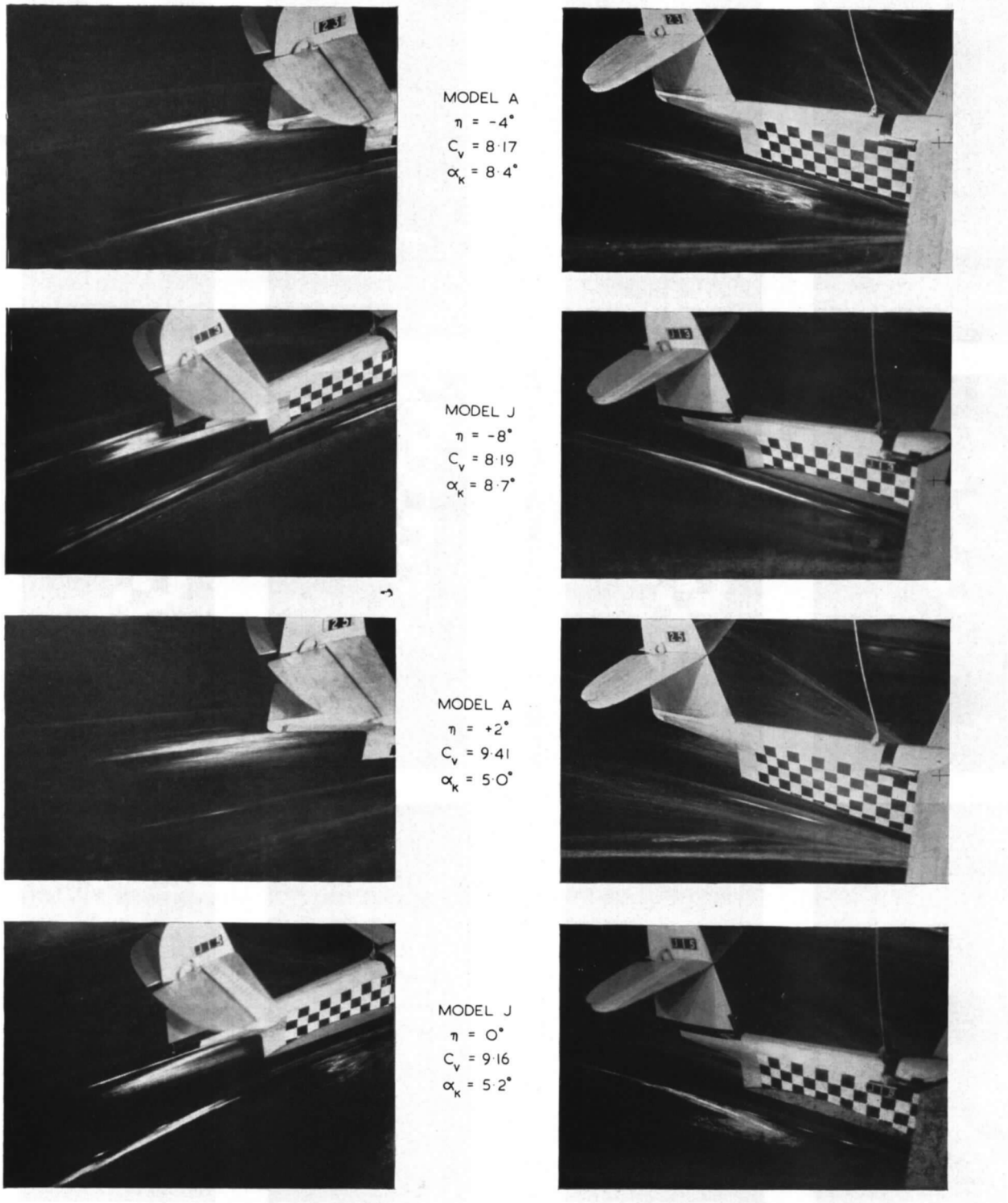

FIG. 103. Wake photographs for Models A and J ($C_{\Delta 0} = 2{\cdot}75$).

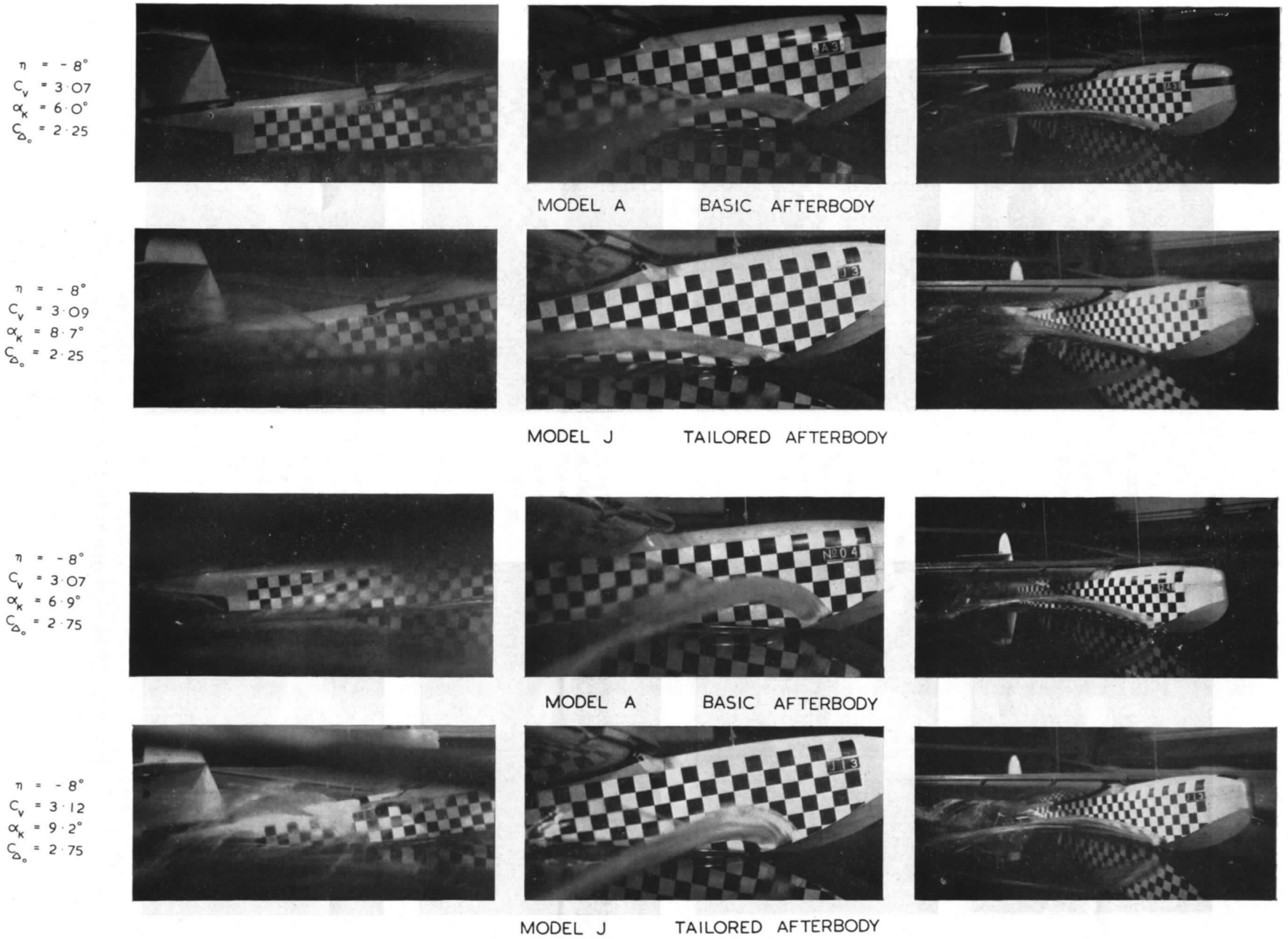

FIG. 104. Effect of a tailored afterbody on spray ($C_v = 3$).

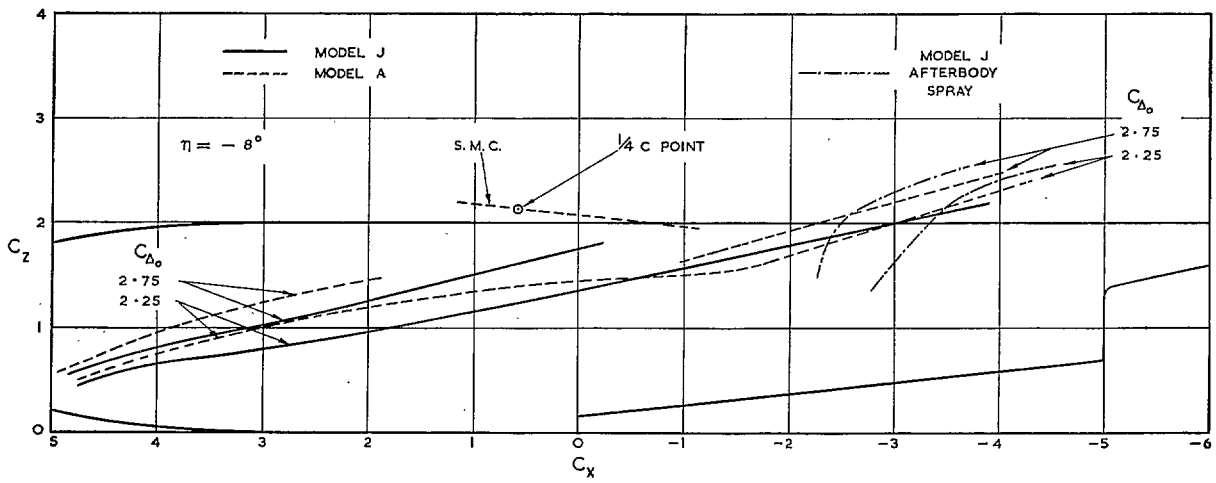

FIG. 105. Effect of a tailored afterbody on spray projections (Model J).

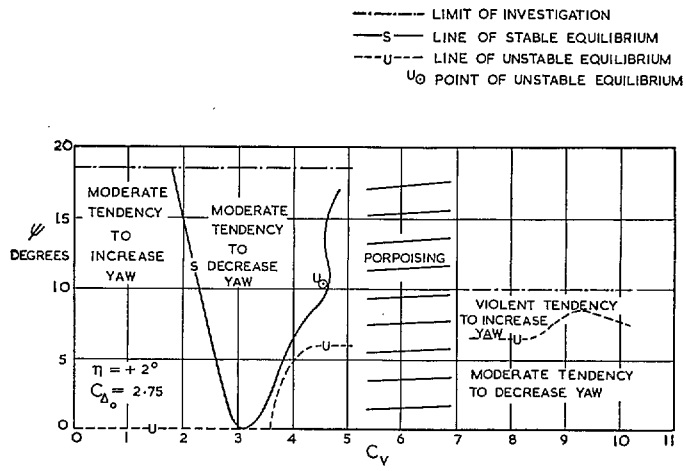

(a) NORMAL AFTERBODY

MODEL A

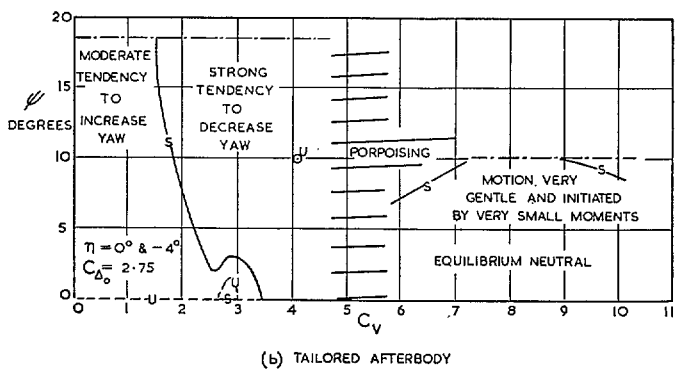

(b) TAILORED AFTERBODY

MODEL J

FIGS. 106a and 106b. Effect of tailored afterbody on directional stability ($C_{v_0} = 2{\cdot}75$).

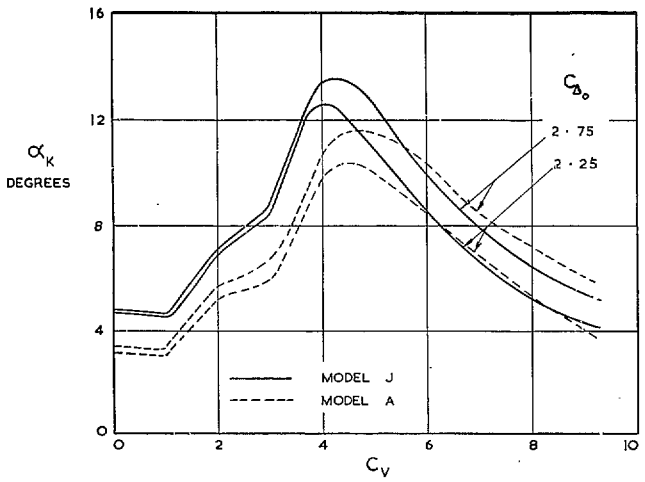

FIG. 107. Effect of a tailored afterbody on trim curves ($\eta = 0$ deg.).

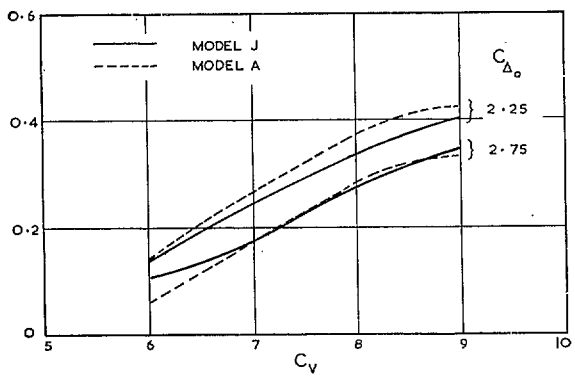

FIG. 108. Effect of a tailored afterbody on elevator effectiveness.

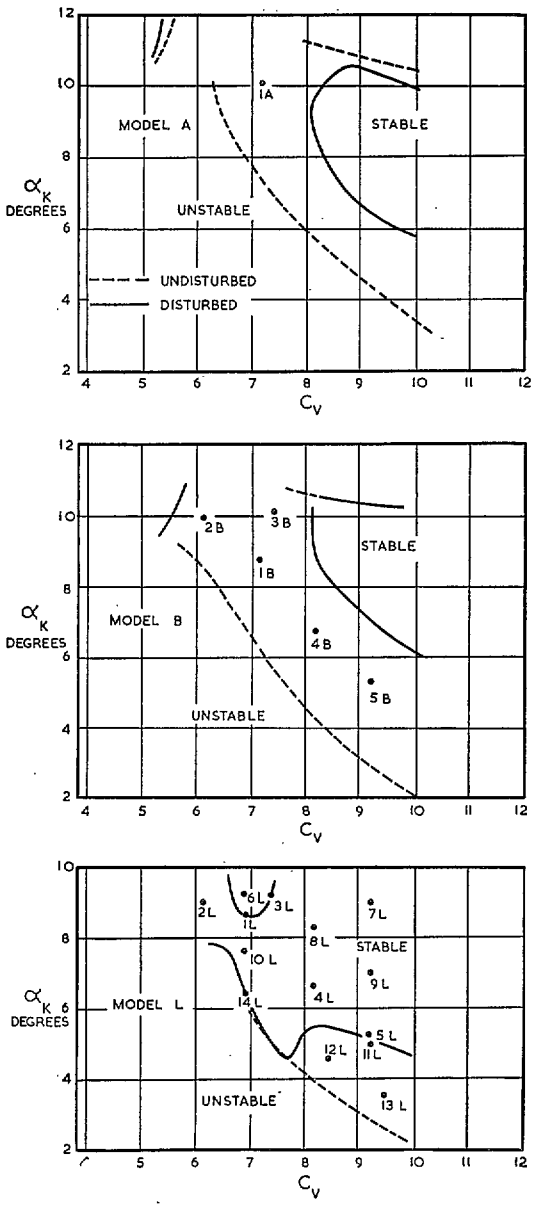

FIG. 109 (1). Relation between points investigated in waves and longitudinal stability limits.

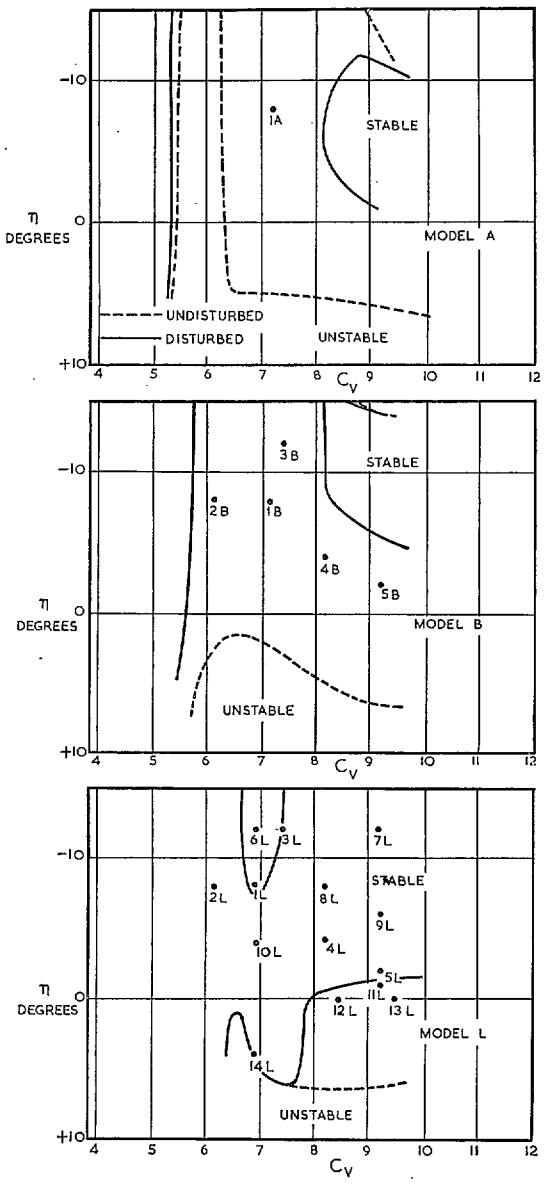

FIG. 109 (2). Relation between points investigated in waves and longitudinal stability limits.

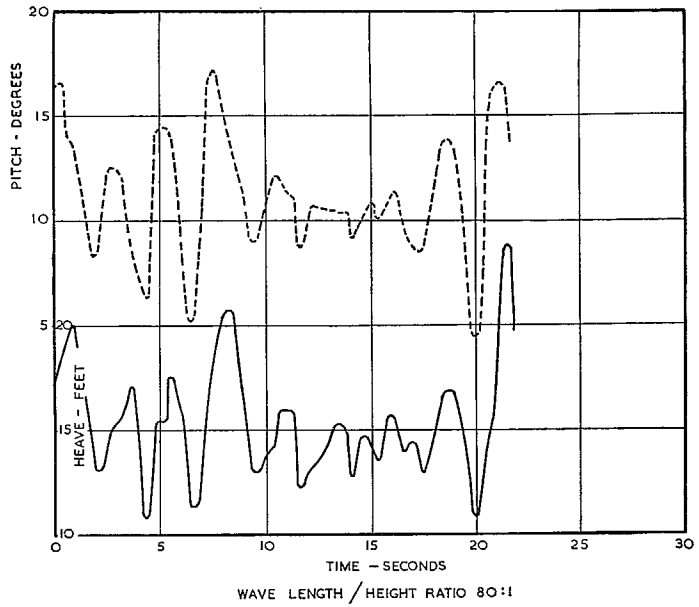

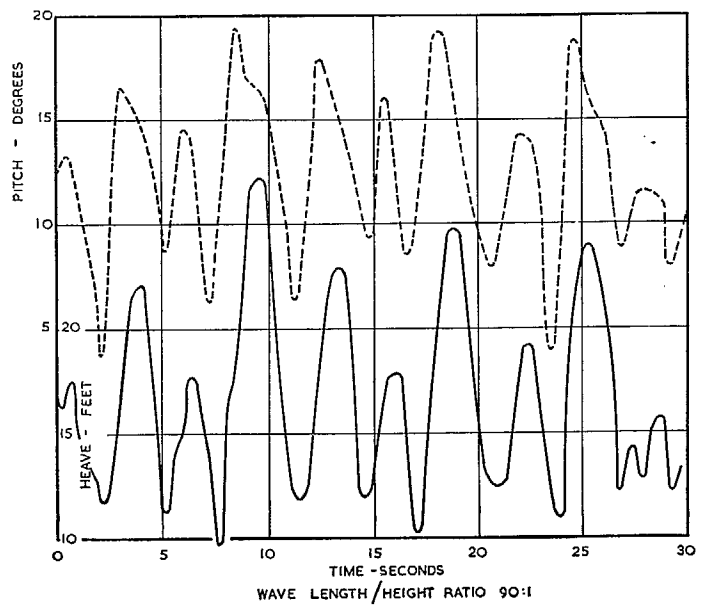

FIG. 110 (1). Motion of Model A in waves of scaled height 2·35 ft.

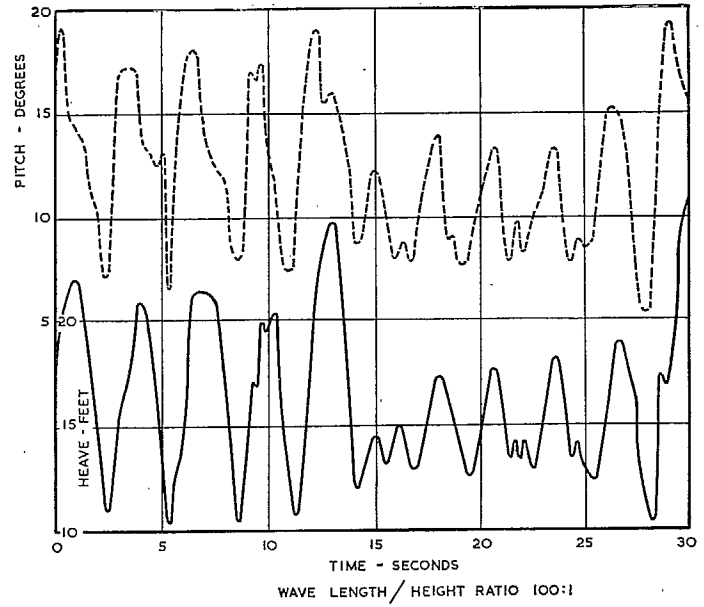

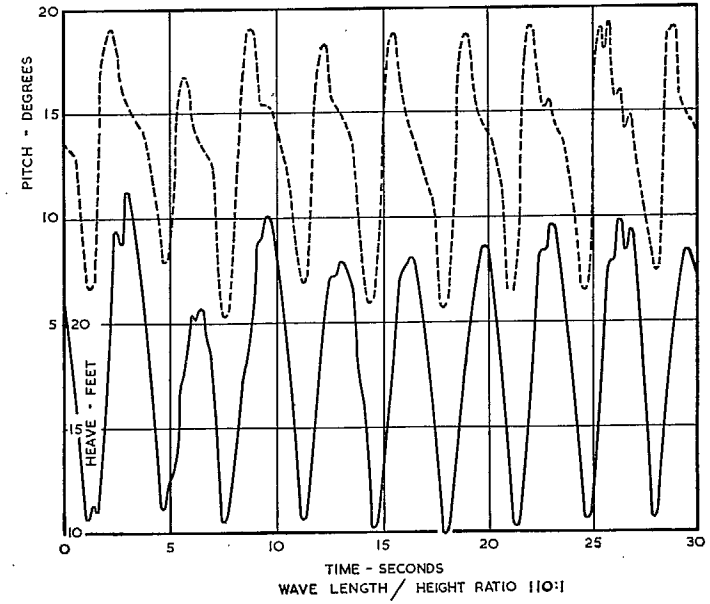

FIG. 110 (2). Motion of Model A in waves of scaled height 2·35 ft.

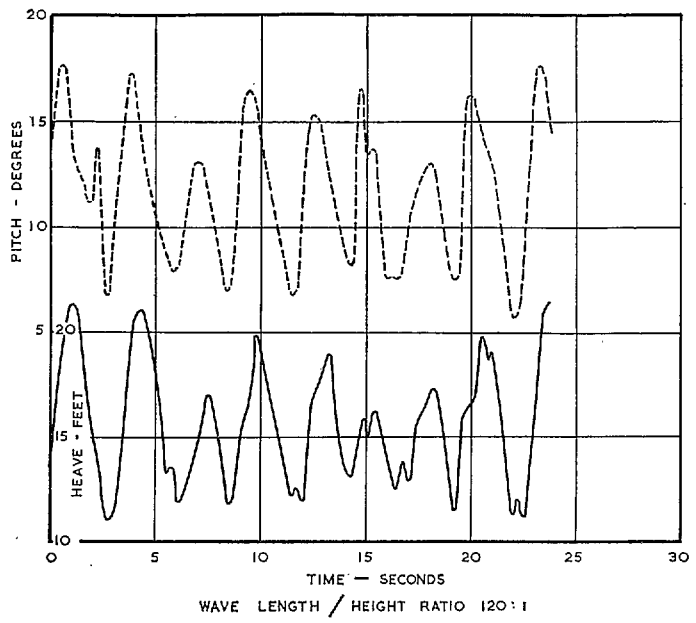

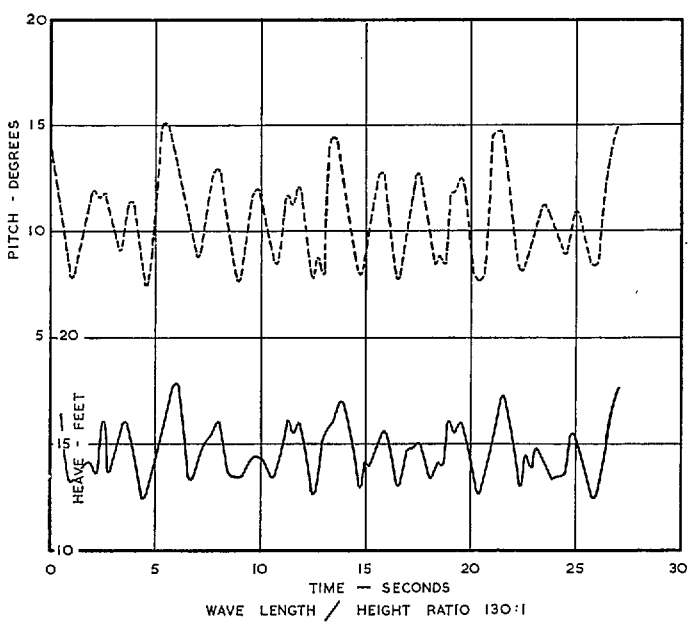

FIG. 110 (3). Motion of Model A in waves of scaled height 2·35 ft.

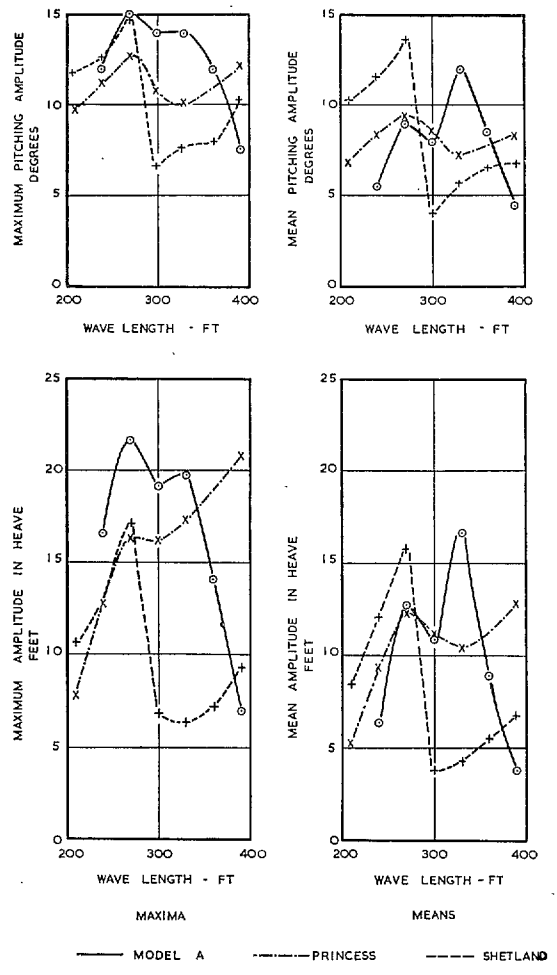

FIG. 111. Comparison of oscillations in waves of Model A *Princess* and *Shetland* scaled to *Princess* size.

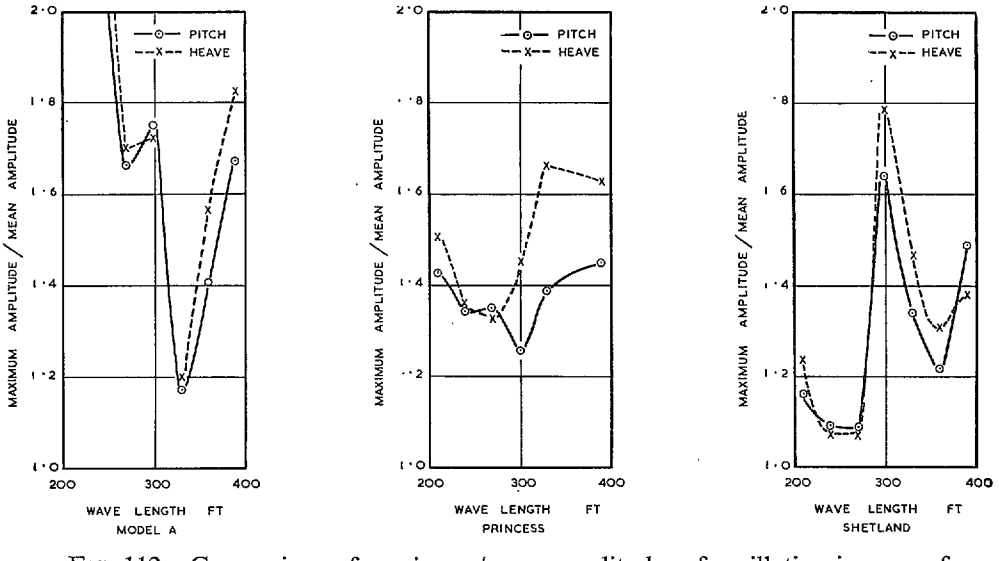

FIG. 112. Comparison of maximum/mean amplitudes of oscillation in waves for Model A *Princess* and *Shetland*

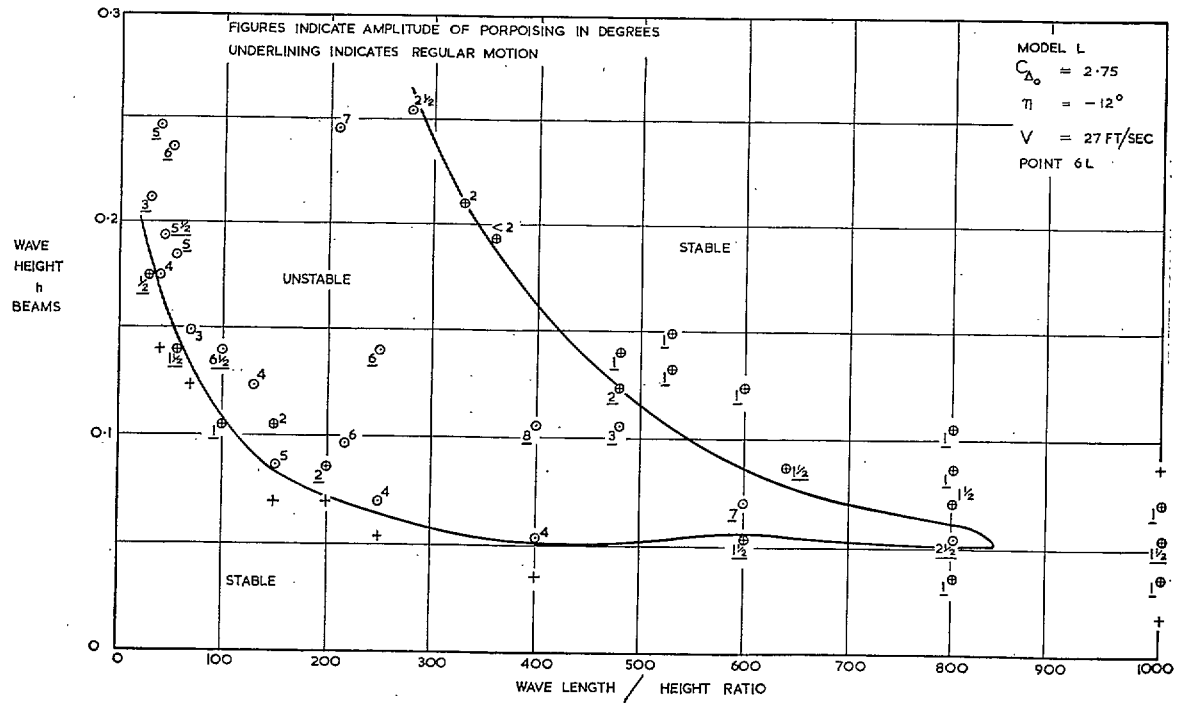

FIG. 113. Typical wave diagram on a wave length/height ratio base.

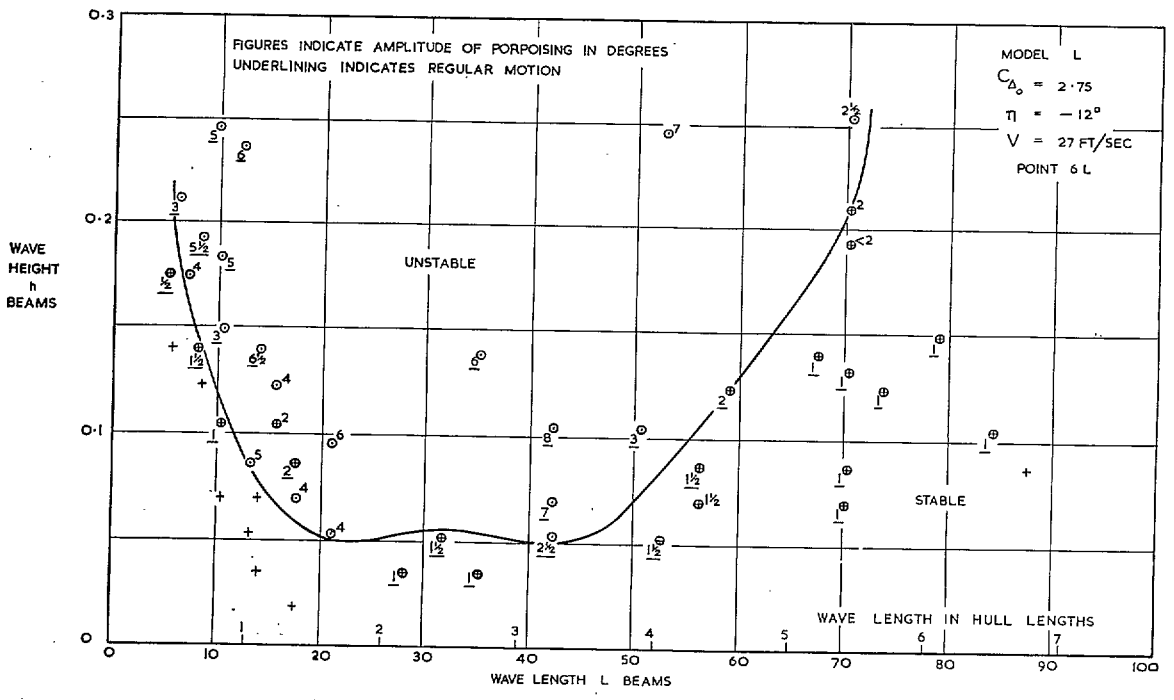

FIG. 114. Typical wave diagram on a wave length base.

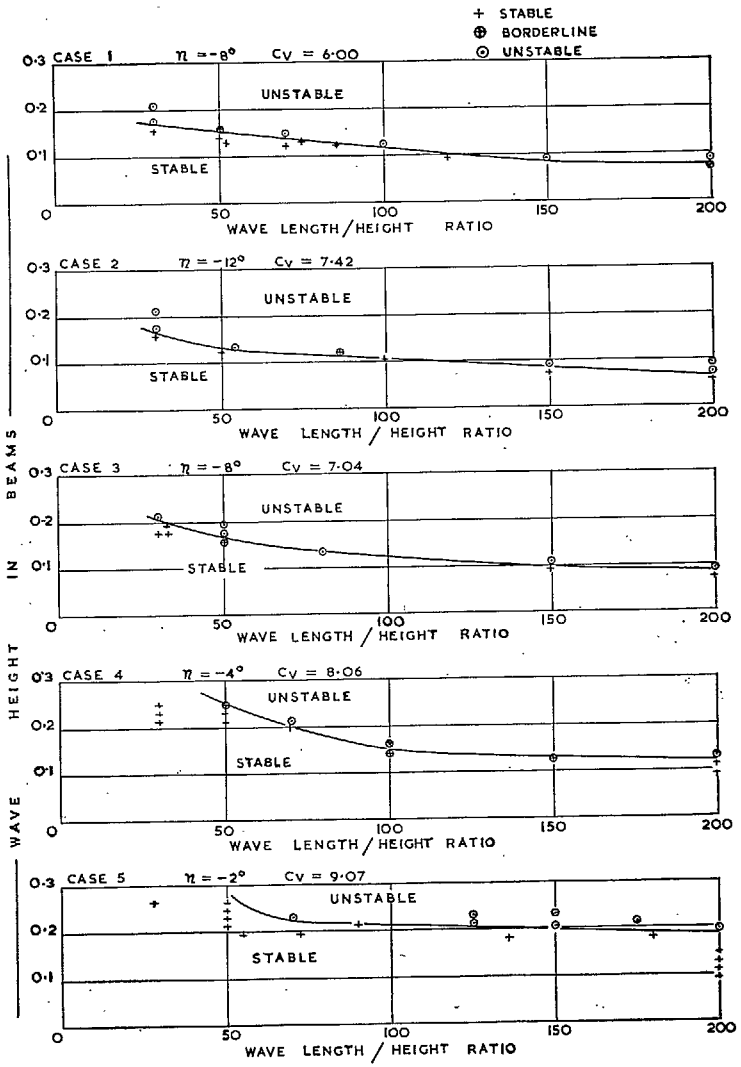

FIG. 115 (1). Model wave diagrams.

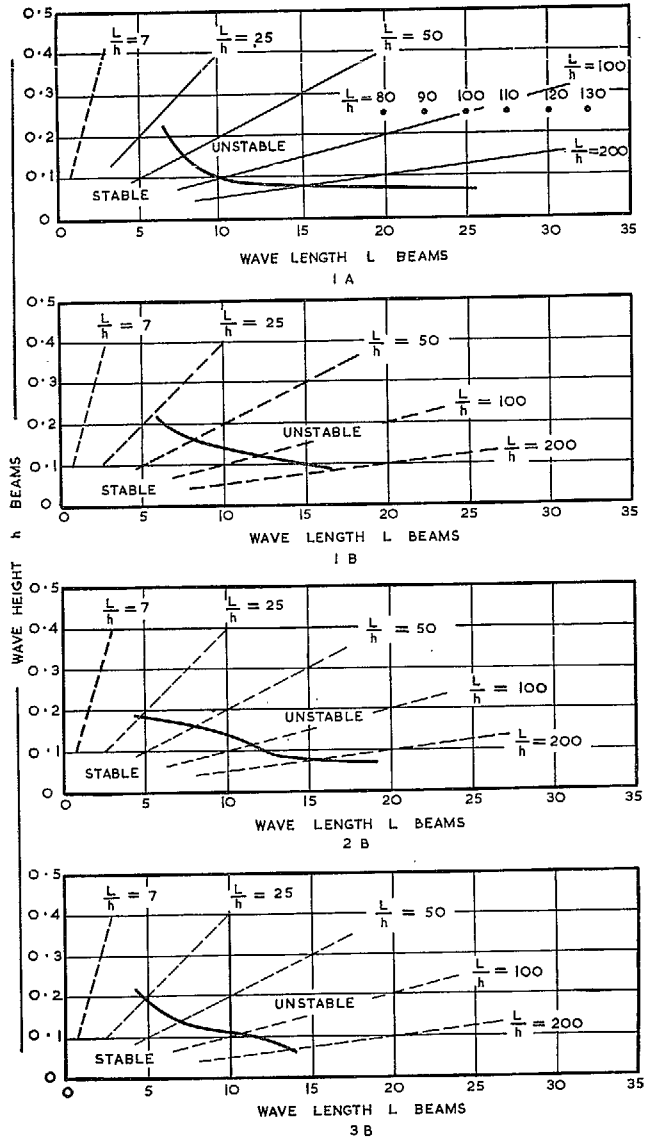

FIG. 115 (2). Model wave diagrams.

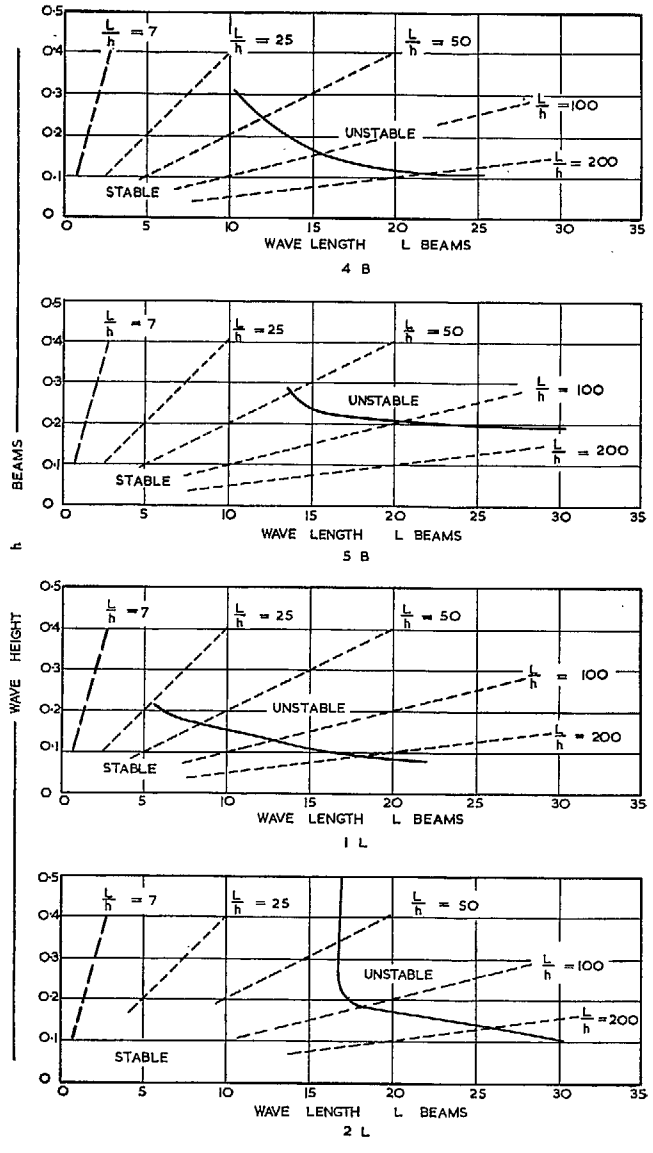

FIG. 115 (3). Model wave diagrams.

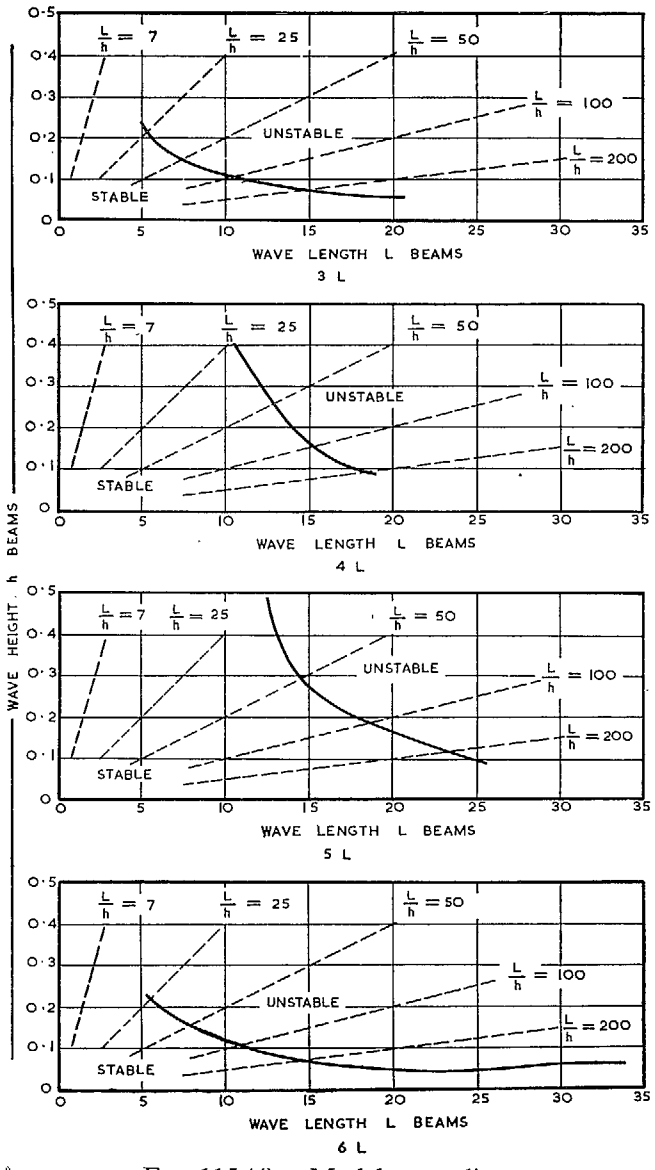

FIG. 115 (4). Model wave diagrams.

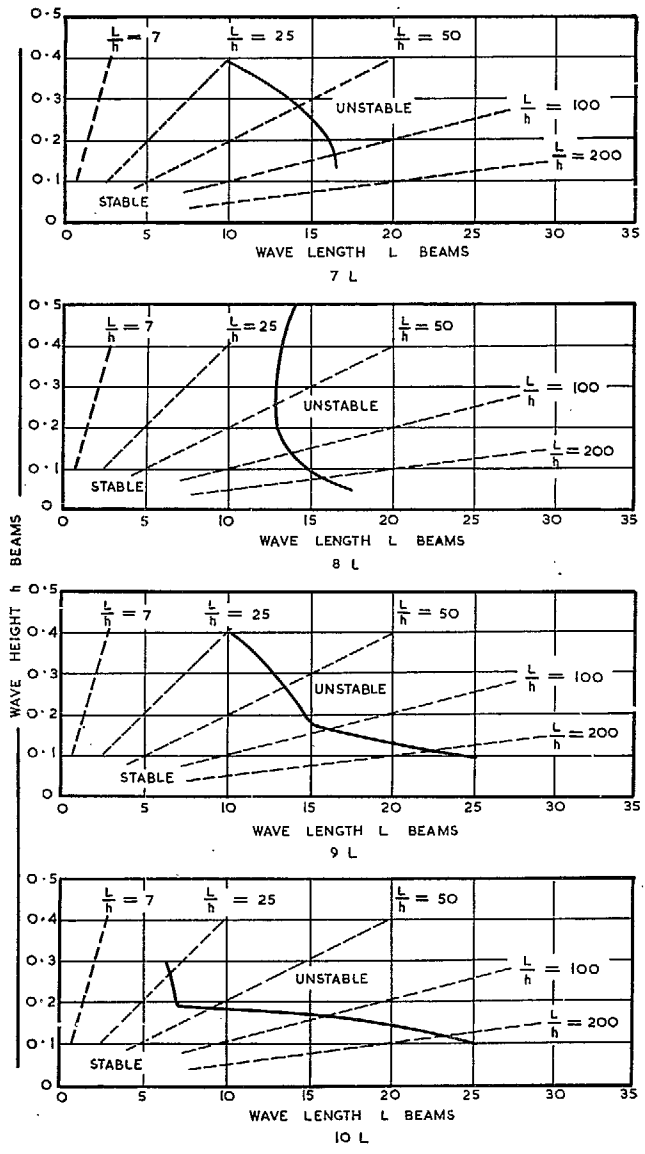

FIG. 115 (5). Model wave diagrams.

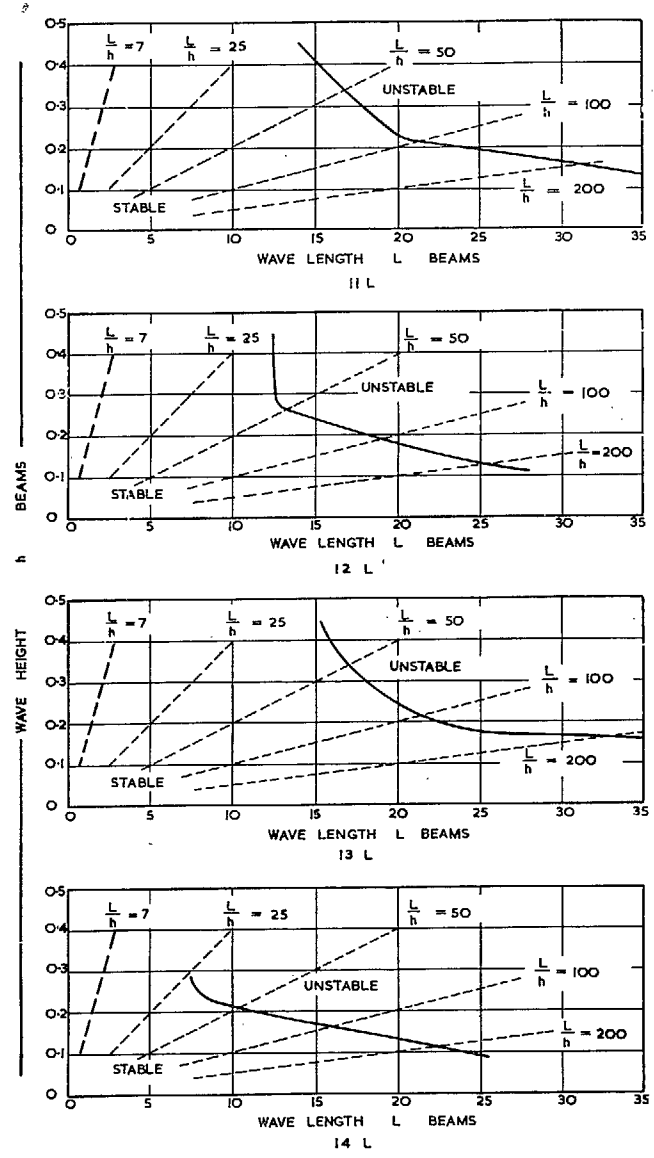

FIG. 115 (6). Model wave diagrams.

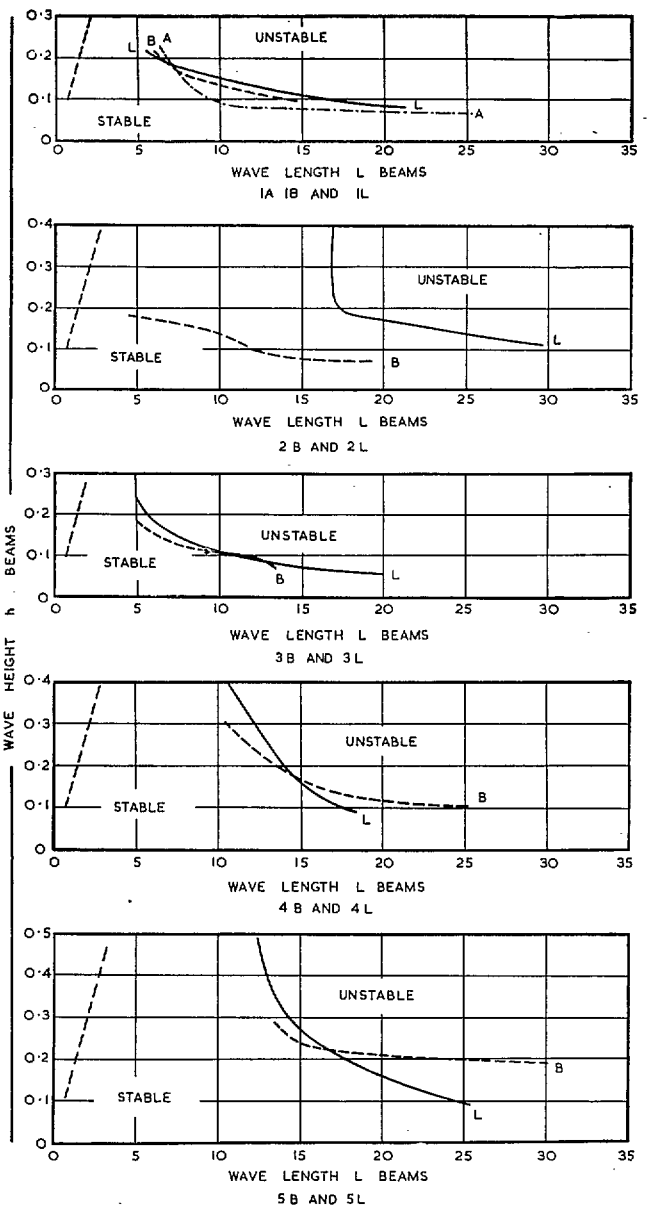

FIG. 116. Comparison of model wave diagrams.

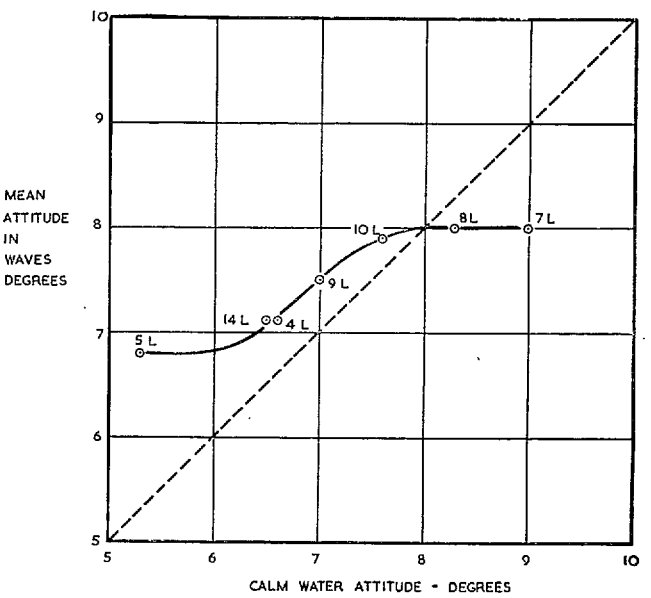

POINT	SPEED	ELEVATOR ANGLE
	C_V	η
7 L	9·2	− 12°
8 L	8·2	− 8°
10L	6·9	− 4°
9 L	9·2	− 6°
4 L	8·2	− 4°
14 L	6·9	+ 4°
5 L	9·2	− 2°

FIG. 117. The effect of waves on attitude.

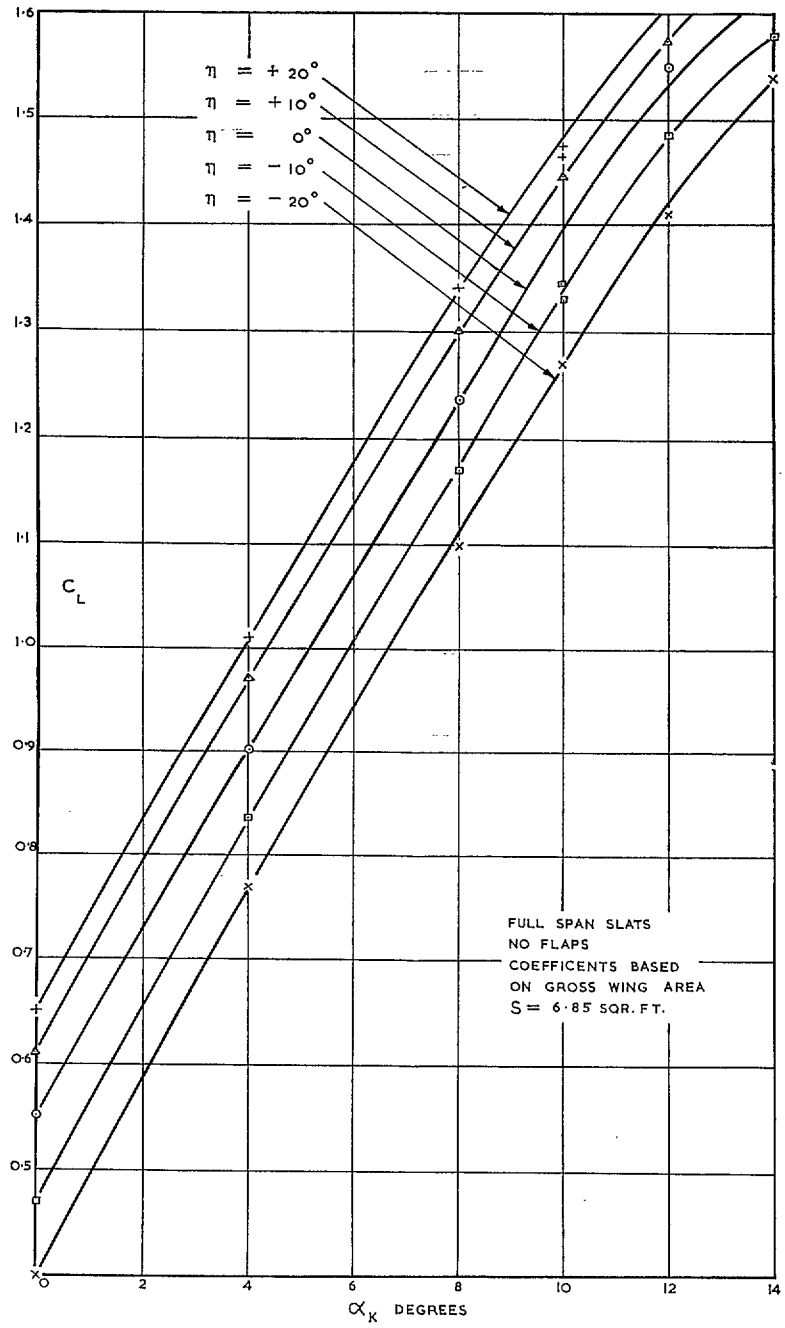

FIG. 118. Model A lift curves without slipstream ($C_{\Delta 0} = 2{\cdot}25$).

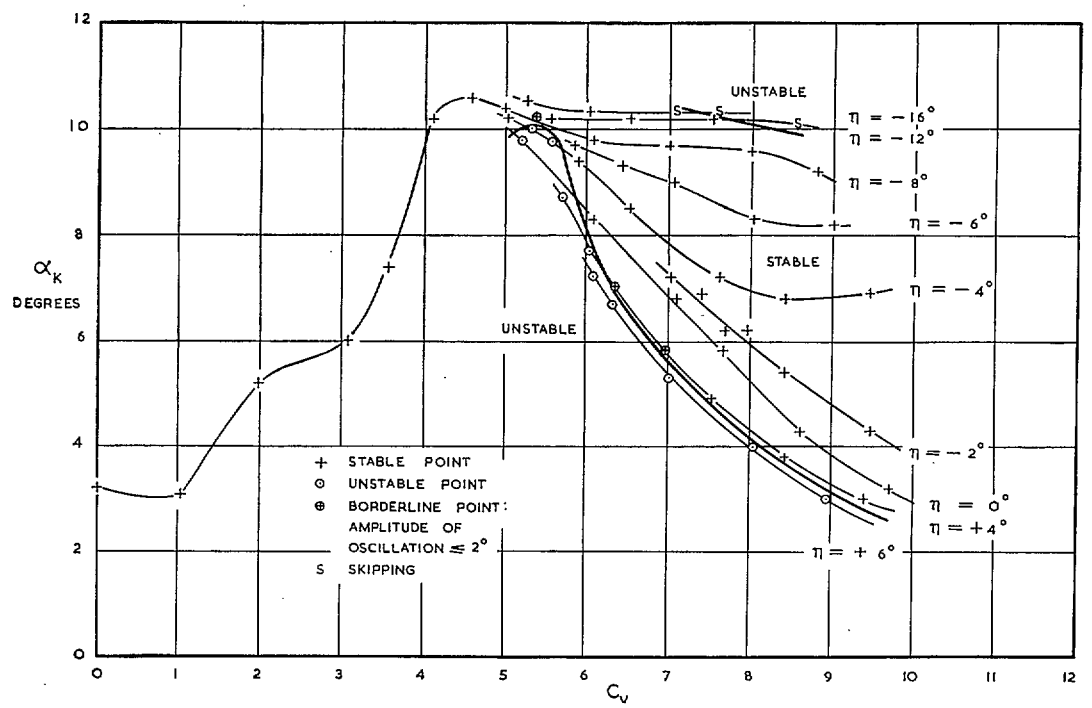

FIG. 119. Model A longitudinal stability without disturbance ($C_{\Delta 0} = 2{\cdot}25$).

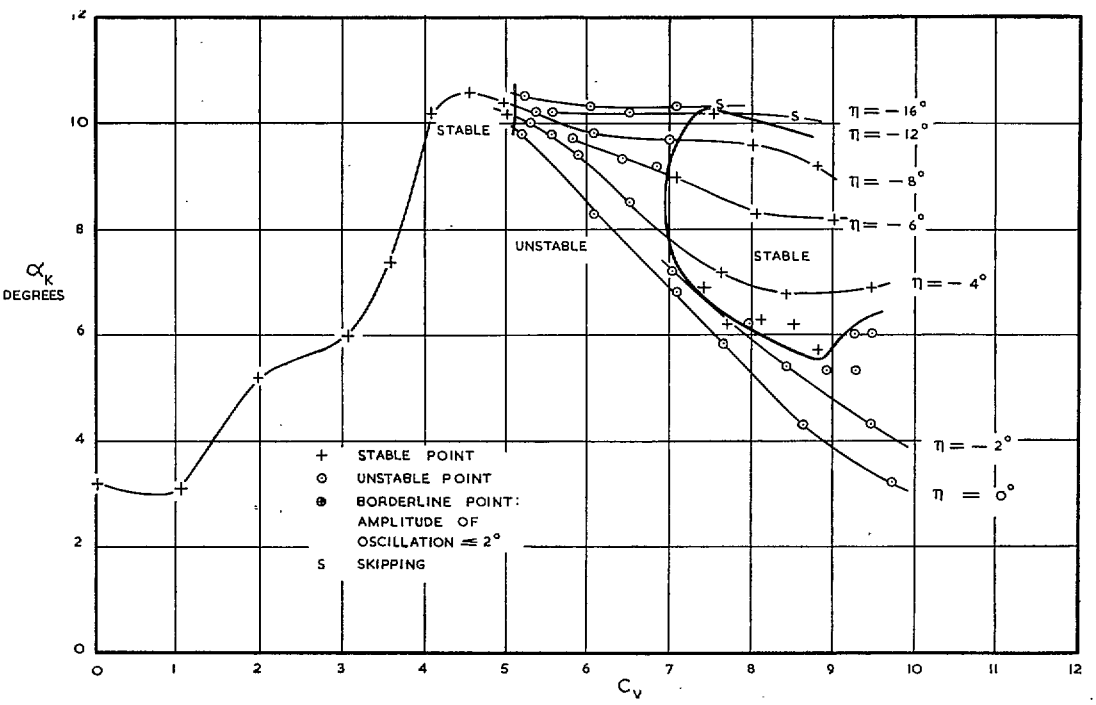

FIG. 120. Model A longitudinal stability with disturbance ($C_{\Delta 0} = 2{\cdot}25$).

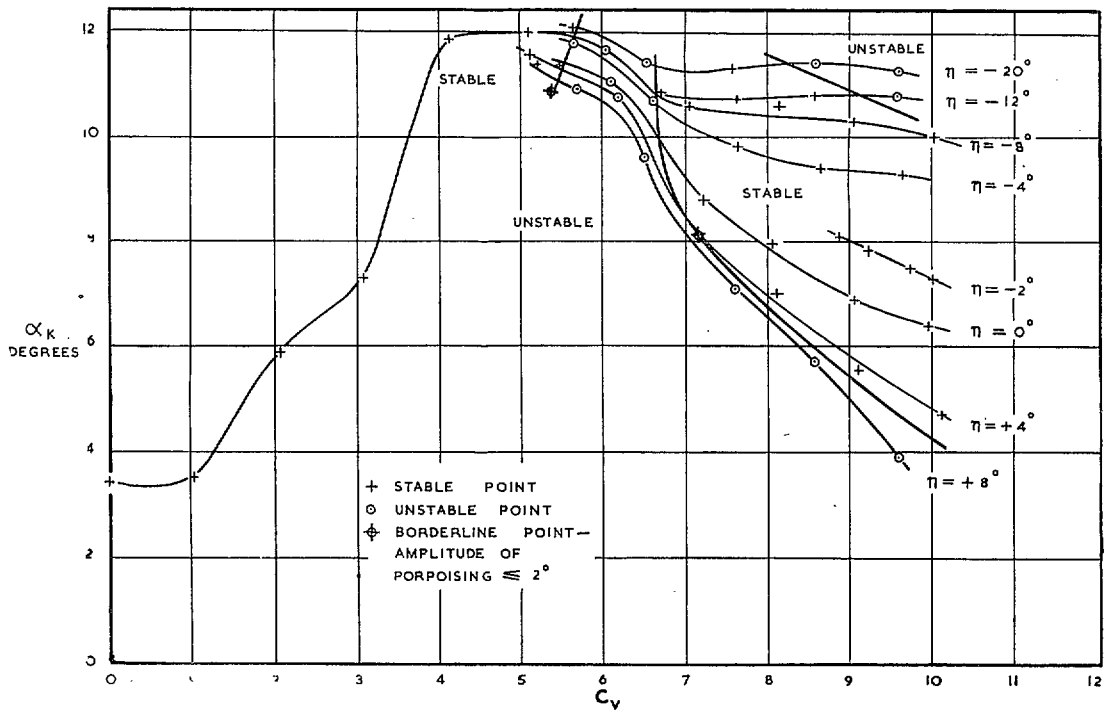

FIG. 121. Model A longitudinal stability without disturbance ($C_{\Delta 0} = 3{\cdot}00$).

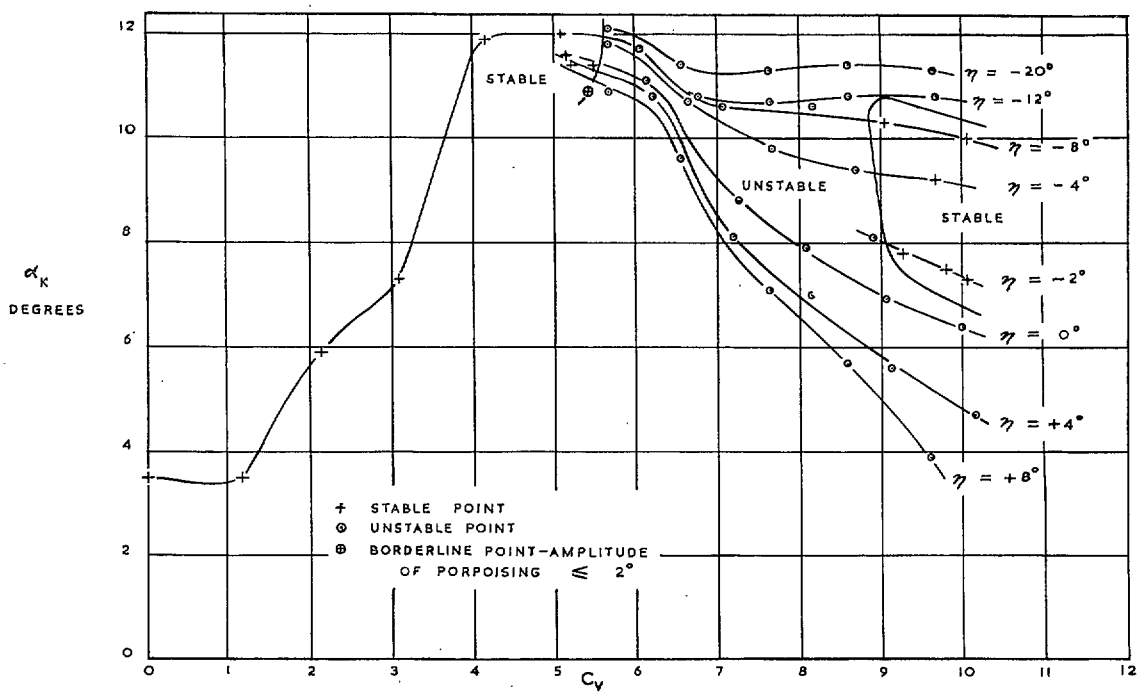

FIG. 122. Model A longitudinal stability with disturbance ($C_{\Delta 0} = 3{\cdot}00$).

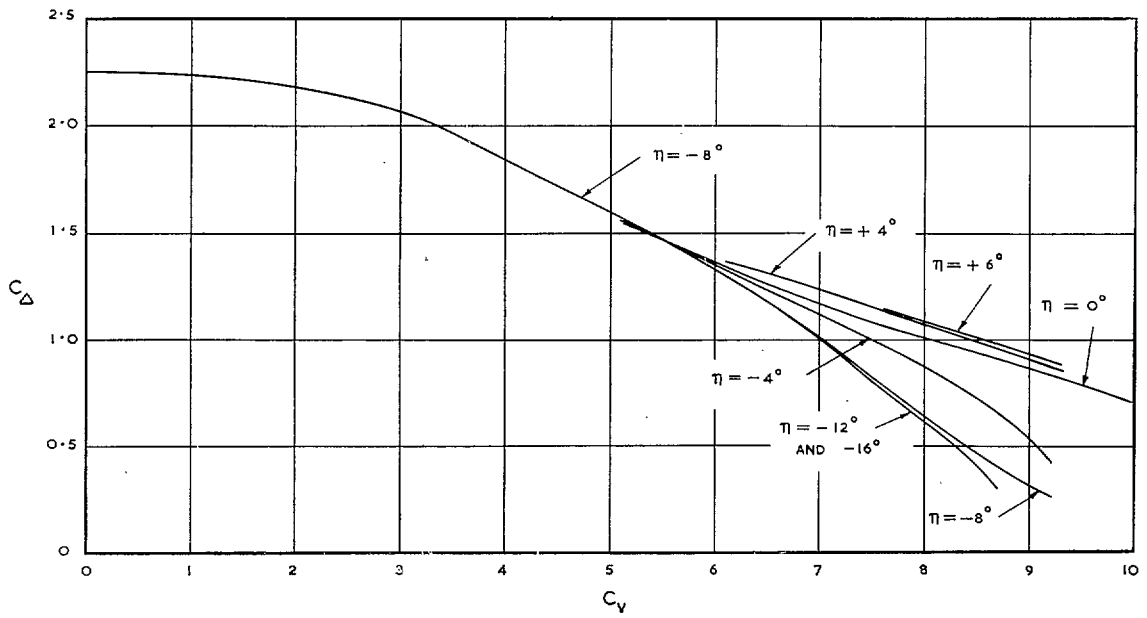

FIG. 123. Model A load-coefficient curves ($C_{\Delta 0} = 2{\cdot}25$).

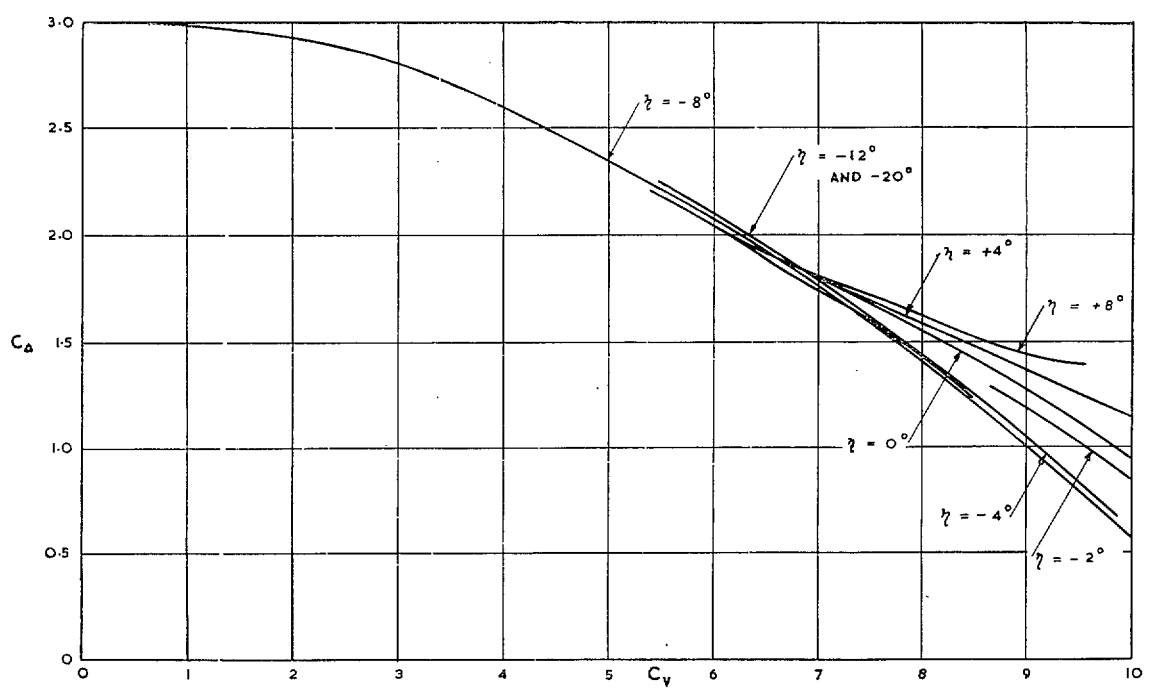

FIG. 124. Model A load-coefficient curves ($C_{\Delta 0} = 3{\cdot}00$).

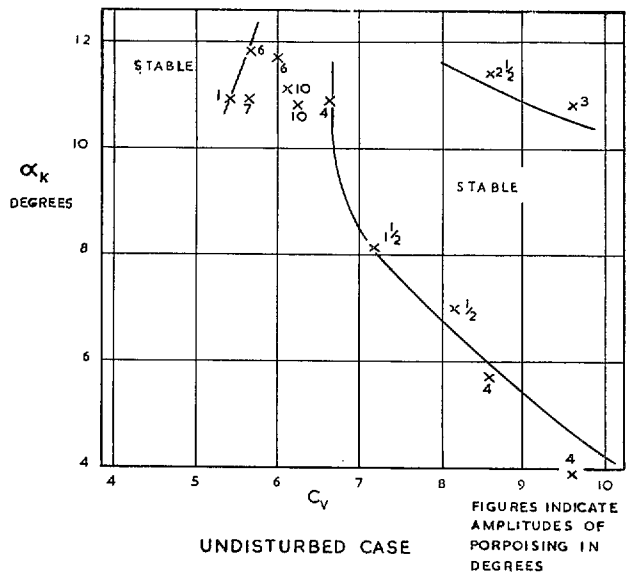

FIG. 125. Model A porpoising amplitudes and stability limits ($C_{A0} = 3{\cdot}00$).

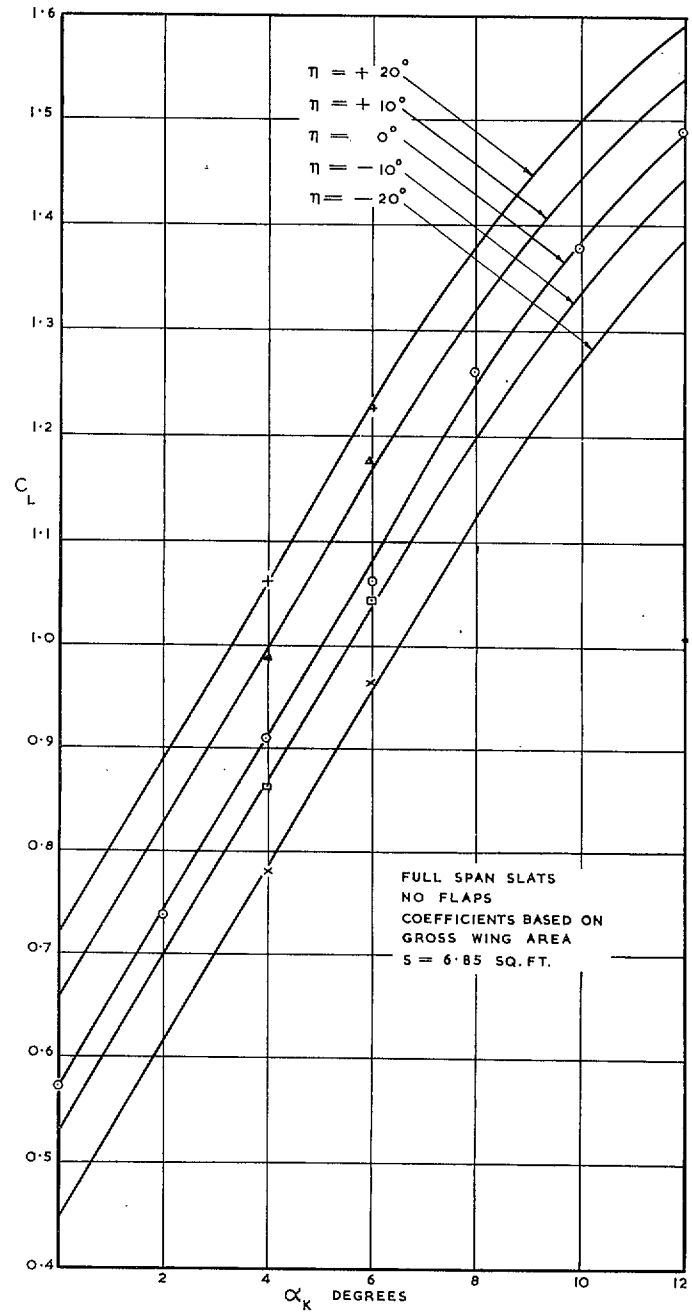

FIG. 126. Model B lift curves without slipstream.

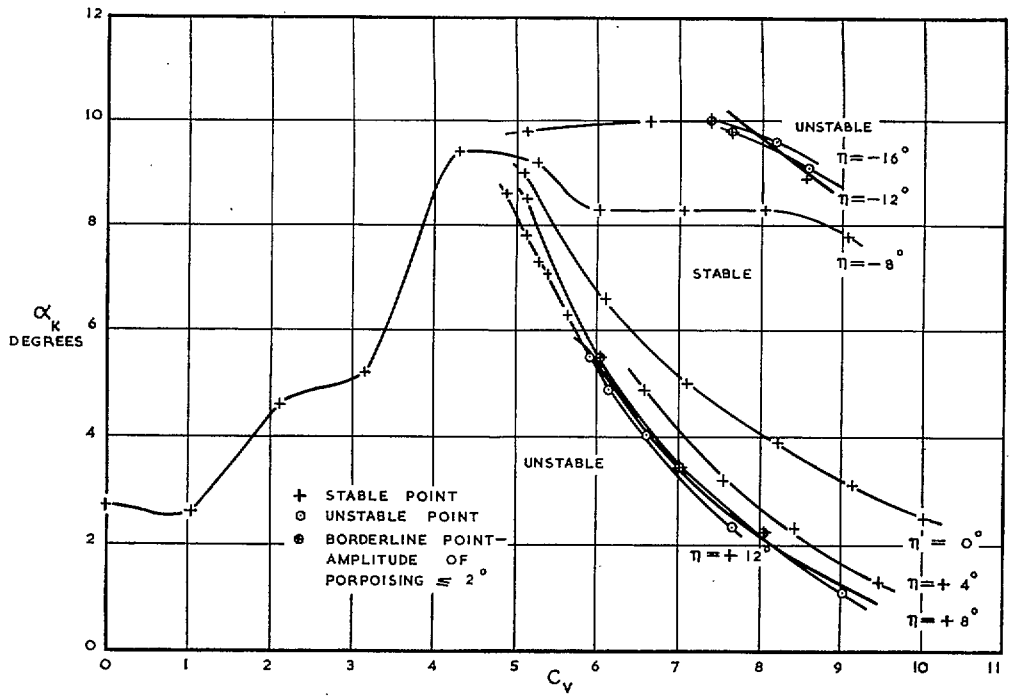

FIG. 127. Model B longitudinal stability without disturbance ($C_{\Delta 0} = 2{\cdot}00$).

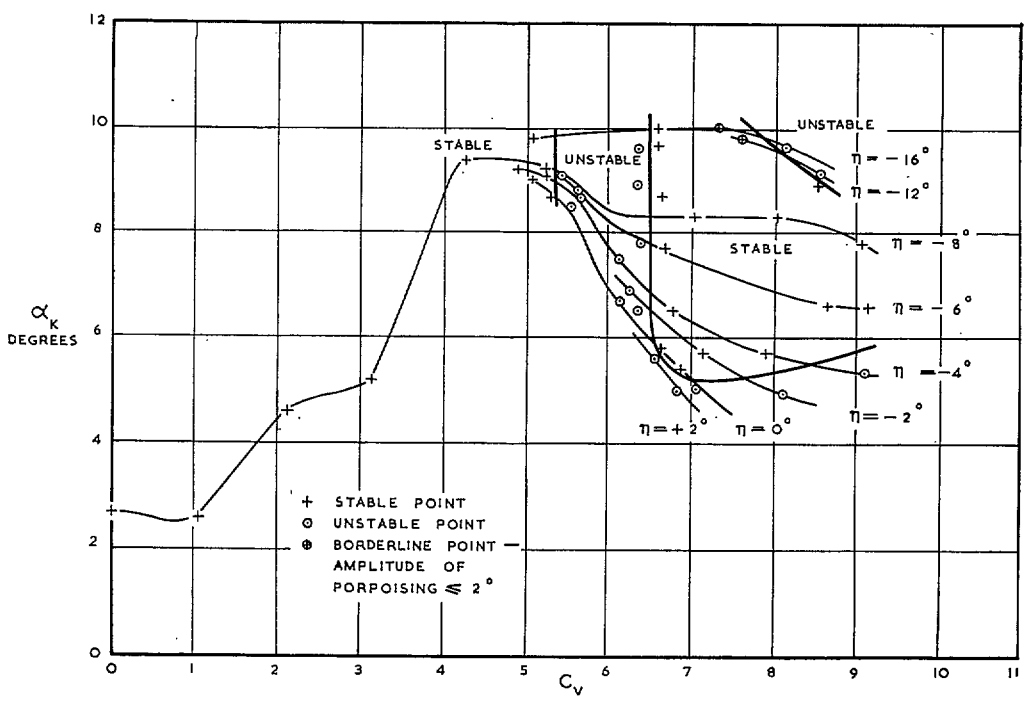

FIG. 128. Model B longitudinal stability with disturbance ($C_{\Delta 0} = 2{\cdot}00$).

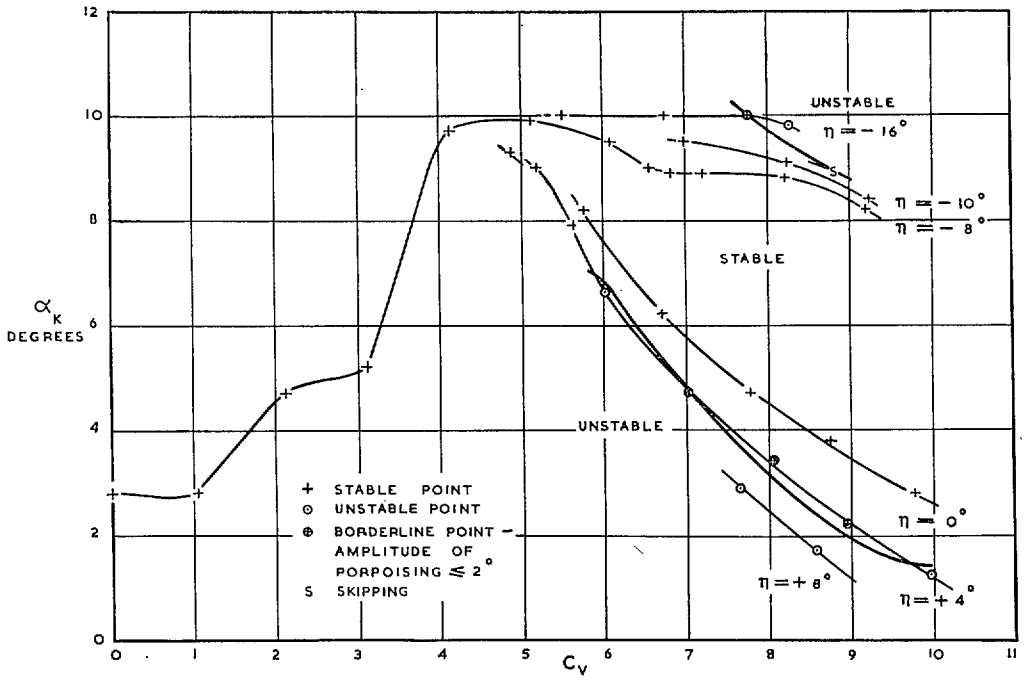

FIG. 129. Model B longitudinal stability without disturbance ($C_{\Delta 0} = 2{\cdot}25$).

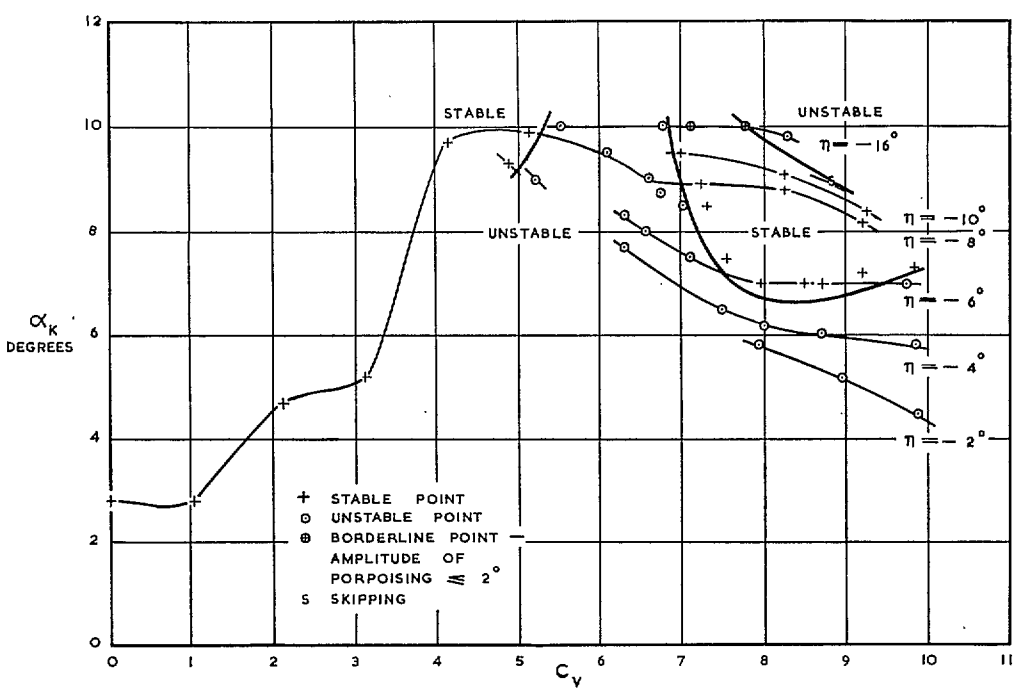

FIG. 130. Model B longitudinal stability with disturbance ($C_{\Delta 0} = 2{\cdot}25$).

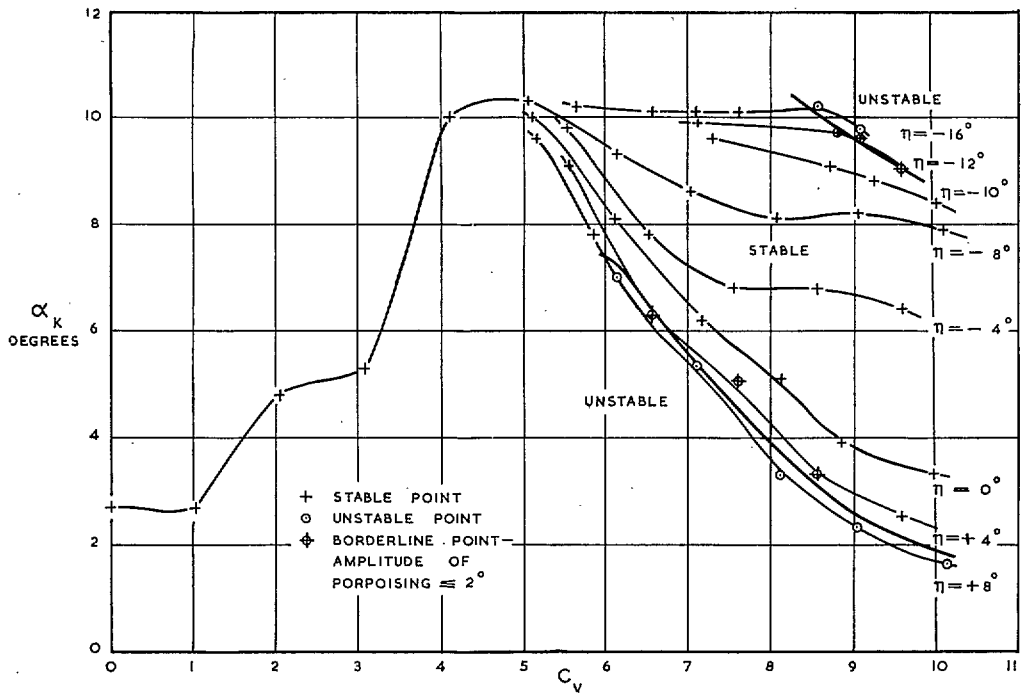

FIG. 131. Model B longitudinal stability without disturbance ($C_{\Delta 0} = 2{\cdot}50$).

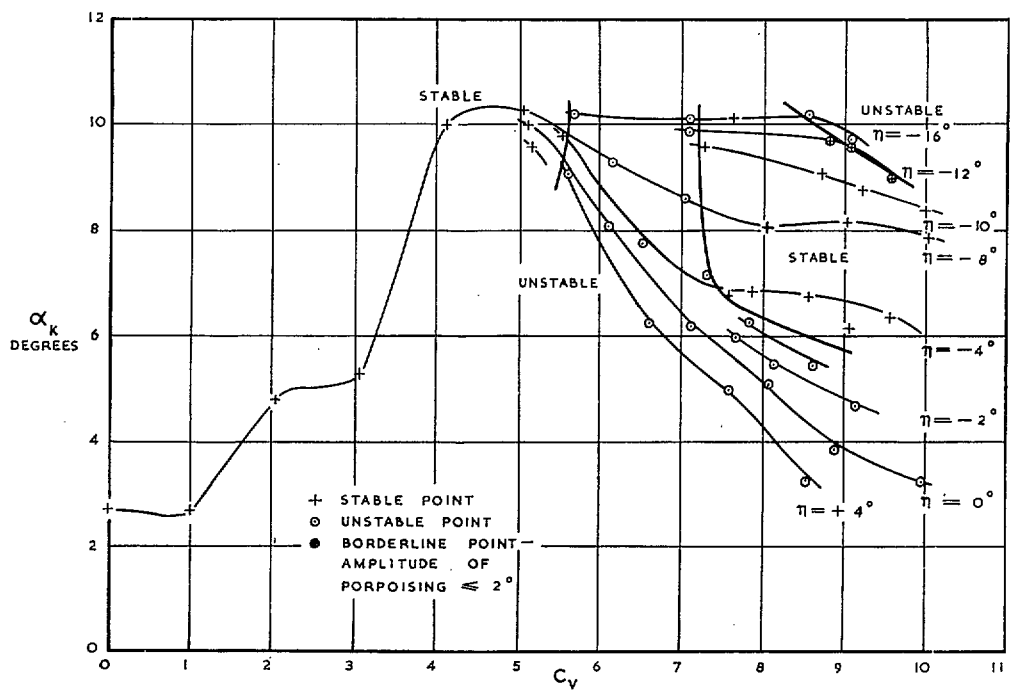

FIG. 132. Model B longitudinal stability with disturbance ($C_{\Delta 0} = 2{\cdot}50$).

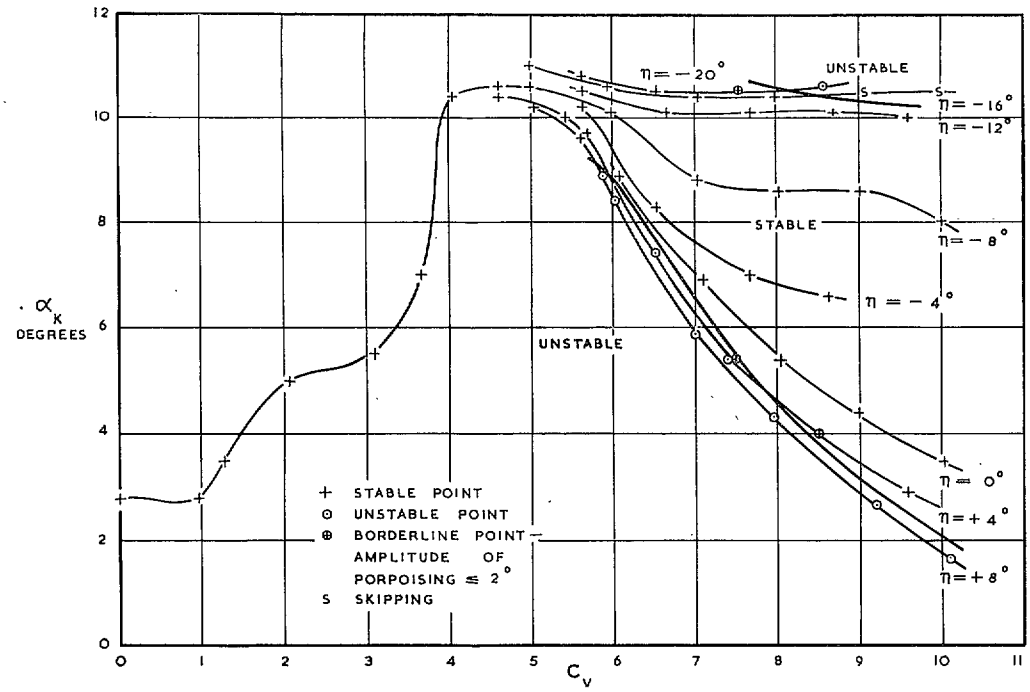

FIG. 133. Model B longitudinal stability without disturbance ($C_{\Delta 0} = 2{\cdot}75$).

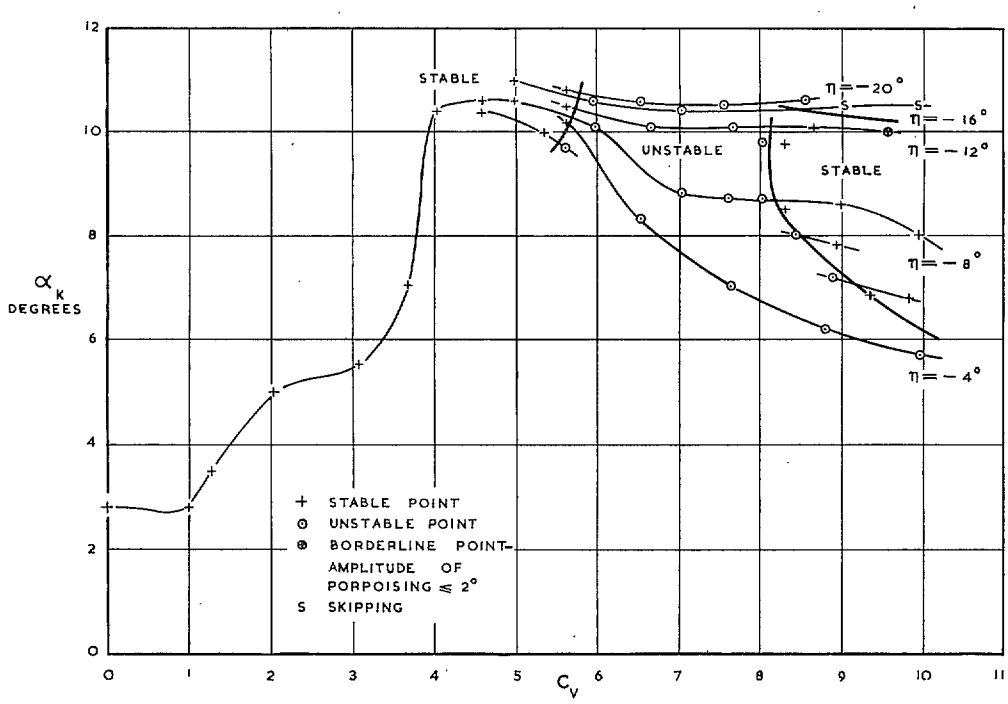

FIG. 134. Model B longitudinal stability with disturbance ($C_{\Delta 0} = 2{\cdot}75$).

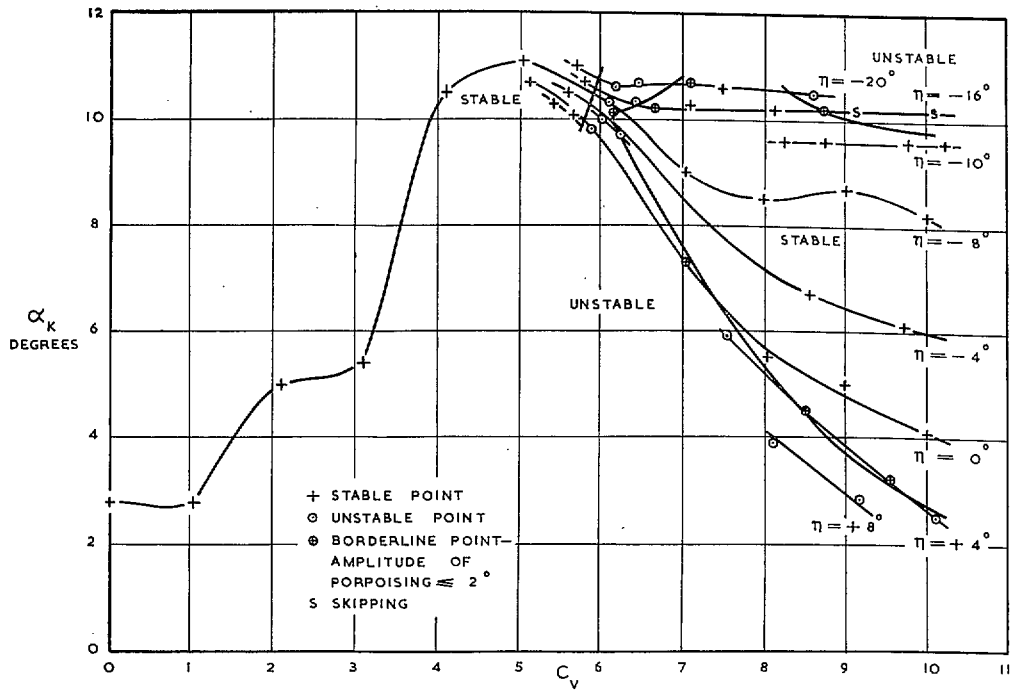

FIG. 135. Model B longitudinal stability without disturbance ($C_{\Delta 0} = 3{\cdot}00$).

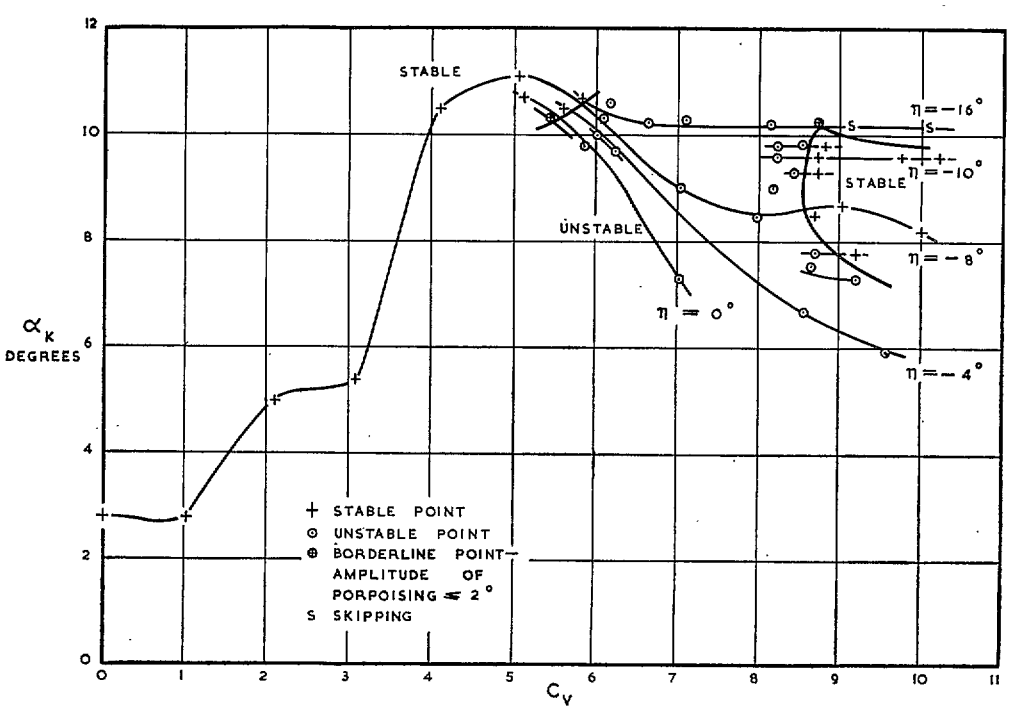

FIG. 136. Model B longitudinal stability with disturbance ($C_{\Delta 0} = 3{\cdot}00$).

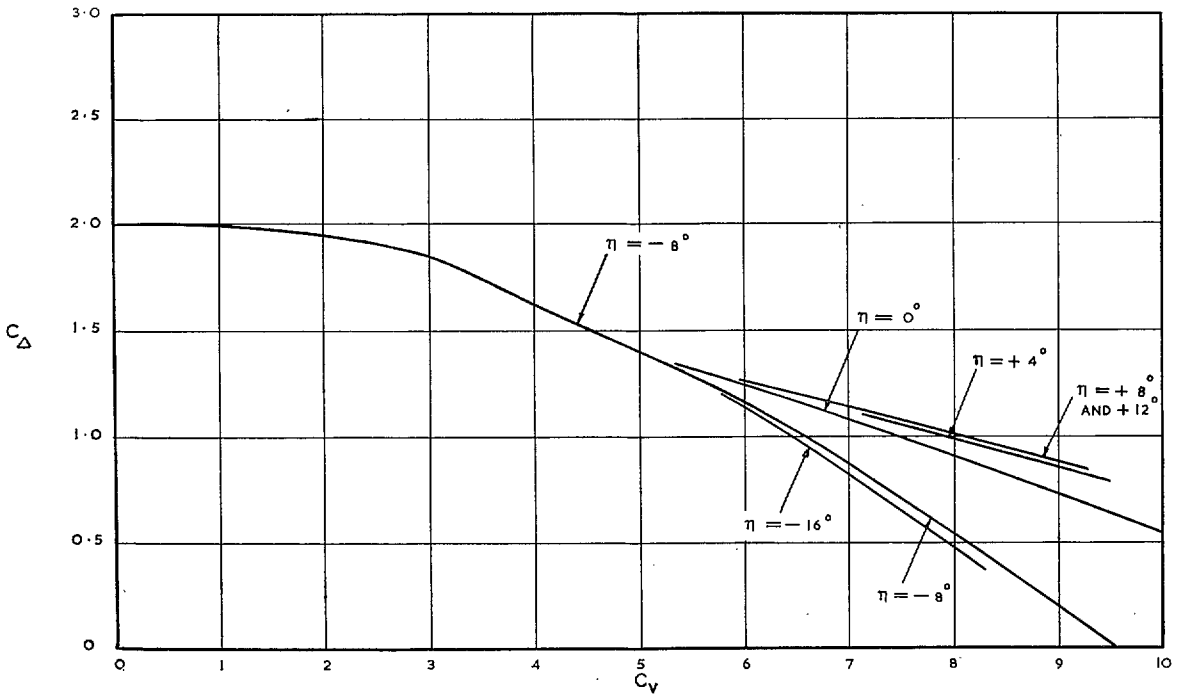

FIG. 137. Model B load-coefficient curves ($C_{\Delta 0} = 2{\cdot}00$).

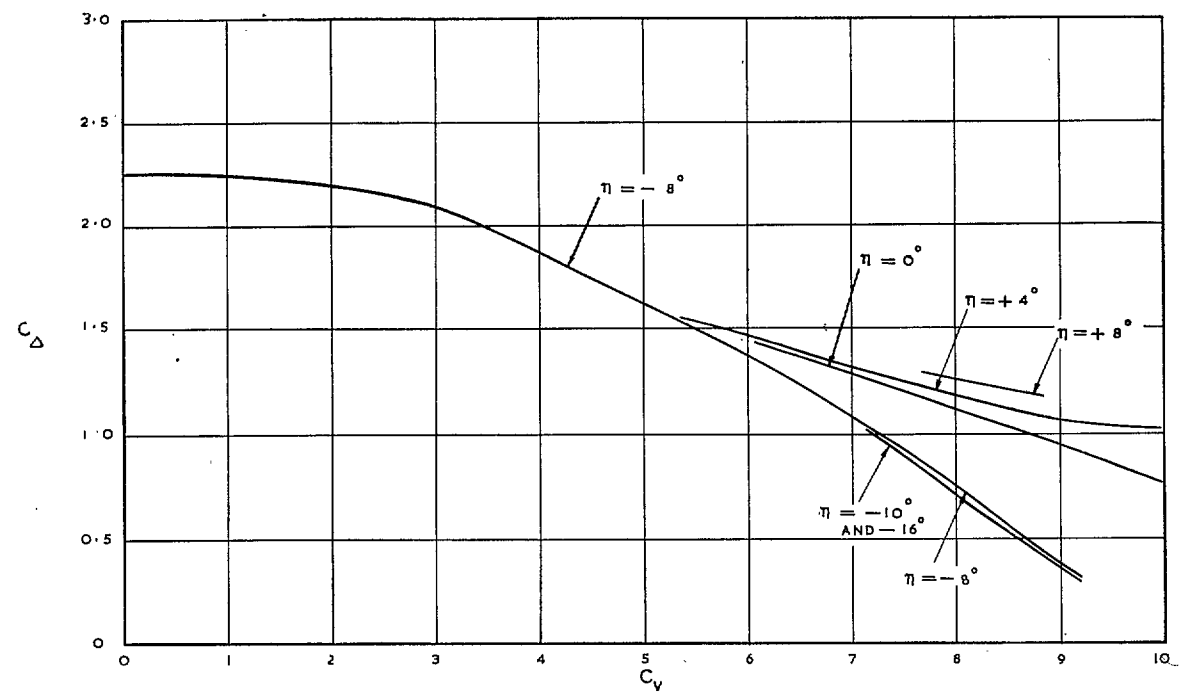

FIG. 138. Model B load-coefficient curves ($C_{\Delta 0} = 2{\cdot}25$).

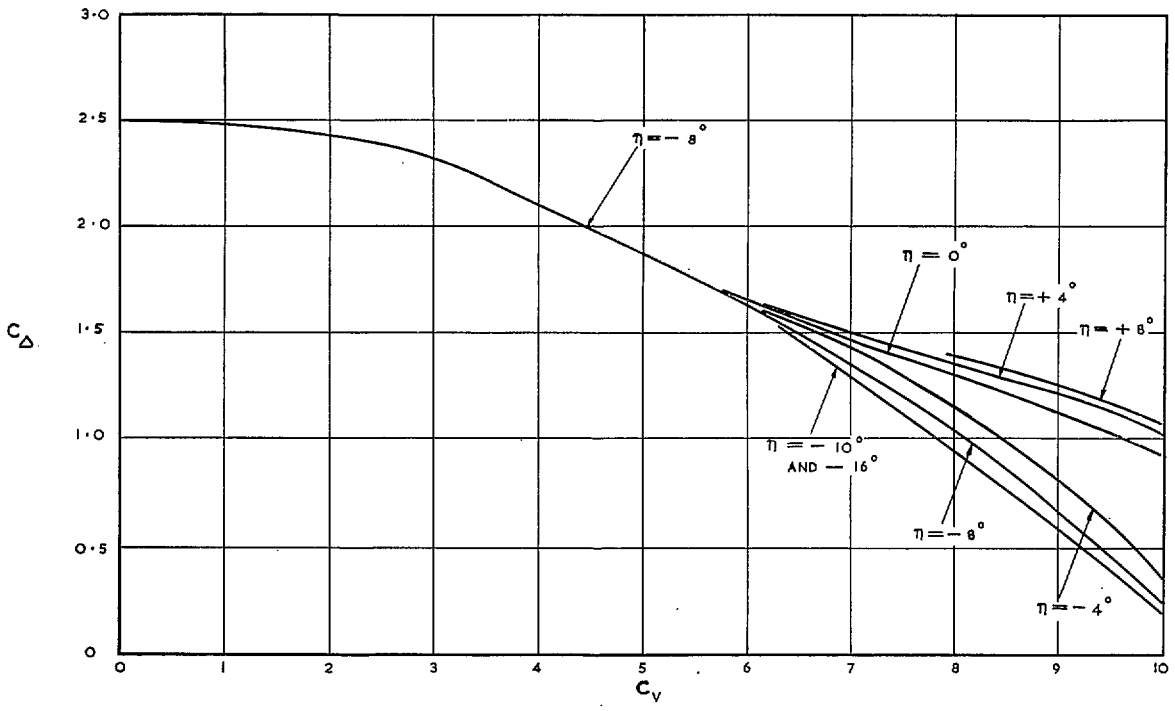

FIG. 139. Model B load-coefficient curves ($C_{\Delta 0} = 2{\cdot}50$).

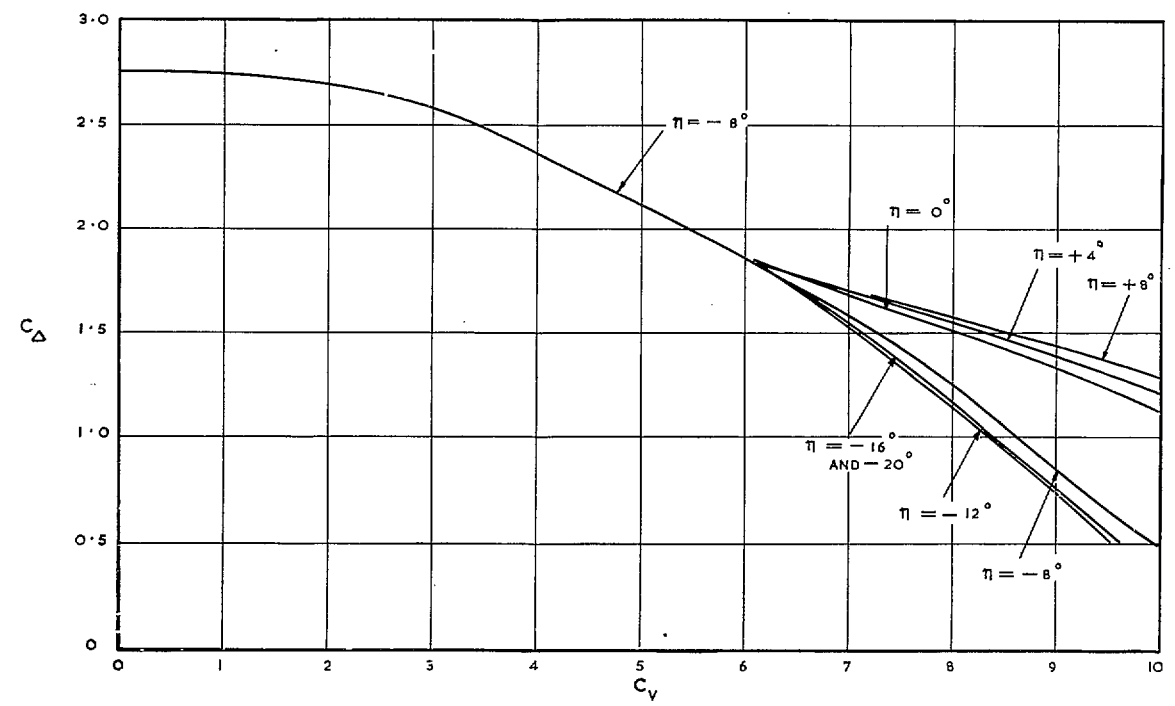

FIG. 140. Model B load-coefficient curves ($C_{\Delta 0} = 2{\cdot}75$).

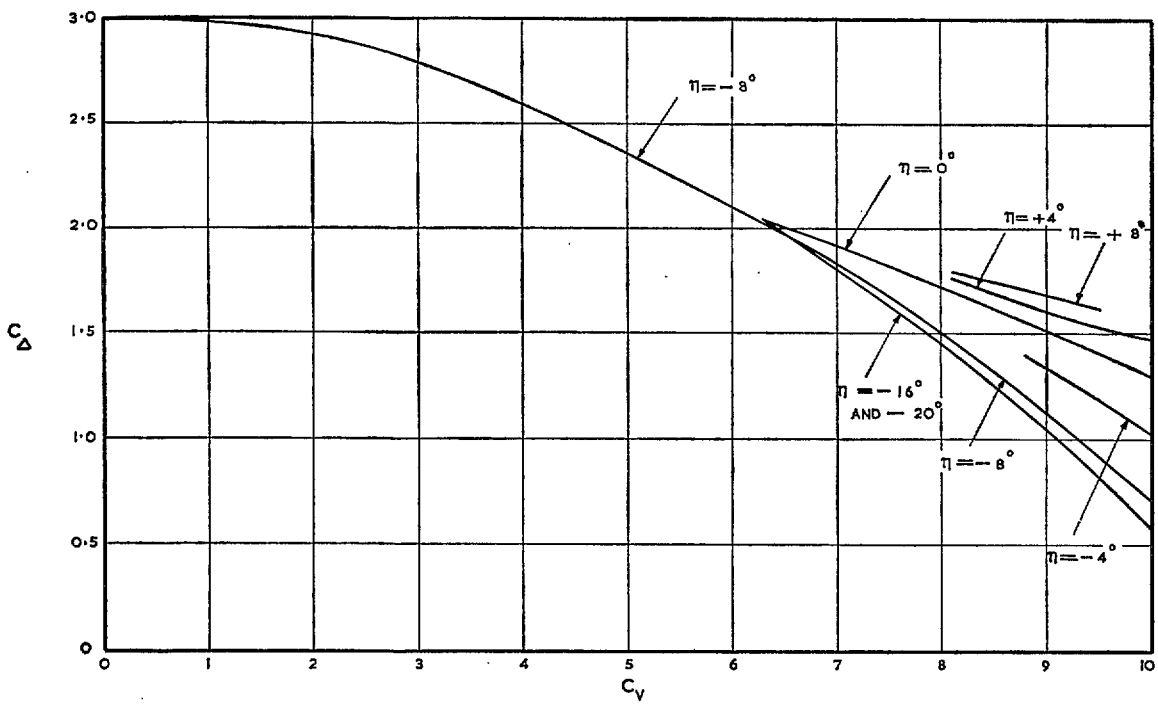

FIG. 141. Model B load-coefficient curves ($C_{\Delta 0} = 3{\cdot}00$).

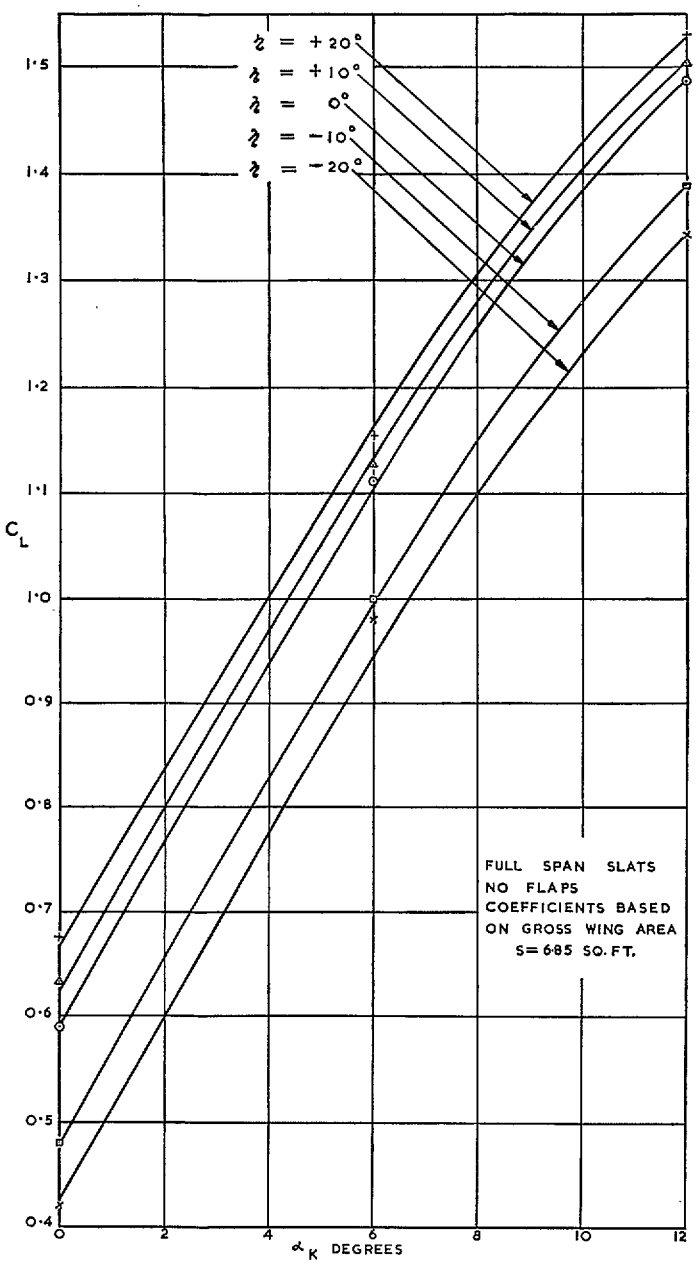

FIG. 142. Model C lift curves without slipstream.

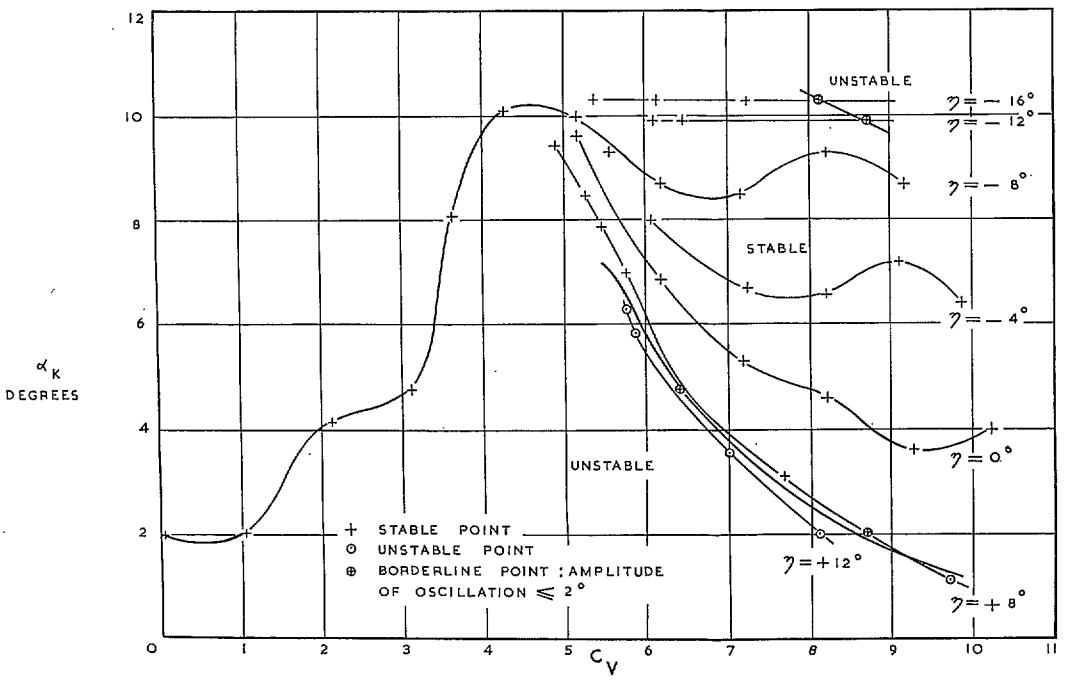

FIG. 143. Model C longitudinal stability without disturbance ($C_{\Delta 0} = 2{\cdot}25$).

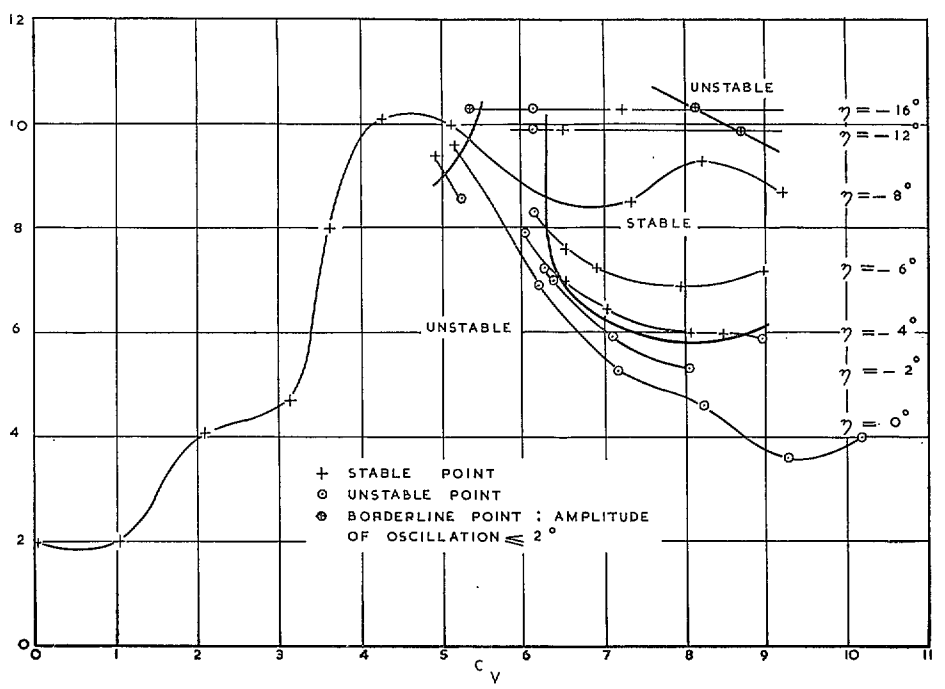

FIG. 144. Model C longitudinal stability with disturbance ($C_{\Delta 0} = 2{\cdot}25$).

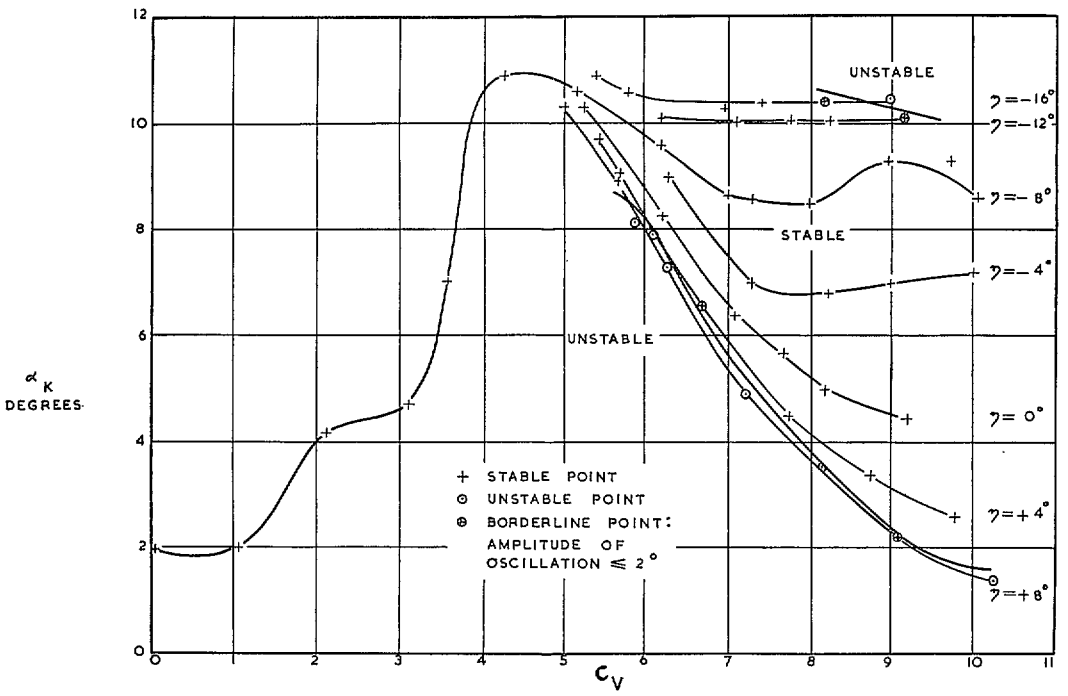

FIG. 145. Model C longitudinal stability without disturbance ($C_{\Delta 0} = 2{\cdot}75$).

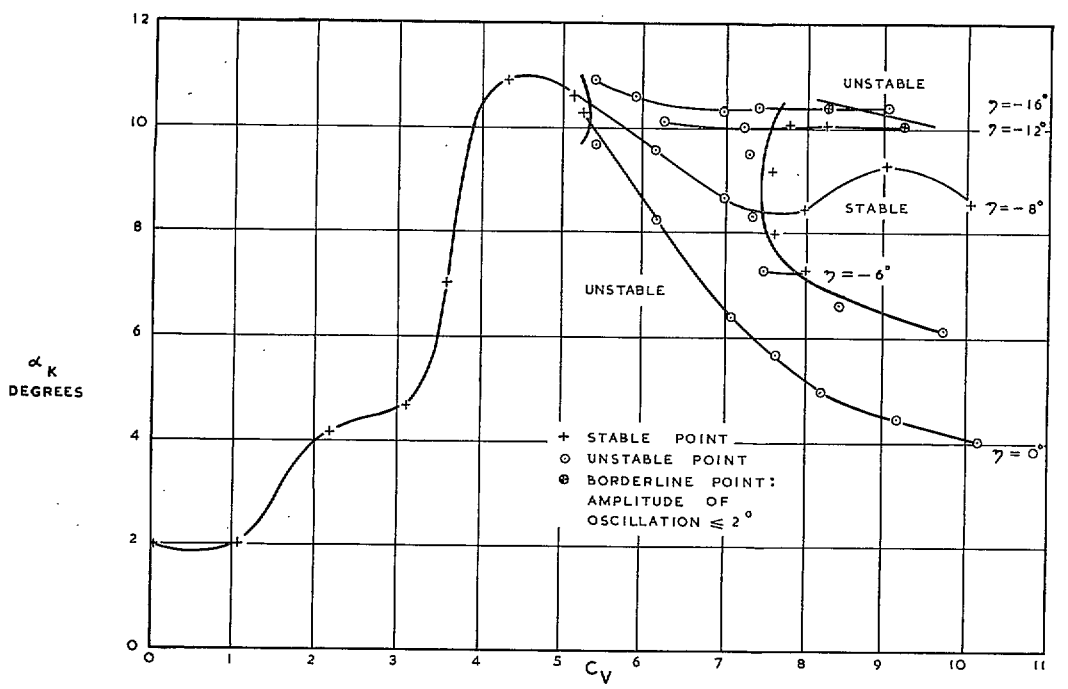

FIG. 146. Model C longitudinal stability with disturbance ($C_{\Delta 0} = 2{\cdot}75$),

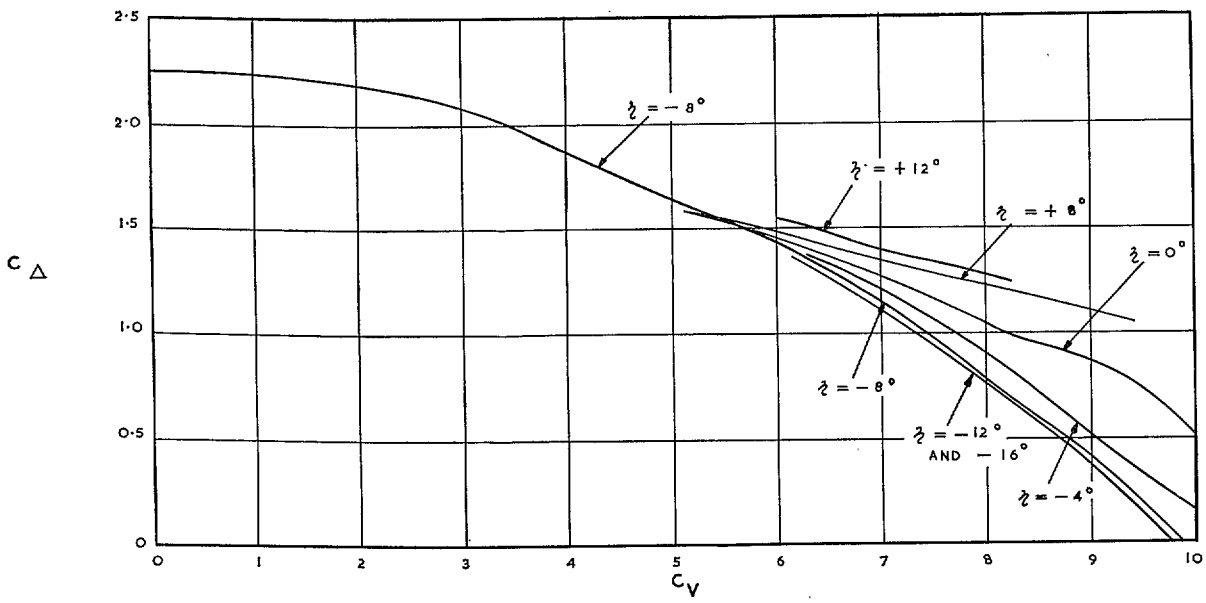

FIG. 147. Model C load-coefficient curves ($C_{\Delta 0} = 2{\cdot}25$).

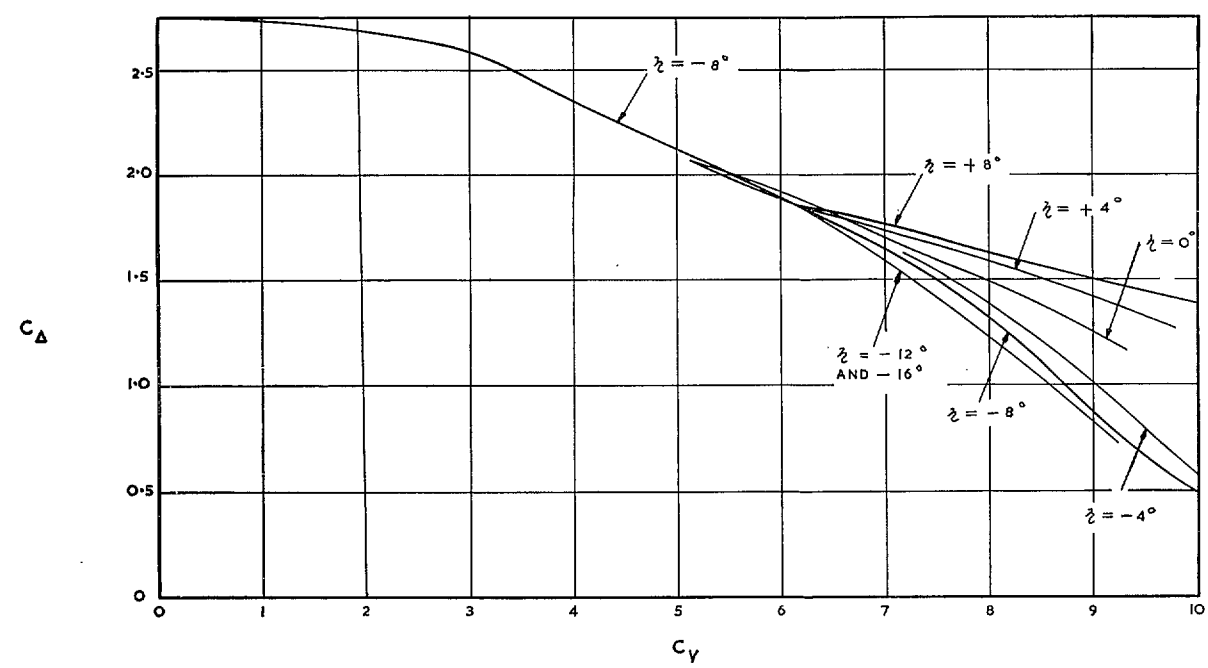

FIG. 148. Model C load-coefficient curves ($C_{\Delta 0} = 2{\cdot}75$).

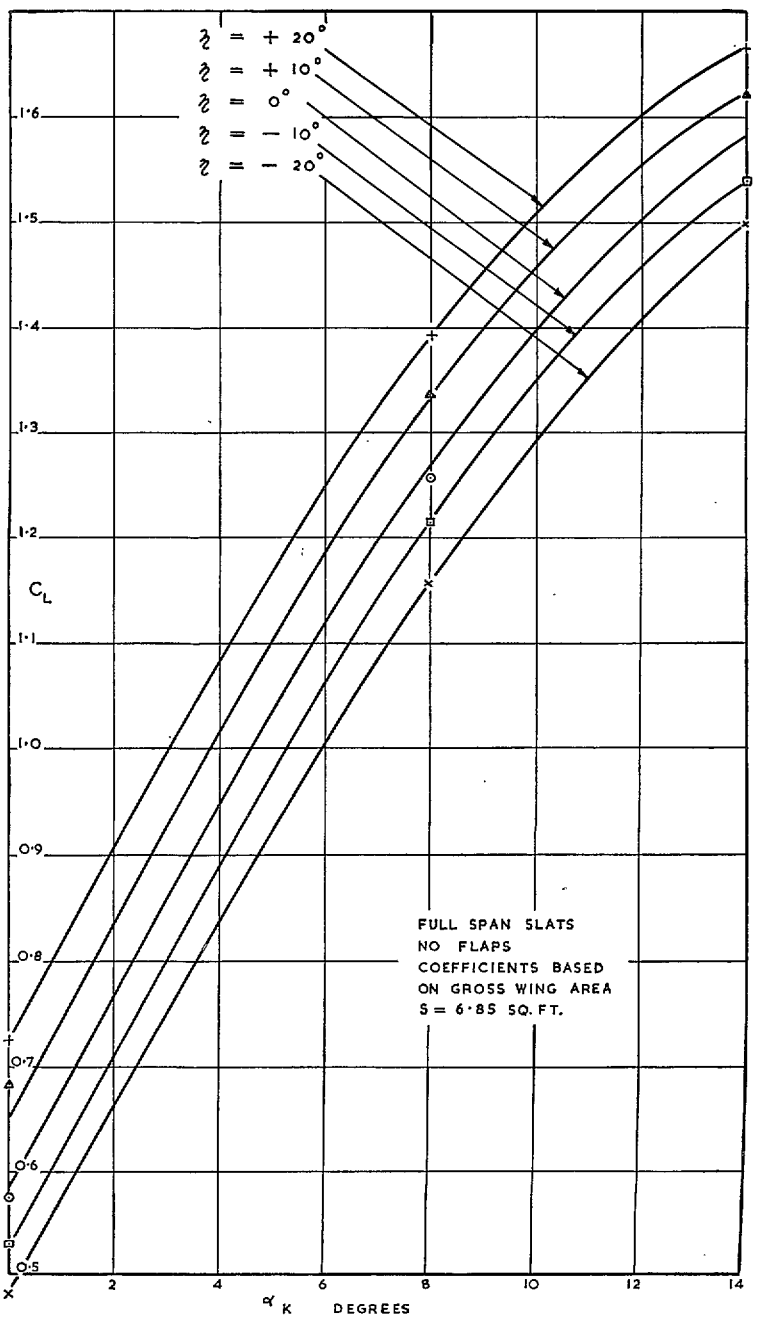

FIG. 149. Model D lift curves without slipstream.

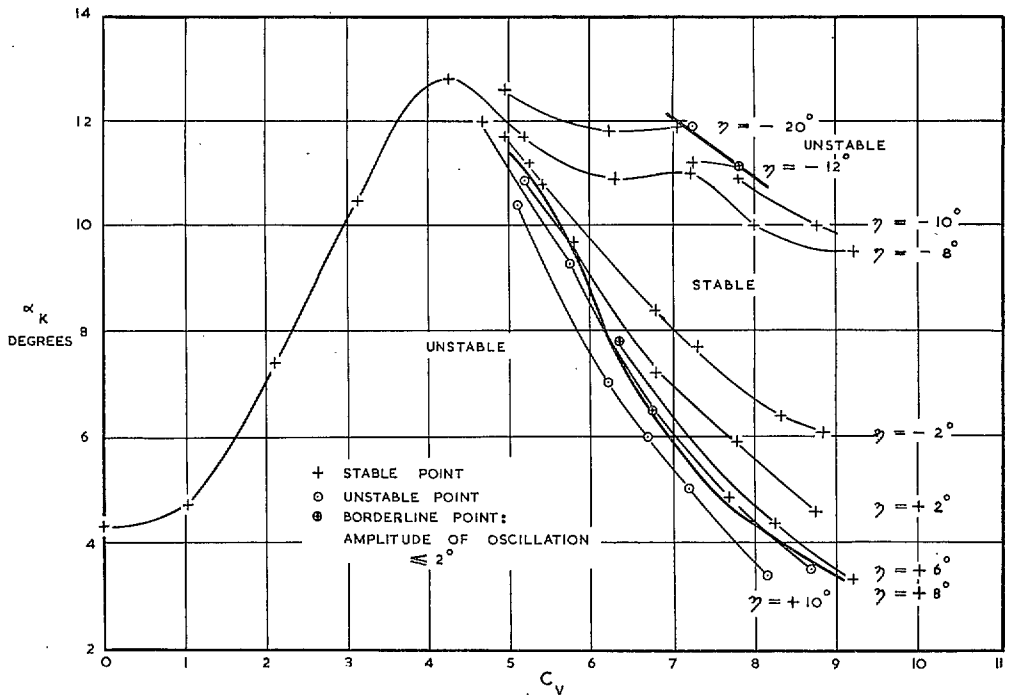

FIG. 150. Model D longitudinal stability without disturbance ($C_{\Delta 0} = 2{\cdot}25$).

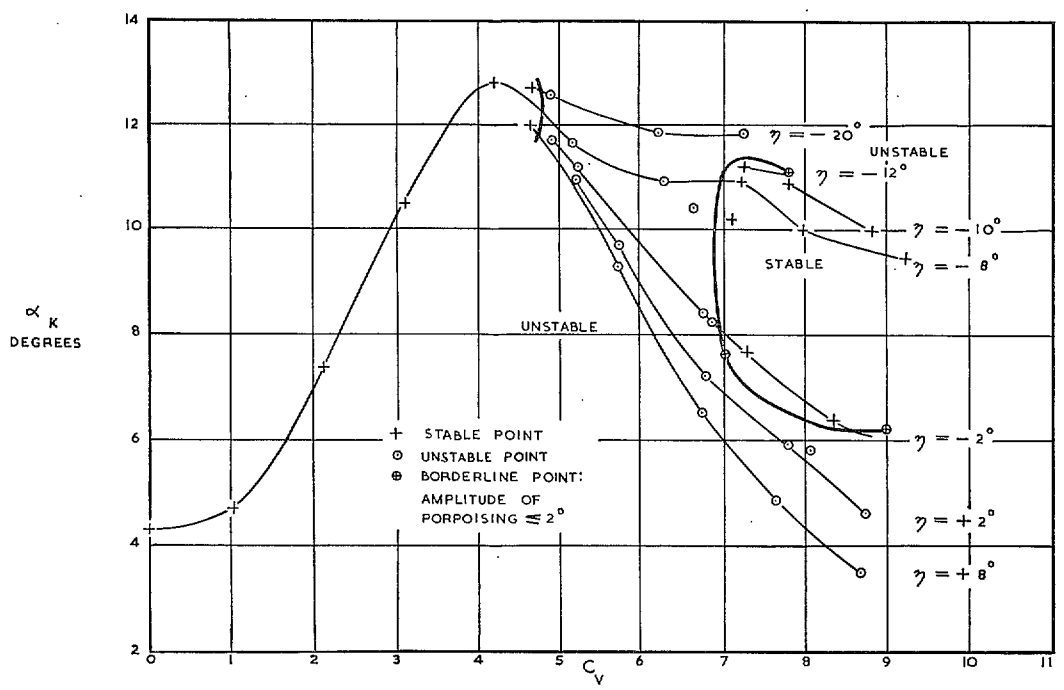

FIG. 151. Model D longitudinal stability with disturbance ($C_{\Delta 0} = 2{\cdot}25$).

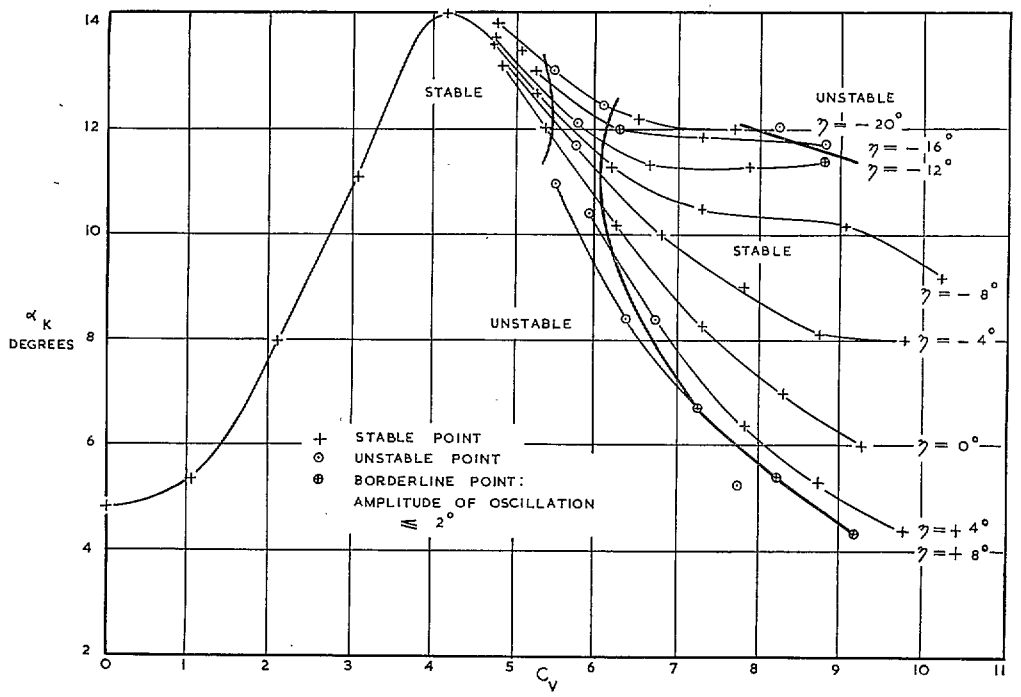

FIG. 152. Model D longitudinal stability without disturbance ($C_{\Delta 0} = 2{\cdot}75$).

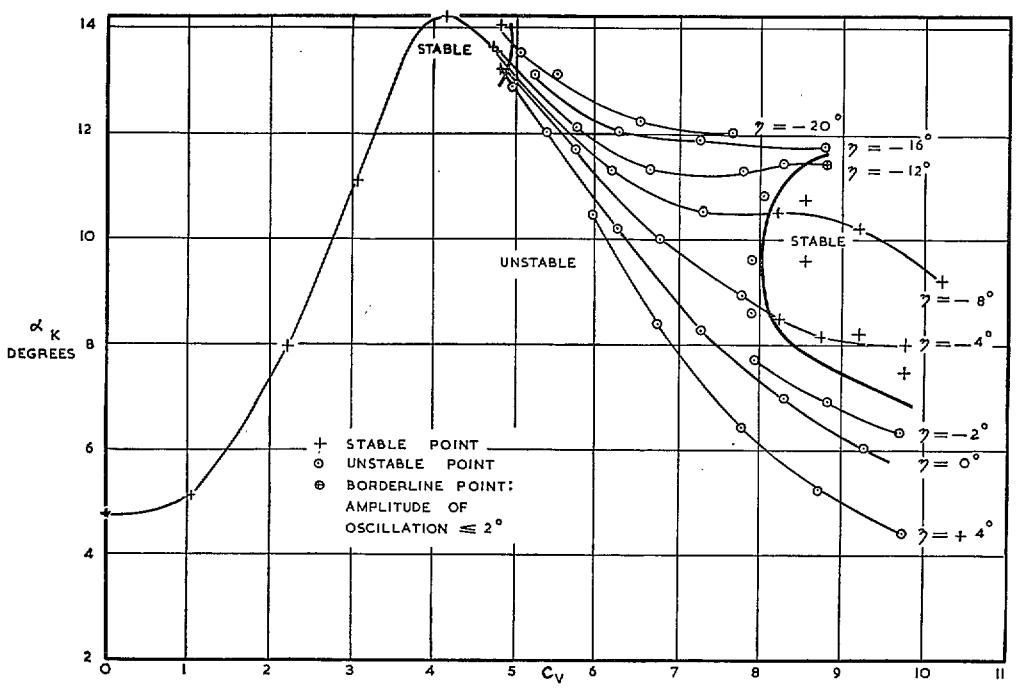

FIG. 153. Model D longitudinal stability with disturbance ($C_{\Delta 0} = 2{\cdot}75$).

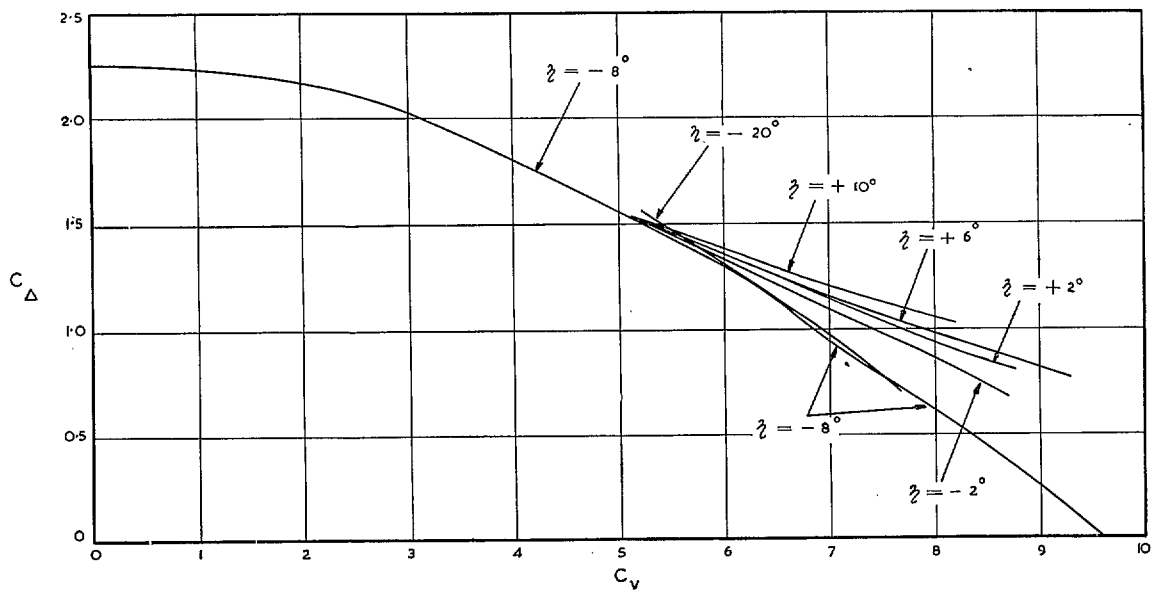

FIG. 154. Model D load-coefficient curves ($C_{\Delta 0} = 2{\cdot}25$).

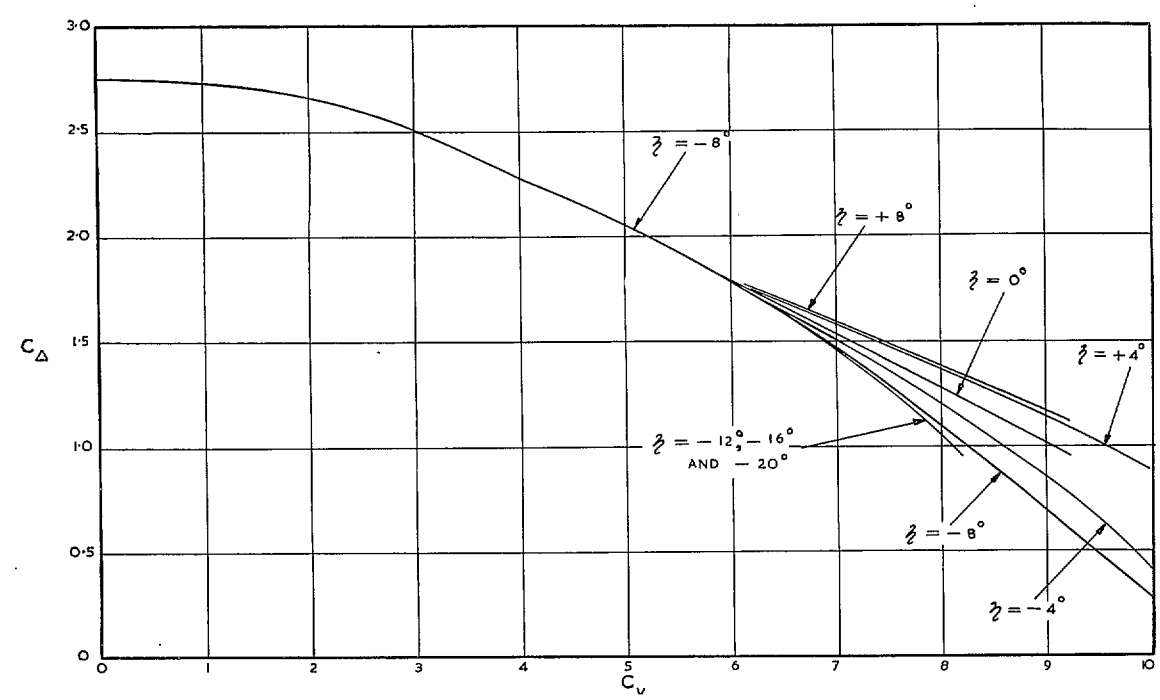

FIG. 155. Model D load-coefficient curves ($C_{\Delta 0} = 2{\cdot}75$).

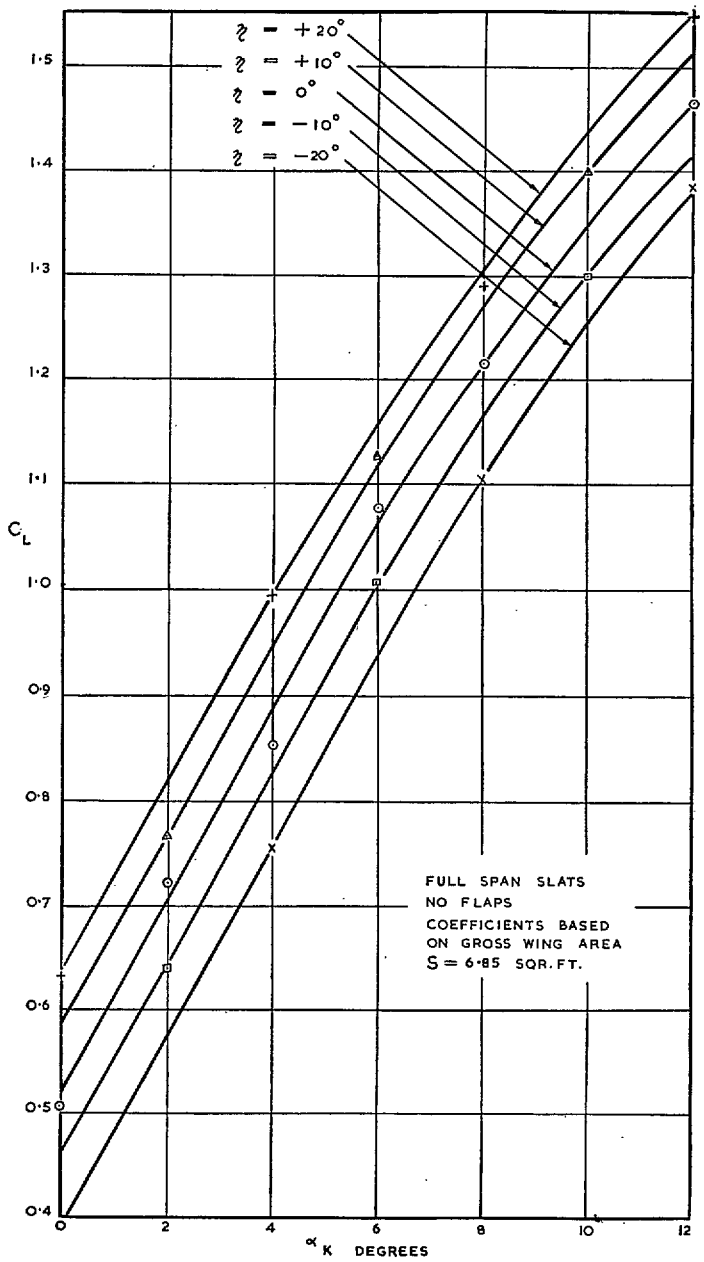

FIG. 156. Model E lift curves without slipstream.

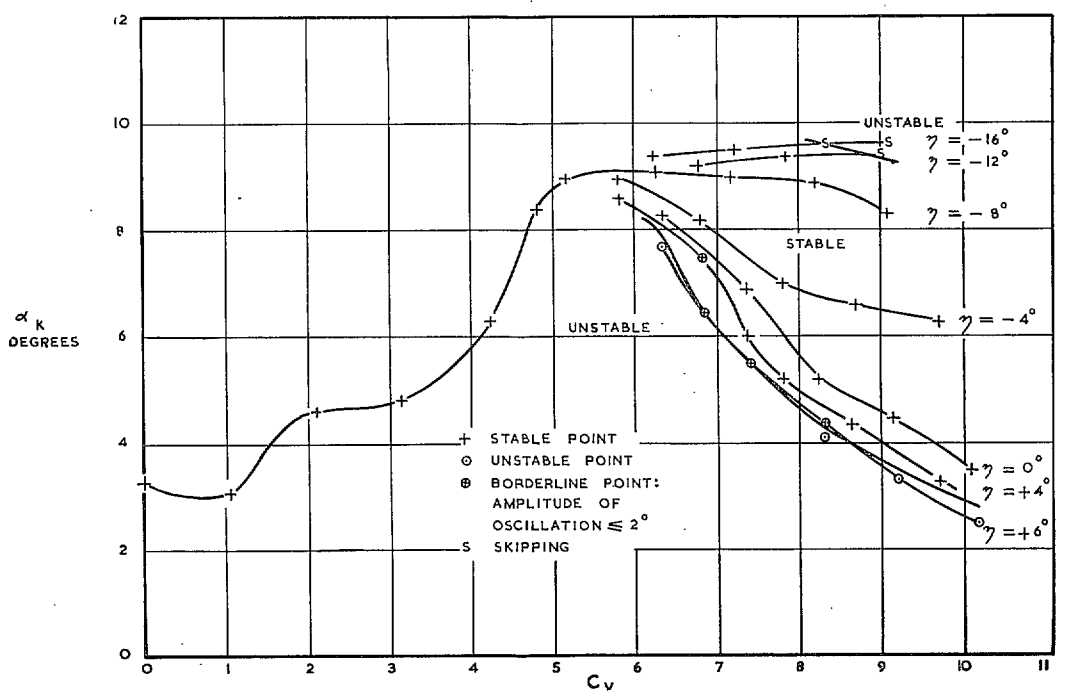

FIG. 157. Model E longitudinal stability without disturbance ($C_{\Delta 0} = 2{\cdot}25$).

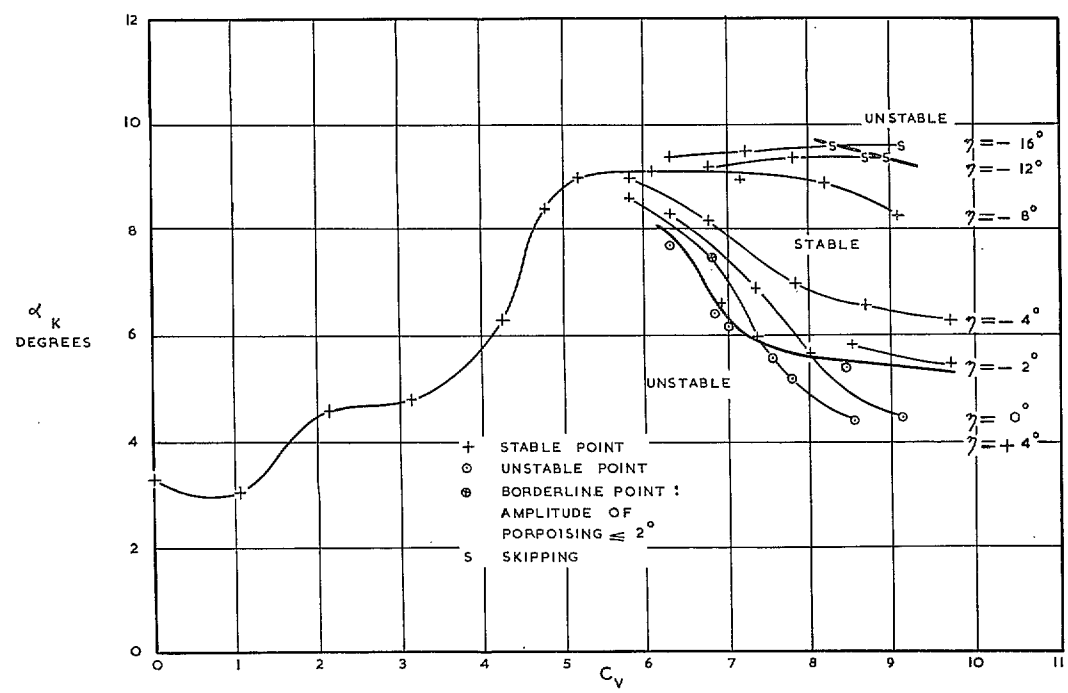

FIG. 158. Model E longitudinal stability with disturbance ($C_{\Delta 0} = 2{\cdot}25$).

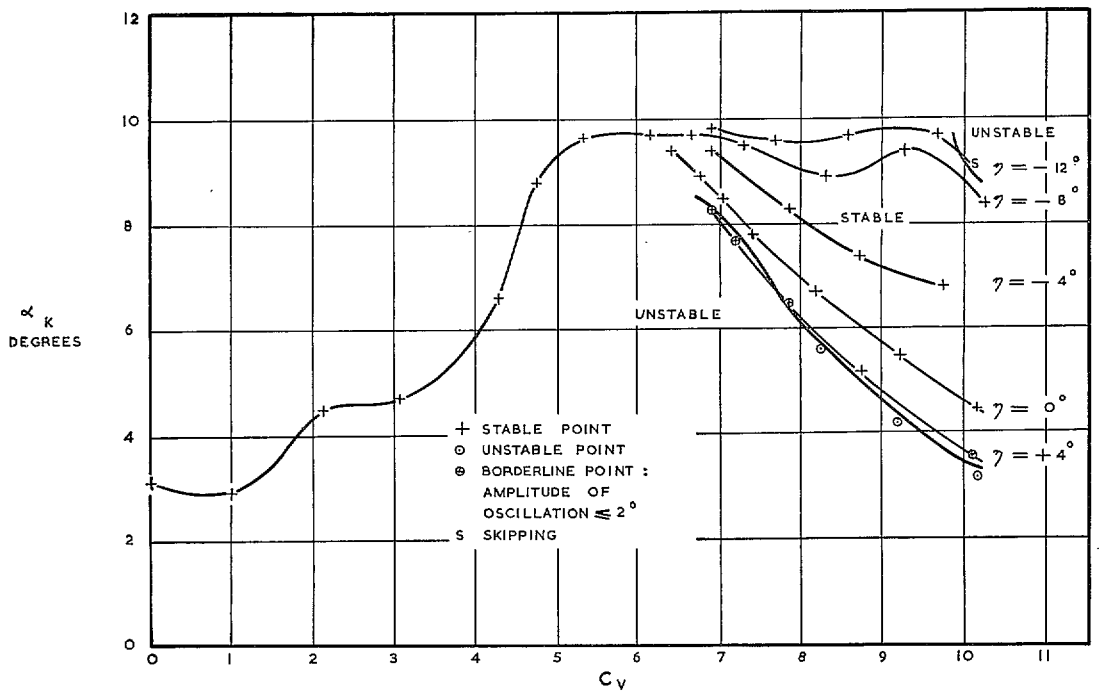

FIG. 159. Model E longitudinal stability without disturbance ($C_{\Delta 0} = 2{\cdot}75$).

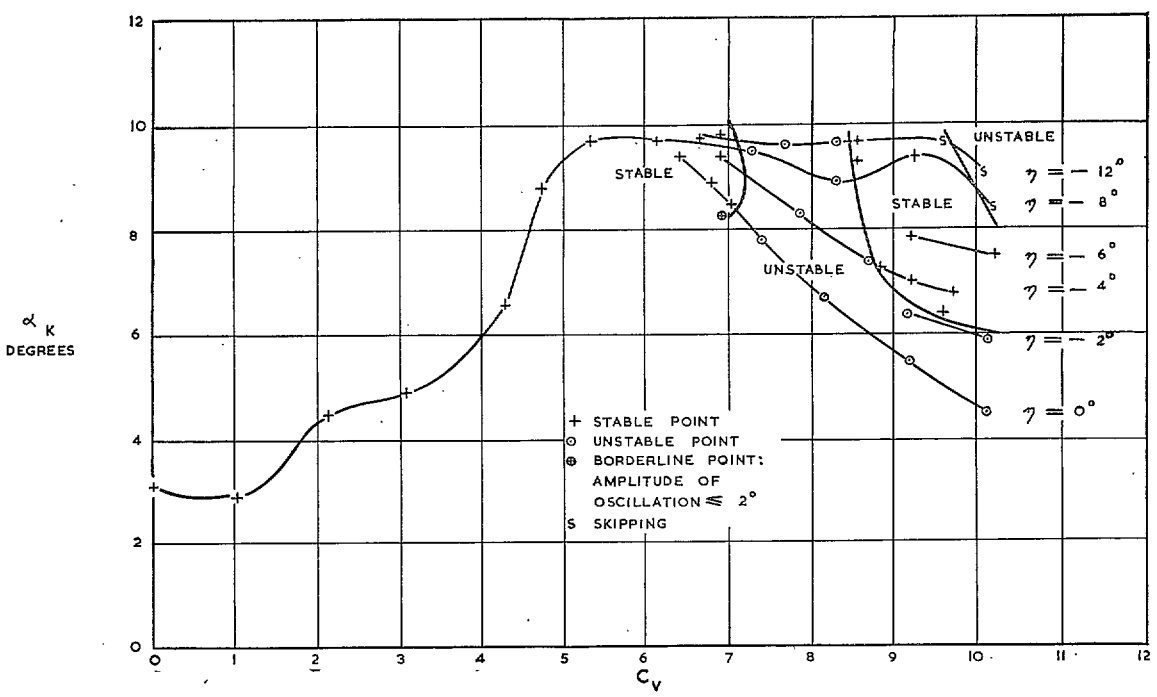

FIG. 160. Model E longitudinal stability with disturbance ($C_{\Delta 0} = 2{\cdot}75$).

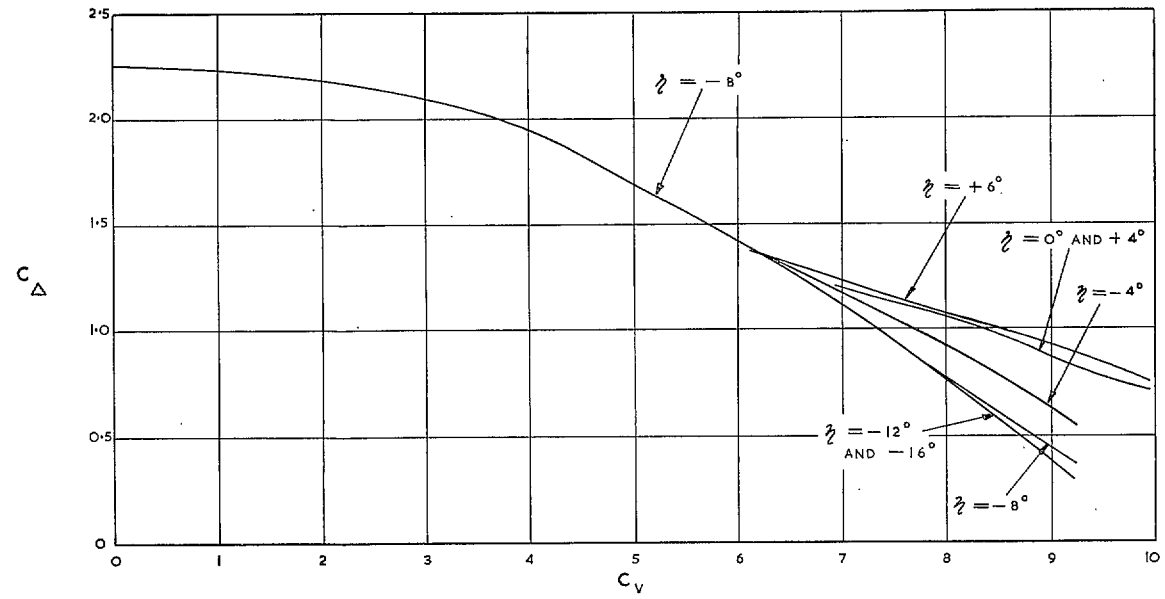

FIG. 161. Model E load-coefficient curves ($C_{\Delta 0} = 2{\cdot}25$).

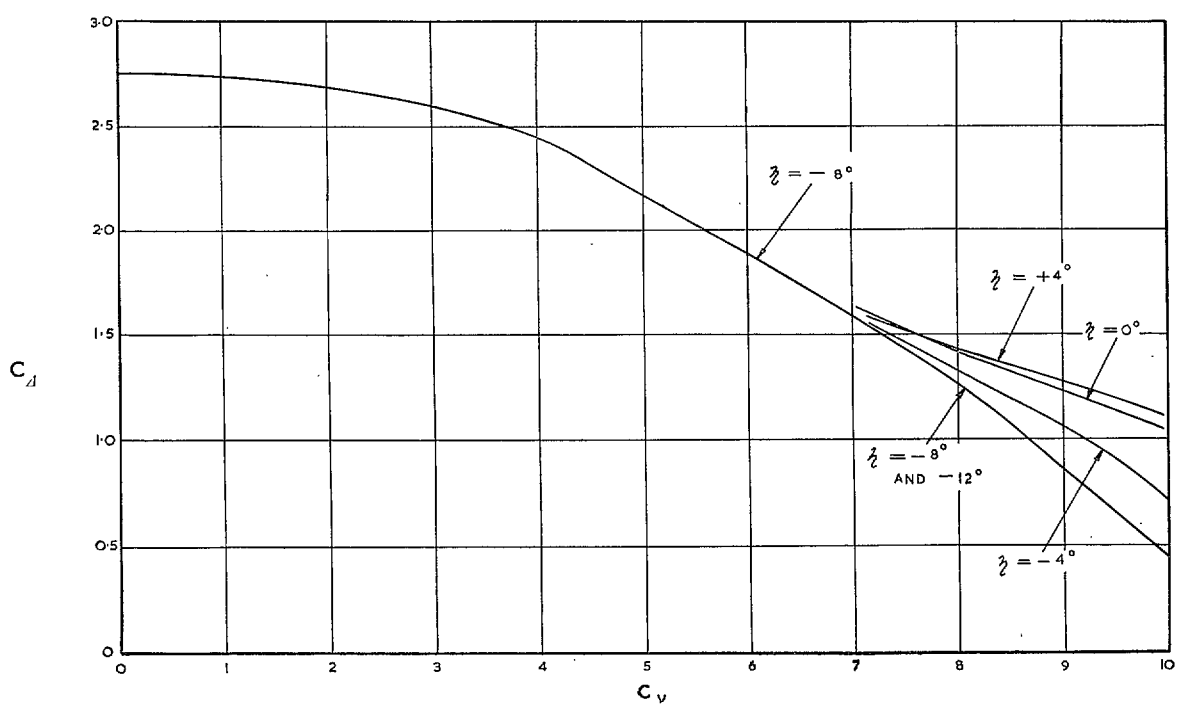

FIG. 162. Model E load-coefficient curves ($C_{\Delta 0} = 2{\cdot}75$).

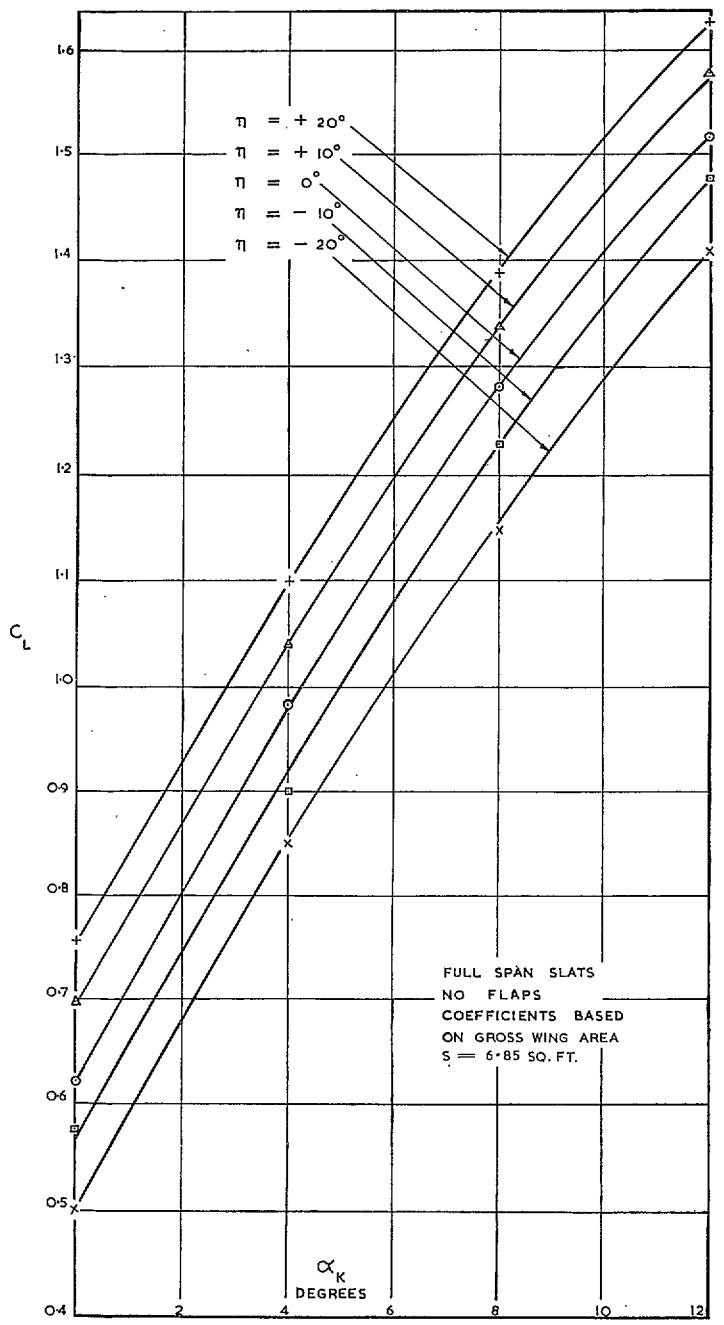

FIG. 163. Model F lift curves without slipstream.

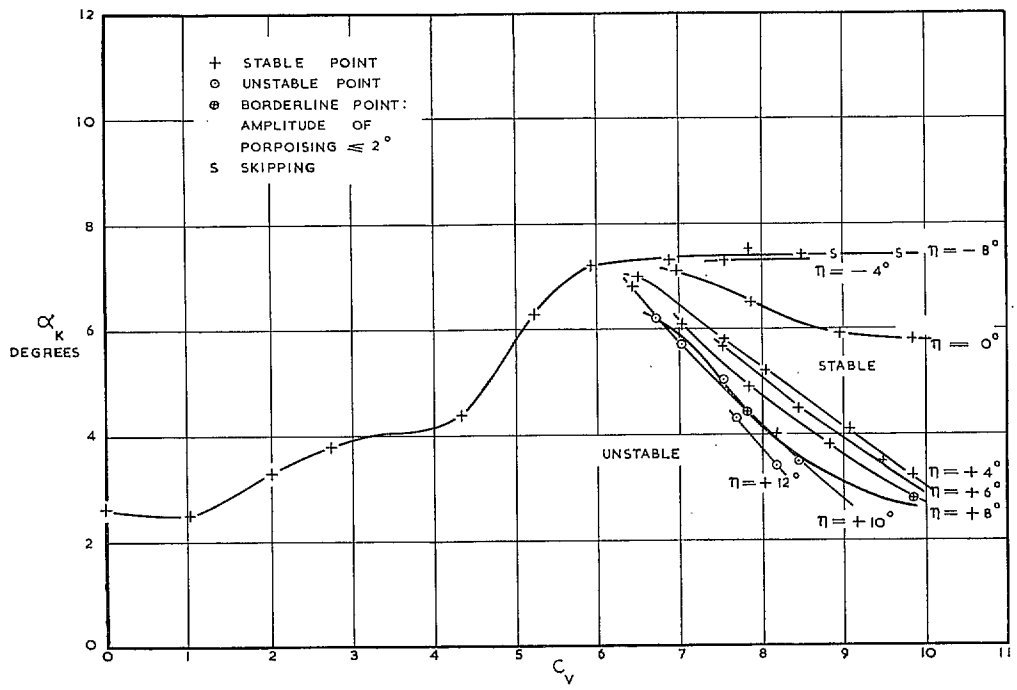

FIG. 164. Model F longitudinal stability without disturbance ($C_{\Delta 0} = 2{\cdot}25$).

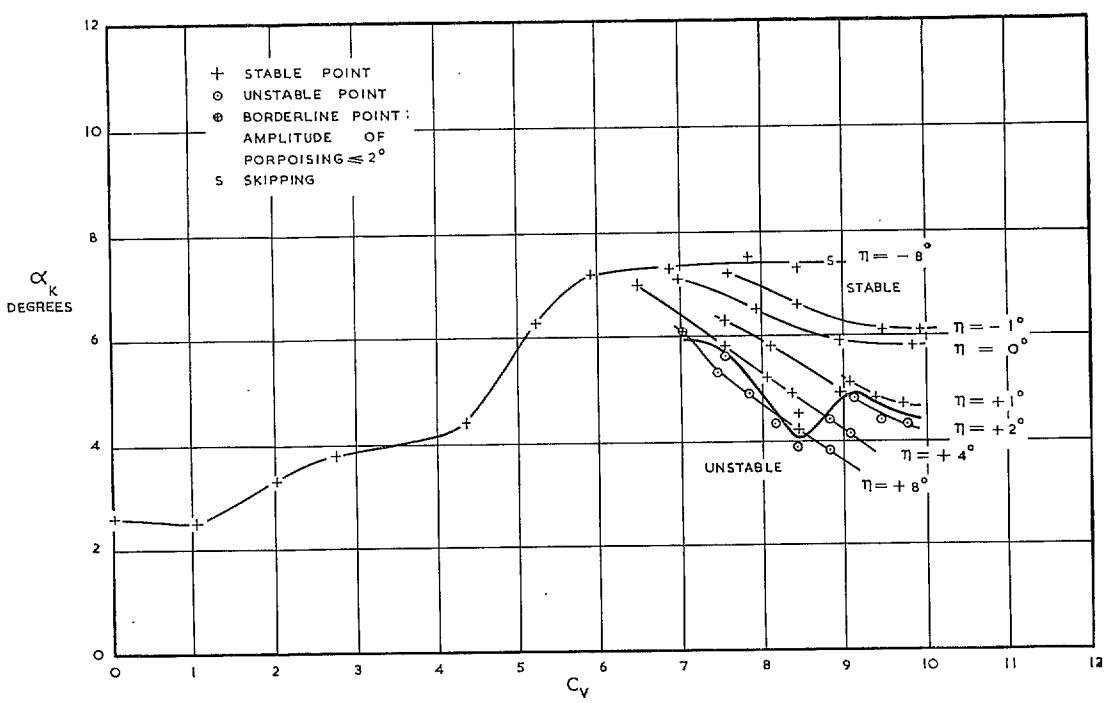

FIG. 165. Model F longitudinal stability with disturbance ($C_{\Delta 0} = 2{\cdot}25$).

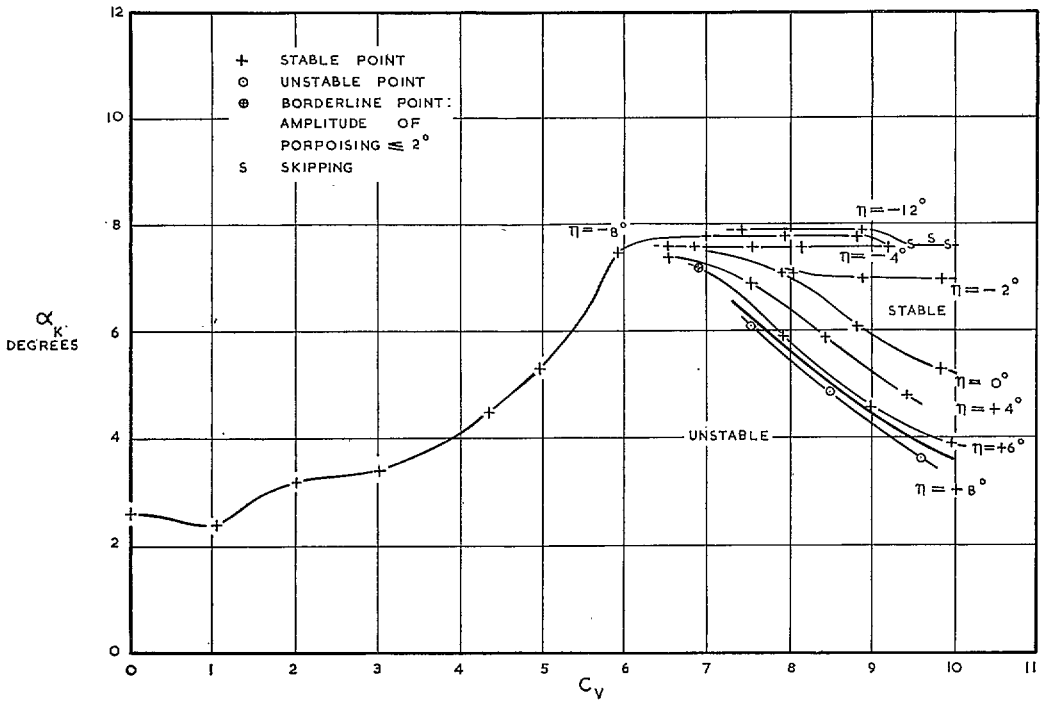

FIG. 166. Model F longitudinal stability without disturbance ($C_{\Delta 0} = 2{\cdot}75$).

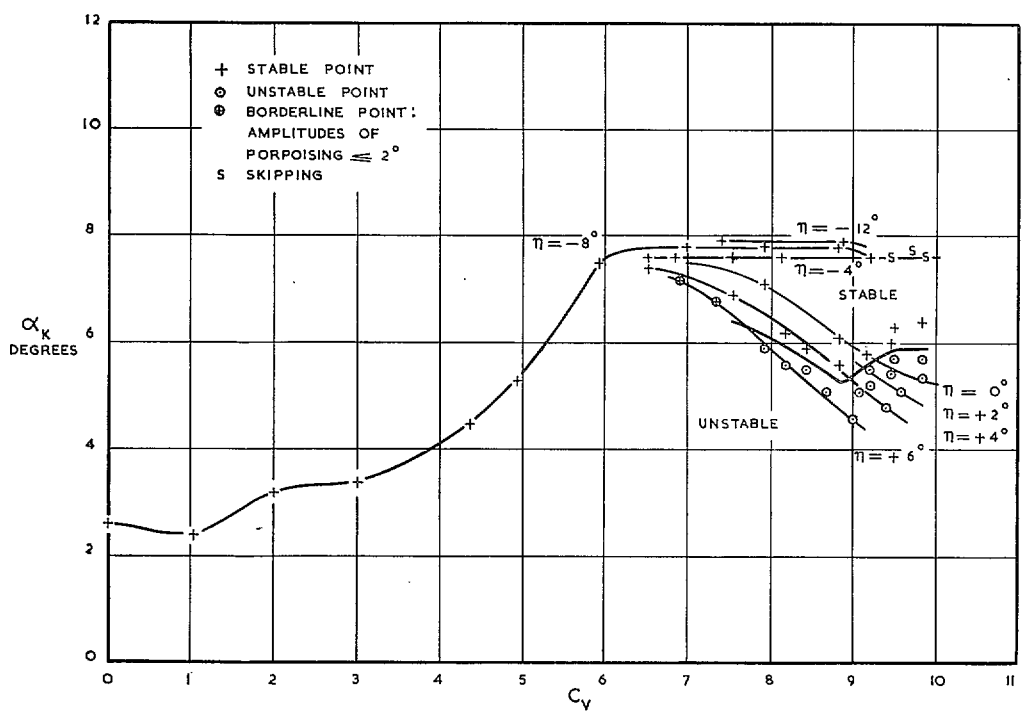

FIG. 167. Model F longitudinal stability with disturbance ($C_{\Delta 0} = 2{\cdot}75$).

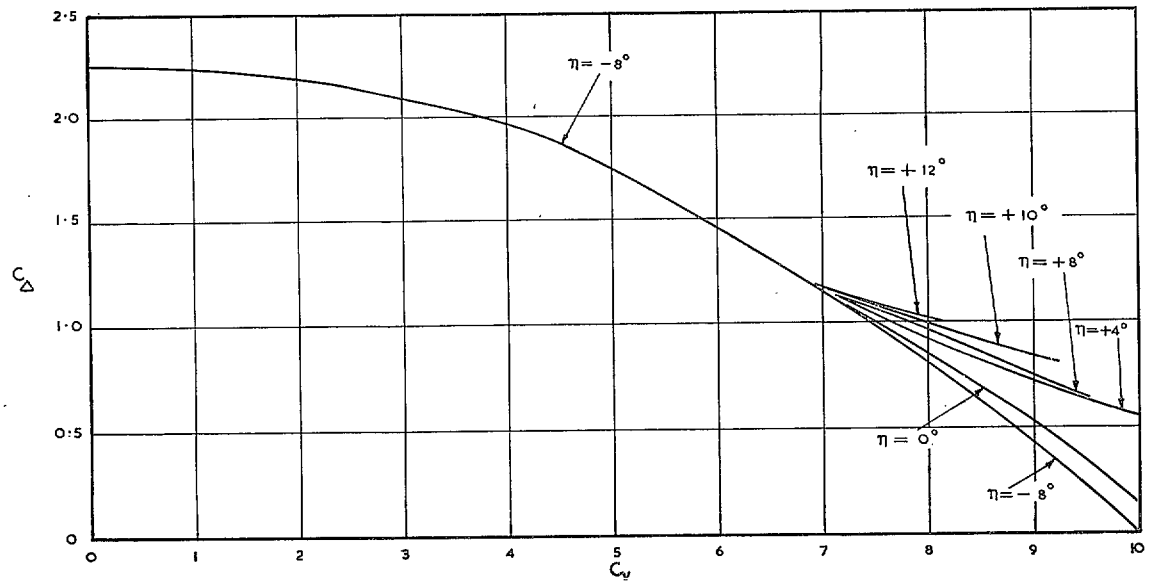

FIG. 168. Model F load-coefficient curves ($C_{\Delta 0} = 2{\cdot}25$).

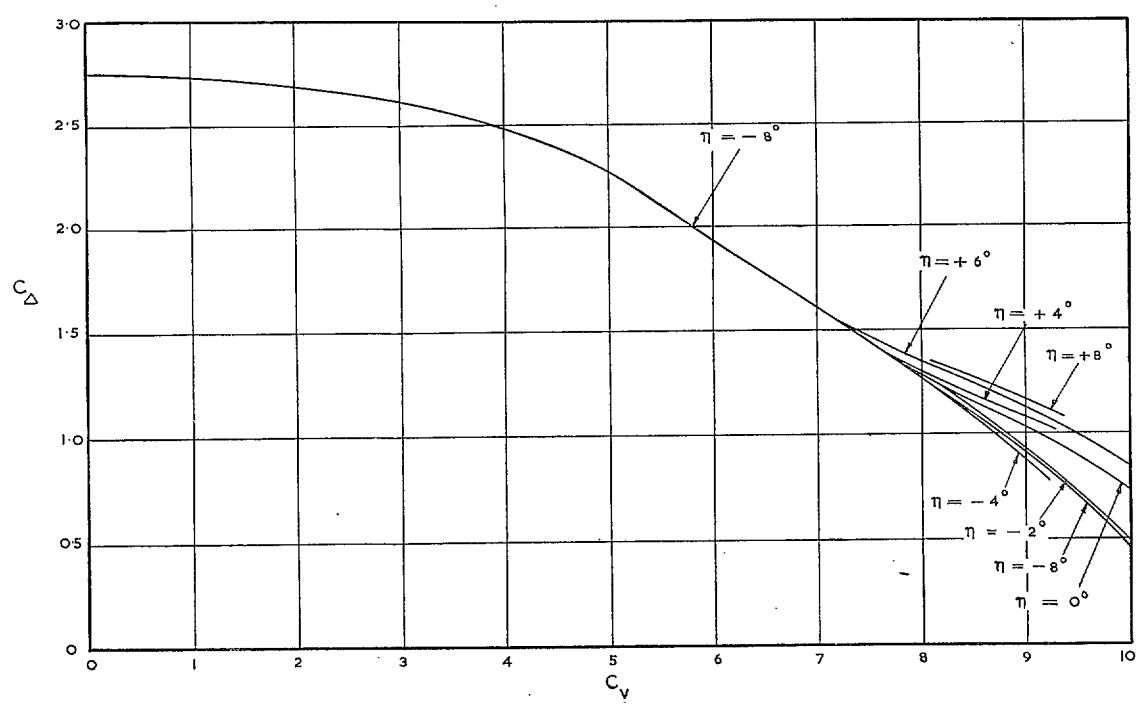

FIG. 169. Model F load-coefficient curves ($C_{\Delta 0} = 2{\cdot}75$).

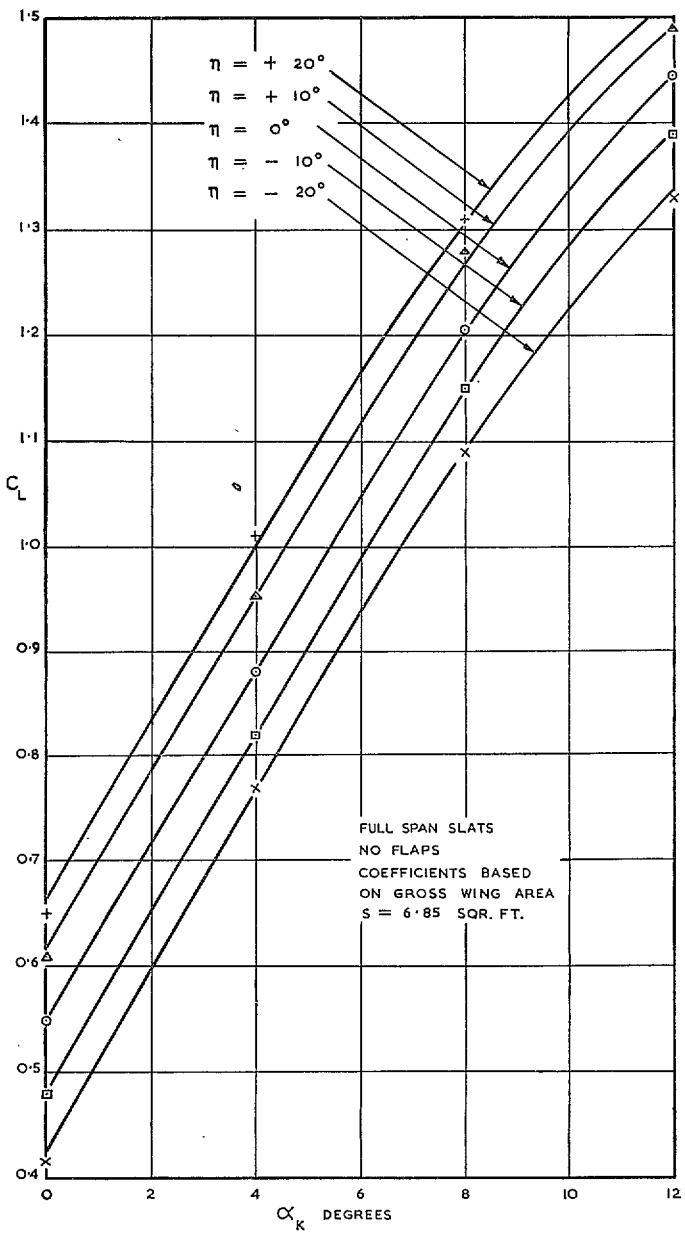

FIG. 170. Model G lift curves without slipstream.

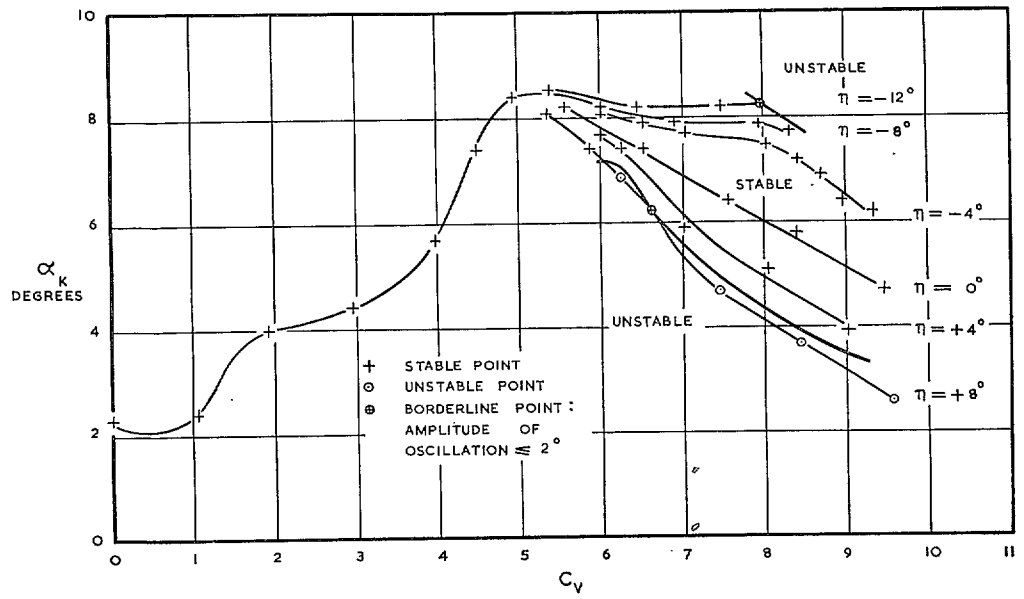

FIG. 171. Model G longitudinal stability without disturbance ($C_{\Delta 0} = 2{\cdot}25$).

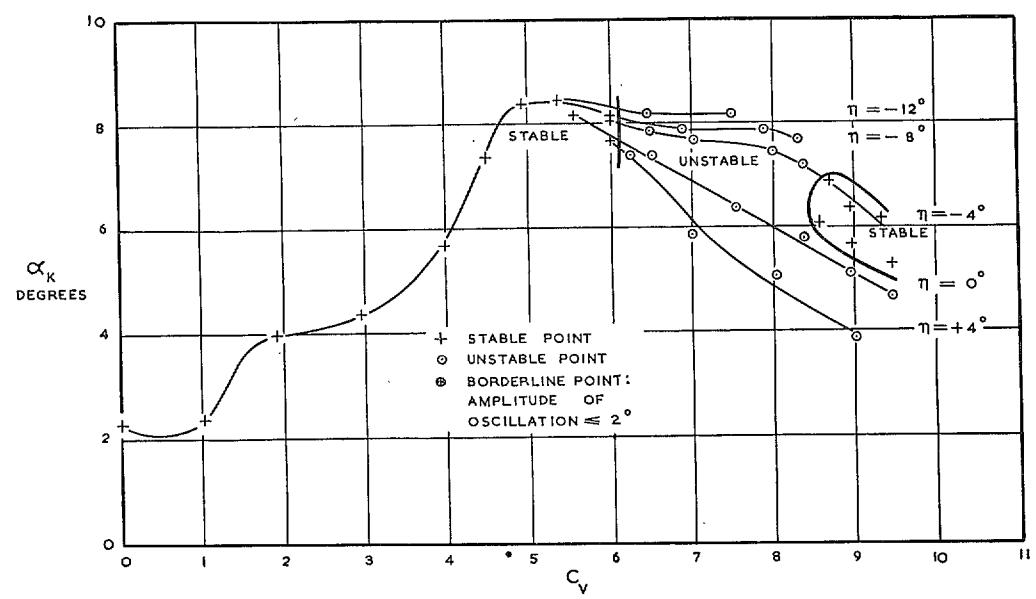

FIG. 172. Model G longitudinal stability with disturbance ($C_{\Delta 0} = 2{\cdot}25$).

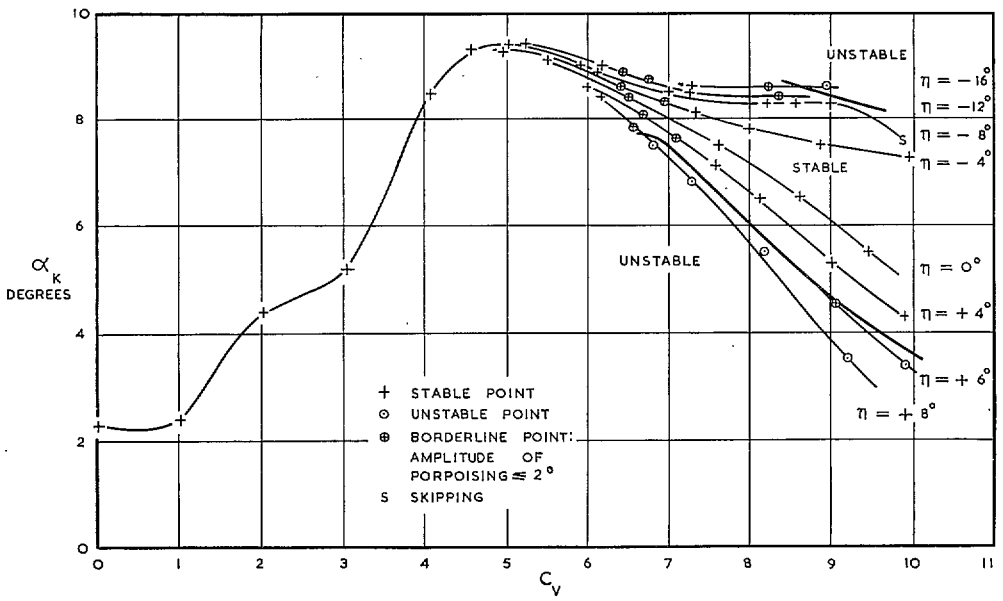

FIG. 173. Model G longitudinal stability without disturbance ($C_{\Delta 0} = 2{\cdot}75$).

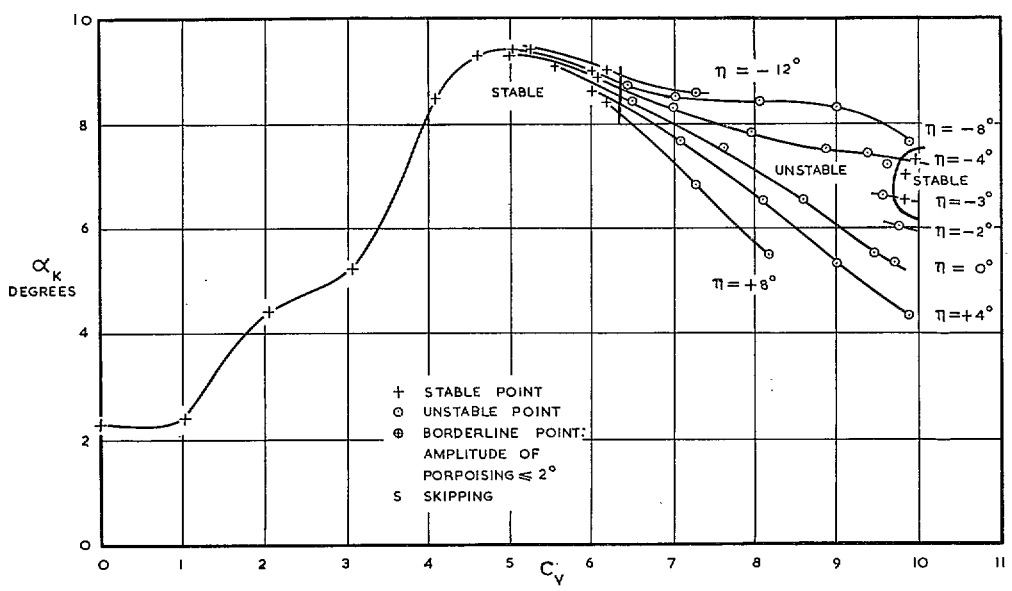

FIG. 174. Model G longitudinal stability with disturbance ($C_{\Delta 0} = 2{\cdot}75$).

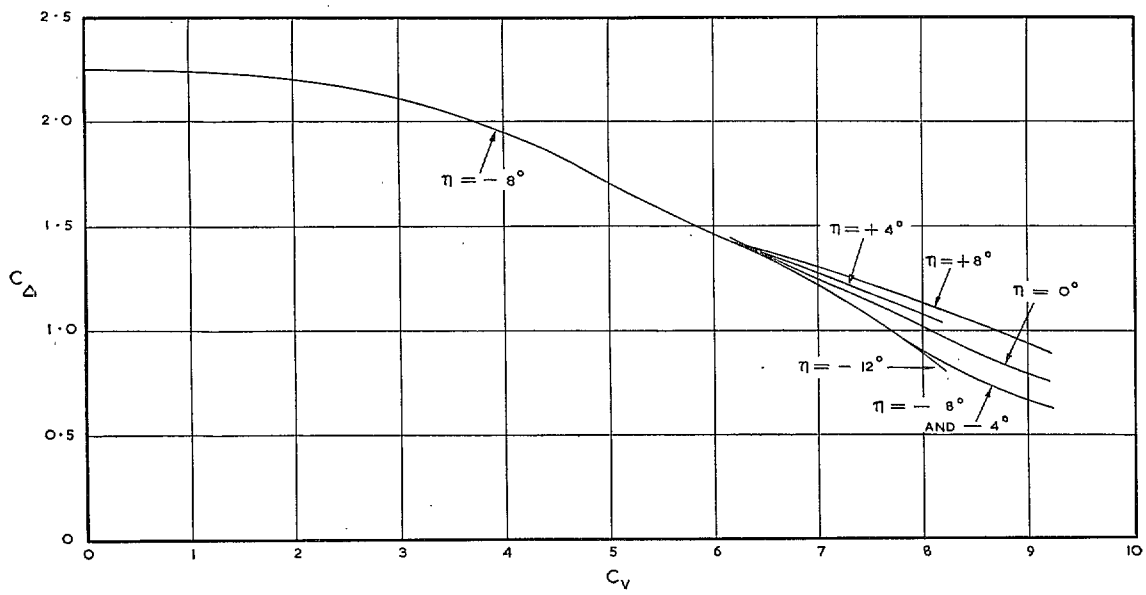

FIG. 175. Model G load-coefficient curves ($C_{\Delta 0} = 2{\cdot}25$).

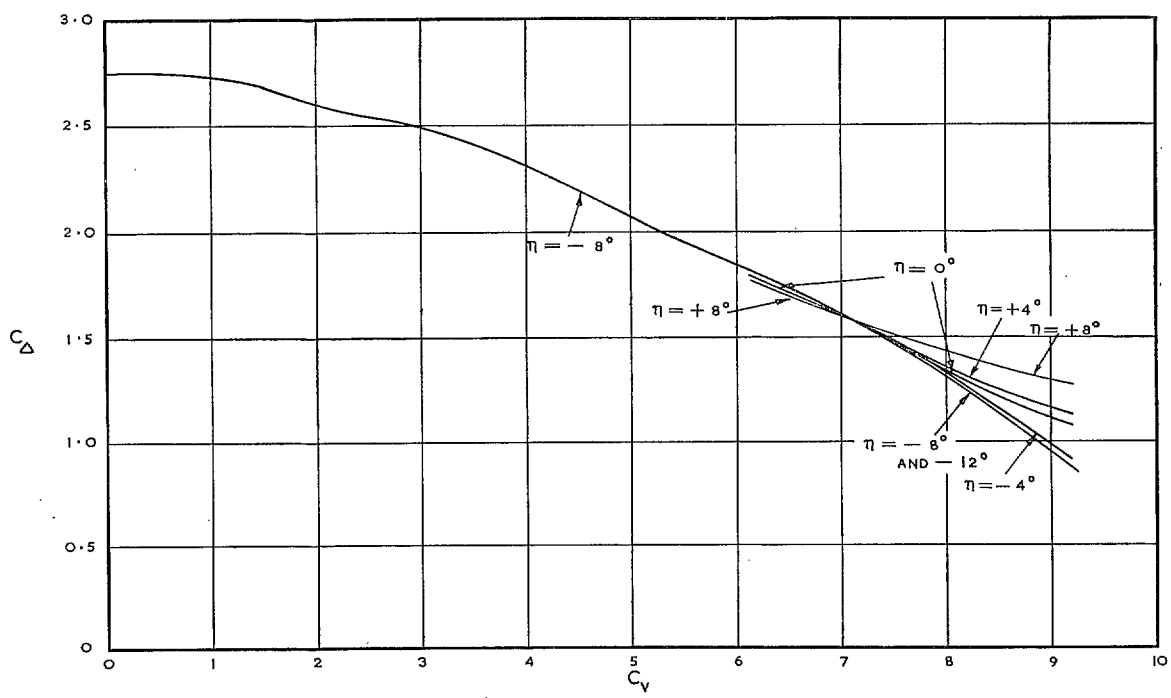

FIG. 176. Model G load-coefficient curves ($C_{\Delta 0} = 2{\cdot}75$).

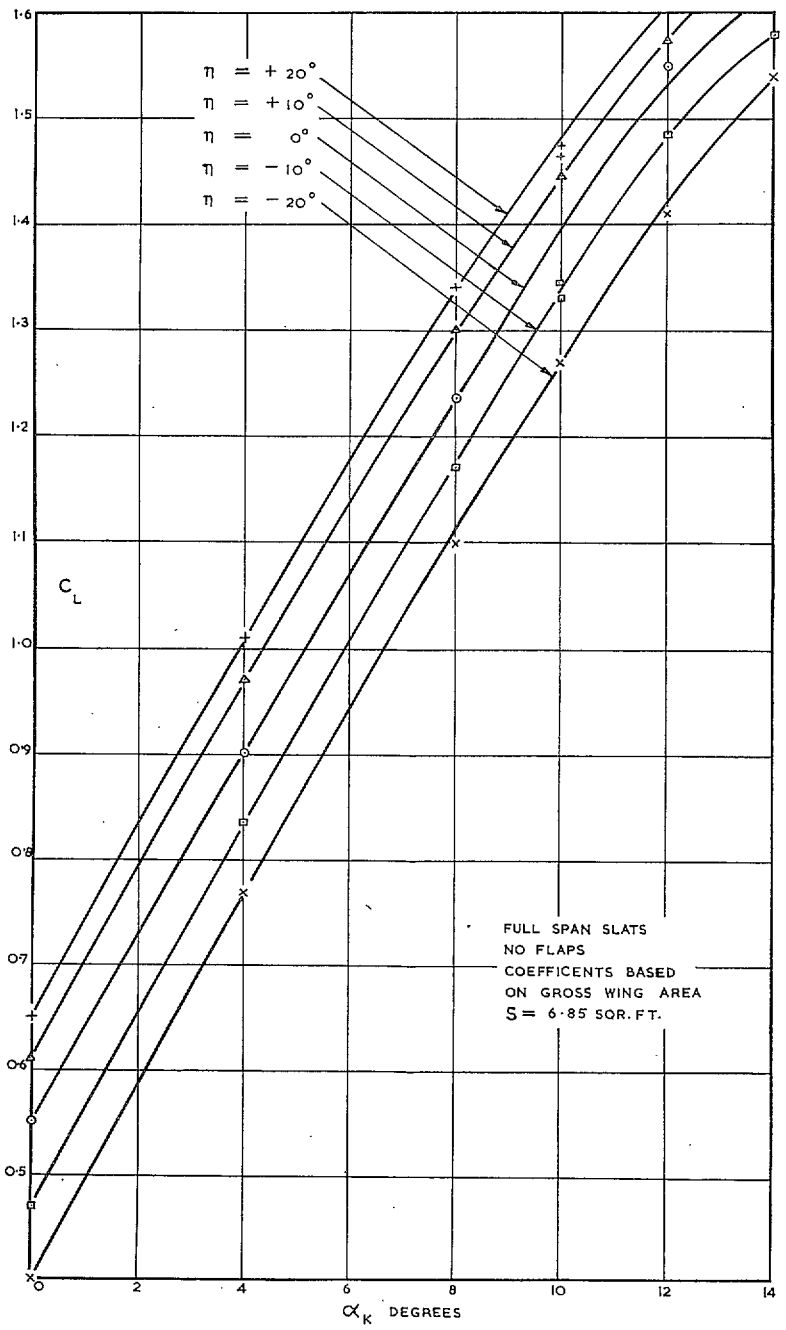

FIG. 177. Model H lift curves without slipstream.

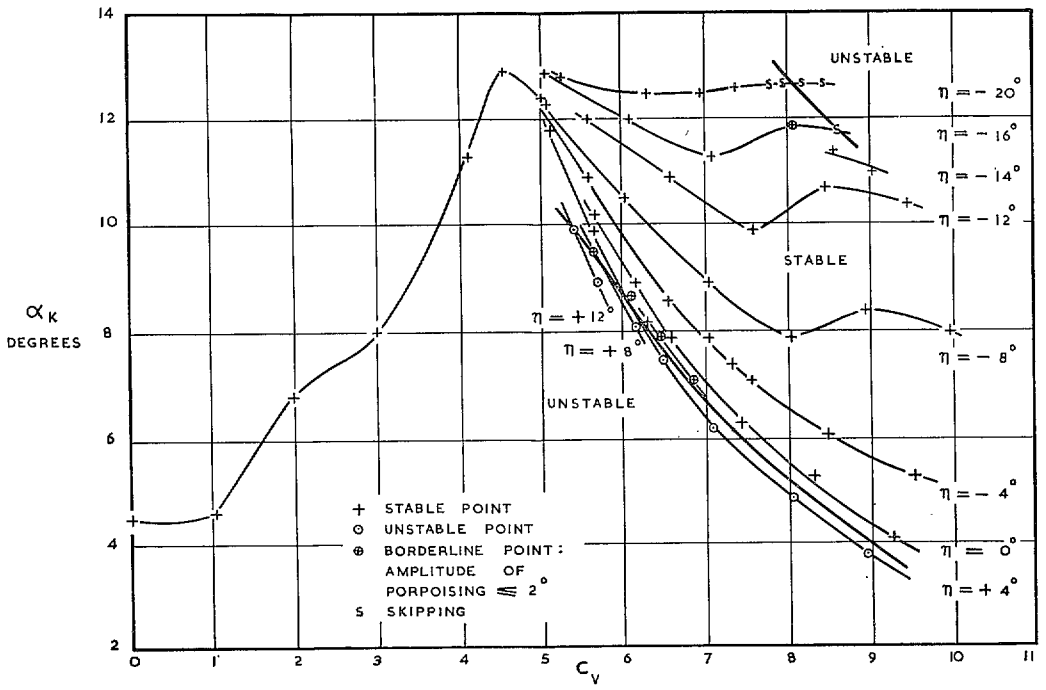

FIG. 178. Model H longitudinal stability without disturbance ($C_{\Delta 0} = 2{\cdot}25$).

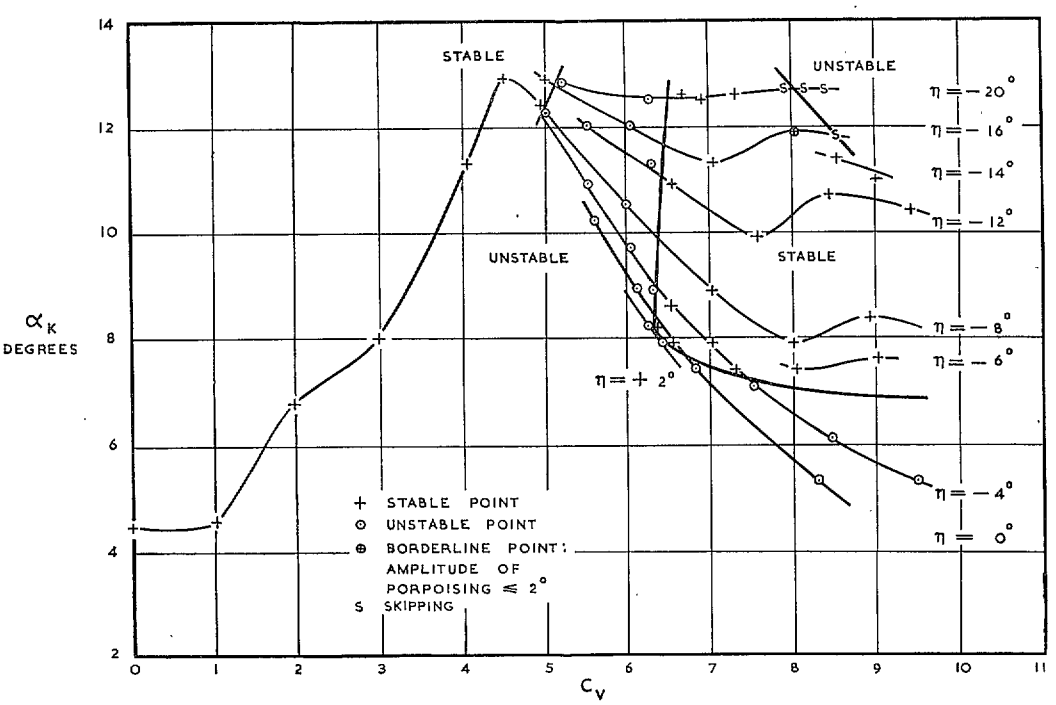

FIG. 179. Model H longitudinal stability with disturbance ($C_{\Delta 0} = 2{\cdot}25$).

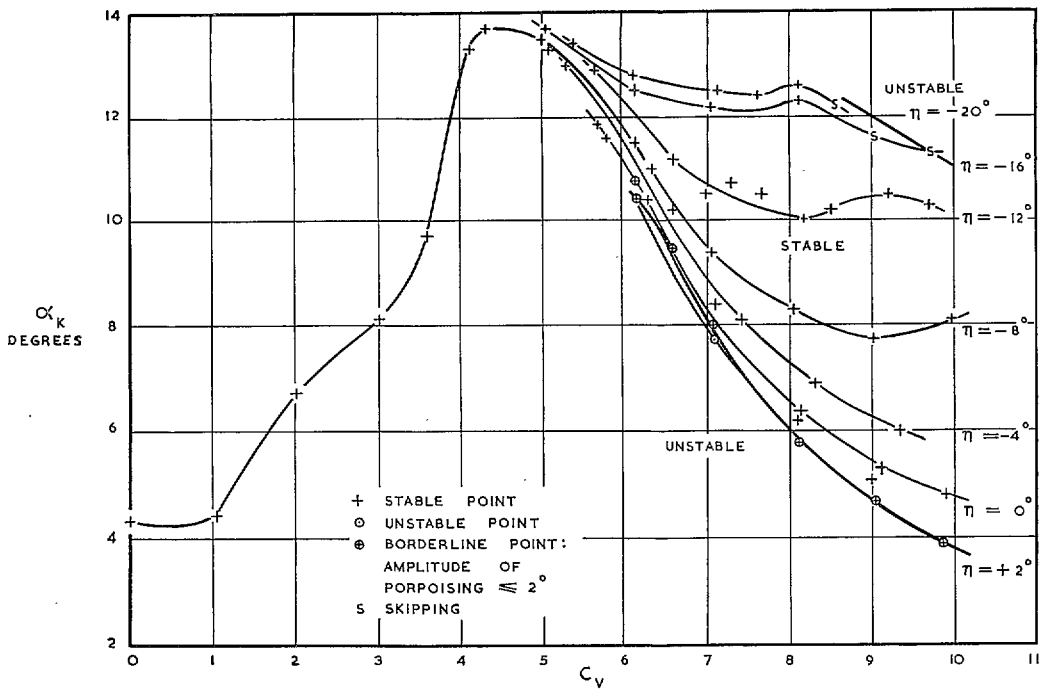

FIG. 180. Model H longitudinal stability without disturbance ($C_{\Delta 0} = 2{\cdot}75$).

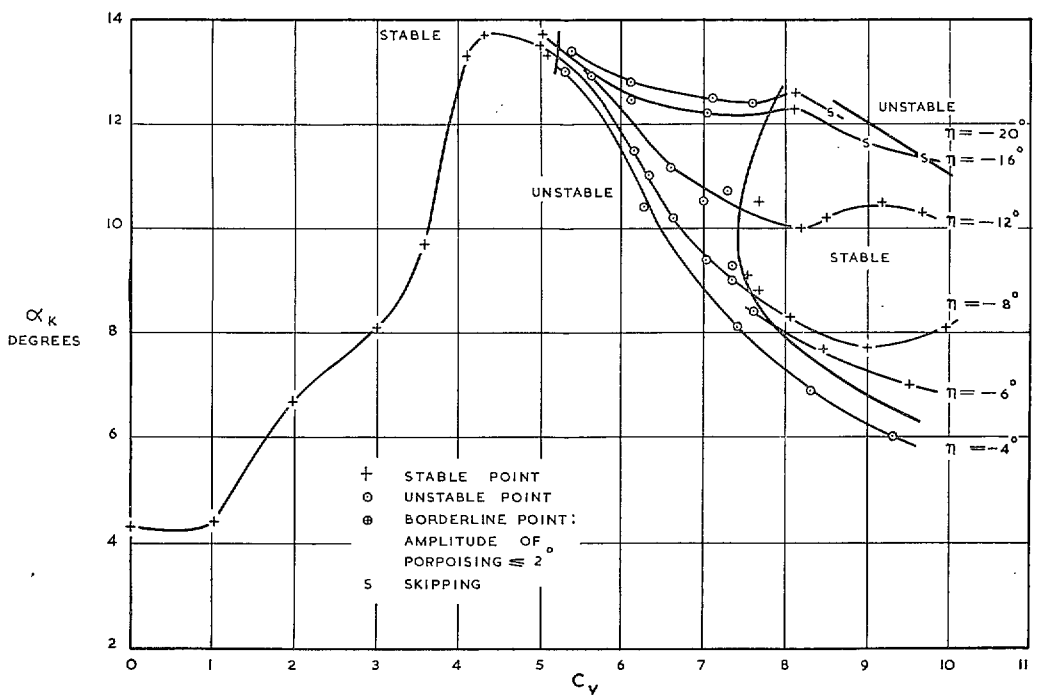

FIG. 181. Model H longitudinal stability with disturbance ($C_{\Delta 0} = 2{\cdot}75$).

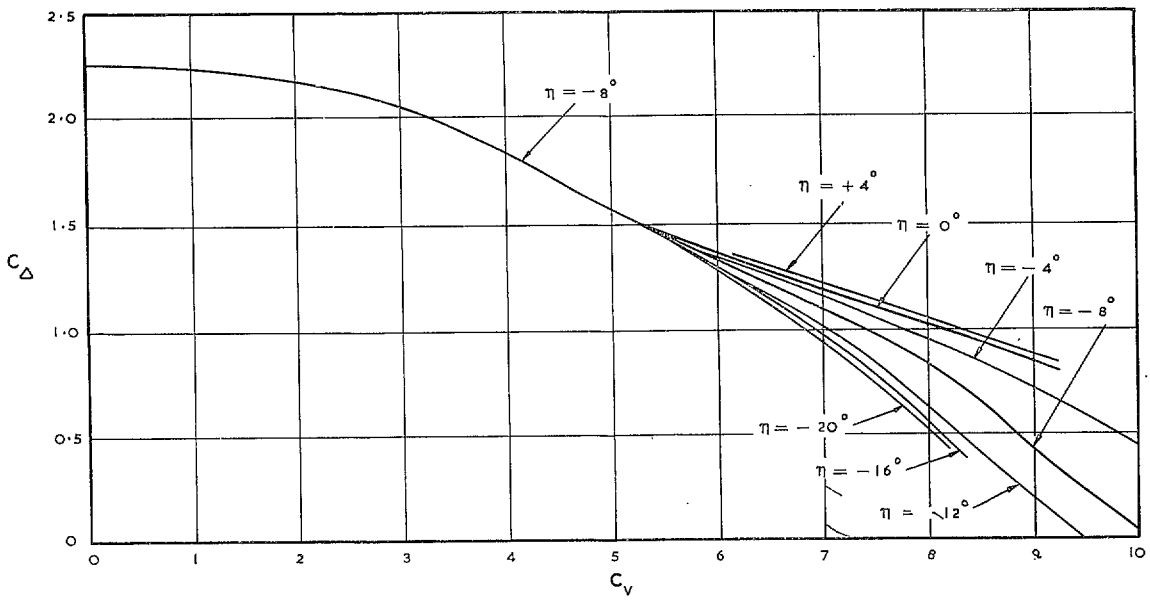

FIG. 182. Model H load-coefficient curves ($C_{\Delta 0} = 2{\cdot}25$).

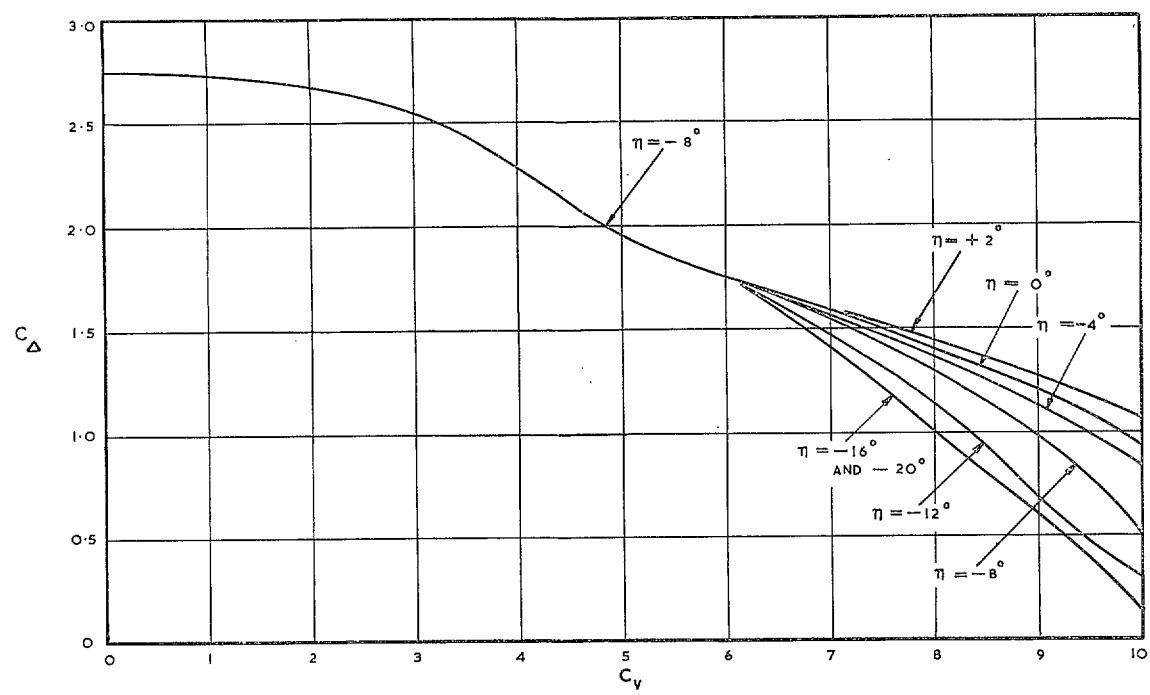

FIG. 183. Model H load-coefficient curves ($C_{\Delta 0} = 2{\cdot}75$).

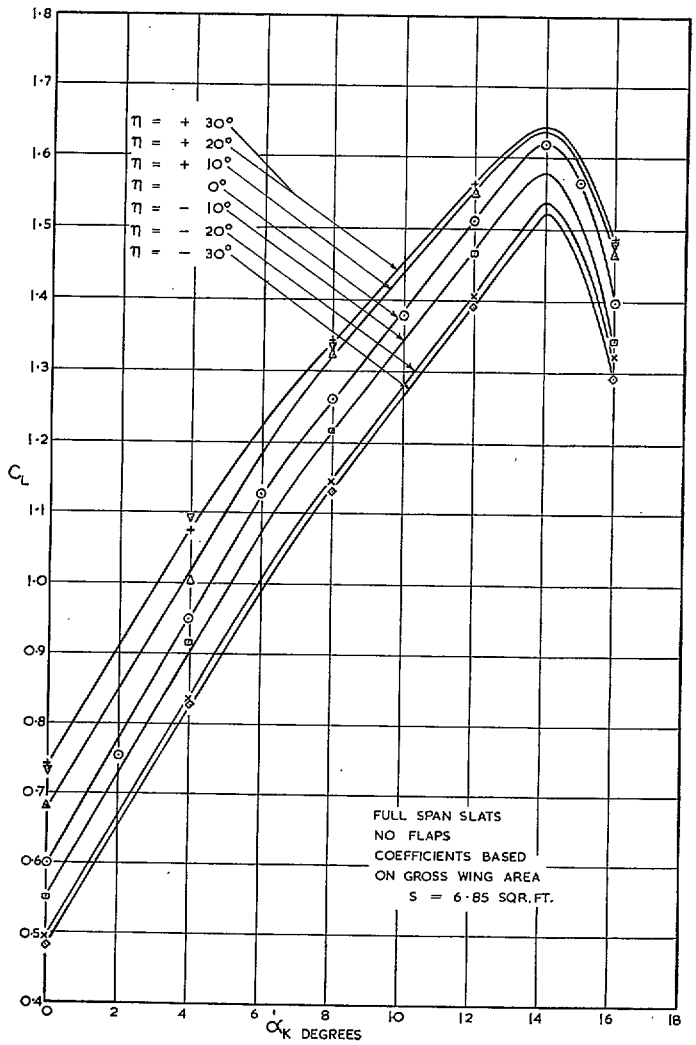

FIG. 184. Model J lift curves without slipstream.

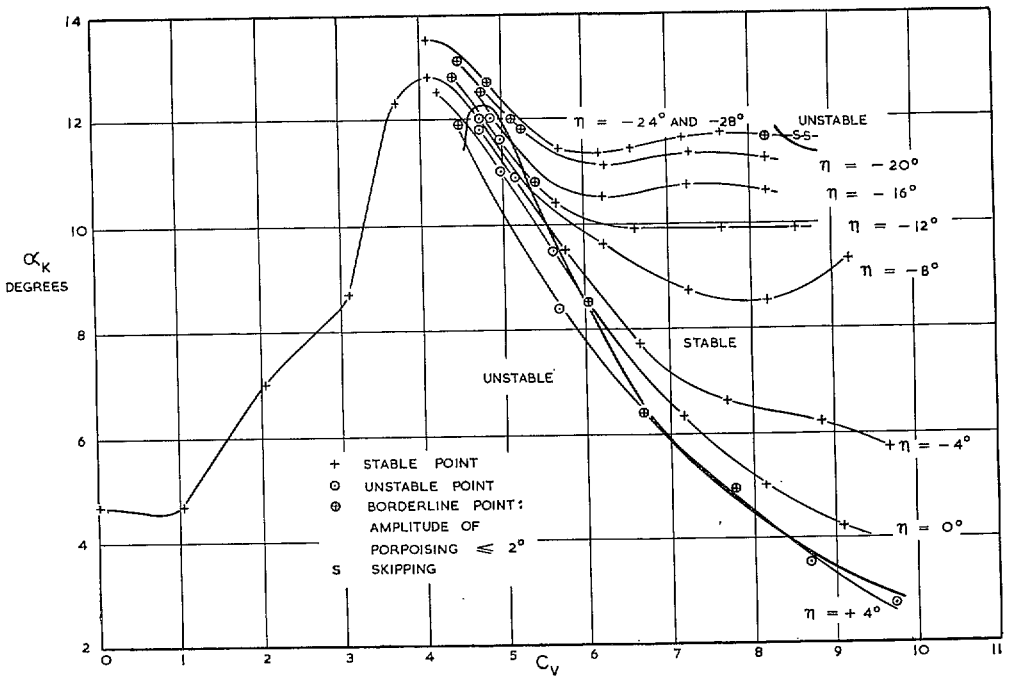

FIG. 185. Model J longitudinal stability without disturbance ($C_{\Delta 0} = 2{\cdot}25$).

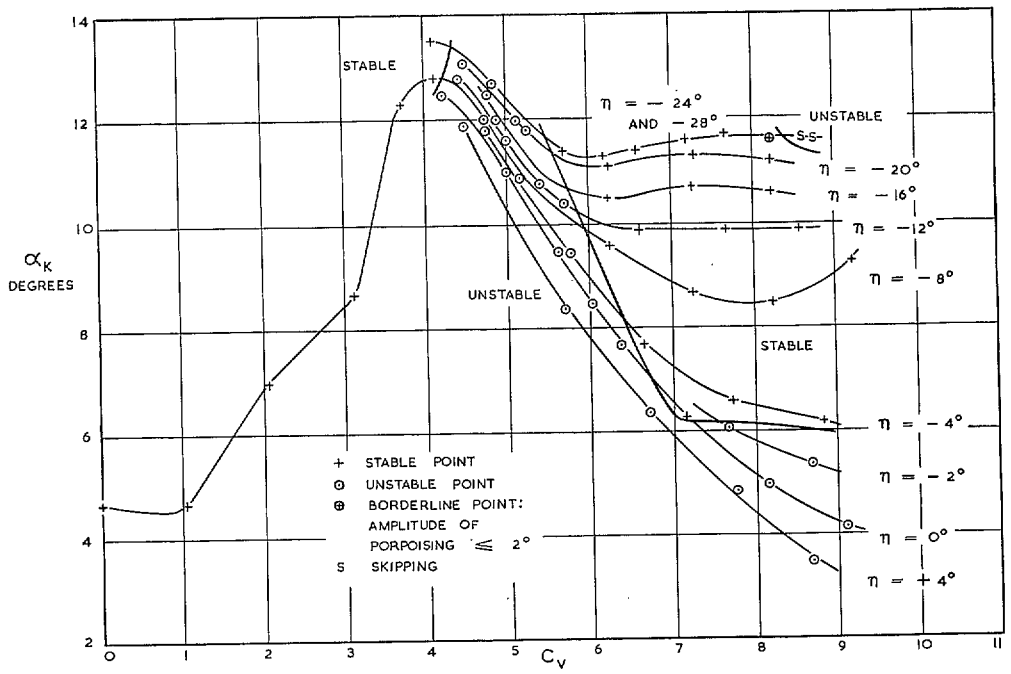

FIG. 186. Model J longitudinal stability with disturbance ($C_{\Delta 0} = 2{\cdot}25$).

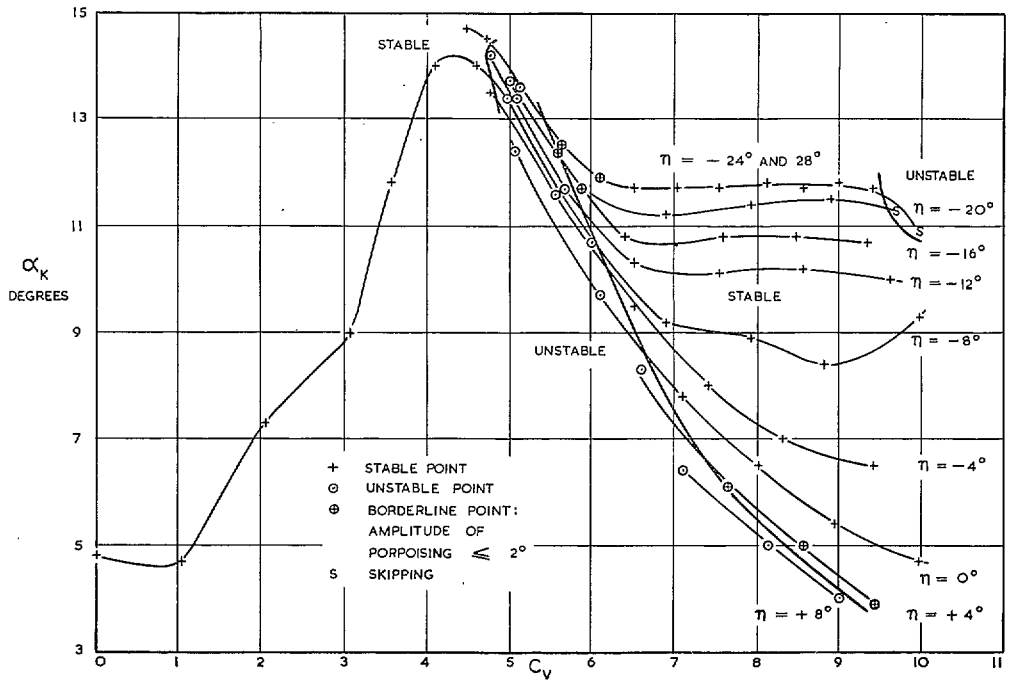

FIG. 187. Model J longitudinal stability without disturbance ($C_{\Delta 0} = 2{\cdot}75$).

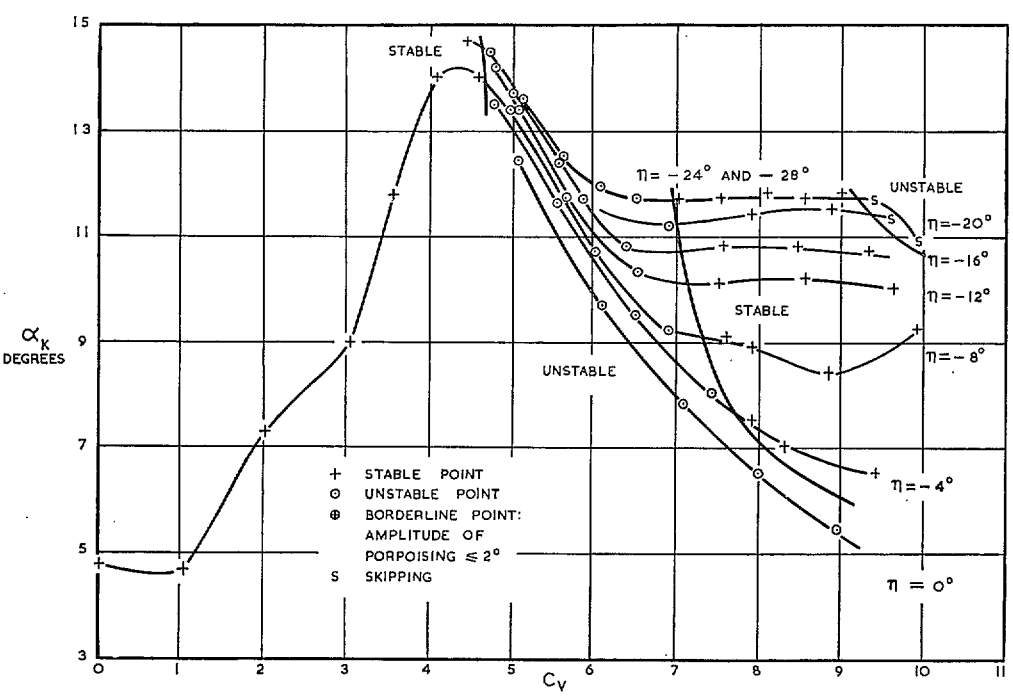

FIG. 188. Model J longitudinal stability with disturbance ($C_{\Delta 0} = 2{\cdot}75$).

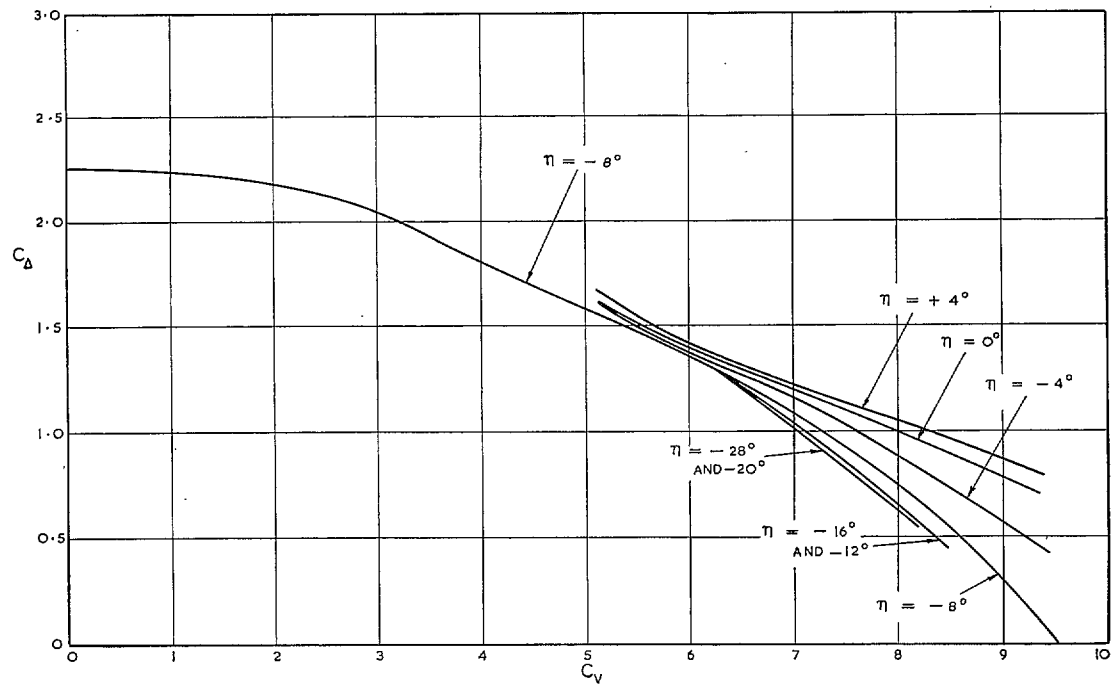

FIG. 189. Model J load-coefficient curves ($C_{\Delta 0} = 2{\cdot}25$).

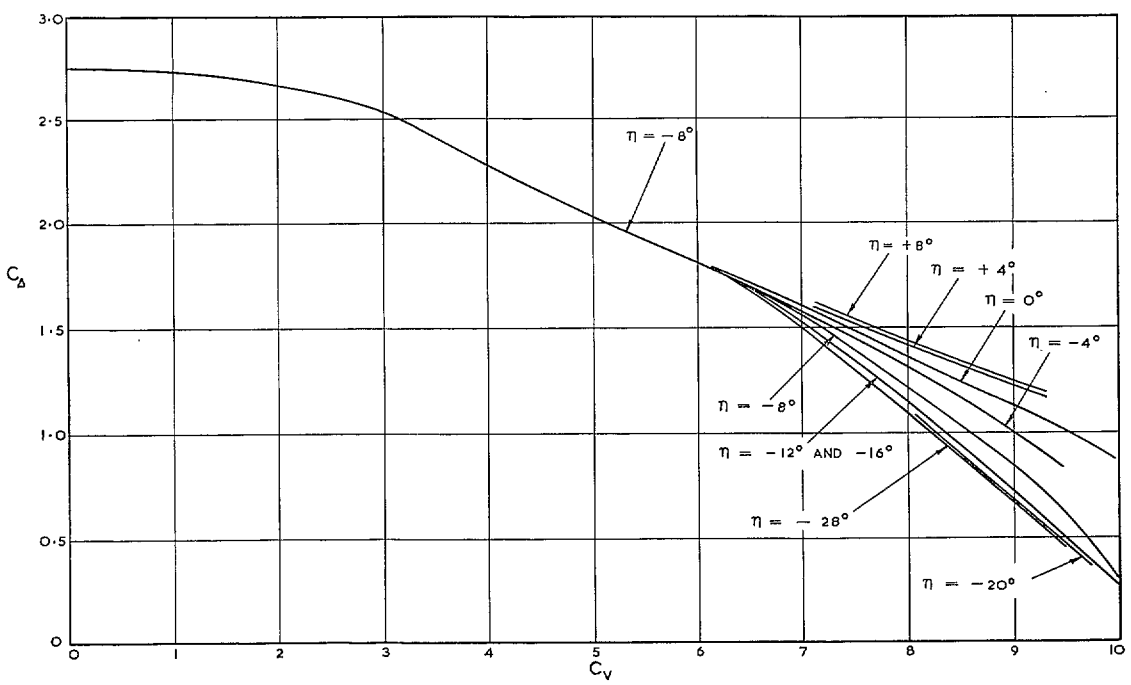

FIG. 190. Model J load-coefficient curves ($C_{\Delta 0} = 2{\cdot}75$).

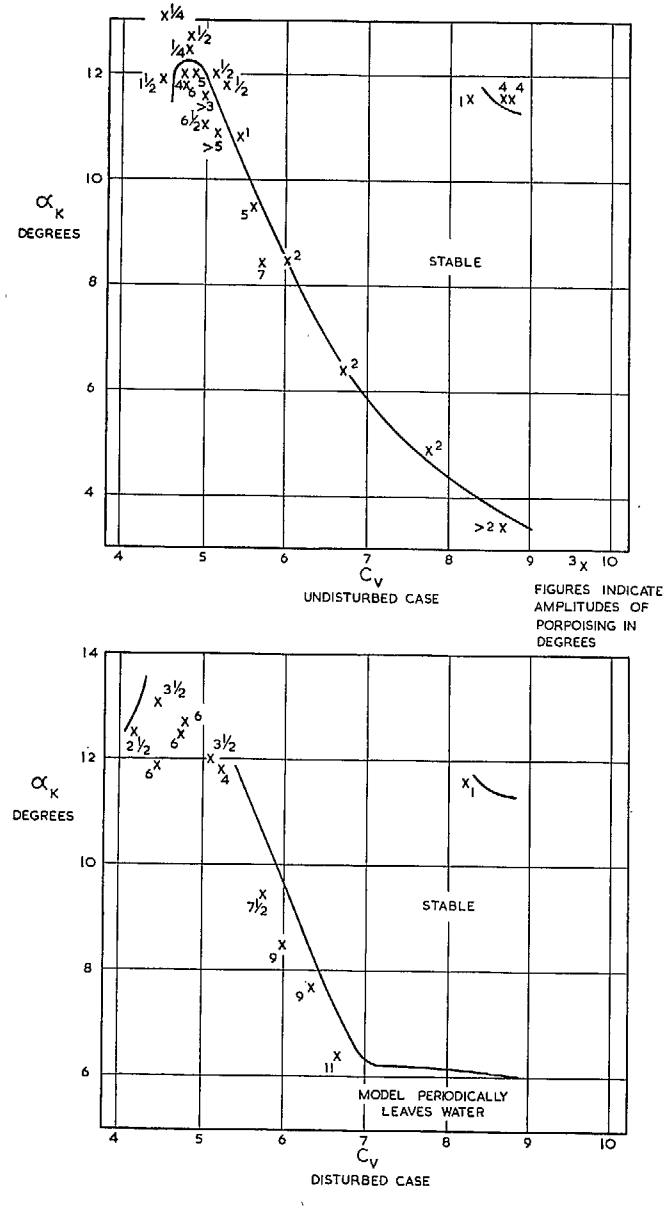

FIG. 191. Model J porpoising amplitudes and stability limits ($C_{\Delta 0} = 2{\cdot}25$).

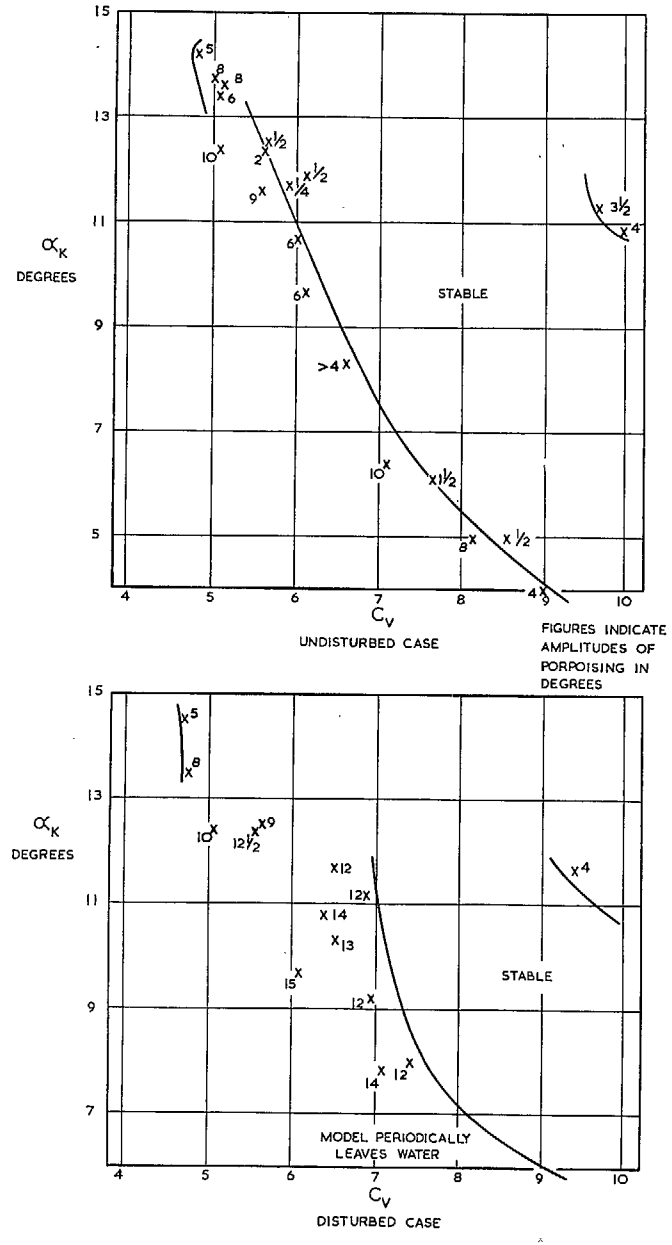

FIG. 192. Model J porpoising amplitudes and stability limits ($C_{\Delta 0} = 2{\cdot}75$).

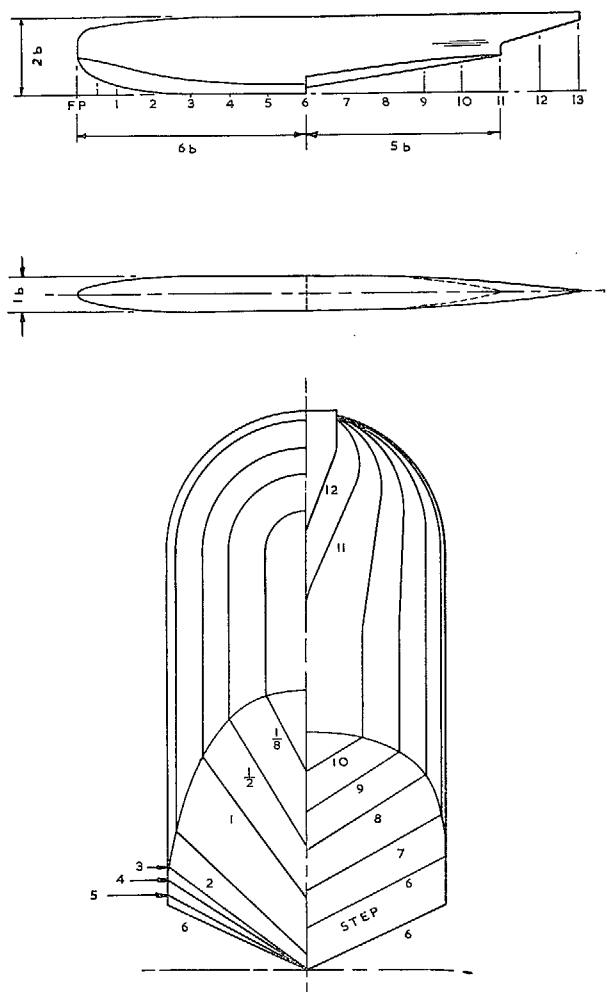

FIG. 193. Model K hull lines.

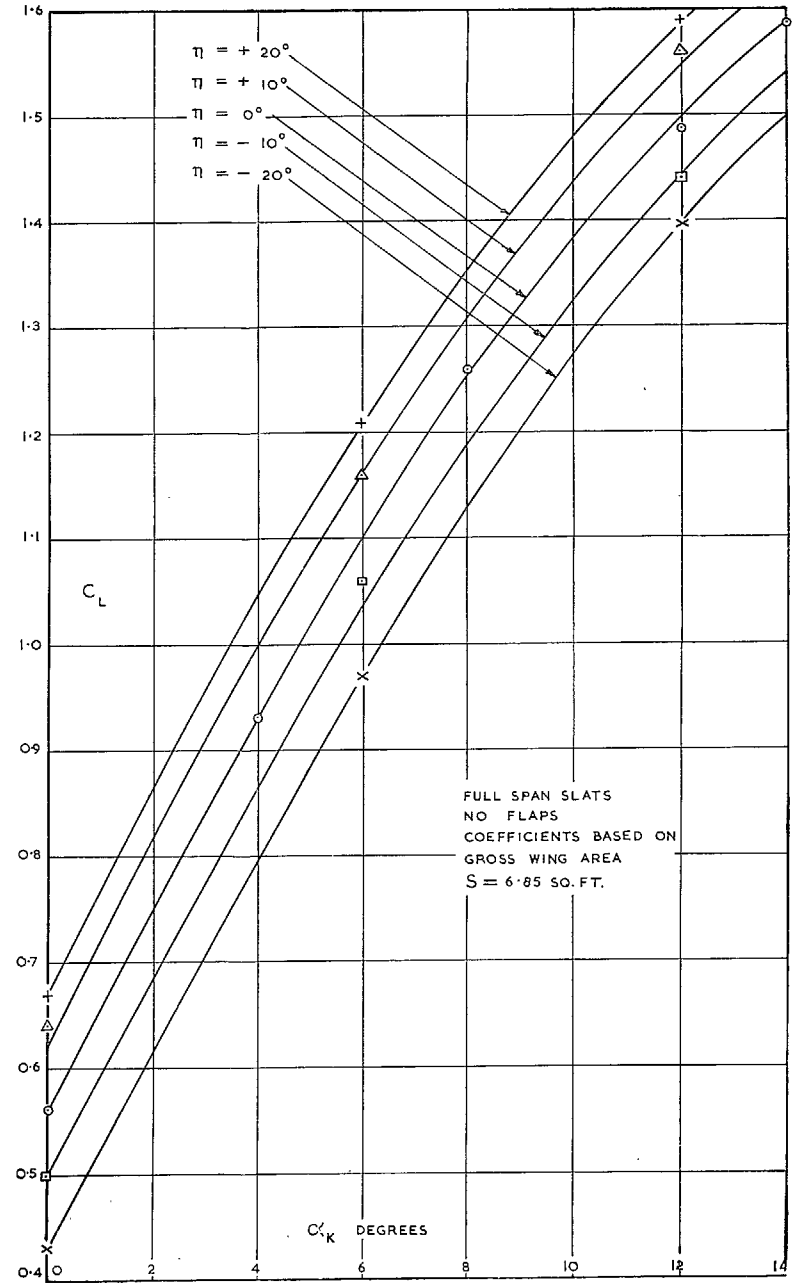

FIG. 194. Model K lift curves without slipstream

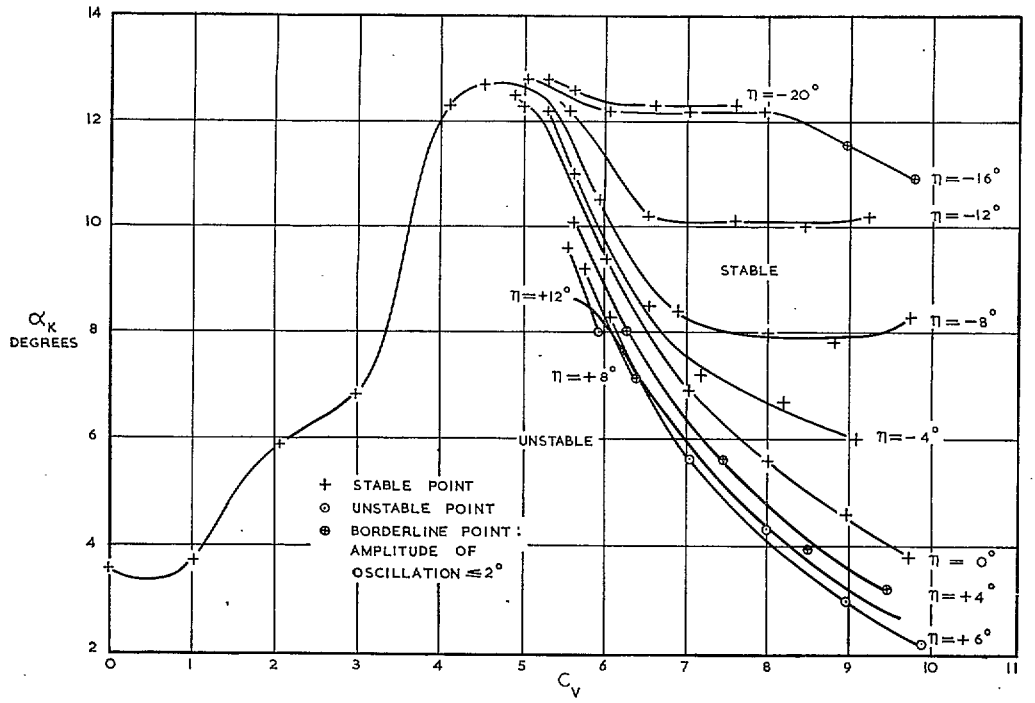

FIG. 195. Model K longitudinal stability without disturbance ($C_{\Delta 0} = 2{\cdot}75$).

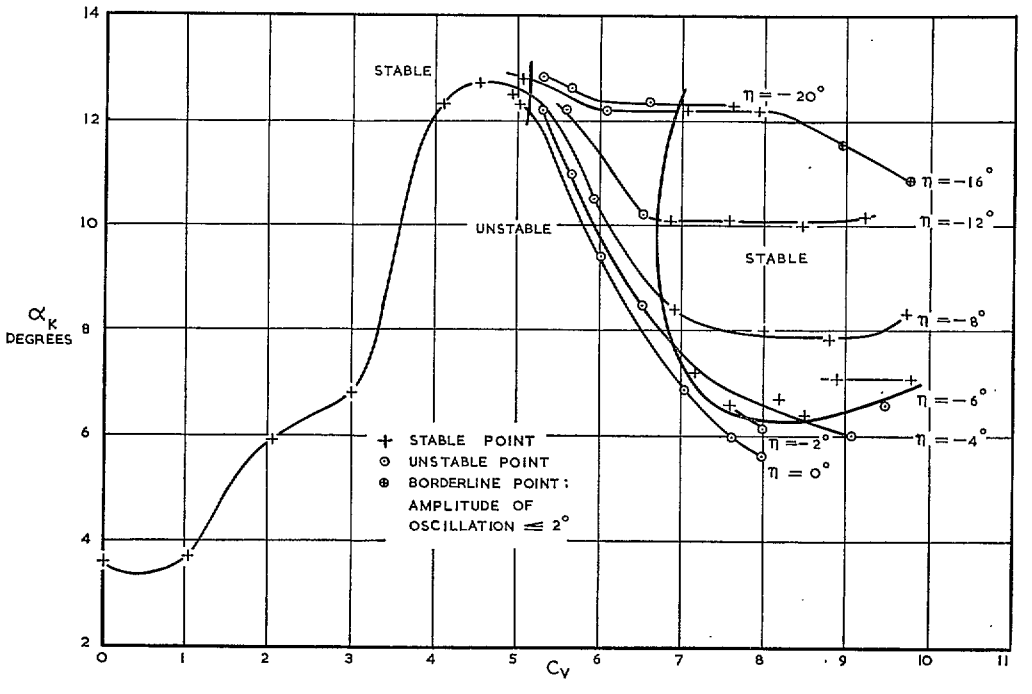

FIG. 196. Model K longitudinal stability with disturbance ($C_{\Delta 0} = 2{\cdot}75$).

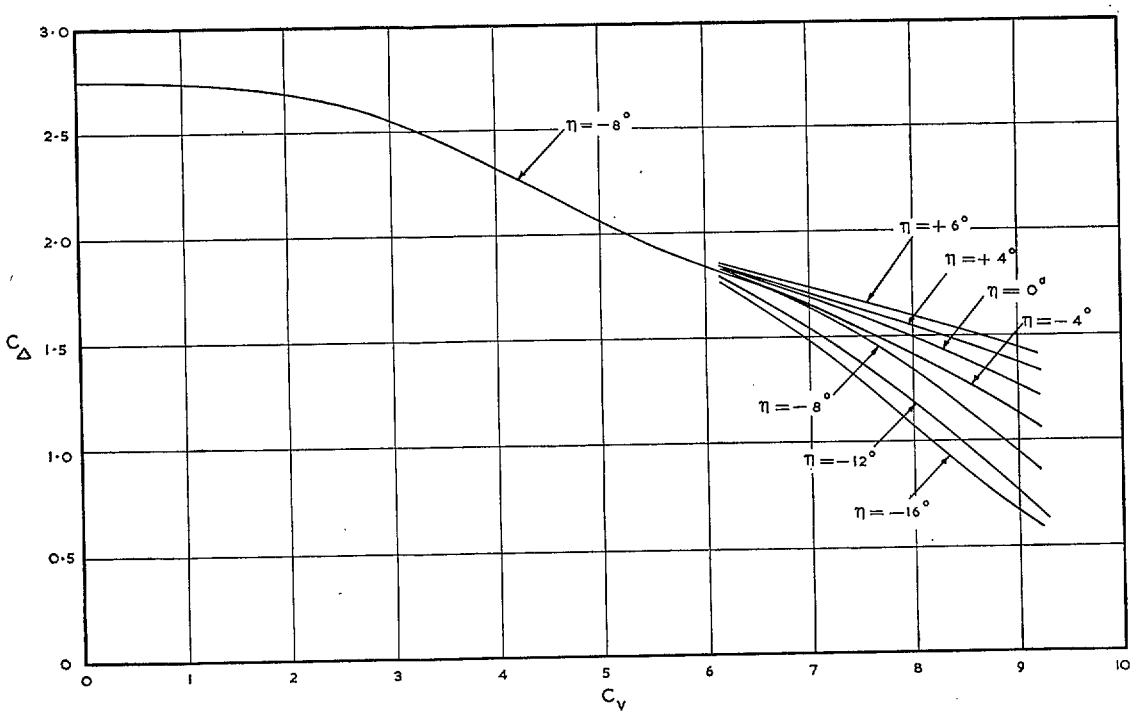

FIG. 197. Model K load-coefficient curves ($C_{\Delta 0} = 2{\cdot}75$).

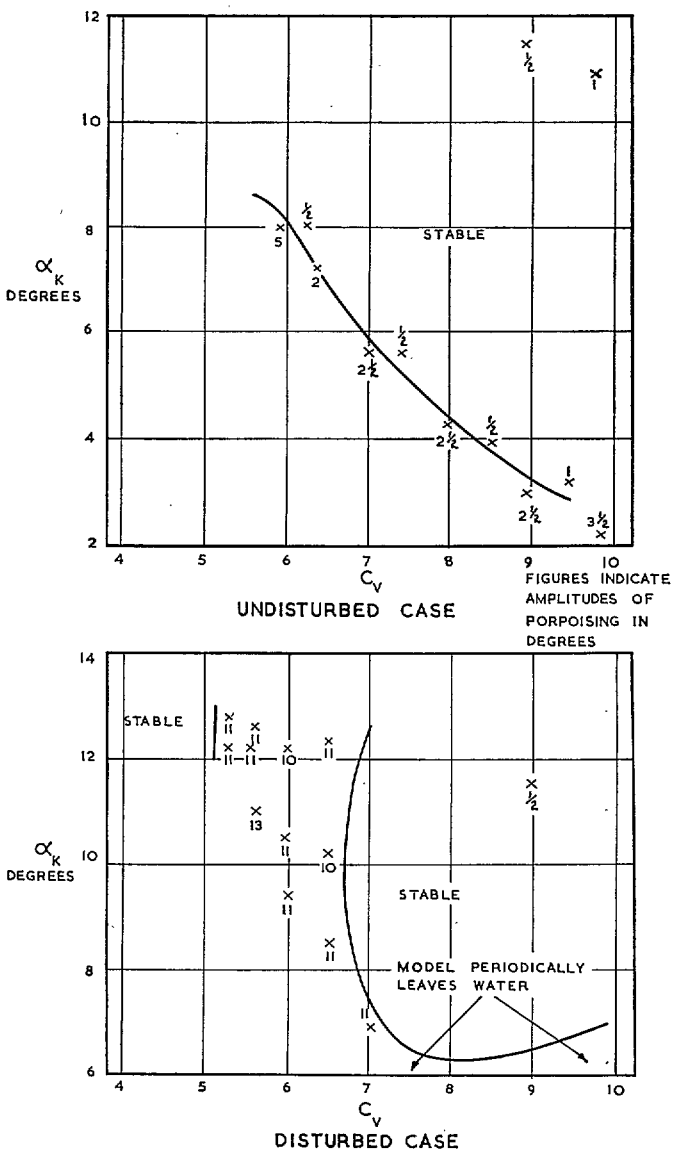

FIG. 198. Model K porpoising amplitudes and stability limits ($C_{\Delta 0} = 2{\cdot}75$).

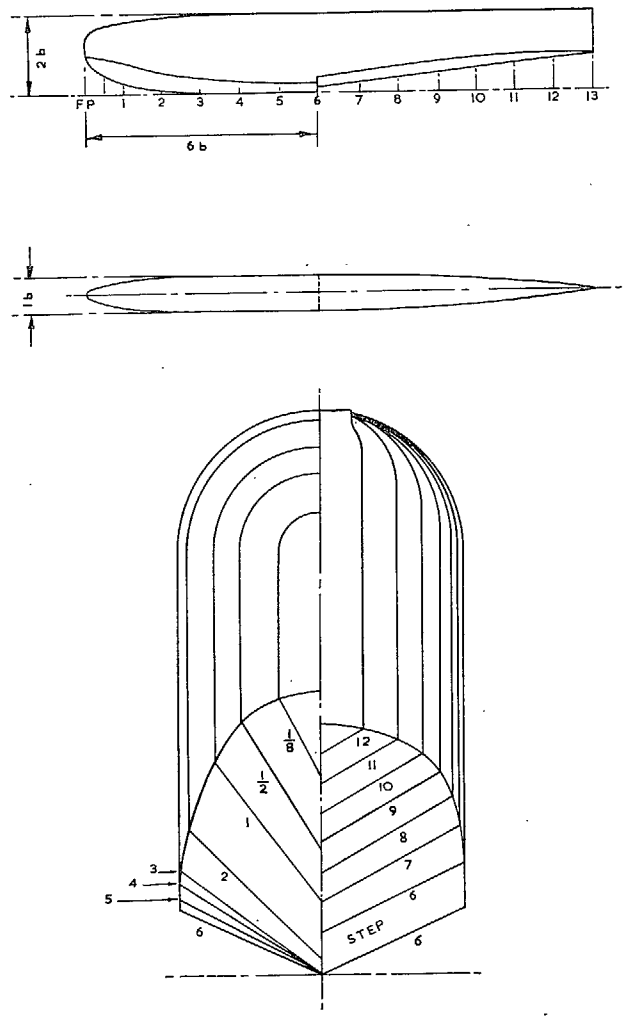

FIG. 199. Model L hull lines.

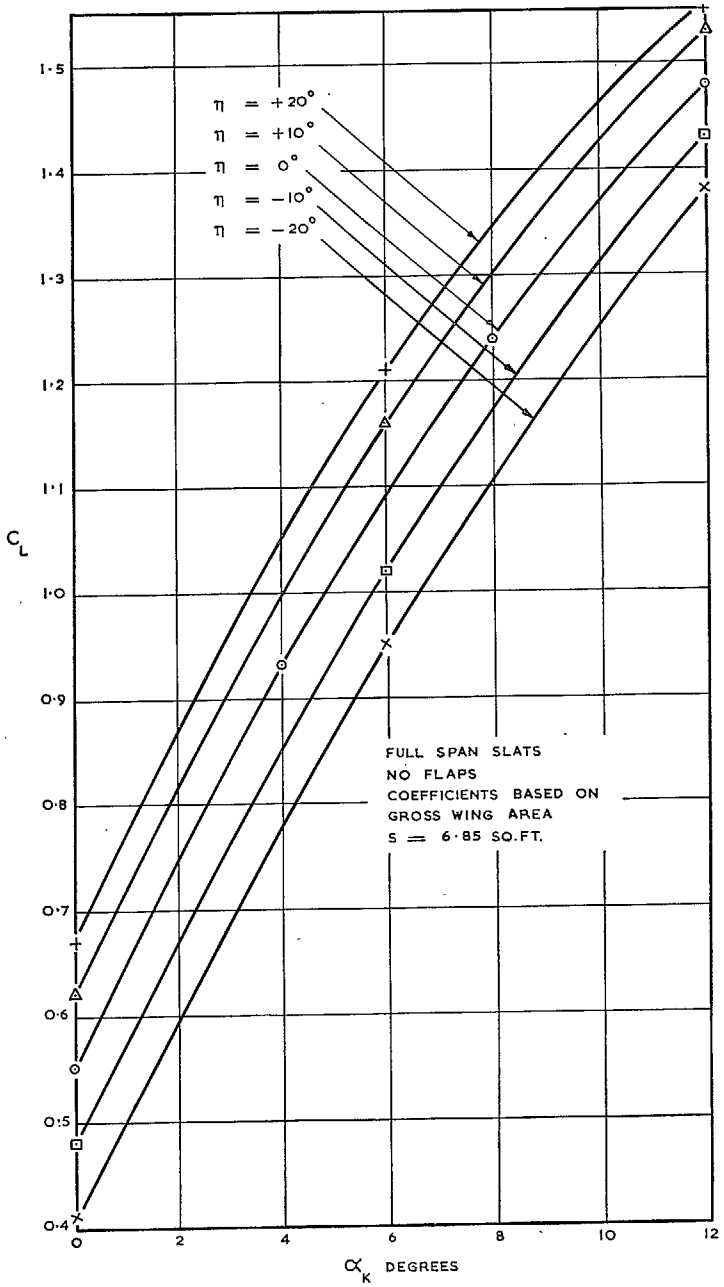

FIG. 200. Model L lift curves without slipstream.

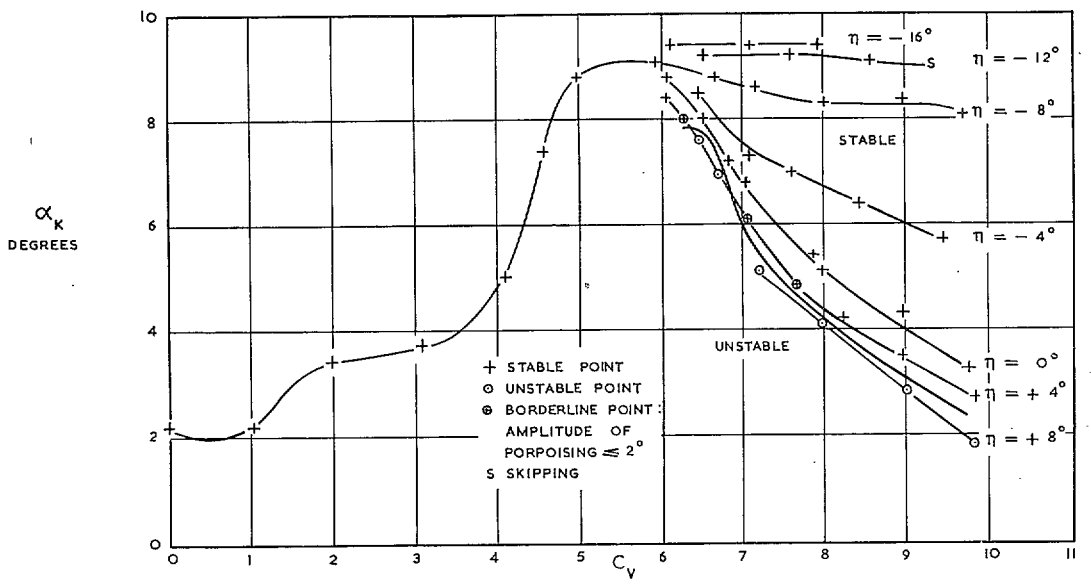

FIG. 201. Model L longitudinal stability without disturbance ($C_{\Delta 0} = 2{\cdot}75$).

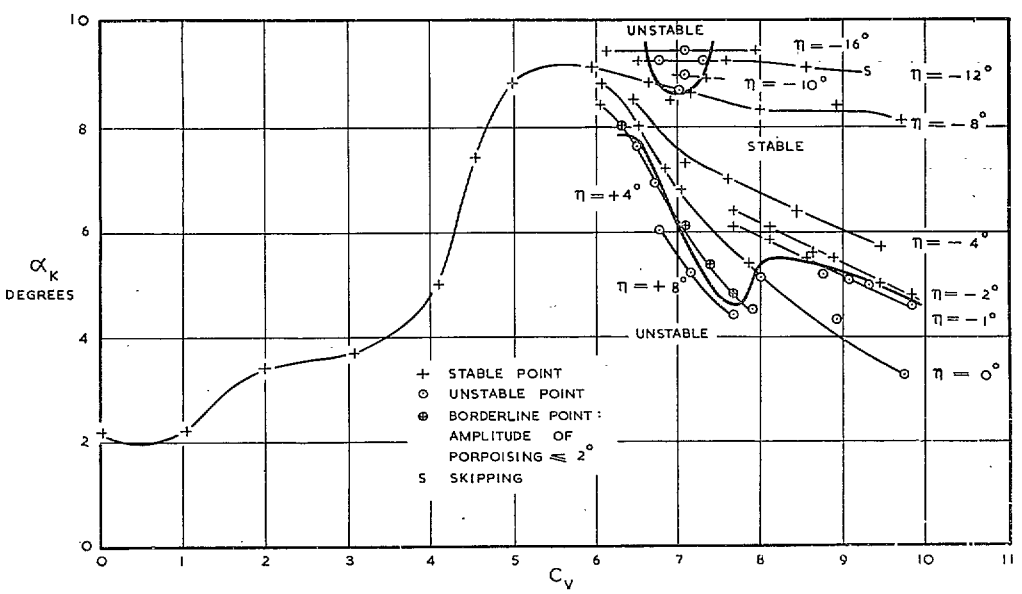

FIG. 202. Model L longitudinal stability with disturbance ($C_{\Delta 0} = 2{\cdot}75$).

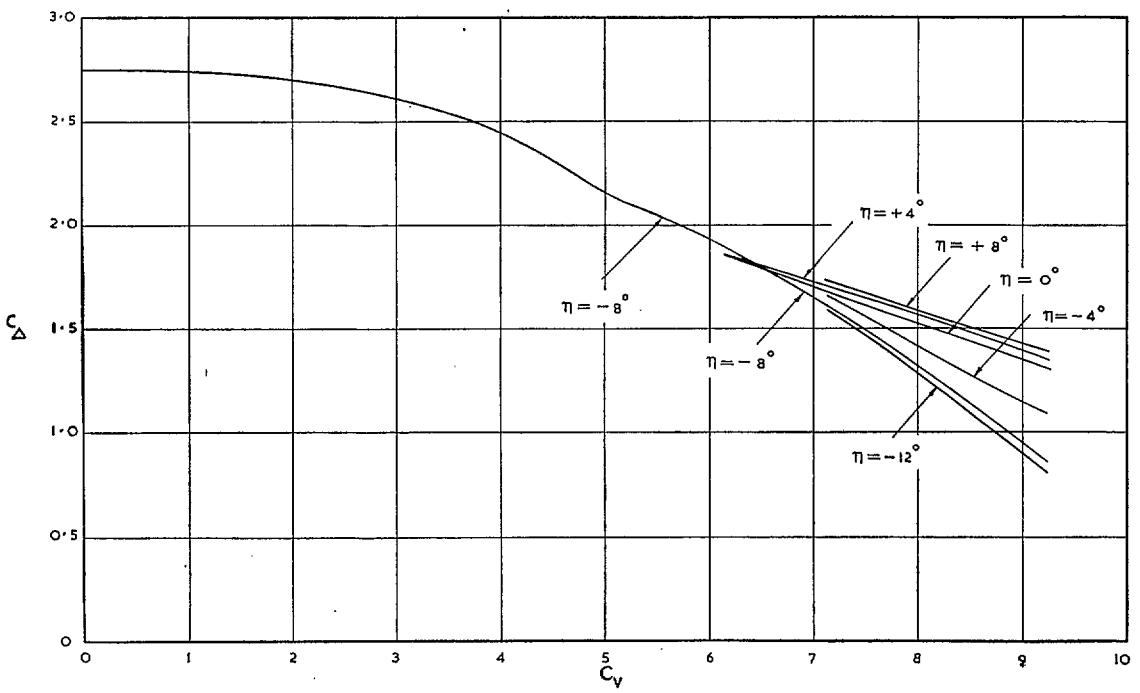

FIG. 203. Model L load-coefficient curves ($C_{\Delta 0} = 2{\cdot}75$).

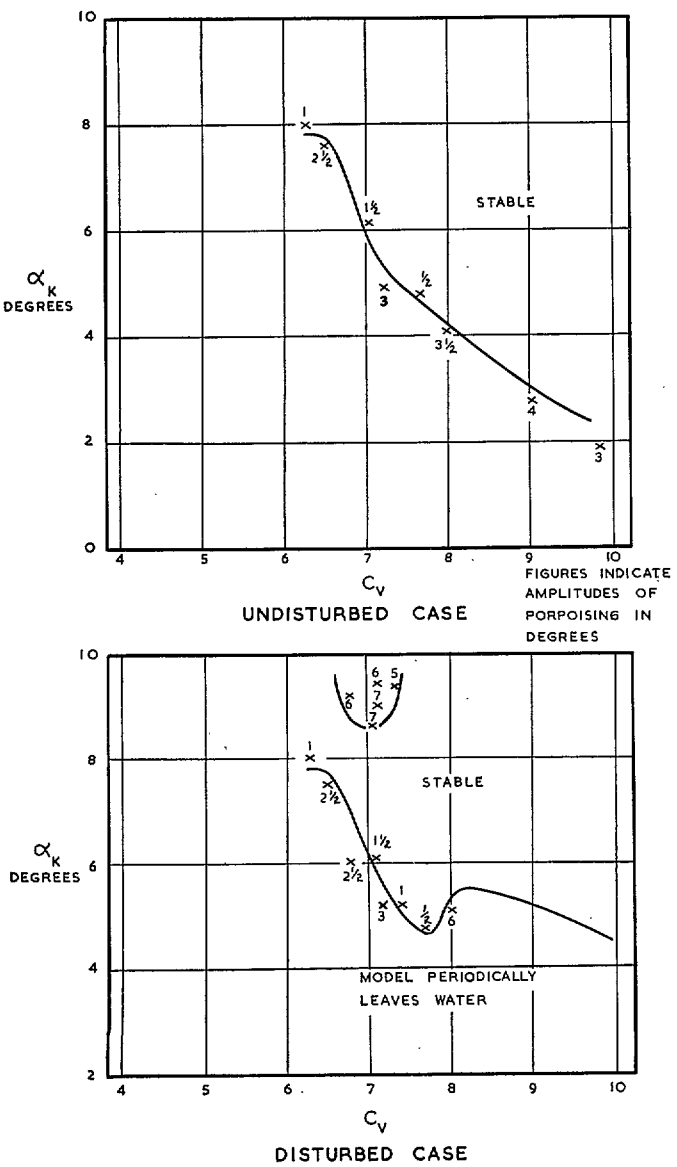

FIG. 204. Model L porpoising amplitudes and stability limits ($C_{\Delta 0} = 2{\cdot}75$).

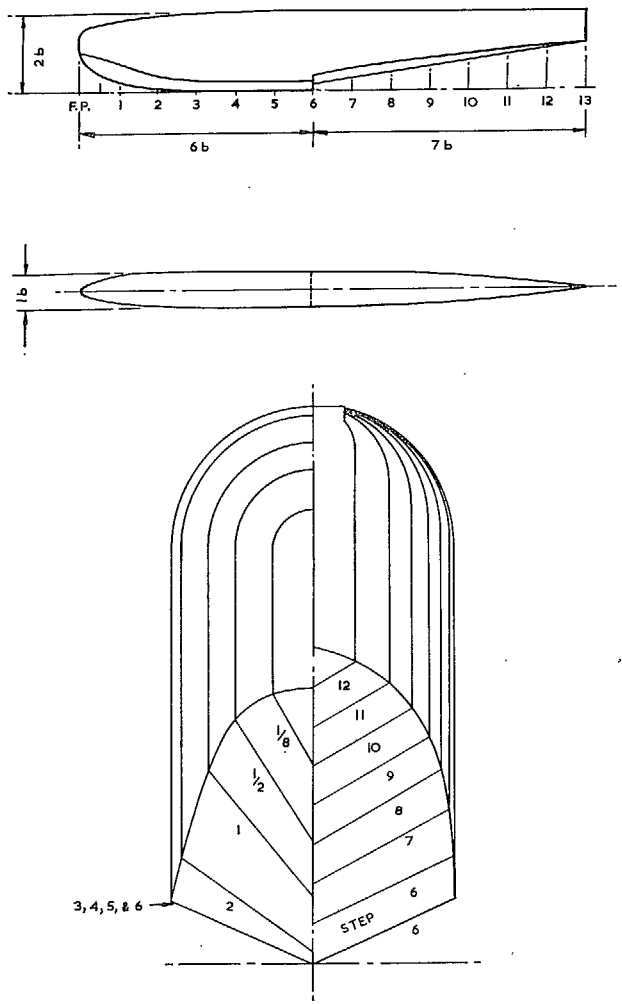

FIG. 205. Model M hull lines.

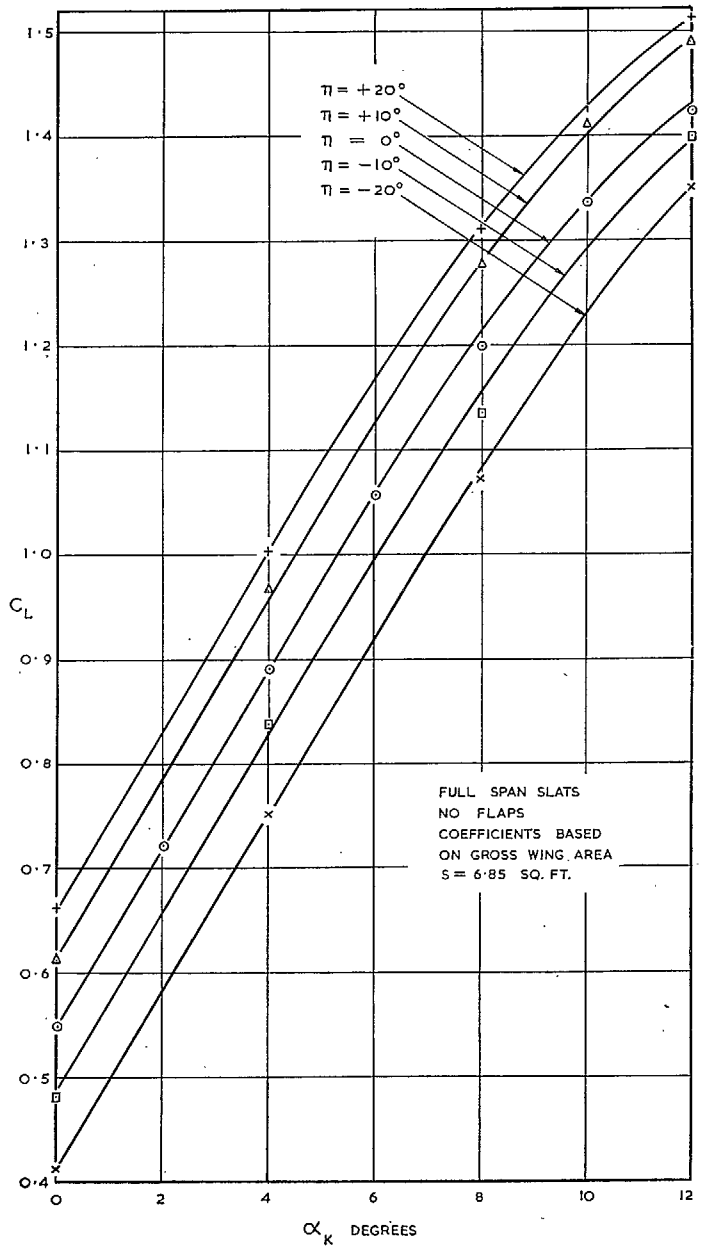

FIG. 206. Model M lift curves without slipstream.

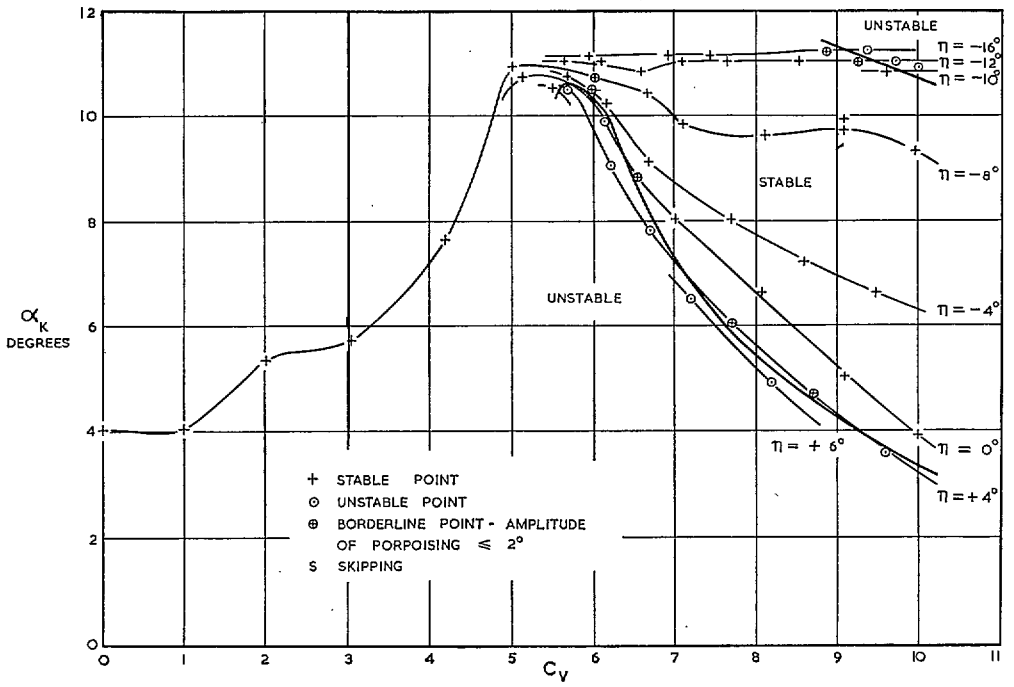

FIG. 207. Model M longitudinal stability without disturbance ($C_{\Delta 0} = 2{\cdot}75$).

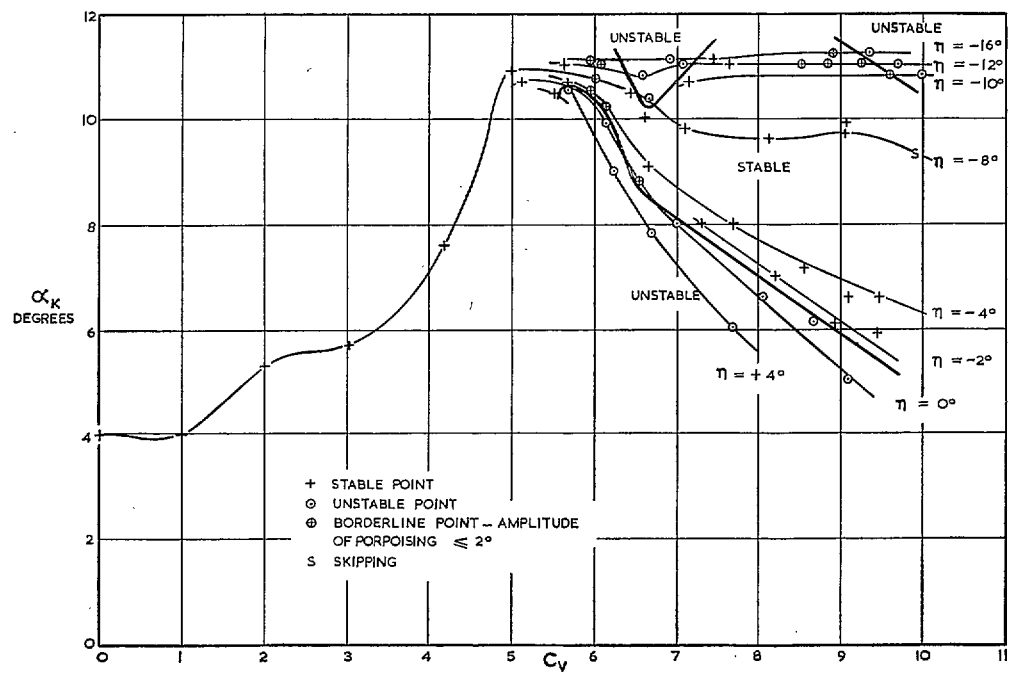

FIG. 208. Model M longitudinal stability with disturbance ($C_{\Delta 0} = 2{\cdot}75$).

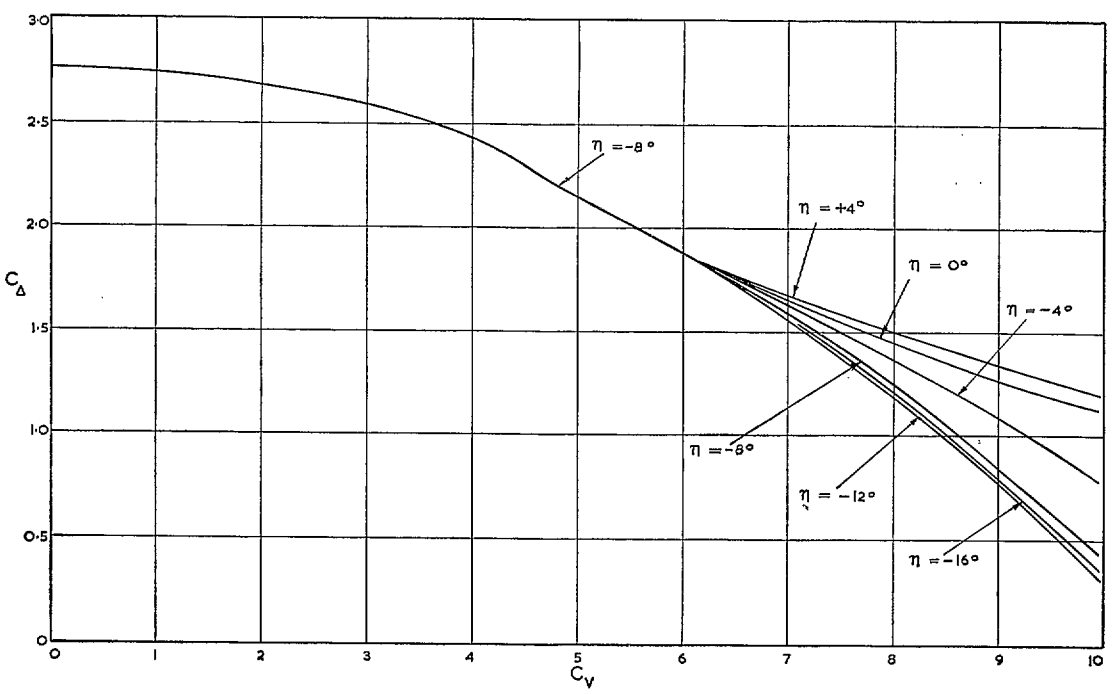

FIG. 209. Model M load-coefficient curves ($C_{\Delta 0} = 2{\cdot}75$).

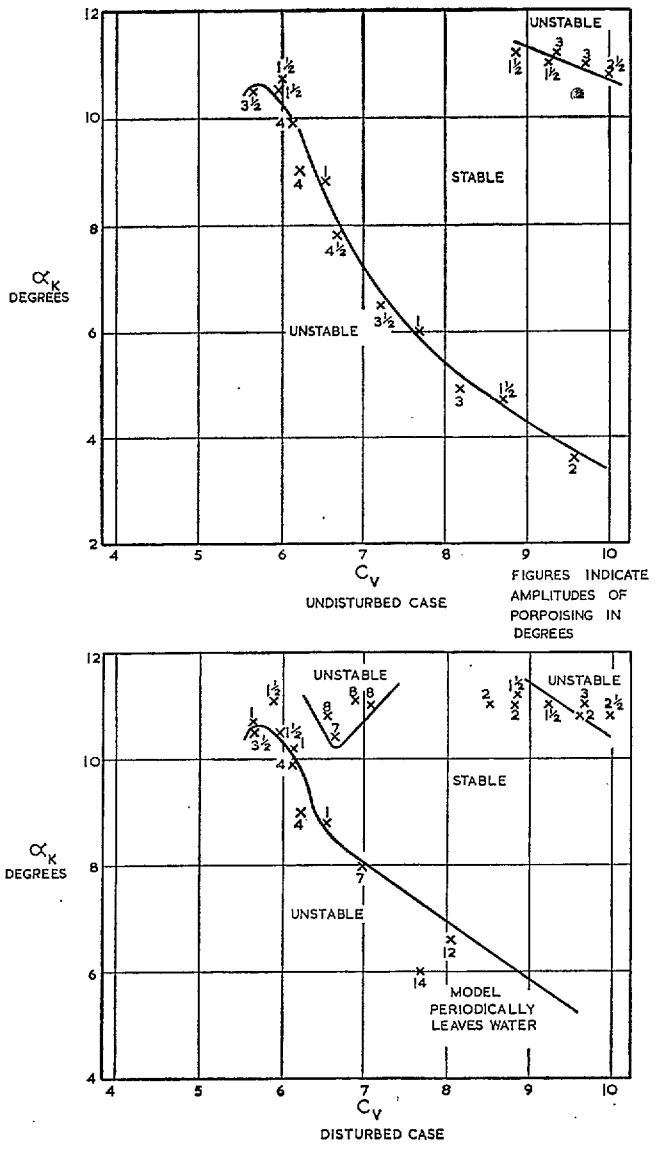

FIG. 210. Model M porpoising amplitudes and stability limits ($C_{\Delta 0} = 2{\cdot}75$).

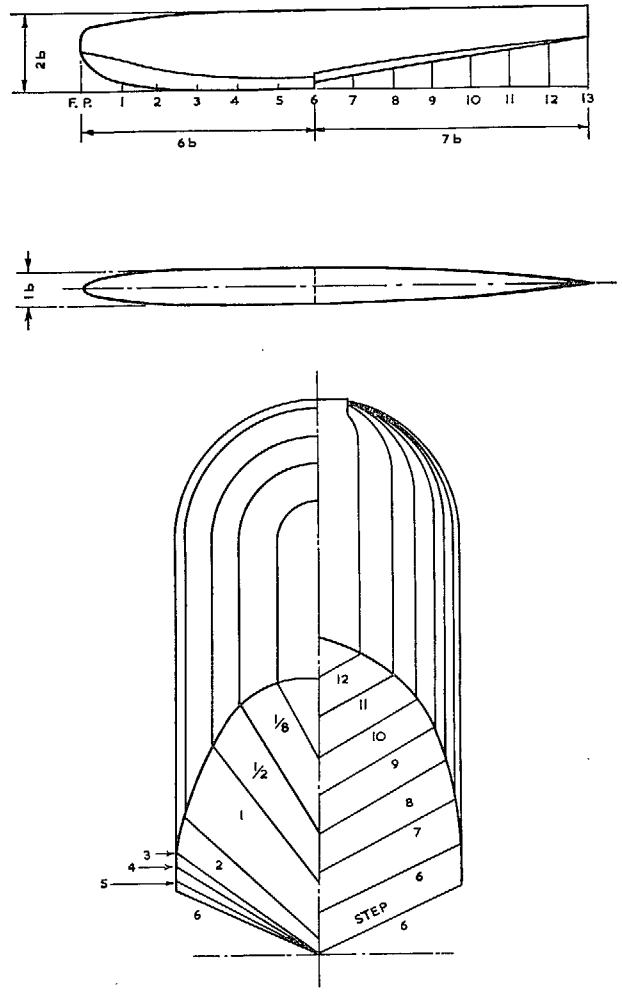

FIG. 211. Model N hull lines.

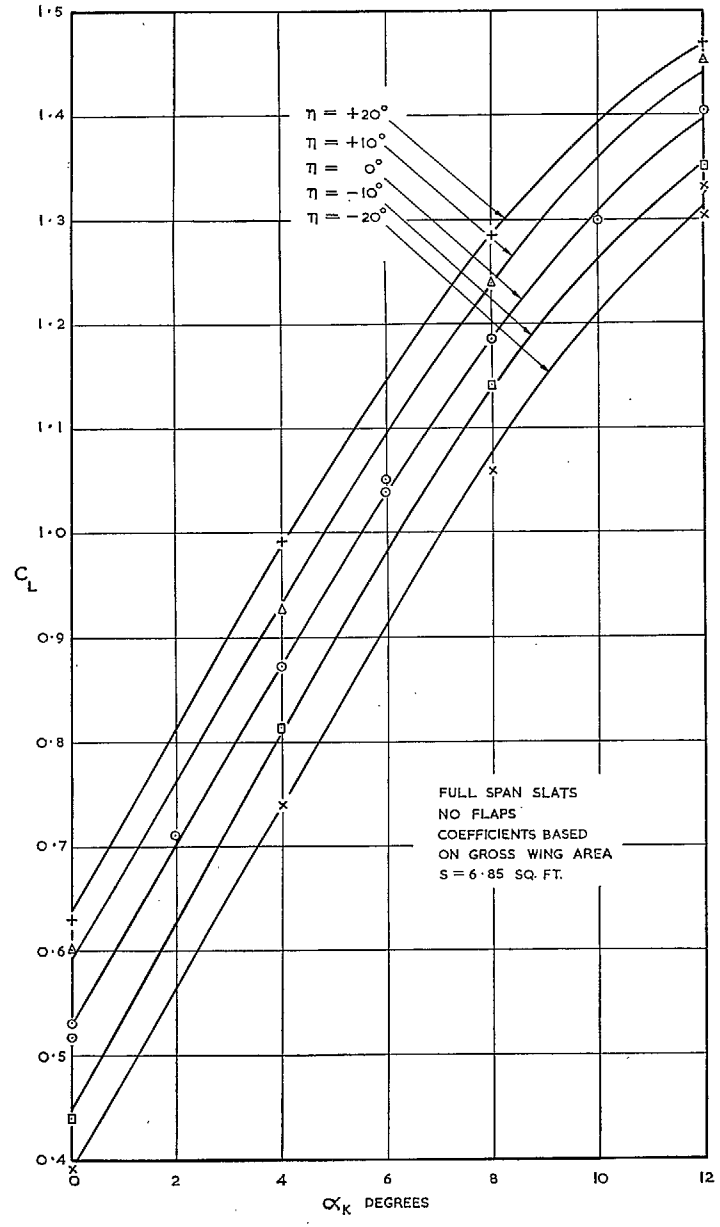

FIG. 212. Model N lift curves without slipstream.

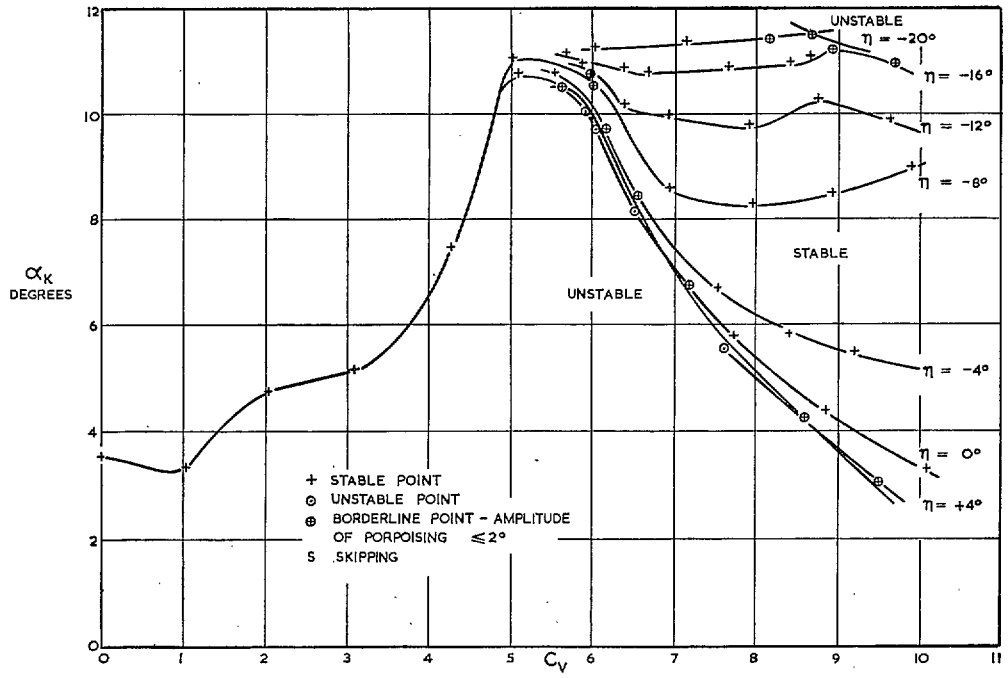

FIG. 213. Model N longitudinal stability without disturbance ($C_{\Delta 0} = 2{\cdot}75$).

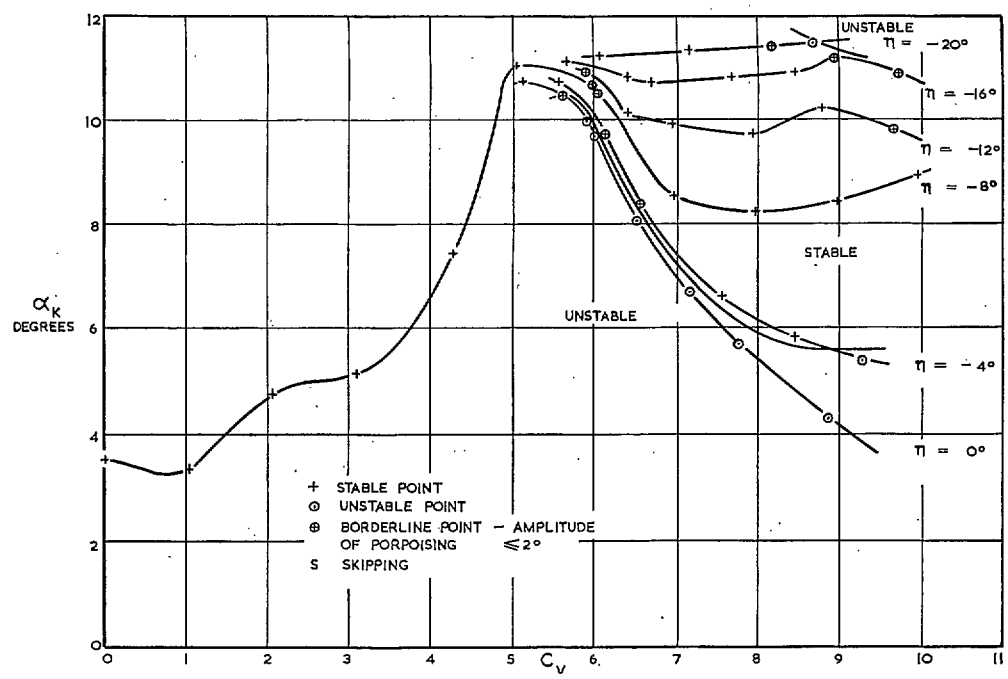

FIG. 214. Model N longitudinal stability with disturbance ($C_{\Delta 0} = 2{\cdot}75$).

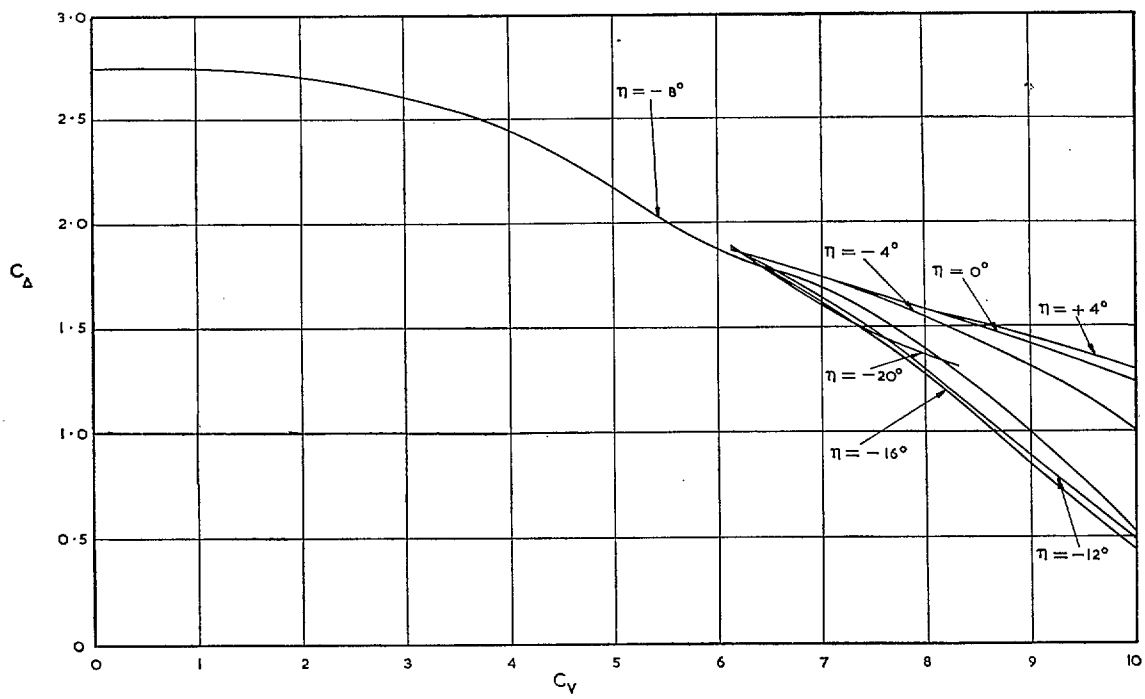

FIG. 215. Model N load-coefficient curves ($C_{\Delta 0} = 2{\cdot}75$).

(73844) Wt. 53/2293 K.5 11/59 Hw.

PRINTED IN ENGLAND

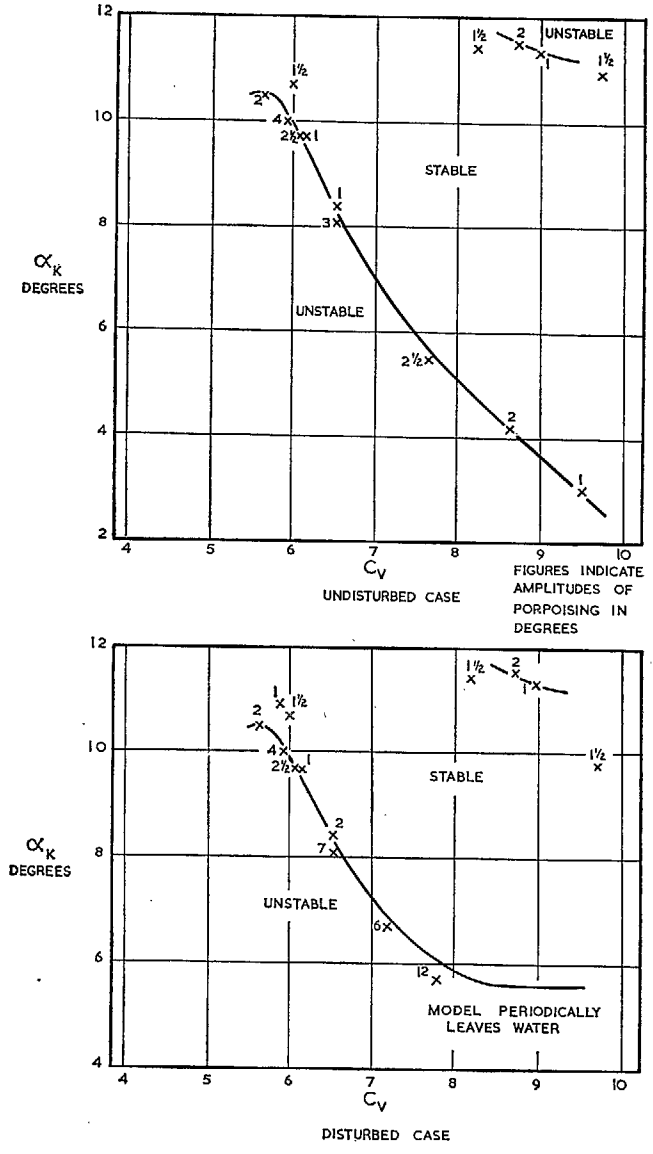

FIG. 216. Model N porpoising amplitudes and stability limits ($C_{\Delta 0} = 2{\cdot}75$).

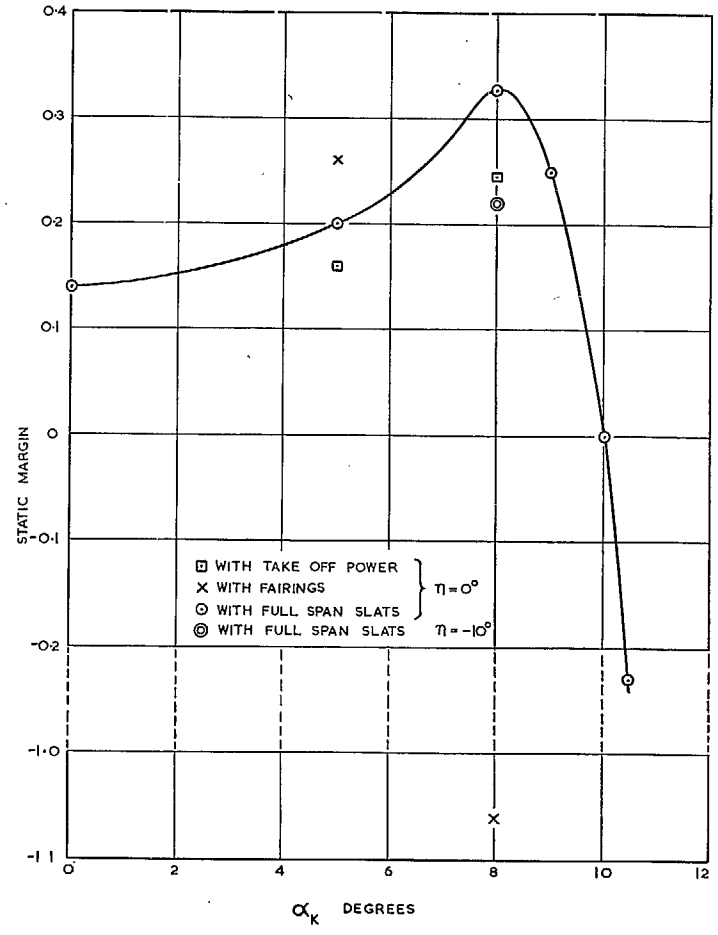

FIG. 217. Variation of static margin with attitude.